

PHYSICAL, CHEMICAL AND BIOLOGICAL PROPERTIES OF AIRBORNE PARTICLES
EMITTED FROM ANIMAL CONFINEMENT BUILDINGS

BY

XUFEI YANG

DISSERTATION

Submitted in partial fulfillment of the requirements
for the degree of Doctor of Philosophy in Agricultural and Biological Engineering
in the Graduate College of the
University of Illinois at Urbana-Champaign, 2010

Urbana, Illinois

Doctoral Committee:

Associate Professor Xinlei Wang, Chair
Professor Yuanhui Zhang
Professor Richard S. Gates
Professor Keith R. Cadwallader
Professor Mark J. Rood
Associate Professor Zhongchao Tan, University of Waterloo

ABSTRACT

Airborne particles emitted from animal confinement buildings have been an environmental concern for some time. Relevant regulations are under discussion. However, one of the major obstacles is a lack of comprehensive understanding of their physical, chemical and biological properties that may be closely related to environmental and health effects. In addition, the use of receptor modeling requires known chemical source profiles. To address the current research need, airborne particles collected from six types of animal confinement buildings were subject to characterization.

First, TSP, PM₁₀ and PM_{2.5} concentrations were determined gravimetrically and their variations were investigated. PM concentrations were significantly affected by animal building type, season (ambient temperature) and feeding systems; while, animal density had no significant effect. Specifically, higher PM concentrations occurred in poultry buildings than swine buildings; PM concentrations decreased with ambient temperature; and wet feeding systems were associated with lower TSP and PM₁₀ concentrations than dry feeding systems. A generalized linear model was established for estimating PM₁₀ concentrations in swine buildings with animal building type, daily average ambient temperature, specific fan area, animal density, and TSP concentrations as predictors. The coefficient of determination (R^2) of the proposed model was 0.907.

Second, some previous studies reported that Federal Reference and Equivalent Method (FRM/FEM) PM samplers oversample PM₁₀ and PM_{2.5} from agricultural sources. They proposed an indirect method that calculates PM₁₀ and PM_{2.5} concentrations from TSP concentrations and the particle size distribution (PSD) of TSP. The conclusion and the proposed calculation method were established based on several assumptions. The present study shows that when different assumptions are employed, different conclusions and calculation results could be obtained. The PM₁₀ and PM_{2.5} concentrations derived from different particle size analyzers could be significantly different. Among the four analyzers under investigation, Aerosizer DSP produced the most comparable PM₁₀ concentrations to the gravimetric method.

Third, the chemical composition of the PM₁₀ and PM_{2.5} samples was examined, including inorganic elements and soluble ions. The present study revealed that PM chemical composition

varied significantly with animal building type. PM samples from certain different types of animal confinement buildings, e.g., manure-belt layer hen and tom turkey, had significantly different chemical compositions, indicating a possibility of applying receptor models to determining PM contributions by different animal building types. Seasons had no significant effect on PM₁₀ and a significant but slight effect on PM_{2.5} chemical compositions- the absence of strong seasonal variations is a good news for PM receptor modeling. Future efforts should be made to apply receptor models to animal production related air quality problems, and to compare receptor models with dispersion models to assess their respective advantages and limitations. PM_{2.5} samples from different types of animal confinement buildings had more similar chemical compositions than PM₁₀ samples. One of the limitations associated with the present study is that the total mass fraction of investigated chemical species was low, typically less than 16%. Future investigations should attempt to characterize the rest of PM mass.

Fourth, a total of 57 odorants were identified and quantified in TSP, PM₁₀ and feed samples. Acetic acid and ethanol were the most abundant odorants; while, phenylacetic acid and (E,E)-2,4-decadienal were the top two odor contributors, considering their low odor thresholds in air. The odorant composition of PM samples varied significantly with animal building type. Compared to the TSP samples, the PM₁₀ samples from different animal buildings were more similar in odorant composition and contributed on average 50% of the odor strength of TSP samples. The effect of seasons was also significant, but less substantial than that of animal building types. A gradual change in odorant composition from hot to mild to cold seasons was observed. TSP and PM₁₀ samples were found to have significantly different odorant compositions and significantly higher odorant contents than feed samples, suggesting that the majority of particle-borne odorants may originate from sources other than feed. Different than the conclusions from some previous studies, the present study suggests that the majority of odorants exist in the gas phase rather than on particles.

Fifth, airborne endotoxins and (1→3)-β-D-glucans in TSP samples were analyzed. Most measured airborne endotoxin concentrations exceeded the exposure limit proposed by Donham et al. (1995; 2000) and the threshold issued by the Dutch Health Council in the Netherlands, which may raise a health concern for farm workers as well as animals grown in confined environments. The present study revealed that animal building types had a significant effect on airborne endotoxins and (1→3)-β-D-glucan concentrations, but no significant effect on the

contents of endotoxin and (1→3)- β -D-glucan in particles. By contrast, seasons had no significant effect on airborne endotoxin and (1→3)- β -D-glucan concentrations but a significant effect on their contents in particles, which increased with the daily average ambient temperature. Elevated indoor temperatures during the summer were considered to facilitate the growth and propagation of bacteria and fungi, thus leading to higher microbial contents in particles. A significant and positive correlation was identified between TSP and airborne endotoxin/ (1→3)- β -D-glucan concentrations, implying a possibility of applying existing dust control techniques for the mitigation of these two bioactive agents.

ACKNOWLEDGEMENT

I would like to express my great gratitude to Dr. Xinlei Wang, my dissertation advisor. Without his instruction, help and support, I cannot imagine where my PhD study would end up with. Thanks, Dr. Wang, for encouraging and giving me opportunities to manage research projects, teach classes, write proposals, participate in professional societies and coordinate conference sessions. I am particularly grateful to him for believing in me, offering me plenty of freedom in research, and, more importantly, sticking with me for over five years. I really appreciate his kindness, patience and other great personalities.

I would like to give many thanks to my committee members: Dr. Yuanhui Zhang, Dr. Richard Gates, Dr. Keith Cadwallader, Dr. Mark Rood and Dr. Zhongchao Tan for spending their precious time on my PhD dissertation. My special thanks go to Dr. Yuanhui Zhang, Dr. Keith Cadwallader and Dr. Roderick Mackie for their continuous support without conservation to the USDA project that I have been working for in past a few years.

Words cannot express my gratefulness to Jongmin Lee and Jingwei Su for helping me accomplish once seemingly never-ending field trips, and to Yaowapa Lorjaroenphon for analyzing odorants and for allowing me to use her data, and to Dr. Ted Funk, Steve Ford and Matt Robert for helping me locate sampling sites, build and repair sampling equipment and for offering me numerous instructions and suggestions.

I am also thankful to my research partners- Dr. Xiangzhen Li, Dr. Peiying Hong and Dr. Takumi Shinkai, and to my graduate colleagues- Sheryl Jerez, Hai Wu, Zhichao Wang, Guo Yu, Wei Yan, Liangcheng Yang, Nan Jiang, Rong Dong, Dongning Li and Doug Barker, and to all the people on- and off-campus who offered their support and assistance during my PhD study.

Finally, I want to give my deep thanks to my family- my wife Liping and daughter Lele (Nancy), my parents, grandma and parents-in-law. Their love is the biggest strength of mine, encouraging me to move forward. I owe them a better life and I promise that will come soon.

TABLE OF CONTENTS

LIST OF FIGURES	VIII
LIST OF TABLES	XII
LIST OF SYMBOLS	XVII
LIST OF ABBREVIATIONS AND ACRONYMS	XX
1. INTRODUCTION	1
1.1 Motivation.....	1
1.2 Objectives	3
1.3 Approach.....	4
2. LITERATURE REVIEWS	6
2.1 Air Pollutants in Animal Confinement Buildings.....	6
2.2 Emissions of Gaseous Air Pollutants from Animal Confinement Buildings.....	10
2.3 Emissions of Airborne Particles from Animal Confinement Buildings	19
2.4 Air Quality Modeling.....	46
2.5 Chemical Speciation of Airborne Particles from Animal Confinement Buildings.....	54
2.6 Source, Health Effects and Measurement of Airborne Endotoxins and (1→3)-β-D-Glucan in Animal Confinement Buildings	62
3. MASS CONCENTRATIONS OF TSP, PM ₁₀ AND PM _{2.5} EMITTED FROM SWINE AND POULTRY CONFINEMENT BUILDINGS	73
3.1 Introduction.....	73
3.2 Materials and Methods.....	75
3.3 Results and Discussions	97
3.4 Limitations and Recommendations.....	137
3.5 Chapter Summary and Conclusions.....	138
4. CHARACTERIZATION OF INORGANIC ELEMENTS AND SOLUBLE IONS IN PM ₁₀ AND PM _{2.5} EMITTED FROM ANIMAL CONFINEMENT BUILDINGS	142
4.1 Introduction.....	142
4.2 Literature Reviews	144
4.3 Materials and Methods.....	145
4.4 Results and Discussions	148
4.5 Limitations and Recommendations.....	168
4.6 Summary and Conclusions	169

5. CHARACTERIZATION OF PARTICLE-BORNE ODORANTS FROM ANIMAL CONFINEMENT BUILDINGS	172
5.1 Introduction.....	172
5.2 Materials and Methods.....	174
5.3 Results and Discussions	178
5.4 Chapter Summary and Conclusions.....	235
6. ASSESSMENT OF AIRBORNE ENDOTOXIN AND (1→3)-BETA-D-GLUCAN IN SWINE AND POULTRY CONFINEMENT BUILDINGS.....	240
6.1 Introduction.....	240
6.2 Approaches	242
6.3 Results and Discussions	245
6.4 Chapter Summary and Conclusions.....	260
7. CONCLUSIONS AND RECOMMENDATIONS	263
7.1 Conclusions.....	263
7.2 Recommendations.....	266
REFERENCES	268
APPENDIX A. FARM INFORMATION OF SAMPLING SITES	300
APPENDIX B. LAYOUT OF ANIMAL FACILITIES UNDER INVESTIGATION.....	315
APPENDIX C. SAMPLING PROCEDURE AND MASS MEASUREMENT.....	322
APPENDIX D. MEASUREMENT OF PSD WITH HORIBA LA-300 PARTICLE SIZER	325
APPENDIX E. MEASUREMENT OF PARTICLE DENSITY WITH PYCNOMETER.....	327
APPENDIX F. LOGNORMAL REGRESSION ANALYSIS OF THE PARTICAL SIZE DISTRIBUTION DATA	329
APPENDIX G. FITTING PERFORMANCE OF PARTICLE SIZE DISTRIBUTION MODELS ON ANIMAL BUILDING DUST.....	341
APPENDIX H. CALIBRATION OF VENTURI ORIFICES	358
APPENDIX I. LIST OF VOLATILE ORGANIC COMPOUNDS ANALYZED IN THIS STUDY	361
APPENDIX J. EXPERIMENTAL PROCEDURE FOR ENDOTOXIN AND (1-3)-BETA-D-GLUCAN ANALYSES	363
AUTHOR’S BIOGRAPHY	367

LIST OF FIGURES

Figure 2.1. Deposition regions of different sized particles in the human respiratory system.	31
Figure 2.2. Comparison of the size-cut curves of the EPA defined FRM PM ₁₀ and PM _{2.5} sampler with the ACGIH defined inhalable, thoracic, and respirable samplers.	33
Figure 2.3. Two basic designs of the PM ₁₀ size separators.	35
Figure 2.4. Structure of an endotoxin (LPS) molecule.	63
Figure 2.5. Structure of a (1→3)-β-D-glucan molecule.	69
Figure 3.1. Schematic of a multi-point TSP sampling system.	77
Figure 3.2. Schematic of a Harvard impactor.	78
Figure 3.3. Sampling setup in an animal building.	80
Figure 3.4. Flowchart for statistical analysis on PM concentrations.	81
Figure 3.5. Process flowchart for examining the validity of indirect calculation method.	83
Figure 3.6. Approaches to determining PM ₁₀ mass fraction on a PSD profile.	86
Figure 3.7. Penetration curves for calculation of PM ₁₀ and PM _{2.5} mass fractions.	89
Figure 3.8. Selection of the characteristic diameter of a size range.	90
Figure 3.9. Simulated size selective sampling by an FRM/ FEM PM ₁₀ sampler: a- an assumed lognormal penetration curve (D ₅₀ =10 μm and S=1.5), b- an assumed lognormal PSD curve of a TSP sample (MMD=15, GSD=1.5), and c- the PSD curve of the collected PM ₁₀ versus that of the TSP sample.	93
Figure 3.10. Parts of the results of mass concentration measurements. The errors bars represent the standard deviation of PM concentrations.	98
Figure 3.11. Percentile plot of measured PM ₁₀ and PM _{2.5} concentrations.	105
Figure 3.12. QQ plot of TSP concentration data before (a) and after transformation (b).	106
Figure 3.13. Effect of animal building type on PM concentrations and mass ratios.	109
Figure 3.14. Effect of animal density on PM concentrations and mass ratios.	110
Figure 3.15. Effect of seasons on PM concentrations and mass ratios.	111
Figure 3.15. (cont.).....	112
Figure 3.16. Effect of ambient temperature on PM concentrations and mass ratios.	113
Figure 3.17. Effect of feeding system on PM concentrations and mass ratios.	114
Figure 3.18. Measured versus predicted PM ₁₀ concentrations: A- datasets for regression, B- datasets for validation, error bars represent the 95% confidence level.	119
Figure 3.19. Comparison of R _{PM10} values derived from different approaches and different particle size analyzers.	124

Figure 3.20. Comparison between a measured and an assumed PSD curve with identical MMD and GSD. The measured PSD curve has a tail peak in the size range of 0.5 to 5 μm	125
Figure 3.21. Comparison of the penetration curve of an ideal PM_{10} sampler to the assumed lognormal penetrative curve ($D_{50}= 10 \mu\text{m}$ and slope=1.5).....	126
Figure 3.22. Comparison of calculated to measured PM_{10} concentrations (approach B, d_j -average diameter). The blue dash line represents the 95% confidence interval of slope.	130
Figure 3.23. Effects of correction on calculated PM_{10} concentrations. Only the data available from all the four analyzers were shown herein.	132
Figure 3.24. Hierarchical plot of calculated and measured PM_{10} concentrations.....	133
Figure 4.1. EDXRF spectra for two PM_{10} samples (excitation condition #2)	149
Figure 4.2. Correlation between EDXRF counts (from the 2 nd excitation condition) and the mass of an element determined by ICP-AES.	151
Figure 4.3. Average mass fraction of inorganic elements and soluble ions in PM samples.....	153
Figure 4.4. Correlation distance-based PCoA plot of PM samples from different types of animal buildings: (a) PM_{10} and (b) $\text{PM}_{2.5}$ samples.....	157
Figure 4.5. Schematic of swine production cycle used in the Midwest.....	162
Figure 4.6. Correlation distance-based PCoA plot of PM samples from different seasons: (a) PM_{10} and (b) $\text{PM}_{2.5}$ samples.....	164
Figure 4.7. Correlation distance-based PCoA plot of PM_{10} versus $\text{PM}_{2.5}$ samples.	165
Figure 4.8. PCA scree plot for chemical composition of PM_{10} and $\text{PM}_{2.5}$ samples.	166
Figure 4.9. Correlation distance-based PCoA plot of chemical species in PM samples.	167
Figure 5.1. Effect of animal building type on (a) total mass fraction and (b) Simpson's diversity index of odorants in TSP samples.	194
Figure 5.2. Non-metric MDS plot of TSP samples from different types of animal confinement buildings based on mass fraction of odorants.	196
Figure 5.3. Effect of animal building type on (a) COI_p and (b) COI of TSP samples.....	201
Figure 5.4. Effect of animal building type on Simpson's diversity index of OAV_p -based odorant composition in TSP samples.	202
Figure 5.5. Effect of animal building type on odor strength per mass of odorants in TSP samples.	203
Figure 5.6. Non-metric MDS plot of TSP samples from different types of animal confinement buildings based on OAV_p of odorants.....	204
Figure 5.7. Non-metric MDS plot of PM_{10} samples from different types of animal confinement buildings based on mass fraction of odorants.	208

Figure 5.8. Effect of animal building type on odor strength per mass of odorants in PM ₁₀ samples.	211
Figure 5.9. Non-metric MDS plot of PM ₁₀ samples from different types of animal confinement buildings based on OAV _P of odorants.....	212
Figure 5.10. Correlation distance-based PCoA plot of particle samples from different types of animal confinement buildings: (a) TSP samples, mass fraction; (b) TSP samples, OVA _P ; (c) PM ₁₀ samples, mass fraction; (d) PM ₁₀ samples, OVA _P	215
Figure 5.11. Non-metric MDS plot of TSP samples collected in different seasons- (a) mass fraction-based and (b) OVA _P based odorant composition.	220
Figure 5.12. Non-metric MDS plot of PM ₁₀ samples collected in different seasons- (a) mass fraction-based and (b) OVA _P based odorant composition.	222
Figure 5.13. Comparison among TSP, PM ₁₀ and feed samples in terms of (a) total mass fraction of identified odorants, (b) Simpson's index for mass fraction-based odorant composition, (c) COI _P , and (d) Simpson's index for OAV _P -based odorant composition.	224
Figure 5.14. Bray-Curtis dissimilarity-based non-metric MDS and correlation distance-based PCoA plots of TSP, PM ₁₀ and feed samples- (a) Non-metric MDS plot based on mass fraction of odorants, (b) PCoA plot based on mass fraction of odorants, (c) Non-metric MDS plot based on OAV _P of odorants; (d) PCoA plot based on OAV _P of odorants.....	226
Figure 5.15. PCoA plots of identified odorants in (a) TSP and (b) PM ₁₀ samples.....	230
Figure 5.16. Proposed sample setup for collection of particle-borne odors	235
Figure 6.1. Variations in (a) endotoxin and (b) (1→3)-β-D-glucan levels with animal building type.....	253
Figure 6.2. Effect of seasons on endotoxin and (1→3)-β-D-glucan levels.	255
Figure 6.3. Effect of ambient temperature on endotoxin and (1→3)-β-D-glucan levels.....	256
Figure 6.4. Indoor and ambient temperature in different seasons.....	257
Figure 6.5. Airborne endotoxin/ (1→3)-β-D-glucan concentration versus TSP concentration.	259
Figure B.1. Layout of animal buildings.	315
Figure B.1. Layout of animal buildings (cont. 1)	316
Figure B.1. Layout of animal buildings (cont. 2)	317
Figure B.1. Layout of animal buildings (cont. 3)	318
Figure B.1. Layout of animal buildings (cont. 4)	319
Figure B.1. Layout of animal buildings (cont. 5)	320
Figure B.1. Layout of animal buildings (cont. 6)	321
Figure C.1. Sampling setup in an animal building.....	323

Figure D.1. A PSD profile measured by Horiba.	326
Figure F.1. Linear regression of a PSD example on an Excel sheet.	331
Figure F.2. Examples of PSD profiles with different peak characteristics: a- the 21 st dataset, b- the 3 rd dataset, c- the artificial (A) dataset, and d- the 7 th dataset; Left-measured data (open square) and linear regression line (blue dash line) on the log-probability graph, and Right- observed PSD curve (open square), PSD curve from nonlinear regression (red solid line) and PSD curve from linear regression (blue dash line).	334
Figure F.2. (cont.)	335
Figure F.3. Percentile plot of C values from different particle size analyzers.	338
Figure F.4. Scatter plot of R^2_{linear} versus $R^2_{\text{nonlinear}}$ from different particle size analyzers.	339
Figure F.5. Two extreme PSD examples: a- point 'a' in Figure F.4 (Malvern, $R^2_{\text{linear}}=0.8774$, $R^2_{\text{nonlinear}}=0.9503$); b- point 'b' in Figure F.4 (Coulter, $R^2_{\text{linear}}=0.9759$, $R^2_{\text{nonlinear}}=0.7018$).	339
Figure G.1. PSD curves predicted by different models.	347
Figure G.2. Fitting performance of six particle size distribution models on data derived from four different particle size analyzers; L= lognormal, W= Weibull, G= Gamma, E= exponential, K= Khragian-Mazin, and C= Chen's empirical.	348
Figure G.2 (cont.)	349
Figure G.3. Rank of fitting performances of six models on PSD data derived from: a- Horiba, b- DSP, c- Coulter, and d- Malvern.	350
Figure G.4. PSD curves of one-parameter models: a- exponential, b- Khragian-Mazin, c- Chen's empirical.	352
Figure G.5. Comparison of a measured PSD curve versus regression curves predicted by the exponential ($R^2=-0.5132$), Khragian-Mazin ($R^2=-1.3017$) and Chen's empirical models ($R^2=-1.0584$).	353
Figure H.1. Calibration curves for venturi orifices used for TSP samplers- bench test.	358
Figure H.2. Calibration curves for venturi orifices used for PM ₁₀ and PM _{2.5} samplers- bench test.	359
Figure H.3. Effect of airflow rate on 50% cut size (D_{50}) of PM samplers.	360
Figure J.1. Layout of the 96-well microplate for endotoxin analysis.	365
Figure J.2. Determination of the reaction time on an absorbance curve.	365

LIST OF TABLES

Table 1.1. Analytical methods used in current study.....	5
Table 2.1. Threshold limit values for typical air pollutants in animal confinement buildings	6
Table 2.2. Comparison of commonly used dispersion and receptor models	53
Table 2.3. Summary of airborne endotoxin test results in swine and poultry buildings.....	68
Table 3.1. Sampling sites for PM collection.....	75
Table 3.2. List of samplers and filters in current study	78
Table 3.3. Comparison of particle size analyzers used in this study	84
Table 3.4. Approaches to determining the mass fractions of PM ₁₀ and PM _{2.5} in a TSP sample.....	86
Table 3.5. Penetration curve of an ideal PM ₁₀ sampler (CFR, 1987).	87
Table 3.6. Penetration curve of an ideal PM _{2.5} sampler (CFR, 1997).	87
Table 3.7. Penetration curve of an ideal PM _{2.5} sampler with a PM ₁₀ inlet.	88
Table 3.8. Summary of PM mass concentrations (I): animal building type.	99
Table 3.9. Summary of PM mass concentrations (II): season.	100
Table 3.10. Summary of PM mass concentrations (III): animal building type × season.....	101
Table 3.11. PM mass concentrations in animal confinement buildings.	103
Table 3.12. Threshold limits of PM concentrations.....	104
Table 3.13. Frequency of measured PM concentrations exceeding threshold limits.....	105
Table 3.14. Normality of PM concentration data before and after transformation.....	106
Table 3.15. Normality of PM mass ratio data before and after transformation.	106
Table 3.16. Pairwise one-way ANOVA test on PM concentrations and mass ratios with animal building type as a factor.	108
Table 3.17. Correlation between animal density and PM concentrations (mass ratios).	111
Table 3.18. Paired t-tests on PM concentrations and mass ratios with season as a factor.....	113
Table 3.19. Correlation between ambient temperature and PM concentrations (mass ratios).....	113
Table 3.20. ANOVA tests on PM concentrations and mass ratios- dry versus wet feeding systems.	114
Table 3.21. Parameter estimates and goodness-of-fit of PM concentration models.....	117
Table 3.22. Parameter estimates and goodness-of-fit of modified PM concentration models.	118

Table 3.23. Sensitivity coefficients and measurement errors of predictors in the modified PM ₁₀ concentration model.....	121
Table 3.24. Ratios of calculated to measured PM ₁₀ and PM _{2.5} concentrations- A summary.....	122
Table 3.25. Normality of the original and log-transformed ratio data.....	123
Table 3.26. Paired t-tests on PM ₁₀ concentrations derived from different approaches.	124
Table 3.27. Paired t-tests on PM _{2.5} concentrations derived from different approaches.....	126
Table 3.28. Paired t-tests on PM concentrations derived from different particle size analyzers (N=35, d _j - average diameter).....	127
Table 3.29. Geometric mean and geometric standard deviation of R _{PM10} values derived from different particle size analyzers and approaches.	131
Table 3.30. Paired t-tests on PM ₁₀ concentrations calculated with different d _j : average versus maximum diameter.	134
Table 3.31. Summary of errors for PM mass measurements without post-conditioning.	135
Table 3.32. Summary of parameter estimates for Equation 3.27.....	136
Table 4.1. Summary of field sampling.....	145
Table 4.2. Excitation conditions applied on the KeveX 770 EDXRF analyzer.....	146
Table 4.3. Mass fraction of inorganic elements and soluble ions in PM ₁₀ samples (in ng/mg dust).....	154
Table 4.4. Mass fraction of inorganic elements and soluble ions in PM _{2.5} samples (in ng/mg dust).....	155
Table 4.5. Summary of ANOSIM test on PM ₁₀ and PM _{2.5} samples from different type of animal confinement buildings ^{x,y}	158
Table 4.6. Major chemical species in PM ₁₀ samples that contribute to variations in chemical composition among different types of animal confinement buildings.	160
Table 4.7. Major chemical species in PM _{2.5} samples that contribute to variations in chemical composition among different types of animal confinement buildings.	161
Table 4.8. ANOSIM test on PM ₁₀ and PM _{2.5} samples from different seasons.	163
Table 4.9. Summary of ANOSIM test on PM samples from the same types of animal confinement buildings but differing in particle size (PM ₁₀ versus PM _{2.5}).....	166
Table 5.1. Summary of field sampling.....	174
Table 5.2. Frequency of occurrence of the odorants identified in TSP, PM ₁₀ and feed samples and comparison with references.	179
Table 5.2. (cont. 1).....	180
Table 5.2. (cont. 2).....	181
Table 5.3. Thresholds, sensory characteristics and sources of the odorants identified in this study.	181

Table 5.3. (cont. 1).....	182
Table 5.3. (cont. 2).....	183
Table 5.4. Summary of quantitative analysis results- mass fraction of odorants in particle and feed samples (in ppm).	184
Table 5.4. (cont. 1).....	185
Table 5.4. (cont. 2).....	186
Table 5.4. (cont. 3).....	187
Table 5.4. (cont. 4).....	188
Table 5.4. (cont. 5).....	189
Table 5.5. Most abundant odorants in particle and feed samples.	190
Table 5.6. Top odor-contributing compounds in particle and feed samples.....	192
Table 5.7. Total mass fraction and Simpson’s diversity index of odorants in TSP samples from different types of animal confinement buildings.....	193
Table 5.8. Summary of ANOSIM test on TSP samples from different types of animal confinement buildings based on mass fraction of odorants (R global =0.416, p<0.001) ^{a,b}	197
Table 5.9. Major odorants in TSP samples that contribute to variations in mass fraction-based odorant composition among different animal building types.	199
Table 5.10. Total mass fraction and Simpson’s diversity index of odorants in TSP samples from different types of animal confinement buildings.....	200
Table 5.11. Summary of ANOSIM test on TSP samples from different types of animal confinement buildings based on OAV _P of odorants (R global =0.495, p<0.001) ^{a,b}	205
Table 5.12. Major compounds in TSP samples that contribute to variations in OAVP-based odorant composition among different animal building types.	206
Table 5.13. Total mass fraction and Simpson’s diversity index of odorants in PM ₁₀ samples from different types of animal confinement buildings.....	207
Table 5.14. Summary of ANOSIM test on PM ₁₀ samples from different types of animal confinement buildings based on mass fraction of odorants (R global= 0.267, p<0.001) ^{a,b}	209
Table 5.15. Major compounds in PM ₁₀ samples that contribute to variations in mass fraction-based odorant composition among different animal building types.....	209
Table 5.16. Total mass fraction and Simpson’s diversity index of odorants in PM ₁₀ samples from different types of animal confinement buildings.....	210
Table 5.17. Summary of ANOSIM test on PM ₁₀ samples from different types of animal confinement buildings based on OAV _P of odorants (R global=0.291, p<0.001) ^{a,b}	213
Table 5.18. Major compounds in PM ₁₀ samples that contribute to variations in OAV _P -based odorant composition among different animal building types.	213

Table 5.19. Summary of ANOSIM test on particle samples from different types of animal confinement buildings-based on correlation coefficient ^{a,b}	215
Table 5.19. (cont.).....	216
Table 5.20. Characteristic odorants or ratios for each type of animal confinement buildings.....	218
Table 5.21. Summary of total mass fraction of odorants, COI _P , COI and the Simpson's diversity index of TSP samples from different seasons.....	219
Table 5.22. Summary of ANOSIM test on TSP samples from different seasons ^{a,b}	220
Table 5.23. Summary of total mass fraction of odorants, COI _P , COI and the Simpson's diversity index of PM ₁₀ samples from different seasons.....	221
Table 5.24. Summary of ANOSIM test on PM ₁₀ samples from different seasons.....	222
Table 5.25. Summary of total mass fraction of odorants, Simpson's diversity index, COI _P and COI for TSP, PM ₁₀ and feed samples.....	223
Table 5.26. A comparison of COI and COI _P between TSP and PM ₁₀ samples- effects of animal building type and season	224
Table 5.27. Summary of ANOSIM tests on TSP, PM ₁₀ and feed samples ^a	226
Table 5.28. An incomplete comparison of odorant concentrations in gas and particle phase.....	231
Table 5.29. Comparison of odor thresholds of several compounds in air and in water ^a	232
Table 6.1. Summary of field sampling.....	242
Table 6.2. Summary of measured airborne endotoxin concentrations ^x	246
Table 6.3. Comparison of airborne endotoxin concentrations in swine and poultry buildings.....	247
Table 6.3. (cont.).....	248
Table 6.4. Summary of airborne (1→3)-β-D-glucan concentrations ^x	250
Table 6.5. Comparison of airborne (1→3)-β-D-glucan concentration in animal buildings.....	251
Table 6.6. Paired t-test on endotoxin and (1→3)-β-D-glucan levels in different seasons.....	255
Table 6.7. Correlation of ambient temperature to endotoxin and (1→3)-β-D-glucan levels.....	256
Table 6.8. Correlation of TSP to airborne endotoxin and (1→3)-β-D-glucan concentrations.....	258
Table A.1. Basic information of sampling sites.....	300
Table A.2. Distance Matrix of sampling sites ^a (km).....	301
Table A.3. Basic information of sampling sites.....	302
Table A.3. (cont. 1).....	303
Table A.3. (cont. 2).....	304

Table A.3. (cont. 3).....	305
Table A.3. (cont. 4).....	306
Table A.3. (cont. 5).....	307
Table A.3. (cont. 6).....	308
Table A.3. (cont. 7).....	309
Table A.3. (cont. 8).....	310
Table A.3. (cont. 9).....	311
Table A.3. (cont. 10).....	312
Table A.3. (cont. 11).....	313
Table A.3. (cont. 12).....	314
Table E.1. Summary of density test results.....	328
Table F.1. A PSD example measured with Horiba LA-300 particle sizer.....	330
Table F.2. Summary of MMD and GSD determined by different methods.	332
Table F.2. (cont.).....	333
Table F.3. Summary of lognormality tests on PSD profiles from different instruments.....	337
Table G.1. Summary of particle size analyzers used in this study.	343
Table G.2. Particle size distribution models to be tested.....	343
Table G.3. Paired t-tests on adjusted R ² values.	351
Table G.4. Properties of the lognormal, Weibull and gamma distributions.	352
Table G.4. (cont.).....	353
Table G.5. Regression coefficients and key parameters of lognormal, Weibull and gamma models ^a	354
Table G.6. Paired t-tests on mean and median diameters and variances derived from the lognormal, Weibull and gamma models.	355
Table H.1. Calibration results from the simulated field test.....	359
Table I.1. Melting and boiling points of analyzed volatile organic compounds ^a	361
Table I.1. (cont.).....	362

LIST OF SYMBOLS

A_i	Factor of animal building type
a_{ik}	Mass fraction of the specie i in air pollutants from the source k
BC_{jk}	Bray-Curtis dissimilarity between the j^{th} and the k^{th} sample
C_{ca}	Slip correction factor for d_a
C_{ce}	Slip correction factor for d_e
COI	Comprehensive odor intensity index
COI _p	Comprehensive particle odor intensity index
C_i	Concentration of the i^{th} specie at the receptor site
C_p	Mass concentration of airborne particles
c_p	True concentration of a particle-borne odorant
$c_{p,\text{meas}}$	Measured concentration of a particle-borne odorants
$C_{\text{PM}_{10}}$	Mass concentration of PM_{10}
$C_{\text{PM}_{2.5}}$	Mass concentration of $\text{PM}_{2.5}$
C_{TSP}	Mass concentration of TSP
$(\text{CO}_2)_i$	Indoor CO_2 concentration
$(\text{CO}_2)_p$	Production rate of CO_2
D	Animal density
$D_{15.9}$	Diameter that corresponds to 15.9% cumulative mass fraction
D_{50}	50% cut size (in chapter 3)
D_{50}	Diameter that corresponds to 50% cumulative mass fraction
$D_{84.1}$	Diameter that corresponds to 84.1% cumulative mass fraction
d_a	Aerodynamic diameter
d_e	Equivalent volume diameter
d_j	Characteristic diameter of a size range
d_{jk}	Correlation distance between the j^{th} and the k^{th} sample
d_p	Diameter of particles
$f_{i,j}$	Fraction of the i^{th} specie in pollutants from the j^{th} source
$F_{\text{PM}_{10}}$	Mass fraction of PM_{10} in TSP
$F_{\text{PM}_{2.5}}$	Mass fraction of $\text{PM}_{2.5}$ in TSP
K_p	Gas/particle portioning coefficient

M_0	Mass of a filter before sampling
$M_{f,a}$	Mass of a filter after filter conditioning
$M_{f,b}$	Mass of a filter before filter conditioning
$M_{p,a}$	Mass of particles after filter conditioning
$M_{p,b}$	Mass of particles before filter conditioning
M_t	Mass of a filter after sampling
N or n	Number of datasets as model input
$n(x)$	Number distribution density function
OAV	Odor activity value
OAV _P	Particle odor activity value
P or p	Number of predictors
PE	Penetration efficiency
PM	Concentration of particles
P_{std}	Standard barometric pressure (101.325 kPa)
P_s	Indoor barometric pressure
Q_b	Ventilation rate of the building
Q_s	Sampling flow rate
r	Pearson's correlation coefficient
r_b	Mean rank of distances between groups
r_w	Mean rank of distances within individual groups
R	Rho, a statistic used in ANOSIM and Mental test
R^2	Coefficient of determination
R_{PM10}	Ratio of calculated to measured PM_{10} concentration
$R_{PM2.5}$	Ratio of calculated to measured $PM_{2.5}$ concentration
S_j	Contribution of the j^{th} source to pollution at the receptor site
t_s	Sampling duration time
$t_{n-p}^{\alpha/2}$	t-critical value at $(1-\alpha)$ confidence level on n-p degree of freedom
T	Daily average ambient temperature
T_s	Indoor temperature during sampling
T_{max_out}	Maximum outdoor temperature
T_{std}	Standard temperature (273.2K)
V	Maximum ventilation capacity (in chapter 3)

V	Volume of sampled air (in chapter 5)
$V_{\min,f}$	Minimum volume of air required to saturate the adsorption of an odorant on filters
$v(x)$	Volume distribution density function
X	Vector of regression coefficients
x_0	Vector of a set of model input
x_{ij}	Mass concentration of the specie i in the sample j
Y_{ij}	Estimated PM concentration
β	Correlation coefficient
Δ	Difference
ε	Measurement error
$\eta_{PM_{10}}(d)$	Collection efficiency of an ideal PM_{10} sampler at diameter d
$\eta_{PM_{2.5}}(d)$	Collection efficiency of an ideal $PM_{2.5}$ sampler at diameter d
λ	Mean free path of the air
ρ_0	Unit density (1000 kg/m^3)
ρ_p	True density of particles
σ	Residual standard error
$\sigma_{\log[PM_{10}]}^A$	Uncertainty of estimated PM_{10} concentration induced by measurement error of predictors
$\sigma_{\log[PM_{10}]}^B$	Uncertainty of estimated PM_{10} concentration associated with prediction interval
σ_g^2	variance
χ	Shape factor

LIST OF ABBREVIATIONS AND ACRONYMS

ACGIH	American Conference of Governmental Industrial Hygienist
AERMOD	American Meteorological Society/ Environmental Protection Agency Regulatory Model
AIC	Akaike information criterion
ANOSIM	Analysis of similarity
ANOVA	Analysis of variance
APECAB	Aerial Pollutant Emissions from Confined Animal Buildings
AU	Animal unit
CAMx	Comprehensive air quality model with extensions
CBL	Convective boundary layer
CEN	European Committee for Standardization
CFD	Computational fluid dynamics
CFU	Colony forming unit
CI	Confidence interval
CMAQ	Community multi-scale air quality
CMB	Chemical mass balance
CFR	Codes of Federal Regulations
DGGS	Distiller's dried grains with solubles
EC	Elemental carbon
EDS	Energy dispersive spectroscopy
EDXRF	Energy dispersive X-ray florescence
EIA	Inhibition enzyme immunoassay
ELISA	Enzyme linked immunosorbent assay
EOF	empirical orthogonal functions
ESD	Equivalent spherical diameter
ESP	Electrostatic precipitator
EU	Endotoxin unit
FA	Factor analysis
FAA	Flame atomic absorption
FDA	Food and Drug Administration

FDMS	Filter dynamic measurement system
FEF ₂₅₋₇₅	Force expiratory flow 25-75%
FEV ₁	Forced expiratory volume in one second
FEM	Federal equivalent method
FPD	Flame photometric detector
FRM	Federal reference method
FVC	Force vital capacity
GC-ECD	Gas chromatograph with electron capture detector
GC-FID	Gas chromatograph with flame ionization detector
GC-MS-O	Gas chromatography-mass spectrometry- olfactometry
GFAA	Graphite furnace atomic absorption
GSD	Geometric standard deviation
GWP	Global warming potential
HP	Hypersensitivity pneumonitis
HPLC	High performance liquid chromatography
HPS	Hantavirus pulmonary syndrome
HVAC	Heating, ventilation and air conditioning
IARC	International Agency for Research on Cancer
IC	Ion chromatography
ICP-AES	Inductively coupled plasma-atomic emission spectroscopy
ICP-MS	Inductively coupled plasma-mass spectrometry
IMPROVE	Interagency monitoring of protected visual environments
IPCC	Intergovernmental Panel on Climate Change
ISCST	Industrial source complex short-term model
IUPAC	International Union of Pure and Applied Chemistry
KLARE	Kinetic limulus assay with resistant-parallel-line estimation
LAL	Limulus amoebocyte lysate
LPM	Liter per minute
LPS	Lipopolysaccharide
MDS	Multidimensional scaling
MMD	Mass median diameter
MSE	Mean square error

NAA	Neutron activation analysis
NAAQS	National Ambient Air Quality Standards
NAEMS	National Air Emissions Monitoring Study
NAMS	National air monitoring stations
NaPMP	Sodium polymetaphosphate
NAS	National Academy of Science
NIOSH	National Institute for Occupational Safety and Health
NMOC	Non-methane organic compounds
OC	Organic carbon
OSHA	Occupational Safety and Health Administration
ODT	Odor detection threshold
ODTS	Organic dust toxic syndrome
OU	Odor unit
OU _E	European odor unit
PANs	Peroxyacyl nitrates
PBL	Planetary boundary layer
PCA	Principal component analysis
PCoA	Principal coordinate analysis
PEL	Permissible exposure limit
PESA	Particle elastic scattering analysis
PFW	Pyrogen-free water
PIGME	Particle induced gamma-ray emission
PIXE	Particle induced X-ray emission spectroscopy
PM	Particulate matter
PMF	Positive matrix factorization
PLA	Partial least-squares
PPC	Positive product control
PSD	Particle size distribution
PTSD	Posttraumatic stress disorder
PVC	Polyvinyl chloride
RH	Relative humidity
RPI	Research Triangle Institute

RSS	Residue sum of squares
SIMPER	Similarity percentage
SBL	Stable boundary layer
SDS	Sodium dodecyl sulfate
SEM	Scanning electron microscope
SLAMS	State and local air monitoring stations
SOAs	Secondary organic aerosols
S-XRF	Synchrotron induced X-ray florescence
TEOM	Tapered Element Oscillating Microbalance
TLV	Threshold limit values
TLV-C	Threshold limit values-ceiling
TLV-STEL	Threshold limit values-shot term exposure limit
TLV-TWA	Threshold limit values- time weighed average
TSP	Total suspended particles
TSS	Total sum of squares
TXRF	Total reflection X-ray florescence
VOC's	Volatile organic compounds
VSCC	Very sharp cut cyclone
USEPA	The United States Environmental Protection Agency
USDA	The United States Department of Agriculture
UV	Ultra violet
WDXRF	Wavelength dispersive X-ray florescence
WINS	Well Impactor Ninety-Six
XRF	X-ray florescence

1. INTRODUCTION

1.1 Motivation

The United States has one of the largest poultry and livestock production industries in the world. In 2008, a total of 9.01 billion broiler chickens, 370 million egg chickens, 273 million turkeys, and 67.4 million pigs were raised in the United States (USDA, 2009). Illinois is a leading agricultural state and has the fourth largest pig production industry (2.2 million head in 2008) in this country. Poultry and livestock production has become increasingly concentrated in past decades, a result of shrinking profit margins for small operations and also due to the emergence of advanced feeding and environmental control technologies. For example, in the United States the number of pig operations dropped by 80% from 1984 to 2008 while pig production increased by 26% (USDA, 2009). Today, a single manure-belt layer hen building can house half a million birds. Such intensive animal production activities have created a number of environmental issues on air and water pollution, solid waste management and occupational health. Aerial pollutant emission from animal buildings is one of them.

Until recently, the investigation of pollutant emissions from animal feeding and other agricultural operations was mostly conducted on gaseous pollutants (e.g., NH_3 and H_2S). There is, however, a lack of information about airborne particles emitted from animal confinement buildings. Particle emissions have received increasing attention due to rapid growing populations in rural communities near animal buildings. Unlike odor, particles are not easily perceived by residents, but they could be more detrimental to both health and the environment.

The PM concentrations in rural areas are generally lower than those in urban and suburban areas, where industrial activities produce large amounts of primary particles. The large number of automobiles in urban and suburban areas also creates an intensive emission of primary particles, as well as NO_x , HC and CO. NO_x and non-methane organic compounds (NMOCs) can be photochemically converted into O_3 , peroxyacyl nitrates (PANs), aldehyde, and other chemical compounds. O_3 can further react with aromatic compounds and analogues to form secondary organic aerosols (SOAs). NO_x and SO_2 (mainly from the combustion of sulfur-containing fossil fuels or biomass) can also react with NH_3 to generate secondary inorganic aerosols, e.g., NH_4NO_3 (Seinfeld and Pandis, 1998). Rural areas are less industrialized and have no significant

NO_x, SO₂ and CO emissions. However, particle concentrations near animal confinement buildings can still reach relatively high levels. The concern is that airborne particles emitted from animal buildings are very complex in composition and may contain toxic, allergenic, pathogenic, and carcinogenic components, and may transport for a long distance. For example, bioaerosols in animal buildings consist of “organic dust (e.g., proteins, poly-carbohydrates), biologically active components (e.g., endotoxins, β-glucans) and some potentially pathogenic microorganisms (e.g., bacteria, fungi)” (Hirst, 1995). As a result, the adverse health effects of airborne particles emitted from animal confinement buildings could be underestimated if we evaluate these effects based on data and protocols derived from previous research on urban aerosols or other particle sources. The adverse health effects of airborne particles from animal buildings and other agricultural operations have become a major concern for the United States Environmental Protection Agency (USEPA) and the United States Department of Agriculture (USDA). Airborne particle emissions for animal confinement buildings may be subject to more state and federal regulations.

One of the technical obstacles to developing these regulations is lack of a complete and systematic understanding of the physical, chemical and biological properties of airborne particles emitted from animal confinement buildings. As a consequence, the transport and fate of these particles in the atmosphere and in human respiratory systems are yet unclear. A viable control strategy should be developed based on the knowledge of production, emission, transport and the health effect of these particles. Although there is limited information available for airborne particles emitted from animal confinement buildings, they, at least, should not be considered to be homogeneous in their physical, chemical, or biological properties (Seedorf, 2004). It should be considered a false assumption that particles emitted from animal buildings are physically, chemically and biologically similar to urban and ambient aerosols that have been extensively studied. If inappropriate data is used to develop regulations and control strategies for animal building particle emissions, it would possibly place an excessive economic burden on animal owners due to an overestimation of the environmental influences, or be unfair to nearby residents due to an underestimation of the potential health effects. Therefore, an experimental study in the characterizations of these particles is urgently needed.

A few experimental studies have been conducted in Europe and Asia concerning the mass concentration, chemical composition and health effects of airborne particles emitted from animal buildings and animal farms. Takai et al. (1998) investigated the overall mean inhalable and

respirable dust concentrations and emission rates in a number of cattle, pig and poultry buildings in England, the Netherlands, Denmark and Germany, and found dust concentrations and emission rates varied with the type of animal and season, and occasionally with the country. Chang et al. (2001) measured the concentrations of airborne endotoxins, dust (mass concentration) and gases (NH_3 , H_2S and CO_2) in five types of swine buildings (breeding, farrowing, nursery, growing, and finishing buildings) in southern Taiwan, and assessed the exposure risks based on published reports. Lammel et al. (2004) studied the mass concentration, trace gases (NH_3 and HNO_3), inorganic ions, aliphatic dicarboxylic acids, total element concentration, element and organic carbons, and morphology of particles on upwind and downwind sites, and directly from a livestock farm in southern Germany, and observed a rapid formation of secondary aerosols (e.g., ammonia haze droplets) downwind of the farm. Only a few similar studies, however, have been done in the United States despite the large number of animal buildings and animal farms. The USDA began support of a research project at Texas A&M University in 2006 to characterize particle emissions from large animal open feed lots. But particle emissions from an open cattle feed lot may be quite different from animal confinement buildings, especially those from swine and poultry buildings where the feed formula, animal digestion system, building ventilation, and waste storage and management are substantially different. The TAMU study is also limited to only the physical and chemical properties of PM. The biological properties of PM, however, are also very important in evaluating its adverse health effect on humans and animals.

1.2 Objectives

The purpose of this study is to investigate the physical, chemical, and biological properties of airborne particles emitted from animal confinement buildings. This study aims to provide a database for future research in particle source apportionment and help the evaluation of health effects, that is, a fundamental understanding of how particle emissions from animal buildings could influence public health in neighboring communities and also the health of animals and workers in animal buildings. The specific objectives of this study are as follows:

1. To measure the mass concentrations of airborne particles (TSP, PM_{10} and $\text{PM}_{2.5}$) emitted from animal confinement buildings.

2. To study inorganic elements and soluble ions in airborne particles (PM_{10} and $PM_{2.5}$) emitted from animal confinement buildings.
3. To investigate particle-borne odors and their variations with animal building type, seasons and particle size (TSP and PM_{10})
4. To examine the concentration of airborne endotoxins and (1→3)- β -D-glucans in animal confinement buildings.

1.3 Approach

The general approach for this study was as follow:

1. Selecting the sampling sites. A total of 18 animal buildings, including 12 swine and six poultry buildings were selected in the states of Illinois and Indiana. These buildings belong to six different types- swine: gestation, farrowing, nursery and finishing; poultry- tom turkey and manure belt layer hen. To study the seasonal variation, each building was visited three times in cold, mild and hot seasons.
2. Developing the sampling protocol. A multi-point sampling system was developed as described by Wang (2000). High volume samplers were selected in order to collect the sufficient amount of airborne particles for subsequent analysis. Sampling equipment and protocols were preliminarily tested at the University of Illinois Swine Research Center (Champaign, IL).
3. Conducting the field sampling. Samplers were installed right before exhaust fans in an animal building. Airborne particles (TSP, PM_{10} and $PM_{2.5}$) were collected onto filters. Important environmental and operational parameters (e.g., indoor temperature and humidity), as well as essential building information, were measured and recorded.
4. Performing physical, chemical and biological analyses. Filters with particles were weighed and then analyzed in the Bioenvironmental Engineering (BEE) Lab or sent to other labs on campus for analytical tests (Table 1.1).
5. Conducting data analysis. The test results were analyzed using statistical tools (general statistical packages: R, MATLAB and SPSS; professional packages: Primer, PAST and PMF) to evaluate errors and uncertainties, to develop regression models, and to determine

the significance of variations in particle properties with environmental and operational parameters.

Table 1.1. Analytical methods used in current study.

Properties	Analytical Methods
Mass concentration	Gravimetric measurement
Elemental composition	Energy dispersive X-ray fluorescence (EDXRF) Inductively coupled plasma-atomic emission spectroscopy (ICP-AES)
Soluble ions	Ion chromatography (IC) Colorimeter
Odorants	Stable-isotope dilution GC/MS
Endotoxin	Kinetic chromogenic LAL assay
(1→3) β -D-glucans	

2. LITERATURE REVIEWS

2.1 Air Pollutants in Animal Confinement Buildings

The issue of air pollutant emission from animal confinement buildings is a natural consequence of poor indoor air quality in these buildings. Air pollutants are carried by the airflow driven by mechanical ventilation systems or by natural convection, and are then discharged into the atmosphere to create pollution. Air pollution in animal confinement buildings has been recognized and studied by industrial hygienists, animal scientists and engineers for many years. Toxic gases and hazardous airborne particles can be produced, or released from the animal themselves, animal feces, feed, and contaminated construction materials (Zhang, 2005). Because of the relatively enclosed environment and the large population of animals, air pollutants can accumulate and reach harmful levels in an animal confinement building. The American Conference of Governmental Industrial Hygienists (ACGIH, 2000) has published a number of threshold limit values (TLVs), including the time weighted average (TLV-TWA), short term exposure limit (TLV-STEL) and ceiling (TLV-C), for air pollutants that had been found in animal confinement buildings (Table 2.1). Although these values are recommended and not mandatory, they are widely used by industrial hygienists in practice as a guideline to evaluate occupational exposure and to develop related control strategies. The permissible exposure limits (PELs) promulgated by the Occupational Safety and Health Administration (OSHA) are enforced by law. However, they were developed over 40 years ago based on the TLVs recommended by the ACGIH in 1968, and have been considered by many researchers to be insufficiently protective.

Table 2.1. Threshold limit values for typical air pollutants in animal confinement buildings.

Contaminant	TLV-TWA	TLV-STEV	TLV-C	TVL basis- critical effect(s)
	ppmv for gases, and mg/m ³ for dust			
Ammonia ^a	25	35		Irritation
Carbon dioxide ^a	5,000	30,000		Asphyxiation
Hydrogen sulfide ^a	10	15		Irritation
Methane ^a	1,000		50,000	Asphyxiation
Animal building dust, inhalable ^b	2.5 (swine), 2.4 (poultry)			
Animal building dust, respirable ^b	0.23 (swine), 0.16 (poultry)			

a- ACGIH (2000)

b- Donham (2000)

To assess the risk of exposure of workers to the indoor air pollutants, a variety of methodologies and equipment have been developed and employed for sample collection and analysis. Personal samplers, installed near the nose of a worker, are widely used for exposure assessment because they measure the real exposure that an individual person experiences. Hand-held infrared gas analyzers, electrochemical sensors, gas sampling bags, and gas adsorption tubes are also very popular because they are portable, convenient and relatively inexpensive. The instruments originally designed for ambient air quality monitoring have been frequently used in recent years, as these instruments are becoming less expensive and can provide better performance in terms of precision, sensitivity, linearity, real-time measurements, and computer assisted data logging and management.

For gaseous pollutants such as NH_3 , CO_2 , H_2S , and CH_4 , the measured concentrations seldom exceeded the TLV-TWA. Reynolds et al. (1996) measured the NH_3 concentrations in swine farms using personal samplers and found the average NH_3 concentrations were 5.42 ppm. Zhu et al. (2000) measured the daily variation of NH_3 and H_2S concentrations in poultry and swine buildings and found that NH_3 and H_2S concentrations ranged from 2 to 15 ppm and from 40 to 3400 ppb, respectively. Ni et al. (2002a) conducted a half year's continuous monitoring of H_2S in a swine finishing building and found the H_2S concentrations ranged from 38 to 536 ppb. A study done by Radon et al. (2002) showed the NH_3 concentration ranged from 5 to 14 ppm in 40 swine farms in Denmark and from 5 to 40 ppm in 36 poultry farms in Switzerland. Snell et al (2003) measured the NH_3 and CH_4 concentrations in four naturally ventilated dairy houses and found the average NH_3 and CH_4 concentrations varied from 5.5 to 12.6 ppm and from 53 to 93 ppm, respectively. Sun et al. (2008) measured the NH_3 , H_2S and CO_2 concentrations in two swine finishing buildings during three different seasons (summer, fall and winter) in Canada and found that the average NH_3 , H_2S and CO_2 concentrations varied from 5 to 32 ppm, from 6 to 615 ppb and from 508 to 4030 ppm, respectively. Blunden et al. (2008) studied the seasonal variation of NH_3 and H_2S concentrations in a swine finishing building in North Carolina. The measurement results showed seasonally average NH_3 and H_2S concentrations ranged from 2.45 to 8.91 ppm and from 47 to 673 ppb, respectively. In summary, NH_3 concentrations in animal confinement buildings are relatively high and occasionally surpass the TLV-TWA; CO_2 , H_2S and CH_4 concentrations were generally below the unhealthy levels. However, H_2S can cause odor nuisance even at such low concentrations (Patnaik, 2003).

In contrast, airborne particle concentrations in animal confinement buildings can be substantially higher than the TLV-TWA, especially during the winter when the ventilation rate is relatively low. Reynolds et al. (1996) measured the exposure of workers to airborne particles in swine farms and found the average concentrations of inhalable and respirable particles were 4.0 mg/m^3 and 0.25 mg/m^3 , respectively. Takai et al. (1998) investigated the inhalable and respirable airborne dust in cattle, swine and poultry buildings in four European countries; and the measurement results revealed that in swine and poultry buildings, inhalable and respirable dust concentrations easily exceeded the TLV-TWA. The maximum dust concentrations occurred in poultry buildings, followed by swine buildings. The overall mean inhalable and respirable dust concentrations for poultry buildings were 3.60 mg/m^3 and 0.45 mg/m^3 , respectively, over 50% greater than the threshold values. A recent study by Kim et al (2008a) in Korea reported the inhalable and respirable particle concentrations in swine buildings varied from 0.6 to 6.7 mg/m^3 and from 0.3 to 3.5 mg/m^3 , respectively, during spring and fall. Banhazi et al. (2008) found the average inhalable and respirable particle concentrations were 4.32 mg/m^3 and 0.84 mg/m^3 , respectively, from a four months' monitoring event covering 17 broiler buildings in Australia. The measurements in this study also show the total suspended particle (TSP) concentrations, approximately equivalent to inhalable particles, were up to 15.6 mg/m^3 in poultry buildings. In summary, the concentrations of airborne particles are relatively high in animal confinement buildings, especially in poultry buildings where feathers can be a significant particle source.

Odor and bioaerosols in animal confinement buildings are also of public concern, although they are currently not regulated by OSHA or included in the ACGIH TLV table. Many chemical compounds were found to contribute to the odor, including a few inorganic compounds such as H_2S and NH_3 , and a number of volatile organic compounds (VOC's) such as indoles, skatoles, alcohols, p-cresols, alkyl sulfides, mercaptans, phenols, and fatty acids (Mackie et al., 1998; Ronald, 1995). Several different methods are currently available for odor analysis. The most direct and also the most commonly used one is olfactometry that utilizes the human sense of smell for odor detection. Odor strength is quantified in terms of odor unit (OU). Lim et al. (2001) measured the odor concentrations in two swine weaning buildings and found the odor concentrations varied from 94 to 635 OU/m^3 at the exhaust, and from 7 to 85 OU/m^3 at the inlet. Jerez et al. (2005) conducted similar measurements in a swine farrowing building and found the odor concentration ranged from 31 to 266 OU/m^3 near the inlet and from 275 to $2,217 \text{ OU/m}^3$ at

the exhaust. A recent study done by Sun et al. (2008) in Canada showed the average odor concentrations at the exhaust varied from 406 to 3040 OU/m³ in two swine weaning buildings. However, there are currently no federal regulations on the permissible odor levels in working environments. One of the reasons is the measurement results using olfactometry lack consistency and replicability. The measurement uncertainty can be up to 250 OU/m³ (van Kempen et al., 2002) or 50% (Lee and Zhang, 2008). To overcome the instrumental limitation of olfactometry, a gas chromatography-mass spectrometry-olfactometry (GC-MS-O) has recently been used to identify and quantify the malodorous chemical compounds in animal confinement buildings (Cai et al., 2006; Wright et al., 2005).

Bioaerosols are defined as a collection of airborne biological particles. Bioaerosols are airborne particles, large molecules or volatile compounds that are living, contain living organisms or were released from living organisms (Cox and Wathes, 1995). Because of the complexity of bioaerosols in terms of composition, size, source, and health effects, there is no single general index for quantifying the strength of bioaerosols. Culturable bacterial and fungal concentrations are two of the most commonly used indices for assessing the bioaerosol contamination in animal facilities. A study done by Butera et al. (1991) in Canada showed the culturable bacterial concentrations varied from 1.48×10^5 to 9.20×10^5 CFU/m³, while the culturable fungi concentrations ranged from 140 to 6,440 CFU/m³ inside a swine finishing building. Radon et al. (2002) measured the culturable bacteria and fungi in a total of 76 swine and poultry buildings in Denmark and Switzerland; the average culturable bacterial and fungal concentrations were found to be 3.8×10^5 colony forming unit (CFU)/m³ and 5.8×10^6 CFU/m³ in swine buildings and 4.4×10^5 CFU/m³ and 7.9×10^7 CFU/m³ in poultry buildings. Predicala et al. (2002) reported an overall mean culturable bacterial concentration of 8.6×10^5 CFU/m³ in two swine buildings in northern Kansas. Lee (2009) recently measured the culturable bacterial concentrations in six swine buildings and three layer-hens buildings during three different seasons and found the concentrations varied from 1.2×10^4 to 1.6×10^4 CFU/m³ in swine buildings and from 1.9×10^4 to 2.8×10^4 CFU/m³ in layer-hens buildings. Although there are currently no regulations on airborne bacteria and fungi because of the lack of essential dose-response data, certain exposure limits have been proposed by public health researchers. Reponen et al. (1992) proposed a threshold limit value of 5,000 CFU/m³ for culturable airborne bacteria. Wheeler et al. (2001) proposed a strict value of 1,000 CFU/m³. For culturable airborne fungi, a concentration of

even less than 100 CFU/m³ could be harmful to immunosuppressed people, according to the ACGIH (1989). In summary, bioaerosols are major contaminants in animal confinement buildings; the measured concentrations of culturable bacteria and fungi are often higher than the proposed exposure limits.

In order to properly assess the seriousness of indoor air pollution, the spatial distribution of air pollutants in an animal confinement building must be considered. Wang (2000) and Jerez (2007) investigated the spatial distribution of airborne particles, CO₂ and NH₃ in swine buildings through field measurements and computer simulation. They found that air pollutants were not uniformly distributed in an animal building and the ratio of the maximum to the minimum concentration of a pollutant could be over six. Computer simulation (e.g., computational fluid dynamics [CFD]) was found to be a useful tool for estimating the spatial distribution of an air pollutant. The number and location of the samplers must be carefully selected based on experimental and/or simulation results so as to improve the representativeness of the measurement data. Additionally, Jerez (2007) found that the concentrations of air pollutants at the exhaust can be significantly different from the indoor average. Therefore, the results from the indoor air quality monitoring, in which the samplers were generally installed at the center of a room, are not readily used for estimation of the emission rate, unless they are proven to have a well-defined mathematical relationship to the air pollutant concentrations at the exhaust. Similarly, the results from the emission measurements at the exhaust do not represent the average indoor air quality.

2.2 Emissions of Gaseous Air Pollutants from Animal Confinement Buildings

Air pollutants emitted from animal confinement buildings can be classified into two categories according to the scope of their environmental impacts. Air pollutants that cause global environmental issues or primarily come from animal facilities include NH₃, CH₄ and N₂O. Others, including airborne particles, odor, H₂S, and bioaerosols, affect the ambient air quality more locally. This section will address the property, source, environmental consequence, and emission measurement of gaseous air pollutants from animal confinement buildings.

2.2.1 Ammonia (NH₃)

Ammonia is a caustic and hazardous gas with an irritating odor and also the most abundant gaseous alkaline chemical species in the troposphere (Seinfeld and Pandis, 1998). The background concentrations of NH₃ vary from 0.1 to 10 ppb across continents. The residence time of NH₃ in the troposphere is relatively short (~10 days), because NH₃ can be easily absorbed by surface or atmospheric water or converted to secondary aerosols. Globally, 45.0 Tg N-NH₃ (1 Tg = 10¹² g) is annually released into the atmosphere and two-thirds (30.4 Tg N-NH₃) is from anthropogenic sources. Animal production contributes 22.0 Tg N-NH₃, 49% of the total emission (Dentener and Crutzen, 1994), which is primarily from the bacterial decomposition of urea or uric acid in animal waste. Animal production is the largest source of NH₃ in the United States. Eighty percent of the nationwide NH₃ emission is from animal waste (Battye et al., 1994). Since NH₃ is a basic gas, it can react with acidic air pollutants such as sulfur oxides, nitrogen oxides, nitric acid, sulfuric acid, and hydrochloride, leading to the formation of secondary inorganic aerosols, e.g., NH₄NO₃ and (NH₄)₂SO₄ (Renard et al., 2004). NH₄NO₃ and (NH₄)₂SO₄ have been found to be the major components of atmospheric aerosols in some regions. For example, the mass fraction of NH₄NO₃ and (NH₄)₂SO₄ were up to 55% in PM_{2.5} in Beijing, China (Pathak et al., 2009), and accounted for 40% in PM_{2.5} in southeastern Spain (Nicolas et al., 2009). These fine ammonium-containing aerosols have been considered to be responsible for the visibility impairment by enhancing the light scattering (Barthelmie and Pryor, 1998), and for the acid rain and the eutrophication of water bodies (Aneja et al., 2001). NH₃ is also a major contributing factor to the nuisance odor from animal facilities. Therefore, the measurement, modeling and mitigation of NH₃ emission from animal facilities have been of great interest to atmospheric scientists, agricultural engineers and environmental scientists in the last 20 years.

Field measurements of NH₃ emission rates have been extensively conducted (Blanes-Vidal et al., 2008; Gay et al., 2003; Harper et al., 2009; Mosquera et al., 2005; Ni et al., 2002a; Svennerstedt, 1999). Because the emission rate is the product of the pollutant concentration and the ventilation rate, these two must be monitored simultaneously for calculation of the emission rate. To measure the exhaust concentration of NH₃, gas samplers or analyzers are generally installed at the exhaust, in most cases right before the exhaust fans. NH₃ concentrations are measured either intermittently or continuously, depending on the analysis method in use. The commonly used instruments for NH₃ measurements are: (1) Gas sampling bags – gas samples are

collected, shipped to the lab, and then analyzed using detection tubes (Zhu et al., 2000); (2) Impingers – NH₃ gas is absorbed with a liquid medium and then analyzed using UV-VIS spectrometry or ion chromatography (IC) (Kim et al., 2008b); (3) Electrochemical sensors (Gates et al., 2005); (4) Chemiluminescence NH₃ analyzers (Blunden et al., 2008; Koerkamp et al., 1998); and (5) Photoacoustic gas analyzers (Ngwabie et al., 2009). The last two instruments can offer real-time measurement data with great accuracy and high resolution, and as a result are becoming increasingly widely used.

To measure the ventilation rate, the most common way is to continuously monitor the operation status of all exhaust fans. For constant-flow fans, vibration or frequency sensors can be used to monitor the on/off state. For variable speed exhaust fans, anemometers can be used to measure the average air velocity, from which the airflow rate can be calculated. The airflow rate data for the constant-flow exhaust fans are available from the manufacturers. However, essential calibrations are needed because the real airflow rate of an exhaust fan can be substantially different from the factory value (Gates et al., 2005). Fan calibration is quite expensive and time-consuming. Regretfully, most of the existing studies did not include the fan calibration process, and therefore, did not provide reliable data about the ventilation rates. Another way for estimating the ventilation rate is to use trace gas, e.g., CO₂. This method is based on mass balance as shown in Equation 2.1.

$$Q_b = \frac{(CO_2)_p}{[(CO_2)_i - (CO_2)_o]} \quad (2.1)$$

Where Q_b is the building's ventilation rate, (CO₂)_p is production rate of CO₂, (CO₂)_i is the indoor concentration, and (CO₂)_o is the outdoor concentration (Zhang, 2005). This method has been used for determination of the ventilation rate of livestock buildings (Hinz and Linke, 1998; Takai et al., 1998). However, it is less accurate and is currently seldom used. Another big challenge for measuring the emission rate is the limited number of sampling points. A manure-belt layer hen building can have up to 154 fans. It is impractical to set up samplers and sensors at all exhaust fans, and in reality only a small number of fans were selected for monitoring. As stated in previous sections, the concentrations of an air pollutant can be significantly different at different sampling points because of the non-uniform spatial distribution of the pollutant in an animal building. NH₃ concentrations at the unmonitored exhaust fans can be remarkably different from those monitored at a limited number of selected fans. As a consequence, there are significant

uncertainties, variations and even controversy with the existing emission rate data. The obtained NH_3 emission data can be used for calculation of emission factors, generally expressed in unit of $\text{g N-NH}_3/\text{AU-day}$, where AU refers to animal unit that is defined to be equal to 500 kg of body weight of animals. The emission factors can then be input into air quality models to simulate or predict the environmental impacts of NH_3 emission.

Zhu et al. (2000) reported a daily variation of NH_3 emission rates from swine and broiler buildings. A swine finishing building with natural ventilation was found to have the highest emission rate with the maximum value of 0.17 mg/s/m^2 . However, the representativeness of their data is questionable because the monitoring lasted only 12 hours in each building. In order to ensure the reliability of the calculated emission factors, a long-term continuous monitoring is required. Ni et al. (2000) conducted a three months' continuous monitoring of NH_3 emission from a swine finishing building and found the emission factor to be $145 \text{ g N-NH}_3/\text{AU-day}$. The unusually high emission factor was explained due to the warm weather that enhanced the volatilization of NH_3 from animal waste. Sun et al. (2008) measured the NH_3 emission from two identical mechanically-ventilated swine finishing rooms in summer, fall and winter. Each monitoring lasted two days. The measurement results showed the NH_3 emission factor varied with rooms and seasons, and was highest ($120.8 \text{ g N-NH}_3/\text{AU-day}$, by averaging the two rooms) in summer and lowest ($71.85 \text{ g N-NH}_3/\text{AU-day}$) in the fall. Blunden et al. (2008) investigated seasonal variation in NH_3 emission from a mechanically ventilated swine finishing building and found the NH_3 emission factor was higher in winter and spring (33.6 ± 21.9 and $30.6 \pm 11.1 \text{ g N-NH}_3/\text{AU-day}$) and lower in summer and fall (24.3 ± 12.4 and $11.8 \pm 7.4 \text{ g N-NH}_3/\text{AU-day}$). Their findings were inconsistent with those by Sun et al (2008) who observed the highest emission factor in summer. A few review papers are available (Arogo et al., 2003; Misselbrook et al., 2000) on the topic of NH_3 emission factors for animal facilities. In summary, there are significant variations and uncertainties in the existing data for NH_3 emission factors. The ratio of the highest to the lowest value is over 100, even for the same type of animal facilities (Arogo et al., 2003). The NH_3 emission rate varies considerably with building type, room size, animal age, animal density, floor type, manure management, season, ventilation strategy, and many other factors. Therefore, it seems impractical to have a universal, representative NH_3 emission factor for the same type of animal facilities (e.g., swine finishing building). The emission factors must be specific enough to account for at least the strongest influential factors.

Other methods have also been used for estimating the NH₃ flux from animal confinement buildings, such as nitrogen balance methods, micrometeorological techniques, chamber methods, and modeling methods (process-based models, dispersion models, and regression models) (Arogo et al., 2003). However, as a direct method, field measurements of emission factors have been most frequently employed so far.

2.2.2 Methane (CH₄) and nitrous oxide (N₂O)

CH₄ and N₂O are both greenhouse gases that are responsible for global warming. Although they exist in the atmosphere at much lower concentrations than CO₂, both of them have very high global warming potentials (GWPs) and contribute significantly to global warming. CH₄ is the second most contributing greenhouse gas, only next to CO₂. The 20-year GWP of CH₄ is 62, which means its greenhouse effect per molecule is over 60 times stronger than CO₂. Annually 535 Tg CH₄ is released to the atmosphere and 25 Tg CH₄ comes from anaerobic digestion of animal waste (IPCC, 1995). The average CH₄ concentration in the atmosphere is presently 1720 ppb, substantially greater than that (~700 ppb) in the pre-industrial age (Dlugokencky et al., 1994). N₂O is an even stronger greenhouse gas, with a 20-year GWP value of 290. Because N₂O has a very long retention time in the atmosphere (~120 years), its impact on the global climate is more persistent than CO₂ and CH₄. The global N₂O emission rate is about 14.7 Tg N-N₂O yr⁻¹ and 3.9 Tg N-N₂O yr⁻¹ is from the agricultural activities. Livestock, primarily beef and dairy cattle, contribute to 0.4 Tg N-N₂O yr⁻¹, around 7% of the total N₂O emission (IPCC, 1995). The background N₂O concentration has increased from 276 ppb in the pre-industrial age to currently 311 ppb (Machida et al., 1995). Although animal production only accounts for a small fraction of the global CH₄ and N₂O emission, efforts have been made to quantify the emission rate and to control the emission from animal confinement buildings, as global warming has become a top public concern in recent years and greenhouse gas emissions from the animal production industry are believed to have the potential to be reduced.

The methods used to determine the NH₃ emissions also apply to the CH₄ and N₂O emissions from animal facilities. CH₄ can be analyzed with either gas chromatography with a flame ionization detector (GC-FID) (Berges and Crutzen, 1996) for intermittent measurements, or photoacoustic gas analyzers (Costa and Guarino, 2009; Snell et al., 2003) for continuous real-time monitoring. Similarly, N₂O can be analyzed with either gas chromatography with an

electron capture detector (GC-ECD) (Prinn et al., 1990; Sneath et al., 1997) or photoacoustic infrared analyzers (Sneath, 1996).

Because most measurements of CH₄ and N₂O emissions from animal confinement buildings just started recently in the United States, only a few data are available. The majority of the existing data are from Europe. Osada et al. (1998) continuously monitored CH₄ and N₂O emissions from a swine finishing building in Denmark and found the emission rates varied diurnally and with the animal age. The average CH₄ and N₂O emission factors were calculated to be 17.5 g CH₄/AU-day and 0.55 N₂O /AU-day, respectively. Ni et al. (2008) conducted a nearly one year monitoring in two identical mechanically ventilated swine finishing buildings in northern Missouri and reported the yearly average CH₄ emission factor was 36.2±2.0 g CH₄/AU-day for building #1 and 26.8±1.8 g CH₄/AU-day for building #2. Ambient temperature was found to be a top influential factor on the CH₄ concentrations and emission rates. Costa et al. (2009) investigated CH₄ and N₂O emissions from a farrowing, gestation, weaning, and a finishing room on a swine farm in Italy and found the emission factors for CH₄ and N₂O varied significantly with seasons and building types. The yearly average CH₄ emission factor was 4.68 g CH₄/AU-day for the farrowing room, 132.1 g CH₄/AU-day for the gestation room, 24.6 g CH₄/AU-day for the weaning room, and 189.8 g CH₄/AU-day for the finishing room. The yearly average N₂O emission factor was 0.66 g N₂O/AU-day for the farrowing room, 2.72 g N₂O /AU-day for the gestation room, 3.62 g N₂O /AU-day for the weaning room, and 3.26 g N₂O /AU-day for the finishing room. Ngwabie et al. (2009) measured the CH₄ emission from a naturally ventilated dairy farm in Sweden for three months and reported the CH₄ emission factor ranged from 216 to 314 g CH₄/AU-day. In summary, similar to the case of NH₃ emission, the emission factors of CH₄ and N₂O are affected by building type, ventilation rate, room size, animal age, animal density, floor type, manure management, ambient temperature, and many other factors; there are significant variations in the existing data. Validity and representativeness of the existing monitoring data must be properly assessed before they are used as the input to global climate models.

2.2.3 Hydrogen sulfide (H₂S)

H₂S is a colorless, toxic, flammable, and malodorous gas. The production of H₂S in animal facilities is mainly due to the bacterial decomposition of sulfur containing organic compounds,

e.g., protein. Exposure to high concentrations of H₂S can result in dizziness, incoordination, headache, pulmonary edema, asthma, reduction of lung function, and even temporary consciousness if the H₂S concentration is extremely high (750~1,000 ppm) (Milby and Baselt, 1999). The global annual emission of H₂S is 0.98 to 3.44 Tg S-H₂S, primarily from volcano eruptions (Seinfeld and Pandis, 1998). The contribution of animal production is negligible on the global scale. As mentioned in the previous section, H₂S concentrations in animal confinement buildings were generally lower than 10 ppm, the TLV-TWA recommended by the ACGIH. However, the recognition threshold of H₂S is very low, only 0.0047 ppm (Patnaik, 2003), which means even at low concentrations H₂S can still cause an unpleasant odor. An increasing number of complaints against odor from animal facilities have been filed by neighboring residents, a result of expansion of nearby residential communities and the ever-increasing recognition of environmental issues by the public. There is a need to regulate H₂S emissions from animal facilities. Because field measurements of H₂S emissions can offer essential data for regulation development, they have attracted much attention in recent years.

The methods used to determine the NH₃ emissions also apply to H₂S. H₂S concentrations are generally monitored using H₂S fluorescence analyzers (e.g., Model 450C H₂S/SO₂ pulse fluorescence analyzer, Thermal Fisher Scientific, Inc., Waltham, MA) (Blunden et al., 2008; Ni et al., 2002b) or hand-held H₂S analyzers (Zhu et al., 2000). The former one has become increasingly popular because it can provide accurate high-resolution real-time measurements. H₂S emission factors have been calculated based on the measurement data. Ni et al. (2002b) continuously monitored H₂S emissions from two identical swine finishing buildings in Illinois for six months and reported the building-average H₂S emission factor was 6.2 g H₂S/AU-day. Schmidt et al. (2002) measured H₂S emissions from swine, dairy and poultry buildings, and found the H₂S emission factor from the swine buildings was highest during the winter. Blunden et al. (2008) studied the seasonal variation in H₂S emission from a mechanically ventilated swine finishing building in North Carolina and found the H₂S emission factor, similar to the NH₃ emission factor, was higher in winter and spring (4.2±2.1 and 3.3±1.0 g H₂S/AU-day) and lower in summer and fall (1.2±0.7 and 1.7±0.5 g H₂S/AU-day). A recent study by Sun et al. (2008) showed the building-average H₂S emission factor was highest (4.50 g H₂S/AU-day) in summer and lowest (1.30 g H₂S/AU-day) in fall. In summary, the emission factor of H₂S from animal confinement buildings was substantially lower than that of NH₃; however, due to the extremely

low sensory threshold of humans to H₂S, although the emission rates are generally low, H₂S is still considered to be a major odor contributor. Accordingly, H₂S was sometimes used as a surrogate gas for assessing the odor in and from animal facilities.

2.2.4 Odor

A number of chemical compounds have been identified to contribute to the odor in animal facilities (Mackie et al., 1998; Ronald, 1995). Although there are no federal regulations regarding odor, some states and cities in the United States have implemented air quality standards for odor in the ambient air (Mahin, 2001). These published odor standards are mainly for short-term exposure and range from 1 to 7 OU/m³. As more communities are being built near animal facilities, there has been a significant increase in complaints against the odor from animal confinement buildings.

The methods used to investigate the NH₃ emissions can also be used to determine the emission factors of odor from animal facilities. The most frequently used analytical method for odor detection is olfactometry. It is basically a dilution-to-threshold method. A simple procedure is as follows: (1) odorous gas samples are collected using the sampling bags and then shipped to a lab; (2) gas samples are diluted and, ideally, smelled by a group of trained persons (a panel) on the olfactometer; (3) the second step is repeated until the odor cannot be detected by half of the panel members and by definition reaches the odor detection threshold (ODT); (4) odor strength is quantified with the dilution ratio and presented in unit of odor unit (OU). In this method, the olfactometer is used for dynamic dilution of gas samples, experimental condition control and data recording. It should be noted that a European odor unit (OU_E) is defined by the European Committee for Standardization (CEN, 2003) as the odor strength of 123 µg n-butanol/m³. The definitions of OU_E and OU are different and, hence, they cannot be directly compared. Other techniques have also been used for odor detection, such as gas chromatograph-mass spectrometry (GS-MS) (Lee and Noble, 2003), Fourier transform infrared spectroscopy (FTIR) (van Kempen et al., 2002) and electronic noses (Hudon et al., 2000). However, the use of these methods, in most cases, relies on the reference standards provided by olfactometry. Their applications so far are still very limited. Because the odor detection with olfactometry must be done in a lab, only intermittent measurement data are available. A study by Zhu et al. (2000) reported the building average emission factor of odor from swine buildings was 149 OU/AU-sec. Lim et al. (2001) measured the odor emissions from two mechanically ventilated swine nursery

buildings in Indiana and reported the time-average emission factors of odor were 18.3 and 62.5 OU/AU-sec, respectively. The significant difference was ascribed to the different manure characteristics (e.g., water content, soluble ions and pH) in the two buildings. Gallmann et al. (2001) conducted a three-finishing-cycle, a total of 13-months monitoring in a mechanically ventilated and a naturally ventilated swine finishing building. They found there was no significant difference between the two buildings during cycle 1 and 2. However, the time average emission factor of odor in the mechanically ventilated building (193 OU_E/AU-sec) was significantly higher than that in the naturally ventilated building (105 OU_E/AU-sec) during cycle 3. The overall range of the measured odor emission factors for both buildings was 4 to 550 OU/AU-sec. Lim et al. (2004) investigated the effects of manure removal strategies on odor emissions from two swine finishing buildings in Indiana and found the odor emission rate decreased as the manure accumulation/cleaning cycle increased. The geometric mean emission factor of odor was 29 OU/AU-sec when the cycle was 14 days. Sun et al. (2008) investigated the diurnal and seasonal variations of odor emissions from two identical swine finishing buildings and reported the building-average odor emission factor was higher (124.4 OU/AU-sec) in summer and lowest (105.8 OU/AU-sec) in fall. The same trends were found in the cases of NH₃ and H₂S emissions. A strong correlation between odor and NH₃ emissions, and between odor and total reduced sulfur (TRS) emissions, were observed by Gay et al. (2003) from field measurements in over 200 animal facilities in Minnesota. In summary, the emission rates of odor from animal facilities are affected by animal age, animal density, ventilation system and operation, manure management, manure characteristics, ambient and indoor air temperature, and many other factors; inherent measurement error of the olfactometry method is another source of uncertainty in existing emission factor data.

2.2.5 Non-methane organic compounds (NMOCs)

The photochemical reaction of NMOCs and NO_x leads to the formation of ozone, a major chemical ingredient in photochemical smog. Globally, the anthropogenic emission rate of NMOCs is 142 Tg/yr (Seinfeld and Pandis, 1998). The majority of NMOCs emissions are from fuel consumption. Although the contribution of animal production is insignificant, several measurement projects are underway in the United States., and one of them is being conducted by researchers at Purdue University. Methods to determine the emission factors of NH₃ also apply

to NMOCs. Concentrations of NMOCs can be quantified using GC-FID. No data are available at this time, as all related projects just recently started.

2.3 Emissions of Airborne Particles from Animal Confinement Buildings

2.3.1 Particle sources

Airborne particles from animal facilities are very complex in composition and originate from a variety of sources such as feed, feces, animal skin and hair (or feathers for poultry), construction materials, insects, and microorganisms (Zhang, 2005). Airborne particles from animal facilities can be classified into inorganic, organic and biological particles according to their chemical composition and origins. The biological ones are often referred to as bioaerosols. However, a single airborne particle can be a mixture of inorganic, organic and biological components, or be an agglomerate of primary particles with inorganic, organic and biological origins. In fact, many airborne particles in animal buildings are formed by agglomeration of smaller particles, possibly from different sources (Koon et al., 1963). Therefore, it can be extremely difficult to correctly identify the source of a single airborne particle.

Source identification and apportionment of airborne particles can be conducted on a bulk scale or on individual particles. The results of source apportionment are generally presented in unit of particle number fraction (%). Although the formation of particle agglomerates may undermine the validity of individual particle based methods, many studies on source identification of airborne particles are done by examining the shape and size of individual particles with optical or electron microscopy (Donham et al., 1986b; Heber et al., 1988a) and accordingly determine a classification.

Previously, feed was considered to be the primary source of airborne particles from animal facilities (Curtis et al., 1975; Donham et al., 1986b; Heber et al., 1988a). Curtis et al. (1975) compared the crude-protein (CP) contents in the feed, settled dust and airborne particles under different diet conditions in a swine building and found the CP contents in airborne particles were consistently close to those in the feed and settled dust. Based on that, they concluded that the majority of airborne particles were feed particles. Donham et al. (1986b) studied the sources of airborne particles collected from 21 swine buildings in Iowa by light microscopic analysis and found the airborne particles were primarily from feed (starch, grain meal, plant trichomes, and

corn silk) and fecal materials (microorganisms, animal cells and undigested feed) and the feed content increased with the size of pigs. They also observed the existence of dander, mold pollens, insect parts and minerals in airborne particles. To improve the contrast of images, starch granules and fecal materials were dyed with Iodine and Nile Blue Sulfate stains, respectively. Heber et al. (1988a) collected airborne particle samples from 11 swine buildings in Kansas with eight field trips for each building and then used an optical and a scanning electron microscope (SEM) to identify the particles. They found the majority of airborne particles were from feed. Around 65% (number) of particles were grain meal particles and 13.5% were starch granules. Most of the starch granules were larger than 6.7 μm . Grain meal particles were on average smaller but most of them were still larger than 3.0 μm . Identification work was performed on the SEM because it provided a much better resolution (1.5 μm) than the optical microscope (5.4 μm). In fact, in their experiments, the resolution of the SEM images was limited by the rough surface of the glass fiber filters used for particle collection and SEM observation. If polycarbonate filters had been used, the results would have been more reliable, especially for smaller particles.

A later study by Feddes et al. (1992) showed fecal materials were the major source of respirable airborne particles in turkey buildings. Their conclusions looked inconsistent with those made by other researchers at first glance. However, it must be noted that Feddes and his colleagues measured only the respirable particles with a 50% cut-size (D_{50}) of 4 μm , while inhalable particles ($D_{50}=100 \mu\text{m}$) were collected and analyzed in previously mentioned studies. The study by Heber et al. (1988a) showed that the composition of airborne particles varied with particle size and the feed contents were actually lower for smaller particles. Animal type could be another possible affecting factor. The study by Feddes et al. (1992) was done in turkey buildings, while most other studies were done in swine buildings. The feed, housing and feeding system, animal activities and feces composition are totally different for swine and turkey.

Source identification and apportionment can provide valuable information for development of control strategies. Once the major sources of airborne particles are determined, measures can be implemented to reduce the production rate at those sources. For example, adding fat to the feed was found to be an effective way to reduce the aerosolization of the feed (Chiba et al., 1985). From the emission control point-of-view, future source identification studies should focus on fine particles, because once released from the animal facilities, large particles will quickly settle

down but the fine particles will travel a relatively long distance in the atmosphere, reaching neighboring communities and creating air pollution problems.

2.3.2 Particle properties

Particle size

Particle size is one of the most important physical characteristics of airborne particles. For a spherical particle, the particle size equals its own diameter. However, most airborne particles collected in polluted environments are non-spherical and irregular in shape. In order to apply the concept of particle size to non-spherical particles, several equivalent diameters were defined by transforming a real particle to an imaginary spherical particle while keeping one of the particle properties constant during the transformation. Two commonly used equivalent diameters are: (1) equivalent volume diameter, defined to be equal to the diameter of a sphere with identical volume to the original particle, and (2) aerodynamic diameter, defined to be equal to the diameter of a unit density ($\rho=1000 \text{ kg/m}^3$) sphere with the same aerodynamic behaviors (e.g., settling velocity) as the original particle (Hinds, 1982). Airborne particles collected in real environments are unexceptionally non-uniform in size (polydisperse). A particle size distribution (PSD) profile can be obtained by classifying the particles into a number of size classes. The y-axis of the obtained PSD profile can be particle number (count), mass, or count or mass frequency. Quantities used to define the location of a PSD include arithmetic mean, geometric mean, median, and mode diameter (Zhang, 2005). Among them, the mass median diameter (MMD) is most frequently used. The spread of a PSD is generally quantified with the geometric standard deviation (GSD). The shape of a PSD can be modeled with mathematical equations (Chen et al., 1995). In fact, most of the measured PSD profiles are approximately log-normal, and accordingly log-probability graphs are frequently used for interpretation and analysis of measured PSD data.

Particle size is closely related to the human health effects of particles. The smaller a particle is, the more deeply it may penetrate into the respiratory tract. Also, smaller particles can travel a longer distance in the atmosphere than larger ones. Therefore, in order to properly assess the environmental health effects, field measurement of size distribution of airborne particles from animal confinement buildings is of great importance.

There are numerous analytical instruments currently available for measuring the PSD of airborne particles. According to their working principles, these instruments can be classified into several categories: (1) Direct observation – measuring the size of individual particles with microscopes and then summarizing the results. The SEM and optical microscope are two examples of this category; (2) Inertial classification –fractioning particles into a number of size groups based on the aerodynamic behavior of particles, e.g., inertia. The aerodynamic particle sizer (APS) (TSI Inc., St. Paul, MN), the aerosizer DSP (TSI Inc., St. Paul, MN) and the Anderson multi-stage cascade impactors (Thermal Fisher Scientific Inc., Waltham, MA) belong to this category; (3) Light scattering – measuring the intensity of light scattered by the given particles. The intensity is proportional to the sixth power of the particle diameter. Examples include the Climate CI-500 (Climet Instruments Co., Redlands, CA) and the Horiba LA-300 (Horiba Group, Edison, NJ); (4) Electrical mobility – classifying electrically charged particles according to their mobility in an electric field. The scanning mobility particle sizer (SMPS) and Differential Mobility Analyzer (DMA) (TSI Inc., St. Paul, MN) is in this category. Some instruments are designed for in-situ field measurements, e.g., APS, DSP and SMPS; while some others must be operated in the lab and, hence, require particle samples to be collected on filters or other media prior to analysis, e.g., Horiba LA-300 and Coulter Counter Multisizer.

Airborne particles from animal confinement buildings have been found to include more large particles than atmospheric aerosols (Heber et al., 1988a). Larger particles are suspended or resuspended in the air because of the turbulent airflow and the animal movement inside the animal barns. As a result, the MMDs measured at animal facilities are generally over 10 μm , in terms of both geometric and aerodynamic diameters (Donham et al., 1986b; Jerez, 2007; Lee, 2009; Maghirang et al., 1997; Redwine et al., 2002). Donham et al. (1986b) studied the size distribution of airborne particles from 21 swine buildings in Iowa using cascade impactors, and found the MMD was 10.7 μm , although 66% (number) of particles were smaller than 4.6 μm . Maghirang et al. (1997) used the same methods to investigate airborne particles from a mechanically ventilated swine weaning building, and reported the MMDs ranged from 10 to 19 μm . Redwine et al. (2002) measured the size distribution of particles from four tunnel ventilated broiler buildings using a Coulter Counter Multisizer. The results showed the MMDs ranged from 24 to 27 μm and increased with the bird age. Jerez (2007) investigated the PSD at the exhaust of a mechanically ventilated swine finishing building using a Horiba LA-300 particle sizer, and

reported the average MMD was 26.8 μm . Lee (2009) measured the size distribution of particles from six poultry and nine swine buildings using four different particle sizers (a Horiba LA-300, a Coulter Counter Multisizer, an Aerosizer DSP, and a Malvern Master-Sizer), and reported the MMDs ranged from 8.6 to 19.3 μm . The MMDs measured with the Horiba LA-300 was significantly greater than with the other three instruments. A log-normal distribution was observed in most cases, but occasionally a bimodal size distribution was detected.

Particle shape

Airborne particles from animal confinement buildings are mostly irregular in shape. Particle shape significantly affects the aerodynamic behavior of airborne particles and is also a critical parameter for engineering design or selection of air cleaning equipment (Zhang, 2005). The particle shape is generally determined by image analysis. The modern particle imaging systems can provide size and shape information simultaneously and automatically, e.g., PSA300 (Horiba Group, Edison, NJ) and Morphology G3 (Malvern Instruments Ltd., Worcestershire, United Kingdom). However, most of the previous studies were done using general microscopes in the lab. The measurement of the particle shape can provide valuable information for particle classification, source identification and for determination of particle shape factors, surface area and other important properties (Wang et al., 2008). The particle shape factors are necessary for conversion of equivalent volume diameter to aerodynamic diameter, and vice versa, as shown in Equation 2.2 (Zhang, 2005):

$$d_a = d_e \left(\frac{C_{ce} \rho_p}{C_{ca} \rho_0 \chi} \right)^{\frac{1}{2}} \quad (2.2)$$

Where d_a is the aerodynamic diameter, d_e is the equivalent volume diameter, C_{ce} and C_{ca} are slip correction factors for d_a and d_e , ρ_p is the “true” particle density, ρ_0 is the unit density (1000 kg/m^3), and χ is the shape factor.

So far only a few publications are available concerning the shape of airborne particles from animal facilities. Heber et al. (1988a) studied the size and shape of airborne particles from 11 swine finishing buildings with scanning electron microscopy. Starch granules, grain meal and skin particles were identified based on their shape and size. The unidentified particles were classified into irregular, rounded and cylindrical particles. Hiranuma et al. (2008) investigated the shape of airborne particles from an open-air cattle feedlot and classified the particles into

three types: (A) smooth, rounded particles, (B) rough-surface, amorphous particles, and (C) fine particle agglomerates. Most particles were identified as Type B.

Particle density

Particle density is also called true particle density, to distinguish it from bulk density of particles. In addition to particle shape, particle density is another important factor affecting the aerodynamic behavior of airborne particles. Particle density is required for conversion between equivalent volume diameter and aerodynamic diameter, as shown in Equation 2-2, and for conversion of particle number based PSD data to mass based PSD data (Almuhanna, 2007). Particle density can be measured with a pycnometer, but the pycnometer has certain limitations when applied to the case of airborne particles. Taking the AccuPyc II 1340 pycnometer (Micromeritics Instrument Cop., Norcross, GA) as an example, the bulk volume of test samples should be no less than 0.5 cm^3 . This means at least $\sim 200 \text{ mg}$ of airborne particle samples need to be collected in the field, which in reality is almost impossible. Moreover, as reported by Heber et al. (1988a), smaller particles had different composition than bigger particles, from which it can be concluded that particle density may change with particle size. To accurately assess the density of particles within a certain size range, airborne particle samples must first be fractionated to different size ranges using a particle size separator. However, in reality, the mass of particles collected after size separation are too small to be analyzed by the pycnometer. Therefore, previous studies (Jerez, 2007; Lee, 2009; Lee et al., 2008) assumed that particle density was identical for all size fractions in Equation 2.2. They also assumed that the density of airborne particles was equal to that of the settled dust in the same animal building, and used the test data for the settled dust to represent the density of airborne particles. Particle density can also be calculated from Equation 2-2 if the particle shape factor, the aerodynamic diameter and the equivalent volume diameter are known. But this requires a simultaneous measurement of both diameters and was seldom used because of the complexity of the measurement system (Hering and Stolzenburg, 1995).

Almuhanna (2007) studied the properties of particles in a swine finishing building in Kansas and reported the average particle density was 1.84 g/cm^3 . Jerez (2007) measured the density of the settled dust in a mechanically ventilated swine finishing building and reported the average particle density was 1.45 g/cm^3 . Lee (2009) investigated the airborne particles from six poultry

and nine swine buildings in three different seasons and reported the particle densities ranged from 1.46 to 2.01 g/cm³. Particles from swine farrowing buildings were found to have the highest average density (1.75 g/cm³) while particles from swine gestation buildings had the lowest value (1.58 g/cm³). No significant seasonal variation was observed.

Carrier of odorous compounds and microorganisms

Airborne particles from animal facilities have been considered to be a major cause of odor nuisance for neighboring communities (Bottcher, 2001). Previous studies have revealed the existence of malodorous compounds in airborne particles from animal confinement buildings (Bottcher, 2001; Burnett, 1969; Hammond et al., 1979; Hammond et al., 1981; Lee and Zhang, 2008; Wang et al., 1998). Those odorous compounds may have come from fecal materials contained in the airborne particles, or originated from other sources but later become adsorbed on the particle surface. Investigation of odorants in airborne particles is of great importance for odor emission control, because the control strategies and dispersion models developed for airborne particles are also applicable to these particle-phase odorants.

Hammond et al. (1981) investigated the odorous organic compounds in airborne particles emitted from a swine building and found the concentrations of butyric acid and p-cresol were over tens of million times greater than those in the gas phase. Donham et al. (1986b) measured the amount of NH₃ gas adsorbed on settled dust and reported the value was 3.9 mg NH₃/g dust. Because settled dust is a potential source of airborne particles, it is reasonable to conclude that NH₃ gas can be carried by airborne particles. Wang et al. (1998) investigated the odor carrying characteristics of the settled dust collected in a swine finishing building and identified up to 100 volatile compounds using a GC-FID. Lee and Zhang (2008) studied the odor emission from the settled dust collected in poultry, swine and cattle buildings with the low temperature thermal desorption technique and found the NH₃-carrying capacity and desorption rate were significantly affected by animal type. However, no carrying capacity data were provided because in their study each desorption experiment took two hours, but after that the desorption process still continued. In the current study, a total 57 organic compounds were identified and quantified in airborne particles from poultry and swine confinement buildings. Many compounds were related to odor.

Although NH₃ has been found to be contained in airborne particles, the majority of NH₃ still exists in the gas phase. Assuming the concentration of airborne particles is 10 mg/m³ in an animal building and the NH₃ carrying capacity is 10 mg NH₃/g, the concentration of NH₃ in the particulate phase would be 0.1 mg/m³, or 0.17 ppmv, which is much less than the concentration of gas phase NH₃ in animal confinement buildings (several to tens of ppmv). But for VOC's, the situation can be reversed, as reported by Hammond et al. (1981).

Airborne particles from animal confinement buildings have also been revealed to be a carrier of microorganisms. Bacteria, fungal spores and viruses can be attached on the surface of airborne particles by means of van der Waals forces or electric forces. Airborne bacteria generally do not exist as individual particles but mostly adhere to airborne particles larger than 4 µm in diameter (Robertson and Frieben, 1984). Therefore, technologies used for mitigation of airborne particles can also be useful for removal of airborne microorganisms from the exhaust air. In contrast to airborne bacteria, most of the bacterial and fungal spores are present in the air as individual particles.

2.3.3 Environmental health effects

It has been recognized for many years that airborne particles from animal facilities are detrimental to animal and human health and exposure to these airborne particles can cause infectious diseases, respiratory diseases and even cancer among farm workers and their family members (Donham, 1986; Donham et al., 1984b; Donham et al., 1977; Kirkhorn and Garry, 2000; Larsson et al., 1994; Schenker et al., 1998). Occupational health issues are very common for workers and veterinarians working in animal confinement buildings. It was estimated that 25 to 70% of workers and up to 93% of veterinarians suffer from certain respiratory diseases (Donham et al., 1989; Donham et al., 1977; Donham et al., 1986a; Donham et al., 2007)

Airborne particles from animal confinement buildings originate mainly from organic sources, such as feed, fecal materials and animal skin and hair (Donham, 1986; Donham et al., 1986b; Heber et al., 1988b). Inorganic dusts only account for a small portion of the total mass and generally do not contain biologically active materials such as asbestos and silica (Donham, 1986). Adverse health effects are mainly caused by the hazardous agents contained in organic dusts (Donham et al., 1977; Kirkhorn and Garry, 2000), and are listed as follows:

- Bacteria and fungi. Fungi and thermophilic bacteria are sources of allergens associated with hypersensitivity pneumonitis (HP) previously called farmer's lung disease. Fungi are also sources of type I allergens (IgE binding allergens) that cause allergic respiratory symptoms, especially asthma, and sources of β (1 \rightarrow 3) glucans. Endotoxin and peptidoglucans are released by Gram-negative and Gram-positive bacteria, respectively. Moreover, the bacteria and fungi found in animal confinement buildings include some pathogenic and infectious species (Douwes et al., 2003).
- Endotoxin. Endotoxin (lipopolysaccharide, LPS) is a cell envelope component of Gram-negative bacteria and is released mainly by lysed cells. Inhalation of endotoxins can cause fever, shivering, pulmonary inflammation, non-allergic asthma, airway obstruction, and deterioration of lung functions (Kirkhorn and Garry, 2000). Endotoxin has been identified to be significantly related to the deterioration of lung functions in terms of "forced expiratory volume in one second" (FEV₁) through dose-response studies (Donham et al., 1989; Donham et al., 1986a). Recent epidemiological studies show early exposure to low levels of endotoxin may have a protective effect against the development of atopy and allergic asthma (Liu and Leung, 2000; Von Ehrenstein et al., 2000). However, exposure to high levels of airborne endotoxin is still widely believed to be highly risky (Heederik et al., 2007; Schenker et al., 1998).
- (1 \rightarrow 3) β -D-glucans. (1 \rightarrow 3)- β -D-glucans are insoluble D-glucose polymers linked by β (1 \rightarrow 3) glycosidic bonds, released by fungi and some bacteria as a cell envelope component. Similar to endotoxin, (1 \rightarrow 3)- β -D-glucans are strongly inflammatory but non-allergic and are generally considered to be related to respiratory symptoms, pulmonary inflammation and deterioration of lung functions (Wan and Li, 1999). (1 \rightarrow 3)- β -D-glucans may have synergistic effects with endotoxin, exotoxins and phytotoxins in causing pulmonary inflammations (Fogelmark et al., 1992).
- Mycotoxins. Mycotoxins are a wide category of toxins released by fungi. They are generally low-molecular-weight secondary metabolites. Most fungal species isolated in animal confinement buildings belong to the genera of *Aspergillus* and *Penicillium* growing on animal feed. Aflatoxins are produced by the *Aspergillus* species of fungi, with four major different types (B1, B2, G1, and G2). Aflatoxins are well defined

carcinogens and Aflatoxins B1 is the most carcinogenic naturally-occurring compounds ever known (Squire, 1981). Ochratoxins are released by *Penicillium* and several *Aspergillus* species, with three different types (A, B and Mellein). Ochratoxin A is potentially carcinogenic once ingested by humans and animals (Turner et al., 2009). However, little is known about the health effects of airborne mycotoxins due to the lack of dose-response data (Donham, 1986; Douwes et al., 2003; Schenker et al., 1998).

- Allergens. Allergens released from animal confinement buildings include animal dander, dust mites, insect fragments, pollens, fungal molds, bacteria, and allergenic components in grain dust (Kirkhorn and Garry, 2000). Possible allergenic effects include upper respiratory allergies, asthma and most frequently bronchial hyperactivity (Von Essen and Donham, 1999).

Because of the presence of biologically active, hazardous agents, the following diseases may be caused by exposure to airborne particles from animal confinement buildings:

- Infectious diseases. Infectious diseases are caused by pathogenic microorganisms including viruses, bacteria, fungi, protozoa, multi-cellular parasites, and occasionally aberrant proteins. These pathogens can be transmitted from a reservoir or host to a susceptible host through water, food, blood, and airborne particles. Typical infectious diseases associated with exposure to airborne particles from animal confinement buildings include Q-fever, swine influenza, avian influenza, anthrax, and Hantavirus pulmonary syndrome (HPS) (Douwes et al., 2003; Gilchrist et al., 2007; Kirkhorn and Garry, 2000). A recent study reported swine farm workers and veterinarians had a much higher odd ratio for infection by H1N1 and H1N2 swine influenza viruses than adults without exposure to swine (Myers et al., 2006). The outbreak of the H1N1 swine flue in last year is a perfect example of how an infectious disease originated from swine confinement buildings eventually became a serious public health challenge throughout the world.
- Respiratory diseases. Animal farm workers and veterinarians may suffer from non-allergic and/or allergic respiratory diseases. The non-allergic respiratory diseases include non-allergic asthma, non-allergic rhinitis, chronic bronchitis, chronic airway obstruction and organic dust toxic syndrome (ODTS). The allergic respiratory diseases include

allergic asthma, allergic rhinitis, and hypersensitivity pneumonitis (HP) (Douwes et al., 2003). Exposure to airborne particles as well as CO₂ and H₂S was found to be related to acute but temporary deterioration of pulmonary functions in terms of “force vital capacity (FVC)” and “force expiratory flow 25-75%” (FEF₂₅₋₇₅) (Donham et al., 1984b).

- Cancer. Aflatoxins are widely believed to be a human carcinogen particularly related to liver cancer. Ochratoxin A has been classified by the International Agency for Research on Cancer (IARC) as a possible carcinogen and mutagen (Robbiano et al., 2004). Exposure to animal feed was found to increase the risk of liver cancer and other cancers among workers (Olsen et al., 1988).

The health effects discussed above may not result from exposure to airborne particles only, but sometimes should be considered as a result of synergistic effects of airborne particles and other potentially harmful gases (e.g., NH₃, H₂S, odor, CO₂ and CH₄) from animal confinement buildings (Donham, 1986; Donham et al., 2002). Because of the presence of synergistic effects, a pollutant may exhibit obvious adverse health effects even at levels much lower than the ACGIH TLV-TWA. Donham et al. (2000) proposed the exposure limit for NH₃ gas was 7 ppmv for swine buildings and 12 ppmv for poultry buildings. Both are appreciably lower than the ACGIH TLV-TWA value, 25 ppmv.

Increased antibiotic resistance in human pathogens is also of public health concern, due to the excessive use of antibiotics in animal production. It was estimated that annually 40% to 87% of antibiotics are used for animals in the United States (Levy, 1998; UCS, 2001). Transmission of antibiotic resistant bacteria can take place from animals to farm workers and then from farm worker to other people (Armand-Lefevre et al., 2005; Voss et al., 2005). Antibiotic resistant genes can be transferred from one group of bacteria to another and possibly to human pathogens (Levy, 1998), resulting in serious illness. Recent studies show that airborne particles from animal confinement buildings may contain antibiotics (Hamscher et al., 2003), antibiotic resistant bacteria (Chapin et al., 2005) and antibiotic resistant genes (Sapkota et al., 2006). Therefore, in addition to food, groundwater and soil, airborne particles may also contribute to the transmission of antibiotic resistance bacteria and genes from animal confinement buildings to public communities.

Most previous studies focused on the adverse health effects of poor indoor air quality on farm workers and veterinarians. Recent studies revealed that a number of physical and mental health issues in neighboring communities may be a consequence of air pollutant emission from animal confinement buildings. The identified health issues include excessive respiratory symptoms (e.g., asthma, wheeze and chronic airway obstruction), depression, anxiety, and post-traumatic stress disorder (PTSD) (Bullers, 2005; Schiffman et al., 2002; Thu, 2002). However, there is a lack of essential exposure and health response data. Consequently, it is difficult to determine whether these health effects are due to airborne particles, toxic gases or synergistic effects of airborne particles and gaseous pollutants.

2.3.4 Sampling techniques and instruments

Particle size is probably the most important physical property of airborne particles associated with their effect on the environment and public health. As mentioned in Section 2.3.2, smaller particles can penetrate the human respiratory system more deeply than larger particles. Also, smaller particles can travel a longer distance in the atmosphere. Therefore, particle size-selective sampling is of great significance and is generally required for assessment of environmental and health consequences of polydisperse airborne particles.

Inhalable, thoracic and respirable particles

For assessing the occupational exposure to airborne particles of different sizes in a workplace, the concepts of inhalable, thoracic and respirable particles were defined by the ACGIH (1985) according to the compartments they can reach in the human respiratory system, shown in Figure 2.1. Threshold limit values were developed regarding the concentrations of these particles in the workplace.

- Inhalable particles ($D_{50} = 100 \mu\text{m}$). These particles can be inhaled through the nose or mouth and enter the upper respiratory tract.
- Thoracic particles ($D_{50} = 10 \mu\text{m}$). As a subfraction of inhalable particles, these particles can pass through the upper respiratory tract and reach the lower respiratory tract (thoracic airways).

- Respirable particles ($D_{50} = 4 \mu\text{m}$). As a subfraction of thoracic particles, these fine particles can penetrate through the lower respiratory tract and enter the gas exchange region of the lung.

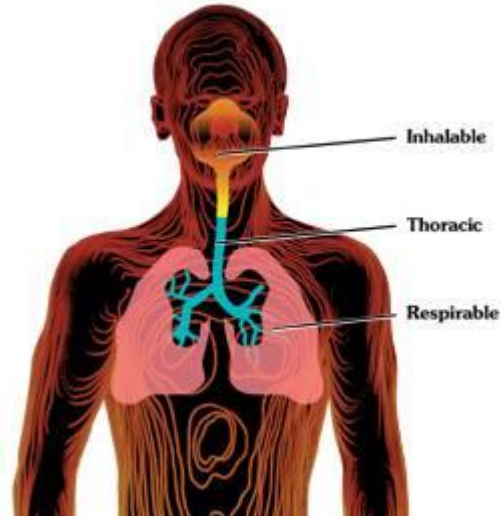


Figure 2.1. Deposition regions of different sized particles in the human respiratory system.

(Photo from: <http://www.skcinc.com/headlns/pic.jpg>)

Particle samplers were designed to screen larger particles and collect only smaller particles that can enter the airway region of interest. Accordingly, inhalable, thoracic and respirable samplers have 50% cut-points (D_{50}) at $100 \mu\text{m}$, $10 \mu\text{m}$, and $4 \mu\text{m}$, respectively. They are all personal samplers, installed near the nose of an individual. Inhalable samplers are generally simple in structure and have a rounded, open inlet occasionally covered with a plastic or metal mesh (e.g., IOM inhalable dust sampler, SKC button sampler for inhalable dust, SKC Inc., Eighty Four, PA). Thoracic samplers generally consist of an impactor or a cyclone for removal of larger particles (e.g., thoracic parallel particle impactor, personal particulate sampler and SKC personal modular impactor by SKC Inc., Eighty Four, PA; CIS Inhalable sampler and high flow thoracic cyclone by BGI Inc., Waltham, MA). Similar to thoracic samplers, respirable samplers utilize an impactor or a cyclone for particle separation (e.g., SKC aluminum cyclone, GS-1 and GS-3 cyclones, and respirable parallel particle impactor by SKC Inc., Eighty Four, PA; CIS respirable sampler, respirable dust cyclone and high flow respirable cyclone by BGI Inc., Waltham, MA). Vacuum pumps and flow control units are used to provide a constant sampling flow rate, which is critical for size-selective sampling efficiency. Particles are collected on filters or introduced to particle counters or sensors for real-time measurements.

TSP, PM₁₀ and PM_{2.5}

In contrast to inhalable, thoracic and respirable particles, the concepts of total suspended particles (TSP), PM₁₀ and PM_{2.5} are defined by the USEPA (Wilson et al., 2002). TSP once was an indicator for particulate matter (PM) in the National Ambient Air Quality Standards (NAAQS). However, it has been replaced by PM₁₀ since 1987 (FR, 1987). TSP is not defined by a certain cut-size but refers to airborne particles that can be collected by the High Volume Sampler (hivol). In reality, the 50% cut-size of the hivol ranges from 25 to 40 µm depending on the wind speed and direction (Wilson et al., 2002).

PM₁₀ refers to airborne particles 10 µm or less in size, according to the USEPA (2009b). However, this definition is somehow not clear because it does not specify what the “size” refers to. Another definition is published by researchers at the University of Georgia (UGA), Athens, Georgia that PM₁₀ refers to particles with an aerodynamic diameter less than or equal to 10 µm (UGA, 2009). However, it is impossible to collect “pure” PM₁₀ using either impactors or cyclones. The size cut curve of a PM₁₀ sampler can be very sharp but definitely not “ideal.” Moreover, the size cut curves of PM₁₀ samplers are measured in a lab under controlled, constant environmental conditions and with artificial standard dusts with known particle size. However, during a field measurement, the environmental conditions may vary with time and can be substantially different from the lab conditions. Also, the ambient aerosols are very complex in shape and composition and may contain semi-volatile compounds that can be lost during the sampling period, thus creating sampling errors (Wilson et al., 2002). Therefore, it is extremely difficult to determine the accuracy of PM₁₀ measurements in an absolute sense based on the USEPA’s definition of PM₁₀. To overcome such a difficulty, the USEPA has developed a reference method (Appendix J, Title 40, Part 50 of the Code of Federal Regulations [CFR]) by specifying the sampler performance (e.g., cut size), criteria for selection of filters, sampling procedures, calibration procedures, and calculation methods for PM₁₀ measurements (CFR, 2001a). According to the CFR, PM₁₀ reference samplers should have 50% collection efficiency for particles with an aerodynamic diameter at 10±0.5 µm (CFR, 2001a). A number of PM₁₀ sampling methods (samplers) have been accepted by the USEPA to become the EPA-designated reference (also known as Federal Reference Method, FRM) or equivalent methods (Federal Equivalent Method, FEM), as they successfully satisfy the acceptance criteria of being an FRM or FEM for PM₁₀ according to Title 40, Part 53 of the CFR (CFR, 2001c). The measurement

accuracy was defined by the CFR to be the agreement of a PM₁₀ candidate method with a reference method during lab test and field sampling (CFR, 2001c; Williams et al., 2000). PM₁₀ and thoracic samplers have the identical 50% cut size (10 μm). However, the size cut curve of the FRM PM₁₀ samplers is slightly steeper than that of thoracic samplers (Figure 2.2).

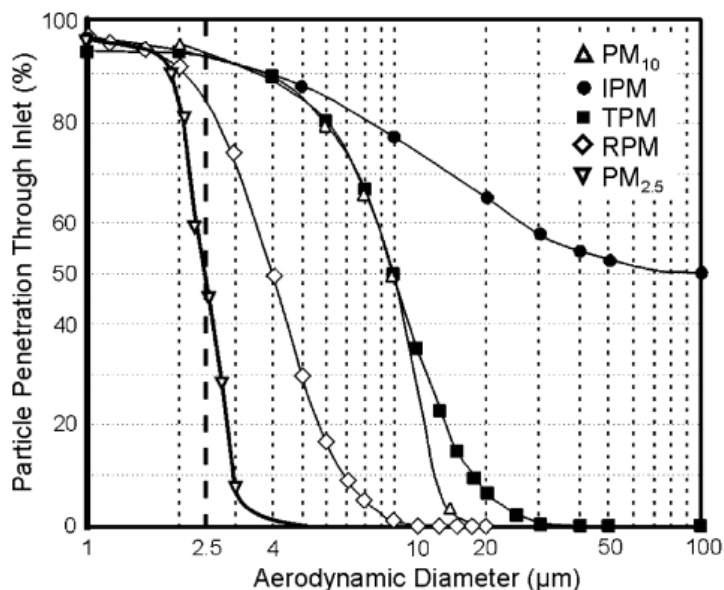


Figure 2.2. Comparison of the size-cut curves of the EPA defined FRM PM₁₀ and PM_{2.5} sampler with the ACGIH defined inhalable, thoracic, and respirable samplers.
(Cited from Wilson et al. [2002])

PM_{2.5} refers to particles with aerodynamic diameters up to 2.5 μm. The NAAQS for PM_{2.5} was implemented in 1997. Similar to the case of PM₁₀, the presence of numerous uncertainties during field sampling leads the assessment of measurement accuracy for PM_{2.5} to be very difficult in an absolute sense (Noble et al., 2001). A reference method for PM_{2.5} measurements (Appendix L, Title 40, Part 50 of the CFR) has been promulgated by the USEPA, which not only defines the range and precision, sampling procedures, calibration procedures and calculation methods for PM_{2.5} measurements, but also specifies technical details in filter specifications, sampler design and flow rate control (CFR, 2001b). According to the CFR, only two PM_{2.5} particle size separators are currently qualified to be used in FRMs and FEMs. They are Well Impactor Ninety-Six (WINS) and BGI PM_{2.5} Very Sharp Cut Cyclone (VSCCTM), both working at a flow rate of 16.7 liter per minute (LPM). The measurement accuracy for PM_{2.5} was defined in a relative sense, as the degree of agreement of a candidate PM_{2.5} sampler with a reference method (CFR, 2001b).

The WINS impactor was designed and calibrated by researchers from the Research Triangle Institute (RPI) and the USEPA National Exposure Research Lab, Research Triangle Park, North Carolina (Peters et al., 2001a; Peters et al., 2001b; Peters et al., 2001c) and became the first EPA-approved reference method for PM_{2.5} separation. Unlike conventional impactors, the WINS impactor uses a collection cup instead of a collection plate to minimize particle bounce. The 50% cut size (D₅₀) of the WINS impactor is 2.48 μm and the geometric standard deviation (GSD), which measures the sharpness of a cut curve, is 1.18 (Peters et al., 2001). However, the mineral oils in the collection cup may become frozen under extremely cold weather conditions and the size cut curve may shift due to the accumulation of excessive particles in the collection cup (Vanderpool et al., 2001a; Vanderpool et al., 2001b). As a result, the WINS impactor is becoming less frequently used in field sampling.

BGI PM_{2.5} VSCC™ cyclone was developed by researchers from the Health and Safety Laboratory, Sheffield, United Kingdom and BGI Inc., Waltham, Massachusetts (Kenny et al., 2000; Kenny et al., 2004), based on the design of the SRI-II cyclone (Smith et al., 1979). The principal dimensions of the PM_{2.5} VSCC™ cyclone were determined using an empirical model developed by Kenny and Gussman (1997) for the GK and SRI cyclone families. BGI PM_{2.5} VSCC™ cyclone was originally an EPA-designated equivalent method (FEM) but officially became a reference method (FRM) for PM_{2.5} measurements in 2006 (USEPA, 2006). Compared to the WINS impactor, the BGI PM_{2.5} VSCC™ cyclone does not need mineral oils and, hence, can work in extremely cold weather conditions. Also, the BGI PM_{2.5} VSCC™ cyclone has been demonstrated to have better performance in terms of D₅₀ and GSD under heavy loading conditions (Kenny et al., 2000). The BGI PM_{2.5} VSCC™ cyclone is currently the most popular PM_{2.5} size separator in use.

By August 2009, the USEPA had designated 17 PM₁₀ and 22 PM_{2.5} samplers as the FRMs and seven PM₁₀ and six PM_{2.5} samplers as the FEMs (USEPA, 2009c). All FRMs are filter-based, gravimetric methods in accordance to the CFR (CFR, 2001a; CFR, 2001b); while currently all FEMs are non-filter-based, automated monitoring methods (Class III equivalent methods) except the Thermo Scientific Partisol 2000-D dichotomous air sampler (EQPS-0509-177) (CFR, 2001c).

Although 17 PM₁₀ FRMs are currently available, there are actually only two basic designs of particle size separators as shown in Figure 2.3. Both designs are based on the impaction

mechanism: particles with an aerodynamic diameter larger than 10 μm are separated from the curved air stream due to their large inertia. In the first design (unofficially but often referred to as the PM_{10} inlet), the airflow rate is 16.7 LPM, that is, 1 m^3/hr ; while in the second design (also called high-volume sampler), the flow rate can be much higher, e.g., 1.13 m^3/min for the Ecotech Model 3000 PM_{10} High Volume Air Sampler (Ecotech Inc, Knoxfield, Australia). The first design is currently more popular because it can be used separately or as the pre-separator for a $\text{PM}_{2.5}$ size separator (Figure 2.3). In fact, the current 22 FRMs for $\text{PM}_{2.5}$ measurements all consist of a PM_{10} inlet and a $\text{PM}_{2.5}$ adaptor- either the WINS impactor or the BGI (or URG) $\text{PM}_{2.5}$ VSCC™ cyclone.

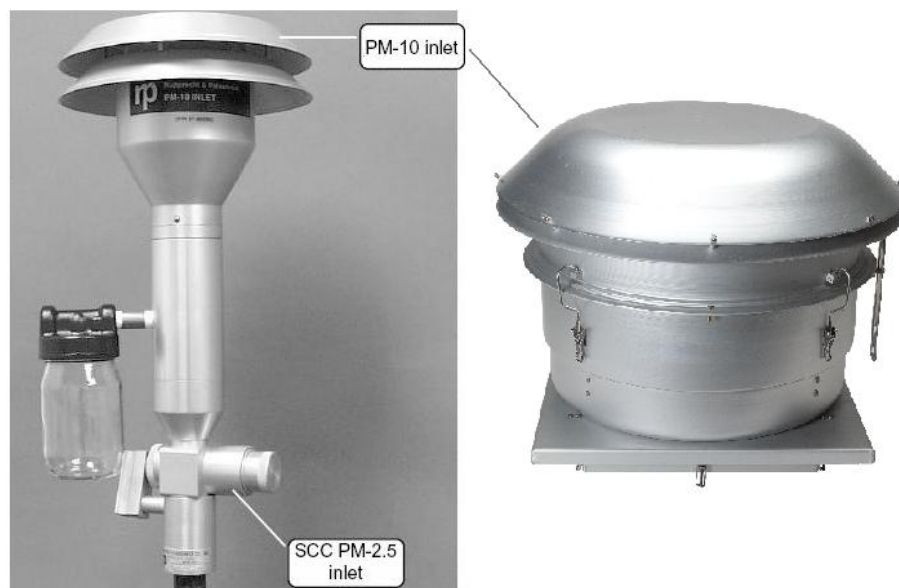


Figure 2.3. Two basic designs of the PM_{10} size separators.

(Photos from: left- <http://www.atmospheric-research.com> and right- <http://www.hi-q.net>)

In the non-filter-based, automated FEMs, airborne particles, after selection with particle size separators mentioned previously, are not collected on filters for subsequent gravimetric measurements in a lab but are introduced to particle mass sensors such as the beta gauge, harmonic oscillating elements, piezoelectric crystals and nephelometer (McMurry, 2000). Among them, the Tapered Element Oscillating Microbalance (TEOM) is one of the most frequently used methods for continuous measurement of airborne particle emissions from animal facilities. Although the TEOM is listed by the USEPA only as a FEM for PM_{10} measurements, it has been used by many researchers for continuous monitoring of TSP and $\text{PM}_{2.5}$ mass concentrations (Heber et al., 2006; Jerez et al., 2006). The TEOM can be configured to measure

TSP or PM_{2.5} by replacing the PM₁₀ inlet with a TSP inlet, or adding a BGI PM_{2.5} VSCC™ cyclone after the PM₁₀ inlet (Figure 2.3), respectively.

The Thermo Scientific Partisol 2000-D dichotomous air sampler is currently the only one filter-based, manual FEM for PM_{2.5} monitoring. It contains a PM₁₀ inlet and a virtual impactor that fractions the PM₁₀ into fine (PM_{2.5}) and coarse (PM_{10-2.5}) particles. A virtual impactor does not have the problem of particle bounce but undersamples PM_{2.5} by 10% because a fraction (10%) of fine particles will follow the air stream of the minor flow and then be collected on the filter for coarse particle.

Other than the FRMs and FEMs, there are many other samplers commercially available for TSP, PM₁₀ and PM_{2.5} monitoring, e.g., Harvard impactors, URG PM₁₀ cyclones and SKC deployable sampler systems. Some of them, e.g., Harvard impactors, have been found to have a comparable performance with the FRMs and FEMs during lab tests and/or field sampling (Babich et al., 2000; Demokritou et al., 2004; Turner et al., 2000). However, these samplers generally employ different designs of PM₁₀ and PM_{2.5} size separators than those used in the FRMs and FEMs. It is very costly and time consuming for those unique designs to be accepted as the FRMs or FEMs, because current criteria are very strict and elaborative (Noble et al., 2001). As a perfect example, it took ten years (1997 to 2006) for the BGI PM_{2.5} VSCC™ cyclone to be promoted from an FEM-level to an FRM-level PM_{2.5} size separator. These non-FRM and non-FEM samplers are generally less expensive and more transportable. Therefore, they have been widely used in situations where the monitoring data are not necessarily USEPA-approved.

Isokinetic sampling

As mentioned previously, TSP (total suspended particles) is defined as airborne particles collected by a high volume sampler (hivol), the only FRM TSP sampler designated by the USEPA. The D₅₀ of the hivol sampler varies with wind speed and direction but is generally from 25 to 40 μm (Wilson et al., 2002). The hivol sampler is specifically designed for sampling airborne particles in an open-air, ambient environment where wind may change in direction and velocity. The rain cap can prevent rain droplets from entering the inside of the sampler. Ambient aerosols are generally small in size (Seinfeld and Pandis, 1998) because otherwise they would quickly settle down due to the gravity force. Therefore, the hivol sampler can roughly collect all ambient aerosols in accordance to the apparent definition of the TSP sampler. However, airborne

particles from animal confinement buildings generally contain a large portion of large particles with geometric diameters up to 200 μm (Lee, 2009). The hivol sampler may undersample airborne particles from animal confinement buildings because of its low collection efficiency for large particles. Moreover, in animal confinement buildings particle samplers are generally installed right before the exhaust fans where a constant airflow velocity and direction are available. In this case, isokinetic sampling is a better choice than the hivol sampler.

Isokinetic sampling is a technique that has 100% collection efficiency for all sized airborne particles according to the definition by IUPAC (1997). To ensure an isokinetic sampling, two requirements must be satisfied concurrently: (1) the sampling probe is in alignment with the air streamline; and (2) the air velocity at the sampling probe (U_s) equals to that of the air being sampled (U_0) (Zhang, 2005). The sampling probe is generally made of a thin metal nozzle with a sharp edge in order to minimize the disturbance to the sampled airflow. Anisokinetic sampling occurs when the requirements for isokinetic sampling are not satisfied and may lead to oversampling or undersampling of airborne particles. There are three different cases of anisokinetic sampling: misalignment, superisokinetic sampling and subisokinetic sampling. Misalignment refers to the case when the axis of the sampling probe is not parallel to the air streamline. If $U_s = U_0$, misalignment would result in undersampling of airborne particles, especially of larger particles, because larger particles have a greater chance to be separated from the curved air streamline due to their larger inertia and, hence, are less likely to be collected. Superisokinetic sampling occurs when $U_s > U_0$. In such a case, the air streamlines converge near the sampling probe. Superisokinetic sampling leads to undersampling of airborne particles because of the loss of large particles that cannot follow the converged air streamlines due to their inertia. In contrast, subisokinetic happens when $U_s < U_0$. In this situation, the air streamlines diverge near the sampling probe, leading to oversampling of large airborne particles. In reality, anisokinetic sampling may occur in the form of a combination of misalignment and subisokinetic or superisokinetic sampling. Sampling efficiency is defined as the ratio of the concentration of particles entering the sampling probe to that in the air being sampled and may be greater or less than one when anisokinetic sampling occurs. Isokinetic samplers have been used for collection of airborne particles from animal confinement buildings for many years (Jerez, 2007; Lee, 2009; Wang, 2000). However, the exhaust fans of animal buildings may be automatically turned off or operated at reduced flow rates when the ambient temperature drops down. The isokinetic

sampling system should accordingly be turned off until the fans return to their full operation modes. Otherwise, the sampling bias would be significant.

Isokinetic sampling does not work when there is no air movement. Consequently the isokinetic sampling probe should be removed or replaced by other samplers under calm air conditions. Particle sampling in calm air turns out to be a major technical challenge in animal buildings. The sampling efficiency is generally affected by two factors: the settling velocity and the particle inertia. They are also the two major sources of sampling bias, especially for large particles. The particle settling would lead to an overestimation of particle concentrations if the sampling probe faces upwards, or an underestimation if the probe faces downwards (Hinds, 1982). By aligning the axis of the sampling probe horizontally, the sampling bias due to the settling velocity can be minimized. However, the sampling airflow will inevitably induce the converged air streamlines around the sampling probe in calm air. A portion of large particles would be lost due to their large inertia, similar to the previous discussion for superisokinetic sampling. Certain criteria for the sampler setup in calm air were proposed by Davies (1968) to ensure the loss due to the particle settling and inertia is negligible. However, according to his criteria, particle sampling in calm air works well only for particles with aerodynamic diameters equal or less than $\sim 20 \mu\text{m}$. For particles larger than $\sim 20 \mu\text{m}$, the loss due to the particle settling cannot be neglected (Wang, 2000).

Issues on particle sampling at animal facilities

Overloading is one of the most serious issues associated with particle sampling at animal facilities. Because airborne particles from animal facilities are generally more concentrated and comprise more large particles than ambient aerosols, particle samplers can be overloaded more quickly than the case of ambient aerosol sampling. Overloading can occur for both size separators and filters.

Overloading of the filters is uncommon but can be found during particle sampling in poultry buildings where airborne particle concentrations are extremely high. When excessive particle mass is being accumulated on a filter, the particle layer will gradually lose its integrity. Filter material is a major affecting factor on the probability of the occurrence of overloading. For example, glass fiber filters tend to be able to retain more particle mass than Teflon filters because of their rough surface texture. The source of airborne particles is another affecting factor.

Airborne particles from poultry buildings contain a large portion of feathers and tend to form a relatively loose particle layer on the filters. Consequently, they can quickly overload the filters.

Overloading of the size separators is a more common issue and should receive extraordinary attention (Zhao et al., 2009). The EPA-designated FRMs and FEMs were originally developed for sampling of ambient aerosols, and have not been systematically evaluated under extremely high loading conditions. An FRM sampler for PM_{2.5} should be able to work at a PM_{2.5} concentration as high as 200 µg/m³ for 24 hours, according to the CFR 40, Part 50, Appendix J (CFR, 2001b). However, the document does not specify the loading capacity of an FRM PM_{2.5} sampler, that is, the upper limit of particle mass that an FRM PM_{2.5} sampler can draw in without loss in performance. Vanderpool et al. (2001a) investigated the loading characteristics of the EPA WINS PM_{2.5} separator with Arizona test dust and found the 50% cut size (D₅₀) of the WINS impactor decreased from 2.48 to 2.21 µm after three days. The mean mass concentration during the test was 332 µg/m³, much lower than the typical particle concentrations found at animal facilities. Moreover, the Arizona test dust used in their study, with a MMD of 5 µm and a GSD of 2, is substantially smaller than airborne particles from animal facilities. Therefore, the real performance of the WINS impactor is questionable when used for measurements of airborne particles from animal confinement buildings. The BGI PM_{2.5} VSCCTM cyclone has been found to have better performance under heavy loading conditions (Kenny et al., 2000). The 50% cut size (D₅₀) of the BGI PM_{2.5} VSCCTM cyclone shifted from 2.50 to 2.35 µm after 6 mg of PM_{2.5} was collected. However, the airborne particles used in their study are significantly smaller than those from animal facilities. The mass ratio of PM₁₀ to PM_{2.5} is less than two, which is much smaller than the typical ratio (~10) found at animal facilities (Burns et al., 2008). In order to avoid potential overloading, the BGI PM_{2.5} VSCCTM cyclone should be cleaned frequently, e.g., every three days as proposed by Professor Robert Burns and his colleagues. In addition, little information is known about the loading characteristics of the EPA PM₁₀ inlet because most of the ambient aerosols are smaller than 10 µm. However, this is not the case for airborne particles from animal confinement buildings. In recent APECAB (Aerial Pollutant Emissions from Confined Animal Buildings) and NAEMS (National Air Emissions Monitoring Study) projects, the PM₁₀ inlets of the TEOM were cleaned every week in order to prevent the occurrence of overloading. However, in poultry buildings where TSP concentrations easily exceed 10 mg/m³, this cleaning cycle may not be short enough.

Applicability of the TEOM to particle sampling at animal facilities is another unresolved issue. In a TEOM, airborne particles are collected on a filter fixed on a hollow, tapered tube. The tube with the filter oscillates at a certain frequency that decreases as the mass of particles on the filter increments. The relationship is described by a mathematical equation for the simple harmonic oscillator. The mass sensor of TEOM has a lower detection limit of 0.01 μg , which makes it particularly suitable for measurements of ambient aerosols that generally have a very low mass concentration. The filter, tapered tube and mass transducer are normally operated at 50°C to remove the particle-bounded water (Patashnick and Rupprecht, 1991). However, this may lead to the loss of the volatile and semi-volatile compounds (e.g., NH_4NO_3), thereby resulting in a significant underestimation of particle mass concentrations, especially the $\text{PM}_{2.5}$ concentrations (Hodzic et al., 2005; Lee et al., 2005; Soutar et al., 1999). To overcome this limitation, certain modifications were made with the sample equilibrium system (SES) on the conventional TEOM unit (Meyer et al., 2000; Patashnick et al., 2001), and one of them recently became commercially available. It is known as the filter dynamic measurement system (FDMS) (Thermo Scientific 8500C FDMS system, Thermo Fisher Scientific Inc., Franklin, MA). TEOM/FDMS was recently accepted by the USEPA as a new FEM for $\text{PM}_{2.5}$ monitoring (USEPA, 2009c). By comparing the TEOM measured data with those measured by the TEOM/FDMS and/or filter-based FRMs from the same sampling events, the correction factors have been calculated for reprocessing of the old data and for calibration of the still-prevalent conventional TEOM units (Charron et al., 2004; Favez et al., 2007; Gehrig et al., 2005; Green et al., 2001). Unfortunately, the possible underestimation due to the limitation of the TEOM has not been properly assessed for airborne particles from animal facilities, although a large amount of data have been produced from continuous measurements with the TEOM in last ten years. Jerez et al. (2006) compared the TSP concentration data measured by the TEOM and by the UIUC TSP nozzle and found the TEOM underestimated the TSP concentrations by up to 54%. But this may mainly result from the difference in collection efficiencies between the TEOM TSP inlet and the UIUC TSP nozzle. The latter one is specifically designed for isokinetic sampling. In fact, airborne particles from animal facilities may consist of a large portion of volatile and semi-volatile organic compounds, especially in fine particles because they are formed predominantly from fecal materials. Therefore, there is potentially a significant underestimation of fine particle

concentrations by the TOEM. Efforts should be made in the future to determine the degree of underestimation and the associated correction factors.

Previous studies reported that the FRM/FEM size selective PM samplers may significantly overestimate mass concentrations of airborne particles from animal facilities or other agricultural sources (Buser et al., 2007a; Buser et al., 2007b; Buser et al., 2007c; Wang et al., 2005a; Wang et al., 2005b). Because aerodynamic MMDs of these particles are generally larger than 10 μm , the FRM/FEM PM_{10} and $\text{PM}_{2.5}$ samplers tend to collect more particles larger than the D_{50} than particles smaller than D_{50} in terms of mass, thereby leading to an oversampling of mass concentrations. To correct this sampling error, the size distribution of TSP particles was measured. The correction factors were calculated by comparing the measured PSD profile with the size cut curve of the FRM/FEM PM samplers (Wang et al., 2005b). Subsequently, the “true” mass concentrations were determined. These claims are absolutely true in theory. However, the “true” mass concentration can never be obtained in reality because of the existence of numerous uncertainties during field sampling. The unpredicted PSD is only one of them. Because of that, the USEPA defines the accuracy for PM measurements in a relative sense, as the agreement of a candidate method with a reference method. As an administrative standard, the CFR has specified the validity of the PM_{10} and $\text{PM}_{2.5}$ data: only those collected with FRMs or FEMs can be referred to as PM_{10} and $\text{PM}_{2.5}$. This should be considered to be a practical definition of PM_{10} and $\text{PM}_{2.5}$ (Kenny et al., 2000). On the other hand, the development of PM_{10} and $\text{PM}_{2.5}$ standards was driven by epidemiological evidence showing the adverse health effects of fine particles. PM_{10} is often selected as an indicator of particles that can enter the thoracic region (Wilson et al., 2002), while $\text{PM}_{2.5}$ is frequently used in epidemiological studies as an exposure index for respirable particles (Brunekreef and Holgate, 2002). Both thoracic and respirable particles are defined by the characteristic size cut curve of a certain compartment in the human respiratory system (Wilson et al., 2002). Therefore, an oversampling of large particles by the FRM/ FEM samplers is not a significantly important issue because those large particles would also likely be collected by the corresponding compartment in the human respiratory system. Another problem with the “true” mass concentration is that in the method proposed for calculation of the correction factors, the degree of oversampling is very sensitive to the slope of the PSD curve near the D_{50} of a PM sampler, because the size cut curves of the FRM/FEM samplers are generally very sharp. Unfortunately, most particle sizers currently available cannot provide a very accurate and

reliable measurement of the slope due to the limited number of channels and the measurement uncertainty with each channel. A Coulter Counter Multisizer was used to measure the PSD data for evaluation of oversampling (Buser et al., 2008; Wang et al., 2005a). However, first it is a filter based method, i.e., particles must first be collected on filters and then transferred into a solution for analysis. This inevitably creates certain errors because of the sampling bias and the size change due to disintegration and/or aggregation of particles in a solution. Second, the Coulter Counter Multisizer only measures the equivalent spherical diameter (ESD), while the size cut curve of PM samplers is in unit of aerodynamic diameter. These two diameters obviously cannot be directly compared and, unfortunately, there is no easy way to convert one to another.

2.3.5 Emission factors of airborne particles from animal facilities

Similar to the case of NH_3 , the emission rate of airborne particles is the product of the particle concentration and ventilation rate. The emission factor is calculated by averaging the emission rate over the weight (or number) of animals, generally presented in unit of g/AU-day. Airborne particle concentrations can be measured either with filter-based, gravimetric methods or non-filter-based, automate methods, e.g., TEOM. Ventilation rates can be determined with the same methods as discussed in Section 2.2.1.

Some of the previous studies used inhalable and respirable samplers for particle collection and measurements (Predicala and Maghirang, 2002; Seedorf, 2004; Takai et al., 1998). However, since inhalable and respirable particles are not NAAQS regulated, only PM_{10} and $\text{PM}_{2.5}$, and occasionally TSP and PM_1 data will be reviewed in this section.

Lacey et al. (2003) measured the TSP and PM_{10} emissions from four tunnel-ventilated broiler buildings in central Texas. A total of 120 filter samples were collected, throughout three grow-out cycles of flocks. According to their report, the time average emission factor was 245 g/AU-day for TSP and 12.9 g/AU-day for PM_{10} . However, the PM_{10} concentrations in their study were calculated from the TSP concentrations and the PSDs measured by a Coulter Counter Multisizer. The reliability of their PM_{10} data is, therefore, questionable. Lim et al. (2003) conducted a seven days' continuous monitoring using the TEOM in a belt-and-battery layer-hens building in Indiana and reported the average emission factors were 63 ± 15 , 15 ± 3.4 and 1.1 ± 0.3 g/AU-day for TSP, PM_{10} and $\text{PM}_{2.5}$, respectively. Jacobson et al. (2004) conducted a preliminary

study on PM emissions from four pig and two poultry buildings in six states. They found that the PM₁₀ emission factors ranged from 2.0 to 10.0 g/AU-day for high-rise layer-hen buildings. Roumeliotis and Van Heyst (2007) measured the emissions of PM₁₀, PM_{2.5} and PM₁ from a broiler building in Ontario, Canada, using DustTrak aerosol monitors. The monitoring event covered three complete grow-out cycles. It was found that the PM emission rates increased with the bird age but had no significant seasonal variation. Similar observations were reported recently by Burns et al. (2008). The time-average emission factor was 5.79±0.19 g/AU-day for PM₁₀, 1.22±0.05 g/AU-day for PM_{2.5} and 0.99±0.04 for PM₁.

Compared to poultry buildings, swine buildings tend to have lower emission factors. As a part of the APECAB project, Jacobson et al. (2005) conducted a 15-month measurement in two swine gestation buildings in Minnesota using the TEOM. They found that the PM₁₀ emission factors were relatively stable during the winter (0.75 to 1.4 g/AU-day) but fluctuated greatly during the summer (0.95 to 3.8 g/AU-day), probably because the ventilation stages varied more greatly and frequently during the summer than winter. Under the same APECAB project, Hoff et al. (2005) and Koziel et al. (2005) reported the PM₁₀ emission factors ranged from 0.7 to 4.3 g/AU-day in swine finishing buildings, while Jerez et al. (2005) reported an average PM₁₀ emission factor of 1.2 g/AU-day in a swine farrowing building. Professor Annamaria Costa and her colleagues (Costa and Guarino, 2009; Costa et al., 2007) measured the PM₁₀ emissions from four different types of swine buildings (farrowing, gestation, weaning and finishing) in Italy and reported that the yearly average PM₁₀ emission factor was 0.09 g/AU-day for the farrowing building, 1.23 g/AU-day for the gestation building, 2.0 g/AU-day for the weaning building, and 2.59 g/AU-day for the finishing building. No significant seasonal variation was observed in their study.

Although in recent years, many efforts have been made to produce reliable and representative data for airborne particle emissions from animal confinement buildings, additional efforts are still needed for development of a complete and comprehensive emission inventory. The existing data are not enough to characterize the variability in particle emission factors due to different building design, animal type, animal age, season, manure management, and many other operational and environmental factors (Roumeliotis and Van Heyst, 2008). Emission factors reported by researchers from other countries are not readily applied to the United States because of the possible difference in management practices (Roumeliotis and Van Heyst, 2008). The

recently completed NAEMS and a few other similar projects are expected to produce more reliable data in the near future.

It must be noted that animal confinement buildings are nationwide only a minor source of airborne particles. It was estimated that in 2005, 2.2 million tons of PM₁₀ and 1.2 million tons of PM_{2.5} were emitted from anthropogenic sources in the United States (USEPA, 2009a). Assume 15 g/AU-day and 3 g/AU-day are representative values of PM₁₀ emission factors for broilers and pigs, respectively, and the average weight is estimated to be 1.6 kg for broilers and 60 kg for pigs, then the total PM₁₀ emissions in 2005 would be approximately 29,000 tons from broiler buildings and 8,200 tons from pig buildings. Therefore, animal confinement buildings are nationwide a minor source but can be a regionally or locally major source of airborne particles in the areas where animal production is concentrated.

2.3.6 Influential factors and control strategies

A successful control strategy can only be developed based on a good understanding of the operational and environmental factors that affect the production of airborne particles in animal confinement buildings. Heber et al. (1988b) summarized a number of factors that may influence the airborne particle concentrations in swine buildings as follows:

- Outside temperature. Particle concentrations tend to decrease as the outside temperature goes up. Because the ventilation rate increases with the outside temperature, the airborne particles in the animal barns will be diluted by an increased volume of fresh air.
- Ventilation system. Compared to the mechanical ventilation systems, the natural ventilation systems are generally associated with higher indoor airborne particle concentrations because of their lower ventilation rates.
- Air velocity in the barns. The effects of air velocity are relatively complex. Increased air velocity may enhance the suspension and re-suspension of particles, but at the same time an increasing amount of particles may be removed due to the enhanced inertial impaction on building surfaces and other objects.
- Moisture. Particle concentrations decrease with the relative humidity (RH). The adsorption of water on airborne particles enlarges the particle size, thereby lowering the possibility

of re-suspension. However, the effect of a moisture becomes significant only under very high RH conditions, e.g., RH greater than 85%.

- Animal activity. Increased animal activity leads to higher particle concentrations. Animal activity is affected by indoor temperature, feeding method, feed type, light and human activity in the animal barns.
- The quantity of feed per animal. Feed delivery is a major source of airborne particles. An excessive amount of feed may lead to high particle concentrations.
- Building cleanliness. The dusty floor and wall surfaces are sources of airborne particles and also enhance the possibility of particle re-suspension.

These factors also apply to poultry buildings. But in the latter case, the manure management system is additionally a major affecting factor. Unlike swine manure stored in a pit or lagoon, poultry manure is either collected, dried (e.g., in the high-rise layer-hens buildings) and then sent off as fertilizer, or directly settled on the floor covered with bedding materials (e.g., in the broiler buildings). In the first case, drying manure enhances the chance of aerosolization, but on the other hand such a concentrated manure management practice may reduce the particle emission rate per animal by avoiding the potential disturbance by animal activity. In the second case, airborne particles can be produced from suspension of fecal materials on the floor due to animal movements and turbulent airflow.

To reduce the production of airborne particles in the barns, the following control strategies can be employed (Roumeliotis and Van Heyst, 2008):

- Feed additives. Adding animal fat into the feed diet can effectively reduce the particle production by suppressing the aerosolization of feed (Chiba et al., 1985; Takai et al., 1996). Soybean oil is another effective feed additive according to Gast and Bundy (1986).
- Oil sprinkling. Spraying vegetable oils into the room air facilitates the agglomeration of fine particles in the air, in the manure or feed and, thus, suppresses the particle production (Rule et al., 2005; Zhang et al., 1996).

A number of aftertreatment techniques are currently available to mitigate the emission of already airborne particles from animal facilities (Tan and Zhang, 2004; Ullman et al., 2004).

They are:

- Wet scrubber. In a wet scrubber, an aqueous solution, generally water, is sprayed into the exhaust gas to remove gaseous pollutants and airborne particles simultaneously. The removal efficiency of airborne particles is significantly affected by and decreases with the ventilation rate (Bottcher et al., 1999).
- Biofilter. Bacteria and other microorganisms are grown on the surface of packing materials in a biofilter. When air pollutants pass through a biofilter, they are absorbed and/or adsorbed on the surface of packing materials and then biodegraded by the microorganisms. Biofilters were found to be able to remove both gaseous pollutants and airborne particles effectively (Martinec et al., 2001)
- Electrostatic precipitator (ESP). In an ESP, airborne particles are charged with an electric field of high voltage and then collected on an electrode or a dust tray. Previous studies in poultry buildings found that ESP had very high removal efficiencies but its performance declined quickly because of the rapid accumulation of particles on the electrode (Chai et al., 2009; Mitchell et al., 2003).
- Cyclone. Cyclone is basically an aerodynamic deduster. Airborne particles are separated from the air vortex due to their inertia and then collected in a dust bunker. Uniflow cyclones were recently developed by researchers at UIUC and have shown substantially lower pressure drops than conventional return-up cyclones (Zhang et al., 2005). A preliminary test in a swine finishing building showed the emission of airborne particles was reduced by 90% with a uniflow cyclone (Zhang et al., 2001).

Among the techniques discussed above, oil sprinkling and biofilter are most promising to be widely practiced in animal confinement buildings. Other techniques, however, are either too expensive or technically underdeveloped. Since airborne particles are carriers of odorous compounds and microorganisms, the control strategies mentioned above should also be effective for odor and pathogenic microorganisms.

2.4 Air Quality Modeling

A main purpose of emission measurements is to provide input data for air quality models so that the contribution of animal facilities to the air quality issues in the area of interest can be determined; and based on that, the essential emission regulations and the effective control

strategies can be developed and implemented. The commonly used air quality models can be classified into three categories: photochemical models, dispersion models and receptor models. The first two require input of emission factors or rates, while receptor models need input of chemical speciation information.

2.4.1 Photochemical models

Photochemical air quality models include several very complex chemical transport models, e.g., community multi-scale air quality (CMAQ) modeling system, and comprehensive air quality model with extensions (CAMx). Although theoretically these models can be applied on local and regional scales, they are generally used to simulate and predict the air quality over large spatial scales (Matthias et al., 2009; Odman et al., 2009). The operation of these models requires a comprehensive emission inventory. But minor sources are usually neglected because of the priority issue and accordingly the limited emission data for minor sources. Since animal confinement buildings are a primary source of NH_3 , an important precursor of secondary inorganic aerosols modeled in the CMAQ (Binkowski, 1999), they are often included in the NH_3 emission inventory for photochemical modeling. In contrast, animal confinement buildings are only a minor source of airborne particles on a global, national or even regional scale. As a consequence, they are normally excluded from the PM emission inventory for photochemical modeling. Because airborne particles from animal confinement buildings are normally a local environmental issue, particle concentrations within the limited affected area are expected to have a quick response to the variation of the source emission rate that indeed fluctuates frequently and greatly with time. However, current photochemical models do not offer sufficient temporal and spatial resolutions to depict this type of quickly varying, locally occurring air pollution scenario. In addition, airborne particles from animal facilities are unlikely to change chemically within a short transport distance and, therefore, a simulation of chemical transformation by photochemical models would be unnecessary. Also, the photochemical modeling is very time and labor consuming. In conclusion, the measured emission factors of airborne particles from animal confinement buildings are unlikely to be used in photochemical models.

2.4.2 Dispersion models

Dispersion models may be a more reasonable choice considering the characteristics of airborne particle emission from animal confinement buildings. Dispersion models use

mathematical formulas to describe the transport and removal of an air pollutant in the atmosphere and to calculate its concentrations in the area of interest (Holmes and Morawska, 2006). Dispersion models were first promulgated by the USEPA for regulatory modeling applications in the 1977 Clean Air Act (Schnelle and Dey, 2000). According to their mathematical principles, dispersion models can be classified into four types: box models, Gaussian models, Lagrangian models, and computational fluid dynamic (CFD) models (Holmes and Morawska, 2006). Among them, Gaussian models are currently most frequently employed. Compared to photochemical models, dispersion models are more suitable for simulating the atmospheric transport of primary and non-reactive pollutants with less required input data (USEPA, 2004b). In fact, Eulerian grid models used in CMAQ and CAMx are in principle very similar to box models but have been incorporated in with the chemical transformation modules. Consequently, these two photochemical models can handle reactive and secondary pollutants by modeling the associated photochemical reactions, but require significantly more input data. A number of dispersion models have been used to simulate the transport of air pollutants, mostly NH₃ and odor, from animal facilities (Guo et al., 2001; Hayes et al., 2006; Sheridan et al., 2004; Smith, 1995) or to calculate the emission factor in a backward way (Wang et al., 2006). However, so far no studies have been reported in the literature using dispersion models to simulate airborne particle emissions from animal facilities. Commonly used models in the United States for local dispersion modeling (<50 km) include the Industrial Source Complex Short-Term Model (ISCST3) and its recent replacement, the American Meteorological Society/Environmental Protection Agency Regulatory Model (AERMOD) (Bunton et al., 2007). CALPUFF was used by some agricultural engineers for simulating the transport of gaseous pollutants on a local scale (Wang et al., 2006). However, it was designed primarily for regional dispersion modeling (>50 km).

ISCST3 is a steady state Gaussian plume model designed for assessment of pollutant dispersion from a variety of industrial sources: point, area, volume, and open pit sources (USEPA, 1995). The model requires at least two input files: a runstream and a meteorological data file. The runstream file is used for specifying the modeling options (e.g., buoyancy-induced dispersion, stack-tip downwash, and final plume rise), source parameters (e.g., type, location, dimension, and emission rate), receptor locations, meteorological data file specifications and output file options. The meteorological data file contains the information of temperature, wind

speed, atmospheric stability, mixing height and many other dispersion related parameters. ISCST3 can be used to calculate the short-term variations in airborne particle concentrations with varying emission rates and meteorological conditions. However, ISCST3 has certain limitations: first, the surface roughness was oversimplified into only two types: urban and rural; second, the effects of atmospheric stratification were interpreted with the outdated Pasquill-Gifford stability classification developed in the 1960s (Tirabassi and Rizza, 1993). ISCST3 was once a USEPA recommended model but was replaced by AERMOD in 2005 (CFR, 2005).

AERMOD is a near field steady state Gaussian plume model developed based on the advanced knowledge of planetary boundary layer (PBL) (USEPA, 2004a). Like ISCST3, AERMOD assumes that in the stable boundary layer (SBL) both the horizontal and vertical distributions of air pollutants are Gaussian. However, in AERMOD, the vertical distribution in the convective boundary layer (CBL) is assumed to follow a bi-Gaussian probability density function and the Monin-Obukhov length replaces the Pasquill-Gifford stability to characterize the effects of atmospheric stratification. As a result, more meteorological data are required by AERMOD (USEPA, 2003). The model input includes at least three files: a runstream and two meteorological data files. The format of the runstream file in AERMOD is very similar to ISCST3 since AERMOD was actually modified from ISCST2. One of the meteorological data files contains the surface scalar parameters and the other one consists of the vertical profiles of meteorological data. Both meteorological data files are produced by AERMET, a meteorological preprocessor specifically designed for AERMOD. AERMAP is the terrain preprocessor for AERMOD and used when the effect of elevated terrain needs to be considered. Previous studies on comparison of different dispersion models showed AERMOD could under-predict the pollutant concentrations while ISCST3 might cause significant over-prediction (Hanna et al., 2001).

The measured emission factors need be processed before input into dispersion models. An animal confinement building can generally be considered as a point source, because the distance between the building and the receptor site of interest is normally much larger than the building size. In this case, the emission rate is presented in unit of g/h (or day/week, depending on the time scale of interest), and can be calculated by multiplying the emission factor by total animal weight in unit of AU. However, in some cases the receptor site of interest is relatively close to the animal building and, accordingly, the building may need to be considered as an area or

volume source with the emission rate expressed in unit of $\text{g}/\text{m}^2\text{-h}$ or $\text{g}/\text{m}^3\text{-h}$, respectively. Besides, it should be noted that in ISCST3 and AERMOD the maximum temporal resolution for both input and output data is one hour (Faulkner et al., 2007).

2.4.3 Receptor models

Receptor models use quite a different approach for determination of the source contribution. In photochemical and dispersion models, the transport of air pollutants in the atmosphere is described by a variety of dispersion algorithms. However, in reality, the transport process is very complicated and is affected by numerous uncertainties. It is very common that the predicted air pollutant concentrations at the receptor locations are different by a factor of two to three from the measured values (Holmes and Morawska, 2006). To overcome the difficulty in modeling the air pollutant transport, an alternative way is to directly establish a mathematical or statistical relationship of air pollutant emissions at the source to the air pollution profile at the receptor site. This is the origin and the key concept of receptor modeling. In receptor models, the air pollution profile at a receptor site is considered to be a result of a mixing of various air pollutants from multiple separate sources. Non-reactive air pollutants are assumed to be mass conservative during the transport process. For reactive air pollutants, a gain or loss of mass is likely to occur due to the chemical transformation. Based on the assumption of mass conservation, a mass balance equation can be established (Equation 2.3) (Hopke, 1999), where x_{ij} is the mass concentration of the specie i in the sample j at the receptor site, a_{ik} is the mass fraction of the specie i in air pollutants from the source k , and f_{kj} is the contribution of the source k to the sample j in terms of mass concentration. Therefore, once the mass concentrations of multiple non-reactive species are known at both sources and the receptor site, the source contributions can be calculated from mass balance. Receptor models are especially suitable for particle source apportionment because airborne particles are usually complex in chemical composition and may contain a number of non-reactive species that can be used to establish the mass balance. Inorganic elements (especially metals) and soluble ions are often selected for receptor modeling. Recently, low reactive organic compounds were introduced into the models to increase the dimension of the matrix (Jorquera and Rappengluck, 2004).

$$x_{ij} = \sum_{k=1}^p a_{ik} f_{kj} \quad (2.3)$$

There are numerous receptor models currently available for particle source apportionment, including enrichment factors, chemical mass balance (CMB), linear regression, empirical orthogonal functions (EOF), factor analysis (FA), principle component analysis (PCA), partial least-squares (PLA), positive matrix factorization (PMF), artificial neural networks, genetic algorithm and edge detection (Watson et al., 2002). According to their mathematical or statistical principles, these models can be classified into chemical mass balance, multivariate calibration and factor analysis methods (Hopke, 1999). USEPA currently provides three receptor modeling tools free to the public: CMB, PMF and UNMIX. The first two are also the most commonly used receptor models today.

The CMB model was directly developed based on Equation 2-3. It is often used to determine the contributions of known sources but requires a complete source chemical profile database. However, to obtain that database is usually a big challenge and may require a lot of field measurement work. There are several assumptions in the CMB model: (1) the source chemical profiles are relatively constant over time; (2) the selected chemical species are non-reactive; (3) all contributing sources have been included and measured; (4) the number of selected species are greater than or equal to the number of sources or source groups; (5) all sources are independent from one another; and (6) measurement errors are independent and follow the normal distribution (Coulter, 2004). Any deviations from these assumptions in a real case will cause an increase in uncertainties in the model output. A validation procedure is necessary before modeling. The assumptions in the CMB model are also part of its limitations. Especially the third and fifth assumptions are very difficult to satisfy in reality. The CMB software was originally developed in 1978 and since then, a lot of modifications have been implemented. The effective variance weighted least squares algorithm is used in the current CMB software (EPA-CMB8.2) for solving the overdetermined matrix equations of mass balance.

As a factor analysis method, the PMF model does not require input of source chemical profiles but needs a lot more chemical profile data from the receptor sites. The PMF model is useful in determining the presence and contribution of major sources but alone cannot identify the specific sources. The PMF model was proposed by a group of Finnish scientists (Juntto and Paatero, 1994; Paatero and Tapper, 1994) in an effort to overcome the negative contributing factors produced by the PCA, a previously very popular receptor model. In the PMF model, a new objective function is defined and this function set a constraint on the solution matrix so that

all values in this matrix will be non-negative. Assumptions in the CMB model also apply to the PMF model except for the second and third. The PMF model can use somewhat reactive species as tracers, in addition to non-reactive species. The current PMF software (EPA PMF v3.0) requires two separate input files: a concentration and an uncertainty data file (USEPA, 2008). The software provides three different modeling options (algorithms): base, bootstrap and Fpeak model. It also offers an input data analysis module for assessing signal-to-noise, concentration time series and other statistical characteristics of raw data before modeling.

2.4.4 Implications to this project

Both the dispersion and receptor models can be used to determine the contribution of airborne particle emissions from animal confinement buildings to a local air quality problem. These two types of models both have their own advantages and limitations but can be complementary to each other. The best way might be to use both the dispersion and receptor models and then integrate their results together to obtain a comprehensive view (NAS, 2003). A comparison of the commonly used dispersion and receptor models is shown in Table 2.2.

The greatest challenge in using the dispersion models is that the emission factor of airborne particles from animal confinement buildings varies significantly from building to building because of differences in geographic location, building dimension, animal age and density, ventilation strategy and many other unpredictable factors. The “typical” emission factors generated from monitoring a limited number of animal buildings might be appropriate for estimation of a nationwide or regionally total airborne particle emission from animal facilities. But can they be applied to an individual animal building? If we do so, an assumption behind this would be the emission factors are identical or at least numerically similar among all animal confinement buildings of the same type.

Can the receptor models be a better choice? As mentioned previously, the receptor models assume the source chemical profiles are relatively constant, which means airborne particles from different animal confinement buildings but of the same type would have a similar chemical composition. Deviations from this assumption are inevitable in reality. Changes in the diet of animal feed, manure management, animal age and animal activity would all possibly alter the chemical composition of airborne particles. But compared to the assumption for the dispersion models, which is more robust? This study will try to provide essential data for making this

judgment. If the final answer favored the receptor models, then the data generated from this study would be useful for particle source apportionment through receptor modeling (e.g., CMB).

Table 2.2. Comparison of commonly used dispersion and receptor models.

		Input	Output	Assumptions
Dispersion models	ISCST3	Dispersion options: Average time; Source information: <i>source type, emission rate, temperature, source dimensions, building dimensions;</i> Receptor locations; Meteorological data;	Air pollutant concentration at the receptor site(s).	Gaussian distribution in both the horizontal and vertical directions; No physical and chemical transformation.
	AERMOD	Similar to ISCST3, but needs two meteorological data files.	Air pollutant concentration at the receptor site(s).	Gaussian distribution both horizontally and vertically in the SBL, and bi-Gaussian distribution vertically in the CBL; No physical and chemical transformation.
Receptor models	CMB	A complete source chemical profile database (multiple sources); Chemical profiles at the receptor site(s) (# of sites ≥ 1).	Contributions of specific sources to the air pollution at the receptor site(s).	Constant source chemical profiles; Nonreactive chemical species; All contributing sources are counted; # of selected species \geq # of sources; No interdependent sources; Normally distributed measurement errors.
	PMF	Chemical profiles at multiple receptor sites, or at limited number of sites but with multiple samples for each site at different time points.	Presence and contributions of potential sources in a polluted area.	Constant source chemical profiles; # of selected species \geq # of sources; No interdependent sources; Normally distributed measurement errors.

The receptor models can also be used to determine the sources of indoor air pollutants (Chao and Cheng, 2002). In that case, an exhaust fan would be considered as a receptor site. By collecting multiple airborne particle samples at the exhaust and measuring their chemical compositions, the major airborne particle sources and their respective contributions could be determined with factor analysis (e.g., PMF). Because in the animal confinement buildings, the air exchange rate is typically high and the retention time of an air pollutant is likely very short. In such a case, the selected species for receptor modeling are not necessarily non-reactive. This indicates that the source apportionment of malodorous VOC's in an animal building is plausible through receptor modeling.

2.5 Chemical Speciation of Airborne Particles from Animal Confinement

Buildings

Using receptor models for particle source apportionment requires a measurement of chemical compositions of airborne particles at the sources or receptor sites. Also, chemical speciation can provide valuable information for assessment of health effects of airborne particles from animal confinement buildings since health effects are closely related to physical, chemical and biological properties of airborne particles. There is little knowledge so far about the chemical composition of airborne particles from animal confinement buildings (Lammel et al., 2004; Martin et al., 2008). However, it should be expected that these airborne particles have significantly different chemical properties than ambient aerosols that have been extensively studied. This means the chemical speciation methods developed for ambient aerosols may not be optimal or appropriate for characterizations of airborne particles from animal confinement buildings. However, to ensure the data compatibility that is required by the application framework for receptor modeling, the EPA recommended methods and protocols should be followed in practice.

According to “Particulate matter (PM_{2.5}) speciation guidance” (USEPA, 1999b), the major chemical components in ambient PM_{2.5} aerosols are sulfate, nitrate, ammonium, organic carbon (OC), elemental carbon (EC) (graphite carbon or soot), sodium chloride, water and geological materials. The target chemical species include OC and EC, chemical elements and soluble ions, and are studied separately with different sampling and analytical protocols. OC and EC are generally determined through thermal optical analysis (Wilson et al., 2002). However, there is obviously no EC production in animal confinement buildings. The OC measurement results can provide the concentration of carbon atoms contained in organic compounds by comparing to reference materials but cannot directly offer the content of organic compounds in airborne particle samples (El-Zanan et al., 2005). Consequently, OC and EC measurements seem to be unnecessary for airborne particles from animal confinement buildings and, therefore, would be excluded from this section.

2.5.1 Methods for elemental composition measurement

There are several techniques currently recommended by USEPA (1999a) for determining the elemental composition of ambient aerosols, including flame atomic absorption (FAA), graphite

furnace atomic absorption (GFAA), neutron activation analysis (NAA), particle induced X-ray emission spectroscopy (PIXE), X-ray fluorescence (XRF), inductively coupled plasma spectroscopy-atomic emission spectrometry (ICP-AES), and inductively coupled plasma-mass spectrometry (ICP-MS). The selection of these techniques is generally dependent upon the specific sampling protocol (e.g., selected filters, samplers and sampling flow rate), the purpose of analysis (e.g., specific elements, non-destructive or destructive methods, and sensitivity), the sample matrix (e.g., possible major and trace elements), the availability of instrumentation and certainly the project budget.

X-ray fluorescence (XRF)

X-ray fluorescence (XRF) bombards the atoms with X-rays or γ -rays, and then analyzes the element-specific secondary (fluorescent) X-ray emissions (Skoog et al., 1998). Quantification of an element is done by comparing the X-ray intensity emitted from the test sample to that from a standard material. The basic physical process is as follows. The absorption of X-rays or γ -rays by an inner shell electron will possibly cause the release of this electron from the atom, creating a vacancy in the inner atomic shell. A higher energy electron at the outer shell in the same atom will then fall into the inner orbital to occupy the vacancy and during this transition a fluorescent X-ray photon will be released. The energy of this photon is element characteristic and, thus, can be used as an evidence for element identification. According to the atomic orbital theory, only several transition routes are available, including L \rightarrow K transition ($K\alpha$), M \rightarrow K transition ($K\beta$), M \rightarrow L transition ($L\alpha$), and so on. $K\alpha$ is often used for identification of light elements, while $L\alpha$ is very useful for determination of heavy metals (Watson et al., 1999).

There are two basic types of XRF instruments: wavelength dispersive X-ray fluorescence (WDXRF) and energy dispersive X-ray fluorescence (EDXRF). WDXRF uses a crystal (single channel WDXRF) or crystals (multi-channel WDXRF) to disperse the fluorescent X-ray into its component wavelengths and detects the monochromatic X-ray with a semiconductor detector. WDXRF has greater spectral resolution but is less sensitive than EDXRF. To improve the sensitivity, a high intensity X-ray irradiation is required, which may cause damage to particle filters.

EDXRF uses a polychromatic X-ray source and a silicon (lithium) semiconductor detector. In the detector, an arrived X-ray photon would create a voltage pulse that is proportional to the

photon energy, the critical information for elemental identification. The voltage pulses are amplified and then measured and counted by a multichannel pulse-height analyzer. Accordingly, a count versus energy XRF spectrum can be obtained. EDXRF has poorer spectral resolution than WDXRF. With the development of deconvolution algorithms and computer technology, peak overlap is no longer a big issue but still leads to certain uncertainties in measurement results. The X-ray irradiated on the filter samples can be either directly from the X-ray source or from secondary fluorescers (targets). In the former case, a filter is occasionally used to modulate the original X-rays. In the latter case, a secondary fluorescer is excited by the X-rays from the source, producing secondary X-rays to bombard the filter sample. Compared to WDXRF, EDXRF is non-destructive, cheaper and more sensitive, and consequently, is more frequently used at present. Theoretically, EDXRF can detect all elements heavier than He, but in reality should only be used to quantify elements heavier than Na due to the strong interference of background to light elements. The sensitivity of the EDXRF analysis is adjustable and can be improved by increasing the intensity of the irradiating X-rays and the counting time.

EDXRF has been extensively used for determining the elemental composition of ambient aerosols, especially PM_{2.5} (Martuzevicius et al., 2004; Sillanpaa et al., 2005; Wei et al., 1999). EDXRF is currently in use by the National Ambient Monitoring Stations (NAMS), State and Local Ambient Monitoring Stations (SLAMS) and the Interagency monitoring of Protected Visual Environments (IMPROVE) program as the standard method for elemental analysis of ambient PM_{2.5} (USEPA, 1999b). A standard sampling and analysis protocol has been developed by the USEPA (Compendium Method IO-3.3) (USEPA, 1999a) to normalize the operation procedure and to ensure the quality of outcome data. However, EDXRF has certain limitations when used for studying airborne particles from animal confinement buildings. These limitations would be discussed later in Chapter 4.

Synchrotron induced X-ray fluorescence (S-XRF) and total reflection X-ray fluorescence (TXRF) have recently been used in ambient aerosol analysis and have shown the capability to detect light elements by minimizing the interference of background (Chimidza et al., 2001; Yue et al., 2004). However, the availability of S-XRF and TXRF is quite limited.

ICP-AES

Inductively coupled plasma-atomic emission spectrometry (ICP-AES), also called inductively coupled plasma-optical emission spectrometry (ICP-OES), is probably the most widely used multi-element analysis technique today. ICP is a plasma producing technique (Grohse, 1999; Skoog et al., 1998). An ICP unit generally consists of a quartz glass tube and a coil. When a high frequency time-varying current passes through the coil, a time-varying magnetic field is formed around the coil and in the quartz glass tube. When Ar gas flows through the tube, an inductive current is formed in the gas, which breaks the Ar atoms into electrons and ions (plasma). The temperature of the produced plasma generally ranges from 6000 to 10,000 K. At such high temperatures, most chemicals can be atomized very efficiently. ICP-AES uses a nebulizer to spray a sample solution into a chamber where an ICP torch breaks the sample into atoms and charged ions. The produced atoms and ions are excited by the plasma into excited electronic states that are unstable. The excited atoms and ions would, therefore, return to the ground electronic state and simultaneously release photons (atomic emission). The energy of released photons is element-specific and, hence, can be used for element identification. Such excitation and returning process occurs repeatedly in the ICP torch and, accordingly, a large number of photons can be emitted from a small amount of test sample in the ICP torch. The intensity of atomic emission of a certain element is proportional to the mass of that element introduced into the ICP torch. Therefore, by comparing the intensity of atomic emission of an element in an unknown sample to that in a standard solution, the quantity of that element in the unknown sample can be determined.

According to the geometry of the ICP torch, the current ICP-AES instruments can be classified into two categories: ICP-AES with radial torch and ICP-AES with axial torch. The latter one provides greater sensitivity (<1 ppb) but is generally more expensive.

To use ICP-AES for ambient aerosol analysis, the collected aerosols must be extracted and digested in the presence of acids, e.g., HNO₃, HCl, HClO₄, HF and their mixtures. Therefore, unlike EDXRF, ICP-AES is a destructive method. An acid mixture of HNO₃ and HCl is generally used for sample digestion. However, some refractory minerals, e.g., SiO₂ and TiO₂, may require the use of HF. There are four major acid digestion methods currently available: hot-plate, ashing, ultrasonication, and microwave. Among them, hot plate acid digestion and

microwave assisted acid digestion are recommended by the USEPA for ambient aerosol analysis (Compendium Method IO-3.4) (USEPA, 1999a). In both methods, the acid solution is heated to over 100°C to enhance the digestion rate. The microwave digestion method generally is more efficient, less time-consuming, safer, and more convenient than the hot plate digestion method and consequently is becoming increasingly popular.

Many studies have used ICP-AES to determine the inorganic elements in airborne particles (Espinosa et al., 2002; Gomes et al., 1996; Park and Kim, 2005). A standard sampling and analysis protocol can be found in EPA Compendium Method IO-3.4. Compared with EDXRF, ICP-AES has certain advantages. First, it can detect some light elements, e.g., Li, B, Na, and Mg. Second, the ICP-AES instrument is widely available and the analysis cost is becoming less expensive. Third, the standard solutions are easily prepared or purchased. Fourth, the linear range of ICP-AES is over five orders of magnitude, which means less calibration efforts are required. However, ICP-AES is a destructive method and currently the analysis cost of ICP-AES is still slightly more expensive than EDXRF.

Inductively coupled plasma-mass spectrometry (ICP-MS) is similar to ICP-AES but uses a mass spectrometer to detect the ions produced in the ICP torch. ICP-MS offers the highest detection sensitivity for most elements among existing multi-element analysis instruments. ICP-MS can also measure isotopes that are often used as tracers for source identification studies (Choi et al., 2006). However, the ICP-MS test is currently very expensive and the extremely high sensitivity of the ICP-MS is usually unnecessary for ambient aerosol analysis.

Other techniques

Flame atomic absorption (FAA) uses a flame to atomize a sample solution (Skoog et al., 1998). The aerosols are then illuminated by a light beam. The transmitted light is filtered by a monochromator and then measured by a photomultiplier. Identification of elements is based on the fact that each element has its specific atomic adsorption wavelengths so the transmitted light intensity at those wavelengths would be reduced with the presence of the corresponding element. Quantification is based on Beer's law that the light absorbance is linearly related to the concentration of an element. Graphite furnace atomic absorption (GFAA) is very similar to FAA in terms of working principles, but uses an electrical energy to atomize an analyte (Skoog et al., 1998). GFAA generally has greater sensitivity than FAA. One limitation of both FAA and

GFAA is that they can only quantify a single element each time. And airborne particle samples must be digested before analysis. As a result, today they are only used in ambient aerosol studies when a single or a few elements are of interest.

Neutron activation analysis (NAA) bombards the atoms with high energy neutrons to create artificial radioactive isotopes (Landsberger, 1999). The decay of these isotopes is associated with element-specific γ ray radiations, from which the presence of certain elements can be identified. By comparing the intensity of γ ray radiations from unknown samples to that from standard materials, the elemental composition in unknown samples can then be quantified. NAA has a number of advantages as a method for measuring the elemental compositions of airborne particles. First, it is a non-destructive method. The measured filter samples can subsequently be used for other purposes. Second, NAA is a very sensitive method. It can simultaneously detect nearly all elements found in airborne particles with great sensitivity (ppm) except for Pb and S, and the detection limits can be further improved by extending the irradiation and counting time. NAA was once the standard reference method for sensitive (ppm) multi-element analysis, prior to the advent of PIXE and ICP-AES. NAA has been extensively used for studying the elemental composition of ambient aerosols (Biegalski and Landsberger, 1995; Var et al., 2000). Unfortunately, it has become decreasingly available due to the abolishment of the nuclear reactors since the 1980's.

Particle induced X-ray emission spectroscopy (PIXE) bombards the atoms with light ions, e.g., protons, and then detects the produced X-ray emission (Cohen, 1999). Since the X-ray wavelengths are element specific, the elements in a sample can be identified accordingly. Similar to the case of XRF, quantification of an element can be done by comparing the X-ray intensity of the tested samples to a standard material. PIXE can measure over 20 different elements at once, including Al, Si, P, S, Cl, K, Ca, Ti, V, Cr, Mn, Fe, Co, Ni, Cu, Zn, Br, Sr, Y, Zr, and Pb (USEPA, 1999a). Irradiation of ions on a sample also creates γ ray emission, Rutherford backscattering, elastic scattering, β decay, and ultra-violet (UV) light. Some of them are very useful for determining the elemental composition. Particle induced gamma-ray emission (PIGME) can be used to determine light elements such as Li, B, F, Na, Mg, Al, and Si. Rutherford backscattering is useful for analysis of very light elements including C, N and O. Particle elastic scattering analysis (PESA) can be used for analysis of H. Similar to NAA, PIXE is a non-destructive method. But unlike NAA, PIXE is generally used for airborne particle

samples collected with low volume sampler because PIXE tests require the loaded particle mass should be less than $300 \mu\text{g}/\text{cm}^2$ filter area to satisfy the thin target assumption. In contrast, NAA can handle both high and low particle loading cases. PIXE is one of the most commonly used methods in ambient aerosol study (Artaxo et al., 2002; Cyrus et al., 2003). However, the availability of PIXE instruments is relatively limited compared to FAA, GFAA and ICP-AES.

2.5.2 Methods for determination of soluble ions

There are many water-soluble inorganic and organic ions that have been found in ambient aerosols. As mentioned previously, the mass fraction of NH_4NO_3 and $(\text{NH}_4)_2\text{SO}_4$ can exceed 50% in ambient $\text{PM}_{2.5}$ (Pathak et al., 2009). They are mainly secondary inorganic aerosols formed in the atmosphere as a consequence of NH_3 , NO_x , and SO_2 emissions. Other inorganic ions, e.g., Na^+ , Mg^{2+} , K^+ , Ca^{2+} and Cl^- , may come from sea salts, soil or rock minerals. Organic ions mainly include carboxylic and dicarboxylic acid radicals (Tsapakis et al., 2002). Dicarboxylic acids recently have received much attention because of their potential impacts on global climate (Hsieh et al., 2007). However, in ambient aerosol studies, e.g., NAMS, SLAMS and IMPROVE, the most commonly measured soluble ions are NH_4^+ , Na^+ , Mg^{2+} , K^+ , Ca^{2+} , Cl^- , NO_3^- , and SO_4^{2-} .

Both cations and anions can be analyzed with ion chromatography (IC). IC is structurally very similar to conventional high performance liquid chromatography (HPLC) but uses different separation columns and detectors (Skoog et al., 1998). The working principle of IC is as follows. An analyte solution is injected into an eluent stream (the mobile phase) using a syringe or an autosampling valve. The eluent then flows through an ion-exchange resin column, the stationary phase where the mixed ions are separated because of their different affinities to the resin. Next, the eluent passes through an ion suppressor to reduce the background conductance of the eluent and to convert the ions of interest to their corresponding acidic or base forms. Finally, the eluent is introduced into a conductivity detector to finish the analysis. The presence of ions would cause the change in conductivity and, thus, the already separated ion species are detected by the IC as a number of discrete peaks on a chromatogram. Similar to the case of HPLC, the retention time is used for identification of ions and, thus, a chromatogram of a standard solution is needed as a reference for comparison. Quantification can be done by comparing the peak area of an ion in the unknown sample to the calibrating curve developed with standard solutions. A single IC

instrument cannot analyze cations and anions simultaneously. The analysis of cations requires a different eluent, ion-exchange resin column and ion suppressor than the analysis of anions. IC is a very sensitive analytical method. The lower detection limits are typically less than 50 µg/L, which is normally sufficient for ambient aerosol analysis (Chow and Watson, 1999).

To use IC for determining soluble ions in airborne particles, airborne particles are usually collected on Nylon and Teflon filters and then are extracted into ultra pure water (e.g., ASTM I ultra pure water) by ultrasonication. Like HPLC, IC requires the sample to be particle free, so the extracted analyte solutions must be filtered to remove suspended particles before injection. USEPA Compendium Method IO-4.2 provides a standard sampling and analysis protocol for using IC in ambient aerosol analysis (USEPA, 1999a).

Concentrations of soluble ions in ambient aerosols can provide valuable information for source apportionment and for investigation of chemical transformations in the atmosphere. A lot of studies have used IC to determine the soluble ions in ambient aerosols (Lin, 2002; Marenco et al., 2006). Cations are occasionally analyzed with other methods. NH_4^+ can be analyzed with an automated colorimeter (EPA Method 1690); while FAA, GFAA and ICP-AES can be used to analyze metal cations such as Na^+ , Mg^{2+} , K^+ and Ca^{2+} .

2.5.3 Existing results

Only a few studies have been done concerning the chemical composition of airborne particles in or from animal facilities. Lammel et al. (2004) investigated airborne particles from a livestock farm with 170 cattle, 1,200 pigs and 17,400 chickens in southern Germany. EDXRF and IC were used to determine the inorganic elements and soluble ions in collected TSP samples. Eight inorganic ions (NH_4^+ , Na^+ , Mg^{2+} , K^+ , Ca^{2+} , Cl^- , NO_3^- , and SO_4^{2-}) and 20 elements (Al, P, S, Cl, K, Ca, Ti, V, Cr, Mn, Fe, Co, Ni, Cu, Zn, As, Br, Pb, Ba, and Rb) samples were analyzed in their study. By comparing airborne particles emitted from the farm to background particles, they found the livestock farm was a source for NH_4^+ and NO_3^- but not for other elements or soluble ions. However, in their study only a few particle samples were collected. Moreover, because samplers were installed outside the animal buildings, the collected airborne particles were highly diluted with background particles and, thus, had very low concentrations. Their conclusions, therefore, are questionable. A recent study by Martin et al. (2008) was conducted in a swine finishing building in Iowa. PM_{10} and $\text{PM}_{2.5}$ samples were collected using MiniVol portable air

samplers downwind of the building. IC was used to determine soluble ions in collected particle samples. The elevated concentrations of Ca^{2+} , NH_4^+ , NO_3^- , and SO_4^{2-} were observed downwind and were explained by the particle emission from the swine building. However, no chemical speciation information was known for airborne particles in or just emitted from the swine finishing building.

2.6 Source, Health Effects and Measurement of Airborne Endotoxins and (1→3)-β-D-Glucan in Animal Confinement Buildings

Airborne particles from animal confinement buildings may contain a number of inorganic elements and soluble ions. However, most of these chemicals do not have significant health effects. The major concern is over biologically active components in those airborne particles. Among them, airborne endotoxins and (1→3)-β-D-glucans are of great interest.

2.6.1 Endotoxin

Endotoxin (lipopolysaccharide, LPS) is a cell envelope component mainly released by lysed Gram-negative bacteria, e.g., genera *Pseudomonas*, *Bacillus*, *Corynebacterium*, *Pasteurella*, *Vibrio*, and *Enterobacter* (Cox and Wathes, 1995). A LPS molecule consists of three parts: O-antigen, core polysaccharide and lipid A (Figure 2.4). Among them, lipid A is widely believed to be responsible for the toxicity of endotoxin. Lipid A comprises two glucosamine groups with several acyl chains (fatty acids) and a phosphate attached onto each group. Different Gram-negative bacteria may differ in the number, length and attachment site of acyl chains, resulting in different degrees of toxicity (Milton et al., 1992). Even for the same bacterial specie, the structure of lipid A may change when the bacteria grow at different lifetime periods or under different environmental conditions. Endotoxins are relatively heat-tolerant and can survive at 121°C for 1 h without losing their biological activity. But they can be deactivated by advanced oxidation using, e.g., Cl_2 , NH_2Cl , or KMnO_4 (Anderson et al., 2003).

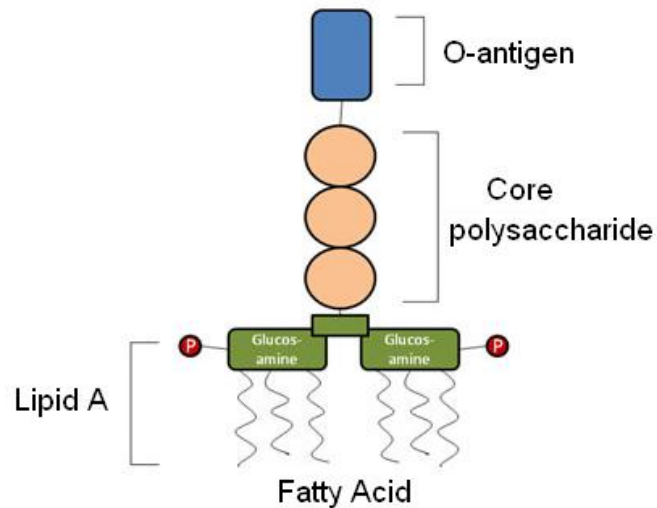


Figure 2.4. Structure of an endotoxin (LPS) molecule.
 (Photo from: http://www.glycosan.com/what_endotoxin.html)

Endotoxins are toxic to most mammal animals. Upon injection to the blood, endotoxins immediately initialize a series of immunoreactions, leading immune cells such as macrophages and endothelial cells to release pro-inflammatory cytokines. A variety of symptoms can be observed, including “fever, change in white blood cell counts, disseminated intravascular coagulation, hypotension, shock, and death” (Todar, 2008). Humans are, unfortunately, more sensitive to infection with endotoxins than most other mammals. A dose of 2 ng of *Salmonella abortus-equi* endotoxin/kg body weight can cause an increase in body temperature of 1.9°C (Anderson et al., 2002). To prevent pharmaceuticals and medical devices from endotoxin contamination, a Class II special controls guidance has been issued by the United States Food and Drug Administration (FDA) (2003).

Other than injection, inhalation of airborne endotoxins also leads to a number of symptoms, including fever, shivering, pulmonary inflammation, non-allergenic asthma, airway obstruction, and deterioration of lung functions (Kirkhorn and Garry, 2000). The adverse health effect of endotoxins can be either acute or chronic. Acute lung function impairment (e.g., decreased FVC and FEV₁), acute decrease in lung diffusion capacity and acute bronchial obstruction have been found to be highly dose-dependent among swine farm workers (Donham et al., 1989; Donham, 1990; Donham et al., 1984b; Donham et al., 1986a). Dust control by oil sprinkling was found to alleviate the acute health effects associated with endotoxins by reducing airborne endotoxin concentrations at the same time (Senthilselvan et al., 1997). Chronic bronchial obstruction and

hyperactive airways were found among swine farm workers as a result of long-term exposure to airborne endotoxins (Donham et al., 1984a). Efforts have been made to develop the exposure limit for airborne endotoxins through dose-response studies (Donham et al., 1989; Michel et al., 1997; Zock et al., 1998). The Dutch Health Council in the Netherlands has proposed an eight-hour TLV-TWA of 4.5 ng/m^3 ($\sim 50 \text{ Endotoxin Unit (EU)/m}^3$) for airborne endotoxins. Donham et al. (2000) recommended an exposure limit of 100 EU/m^3 for swine buildings and 614 EU/m^3 for poultry buildings.

Endotoxins are normally embedded into the outer membrane of Gram-negative bacterial cells and are released and become biologically active when bacteria cells are lysed or at the multiplication stage (Todar, 2008). Previous studies have revealed the ubiquitous presence of Gram-negative bacteria in airborne particles from animal confinement buildings. Martin et al. (1996) investigated bacterial and fungal flora of deposited dust in a swine finishing building. Five Gram-negative bacilli were identified, including *Acinetobacter Calcoaceticus*, *Enterobacter agglomerans*, *Pasteurella*, *Vibro*, and non-fermentative bacillus. Predicala et al. (2002) collected airborne bacterial and fungal samples in a swine finishing building in Kansas and reported the presence of genera *Pseudomonas*, *Vibro* and Gram-negative *Bacilli*. Both studies used culture based methods, with which only culturable bacterial and fungal species can be identified. To overcome this difficulty, a recent study by Nehme et al. (2008) used culture-independent molecular methods for determination of bacterial diversity and species in airborne particles from eight swine confinement buildings in Canada. Through 16S rDNA gene clone libraries analysis, they found the airborne Gram-negative bacteria mainly belonged to genera *Moraxella*, *Bacteroides* and *Pseudomonas*.

Endotoxins can be analyzed with either Limulus amoebocyte lysate (LAL) assays or GS-MS. The GS-MS method measures 3-hydroxylated fatty acids (3-OH FAs) in lipid A, a major component of LPS (Mielniczuk et al., 1993). As mentioned previously, the number and length of 3-OH FAs (acyl chains) in a LPS molecule vary with bacterial species and their growth conditions. The typical chain lengths of 3-OH FAs are C₁₀, C₁₂, C₁₄, C₁₆, and C₁₈ (Liu et al., 2000). To use GS-MS for airborne endotoxin analysis, endotoxins are first extracted from the filter samples in a hot methanolic HCl solution. Next, the products are subject to trimethylsilyl derivatization. The trimethylsilyl derivatives are then analyzed using GS/MS or GS/MS/MS (Saraf et al., 1999). Airborne endotoxin concentrations were presented in unit of ng 3-OH

FAs/m³. GC-MS have become increasingly popular in recent years (Laitinen et al., 2001; Lee et al., 2004; Liu et al., 2000). Because it measures specific chemical compounds with well-defined wet chemistry procedures and is a highly reliable instrument, the analysis results are highly replicable (Reynolds et al., 2005). This is an advantage of the GS-MS method over the LAL assay method. However, 3-OH FAs concentration is not a direct measure of toxicity of endotoxins. The toxicity in reality is often of primary interest instead of the concentration.

LAL assay method is more conventional but is still the default standard method for endotoxin analysis. Limulus amoebocyte lysate (LAL) is an aqueous solution extracted from the blood of the horseshoe crab, *Limulus polyphemus*. This animal is very sensitive to infection by Gram-negative bacteria, and once infected, blood clotting would quickly occur (Williams, 2007). There are five different types of LAL assays currently available, including gel clot LAL assay, endpoint fluorescent assay, endpoint chromogenic LAL assay, kinetic chromogenic LAL assay, and kinetic turbidimetric LAL assay. Among them, the gel clot LAL assay is the cheapest and most convenient one and is mainly used for qualitative or semi-quantitative analysis; while the other four assays are all quantitative methods. Kinetic chromogenic LAL assay has the highest sensitivity (0.005 EU/mL) and the largest detection range (0.005 to 50 EU/mL), but requires an incubating microplate reader. Endpoint chromogenic LAL assay can use a less expensive, conventional microplate reader or spectrophotometer, but has poorer sensitivity (0.1 EU/mL) and smaller detection range (0.1 to 1.0 EU/mL). Currently these two chromogenic assays are most widely used for airborne endotoxin analysis.

A chromogenic LAL assay consists of a colorless substrate and a proenzyme extracted from amoebocyte cells in the blood of horseshoe crabs. The proenzyme can be converted to an active enzyme in the presence of an endotoxin as a catalyst. The enzyme then catalyzes the dissociation of the colorless substrate into a short peptide segment (Ac-Ille-Glu-Als-Arg) and a p-nitroaniline (pNA). The pNA is a yellow organic compound that can be photometrically quantified at 405 nm with a microplate reader or a conventional spectrophotometer. The difference between kinetic and endpoint chromogenic LAL assay is as follows. In the kinetic assay, the pNA-associated color development is continuously measured at 37°C with an incubating microplate reader, and the reaction time (onset time) of an unknown sample is then compared with the reaction time of endotoxin standards to calculate the endotoxin concentration in the unknown sample. In the endpoint assay, the pNA-associated color development at 37°C is stopped after a certain time

(e.g., six minutes) by adding a stop reagent, and then the developed yellow color is measured with a conventional microplate reader or spectrophotometer and the endotoxin concentration in an unknown sample is calculated by comparing its absorbance at 405 nm to the absorbance of the standard solutions with a known endotoxin concentration.

For airborne endotoxin analysis, endotoxins must first be extracted from particles into a solution and then the solution should be diluted so as to ensure the endotoxin concentration after dilution is within the detection range of the selected assay. However, so far there is no standard protocol (Spaan et al., 2008). A guideline has been developed by the European Committee for Standardization (CEN) but fails to specify certain important experimental steps (CEN, 2000). Many experimental factors can affect the potency of endotoxins and, thus, change the measurement results. These factors include particle sampling medium, chemical reagents used for extraction, container, extraction method, chemical reagents used for dilution, and dilution ratio. The commonly used sampling media include liquid medium (used in impingers), glass fiber filter, polycarbonate filter, Teflon filter, and polyvinyl chloride (PVC) filter. Using liquid media was found to produce higher endotoxin concentration but lower variance than using PVC filters (Duchaine et al., 2001), polycarbonate filters, and glass fiber filters (Stephenson et al., 2004). Using glass fiber filters was found to yield higher endotoxin concentration than using Teflon filters (Spaan et al., 2007), and polycarbonate filters (Stephenson et al., 2004). Endotoxins are generally extracted with pyrogen-free water (PFW), Tween-20 solution (PFW-Tween), Tris-HCl solution (PFW-Tris), a mixed buffer solution of sodium dodecyl sulfate (SDS), triethylamine and potassium phosphate, or a mixed buffer solution of triethylamine and potassium phosphate (PFW-TAP). Using 0.05% Tween-20 solutions was found to improve the recover efficiency and, thus, produce higher endotoxin concentration than using PFW or PFW-Tris (Spaan et al., 2007). PFW, PFW-Tween, PFW-TAP, or PFW-SDS was previously used for dilution of endotoxin and a recent study revealed that PFW might be the best choice (Spaan et al., 2007). Agitation is often used for endotoxin extraction rather than ultrasonication. Borosilicate glass, “soft” glass or polypropylene containers are normally selected for endotoxin analysis and do not generate significantly different results (Douwes et al., 1995). Effects of different LAL assays were also evaluated and significant differences were found among different assay methods (Reynolds et al., 2002; Thorne et al., 1997). In summary, numerous uncertainties are associated with the experimental process. As a result, it is difficult to compare the results from

different studies. Many efforts have been made to develop a standard protocol in recent years (Douwes et al., 1995; Spaan et al., 2007; Spaan et al., 2008; Thorne et al., 2003). However, as Reynolds et al. (2005) claimed, LAL assays are more suitable for comparing endotoxin contaminations in similar environments. If the environmental conditions are substantially different, but still a direct comparison is desired, the GC/MS method should be considered as the first choice.

Because LAL assay methods are based on enzyme reactions, factors that promote or inhibit the activation and activity of the enzyme can strongly interfere with the analysis results (Williams, 2007). For example, (1→3)- β -D-glucans can also initiate the conversion of the proenzyme to enzyme and, hence, cause a measurement error. To identify and to overcome the possible inhibition or enhancement, a method named “the kinetic limulus assay with resistant-parallel-line estimation (KLARE)” was developed by Milton et al. (1992). This method has been used for measuring the airborne endotoxins in animal facilities (Chang et al., 2001), but was found to possibly underestimate the endotoxin concentration when the glass fiber filters were used (Thorne et al., 1997).

Numerous studies have been conducted on determination of airborne endotoxins in swine and poultry confinement buildings, as partially summarized in Table 2.3. Airborne endotoxin concentrations are generally presented in unit of endotoxin unit (EU)/m³ or ng/m³, depending on the unit (ng or EU) of the selected calibration standard. In general, 1 ng endotoxin approximately equals 10~15 EU. This can be used for a rough comparison of endotoxin test results. It can be seen from Table 2.3 that airborne endotoxin levels in both swine and poultry buildings can easily exceed the exposure limits recommended by Donham et al. (2000). As a comparison, airborne endotoxin concentrations in the urban areas are generally less than 2 EU/m³ (Madsen, 2006). Airborne endotoxins are not only detrimental to workers staying in animal buildings, but after being discharged into the atmosphere, may also cause adverse health effects on people living in neighboring communities. Elevated airborne endotoxin concentrations have been observed in the regions where animal production is intensive (Schulze et al., 2006).

Table 2.3. Summary of airborne endotoxin test results in swine and poultry buildings.

Animal type	Farm sites	Particle size	Mean endotoxin concentration	Method	Reference
Swine	n/a	Total	120 ng/m ³ (n=8)	Gel clot LAL assay	Clark et al. (1983)
Swine farrowing and nursery	The Netherlands	Total	128 ng/m ³ (n=96)	Chromogenic LAL assay	Attwood et al. (1987)
Swine finishing		D ₅₀ ≤8.5 μm	115 ng/m ³ (n=97)		
Swine	Sweden	Total	120 ng/m ³ (n=70)	n/a	Donham et al. (1989)
		D ₅₀ ≤8.5 μm	105 ng/m ³ (n=69)		
Swine	The Netherlands	Total	240 ng/m ³ (n=30)	n/a	Preller et al. (1995)
		Respirable	230 ng/m ³ (n=30)		
Swine	Iowa (Time 1)	Total	112 ng/m ³ (n=161)	Endpoint chromogenic LAL assay	Reynolds et al. (1996)
		Respirable	17.0 EU/m ³ (n=151)		
Swine	Iowa (Time 2)	Total	176.1 EU/m ³ (n=151)	KLARE assay; endpoint assay	Thorne et al. (1997)
		Respirable	11.9 EU/m ³ (n=151)		
Swine	Iowa	Total	8290 EU/m ³		
Swine sows	North Europe	Inhalable	83.5 ng/m ³ (n=44)	Kinetic turbidimetric LAL assay	Seedorf et al. (1998)
		Respirable	7.9 ng/m ³ (n=44)		
Swine weaning	North Europe	Inhalable	172.0 ng/m ³ (n=27)	Kinetic turbidimetric LAL assay	Seedorf et al. (1998)
		Respirable	18.3 ng/m ³ (n=27)		
Swine fattening	North Europe	Inhalable	122.1 ng/m ³ (n=39)	Kinetic turbidimetric LAL assay	Seedorf et al. (1998)
		Respirable	12.2 ng/m ³ (n=39)		
Swine breeding	Taiwan	Total	36.8 EU/m ³ (n=12)	KLARE assay	Chang et al. (2001)
		Respirable	14.1 EU/m ³ (n=10)		
Swine farrowing	Taiwan	Total	82.1 EU/m ³ (n=12)	KLARE assay	Chang et al. (2001)
		Respirable	48.6 EU/m ³ (n=25)		
Swine nursery	Taiwan	Total	298 EU/m ³ (n=12)	KLARE assay	Chang et al. (2001)
		Respirable	20.9 EU/m ³ (n=22)		
Swine growing	Taiwan	Total	145 EU/m ³ (n=12)	KLARE assay	Chang et al. (2001)
		Respirable	21.8 EU/m ³ (n=21)		
Swine finishing	Taiwan	Total	136 EU/m ³ (n=12)	KLARE assay	Chang et al. (2001)
		Respirable	129 EU/m ³ (n=17)		
Swine	Denmark	Total	58.0 ng/m ³ (n=40)	Kinetic chromogenic LAL assay	Radon et al. (2002)
	Germany		76.3 ng/m ³ (n=100)		
Poultry	Switzerland	Total	257.6 ng/m ³ (n=36)	Kinetic chromogenic LAL assay	Radon et al. (2002)
Poultry	n/a	Total	310 ng/m ³ (n=7)	Gel clot LAL assay	Clark et al. (1983)
Poultry/ broiler	North Carolina	Total	40 ng/m ³ (n=3)	Gel clot LAL assay	Jones et al. (1984)
		Respirable	6.0 ng/m ³ (n=3)		
Poultry/ broiler	n/a	Inhalable	3132 EU/m ³	KLARE assay	Reynolds and Milton (1993)
			4593 EU/m ³	Endpoint assay	
Poultry/ chicken brooder	n/a	Inhalable	1274 EU/m ³	KLARE assay	Reynolds and Milton (1993)
				1164 EU/m ³	
Poultry	Iowa	Total	1340 EU/m ³	KLARE assay; endpoint assay	Thorne et al. (1997)
Swine	North Europe	Inhalable	600.0 ng/m ³ (n=43)	Kinetic turbidimetric LAL assay	Seedorf et al. (1998)
		Respirable	43.8 ng/m ³ (n=43)		
Poultry/ broiler	North Europe	Inhalable	785.0 ng/m ³ (n=21)	Kinetic turbidimetric LAL assay	Seedorf et al. (1998)
		Respirable	53.5 ng/m ³ (n=21)		

2.6.2 (1→3) β-D-glucan

(1→3)-β-D-glucan is a major component of the fungal cell wall. It is also contained in the cell wall of certain bacteria and vegetable materials (Rylander, 1999). (1→3)-β-D-glucan is an insoluble D-glucose polymer linked by β (1→3) glycosidic bonds; while one of its analogs, cellulose, is linked by β (1→4) glycosidic bonds. In the fungal cell wall, the backbone of a (1→3)-β-D-glucan chain is constituted of (1→3) β-D-glucoses with many branches attached on the backbone at the (1→6) position (Figure 2.5). (1→3)-β-D-glucan is frequently used as an index for estimation of mold contamination since a direct and accurate measurement of mold is normally very difficult (Iossifova, 2006).

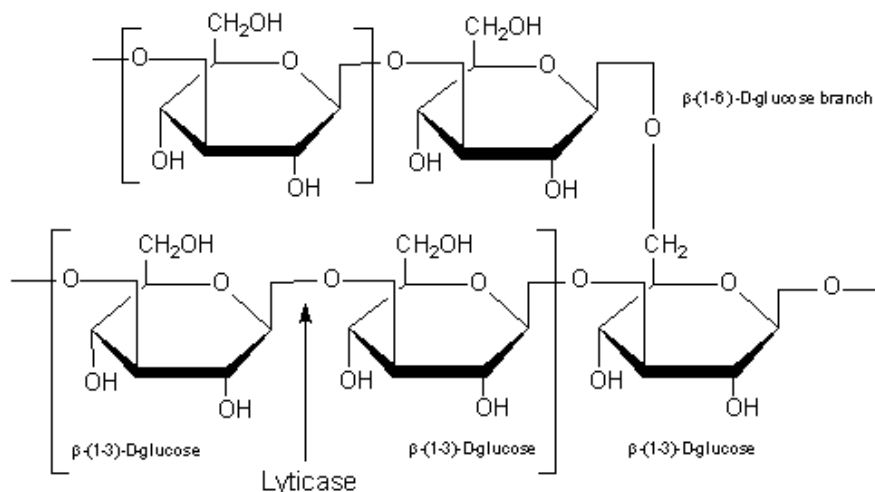


Figure 2.5. Structure of a (1→3)-β-D-glucan molecule.

(Photo from: <http://www.sigmaaldrich.com/life-science/metabolomics/enzyme-explorer/learning-center/carbohydrate-analysis.html>)

The biological activity of (1→3)-β-D-glucans is affected by their molecular weight, shape, structure and source, and is not always detrimental. Because (1→3)-β-D-glucans can activate the immune system, there are a number of potential medical applications, e.g., in therapy for cancer (Hazama et al., 2009) and prevention of infection (Defelippe et al., 1993). However, there is no evidence that airborne (1→3)-β-D-glucans are therapeutically beneficial. Exposure to airborne (1→3)-β-D-glucans is commonly believed to exert adverse effects on human health (Douwes et al., 2003). Similar to endotoxins, (1→3)-β-D-glucans are strongly inflammatory, but non-allergenic agents. Airborne (1→3)-β-D-glucans have been associated with atopy and respiratory symptoms, including non-allergic asthma, airway inflammation and deterioration of pulmonary functions from a number of field studies (Thorn et al., 1998; Wan and Li, 1999). The pro-

inflammatory potential of (1→3)-β-D-glucans has been confirmed by *in vitro* studies showing a significant increase in the cytokine release upon the injection of (1→3)-β-D-glucans into the blood (Sigsgaard et al., 1994). (1→3)-β-D-glucans and endotoxins may have synergistic effects on the secretion of cytokines (Engstad et al., 2002). However, neither official nor recommended threshold limit value is currently available due to the lack of essential dose-response data.

As mentioned previously, airborne (1→3)-β-D-glucans are primarily released by fungi. The temperature and humidity in animal confinement buildings are normally relatively high, which is suitable for the growth of many fungal species. Martin et al. (1996) reported the presence of fungal genera *Absidia*, *Alternaria*, *Cladosporium*, *Penicillium*, *Rhizopus*, and *Scopulariopsis* in a swine finishing building in Canada. Fungal genera *Aspergillus*, *Penicillium*, and *Mucor* were observed by Seedorf et al. (1998) in animal buildings in four European countries. Predicala et al. (2002) found the existence of fungal genus *Penicillium* in airborne particles collected in a swine finishing building in Kansas. All those studies used culture based methods and, thus, failed to consider non-culturable fungal species. In fact, the majority of airborne fungal spores are non-culturable (Rylander and Etzel, 1999). Even so, the culturable airborne fungal concentrations in animal buildings can be up to 10,000 CFU/m³ in poultry buildings (Seedorf et al., 1998).

There are two methods currently available for (1→3)-β-D-glucan analysis: inhibition enzyme immunoassay (EIA) and LAL assay (Rylander, 1999). But unfortunately, so far there is no standard protocol available for airborne (1→3)-β-D-glucan analysis.

EIA method was developed by Douwes et al. (1996) and is basically a competitive enzyme linked immunosorbent assay (ELISA) method with (1→3)-β-D-glucan as the antigen. In this method, a glucan conjugate solution is injected into animals, e.g., rabbits, to create the anti-β (1→3)-glucan antibodies in the blood and then the antibodies are extracted and purified for detection purposes. As an ELISA method, EIA requires a primary and a secondary antibody, prepared with different animals. The secondary antibodies are conjugated with peroxidase enzymes. A simple analysis procedure is described as follows: (1) BSA (bovine serum albumin)-laminarin conjugates are used to coat the microplate well surface; (2) the primary antibodies and sample solutions are added into the wells; (3) the microplate is incubated for a certain time to let antibodies and antigens ((1→3)-β-D-glucans in the sample) to bond together; (4) the microplate is washed to remove the unbounded primary antibodies; (5) the secondary peroxidase-labeled

antibodies are added and then compete with the primary antibodies to form antigen-antibody conjugates; (6) the microplate is washed to remove free antibodies; (7) a solution containing *o*-phenylenediamine ($C_6H_4(NH_2)_2$) and peroxide (H_2O_2) is added; (8) the remaining peroxidase enzymes catalyze the decomposition of H_2O_2 molecules, and during this process, *o*-phenylenediamine is oxidized to *o*-nitroaniline, an orange-colored compound; and (9) the enzyme reaction is stopped and the optical density is measured at 492 nm. The more (1→3)-β-D-glucans exist in the sample, the more secondary antibodies remain after Step 6. This means the optical density at 492 nm is positively related to the concentration of (1→3) β-D-glucans. The EIA method has been used to measure concentrations of (1→3)-β-D-glucans in occupational and home environments (Douwes et al., 2000; Wouters et al., 2006). However, one disadvantage of the EIA method lies in its limited sensitivity. The lower detection limit of the EIA method is 40 ng/mL. To ensure the (1→3)-β-D-glucan concentration in the extract is greater than the detection limit, preparation of 1 mL extract requires 25 mg particles according to Iossifova (2006). But in reality, it is very difficult to collect sufficient airborne particles required by the EIA test.

LAL assay method for (1→3)-β-D-glucan analysis is very similar to that for endotoxin analysis. The only difference is that instead of the activating factor C, the activating factor G is used in the LAL assay for (1→3)-β-D-glucan test. Only (1→3)-β-D-glucans can activate factor G and, thereby, initiate the enzyme-catalyzed color or turbidity yielding process (Douwes, 2005). Kinetic chromogenic LAL assay is often employed because of its large detection range and high sensitivity (1 pg/mL) (Iossifova, 2006). The mechanism of the LAL assay and the associated experimental procedure are very similar to those for endotoxin analysis and, hence, will not be repeated in this section. LAL assay is a very popular method for (1→3)-β-D-glucan analysis. Compared to the EIA method, LAL assay is more sensitive, accurate and specific and does not require an automatic microplate washer (Iossifova, 2006). LAL assay has been extensively used for determination of airborne (1→3)-β-D-glucan in occupational and indoor environments (Gladding et al., 2003; Rylander and Carvalheiro, 2006).

Only a few studies have been reported on measuring airborne (1→3)-β-D-glucans in animal confinement buildings. Douwas et al. (1996) collected inhalable airborne particles in swine buildings and then determined the (1→3)-β-D-glucan concentration with the EIA method. A geometric mean concentration of $4.3 \mu\text{g}/\text{m}^3$ was reported. Rylander and Carvalheiro (2006) investigated the personal exposure of poultry farm workers to bioaerosols in the southern

Sweden. Total airborne particles were collected on filters with personal samplers. An endpoint LAL assay was used to determine the (1→3)-β-D-glucan concentration. It was found that in poultry buildings the concentrations of water insoluble (1→3)-β-D-glucans ranged from 4 to 870 ng/m³, with a mean value of 270 ng/m³. Sander et al. (2008) recently measured airborne (1→3)-β-D-glucan concentrations in poultry and swine buildings in Germany using a novel two-site enzyme immunoassay and reported the concentration ranged from 2 to 972 ng/m³ in the poultry buildings and from 33 to 410 ng/m³ in the swine buildings. However, the quantity of existing data and the scale of previous measurements are very limited. A comprehensive measurement database is desperately needed in order to improve our understanding of the potential risk of exposure to airborne (1→3)-β-D-glucans in animal confinement buildings.

3. MASS CONCENTRATIONS OF TSP, PM₁₀ AND PM_{2.5} EMITTED FROM SWINE AND POULTRY CONFINEMENT BUILDINGS

3.1 Introduction

Particulate matter (PM) emitted from animal confinement buildings has become an environmental concern because of their potential adverse effects on human health and environment (NAS, 2003). Although nationwide animal production is only a minor source of PM, it can be a major contributor in the areas where animal production is concentrated. PM from animal confinement buildings may have significantly different properties than urban aerosols, and may carry toxic, allergenic, pathogenic and carcinogenic components (Douwes et al., 2003; Kirkhorn and Garry, 2000; Schenker et al., 1998). Development of relevant regulations, therefore, requires a profound understanding of potential environmental and health effects, and a comprehensive exposure and emission database.

Particles size is one of the most important physical characteristics related to the environmental and health effects of PM. Fine particles, e.g., PM_{2.5}, have a relatively long retention time in the atmosphere, and can penetrate into the gas exchange region of the lung (Brunekreef and Holgate, 2002). As a result, size selective particle sampling has become of great importance and interest. Previous size selective sampling in animal confinement buildings focused on assessment of personal exposure to indoor PM, in which the ACGIH recommended inhalable, thoracic, and inhalable samplers were widely employed (Donham et al., 1986b; Maghirang et al., 1997; Seedorf, 2004; Takai et al., 1998). In recent years, much attention has been paid to the impacts of PM emissions from animal confinement buildings on ambient air quality. As PM₁₀ and PM_{2.5} are regulated by the National Ambient Air Quality Standards (NAAQS), the emission measurements of PM₁₀ and PM_{2.5} have become a major interest (Burns et al., 2008; Costa et al., 2007; Lim et al., 2003; Roumeliotis and Van Heyst, 2007). Although total suspended particulate matter (TSP) has been no longer regulated by the NAAQS, TSP concentration is still informative and valuable since most airborne particles in and from animal confinement buildings are larger than 10 μm (Donham et al., 1986b; Lee, 2009; Redwine et al., 2002). Accordingly, TSP monitoring still received considerable attention (Lacey et al., 2003; Lim et al., 2003). PM concentrations were mainly used for calculation of emission factors (Burns

et al., 2008; Costa et al., 2007; Lim et al., 2003), which were correlated with environmental and operational parameters to determine major affecting factors (Costa and Guarino, 2009; Jacobson et al., 2005; Roumeliotis and Van Heyst, 2007). However, most previous investigations of PM concentrations were conducted on only one to a few farms. There is a need to monitor and to compare PM concentrations from different types of animal confinement buildings.

A variety of PM samplers have been used for collection and/or monitoring of PM emitted from animal confinement buildings such as Anderson multi-stage impactor (Donham et al., 1986b), tapered element oscillating microbalance (TEOM) (Burns et al., 2008; Jacobson et al., 2005; Lim et al., 2003), beta gauge (Heber et al., 2008) and DustTrak aerosol monitors (Roumeliotis and Van Heyst, 2007). Many of them were originally designed for ambient air quality or industrial hygiene studies. Unexpected difficulties, e.g., sampler overloading, may occur when these instruments are being used in animal confinement buildings (Mcclure, 2009). Some previous studies reported that federal reference method/ federal equivalent method (FRM/ FEM) PM samplers might significantly overestimate PM₁₀ and PM_{2.5} concentrations from animal facilities and other agricultural sources (Buser et al., 2007a; Buser, 2004; Buser et al., 2008; Wang et al., 2005a; Wang et al., 2005b). To overcome this limitation, an alternative method was proposed and has been increasingly practiced in agricultural air quality studies, which basically calculates PM₁₀ and PM_{2.5} concentrations from the particle size distribution (PSD) and the mass concentration of a collected TSP sample (Buser et al., 2008; Cao et al., 2009; Jerez, 2007; Wang et al., 2005a; Wanjura et al., 2005). However, the validity of this method has not been fully assessed due to a lack of essential experimental data. A systematic evaluation of this method is therefore needed.

Chemical and biological characteristics of PM from animal confinement buildings have recently received particular attention (Cai et al., 2006; Cambra-Lopez et al., 2010; Nehme et al., 2008) because they are closely related to adverse effects of PM. Some tests, e.g., particle-bonded odorants and microorganisms, require fresh filter samples so as to minimize possible changes in PM compositions during filter conditioning. This may cause a misestimation of collected PM mass, and subsequently generate unexpected errors for quantitative chemical and biological analysis. It is therefore of importance to investigate a change in the mass of PM samples before and after filter conditioning and to determine whether the induced errors are substantial, which to our knowledge have not been done to date.

Specific objectives of this chapter were as follows:

- To determine TSP, PM₁₀ and PM_{2.5} mass concentrations in eighteen animal confinement buildings under different environmental and operational conditions;
- To investigate variations in PM concentrations with environmental and operational parameters, and to determine the major affecting factors;
- To compare measured PM₁₀ and PM_{2.5} mass concentrations with the values calculated from TSP mass concentrations and PSD data.
- To evaluate effects of filter conditioning on measured PM mass concentrations.

3.2 Materials and Methods

3.2.1 Particle sampling

3.2.1.1 Sampling sites

A total of eighteen animal confinement buildings in Illinois and Indiana were selected, including twelve swine and six poultry buildings (Table 3.1). These buildings belong to six different animal building types. All of them, except for tom turkey, were mechanically ventilated animal buildings.

Table 3.1. Sampling sites for PM collection.

Animal type	Building Type	State ^a	# of buildings
Swine	Gestation	Illinois	3
	Farrowing	Illinois	3
	Weaning	Illinois	3
	Finishing	Illinois	3
Poultry	Layer hens ^b	Illinois and Indiana	3
	Tom turkey	Illinois	3
Total			18

a. Specific locations of those farms are confidential according to an agreement with farm owners.

b. All layer hens buildings were manure belt type.

Each building was visited three times in different seasons: cold, mild and hot. The definition of cold, mild and hot seasons in this study was based on the daily average ambient temperature (T_{mean}) during the sampling period: cold ($T_{\text{mean}} \leq 5 \text{ }^\circ\text{C}$), mild ($5 \text{ }^\circ\text{C} < T_{\text{mean}} \leq 20 \text{ }^\circ\text{C}$) and hot ($T_{\text{mean}} > 20 \text{ }^\circ\text{C}$). Although there were a few exceptions, the bottom-line was to ensure that a significant temperature difference was present between hot, mild and cold weather seasons for each sampling site. Ambient temperature data from the nearest weather stations were selected for classification, so as to avoid the potential “hot island” effect caused by animal buildings. Field

measurement data for indoor and outdoor temperature and humidity were also available. Detailed farm information and field trip records could be found in Appendix A and B.

3.2.1.2 Sampling equipment and materials

A multi-point TSP sampling system (Wang, 2000) was used for TSP collection. This system consisted of a vacuum pump, polyethylene tubing's and six TSP samplers (Figure 3.1); while each sampler consisted of a UIUC TSP nozzle, a 37 mm polycarbonate filter cassette, a venturi orifice and essential tubing's and adaptors. The UIUC TSP nozzle was developed specifically for isokinetic sampling at a constant airflow rate. Two different designs of UIUC TSP nozzles were used in this study, depending on the incoming airflow velocity. Each nozzle was assembled with a 37 mm polycarbonate filter cassette. Following the cassette, a venturi orifice, developed by Wang and Zhang (1999), was used to control the sampling airflow rate at approximately 20 liter per minute (LPM) with relatively low pressure drop. The accurate flow rate was determined through calibration of venturi orifices in the lab (please refer to Appendix H), and used for calculating the actual volume of sampled air. TSP samplers were installed upstream of a continuous-running exhaust fan and their installation positions were determined according to the velocity and direction of incoming airflow, but typically 0.2-0.4 m from the fan face and 1.2-1.4 m in height. In tom turkey buildings, since they were all naturally ventilated, a calm-air particle sampling protocol was employed (Zhang 2005). In this case, no TSP nozzle was used and an open-faced filter cassette was positioned horizontally toward the exhaust air and installed near a downwind end door.

Harvard impactors (Air Diagnostic and Engineering Inc, Harrison, ME), also named MS&T impactors, were used for collection of PM₁₀ and PM_{2.5} samples (Figure 3.2). Harvard impactors were originally developed by researchers in the School of Public Health at Harvard University to collect airborne PM in indoor and occupational environments for exposure assessment; however, they have also been extensively used for collection of ambient aerosols (Cyrus et al., 2003; Martuzevicius et al., 2004). Although Harvard impactors are not EPA designate FRM or FEM samplers, they have been found to have comparable performance with FRM and FEM samplers during both lab tests and field measurements (Babich et al., 2000; Demokritou et al., 2004; Turner et al., 2000). Size separation with Harvard impactors is achieved based on the principle of impaction. The size separator in a Harvard impactor consists of a single round nozzle and an

impacting plate rinsed with mineral or silicon oil. Following the size separation unit, an Anderson filter cassette is used to hold a 37 mm filter air-tightly. The impactor inlet is a slatted aluminum cylinder, and an additional rain hat is available for outdoor sampling. The sampling flow rate was controlled at approximately 20 LPM using a venturi orifice. Harvard impactor was installed with spacing typically of 0.6-1.0 m from the fan face or end door. The installation height was normally 1.2-1.4 m.

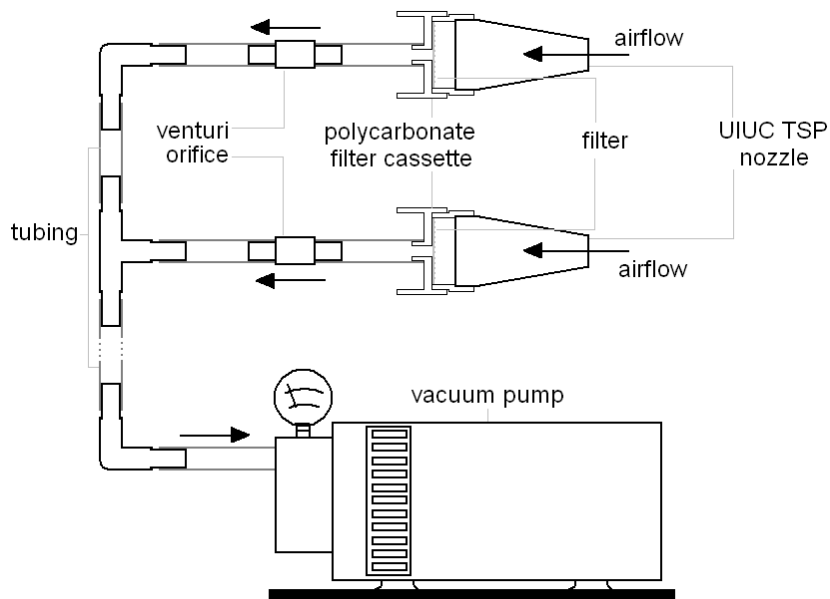


Figure 3.1. Schematic of a multi-point TSP sampling system.

There are a couple of reasons why Harvard impactors were selected in this study. First, as previously mentioned, Harvard impactors have comparable performance with the FRMs and FEMs. Second, Harvard impactors, around \$900 per unit, are much less expensive than FRM and FEM samplers; as a comparison, an FRM PM₁₀ inlet only is over \$1,000. This allows the use of multiple samplers without exceeding the budget cap. Third, Harvard impactors are light and portable. Each unit is less than two pounds in weight, easily transported from farm to farm. Fourth, installation of Harvard impactors is relatively simple, which can reduce the setup time in animal barns and consequently can minimize potential disturbances to animals. Fifth, Harvard impactors allow a high volume sampling with the maximum sampling flow rate of 20 LPM. This is particularly important because a high mass loading of PM was desired by parts of chemical and biological analyses in this study. Besides, a constant flow rate of 20 LPM can be achieved with venturi orifices, which can effectively simplify the sampling system.

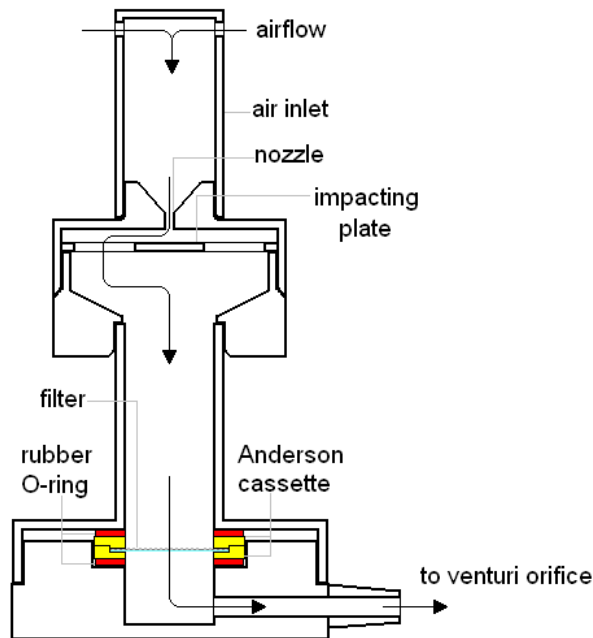


Figure 3.2. Schematic of a Harvard impactor.

Totally seven TSP, three PM₁₀ and two PM_{2.5} samples were collected from each field trip (Table 3.2). Four different types of filters were selected depending on the purpose of analysis, including glass fiber filter (Type A/E, P/N 61652, Pall Corporation, Ann Arbor, MI), Teflon filter (Zefluor™ PTFE member filter w/ support pads, P/N P5RJ037, Pall Corporation, Ann Arbor, MI), ringed Teflon filter (Teflo™ w/ ring PTFE member filter, P/N R2PJ037, Pall Corporation, Ann Arbor, MI), and polycarbonate filter (ISOPORE™ membrane filter, GTTP03700, Millipore Corporation, Billerica, MA). All samples except TSP5 were used for determination of PM mass concentrations.

Table 3.2. List of samplers and filters in current study.

Sampler	Filter	Purpose	Named with
PM1 (PM ₁₀)	Ringed Teflon	Mass and elements	mmddyEL10
PM2 (PM ₁₀)	Ringed Teflon	Mass, ions and endotoxin	mmddyION10
PM3 (PM ₁₀)	Glass fiber	VOC's	mmddyOC1
PM4 (PM _{2.5})	Ringed Teflon	Mass and elements	mmddyEL25
PM5 (PM _{2.5})	Ringed Teflon	Mass, ions and endotoxin	mmddyION25
TSP1	Glass fiber	Mass and VOC's	mmddyOC2
TSP2	Glass fiber	Mass and microbe	mmddyMA
TSP3	Glass fiber	Mass and endotoxin	mmddyEN
TSP4	Glass fiber	Mass and Backup	mmddyBK
TSP5	Polycarbonate	Morphology	mmddySEM
TSP6	Teflon	Mass and PSD	mmddyPSD1
TSP7	Teflon	Mass and PSD	mmddyPSD2

3.2.1.3 Sampling procedure and setup

Filters and support pads were pre-conditioned in desiccators (relative humidity [RH] \leq 30 %) at room temperature (around 22 °C) for 24 for 48 hours, and then weighed on an analytical balance (Model Ag245, Mettler Toledo, Greifensee, Switzerland). After pre-weighing, filters were loaded into polycarbonate filter cassettes and Anderson cassettes. Polycarbonate cassettes were then sealed with plastic caps; while Anderson cassettes were either loaded into Harvard impactors sealed with aluminum foils or stored in 50 mm sterile Petri dishes (NC9074091, Fisher Scientific Inc., Franklin, MA).

Sampler assembling and installation were performed upon arrival at a farm. The UIUC TSP nozzles were installed on a wood or steel frame upstream of an exhaust fan (Figure 3.3) that ran continuously through the whole sampling period. Airflow velocity and direction were measured with a hotwire anemometer, and positions and orientations of TSP nozzles were determined accordingly. Harvard impactors were installed on a table before the same exhaust fan with a distance of at least 0.3 m, so as to avoid excessively high air velocities that might affect the sampler performance. Overloading of Harvard PM₁₀ and PM_{2.5} impactors were found when animal buildings were extremely dusty, which mostly happened during the winter. To overcome such a problem, a time relay was used to run vacuum pumps intermittently during sampling, thereby reducing the total volume of sampled air. Additionally, for PM_{2.5} sampling, a pre-separator was placed upstream of each PM_{2.5} impactor to remove particles larger than 10 μ m from influent air. Each field sampling lasted for 20 to 24 hours. Environmental and operational conditions, such as indoor and outdoor temperature and humidity, were measured and/or recorded during sampling, and so did building information such as number of animals, average weight, building size and ventilation fans.

After sampling was done, polycarbonate cassettes were disassembled from TSP samplers and re-sealed with plastic caps; while Harvard impactors were re-sealed with parafilms and aluminum foils for avoiding possible contaminations during transportation. Upon arrival at the laboratory, filters were immediately moved out from cassettes and weighed on the analytical balance. After that, parts of filters were post-conditioned in desiccators for 24 to 36 hours and weighed again.



Figure 3.3. Sampling setup in an animal building.

3.2.2 Determination of PM concentrations

Mass concentrations were calculated with Equation 3.1, where C_p is mass concentration of airborne particles (mg/m^3), M_t is the mass of a filter with collected particles (mg), M_0 is the mass of that filter before sampling (mg), Q_s is the sampling flow rate (m^3/h), t_s is the sampling duration time (h), T_{std} is the standard temperature (273.2 K), T_s is the indoor temperature during sampling (K), P_s is the indoor barometric pressure (kPa), and P_{std} is the standard barometric pressure (101.325 kPa). However, only maximum indoor temperature was monitored in this study due to lack of essential equipment. A compromise was made accordingly by assuming T_s to be 293.2 K (20 °C), a typical set point temperature for animal barns. Static pressure was not monitored either but generally was less than 0.2 inch water. Therefore, P_s would approximately equal to ambient atmospheric pressure available from local weather stations. Mean PM mass concentrations were averaged from multiple filters that collected the same size of particles, and standard deviations were calculated correspondingly.

$$C_p = \frac{M_t - M_0}{Q_s \times t_s} \times \frac{T_{\text{std}}}{T_s} \times \frac{P_s}{P_{\text{std}}} \quad (3.1)$$

3.2.3 Investigation of variations and affecting factors

Mass concentrations of TSP, PM_{10} and $\text{PM}_{2.5}$ were found to be affected by numerous environmental and operational factors, such as animal type, season, ventilation rate, air velocity, moisture, animal activity, feed system and building cleanliness (Heber et al., 1988b). Many of them were measured and recorded in this study. Accordingly, investigation of variations and affecting factors were conducted by correlating PM concentrations to these factors via statistical

analysis. A brief procedure was shown in Figure 3.4. Other than concentrations, PM mass ratios, e.g., PM_{10}/TSP , were also subject to statistical analysis.

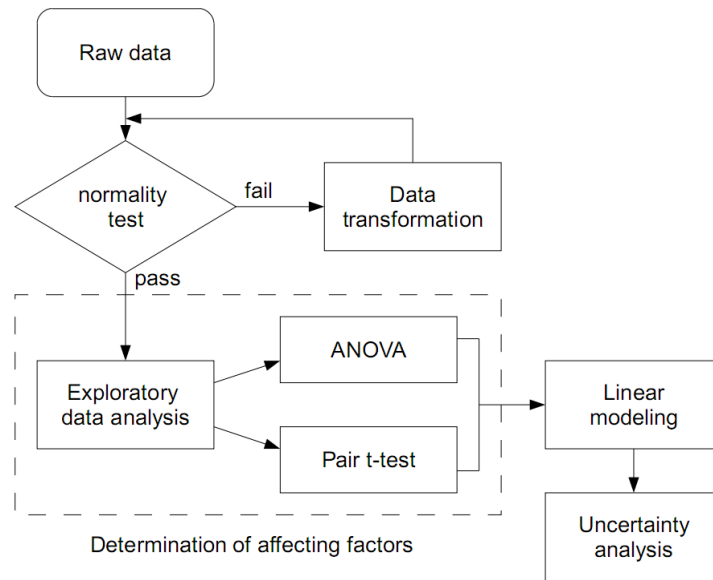


Figure 3.4. Flowchart for statistical analysis on PM concentrations.

- Normality test. The Shapiro-Wilk and Jarque-Bera tests were used to examine normality of data. The null hypothesis of both tests is that a sample population is normally distributed, and this hypothesis is rejected when the calculated p-value is less than the selected level, mostly 0.05. Therefore, a population is not necessarily normally distributed even if it passes these two tests. The p-value is dependent on not only the Shapiro-Wilk value (W) or Jarque-Bera value (JB) but also the size of population (N). Consequently, W and JB values only cannot be used for determine if a population departs from normal distribution. Both the Shapiro-Wilk and Jarque-Bera tests were performed in MATLAB in this study.
- Data transformation. Raw data were transformed into their log forms if they failed in the normality test.
- Exploratory data analysis (EDA). Tools used for EDA included box plots, histograms and scatter plots. The purpose was to determine potential affecting factors and to select appropriate statistical techniques for following data analysis.
- Analysis of variance (ANOVA). ANOVA was employed to determine if there was significant difference in mean PM concentrations with an environmental or operational

factor, e.g., animal type, so that the affecting factors could be identified. One-way ANOVA tests were performed in R (an open-source statistical package) with the Tukey method that did multiple pairwise comparisons among mean PM concentrations of all groups. If the p-value from the Tukey test was less than 0.05, a significant difference was considered to exist between mean PM concentrations from two groups. Multi-way ANOVA tests were also performed in R to identify and quantify sources of variations from potential affecting factors.

- Paired t-test. ANOVA tests performed poorly at the presence of confounding factors and high variances. To overcome this limitation, paired t-tests were performed as a complementary method that compared differences between paired samples. The hypothesis is that no significant difference exists, i.e., the mean difference equals zero. Paired t-test in general is more powerful than ANOVA but requires the data to be paired or matched.
- Linear modeling. A generalized linear model was established to simulate and predict PM concentrations in animal confinement buildings with factors identified by ANOVA and paired t-tests. The model was then simplified with variable selection methods, such as Akaike's Information Criterion (AIC), to reduce the number of predictors, and the significance of each predictor was determined. Regression diagnostics were performed to check error assumptions, model structure and unusual observations. Alternative statistical algorithms, such as weighted least squares, were used if certain problems were present.
- Uncertainty analysis. A propagation-of-error equation was derived based on the developed linear model. Standard deviations of model predictors were either computed or estimated, and were then combined with sensitivity coefficients to calculate the standard uncertainty of the model output, in this case, PM concentrations. The same procedure also applied to the calculation of PM mass concentrations (Equation 3.1).

Prior to statistical analysis, environmental and operational parameters were factorized. Those, assessed on a nominal (e.g., animal building types) or an ordinal scale (e.g., seasons), were treated as dummy variables in linear modeling.

In reality, a major challenge to statistical analysis in this study was that many potential affecting factors, such as building cleanliness, were difficult to be characterized, quantified and factorized. These factors therefore were failed to be considered in linear modeling, which would inevitably cause uncertainties and undermine the predictive power.

3.2.4 Validity of calculating PM_{10} and $PM_{2.5}$ concentrations from PSD data and TSP concentrations

In some previous studies, PM_{10} and $PM_{2.5}$ mass concentrations were calculated from measured TSP concentrations and PSD data (Buser et al., 2008; Cao et al., 2009; Jerez, 2007; Wang et al., 2005a; Wanjura et al., 2005). This method inevitably introduced certain errors that have not been fully examined. In this study, TSP, PM_{10} and $PM_{2.5}$ mass concentrations were gravimetrically determined; while the PSD data for TSP samples were available from a concurrent study conducted by Lee (2009). An experimental evaluation of such an indirect calculation method hence became plausible. A brief procedure was shown in Figure 3.5.

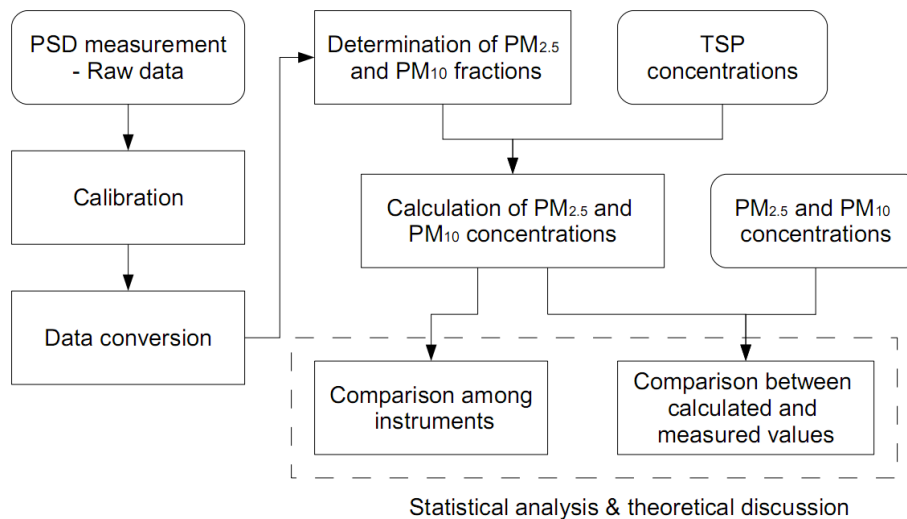


Figure 3.5. Process flowchart for examining the validity of indirect calculation method.

3.2.4.1 PSD measurement and calibration of raw data

Four state-of-the-art particle size analyzers were used to determine the size distribution of PM samples collected in most animal buildings: a Coulter Counter Multisizer (Beckman Coulter Inc., Fullerton, CA), a Horiba LA-300 particle sizer (Horiba Group, Edison, NJ), a Malvern Mastersizer (Worcestershire, UK), and an aerosizer DSP (TSI Inc., St. Paul, MN). An exception

was in swine weaning buildings only Horiba was used for PSD measurements. A simple comparison of those instruments was shown in Table 3.3. Among them, DSP provides in-field real-time measurements of PSD; while the other three analyzers require PM samples to be first collected on Teflon filters and then dispersed in liquid media prior to instrumental analysis. Detailed experimental procedures can be found from Lee (2009). A correction of the raw PSD data were performed with the calibration curves generated from mono-dispersed spherical particles with known size.

Table 3.3. Comparison of particle size analyzers used in this study.

Instrument	Horiba	DSP	Coulter	Malvern
Number of datasets	83	44	45	45
Detection principle	Mie scattering	Time of flight	Electrical Impedance	Mie scattering
Measured diameter	Equivalent volumetric	Aerodynamic	Equivalent volumetric	Equivalent volumetric
Detection range (μm)	0.1 to 600	0.3 to 700	0.4 to 1200	0.02 to 2000
Number of channels	64	100	300	100

3.2.4.2 Conversion of PSD data

Because the definitions of $\text{PM}_{2.5}$ and PM_{10} were based on aerodynamic diameter, the PSD data derived from Horiba, Coulter Counter and Malvern particle sizers were first converted to aerodynamic diameters with Equation 3.2 and 3.3:

$$d_a = d_e \left(\frac{C_{ce} \rho_p}{C_{ca} \rho_0 \chi} \right)^{\frac{1}{2}} \quad (3.2)$$

(For non-spherical particles, $d_e \geq 3 \mu\text{m}$)

$$d_a = \frac{1}{2} \left[\left(6.35 \lambda^2 + 4 d_e^2 \frac{C_{ce} \rho_p}{C_{ca} \rho_0 \chi} \right)^{\frac{1}{2}} - 2.52 \lambda \right] \quad (3.3)$$

(For non-spherical particles, $0.1 \mu\text{m} < d_e < 3 \mu\text{m}$)

where, d_a is the aerodynamic diameter, d_e is the equivalent volume diameter, C_{ce} and C_{ca} are slip correction factors for d_a and d_e , χ is the shape factor, ρ_0 is the unit density (1000 kg/m^3), ρ_p is the “true” particle density and λ is the mean free path of the air ($0.066 \mu\text{m}$ at 101.325 kPa and $20 \text{ }^\circ\text{C}$). Among them, χ and ρ_p were both unknown and needed to be either determined or estimated prior to conversion. Because of a lack of knowledge of particle shape, the shape factor (χ) was commonly assumed to be 1.0 in previous studies (Jerez, 2007; Lacey et al., 2003). The same

assumption was adopted in this study. The true density of particles (ρ_p) was measured in the lab with a pycnometer (AccuPyc II 1340, Micromeritics Instrument Cop., Norcross, GA). However, this equipment requires the volume of test samples to be at least 0.5 mL. This means no less than 200 mg PM samples need to be collected, which is extremely difficult in practice. The settled dust in animal buildings therefore was selected as a surrogate and was assumed to have the same density as PM samples. Details about the procedures of sample collection and density test can be found in Appendix E. After this conversion, all PSD data were presented in terms of aerodynamic diameters.

3.2.4.3 Calculation of PM_{10} and $PM_{2.5}$ mass fractions and concentrations

Calculation of PM_{10} and $PM_{2.5}$ mass concentrations were based on Equation 3.4. Basically, PM_{10} (or $PM_{2.5}$) mass concentration ($C_{PM_{10}(PM_{2.5})}$) equals to the mass fraction of PM_{10} (or $PM_{2.5}$) in a TSP sample multiplied by TSP mass concentration (C_{TSP}). Therefore, a central step was to determine the mass fraction of PM_{10} (or $PM_{2.5}$) from measured PSD data.

$$C_{PM_{10}(PM_{2.5})} = C_{TSP} \times \frac{C_{PM_{10}(PM_{2.5})}}{C_{TSP}} \quad (3.4)$$

Different approaches were used in previous studies for determining the mass fraction of PM_{10} (or $PM_{2.5}$) on a PSD profile, as summarized in Table 3.4 and illustrated in Figure 3.6. The third approach had certain limitations because the linear regression method could significantly misestimate MMD (mass median diameter) and GSD (geometric standard deviation) when a PSD profile was not lognormally distributed. Detailed discussions on the lognormality of PSD data from animal confinement buildings can be found in Appendix F. In this study, two approaches were selected for calculation of PM mass fraction. The first one (approach A) was the same as the first approach in Table 3.4, in which a PSD profile was partitioned into two parts at 10 μm (or 2.5 μm) and the collection of smaller particles was considered to be PM_{10} (or $PM_{2.5}$). The second one (approach B) was similar to the second approach in Table 3.4; however, a major difference was the penetration curve of ideal PM_{10} (or $PM_{2.5}$) samplers would be used in this study.

Table 3.4. Approaches to determining the mass fractions of PM₁₀ and PM_{2.5} in a TSP sample.

#	Approach	References
1 ^a	PM ₁₀ (PM _{2.5}) was the fraction of particles with aerodynamic diameters no greater than 10 μm (2.5 μm) on the PSD profile of a TSP sample.	Buser et al. (2008); Cao et al. (2009); Jerez (2007); Wang et al. (2005a); Wang et al. (2005b); Wanjura et al. (2005).
2 ^b	PM ₁₀ fractions were estimated from the PSD profile and the sampler's penetration curve. The latter was either calculated from the PSD profiles of TSP and PM ₁₀ or assumed by researchers.	Buser et al. (2008); Wang et al. (2005a); Wang et al. (2005b); Wanjura et al. (2005).
3	A lognormal PSD profile was obtained from linear regression of raw PSD data. PM ₁₀ (PM _{2.5}) was the fraction of particles with aerodynamic diameters smaller than 10 μm (2.5 μm) on the regressed PSD profile.	Cao et al. (2009)
A	It is the same as the 1 st approach	This study
B	It is similar to the 2 nd approach but uses the penetration curves of ideal PM ₁₀ and PM _{2.5} samplers specified by the USEPA	This study

- a. The obtained fraction was defined by the authors as the “true” ratio.
 b. The derived fraction was defined by the authors as the “measured” ratio.

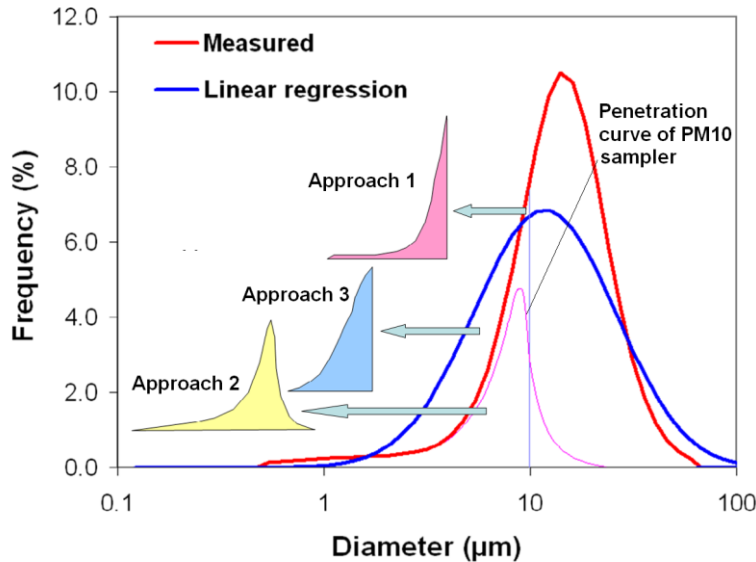


Figure 3.6. Approaches to determining PM₁₀ mass fraction on a PSD profile.

The penetration curves of ideal PM₁₀ and PM_{2.5} samplers were specified by the USEPA (CFR, 1987; CFR, 1997) as administrative standards for evaluating the performance of candidate FRM/ FEM PM samplers. Accordingly, an FRM/ FEM PM sampler, when properly operated, is suppose to work with a penetration curve very similar to the corresponding ideal PM sampler. Unfortunately, the specific penetration curve of an FRM/ FEM PM sampler is often unknown. Ideal PM samplers therefore were selected in this study to simulate size selective sampling by FRM/ FEM PM samplers. The penetration curves of ideal PM₁₀ and PM_{2.5} samplers were shown in Table 3.5 and 3.6, respectively.

Table 3.5. Penetration curve of an ideal PM₁₀ sampler (CFR, 1987).

Diameter (μm)	Collection efficiency	Diameter (μm)	Collection efficiency	Diameter (μm)	Collection efficiency
0.1	1.000	7.0	0.759	16.0	0.000
1.0	1.000	7.5	0.729	17.0	0.000
1.5	0.949	8.0	0.697	18.0	0.000
2.0	0.942	8.5	0.664	20.0	0.000
2.5	0.933	9.0	0.628	22.0	0.000
3.0	0.922	9.5	0.590	24.0	0.000
3.5	0.909	10.0	0.551	26.0	0.000
4.0	0.893	10.5	0.509	28.0	0.000
4.5	0.876	11.0	0.465	30.0	0.000
5.0	0.857	12.0	0.371	35.0	0.000
5.5	0.835	13.0	0.269	40.0	0.000
6.0	0.812	14.0	0.159	45.0	0.000
6.5	0.786	15.0	0.041		

Table 3.6. Penetration curve of an ideal PM_{2.5} sampler (CFR, 1997).

Diameter (μm)	Collection efficiency	Diameter (μm)	Collection efficiency	Diameter (μm)	Collection efficiency
0.100	1.000	2.250	0.707	4.125	0.000
0.500	1.000	2.375	0.602	4.250	0.000
0.625	0.999	2.500	0.480	4.375	0.000
0.750	0.998	2.625	0.351	4.500	0.000
0.875	0.997	2.750	0.230	4.625	0.000
1.000	0.995	2.875	0.133	4.750	0.000
1.125	0.991	3.000	0.067	4.875	0.000
1.250	0.987	3.125	0.030	5.000	0.000
1.375	0.980	3.250	0.012	5.125	0.000
1.500	0.969	3.375	0.004	5.250	0.000
1.675	0.954	3.500	0.001	5.375	0.000
1.750	0.932	3.625	0.000	5.500	0.000
1.875	0.899	3.750	0.000	5.625	0.000
2.000	0.854	3.875	0.000	5.750	0.000
2.125	0.791	4.000	0.000		

It should be noted that in practical FRM/ FEM PM_{2.5} sampling, a PM₁₀ inlet (sampler) is placed upstream of a PM_{2.5} sampler, either WINS impactor or BGI PM_{2.5} VSCCTM cyclone, for pre-separation of larger particles; therefore, the overall performance of such a sampling setup is approximately a combination of an ideal PM₁₀ and an ideal PM_{2.5} sampler. To calculate the penetration curve of this setup, a method of piecewise linear interpolation was used, as described in Equation 3.5 and 3.6. The calculation results were shown in Table 3.7 and were used to calculate the mass fraction of PM_{2.5} because this combination is more similar to practical PM_{2.5} sampling than an ideal PM_{2.5} sampler only.

$$\eta_{\text{overall}}(d) = \eta_{\text{PM}_{10}}(d) \times \eta_{\text{PM}_{2.5}}(d) \quad (3.5)$$

where, d is the diameter listed in Table 3.6, $\eta_{\text{overall}}(d)$ is the overall collection efficiency at a diameter d , $\eta_{\text{PM}_{2.5}}(d)$ is the collection efficiency of an ideal $\text{PM}_{2.5}$ sampler at d and was available from Table 3.6, and $\eta_{\text{PM}_{10}}(d)$ is the collection efficiency of an ideal PM_{10} sampler at d and was calculated as:

For $d \in [d_i, d_{i+1})$,

$$\eta_{\text{PM}_{10}}(d) = \eta_{\text{PM}_{10}}(d_i) + (d - d_i) \frac{\eta_{\text{PM}_{10}}(d_{i+1}) - \eta_{\text{PM}_{10}}(d_i)}{d_{i+1} - d_i} \quad (3.6)$$

where, d_i and d_{i+1} are a pair of nearest diameters listed in Table 3.5.

Table 3.7. Penetration curve of an ideal $\text{PM}_{2.5}$ sampler with a PM_{10} inlet.

Diameter (μm)	Collection efficiency	Diameter (μm)	Collection efficiency	Diameter (μm)	Collection efficiency
0.100	1.000	2.250	0.663	4.125	0.000
0.500	1.000	2.375	0.563	4.250	0.000
0.625	0.999	2.500	0.448	4.375	0.000
0.750	0.998	2.625	0.327	4.500	0.000
0.875	0.997	2.750	0.213	4.625	0.000
1.000	0.995	2.875	0.123	4.750	0.000
1.125	0.978	3.000	0.062	4.875	0.000
1.250	0.962	3.125	0.028	5.000	0.000
1.375	0.943	3.250	0.011	5.125	0.000
1.500	0.920	3.375	0.004	5.250	0.000
1.675	0.904	3.500	0.001	5.375	0.000
1.750	0.881	3.625	0.000	5.500	0.000
1.875	0.848	3.750	0.000	5.625	0.000
2.000	0.804	3.875	0.000	5.750	0.000
2.125	0.743	4.000	0.000		

A major challenge to calculating the mass fraction of PM_{10} (or $\text{PM}_{2.5}$) was that all PSD data in this study were presented in the form of discrete size ranges. The penetration curves (Figure 3.7) are also discrete and can hardly be described by simple equations. Accordingly, it is difficult to calculate PM mass fractions through a simple mathematical integration; instead, we calculated the mass fraction of collected PM_{10} (or $\text{PM}_{2.5}$) in each size range and then added them up over all size ranges, as described by Equation 3.7 and 3.8:

$$F_{\text{PM}_{10}} = \sum_{j=0}^N (f(d_j) \times \eta_{\text{PM}_{10}}(d_j)) \quad (3.7)$$

$$F_{\text{PM}_{2.5}} = \sum_{j=0}^N (f(d_j) \times \eta_{\text{overall}}(d_j)) \quad (3.8)$$

where, d_j is the characteristic diameter of a size range, $F_{PM_{10}}$ is the mass fraction of PM_{10} , $F_{PM_{2.5}}$ is the mass fraction of $PM_{2.5}$, $f(d_j)$ is the fraction of particles in the size range characterized by d_j , and N is the total number of size ranges. Collection efficiencies, $\eta_{PM_{10}}(d_j)$ and $\eta_{overall}(d_j)$, were calculated through piecewise linear interpolation, as presented in Equation 3.9 and 3.10:

For $d_j \in [d_i, d_{i+1})$,

$$\eta_{PM_{10}}(d_j) = \eta_{PM_{10}}(d_i) + (d_j - d_i) \frac{\eta_{PM_{10}}(d_{i+1}) - \eta_{PM_{10}}(d_i)}{d_{i+1} - d_i} \quad (3.9)$$

$$\eta_{overall}(d_j) = \eta_{overall}(d_i) + (d_j - d_i) \frac{\eta_{overall}(d_{i+1}) - \eta_{overall}(d_i)}{d_{i+1} - d_i} \quad (3.10)$$

where, d_i and d_{i+1} are a pair of nearest diameters listed in Table 3.5 for calculation of $\eta_{PM_{10}}(d_j)$ or in Table 3.7 for calculation of $\eta_{overall}(d_j)$.

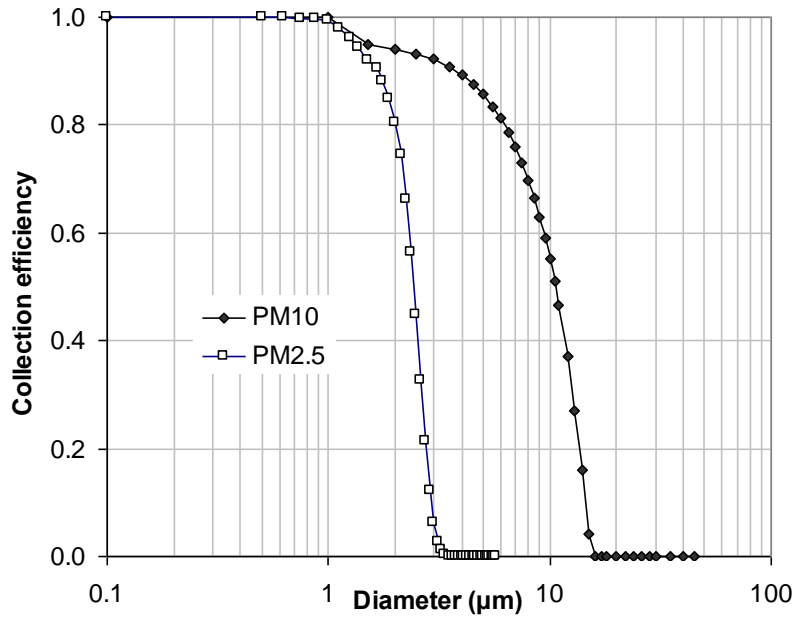


Figure 3.7. Penetration curves for calculation of PM_{10} and $PM_{2.5}$ mass fractions.

It should be noted that Equation 3.7 and 3.8 involved several assumptions:

- The density of particles equals to $1,000 \text{ kg/m}^3$ over all size ranges.
- All particles are solid and spherical so that the mass of particles can be simply calculated as $m = 4\rho\pi r^3/3$.

- All particles within the same size ranges have identical particle diameters

The same assumptions also applied to approach A. In fact, approach A could also be described by Equation 3.7 and 3.8 but with different equations for $\eta_{PM_{10}}(d_j)$ and $\eta_{overall}(d_j)$:

$$\eta_{PM_{10}}(d_j) = \begin{cases} 1, & \text{if } d_j \leq 10\mu\text{m} \\ 0, & \text{if } d_j > 10\mu\text{m} \end{cases} \quad (3.11)$$

$$\eta_{overall}(d_j) = \begin{cases} 1, & \text{if } d_j \leq 2.5\mu\text{m} \\ 0, & \text{if } d_j > 2.5\mu\text{m} \end{cases} \quad (3.12)$$

The average diameter was selected as the characteristic diameter of a size range, d_j (Figure 3.8); however, the maximum diameter of a size range was occasionally used in some previous calculations (Jerez, 2007). For the purpose of comparison, the maximum diameter was also selected in this study.

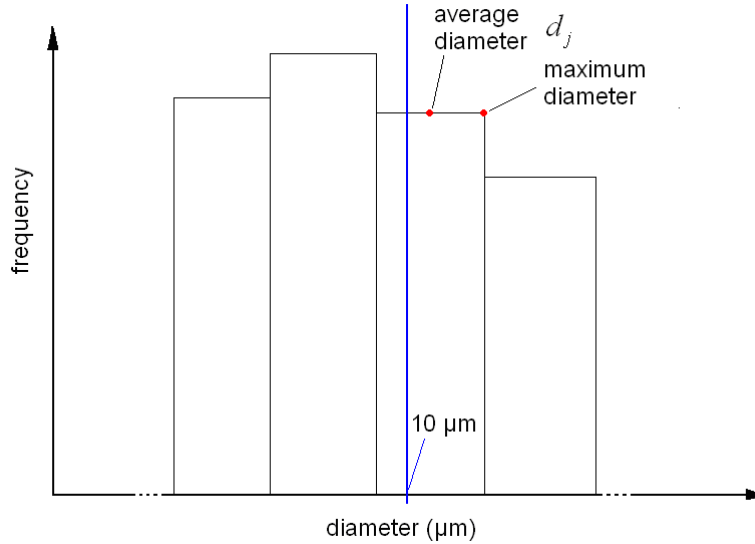


Figure 3.8. Selection of the characteristic diameter of a size range.

Particularly for approach A, when the average diameter was selected as d_j , the collection efficiency of PM_{10} in the size range with $10\mu\text{m}$ in it was calculated as:

$$\eta_{PM_{10}}(d_j) = (10\mu\text{m} - d_j^-) / (d_j^+ - d_j^-) \quad (3.13)$$

Where d_j^+ and d_j^- refer to the maximum and minimum diameters in that size range, respectively.

The purpose was to reduce potential errors of Equation (3.11) and (3.12) that might become

significant when the size range near 10 μm was relatively wide. A similar calculation approach was applied to the case of $\text{PM}_{2.5}$.

A program written in MATLAB 7.0 was developed for calculating the mass fraction of PM_{10} or $\text{PM}_{2.5}$ in a TSP samples. This program made it possible to process a large number of PSD profiles in a single run. Calibration and conversion of the raw PSD data were also integrated into the program. The derived PM mass fractions were then multiplied by TSP concentrations to calculate PM_{10} or $\text{PM}_{2.5}$ mass.

3.2.4.4 Statistical analysis and theoretical discussion

Formation of hypotheses and questions

As mentioned in the introduction section, some previous studies reported that FRM/ FEM PM samplers could significantly overestimate PM_{10} and $\text{PM}_{2.5}$ concentrations from agricultural sources (Buser et al., 2007a; Buser, 2004; Buser et al., 2008; Wang et al., 2005a; Wang et al., 2005b). Potential oversampling of FRM/ FEM PM samplers was investigated both theoretically and experimentally, mostly focused on PM_{10} samplers.

In the theoretical investigation, PM_{10} mass concentrations calculated from approach A were considered to be the ‘true’ PM_{10} concentrations because approach A apparently accords with the theoretical definition of PM_{10} - particles with an aerodynamic diameter no greater than 10 μm . Misestimating PM_{10} concentrations by FRM/ FEM PM samplers was thought to be a result of the departure of the practical penetration curve of FRM/FEM PM_{10} samplers from the ‘ideal’ penetration curve in approach A. Because the penetration curve of FRM/FEM PM_{10} samplers is often unavailable, the collection efficiency of FRM/FEM PM sampler was assumed to follow a lognormal distribution and accordingly the penetration curve could be described by a simple equation as follow:

$$PE(x, D_{50}, S) = 1 - \int_0^x \frac{1}{d_p \sqrt{2\pi \ln S}} \exp \left[\frac{-(\ln d_p - \ln D_{50})^2}{2(\ln S)^2} \right] dd_p \quad (3.14)$$

where, $PE(x, D_{50}, S)$ is the cumulative penetration efficiency of a PM sampler at diameter x , d_p is the particle size, D_{50} is the 50% cut size of this sampler, and S is the slope that represents the

sharpness of the penetration curve. In addition, that the size distribution of agricultural PM was assumed to also follow a lognormal distribution, as described in Equation 3.15:

$$f(x, MMD, GSD) = \frac{1}{x\sqrt{2\pi \ln GSD}} \exp\left[\frac{-(\ln x - \ln MMD)^2}{2(\ln GSD)^2}\right] \quad (3.15)$$

where, $f(x, MMD, GSD)$ refers to the mass fraction density function at diameter x , MMD is the mass median diameter and GSD is the geometric standard deviation of a given PM sample. The PM₁₀ mass fraction, $F_{PM_{10}}$, was then calculated as:

$$F_{PM_{10}} = \int_0^{\infty} PE(x, D_{50}, S) f(x, MMD, GSD) dx \quad (3.16)$$

D_{50} , S , MMD and GSD could be either assumed or estimated: the D_{50} of FRM/ FEM PM₁₀ samplers was specified by the USEPA to be $10 \pm 0.5 \mu\text{m}$ (CFR, 2001a); the slope, S , was assumed to be 1.5 ± 0.1 (Buser et al., 2008; Wang et al., 2005a; Wang et al., 2005b); and previous studies revealed that the MMD of PM from agricultural sources was generally greater than $10 \mu\text{m}$ and the GSD typically ranged from 1.7 to 3.0 (Donham et al., 1986b; Lee, 2009; Redwine et al., 2002). Applying these estimated or assumed values into Equation 3.16, the mass fraction (or mass concentration) of PM₁₀ collected by an FRM/FEM PM₁₀ sampler was calculated and then compared with the ‘true’ PM fraction (or mass concentration) derived from approach A:

$$F_{PM_{10}} = \int_0^{10\mu\text{m}} f(x, MMD, GSD) dx \quad (3.17)$$

From such a comparison, a consistent significant oversampling by FRM/ FEM PM₁₀ samplers was observed and interpreted as follows:

- FRM/FEM PM₁₀ samplers over-sample a portion of particles greater than $10 \mu\text{m}$ but at the same time under-sample a portion of particles smaller than $10 \mu\text{m}$ due to the ‘non-ideal cut’ geometry of their penetration curve (Figure 3.9a).
- The over-sampled part overweighes the under-sampled part (Figure 3.9c). A reason is that the MMD of agricultural PM is generally greater than $10 \mu\text{m}$, which means particles greater than $10 \mu\text{m}$ contribute more mass concentrations than smaller particles (Figure 3.9b). In fact, even if particles were uniformly distributed over all sizes, the penetration

curve described by Equation 3.14 would still lead to an oversampling due to its longer tail in the larger particle size region.

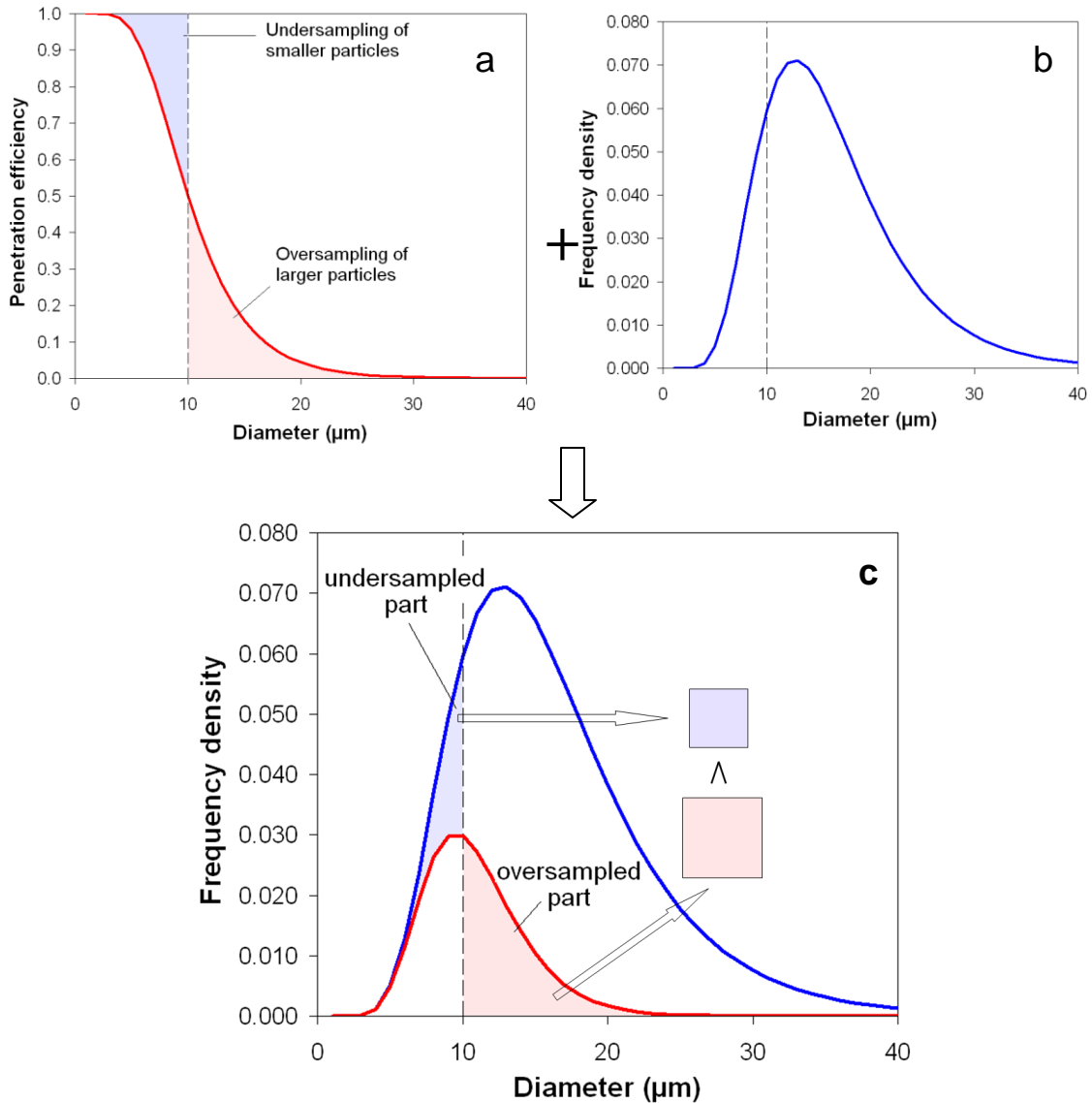


Figure 3.9. Simulated size selective sampling by an FRM/ FEM PM_{10} sampler: a- an assumed lognormal penetration curve ($D_{50}=10 \mu\text{m}$ and $S=1.5$), b- an assumed lognormal PSD curve of a TSP sample ($MMD=15$, $GSD=1.5$), and c- the PSD curve of the collected PM_{10} versus that of the TSP sample.

Theoretical discussions suggested a possible oversampling by FRM/ FEM PM_{10} samplers, and following that, a series of experimental investigations were also conducted. PM_{10} mass concentrations were measured gravimetrically using an FRM PM_{10} sampler, and at the same time were calculated through approach A from TSP mass concentrations and PSD data derived from a

particle size analyzer (e.g., Coulter Counter Multisizer). The measured PM_{10} concentrations were found to be much higher than the calculated concentrations. This phenomenon was considered to be due to the oversampling by FRM/FEM PM_{10} samplers.

However, several issues were associated with the experimental and theoretical investigations mentioned above:

- In the theoretical investigation, both the penetration curves and PSD curves were assumed to follow a lognormal distribution. However, the practical penetration curve of an FRM/ FEM PM_{10} sampler should be more similar to the penetration curve of the ideal PM_{10} sampler (Table 3.5) since the ideal PM_{10} sampler is being employed as a reference standard for the design of FRM/ FEM PM_{10} samplers. Also, field-measured PSD curves may not follow the lognormal distribution. A multimodal distribution, for example, was occasionally observed for agricultural PM (Lee, 2009). Accordingly, a question is- Can the oversampling be reproduced when field-measured PSD data and the penetration curve of the ideal PM_{10} sampler are employed for calculation?
- In the experimental investigation, the PM_{10} mass concentrations calculated through approach A were selected as a reference to assess whether an FRM/FEM PM_{10} sampler overestimates the PM_{10} mass concentrations. However, there was yet no solid evidence ensuring that the PM_{10} mass concentrations derived from the Coulter PSD data are the ‘true’ PM_{10} concentrations. Is there a possibility that the oversampling previously observed is a result of instrumental bias? What if a different particle size analyzer is used? Will it lead to a different conclusion? If the answer was yes, then which particle size analyzers would offer the best estimates of PM_{10} mass concentrations?

From the above discussions, two hypotheses were proposed for statistical tests.

- Hypothesis A- Approach A would consistently produce smaller PM_{10} (or $PM_{2.5}$) mass concentrations than approach B even with field-measured PSD data and the penetration curve of the ideal PM_{10} (or $PM_{2.5}$) sampler.
- Hypothesis B- PSD data derived from different particle size analyzers would produce identical or very similar results of PM_{10} (or $PM_{2.5}$) mass concentration.

Positive results, if produced, would support the statement that current FRM/FEM PM samplers overestimate the mass concentrations of PM₁₀ and PM_{2.5}, and vice versa. Because the calculation method was proposed based on the oversampling statement, negative results, if generated, would undermine the validity of this alternative method.

Data analysis

Statistical analysis followed a similar procedure as illustrated in Figure 3.4, except that there was no linear modeling involved in this case. First, the ratios of the calculated to the measured PM concentrations were calculated. Then, those ratios were subject to a normality test and transformed into their log forms if they failed in the test. Next, univariate analysis (e.g., mean and standard deviation) and exploratory data analysis (e.g., box plot and cluster analysis) were performed to summarize and depict the obtained ratio data. One-way ANOVA and paired t-tests were then used to test the hypothesis A and B, and to determine whether there was a significant difference between measured and calculated PM concentrations, and among PM concentrations calculated from different approaches (A and B) and/or with different d_j selections.

Along with statistical analysis, a theoretical discussion would also be conducted in an effort to interpret the analysis results and to address the issues and questions described in previous paragraphs.

3.2.5 Effects of filter post-conditioning on PM mass measurement.

Some chemical and biological characterizations of PM, e.g., volatile organic compounds (VOC's) and bacterial communities, require fresh PM samples. In these cases, filters need to be weighed immediately after sampling. However, without post-conditioning, water and other volatile impurities adsorbed on filters and collected particles could interfere with the accuracy of mass measurement, leading to an overestimation of PM mass and, accordingly, mass concentration. For most quantitative chemical and biological analyses, the analysis results were normally presented in the form of fractions, e.g., ng analyte per mg PM mass; the overestimation of PM mass thus could be a major uncertainty source. Therefore, one of the objectives in this chapter was to evaluate the effect of filter conditioning on PM mass measurement.

To do that, parts of PM samples were collected on TefloTM and ZefluorTM PTFE filters (PM1, 2, 4, 5 and TSP 6, 7 in Table 3.2) and were weighed before and after post-conditioning; while

other samples, except TSP5, were collected on Type A/E glass fiber filters. Compared to PTFE filters, glass fiber filters are more hygroscopic and have a greater adsorption capacity for VOC's (Chow and Watson, 1999), and consequently may lose more mass during post-conditioning. To address this issue, a laboratory experiment was designed as follows:

- Glass fiber filters were pre-conditioned in desiccators for 24 hrs and then weighed.
- Those filters were conditioned in an environmental chamber at 22°C for 24 hrs. Three separate tests were conducted with the relative humidity (RH) of 50%, 65% and 80%, respectively. For each test, 12 filters were used. The RH set points were selected based on field-measured RH data ($63 \pm 13\%$) in animal buildings.
- Those filters were weighed immediately after taken out from the environmental chamber, and weighed again after post-conditioned in desiccators for 24 hrs.

The mass loss during post-conditioning consisted of two parts: a loss in filter mass and a loss in particle mass. To simulate this process, a mathematical model was established, which assumed that the loss in particle (or filter) mass was proportional to the mass of particles (or a filter) before post-conditioning. This model was presented as:

$$\begin{aligned} M_{p,a} &= \beta_1 M_{p,b}; \quad M_{f,a} = \beta_2 M_{f,b}; \\ M_{p,a} + M_{f,a} &= \beta_1 M_{p,b} + \beta_2 M_{f,b} + \varepsilon \end{aligned} \quad (3.18)$$

Where, $M_{p,a}$ is the mass of PM after conditioning, $M_{p,b}$ is the mass of PM before conditioning, $M_{f,a}$ is the mass of a filter after conditioning, $M_{f,b}$ is the mass of a filter before conditioning, β_1 and β_2 are correlation coefficients, ε is the measurement error. A least square linear regression was then conducted to calculate β_1 and β_2 and their respective 95% confidence intervals.

For laboratory investigation of glass fiber filters, a simpler model (Equation 3.19) was applied because there was no PM collection on filters. The derived β_2 were then used for calculating the mass loss (ΔM) during post-conditioning when glass fiber filters were used for PM collection (Equation 3.20).

$$M_{f,a} = \beta_2 M_{f,b} + \varepsilon \quad (3.19)$$

$$\Delta M = (M_{p,b} + M_{f,b}) - (M_{p,a} + M_{f,a}) \quad (3.20)$$

After that, the calculated results were subject to statistical analysis to determine if the effects of filter conditioning on PM mass measurement were substantial. In this study, $\pm 3\%$ was defined to be the tolerance level for PM mass measurement. Accordingly, a null hypothesis would be that the mass loss due to post-conditioning was equal to or greater than 3%.

3.3 Results and Discussions

3.3.1 Issues associated with field sampling and solutions

A total of 52 field trips were conducted, including nine makeup field trips. A couple of problems were found during field sampling: power failure, disturbance by animals, overloading of PM₁₀ and PM_{2.5} samplers and disturbance by insects. The issue of power failure was solved by connecting two $\frac{3}{4}$ horse power pumps onto separate circuits. Metal fences or poultry meshes were erected in animal barns to prevent the disturbance by animals. To avoid potential overloading, as previously mentioned, we ran sampling pumps intermittently under extremely dusty conditions and additionally installed a PM₁₀ impactor upstream of each PM_{2.5} sampler to remove larger particles. Sampler inlets were covered by metal screens (15×15 mesh size, 73% open area) to prevent small insects entering the inside of samplers.

3.3.2 Summary of field measurement results

3.3.2.1 PM mass concentrations

For each field trip, the mean mass concentrations of TSP, PM₁₀ and PM_{2.5} were calculated from replicate samples and the standard deviations (SD) were also determined. Parts of the results were shown in Figure 3.10. In most cases, the relative standard deviation (GSD) produced from co-located replicate PM samples was relatively small (<15%). TSP, PM₁₀ and PM_{2.5} concentrations differed greatly with animal building type and increased as the weather became colder.

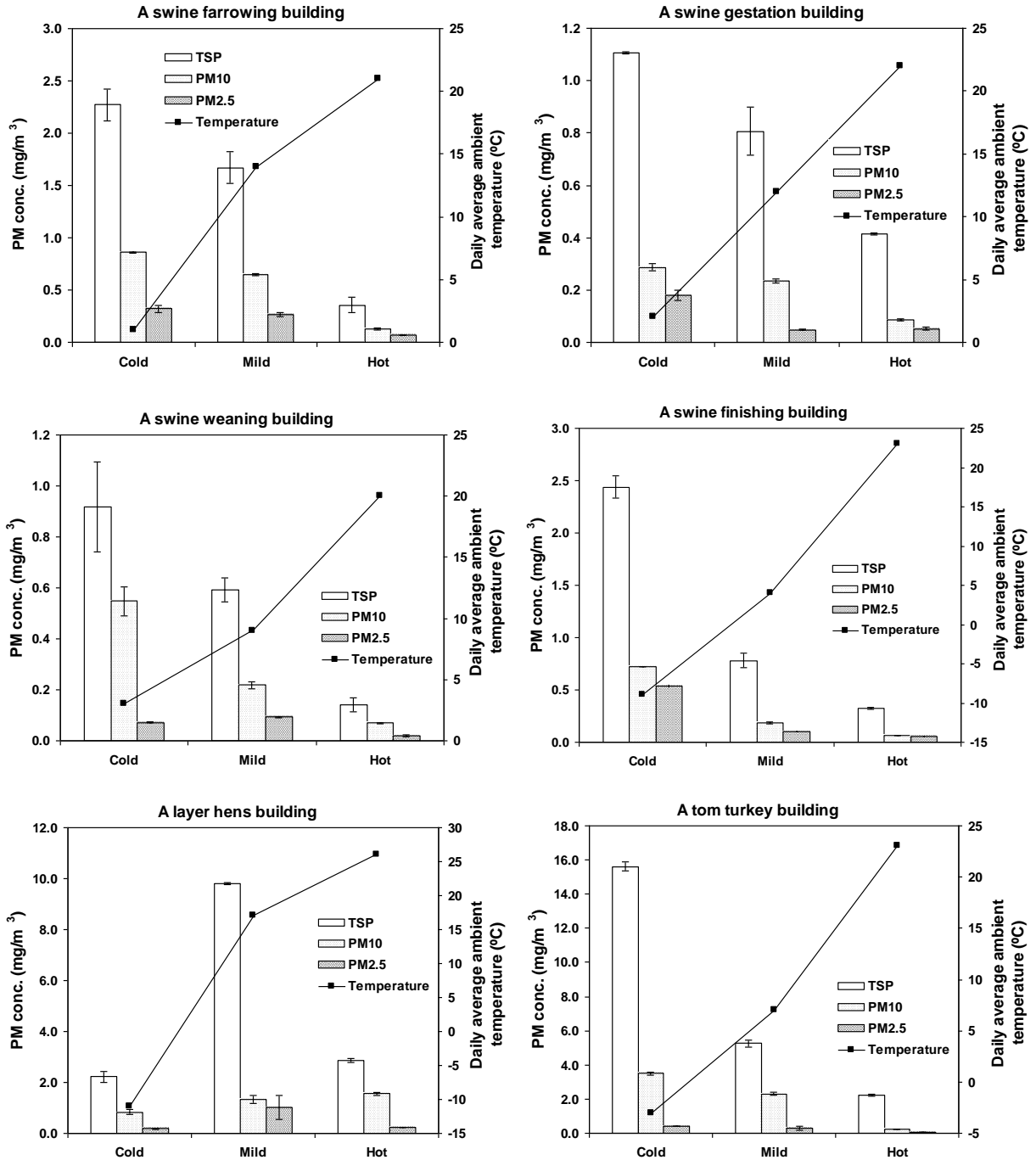


Figure 3.10. Parts of the results of mass concentration measurements. The errors bars represent the standard deviation of PM concentrations.

The measurement results were summarized based on animal building type (Table 3.8). Tom turkey buildings had overall the highest TSP and PM₁₀ concentrations and layer hen buildings had the highest PM_{2.5} concentrations. Both of them are poultry buildings where feathers, which can easily become airborne, may constitute a large portion of PM. In contrast to manure-belt

layer hen buildings, tom turkey buildings have floors bedded with wood shavings. Manures are directly excreted onto floor and mixed with wood shavings replaced every a few to tens of years. The occurrence of higher TSP and PM₁₀ concentrations may be owing to the mechanical suspension, which commonly leads to the formation of coarse particles, of deposited manure and bedding materials by turkeys. Additionally, all tom turkey buildings in this study employ a natural ventilation system. Compared to mechanical ventilation in layer hen buildings, natural ventilation generally has lower ventilation rate and thereby may lead to higher TSP and PM₁₀ concentrations.

Table 3.8. Summary of PM mass concentrations (I): animal building type.

Building type	Statistic	TSP (mg/m ³)	PM ₁₀ (mg/m ³)	PM _{2.5} (mg/m ³)	PM ₁₀ /TSP	PM _{2.5} /TSP	PM _{2.5} /PM ₁₀
All swine (N ^a =35)	Mean	1.20	0.34	0.12	0.32	0.12	0.39
	SD	0.96	0.26	0.12	0.15	0.08	0.20
	Geomean	0.90	0.26	0.09	0.29	0.10	0.34
	GSD	2.23	2.22	2.23	1.59	2.13	1.73
Farrowing (N=9)	Mean	1.00	0.42	0.16	0.44	0.18	0.42
	SD	0.67	0.26	0.10	0.16	0.09	0.16
	Geomean	0.80	0.33	0.13	0.42	0.16	0.39
	GSD	2.12	2.18	1.97	1.34	1.69	1.58
Gestation (N=9)	Mean	0.71	0.20	0.08	0.28	0.11	0.41
	SD	0.30	0.11	0.05	0.10	0.05	0.15
	Geomean	0.65	0.17	0.06	0.26	0.10	0.38
	GSD	1.62	2.01	2.01	1.41	1.69	1.51
Weaning (N=8)	Mean	1.70	0.36	0.08	0.29	0.08	0.26
	SD	1.41	0.29	0.04	0.18	0.06	0.11
	Geomean	1.16	0.28	0.07	0.24	0.06	0.24
	GSD	2.92	2.20	1.84	1.94	2.24	1.59
Finishing (N=9)	Mean	1.48	0.39	0.18	0.26	0.12	0.46
	SD	1.02	0.30	0.20	0.07	0.09	0.30
	Geomean	1.15	0.28	0.10	0.25	0.09	0.36
	GSD	2.28	2.46	2.94	1.33	2.38	2.14
All poultry (N=18)	Mean	4.43	1.32	0.32	0.33	0.08	0.24
	SD	4.08	1.02	0.39	0.16	0.09	0.18
	Geomean	3.15	0.92	0.18	0.29	0.06	0.20
	GSD	2.31	2.60	2.85	1.66	2.09	1.82
Layer hens (N=9)	Mean	2.98	1.07	0.40	0.39	0.12	0.32
	SD	2.77	0.89	0.53	0.19	0.11	0.22
	Geomean	2.25	0.76	0.20	0.34	0.09	0.26
	GSD	2.12	2.55	3.39	1.77	2.14	1.97
Tom turkey (N=9)	Mean	5.88	1.56	0.23	0.27	0.04	0.17
	SD	4.79	1.13	0.17	0.09	0.02	0.08
	Geomean	4.41	1.10	0.17	0.25	0.04	0.16
	GSD	2.26	2.70	2.48	1.50	1.55	1.49

a. N refers to the number of field trips, NOT the number of filter samples.

The lowest PM (TSP, PM₁₀ and PM_{2.5}) concentrations were found in swine gestation buildings where pregnant mother pigs are individually housed in small crates and, thus, their activities are minimized. The use of wet feeding may be another reason accounting for low PM concentrations in gestation buildings because in the wet feeding system animal feed is mixed with water. This may reduce the aerosolization (suspension and re-suspension) of feed particles.

Table 3.9. Summary of PM mass concentrations (II): season.

Building type	Seasons	Statistic	TSP (mg/m ³)	PM ₁₀ (mg/m ³)	PM _{2.5} (mg/m ³)	PM ₁₀ /TSP	PM _{2.5} /TSP	PM _{2.5} /PM ₁₀
All swine	Hot (N=11)	Mean	0.53	0.12	0.05	0.29	0.14	0.46
		SD	0.46	0.06	0.03	0.13	0.09	0.21
		Geomean	0.41	0.11	0.05	0.26	0.11	0.42
		GSD	2.00	1.66	1.68	1.61	2.10	1.63
	Mild (N=12)	Mean	1.26	0.31	0.10	0.27	0.09	0.33
		SD	0.65	0.13	0.07	0.10	0.06	0.15
		Geomean	1.13	0.29	0.08	0.25	0.08	0.29
		GSD	1.62	1.43	1.75	1.54	2.13	1.60
	Cold (N=12)	Mean	1.77	0.59	0.21	0.39	0.14	0.37
		SD	1.20	0.24	0.15	0.17	0.08	0.22
		Geomean	1.48	0.54	0.17	0.36	0.11	0.31
		GSD	1.82	1.56	1.92	1.47	2.03	1.91
All poultry	Hot (N=6)	Mean	2.46	0.63	0.10	0.25	0.04	0.20
		SD	1.65	0.56	0.07	0.15	0.02	0.10
		Geomean	2.10	0.45	0.08	0.22	0.04	0.18
		GSD	1.82	2.45	1.83	1.75	1.61	1.57
	Mild (N=6)	Mean	4.90	1.64	0.62	0.39	0.15	0.39
		SD	2.83	0.92	0.55	0.21	0.13	0.24
		Geomean	4.07	1.40	0.44	0.34	0.11	0.31
		GSD	2.11	1.93	2.51	1.77	2.40	2.15
	Cold (N=6)	Mean	6.40	1.65	0.22	0.29	0.04	0.15
		SD	6.00	1.27	0.15	0.07	0.02	0.04
		Geomean	4.11	1.17	0.17	0.28	0.04	0.14
		GSD	2.93	2.69	2.44	1.28	1.51	1.28

Seasons had a great impact on PM concentrations (Table 3.9). In swine buildings, the highest TSP, PM₁₀ and PM_{2.5} concentrations were observed in cold seasons; while the lowest concentrations occurred in hot seasons. Such a seasonal variation in PM concentrations may be due to a seasonal change in ventilation rates. All swine buildings in this study are mechanically ventilated. The ventilation rate is automatically or manually adjusted so as to maintain the room temperature within a certain range optimal for pig growth, and generally increases with ambient temperature. Lower ventilation rates during the winter mean lower air exchange rates and less dilution, thereby leading to an accumulation of air pollutants, e.g., PM, in swine buildings. A

similar finding was made in tom turkey buildings with natural ventilation (Table 3.10). In tom turkey buildings, the ventilation rate is greatly determined by the openness of curtains, which also tends to increase with ambient temperature.

Table 3.10. Summary of PM mass concentrations (III): animal building type × season.

Building type		Seasons	TSP (mg/m ³)		PM ₁₀ (mg/m ³)		PM _{2.5} (mg/m ³)	
			Mean	SD	Mean	SD	Mean	SD
Swine	Farrowing (N=9)	Hot	0.34	0.09	0.14	0.06	0.08	0.05
		Mild	1.29	0.43	0.45	0.18	0.18	0.08
		Cold	1.39	0.77	0.67	0.19	0.20	0.13
	Gestation (N=9)	Hot	0.36	0.06	0.07	0.02	0.04	0.01
		Mild	0.81	0.04	0.25	0.03	0.06	0.02
		Cold	0.94	0.21	0.33	0.03	0.15	0.03
	Weaning (N=8)	Hot	0.84	0.99	0.13	0.08	0.03	0.01
		Mild	1.79	1.04	0.27	0.08	0.07	0.02
		Cold	2.20	2.07	0.61	0.36	0.11	0.03
	Finishing (N=9)	Hot	0.70	0.58	0.15	0.08	0.05	0.01
		Mild	1.17	0.34	0.24	0.05	0.07	0.05
		Cold	2.55	0.71	0.74	0.10	0.38	0.22
Poultry	layer hen (N=9)	Hot	3.14	2.30	0.94	0.71	0.14	0.08
		Mild	5.00	4.46	1.62	1.33	0.92	0.67
		Cold	1.73	0.58	0.58	0.29	0.11	0.07
	tom turkey (N=9)	Hot	1.78	0.38	0.33	0.10	0.06	0.01
		Mild	4.80	0.44	1.65	0.58	0.31	0.17
		Cold	11.07	4.92	2.71	0.73	0.33	0.09

However, not all types of animal buildings showed the same pattern of seasonal variations as described in the previous paragraph (Table 3.10). PM concentrations in manure-belt layer hen buildings, for instance, did not increase as the weather became colder. This unusual phenomenon was a good example demonstrating that, for even the same type of animal buildings, different ventilation designs may lead to significantly different PM concentrations and/or emissions. Two manure-belt layer hen buildings (Q and P) visited in this study have integrated manure drying zones (Appendix B) where manures are carried by slowly moving rubber belts and dried with the air blew by parts of ventilation fans. Such a manure dewatering approach inevitably elevates the downstream PM concentrations, which, in this case, are not only affected by the ventilation rate but largely dependent on the cleanliness of the manure drying zone, e.g., the amount of manures and deposited dust. The cleanliness of the manure drying zone, however, is mainly determined by the cleaning cycle specified by farm operation guidelines, and accordingly tends to exhibit a periodical but NOT seasonal variation. Comparatively, in the last manure-belt layer hen building (R), manures are transported to a separate house for drying and storage (Appendix B). PM

concentrations were found to decrease with ambient temperature in this building (data not shown). In summary, every animal building can be unique on some aspects. Building-to-building difference is one of the top challenges to investigating PM concentrations and emission rates from animal buildings, and is a major reason why some standard deviation values were fairly big in Table 3.10.

3.3.2.2 Comparison with previous literature

A large variety of PM samplers and monitors have been employed for measurement of PM concentrations in animal buildings, such as TEOM (Burns et al., 2008; Jacobson et al., 2005; Lim et al., 2003), inhalable and respirable personal samplers (Banhazi et al., 2008; Kim et al., 2008a; Takai et al., 1998), PM_{2.5} speciation sampler (Li et al., 2009), DustTrak aerosol monitors (Haeussermann et al., 2008; Roumeliotis and Van Heyst, 2007) and Haz Dust sampler (Costa and Guarino, 2009). Among them, TEOM and inhalable and respirable samplers are most frequently used. Inhalable samplers collect PM with aerodynamic diameter no greater than 100 µm; while isokinetic TSP samplers used in this study collect PM of all sizes. According to the PSD measurement results by Lee (2009), most particles in animal buildings were smaller than 100 µm; therefore, the mass concentration of inhalable PM is comparable to that determined by isokinetic TSP samplers. Respirable samplers have a 50% cut size (D₅₀) of 4 µm, slightly greater than that of PM_{2.5} samplers (2.5 µm). A side-by-side comparison, however, is still informative since both samplers were designed for investigating the respirable fraction of PM.

PM mass concentrations measured in this study were found to be of the same order of magnitude as those reported by previous similar studies (Table 3.11). However, it should be noted that different monitoring methods could generate substantially different measurement results. The advantages and disadvantages of a method must be fully assessed before applying it to a field sampling. For example, a well recognized limitation of TEOM is that it could underestimate the concentration of fine particles, e.g., PM_{2.5}, because of the loss of volatile and semi-volatile components at elevated temperatures, generally 50°C, during detection (Lee et al., 2005; Patashnick et al., 2001).

Table 3.11. PM mass concentrations in animal confinement buildings.

Animal facility	Farm location	Particle size	Mean conc. (mg/m ³)	Method	Reference
Swine farrowing	Illinois	TSP	1.00	Gravimetric	This study
		PM ₁₀	0.42		
		PM _{2.5}	0.16		
Swine gestation	Illinois	TSP	0.71	Gravimetric	This study
		PM ₁₀	0.20		
		PM _{2.5}	0.08		
	Italy	PM ₁₀	0.31	Haz Dust	Haussermann et al. (2008)
Swine weaning	Illinois	TSP	1.70	Gravimetric	This study
		PM ₁₀	0.36		
		PM _{2.5}	0.08		
	Farm 1, Italy	PM ₁₀	0.11	Haz Dust	Haussermann et al. (2008)
Farm 2, Italy	0.40				
Swine finishing	Illinois	TSP	1.48	Gravimetric	This study
		PM ₁₀	0.39		
		PM _{2.5}	0.18		
	Italy	PM ₁₀	0.47	Haz Dust	Haussermann et al. (2008)
	Germany	PM ₁₀	0.73	DustTrak	
	Minnesota	Total ^a	6.86 (w); 0.42 (s) ^b	Personal sampler	Schmidt et al. (2002)
		Inhalable	4.56 (w); 0.64 (s)		
		Respirable	0.44 (w); 0.04 (s)		
		PM ₁₀	1.63 (w); 0.24 (s)		
	Kansas	Inhalable	2.13	Personal sampler	Predicala et al. (2001)
Respirable		0.11			
China	PM ₁₀	0.16	Gravimetric	Wei et al. (2010)	
Swine (unclassified)	North Europe ^c	Inhalable	2.19	Personal sampler	Takai et al. (1998)
		Respirable	0.23		
Turkey	Illinois	TSP	5.88	Gravimetric	This study
		PM ₁₀	1.56		
		PM _{2.5}	0.23		
	Minnesota	Total	4.26 (w); 2.41 (s)	Personal sampler	Schmidt et al. (2002)
		Inhalable	3.54 (w); 2.46 (s)		
		Respirable	0.51 (w); 0.11 (s)		
PM ₁₀	1.11 (w); 0.33 (s)	MiniVol			
Layer hen	Illinois and Indiana	TSP	2.98	Gravimetric	This study
		PM ₁₀	1.07		
		PM _{2.5}	0.40		
	Indiana	TSP	1.887	TEOM	Lim et al. (2003)
		PM ₁₀	0.518		
		PM _{2.5}	0.039		
North Carolina	PM _{2.5}	0.268	Speciation sampler	Li et al. (2009)	
Poultry ^d (unclassified)	North Europe	Inhalable	3.60	Personal sampler	Takai et al. (1998)
		Respirable	0.45		

a. It may refer to TSP but no confirmative information was available.

b. The letters of 'w' and 's' in parenthesis represent winter and summer, respectively.

c. Four countries were included: England, the Netherlands, Denmark and Germany.

d. Layer hen and broiler only.

With a proper calibration, the inconsistency induced by different methods could be minimized. Building characteristics and locations may then become two of the most important factors accounting for the incidence of different PM concentrations in the same type of animal buildings. For example, it is known that animal buildings in Europe are generally smaller than those in the United States. Although the direct influence of building size has not been clear, the corresponding changes in ventilation, feeding, and manure collection and storage systems are expected to have a great impact on PM concentrations. The location and orientation of PM samplers may be another factor. Due to the heterogeneous spatial distribution of PM, a PM sampler installed in the center of an animal building may produce a significantly different PM concentration than that installed near exhaust fans (Jerez, 2007).

3.3.2.3 Comparison with proposed threshold limit values

In this study, PM samplers were installed upstream of exhaust fans. Our measurements targeted at PM concentrations emitted from animal confinement buildings, but on the other hand the measured concentrations also represented the level of indoor PM contaminations near exhausts. Accordingly, two sets of thresholds limit values were used for comparison: the NAAQS and the exposure limits recommended by Donham et al. (2000) (Table 3.12). For the second set of limits, a comparison were undertaken between inhalable and TSP and between respirable and PM_{2.5} concentrations.

Table 3.12. Threshold limits of PM concentrations.

	Threshold limit values (mg/m ³)	Target
NAAQS ^a	PM ₁₀ : 0.150; PM _{2.5} : 0.035	Ambient air quality
Exposure limits (Donham et al., 2000)	Swine- Inhalable: 2.5; respirable: 0.23 Poultry- Inhalable: 2.4; respirable: 0.16	Indoor air quality specifically for animal facilities

a. Averaging time: 24 hours.

Only around 7% PM_{2.5} and 14% PM₁₀ concentration data were below the NAAQS (Figure 3.11), and the percentages differed with animal building types and seasons (Table 3.13). Particularly for poultry buildings, all measured PM₁₀ and PM_{2.5} concentrations exceeded the NAAQS. This indicates that PM contamination on and near an animal farm can be serious and a good air exchange surrounding the farm is desired to dilute exhausted PM to be lower than acceptable levels. Comparatively, most TSP and PM_{2.5} concentrations in swine buildings were below the exposure limits for inhalable and respirable PM, respectively; while, in poultry buildings, over half TSP and PM_{2.5} concentrations exceeded the exposure limits (Table 3.13),

suggesting that indoor PM contamination may be more serious in poultry than in swine buildings. The measured TSP concentrations were also compared with inhalable PM threshold values (TLV-TWA) specified by OSHA (20 mg/m³) and ACGIH (10 mg/m³). Only two data points exceeded the ACGIH standard and none of them exceeded the OSHA standard.

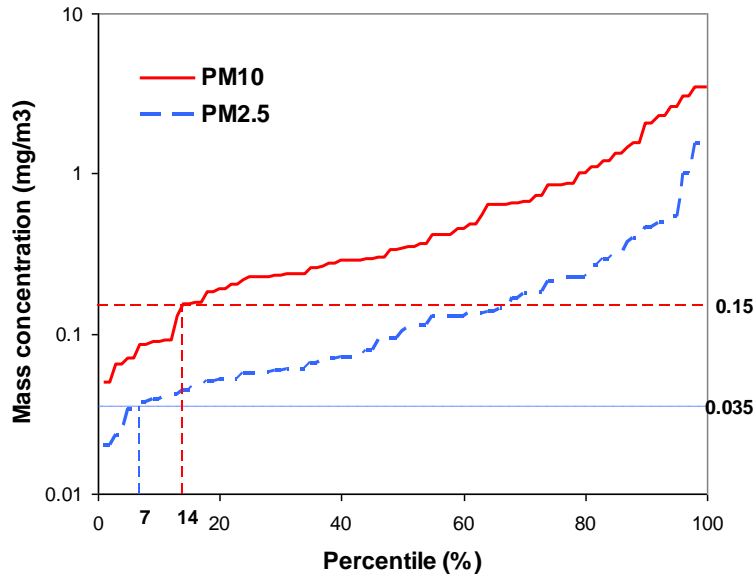


Figure 3.11. Percentile plot of measured PM₁₀ and PM_{2.5} concentrations.

Table 3.13. Frequency of measured PM concentrations exceeding threshold limits.

Building type	Seasons	NAAQS		Exposure limits (Donham et al., 2000)	
		PM ₁₀	PM _{2.5}	Inhalable	Respirable
All swine	All	80%	91%	6%	11%
Farrowing	All	78%	100%	0%	22%
Gestation	All	67%	89%	11%	22%
Weaning	All	88%	88%	13%	0%
Finishing	All	89%	89%	0%	0%
All poultry	All	100%	100%	56%	56%
Layer hen	All	100%	100%	44%	56%
Tom turkey	All	100%	100%	67%	56%
All swine	Hot	36%	73%	0%	0%
	Mild	100%	100%	0%	8%
	Cold	100%	100%	17%	25%
All poultry	Hot	100%	100%	33%	17%
	Mild	100%	100%	83%	83%
	Cost	100%	100%	50%	66%

Because the cut size of PM_{2.5} samplers is smaller than that of respirable samplers, the measured PM_{2.5} concentrations should be less than the real concentrations of respirable PM. Therefore, the numbers shown in Table 3.13 may underestimate the contamination of respirable PM in visited animal confinement buildings.

3.3.3 Variations and Affecting factors

3.3.3.1 Normality tests and data transformation

The original data for TSP, PM₁₀ and PM_{2.5} concentrations failed in the normality test (Table 3.14); accordingly, a data transformation became necessary. Raw concentration data were transformed into their log forms and the normality of the transformed data was found to be improved substantially (Table 3.14 and Figure 3.12).

Table 3.14. Normality of PM concentration data before and after transformation.

Normality test	Statistic	Before transformation			After transformation		
		TSP	PM ₁₀	PM _{2.5}	TSP	PM ₁₀	PM _{2.5}
Shapiro-Wilk	W	0.661	0.726	0.576	0.988	0.982	0.968
	P	<0.001	<0.001	<0.001	0.892	0.632	0.215
Jarque-Bera	JB	184.2	59.2	511.3	0.791	1.032	2.923
	P	<0.001	<0.001	<0.001	0.469	0.597	0.232

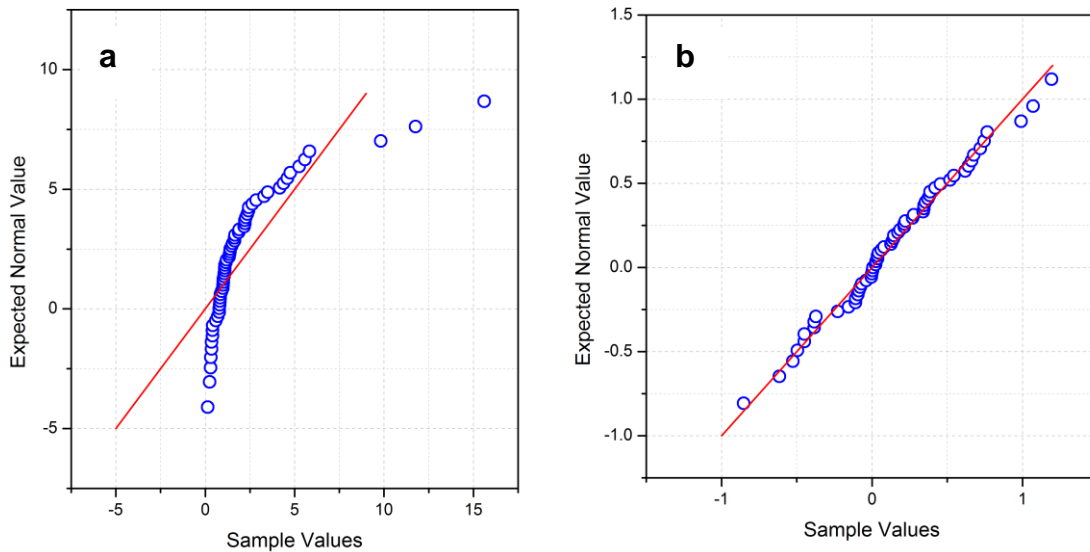


Figure 3.12. QQ plot of TSP concentration data before (a) and after transformation (b).

The same tests and transformation also applied to PM mass ratios (Table 3.15). Although an improvement in normality was less significant, the transformed data passed at least one test and were considered to be acceptable for subsequent statistical analysis.

Table 3.15. Normality of PM mass ratio data before and after transformation.

Normality test	Statistic	Before transformation			After transformation		
		PM ₁₀ /TSP	PM _{2.5} /TSP	PM _{2.5} /PM ₁₀	PM ₁₀ /TSP	PM _{2.5} /TSP	PM _{2.5} /PM ₁₀
Shapiro-Wilk	W	0.925	0.873	0.903	0.988	0.951	0.940
	P	0.003	<0.001	<0.001	0.872	0.031	0.011
Jarque-Bera	JB	14.42	14.52	5.514	0.425	3.303	3.958
	P	<0.001	<0.001	0.063	0.809	0.197	0.138

A poor normality before and an improved normality after log transformation indicates that mean and standard deviation are not appropriate measures for the original PM concentration and mass ratio data. Geometric mean and geometric standard deviation may be more adequate since mathematically they are equal to the mean and standard deviation, respectively, of the log-transformed data. This is a reason why geometric mean and geometric standard deviation were listed in Table 3.8 and 3.9.

3.3.3.2 Determination of affecting factors

Numerous environmental and operational factors are associated with the production and/or elimination of PM in animal buildings, and may consequently affect the mass concentration of PM. Those factors included but not limited to ambient temperature, ventilation system, air velocity in the barns, moisture, animal activity, the quantity of feed per animal, building cleanliness, feeding system, manure management system, and PM control strategy in practice (Heber et al., 1988b). Many of them are difficult to be characterized and quantified. Moreover, the size of the PM concentration database is quite limited in this study, for which a statistical analysis involving too many factors would make no sense. Therefore, only four factors were selected and subject to examination: animal building type, animal density, season (ambient temperature) and feeding system. A description of selected factors was as follows:

- Animal building type- Many factors are dependent on animal building type, i.e., for the same type of animal buildings, similar or even the same ventilation, feeding, and manure management systems and practices tend to be employed. Animal building type was treated as a nominal variable.
- Animal density- Animal density was defined as the weight of animals per cubic meter of room space (kg/m^3). It is determined by the size of a building, the number of animals and animal weight (type and age), and is somehow associated with animal activity.
- Season- As mentioned previously, season was treated as an ordinal variable (cold, mild and hot), classified based on daily average ambient temperature.
- Feeding system- The selection of feeding systems is greatly dependent on animal building types. Two (dry and wet) feeding systems were investigated. Dry feeding systems were used in swine layer hen, tom turkey, swine farrowing and weaning

buildings; while wet feeding systems were used in swine gestation and finishing buildings. Feed system was treated as a normal variable.

Animal building type was found to have a great impact on PM concentrations and PM mass ratios on box charts (Figure 3.13). To determine the level of such an impact, a pairwise one-way ANOVA test (Tukey HSD method) was undertaken and the results were summarized in Table 3.16. Poultry buildings were found to have significantly higher TSP, PM₁₀ and PM_{2.5} concentrations but lower PM_{2.5} fractions than swine buildings. Specifically, tom turkey buildings had significantly greater TSP and PM₁₀ concentrations than all four types of swine buildings but lower PM_{2.5} fractions than swine farrowing and gestation buildings. However, no significant differences in PM concentrations were identified among different types of poultry or swine buildings. Because at least parts of differences in Table 3.16 were of statistical significance, animal building type was considered to be an affecting factor, and thereby was selected as an independent variable for linear modeling.

Table 3.16. Pairwise one-way ANOVA test on PM concentrations and mass ratios with animal building type as a factor.

Building ^a	TSP conc.		PM ₁₀ conc.		PM _{2.5} conc.		PM ₁₀ /TSP ^b		PM _{2.5} /TSP		PM _{2.5} /PM ₁₀	
	Δ ^c	p ^{d,e}	Δ	p	Δ	P	Δ	p	Δ	p	Δ	p
F-G	0.10	0.99	0.27	0.65	0.27	0.66	0.17	0.42	0.18	0.79	0.01	1.00
F-W	-0.16	0.93	0.08	1.00	0.29	0.63	0.24	0.13	0.45	0.03	0.22	0.43
F-FN	-0.16	0.94	0.07	1.00	0.10	0.99	0.23	0.16	0.26	0.47	0.03	1.00
F-L	-0.48	0.06	-0.35	0.37	-0.17	0.93	0.14	0.67	0.31	0.24	0.17	0.63
F-T	-0.74	0.00	-0.52	0.05	-0.12	0.98	0.22	0.16	0.62	0.00	0.40	0.01
G-W	-0.26	0.65	-0.19	0.90	0.02	1.00	0.07	0.98	0.28	0.38	0.21	0.46
G-FN	-0.25	0.67	-0.20	0.88	-0.17	0.94	0.06	0.99	0.08	0.99	0.02	1.00
G-L	-0.58	0.01	-0.61	0.01	-0.45	0.16	-0.04	1.00	0.13	0.93	0.17	0.67
G-T	-0.84	0.00	-0.79	0.00	-0.40	0.27	0.05	0.99	0.44	0.03	0.39	0.01
W-FN	0.00	1.00	-0.01	1.00	-0.19	0.92	-0.01	1.00	-0.20	0.75	-0.19	0.61
W-L	-0.32	0.42	-0.42	0.20	-0.47	0.15	-0.10	0.88	-0.15	0.90	-0.04	1.00
W-T	-0.58	0.02	-0.59	0.02	-0.41	0.26	-0.02	1.00	0.17	0.85	0.18	0.61
FN-L	-0.32	0.40	-0.42	0.21	-0.27	0.69	-0.09	0.92	0.05	1.00	0.14	0.81
FN-T	-0.58	0.01	-0.59	0.02	-0.22	0.85	0.00	1.00	0.36	0.12	0.37	0.03
L-T	-0.26	0.62	-0.17	0.92	0.05	1.00	0.09	0.93	0.31	0.22	0.22	0.35
P-S	0.56	0.00	0.54	0.00	0.31	0.01	-0.02	0.68	-0.25	0.01	-0.23	0.00

a. F-farrowing, G-gestation, W- weaning, FN-finishing, L-layer hen, T- tom turkey, P- poultry, and S- swine; F-G refers to a comparison between farrowing and gestation buildings.

b. PM₁₀/TSP represents the ratio of PM₁₀ to TSP concentrations. The same abbreviation principle applies to PM_{2.5}/TSP and PM_{2.5}/PM₁₀.

c. Δ refers to the difference between the means of two groups.

d. The letter p refers to the p value.

e. The p value was highlighted in bold fonts when smaller than 0.05.

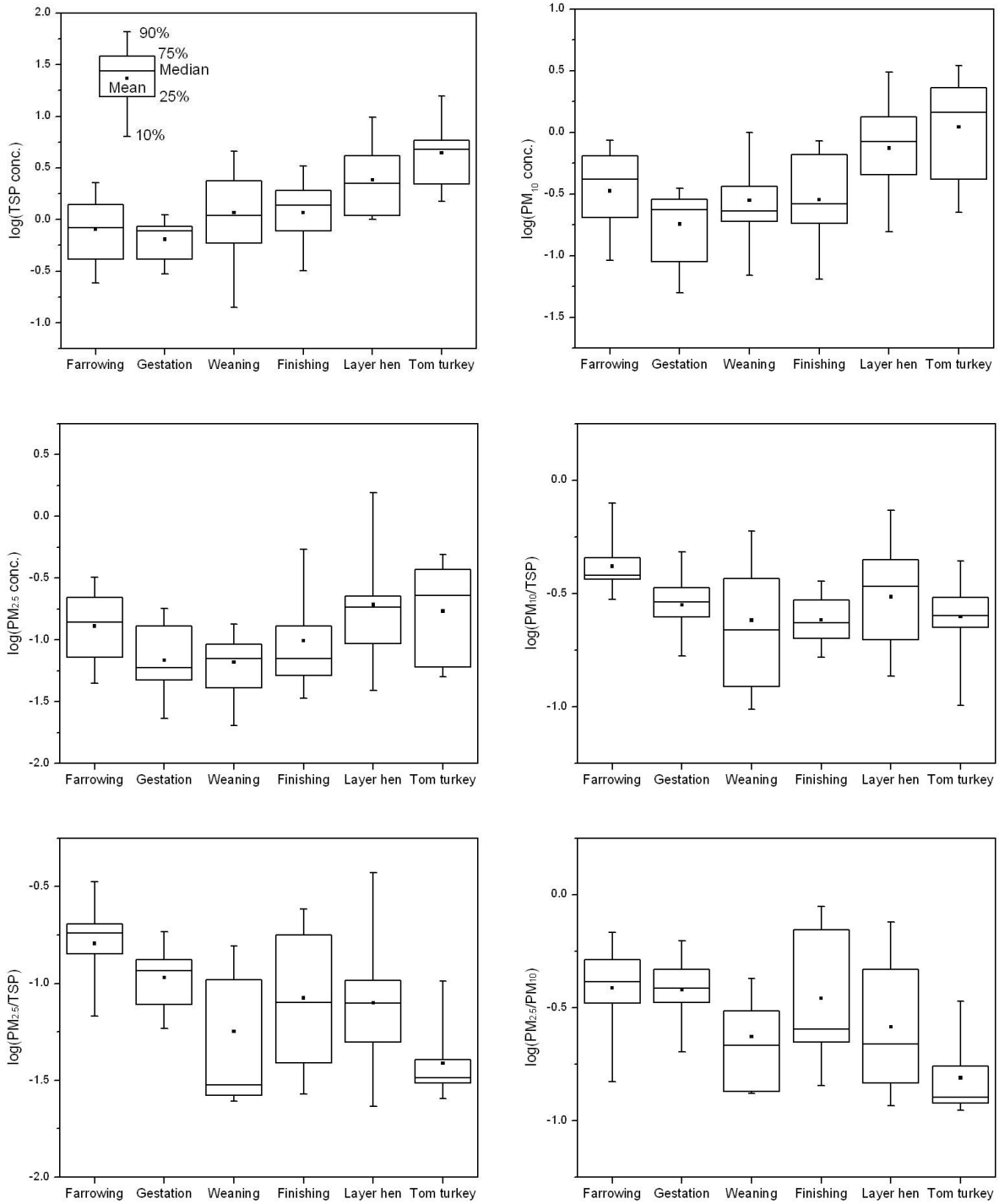


Figure 3.13. Effect of animal building type on PM concentrations and mass ratios.

Animal density was found to have no significant effect on PM concentrations and PM mass ratios (Figure 3.14). The calculation of Pearson's correlation coefficients (r) revealed that PM concentrations and mass ratios were poorly correlated with animal density; all correlations were

insignificant, as indicated by the p values (Table 3.17). It must be noted that the data of animal density in manure-belt layer hen buildings were incomparable with those in other animal buildings because of the multiple-tier battery cage system. Indeed, animal building type is a major factor that defines the range and potential implications of animal density. For example, animal density did not change greatly in gestation and farrowing buildings because only mother pigs and new borne piglets are housed in these buildings and their total body weights were relatively constant. Therefore, a proper assessment of the effect of animal density would require classifying the test data into multiple groups according to animal building type. However, even after grouping (a similar method is ANCOVA but not shown here), no significant effect of animal density was observed (Table 3.17). In finishing and manure-belt layer hen buildings, the calculated correlation coefficients were greater than 0.49 for the case of TSP, PM₁₀ and PM_{2.5} concentrations, suggesting a weak correlation between animal density and PM concentration; however, the corresponding p values were all higher than 0.05, indicating that the identified weak correlation is not statistically significant. In conclusion, animal density is not an affecting factor on PM concentrations or mass ratios.

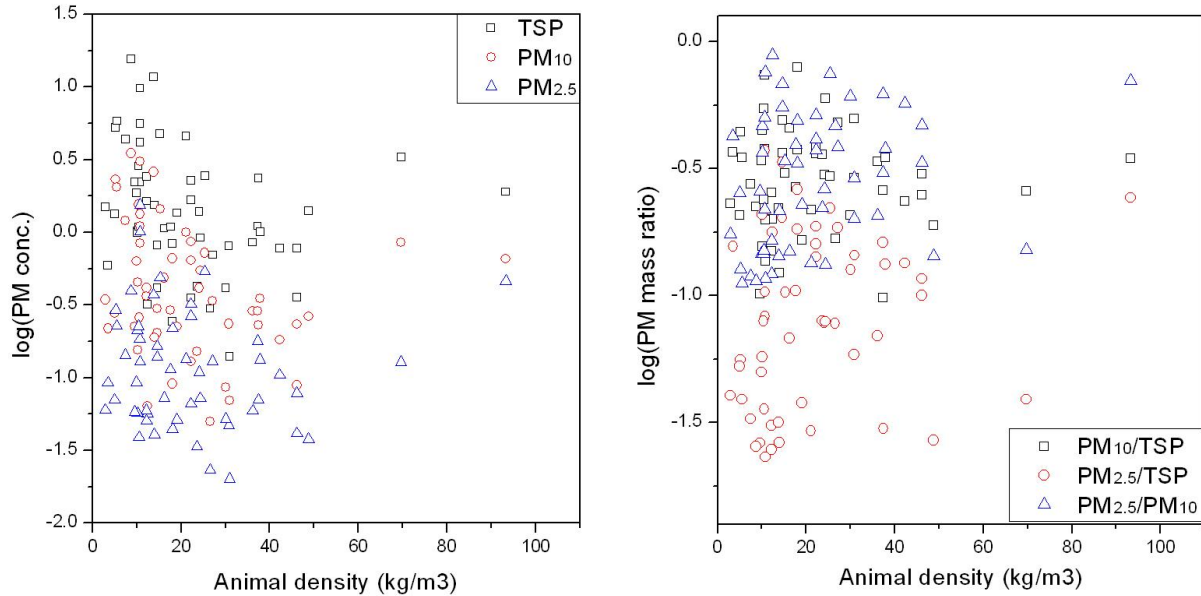


Figure 3.14. Effect of animal density on PM concentrations and mass ratios.

Table 3.17. Correlation between animal density and PM concentrations (mass ratios).

Building type	Statistic	Animal density versus					
		TSP conc.	PM ₁₀ conc.	PM _{2.5} conc.	PM ₁₀ /TSP	PM _{2.5} /TSP	PM _{2.5} /PM ₁₀
All types	r	-0.211	-0.213	-0.069	-0.009	0.191	0.252
	p	0.129	0.126	0.623	0.949	0.171	0.069
Farrowing	r	0.410	0.239	0.151	-0.443	-0.400	-0.183
	p	0.273	0.536	0.699	0.233	0.286	0.637
Gestation	r	0.195	0.167	0.175	0.088	0.056	-0.013
	p	0.615	0.668	0.653	0.822	0.886	0.974
Weaning	r	-0.080	-0.167	-0.302	-0.071	-0.122	-0.111
	p	0.851	0.692	0.468	0.868	0.773	0.793
Finishing	r	0.509	0.615	0.491	0.446	0.125	-0.024
	p	0.162	0.078	0.180	0.229	0.749	0.951
Layer hen	r	0.639	0.527	0.498	-0.048	0.105	0.173
	p	0.064	0.145	0.172	0.903	0.788	0.656
Tom turkey	r	0.231	0.107	0.305	-0.200	0.203	0.429
	p	0.550	0.783	0.424	0.606	0.600	0.249

Season was found to have a great effect on PM concentrations but little effect on PM mass ratios (Figure 3.15). Because each animal building was visited in three different seasons (repeated sampling), paired t-tests, which are statistically more powerful than unpaired t-tests and ANOVA, were employed to evaluate the effect of seasons. As mentioned previously, PM samplers were installed at the manure drying zones in two layer hen buildings (Q and P). The measured PM concentrations were greatly affected the cleanliness of the manure drying zone, and did not exhibit a noticeable seasonal variation. Accordingly, the data of PM concentrations and mass ratios from these two building were excluded in paired t-tests.

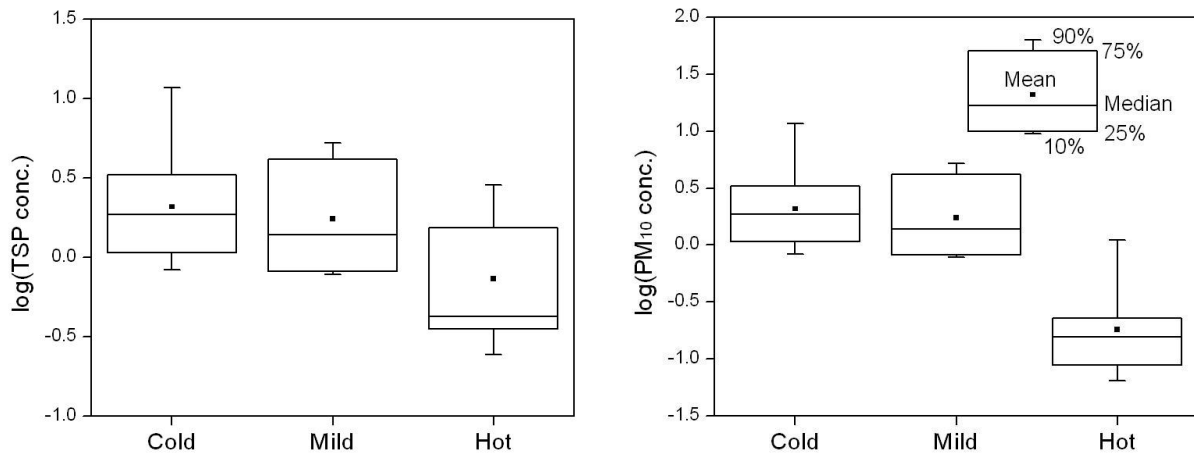


Figure 3.15. Effect of seasons on PM concentrations and mass ratios.

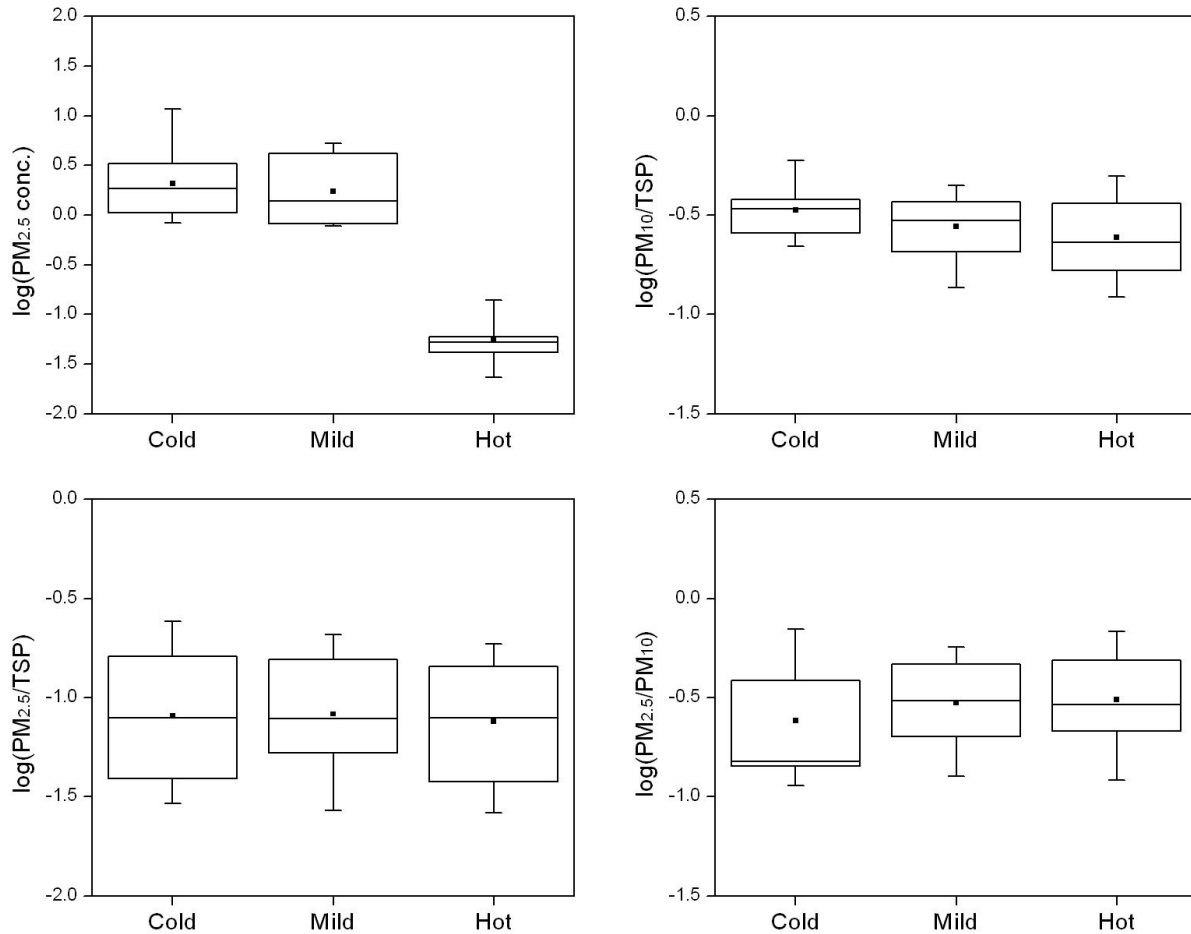


Figure 3.15. (cont.)

The test results (Table 3.18) showed that PM (TSP, PM_{10} and $\text{PM}_{2.5}$) concentrations in cold seasons were significantly higher than those in mild seasons and PM concentrations in mild seasons were again significantly higher than those in hot seasons. Season also had a certain impact on PM mass ratio- the fraction of PM_{10} in TSP in cold seasons was significantly greater than their counterparts in hot seasons. A plausible explanation to this is that lower ventilation rates in cold seasons lead to lower air velocity in animal barns, and accordingly the suspension and re-suspension of larger particles are alleviated. On the other hand, the gravimetric settlement of larger particles was enhanced due to the elongated air retention time in animal buildings. Consequently, TSP samples collected at exhaust likely contain a higher fraction of small particles (PM_{10}) in cold seasons. However, this explanation did not work for the fraction of $\text{PM}_{2.5}$ in TSP and PM_{10} samples ($\text{PM}_{2.5}/\text{TSP}$ and $\text{PM}_{2.5}/\text{PM}_{10}$). There must be some other factors affecting the production and elimination of $\text{PM}_{2.5}$ in animal buildings. We speculated that $\text{PM}_{2.5}$

may originate from different sources and therefore may have different chemical composition and physical properties than TSP and PM₁₀. However, relevant information has been quite limited to date.

Table 3.18. Paired t-tests on PM concentrations and mass ratios with season as a factor.

Seasons	statistic	TSP conc.	PM ₁₀ conc.	PM _{2.5} conc.	PM ₁₀ /TSP	PM _{2.5} /TSP	PM _{2.5} /PM ₁₀
Cold- Mild	Δ	0.162	0.257	0.222	0.094	0.060	-0.035
	p ^a	0.014	<0.001	0.028	0.063	0.560	0.679
Cold- Hot	Δ	0.544	0.716	0.593	0.172	0.049	-0.123
	p	<0.001	<0.001	<0.001	0.001	0.542	0.107
Mild- Hot	Δ	0.389	0.472	0.380	0.083	-0.009	-0.092
	p	<0.001	<0.001	<0.001	0.193	0.892	0.123

a. The p value was highlighted in bold fonts when smaller than 0.05.

PM mass concentrations and mass ratios were also correlated to the daily average ambient temperatures (Figure 3.16). The calculated correlation coefficients and p values (Table 3.19) confirmed the significant effect of seasons on PM mass concentrations. As an affecting factor, season was selected as an independent variable for linear modeling.

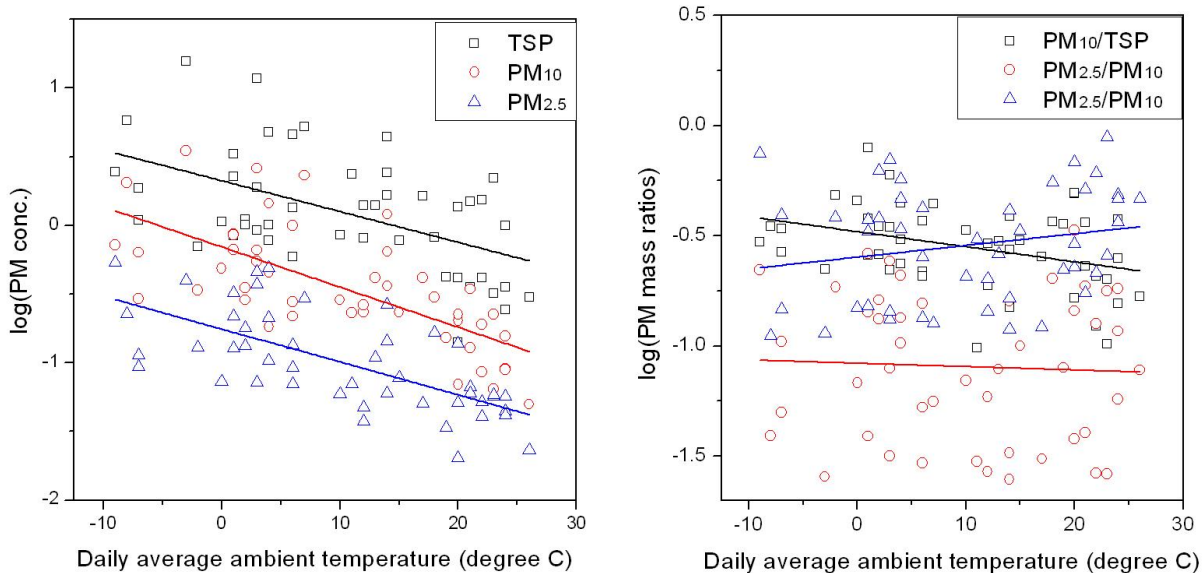


Figure 3.16. Effect of ambient temperature on PM concentrations and mass ratios.

Table 3.19. Correlation between ambient temperature and PM concentrations (mass ratios).

Statistic	Daily average ambient temperature versus					
	TSP conc.	PM ₁₀ conc.	PM _{2.5} conc.	PM ₁₀ /TSP	PM _{2.5} /TSP	PM _{2.5} /PM ₁₀
r	-0.315	-0.414	-0.317	-0.228	0.209	0.028
p ^a	0.022	0.002	0.021	0.100	0.133	0.839

a. The p value was highlighted in bold fonts when smaller than 0.05.

Feeding system was found to have a certain influence on PM concentrations and mass ratios (Figure 3.17). The ANOVA test results (Table 3.20) revealed that animal buildings equipped with dry feeding systems had significantly higher TSP and PM₁₀ concentrations but lower PM_{2.5} to PM₁₀ mass ratios than those with wet feeding systems. As mentioned previously, animal feed (mainly grain meals and starch granules) and water are mixed in wet feeding systems. This reduces the aerosolization of feed particles, thereby leading to lower PM concentrations. However, this feeding approach might be less effective for the control of fine particles such as PM_{2.5} because fine particles were found to have lower feed contents than course particles and might primarily originate from fecal materials (Feddes et al., 1992; Heber et al., 1988a). In this regards, higher PM_{2.5} to PM₁₀ mass ratios (PM_{2.5}/PM₁₀) are a reasonable observation with wet feeding systems.

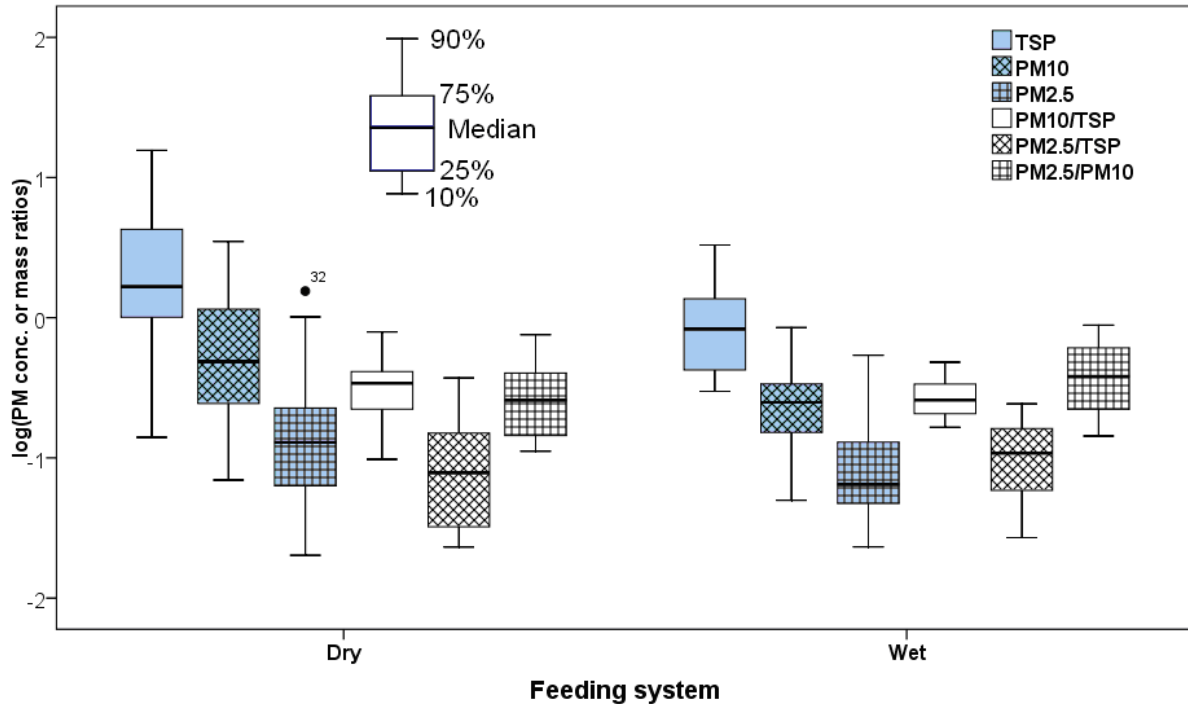


Figure 3.17. Effect of feeding system on PM concentrations and mass ratios.

Table 3.20. ANOVA tests on PM concentrations and mass ratios- dry versus wet feeding systems.

statistic	TSP conc.	PM ₁₀ conc.	PM _{2.5} conc.	PM ₁₀ /TSP	PM _{2.5} /TSP	PM _{2.5} /PM ₁₀
Δ	0.318	0.375	0.205	0.057	-0.113	-0.170
p ^a	0.011	0.003	0.081	0.330	0.257	0.025

a. The p value was highlighted in bold fonts when smaller than 0.05.

It must be noted that the configuration of feed systems is mainly determined by animal building type, and accordingly the differences in PM concentrations and mass ratios between dry and wet feeding systems might be caused by other building type related factors (e.g., ventilation system) than feed system or feed system only. Therefore, although statistically feed system was identified as an affecting factor, it would not be used for subsequent linear modeling.

3.3.3.3 *Linear modeling*

The following variables were used as predictors for linear modeling:

- Animal building type. Only swine buildings were included in the modeling. Poultry buildings were excluded for three reasons: (1) poultry buildings are substantially different from swine buildings and have only a few datasets; (2) tom turkey buildings are incomparable to manure-belt layer hen buildings on many aspects, e.g., ventilation system; (3) the configuration of layer hen building R is appreciably different from building P and Q. These issues inevitably created certain difficulties in linear modeling.
- Seasons. The classification into cold, mild, hot seasons can be ambiguous and inaccurate. To overcome this limitation, daily average ambient temperature was used for linear modeling.
- Specific fan area. In this study, a specific fan area was defined as a ratio of the total fan area over the net volume (space) of an animal confinement building.
- Animal density. Although animal density was not identified as an affecting factor, it may still have certain effects on PM concentrations in swine buildings.

With these variables, a generalized linear model was created as:

$$Y_{ij} = \beta_0 + A_i + \beta_1 T + \beta_2 V + \beta_3 D + \varepsilon_{ij} \quad (3.21)$$

where, Y_{ij} is the estimated PM concentration (in a log form), A_i is the factor of animal building type, T is the daily average ambient temperature ($^{\circ}\text{C}$), V is the specific fan area (m^{-1}), D is the animal density (kg/m^3), β_0 , β_1 , β_2 and β_3 are regression coefficients, and ε_{ij} is the error. Parameter estimation and other relevant analysis were performed with SPSS v17.0. A linear scale response model was selected and a maximum likelihood estimation method was used for model fitting.

For the prediction of TSP concentrations, daily average ambient temperature was found to be of statistical significance; animal building type and specific fan area were also of significance but to a less degree (Table 3.21). However, the low R^2 value suggested that the prediction power of the given model was quite limited. For the prediction of PM_{10} concentrations, animal building type, daily average ambient temperature, animal density and specific fan area were all found to be of significance. The R^2 value was higher than that for TSP concentrations, indicating an improved prediction power. For the prediction of $PM_{2.5}$ concentrations, animal building type and daily average ambient temperature were found of significance; animal density was significant but to a less degree. Overall, PM concentrations decreased with specific fan area but increase with animal density, as indicated by their corresponding regression coefficients. This is understandable because a lower specific fan area means potentially lower building ventilation rates while an increase in animal density may lead to an increase in animal activity.

A similar linear model was created but with non-log-transformed PM concentrations as the dependent variable. Correspondingly, a gamma-with-log-link scale response model was selected in SPSS because the concentration of TSP, PM_{10} and $PM_{2.5}$ followed the gamma distribution fairly well (data not shown here). Similar observations were made from model fitting, e.g., the predictors of significance. The derived R^2 values were even lower: 0.388 for TSP, 0.609 for PM_{10} and 0.502 for $PM_{2.5}$.

The linear models proposed above would not be recommended for predicting PM concentrations in swine buildings because the associated R^2 values were all less than 0.75. A model modification therefore was desired to improve the fitting performance. It is well recognized that TSP monitoring in animal confinement buildings is more convenient and more reliable than PM_{10} and $PM_{2.5}$ monitoring because of issues such as equipment portability and sampler overloading. Many previous studies measured only TSP concentrations and some of them then estimated PM_{10} and $PM_{2.5}$ concentrations from TSP concentrations and PSD data (Cao et al., 2009; Jerez, 2007; Lacey et al., 2003; Wang, 2000). In addition, since the R^2 value for TSP concentration modeling was very low, a field measurement of TSP is of necessity and can hardly be substituted by modeling. So, here comes a question- Can PM_{10} and $PM_{2.5}$ concentrations be predicted with known TSP concentrations?

Table 3.21. Parameter estimates and goodness-of-fit of PM concentration models.

	Parameters	β	Std. error	95% Wald confidence interval		Hypothesis test
				Lower	Upper	Significance
TSP	(intercept)	0.457	0.2066	0.052	0.862	0.027
	Type	-	-	-	-	0.066
	[Type=farrowing]	0.005	0.1375	-0.265	0.274	0.972
	[Type=finishing]	-0.102	0.1327	-0.363	0.158	0.440
	[Type=gestation]	-0.307	0.1470	-0.660	-0.083	0.012
	[Type=weaning]	0 ^a	-	-	-	-
	T	-0.018	0.0046	-0.027	-0.009	0.000
	V	-105.0	62.0	-226.5	16.5	0.090
	D	0.004	0.0028	-0.002	0.009	0.192
Deviance/df= 0.078				R ² = 0.458		
PM ₁₀	(intercept)	-0.100	0.1444	-0.384	0.183	0.487
	Type	-	-	-	-	0.000
	[Type=farrowing]	0.267	0.0961	0.078	0.455	0.006
	[Type=finishing]	-0.113	0.0928	-0.295	0.069	0.224
	[Type=gestation]	-0.290	0.1027	-0.492	-0.089	0.005
	[Type=weaning]	0 ^a	-	-	-	-
	T	-0.026	0.0032	-0.032	-0.020	0.000
	V	-105.5	43.3	-190.5	-20.6	0.015
	D	0.004	0.0020	0.000	0.008	0.036
Deviance/df = 0.038				R ² = 0.727		
PM _{2.5}	(intercept)	-0.874	0.1627	-1.193	-0.555	0.000
	Type	-	-	-	-	0.001
	[Type=farrowing]	0.426	0.1083	0.214	0.638	0.000
	[Type=finishing]	0.080	0.1045	-0.125	0.284	0.446
	[Type=gestation]	-0.028	0.1158	-0.255	0.199	0.807
	[Type=weaning]	0 ^a	-	-	-	-
	T	-0.024	0.0036	-0.031	-0.017	0.000
	V	-56.9	48.8	-152.5	38.77	0.244
	D	0.004	0.0022	0.000	0.008	0.099
Deviance/df = 0.049				R ² = 0.650		

a. Set to zero because weaning buildings were coded as the reference level.

By incorporating an item of TSP concentrations, an alternative linear model was created as:

$$Y_{ij} = \beta_0 + A_i + \beta_1 T + \beta_2 V + \beta_3 D + \beta_4 [TSP] + \varepsilon_{ij} \quad (3.22)$$

Where, [TSP] refers to TSP concentration and β_4 is a new added regression coefficient. Parameter estimation and other relevant analyses basically followed the same protocols as applied to Equation 3.21.

For the prediction of PM_{2.5} concentrations, animal building type, daily average ambient temperature and TSP concentration were found to be of statistical significance (Table 3.22). However, the R² value was only slightly higher than that of the unmodified model, indicating that incorporating TSP concentration did not significantly improve the predictive power. As mentioned previously, the majority of PM_{2.5} may originate from fecal materials; in contrast, most

course particles in TSP may come from feed. In reality, a much poorer correlation ($r = 0.564$) was found between TSP and $PM_{2.5}$ concentration than that ($r = 0.840$) between TSP and PM_{10} concentrations. This may be a reason why the modified $PM_{2.5}$ concentration model had only a slight improvement.

Table 3.22. Parameter estimates and goodness-of-fit of modified PM concentration models.

	Parameters	β	Std. error	95% Wald confidence interval		Hypothesis test
				Lower	Upper	Significance
PM ₁₀	(intercept)	-0.360	0.0899	-0.536	-0.184	0.000
	Type	-	-	-	-	0.000
	[Type=farrowing]	0.264	0.0560	0.154	0.374	0.000
	[Type=finishing]	-0.055	0.0545	-0.161	0.052	0.317
	[Type=gestation]	-0.079	0.0651	-0.207	0.048	0.224
	[Type=weaning]	0 ^a	-	-	-	-
	T	-0.015	0.0023	-0.020	-0.011	0.000
	V	-45.9	26.3	-97.4	5.6	0.081
	D	0.002	0.0012	0.000	0.004	0.081
	TSP	0.568	0.0689	0.433	0.703	0.000
Deviance/df = 0.013				R ² = 0.907		
PM _{2.5}	(intercept)	-0.993	0.1639	-1.314	-0.672	0.000
	Type	-	-	-	-	0.000
	[Type=farrowing]	0.425	0.1022	0.225	0.625	0.000
	[Type=finishing]	0.106	0.0994	-0.089	0.301	0.285
	[Type=gestation]	0.069	0.1188	-0.164	0.301	0.564
	[Type=weaning]	0 ^a	-	-	-	-
	T	-0.019	0.0041	-0.027	-0.011	0.000
	V	-29.5	47.9	-123.4	64.4	0.538
	D	0.003	0.0022	-0.002	0.007	0.208
	TSP	0.261	0.1256	0.015	0.507	0.038
Deviance/df = 0.045				R ² = 0.689		

a. Set to zero because weaning buildings were coded as the reference level.

For the prediction of PM_{10} concentrations, animal building type, daily average ambient temperature and TSP concentration were identified to be of statistical significance; specific fan area and animal density were also significant but to a less degree ($p < 0.1$). By adding TSP concentration as a predictor, the R^2 value was significantly improved from 0.727 to 0.907, making it plausible to apply the modified model for estimating PM_{10} concentrations.

A simplification of the modified PM_{10} concentration model was conducted based on AIC; however, no predictor was removed (data not shown here). The normality of regression residuals was checked with the Shapiro-Wilk test and the result was positive ($W = 0.988$, $p = 0.962$). The model also passed other diagnostic tests (mostly graphic), such as outlier and model structure tests. The Chi-square test of independence revealed that all predictors were independent from each other through (data not shown here).

Two extra sampling datasets, including PM concentrations, building information, and environmental and operational conditions, were employed to test the model performance (Figure 3.18). The first dataset was collected in a finishing building in summer, from which a PM₁₀ concentration was estimated to be 0.150 mg/m³ with a 95% confidence interval (CI) of [0.117, 0.193] mg/m³. The measured concentration, however, was 0.220 mg/m³, 47% higher than the predicted value. The second dataset was from a weaning building in fall. The estimated PM concentration was 0.437 mg/m³ with a 95% CI of [0.355, 0.536] mg/m³; while the measured concentration was 0.352 mg/m³, 19% lower than the predicted value. These examples show that the proposed model can provide a reasonable but rough estimate of PM₁₀ concentration. The estimated PM₁₀ concentrations may be used as a reference for selecting the appropriate sampling period and flow rate before starting an elaborate field trip. Field sampling of PM₁₀ is still essential and should not be replaced by modeling for any reasons.

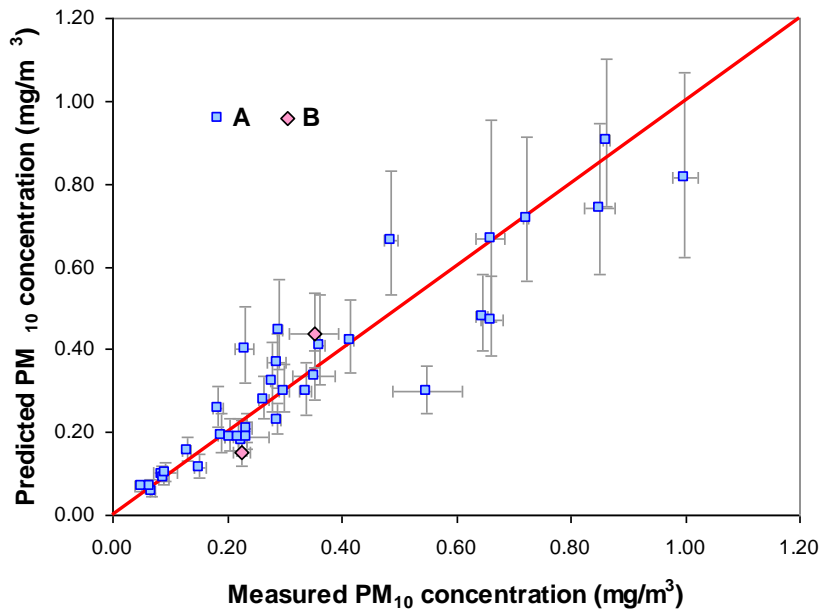


Figure 3.18. Measured versus predicted PM₁₀ concentrations: A- datasets for regression, B- datasets for validation, error bars represent the 95% confidence level.

There were certain limitations of the proposed PM₁₀ concentration model. First, PM₁₀ concentration was assumed to be linearly related to daily average ambient temperature, animal density, specific fan area and TSP concentration. However, such linear relationships are questionable. For example, when ambient temperature is over a certain level, the ventilation rate will reach its highest capacity and cannot be increased furthermore. Consequently, a ventilation-

induced change in PM₁₀ concentrations is likely to have a non-linear response to ambient temperature. Second, the number of datasets was quite limited for modeling. More datasets will be required for parameter estimation and for validating the model performance. Third, all swine buildings visited were located in Illinois; therefore, the proposed PM₁₀ concentration model might only work for the regions with similar meteorological conditions and comparable swine building designs.

3.3.3.4 Uncertainty analysis of the proposed linear model

The modified PM₁₀ concentration model contained seven predictors, and their corresponding sensitivity coefficients were listed in Table 3.23. For animal building type, there was no measurement error; for daily average ambient temperature, the measurement error was estimated to be $\pm 2^\circ\text{C}$; for specific fan area, the measurement error was estimated to be $\pm 5\%$ or $\pm 0.00012 \text{ m}^{-1}$; for animal density, the measurement error was estimated to be $\pm 5\%$ or $\pm 1.2 \text{ kg/m}^3$; for TSP concentration, because each field trip produced a standard deviation, the overall measurement error was estimated to be $\pm 7\%$ or $\pm 0.101 \text{ mg/m}^3$ by averaging the standard deviations from all individual field trips. Accordingly, the uncertainty of the model output induced by measurement errors, $\sigma_{\log[PM_{10}]}^A$, was calculated as:

$$\sigma_{\log[PM_{10}]}^A = \sqrt{(-0.015 \times 2)^2 + (-45.9 \times 0.00012)^2 + (0.002 \times 1.2)^2 + (0.568 \times 0.101)^2} = 0.065$$

The measurement of TSP concentration was found to contribute the most uncertainty, followed by daily average ambient temperature.

Another type of uncertainty is directly associated with the predicted response, presented in terms of the confidence intervals for predictions (also called prediction intervals):

$$y_0 \pm t_{n-p}^{(\alpha/2)} \sigma \sqrt{x_0^T (X^T X)^{-1} x_0}$$

Where, y_0 is the predicted response, in this case, the model estimated PM₁₀ concentration, $t_{n-p}^{(\alpha/2)}$ is the t-critical value at a $(1-\alpha)$ confidence level on $n-p$ degrees of freedom, n is the number of datasets used for linear modeling, p is the number of predictors, σ is the residual standard error on $n-p$ degrees of freedom, x_0 is a set of predictors and X is the vector of regression

coefficients. It can be seen that the confidence intervals for predictions actually vary with predictors.

Table 3.23. Sensitivity coefficients and measurement errors of predictors in the modified PM₁₀ concentration model.

Predictor ^a	Type=farrowing	gestation	weaning	T	V	D	TSP
Sensitivity coefficient	0.264	-0.079	-0.055	-0.015	-45.9	0.002	0.568
Measurement error ^b	0.000	0.000	0.000	2°C	0.00012 m ⁻¹	0.95 kg/m ³	0.101 mg/m ³

a. A_i can be considered as the product of a regression coefficient vector (1×3) multiplied by a dummy variable matrix (3×3) and therefore consists of three independent predictors.

b. A measurement error was presented in terms of standard deviation.

To assess the latter type of uncertainty, the residual standard error was calculated as:

$$\sigma_{\log[PM_{10}]}^B = \sigma = \sqrt{\frac{RSS}{n-p}} = 0.116$$

Where, RSS refers to the residual sum of squares. An extra dataset (finishing, summer) was used to calculate $\sqrt{x_0^T (X^T X)^{-1} x_0}$, 0.478 in this case. So:

$$\sigma_{\log[PM_{10}]}^B = \sigma \sqrt{x_0^T (X^T X)^{-1} x_0} = 0.055$$

Because those two types of uncertainties were independent, the overall uncertainty could be estimated as:

$$\sigma_{\log[PM_{10}]} = \sqrt{(\sigma_{\log[PM_{10}]}^A)^2 + (\sigma_{\log[PM_{10}]}^B)^2} = \sqrt{0.055^2 + 0.065^2} = 0.085$$

This was equivalent to a 95% relative confidence interval of [68%, 148%] for predicted PM₁₀ concentrations (non-log form).

3.3.4 Validity of Calculating PM₁₀ and PM_{2.5} concentrations from PSD data and TSP concentrations

3.3.4.1 Data preparation and transformation

The ratios of the calculated to the measured PM₁₀ and PM_{2.5} concentrations (abbreviated as R_{PM10} and R_{PM2.5}, respectively) were computed and summarized in Table 3.24. DSP and Coulter were found to produce extremely low and, in many cases, even zero PM_{2.5} concentrations, regardless of the calculation approach and selected d_j. For Horiba and Malvern, the situation was

better but still a number of zero $PM_{2.5}$ concentrations were generated. An investigation on measured PSD curves revealed that although the detection sizes of DSP and Coulter stretch into the submicron range, almost no particles smaller than 2.5 μm were detected, which is against a common sense that at least the influent ambient aerosols would contribute certain $PM_{2.5}$ concentrations in animal confinement buildings. Accordingly, the detection capacity of both analyzers on fine particles is questionable. The PSD data derived from DSP and Coulter cannot and should not be used for estimating the concentration of $PM_{2.5}$ or even smaller particles. Comparatively, the calculated PM_{10} concentrations were apparently more reasonable although averagely they were still lower than the measured PM_{10} concentrations.

Table 3.24. Ratios of calculated to measured PM_{10} and $PM_{2.5}$ concentrations- A summary.

d_j	Approach	Particle size analyzer	$R_{PM_{10}}$			$R_{PM_{2.5}}$		
			Mean	SD	N	Mean	SD	N
average diameter	A	Horiba	0.564	0.341	74	0.365	0.521	67
		DSP	0.571	0.179	35	0.007	0.007	32
		Coulter	0.859	0.348	37	0.002	0.008	33
		Malvern	0.809	0.346	37	0.497	0.346	33
	B	Horiba	0.595	0.339	74	0.295	0.410	68
		DSP	0.769	0.232	35	0.010	0.010	33
		Coulter	0.880	0.339	37	0.006	0.020	34
		Malvern	0.794	0.338	37	0.464	0.324	34
maximum diameter	A	Horiba	0.528	0.337	74	0.327	0.469	67
		DSP	0.557	0.176	35	0.006	0.007	32
		Coulter	0.854	0.348	37	0.002	0.007	33
		Malvern	0.778	0.312	37	0.469	0.329	33
	B	Horiba	0.543	0.316	74	0.287	0.387	68
		DSP	0.728	0.219	35	0.009	0.009	33
		Coulter	0.873	0.337	37	0.005	0.019	34
		Malvern	0.755	0.314	37	0.436	0.307	34

The data of $R_{PM_{10}}$ were then subject to normality tests (Shapiro-Wilk test). A substantial departure from the normal distribution was found for the data derived from Horiba, Coulter and Malvern (Table 3.25). Accordingly, a log transformation was conducted, which significantly improved the normality of test data. To be consistent, the ratio data derived from DSP were also transformed. However, for the data of $R_{PM_{2.5}}$, no log transformation was done because of the presence of zero data points.

Table 3.25. Normality of the original and log-transformed ratio data.

d _j	Approach	Particle size analyzer	Original		Log-transformed		N
			W	p ^a	W	p	
average diameter	A	Horiba	0.9002	<0.001	0.9835	0.450	74
		DSP	0.9740	0.562	0.9648	0.318	35
		Coulter	0.9340	0.030	0.9589	0.187	37
		Malvern	0.9250	0.016	0.9707	0.427	37
	B	Horiba	0.9111	<0.001	0.9845	0.503	74
		DSP	0.9634	0.289	0.9702	0.449	35
		Coulter	0.9375	0.039	0.9631	0.253	37
		Malvern	0.9284	0.020	0.9751	0.564	37
maximum diameter	A	Horiba	0.8957	<0.001	0.9822	0.381	74
		DSP	0.9757	0.617	0.9655	0.331	35
		Coulter	0.9323	0.026	0.9579	0.174	37
		Malvern	0.9557	0.147	0.9678	0.352	37
	B	Horiba	0.9002	<0.001	0.9835	0.450	74
		DSP	0.9740	0.562	0.9648	0.318	35
		Coulter	0.9340	0.030	0.9589	0.187	37
		Malvern	0.9250	0.016	0.9707	0.427	37

a. The p value was highlight in bold fonts when greater than 0.05.

3.3.4.2 Test of hypothesis A

Hypothesis A- Approach A would consistently produce smaller PM₁₀ (or PM_{2.5}) mass concentrations than approach B even with field-measured PSD data and the penetration curve of the ideal PM₁₀ (or PM_{2.5}) sampler. The test results were divided into two separate sections according to the selected d_j.

Average diameter as d_j

The data of R_{PM10} derived from approach A and B were compared, as shown in Figure 3.19. For Horiba, DSP and Coulter, approach A produced averagely smaller R_{PM10} values than approach B; while for Malvern, the median R_{PM10} value from approach A was slightly greater than that from approach B. Hypothesis A, therefore, should be rejected. More direct evidence came from paired t-tests on PM₁₀ concentrations calculated from different approaches (Table 3.26). The test results showed that for Malvern, approach A produced significantly higher mean PM₁₀ concentrations than approach B. Additional counter examples against hypothesis A were found from the calculation results derived from Horiba and Coulter, where, in respectively 11% and 46% individual cases, approach A actually generated higher PM₁₀ concentrations than approach B.

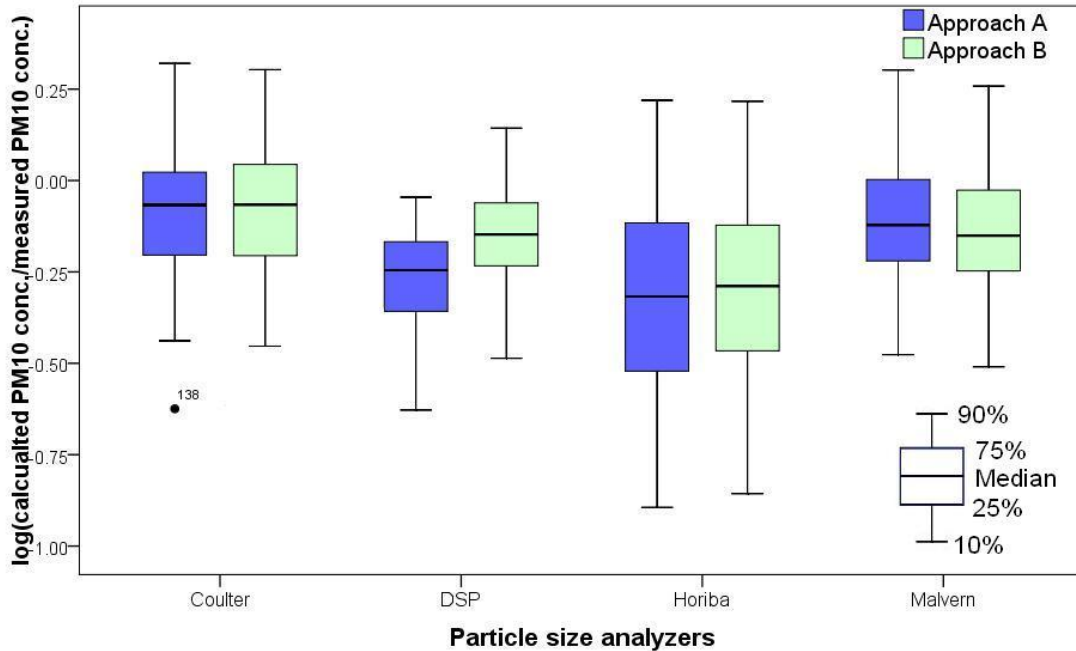


Figure 3.19. Comparison of $R_{PM_{10}}$ values derived from different approaches and different particle size analyzers.

Table 3.26. Paired t-tests on PM_{10} concentrations derived from different approaches.

Approach	Statistic	Horiba	DSP	Coulter	Malvern
A versus B	Δ (mg/m^3)	-0.011	-0.120	-0.004	0.013
	p^a	<0.001	<0.001	0.512	0.017

a. The p value was highlight in bold fonts when smaller than 0.05.

Maximum diameter as d_j

Similarly, for Malvern, approach A produced a slightly higher median $R_{PM_{10}}$ value than approach B. Paired t-test results revealed that for Malvern, PM_{10} concentrations derived from approach A were significantly greater ($\Delta=0.017$ mg/m^3 , $p=0.018$) than those from approach B. Counter examples against hypothesis A were also observed from Horiba and Coulter (41% and 51% of total cases, respectively).

The occurrence of counter examples against hypothesis A was ascribed to two reasons. First, the formation of hypothesis A was based on an assumption that the PSD curves of PM in animal buildings follow a lognormal distribution; however, field-measured PSD profiles were highly diverse and might greatly deviate from the assumed distribution. For instance, a field-measured PSD profile in animal buildings could be left-skewed, or have a minor or a tail peak (Figure 3.20) in the size range less than $10 \mu m$. In any of those cases, the mass fraction of particles smaller than $10 \mu m$ would be higher than that predicted by lognormal distribution, and accordingly

approach A would produce higher PM_{10} concentrations than in the assumed case. Second, another assumption behind hypothesis A is that the penetration curves of FRM/FEM PM_{10} samplers are lognormally distributed; while the penetration curve of ideal PM_{10} samplers is obviously non-lognormal (Figure 3.21). Because of its ‘non-ideal-cut’ penetration curve, the ideal PM_{10} sampler would also over-sample a portion of particles larger than $10\ \mu\text{m}$ while under-sample a portion of particles smaller than $10\ \mu\text{m}$; however, compared to PM_{10} samplers with an assumed lognormal penetration curve, the ideal PM_{10} sampler would over-sample fewer larger particles but under-sample more smaller particles, thereby generating a lower PM_{10} mass concentration. Therefore, it is not surprising that approach B may produce lower PM_{10} concentrations than approach A.

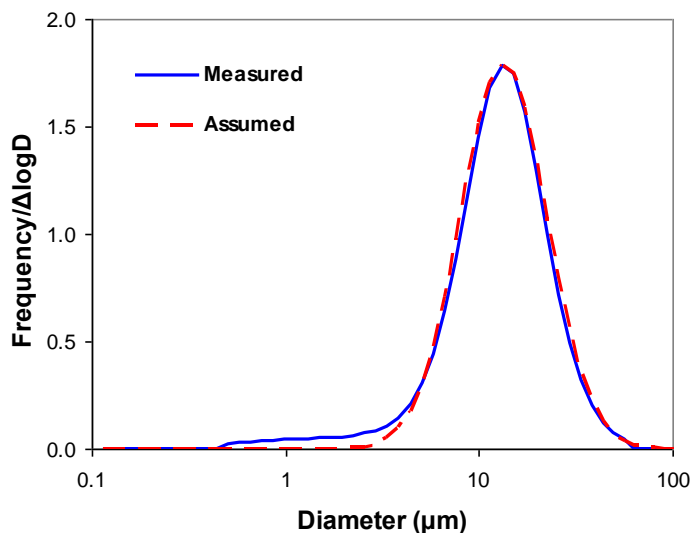


Figure 3.20. Comparison between a measured and an assumed PSD curve with identical MMD and GSD. The measured PSD curve has a tail peak in the size range of 0.5 to $5\ \mu\text{m}$.

Similar examinations were performed on the data of $PM_{2.5}$ but only on those derived from Malvern and Horiba because only these two analyzers offered reasonable estimates of $PM_{2.5}$ concentrations. Paired t-test results showed that, for both Malvern and Horiba, approach A produced significantly higher $PM_{2.5}$ concentration than approach B (Table 3.27). Hypothesis A, therefore, should be rejected. The occurrence of counter examples against hypothesis A may, similarly, be explained by: (1) the deviation of field-measured PSD profiles for the lognormal distribution, and (2) the non-lognormal penetration curve of the ideal $PM_{2.5}$ sampler.

Table 3.27. Paired t-tests on PM_{2.5} concentrations derived from different approaches.

Approach	Statistic	d _i - average diameter		d _i - maximum diameter	
		Horiba	Malvern	Horiba	Malvern
A versus B	Δ (mg/m ³)	0.009	0.006	0.010	0.006
	p ^a	0.004	<0.001	0.006	<0.001

a. The p value was highlight in bold fonts when smaller than 0.05.

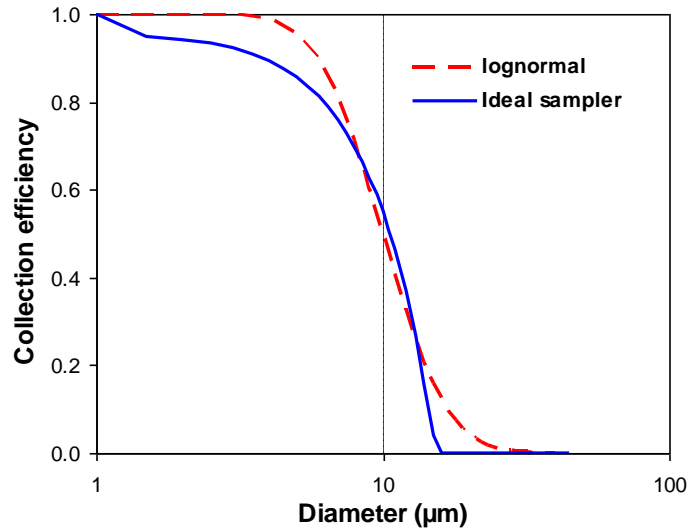


Figure 3.21. Comparison of the penetration curve of an ideal PM₁₀ sampler to the assumed lognormal penetrative curve ($D_{50}= 10 \mu\text{m}$ and slope=1.5).

Because FRM/FEM PM samplers are suppose to have very similar penetration curves to ideal PM samplers, the rejection of hypothesis A indicates that an oversampling by FRM/ FEM PM samplers may not really exist.

3.3.4.3 Test of hypothesis B

Hypothesis B- *PSD data derived from different particle size analyzers would produce identical or very similar PM₁₀ (or PM_{2.5}) mass concentration results.*

It can be seen from Table 3.25 and Figure 3.19 that PM concentrations derived from different particle size analyzers could be substantially different. Hypothesis B, therefore, should be rejected. To further investigate the difference among analyzers, a paired t-test was conducted on the datasets with PSD profiles available from all the four analyzers (Table 3.28). The selected calculation approach was found to have a great influence on the comparison results. For example, with approach A, DSP produced averagely lower PM concentration than Malvern; while, with approach B, the order reversed. Overall, Coulter predicted the highest PM₁₀ concentrations;

while Malvern produced the highest PM_{2.5} concentrations, followed by Horiba. Significantly higher PM_{2.5} concentrations derived from Malvern and Horiba might be related to the detection principle of Mie scattering adopted by both analyzers, which is substantially different from the principle of time-of-flight by DSP and electrical impedance by Coulter; however, the implication of different detection principles is not yet clear. Very similar results were obtained when the maximum diameter was selected as d_j , and, thus, would not be presented here.

Table 3.28. Paired t-tests on PM concentrations derived from different particle size analyzers (N=35, d_j - average diameter).

Analyzer ^a	Approach A				Approach B			
	PM ₁₀		PM _{2.5}		PM ₁₀		PM _{2.5}	
	Δ (mg/m ³)	p ^b	Δ (mg/m ³)	p ^b	Δ (mg/m ³)	p ^b	Δ (mg/m ³)	p ^b
H-D	0.088	0.149	0.084	0.005	0.200	0.010	0.037	<0.001
H-C	-0.239	0.003	0.085	0.005	-0.235	0.002	0.038	<0.001
H-M	-0.125	0.001	-0.005	0.726	-0.104	0.002	-0.011	0.005
D-C	-0.151	0.042	0.001	0.009	-0.035	0.600	0.001	0.132
D-M	-0.037	0.357	-0.089	<0.001	0.095	0.104	-0.048	<0.001
C-M	0.114	0.064	-0.090	<0.001	0.131	0.037	-0.048	<0.001

a. H- Horiba, D- DSP, C- Coulter, M- Malvern; H-D refers to a comparison between Horiba and DSP.

b. The p value was highlight in bold fonts when smaller than 0.05.

3.3.4.4 Comparison with measured PM concentrations.

As concluded from the previous section, different particle size analyzers may produce significantly different PM concentrations. Then, which analyzer should be trusted? If none of them were trustable, which analyzer would offer the best estimates?

In some previous studies, the PSD profiles measured by Coulter were used for calculating PM₁₀ concentrations through approach A, and the calculated concentrations were considered to be the ‘true’ PM₁₀ concentrations (Buser et al., 2007a; Buser et al., 2008; Wang et al., 2005b). However, as revealed by this study, Coulter could not generate reasonable PM_{2.5} concentrations. Because PM_{2.5} is a subfraction of PM₁₀, it is reasonable to question the reliability and ‘trueness’ of PM₁₀ concentrations derived from Coulter.

In the same studies (Buser et al., 2007a; Buser et al., 2008; Wang et al., 2005b), PM₁₀ concentrations measured by FRM/ FEM PM₁₀ samplers were found to be ubiquitously greater than the calculated ‘true’ concentrations. This phenomenon was considered to be due to an oversampling by FRM/FEM PM₁₀ samplers according to the theoretical investigations mentioned previously. However, the rejection of hypothesis A and B revealed that when different assumptions and particle size analyzers were applied, different or even opposite observations

may be obtained. Accordingly, the suggested oversampling may not really exist. Moreover, since the ‘trueness’ of Coulter-derived PM_{10} concentrations is questionable, the occurrence of oversampling becomes debatable.

In fact, the ‘true’ PM_{10} and $PM_{2.5}$ concentrations can hardly be obtained because of the presence of numerous uncertainties during field sampling. The unpredicted PSD is only one of those uncertainties. To address this issue, the USEPA defines the accuracy of PM concentration measurements in a relative sense, as the agreement of a candidate method with a reference method (FRM) (CFR, 2001c; Williams et al., 2000). As an administrative standard, only PM samples collected with FRM and FEM PM samplers may be officially referred to as PM_{10} and $PM_{2.5}$ (Kenny et al., 2000). In other words, if an FRM/FEM PM sampler is properly operated then the measured PM_{10} and $PM_{2.5}$ concentrations will be regulationally trustable. Besides, the penetrative curves of FRM/FEM PM samplers are designed to mimic to the penetration of PM into the human’s respiratory tract; therefore, the ‘oversampled’ particles would also likely enter the corresponding compartment in the human’s respiratory system, and accordingly should not be excluded in evaluation of the health effect of particles. Consequently, we believe that the validity of the calculation method should be determined by how closely its performance is comparable to FRM/ FEM PM samplers, instead of the opposite.

An argument against our point came from a previous experimental study that reported an increase in the 50% cut point (D_{50}) of FRM PM_{10} inlets up to 12.6 μm when sampling cornstarch particles with a MMD of 16 μm (Wang et al., 2005a). This phenomenon, if truly existed, would definitely lead to an oversampling. However, an increase in D_{50} is unlikely to occur to the impactor-based FRM PM_{10} inlet unless the inlet is overloaded and, thus, fails to retain large particles in the impacting cup. Instead, according to Equation 3.24 and 3.25 (Zhang, 2005), an accumulation of large particles in the impacting cup would reduce the distance between the nozzle and the impacting plate (L), thereby leading to a decrease in D_{50} . In addition, in the same study, the D_{50} was determined based on Coulter-derived PSD data. The accuracy of this measurement method is questionable. In summary, there was no solid evidence indicating that the sampling performance of the FRM PM_{10} inlet, if properly operated, would change when used for sampling of agricultural PM.

$$D_x = \frac{D_j + 2L \tan(\alpha_j / 2)}{1 + 1.25 \tan(\alpha_j / 2)} \quad (3.24)$$

$$D_{50} \sqrt{C_c} = \left(\frac{9\eta D_x^3}{4\pi\rho_p U_0 D_j^2} \right)^{1/2} \quad (3.25)$$

where, D_x is the diameter of the air stream when particles start to separate, D_j is the diameter of the nozzle, α_j is the divergence angle, C_c is the slip correction factors at D_{50} , η is the viscosity coefficient of air, ρ_p is the ‘true’ density of particles, and U_0 is the initial air velocity at the nozzle outlet.

Having been used in this study, Harvard impactors were found to have a comparable sampling performance with FRM/ FEM PM samplers (Babich et al., 2000; Demokritou et al., 2004; Turner et al., 2000). It is reasonable to assume that the PM concentrations measured by Harvard impactors are approximately equal to those measured by FRM/ FEM PM samplers. Accordingly, a comparison between the calculated and the Harvard-impactor-determined PM concentrations is expected to offer indirect but valuable information about the performance of the calculation method relative to FRM/ FEM PM samplers.

Two measures were used to evaluate the difference between the calculated and the measured PM concentrations: bias and error. Bias was defined in this study as the average distance between calculated and measured concentrations; while error was defined as the variation in distances. Specifically, in Figure 3.22, the systematic bias was characterized by the slope of a regression line, and decreased to 0 when the slope approached 1; while, the error was characterized by the R^2 value and diminished when the R^2 value improved. Both the bias and error were found to differ greatly with particle size analyzers. For the calculation of PM_{10} concentrations, Coulter produced the lowest bias, DSP produced the lowest error, and the highest bias and the biggest error were both generated from Horiba. For the case of $PM_{2.5}$, Malvern consistently offered the best estimates no matter which approach and/or d_j were selected. However, the slope (<0.35) and the R^2 value (<0.15) were much smaller than 1, indicating that the calculation method should not be applied to estimation of $PM_{2.5}$ concentrations.

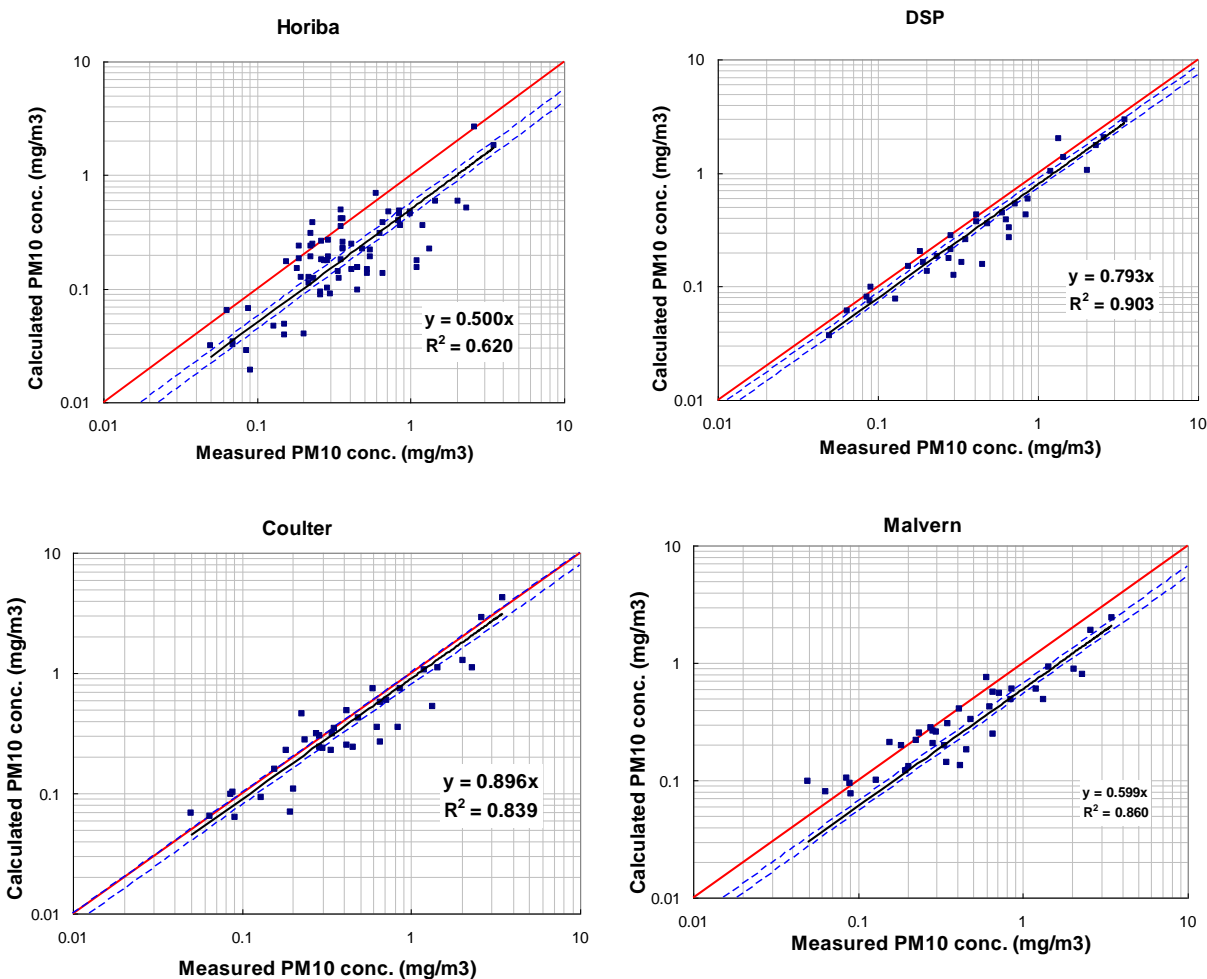


Figure 3.22. Comparison of calculated to measured PM₁₀ concentrations (approach B, d_j- average diameter). The blue dash line represents the 95% confidence interval of slope.

The bias and error could also be characterized by the geometric mean and geometric standard deviation of $R_{PM_{10}}$, respectively. Geometric values were employed because $R_{PM_{10}}$ followed a lognormal distribution. The systematic bias would diminish when the geometric mean of $R_{PM_{10}}$ approached 1; while the error would increase with the geometric standard deviation. It can be seen that Coulter and DSP produced the lowest bias and the lowest error, respectively; while, Horiba again generated the greatest bias and the highest error, regardless of the selected d_j and calculation approaches (Table 3.29).

Table 3.29. Geometric mean and geometric standard deviation of $R_{PM_{10}}$ values derived from different particle size analyzers and approaches.

d_j	Analyzer	Approach A		Approach B	
		Geomean	GSD	Geomean	GSD
Average diameter	Horiba	0.473	1.835	0.509	1.774
	DSP	0.542	1.402	0.734	1.368
	Coulter	0.790	1.540	0.818	1.490
	Malvern	0.743	1.527	0.728	1.530
Maximum diameter	Horiba	0.434	1.902	0.462	1.790
	DSP	0.528	1.404	0.696	1.368
	Coulter	0.785	1.542	0.811	1.490
	Malvern	0.716	1.527	0.695	1.521

In general, a systematic bias can be corrected through calibration with accurate reference standards but an error can not. Accordingly, for calculation of PM_{10} concentrations, DSP was the best PSD data source among the four analyzers. An illustration of the effect of correction was shown in Figure 3.23. The calculated PM_{10} concentrations were corrected by dividing the original calculated values over the geometric mean of $R_{PM_{10}}$. The differences between the calculated and measured PM_{10} concentrations were depicted on a hierarchical plot based on the average Euclidean distance (Figure 3.24). The results showed that DSP-derived PM_{10} concentrations were most similar to the measured concentrations, and all the four analyzers offered better estimates after correction. However, the errors in terms of GSD remained constant after correction and regrettably high even for DSP. This undermines the applicability of the calculation method.

Why does DSP produce the most comparable PM_{10} concentrations to the measured concentrations? There are two possible reasons:

- Among the four analyzers, only DSP measures the aerodynamic diameter of PM; while the other three measure the equivalent volume diameter. To calculate the mass fraction of PM_{10} and $PM_{2.5}$, the measured equivalent volume diameters need to be converted to the corresponding aerodynamic diameters. This conversion is conducted mainly based on two assumptions: (1) the shape factor (χ) is equal to 1, i.e. all particles are solid and strictly spherical, and (2) the particle density (ρ_p) does not vary with particle size and is equal to the density of settled dust. Those two assumptions may generate great uncertainties.

- Only DSP runs an on-field, direct measurement; while all the other three particle size analyzers require PM samples to be first collected on filters, and then extracted and suspended in liquid media for PSD analysis. Such an indirect measurement approach inevitably creates certain uncertainties. For example, particles collected from animal confinement buildings may undergo deformation, disintegration and aggregation on filters and/or in liquid media, all of which would greatly alter the measured PSD profiles.

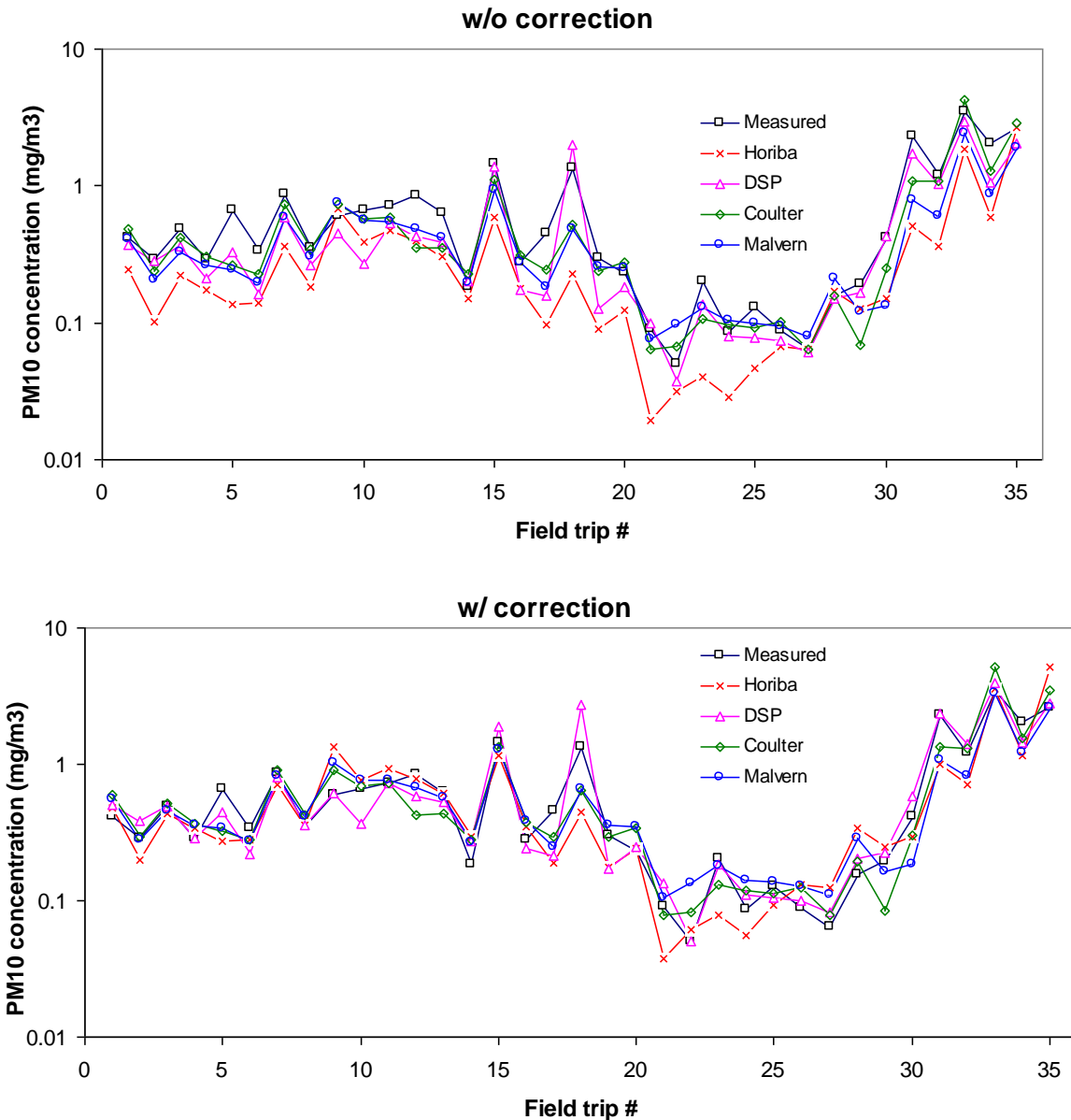


Figure 3.23. Effects of correction on calculated PM₁₀ concentrations. Only the data available from all the four analyzers were shown herein.

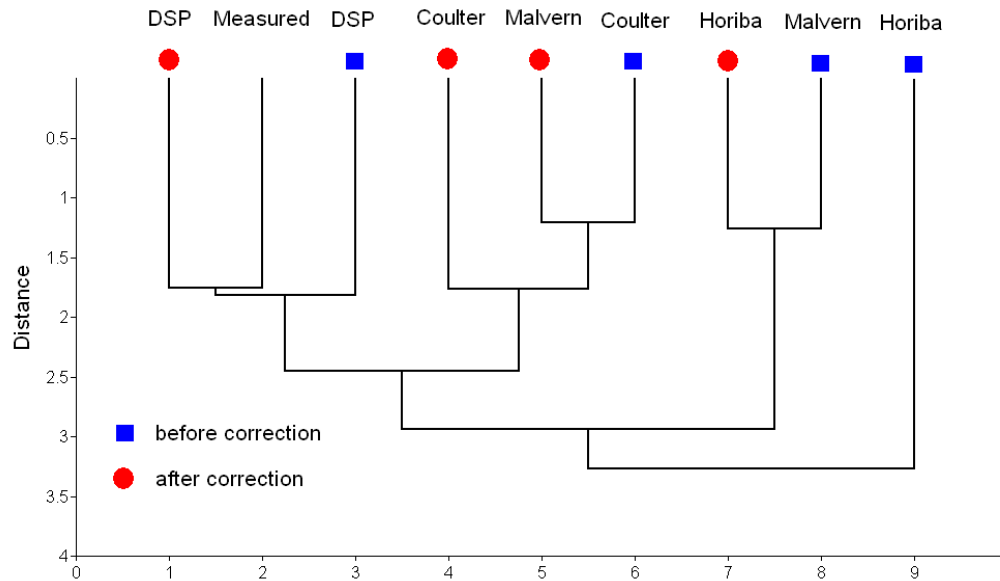


Figure 3.24. Hierarchical plot of calculated and measured PM₁₀ concentrations.

However, there are also a couple of limitations associated with DSP:

- DSP calculates the mass size distribution of PM based on two assumptions: (1) the density of particles is constant over all size ranges; (2) particles are all solid and spherical.
- For each field sampling, the DSP measurement lasted for only around 10 min (twice a day and each for 5 min) because otherwise the analyzer could be easily overloaded. The measured PSD data, therefore, failed to cover a diurnal variation. In contrast, a gravimetric determination of PM concentrations generally requires particle samples to be collected for at least 24 hrs.
- The collection efficiency of the DSP inlet was relatively low for particles larger than 20 μm (Lee, 2009). Therefore, DSP may not actually measure the size distribution of total PM (TSP).

Among the above limitations, the first one was shared with Horiba, Coulter and Malvern; while the other two were for DSP only. Because of these limitations, DSP-derived PM₁₀ concentrations were still far from accurate. The coefficient of determination ($R^2 = 0.903$) between the DSP-derived and the measured PM₁₀ concentrations was even smaller than that ($R^2 = 0.907$) given by the modified PM₁₀ concentration model.

3.3.4.5 Effect of selected d_j on calculation of PM concentrations

Obviously, the average diameter was a more reasonable choice of d_j than the maximum diameter (Figure 3.8), and the calculated PM concentrations would be higher when the average diameter was selected. Paired t-test results revealed that the effect of selected d_j differed with particle size analyzer and calculation approach (Table 3.30):

- The PM_{10} concentrations derived from Horiba, DSP and Malvern were more affected than those from Coulter. Compared to the other three analyzers, Coulter has a much larger number of detection channels. Accordingly, the width of each detection channel is narrower on Coulter. The maximum and the average diameters of a detection channel are more similar.
- The PM_{10} concentrations calculated through approach A were less affected than those from approach B. Selecting maximum diameter gives lower collection efficiency [$\eta_{PM_{10}}(d_j)$] than average diameter. In approach B, this underestimation applies to all detection channels; while, in approach A, this underestimation only occurs in a single channel that crosses 10 μm . Accordingly, approach B is more sensitive to selected d_j .

Table 3.30. Paired t-tests on PM_{10} concentrations calculated with different d_j : average versus maximum diameter.

Approach	Horiba		DSP		Coulter		Malvern	
	Δ (mg/m ³)	p						
A	0.017	<0.001	0.009	<0.001	0.004	0.002	0.012	<0.001
B	0.023	<0.001	0.026	<0.001	0.004	<0.001	0.016	<0.001

The relative error induced by different selections of d_j was found to be up to 11.9% for Horiba, 9.3% for DSP, 1.5% for Coulter and 13.2% for Malvern. In conclusion, the selected d_j has a great influence on calculated PM_{10} concentrations. The average diameter or geometric mean diameter is recommended for future relevant studies.

3.3.5 Effects of filter post-conditioning on PM mass measurement

In Equation 3.17, $M_{f,a}$ can be determined through the weighing of pre-conditioned filters; while $M_{p,a}$ is equal to the mass of a post-conditioned filter sample (with collected PM on it) minus $M_{f,a}$. There is no direct measurement of $M_{p,b}$ or $M_{f,b}$; however, a sum of $M_{p,b}$ and $M_{f,b}$ [$(M_{p,b} + M_{f,b})$] can be determined by weighing a fresh filter sample before post-conditioning. Therefore, if without post-conditioning, an estimate of PM mass ($M_{p,e}$) would be:

$$M_{p,e} = (M_{p,b} + M_{f,b}) - M_{f,a} \quad (3.26)$$

Since $M_{p,a} = \beta_1 M_{p,b}$ and $M_{f,a} = \beta_2 M_{f,b}$, such an estimate can also be presented as:

$$M_{p,e} = (M_{p,a} / \beta_1 + M_{f,a} / \beta_2) - M_{f,a} = M_{p,a} / \beta_1 + M_{f,a} (1 / \beta_2 - 1) \quad (3.27)$$

Then, the relative error of this estimate would be:

$$RE = \frac{M_{p,e} - M_{p,a}}{M_{p,a}} \times 100\% = \frac{(M_{p,a} / \beta_1 + M_{f,a} / \beta_2) - (M_{f,a} + M_{p,a})}{M_{p,a}} \times 100\% \quad (3.28)$$

The calculation results showed that without post-conditioning the PM mass would be overestimated. However, the associated measurement biases were generally small, most likely less than 2.8%. Compared to the standard deviation of replicate samples from the same field trip (averagely, 7.0% for TSP, 3.9% for PM₁₀ and 8.9% for PM_{2.5}), the post-conditioning related biases were much smaller. Particularly, for PM₁₀ and PM_{2.5}, the measurement biases were mostly less than 0.10 mg, only fives times greater than the repeatability of our analytical balance (0.02 mg). Therefore, the cancelation of post-conditioning would not generate significant biases for PM mass determination when PTFE filters were used for sample collection.

Table 3.31. Summary of errors for PM mass measurements without post-conditioning.

	Statistic	TSP	PM ₁₀	PM _{2.5}
Error	Mean	0.55 mg	0.08 mg	0.05 mg
	95% CI of mean	[0.35 mg, 0.75 mg]	[0.06 mg, 0.10mg]	[0.04 mg, 0.06 mg]
	SD	0.58 mg	0.09 mg	0.07 mg
Relative error	Mean	1.4%	1.0%	2.0%
	95% CI of mean	[0.9%, 1.8%]	[0.7%, 1.4%]	[1.2%, 2.8%]
	SD	1.2%	1.9%	3.8%
	N	32	100	97

In order to identify the major source of the measurement bias, a linear regression was performed based on Equation 3.27. No strong correlations were identified between $M_{p,e}$ and $M_{f,a}$, as indicated by the regression coefficient $(1/\beta_2-1)$ (Table 3.32). This observation suggested that the mass change of PTFE filters during post-conditioning was fairly small, and accordingly had little influence on PM mass measurement. The item of $M_{f,a}(1/\beta_2-1)$ was then removed from the linear model because the corresponding p values were greater than 0.05. After removing that item, the regression coefficient $1/\beta_1$ was re-calculated and the results showed that β_1 was fewer than but very close to 1 for TSP, PM₁₀ and PM_{2.5}. Because $(1-\beta_1)$ represented the ratio of the mass loss of particles during post-conditioning, it can be concluded that an overestimation of PM

mass if without post-conditioning was mainly caused by the loss in the mass of particles. But the effect was relatively small, mostly less than 2.0%. The relative errors shown in Table 3.31 and their corresponding $(1 - \beta_1)$ values were slightly different, because they were derived different statistical approaches.

Table 3.32. Summary of parameter estimates for Equation 3.27.

	Statistic	TSP	PM ₁₀	PM _{2.5}
$\frac{1}{\beta_1}$	Estimate	1.0153	1.0061	1.0154
	95% CI	[1.0083, 1.0222]	[1.0035, 1.0086]	[1.0093, 1.0215]
	P	0.000	0.000	0.000
$\frac{1}{\beta_2} - 1$	Estimate	-0.0001	0.0002	0.0001
	95% CI	[-0.0015, 0.0012]	[-0.00004, 0.0004]	[-0.0013, 0.0003]
	P	0.836	0.098	0.527
β_2	Estimate	1.0001	0.9998	0.9999
	95% CI	[0.9988, 1.0015]	[0.9996, 1.0001]	[0.9997, 1.0013]
Upon the removal of $M_{f,a}(1/\beta_2 - 1)$,				
$\frac{1}{\beta_1}$	Estimate	1.0147	1.0078	1.0170
	95% CI	[1.0111, 1.0182]	[1.0063, 1.0093]	[1.0134, 1.0205]
	P	0.000	0.000	0.000
β_1	Estimate	0.986	0.992	0.983
	95% CI	[0.982, 0.989]	[0.991, 0.994]	[0.980, 0.987]

The 95% confidence interval of β_2 in Table 3.32 indicates that the mass of PTFE filters did not change significantly during post-conditioning. In contrast, a slight loss in the mass of glass fiber filters was identified through statistical analysis ($\beta_2=0.9997$, $p=0.000$ for $\beta_2 \geq 1$). No significant difference in β_2 was found between sets of filters conditioned in different humidity conditions (50%, 65% and 80%). An overestimation of filter mass if without post-conditioning was estimated to be averagely 0.03 mg or 0.033%. Compared to that of TSP mass (averagely 0.55 mg), this number was much smaller. This indicated that, for the measurement of PM mass, the mass loss of glass fiber filters during post-conditioning was not of importance.

Because the mass of glass fiber filters was fairly constant with a relative standard deviation of around 0.8%, an overestimation error of 0.03 mg, corresponding to the item of $M_{f,b}(1-\beta_2)$ or $M_{f,a}(1/\beta_2-1)$, could be used for estimating the bias for TSP PM mass measurement. With a sampling time of 24 hrs and a flow rate of 20 LPM, this error would lead to an overestimation of TSP concentrations by averagely 0.001 mg/m^3 , almost negligible compared to the average TSP concentration (2.282 mg/m^3). Taking the mass loss of particles into consideration, it was found that the mean mass loss of TSP samples (including glass fiber filters and particles) during post-conditioning was significantly less than the tolerance level of 3% ($p < 0.001$).

The designed experiment failed to consider the adsorption of VOC's on glass fiber filters, and therefore might underestimate the mass loss of filters, $M_{f,b}(1-\beta_2)$, during post-conditioning. Accordingly, the mass loss of TSP samples might be also underestimated. This issue will be addressed in future relevant investigations. However, because TSP concentrations in this study were substantially higher than ambient PM concentrations, the positive artifact caused by VOC's adsorption was expected to be relatively small (Mader and Pankow, 2001).

3.3.6 Uncertainty Analysis for calculation of PM mass concentrations

Based on Equation 3.1, the measurement error for PM mass concentrations was estimated as:

$$\sigma_{C_p} = \sqrt{\left(\frac{\sigma_{M_t-M_0}}{Q_s t_s} \frac{T_{std}}{T_s} \frac{P_s}{P_{std}}\right)^2 + \left(\sigma_{Q_s} \frac{M_t - M_0}{Q_s^2 t_s} \frac{T_{std}}{T_s} \frac{P_s}{P_{std}}\right)^2 + \left(\sigma_{t_s} \frac{M_t - M_0}{Q_s t_s^2} \frac{T_{std}}{T_s} \frac{P_s}{P_{std}}\right)^2 + \left(\sigma_{T_s} \frac{M_t - M_0}{Q_s t_s} \frac{T_{std}}{T_s^2} \frac{P_s}{P_{std}}\right)^2 + \left(\frac{M_t - M_0}{Q_s t_s} \frac{T_{std}}{T_s^2} \frac{\sigma_{P_s}}{P_{std}}\right)^2} \quad (3.29)$$

Where, $\sigma_{M_t-M_0}$ was estimated to be 1.51 mg for TSP (assuming a relative error of 3.0% based on the previous discussion), 0.04 mg for PM_{10} and 0.04 mg for $PM_{2.5}$ (based on the repeatability 0.02 mg of the analytical balance), σ_{Q_s} was estimated to be 0.05 LPM (0.00005 m³/min), σ_{t_s} was estimated to be 2 min, σ_{T_s} was estimated to be 2 K, σ_{P_s} was estimated to be 0.05 in Hg, and others were estimated to be equal to their corresponding average values. The calculated σ_{C_p} was 0.070 mg/m³ for TSP, 0.005 mg/m³ for PM_{10} and 0.002 mg/m³ for $PM_{2.5}$, and the corresponding relative errors were estimated to be 3.1%, 0.77% and 1.3% respectively. The mass measurement of PM samples was identified to be a major uncertainty source. Compared to the standard deviation of replicate samples from the same field trip, the calculation-associated uncertainties were much smaller. Therefore, the uncertainty associated with the PM concentration measurement may mainly originate from replicate samples that basically reflect the spatial distribution of PM concentrations.

3.4 Limitations and Recommendations

The conclusions obtained in this study were drawn based on a limited number of sampling sites and field trips due to restricted resources. Increasing the number of field trips, sites and sampling points would be required for improving the representativeness of PM concentration

data. This study therefore should be regarded as a preliminary survey and more extensive efforts should be made in the future.

Chicken broiler buildings were not included in this sampling campaign. Considering the scale, 9.01 billion birds per year in the United States (USDA, 2009), and the potential environmental impact (e.g. NH_3) of broiler production, future investigations should certainly include typical broiler buildings in the Midwest.

TSP nozzles and Harvard impactors used in current study are not FRM or FEM samplers. The performance of Harvard impactors in extremely dusty environments has not been fully evaluated. This may raise certain concerns over the reliability and validity of the measurement concentration data.

Glass fiber filters used for sample collection may lead to sampling artifacts because of the adsorption of VOC's and water on filters. Teflon filters or Teflon-coated glass fiber filters should be used in the future to reduce the potential sampling artifacts that may affect the accuracy of PM concentration measurements.

3.5 Chapter Summary and Conclusions

3.5.1 Summary of observations

PM samples were collected in a total of eighteen animal confinement buildings mostly in Illinois. The sampling campaign covered six different types of buildings: swine farrowing, gestation, weaning, finishing, manure-belt layer hen and tom turkey. Each building was visited three times in three different seasons. TSP, PM_{10} and $\text{PM}_{2.5}$ mass concentrations were measured gravimetrically and then subject to statistical analysis. The objectives are: (1) to investigate variations in PM concentrations with selected environmental and operational factors, and, thereby, to identify the major factors; (2) to establish a linear model to predict PM concentrations; (3) to evaluate the effect of post-conditioning on PM mass measurement since fresh PM samples were required by parts of PM characterizations.

In addition to direct measurements, PM_{10} and $\text{PM}_{2.5}$ mass concentrations were calculated from TSP mass concentrations and PSD curves of TSP samples. Two calculation approaches were employed: approach A applied an ideal penetration curve (90° sharp cut), and approach B applied penetration the curves of ideal PM samplers. Another important parameter for

calculation is the characteristic diameter of detection channels. Two different diameters were investigated: maximum and average diameter. A comparison was conducted between the calculated and the measured PM concentrations, and between PM concentrations calculated through different approaches, from different analyzers and/or with different characteristic diameters. The overall goal is to verify the validity of the calculation approach. To achieve this goal, the specific objectives are: (1) to test a hypothesis that approach A would consistently produce smaller PM concentrations than approach B; (2) to test another hypothesis that PSD data derived from different analyzers would produce identical or very similar PM concentrations; (3) to determine which analyzer would offer the best estimates of PM concentrations; and (4) to investigate the effect of the selected characteristic diameters.

The main observations drawn from this chapter are listed as follows:

- The TSP mass concentration was 1.00 ± 0.67 mg/m³ in farrowing, 0.71 ± 0.30 mg/m³ in gestation, 1.70 ± 0.41 mg/m³ in weaning, 1.48 ± 1.02 mg/m³ in finishing, 2.98 ± 2.77 mg/m³ in manure belt layer hen and 5.88 ± 4.79 mg/m³ in tom turkey buildings.
- The PM₁₀ mass concentration was 0.34 ± 0.26 mg/m³ in farrowing, 0.42 ± 0.26 mg/m³ in gestation, 0.36 ± 0.29 mg/m³ in weaning, 0.39 ± 0.30 mg/m³ in finishing, 1.07 ± 0.89 mg/m³ in manure belt layer hen and 1.56 ± 1.13 mg/m³ in tom turkey buildings.
- The PM_{2.5} mass concentration was 0.16 ± 0.10 mg/m³ in farrowing, 0.08 ± 0.05 mg/m³ in gestation, 0.08 ± 0.04 mg/m³ in weaning, 0.18 ± 0.20 mg/m³ in finishing, 0.40 ± 0.53 mg/m³ in manure belt layer hen and 0.23 ± 0.17 mg/m³ in tom turkey buildings.
- Approximately 93% measured PM_{2.5} and 86% PM₁₀ concentrations exceeded the NAAQS. Over 50% measured PM_{2.5} and TSP concentrations from poultry buildings exceeded the exposure limits respectively for respirable and inhalable particles proposed by Donham (2000); while only 5.7% PM_{2.5} and 11% TSP concentrations from swine buildings exceeded the proposed exposure limits.
- Animal building type had a significant effect on PM concentrations and mass ratios. Poultry buildings had significantly higher PM concentrations but lower PM_{2.5} mass ratios (PM_{2.5}/TSP) than swine buildings. However, no significant differences in PM concentrations were identified among different types of poultry or swine buildings. Tom

turkey buildings had overall the highest TSP and PM₁₀ concentrations and manure belt layer hen buildings had the highest PM_{2.5} concentrations; while the lowest PM (TSP, PM₁₀ and PM_{2.5}) concentrations were observed in gestation buildings.

- Animal density had no significant effect on PM concentrations and mass ratios.
- Seasons had a significant effect. PM concentrations in cold seasons were significantly higher than those in mild seasons; while PM concentrations in mild seasons were significantly higher than those in hot seasons. Significantly higher PM₁₀ mass ratios (PM₁₀/TSP) were found in cold than in hot seasons.
- Dry feeding systems were associated with significantly higher TSP and PM₁₀ concentrations than wet feeding systems where a mixing of feed and water reduces the aerosolization of feed particles.
- A generalized linear model were established to predict PM₁₀ mass concentration from animal building type, daily average ambient temperature, specific fan area, animal density, and TSP concentration. The R² value of this model was 0.907.
- Approach A did not consistently produce lower PM₁₀ and PM_{2.5} concentrations than approach B. An oversampling by FRM/FEM PM samplers lacks solid theoretical evidence. The validity of the proposed calculation approach is questionable.
- PM₁₀ and PM_{2.5} concentrations derived from different particle size analyzers could be significantly different. Coulter could not produce reasonable PM_{2.5} concentrations. Because PM_{2.5} is a subfraction of PM₁₀, the accuracy of Coulter-derived PM₁₀ concentrations was questionable. Lower PM₁₀ mass concentrations derived from Coulter than from FRM/ FEM PM₁₀ samplers should not be simply ascribed to oversampling by FRM/FEM samplers but may be caused by uncertainties associated with Coulter method.
- A comparison with the measured PM₁₀ concentrations revealed that Coulter produced the lowest bias and DSP generated the lowest error. After bias correction, DSP was found to produce the best estimates of PM₁₀ concentrations. However, the prediction power was still poor (R²= 0.903). For PM_{2.5}, no particle size analyzer produced good estimates.

- The PM₁₀ concentrations derived from Horiba, DSP and Malvern were significantly affected by the selected characteristic diameter (d_j). The average diameter or geometric mean diameter would be recommended for future relevant studies.
- The cancellation of filter post-conditioning would result in an overestimation of PM mass. The bias for PM mass measurement without post-conditioning was found to be mostly less than 2.8%, much lower than the standard deviation of replicate samples from the same field trip. When PTFE filters were used for PM collection, the bias for PM mass measurement was predominantly caused by the mass loss of particles. When glass fiber filters were used for PM collection, the adsorption of water led to an overestimation of PM mass by averagely 0.03 mg. In general, the effect of filter post-conditioning was statistically significant but not substantial on the measurement of PM mass.

3.5.2 Conclusions

TSP, PM₁₀ and PM_{2.5} samples were collected from six different types of animal confinement buildings and their concentrations were determined gravimetrically. The present study revealed that PM concentrations were significantly affected by animal building type, season (ambient temperature) and feeding systems; while animal density had no significant effect. Specifically, higher PM concentrations occurred in poultry buildings than swine buildings; PM concentrations increased as ambient temperature decreased; and wet feeding systems were associated with lower TSP and PM₁₀ concentrations than dry feeding systems. A generalized linear model was established for estimating PM₁₀ concentrations in swine buildings with animal building type, daily average ambient temperature, specific fan area, animal density, and TSP concentration as predictors. The coefficient of determination (R^2) of the proposed model was 0.907.

Some previous studies reported that FRM/FEM PM samplers oversample PM₁₀ and PM_{2.5} from agricultural sources, and accordingly proposed an indirect method that calculates PM₁₀ and PM_{2.5} concentrations from TSP concentrations and the PSD of TSP. The conclusion and the proposed calculation method were established based on several assumptions. The present study shows that when different assumptions are employed, substantially different conclusions and calculation results could be obtained. The PM₁₀ and PM_{2.5} concentrations derived from different particle size analyzers could be substantially different. Among four analyzers under investigation, Aerosizer DSP produced the most comparable PM₁₀ concentrations to gravimetric method.

4. CHARACTERIZATION OF INORGANIC ELEMENTS AND SOLUBLE IONS IN PM₁₀ AND PM_{2.5} EMITTED FROM ANIMAL CONFINEMENT BUILDINGS

4.1 Introduction

Particulate matter (PM) emanating from animal confinement buildings has received much attention in recent years as an environmental concern (Cambra-Lopez et al., 2010; Heederik et al., 2007). Compared with ambient and urban aerosols, PM from animal confinement buildings comprises a large portion of bioaerosols and may contain toxic, allergenic, pathogenic (Douwes et al., 2003; Kirkhorn and Garry, 2000; Schenker et al., 1998) and even carcinogenic components (Shenker et al., 1998)) detrimental to the health of human and animals and may carry NH₃ and other malodorous compounds, thereby creating an odor nuisance in neighboring communities (Bottcher, 2001; Lee and Zhang, 2008; Oehrl et al., 2001). Regulations for animal feeding operations emissions are under discussions by USEPA and USDA. However, one of major obstacles for regulation development is lack of a complete and comprehensive emission database.

Many efforts have been made to measure PM emissions from animal confinement buildings (Jacobson et al., 2005; Lim et al., 2003; Predicala and Maghirang, 2002), including the recently completed NAEMS (National Air Emissions Monitoring Study) project. Most of them aimed to determine representative PM emission factors such that a nationwide or a regional PM emission rate from animal confinement buildings can be estimated. However, the derived PM emission factors can hardly be applied to individual animal confinement buildings, and it is obviously impractical to monitor PM emission from all buildings.

Based on existing data of emission factors, animal confinement buildings are a minor source of primary PM. It was estimated that in 2005, a total of 2.2 million tons of PM₁₀ were emitted from anthropogenic sources in the United States (USEPA, 2009a). Assume 15g/AU-day and 3 g/AU-day are representative PM₁₀ emission factors for broilers and pigs, respectively, and the average body weight is 1.6 kg for broilers and 60 kg for pigs. Then the total PM₁₀ emissions in 2005 would be 29,000 tons from broiler and 8,200 tons from pig buildings. Therefore, PM emissions from animal confinement buildings are nationwide a minor source but can be regionally or locally a major source in areas where animal production is intensive.

For examining a regional or local PM pollution problem, two types of air quality models are commonly used- dispersion models and receptor models. A big challenge to dispersion modeling is that it requires a known PM emission rate which is usually challenging to measure.. A better strategy, according to a report by the National Academy of Sciences (NAS, 2003), may be a combination of dispersion and receptor modeling.

Receptor modeling does not require known PM emission rates but requires known chemical compositions of PM at receptor sites and/or at sources. Chemical speciation of PM therefore becomes necessary. Non-reactive chemical species are usually selected since receptor modeling is generally based on the principle of mass balance; while reactive chemical species may change in their mass during the transport in the atmosphere. Currently in ambient aerosol studies, e.g., NAMS (National Air Monitoring Stations), SLAMS (State and Local Air Monitoring Stations) and IMPROVE (Interagency Monitoring of Protected Visual Environments), the commonly selected chemical species include organic carbon and elemental carbon (OC/EC), inorganic elements, and soluble ions (USEPA, 1999b). Because there is no significant EC source in animal confinement buildings, in this study we only targeted on inorganic elemental and soluble ions.

Only a few studies have been done in an effort to identify and quantify inorganic elements and soluble ions in PM from animal confinement buildings (Cambra-Lopez and Toores, 2008; Lammel et al., 2004; Li et al., 2009; Martin et al., 2008). All of them focused on one or a few buildings. Accordingly, only limited information has become available. There is a lack of a comprehensive and systematic survey on PM from different types of buildings. To address this issue, in this study we selected three each of six different types of animal production facilities for a total of 18 animal confinement buildings found in the Midwest. The main research objectives were:

- To measure and characterize chemical composition (in terms of inorganic elements and soluble ions) of PM_{10} and $PM_{2.5}$ emitted from each type of animal confinement building;
- To examine variations in PM chemical composition with animal building type, season and particle size.

4.2 Literature Reviews

PM from animal confinement buildings may originate from a variety of sources such as feed, fecal materials, animal skins and hairs, insect segments, construction materials and ambient aerosols (Zhang, 2005). Among them, feed and fecal materials are generally considered to be two major sources (Donham et al., 1986b; Feddes et al., 1992; Heber et al., 1988a). A brief literature review was conducted regarding the inorganic elements in animal feed and manures.

- Feed- Corn and soybean meal are generally the top two abundant components in animal feed currently applied in the United States. Dried Distiller grain with solubles (DDGS) is occasionally but increasingly used as a feed additive. Limestone (mainly CaCO_3), dolomite (mainly $\text{CaMg}(\text{CO}_3)_2$), salts and other minerals (e.g., MgO , MnO , CuO and ZnO) are also often included in the diet of animal feed (Kellems and Church, 1998). All of these feed components can be potential sources of PM. A number of inorganic elements have been identified in corn and soybean such as B, N, P, S, K, Ca, Cr, Ni, Cu, Zn, Mo, Cd, and Pb (Lavado et al., 2001). The relative abundance of each element is affected by soil type, fertilizer application, tillage, crop type and heavy metal pollution sources in nearby regions (Berti and Jacobs, 1996; Bingham, 1979; Lavado et al., 2001; Liu et al., 2005), but is relatively constant under normal growth conditions. DDGS is a byproduct from the dry-mill ethanol production process, thus inorganic elements in DDGS are expected to be similar to those in corn since corn is the main raw material for ethanol production currently in the United States. Salts in animal feed generally include NaCl , KCl , CaCl_2 , MgCl_2 and MgSO_4 , as well as micro minerals required for animal health such as Mn, Fe, Co, Cu, Zn and I.
- Manures- Fecal material is another major component in PM from animal confinement buildings, especially in small particles (Feddes et al., 1992; Heber et al., 1988a). Animal manures have been revealed to contain numerous inorganic elements including B, Na, Mg, P, S, Cl, K, Ca, Mn, Fe, Cu, Zn, As, Se, Hg and Pb (Day, 1988). The species of inorganic elements in animal manures are similar to those in animal feed for obvious reasons; however, the relative abundance of each element can be substantially different because of a difference in the uptake ratio of elements by animals.

In summary, the following inorganic elements may exist in PM from animal confinement buildings: B, Na, Mg, P, S, Cl, K, Ca, Cr, Mn, Fe, Co, Ni, Cu, Zn, As, Se, Mo, Cd, I, Hg and Pb. Some of them (e.g. Na and Cl) may at least partly exist in the form of soluble ions. Besides, certain crustal inorganic elements may be present, e.g., Si and Ti, possibly from construction materials, soil dust and ambient aerosols.

4.3 Materials and Methods

4.3.1 Particle sampling

Field sampling was conducted in twelve swine and six poultry confinement buildings (Table 4.1). Each building was visited three times in different seasons: winter, spring or fall, and summer. Additionally, we collected PM samples in a cage-free layer hen and a chicken broiler building but only a single visit in summer was conducted. Detailed building information can be found in Appendix A.

Table 4.1. Summary of field sampling.

Animal type	Building Type	Location	# of buildings	# of visits
Swine	Gestation	Illinois	3	9
	Farrowing	Illinois	3	9
	Weaning	Illinois	3	^x 8
	Finishing	Illinois	3	9
Poultry	Manure-belt layer hen	Illinois and Indiana	3	9
	Tom turkey	Illinois	3	9
	Cage-free layer hen	Indiana	1	1
	Broiler	Kentucky	1	1
Total			20	55

x. A weaning building was closed down before our last visit, so no summer data were available.

PM₁₀ and PM_{2.5} samples were collected on pre-conditioned and pre-weighed ringed Teflon filters (Teflo™ w/ ring PTFE membrane filter, P/N R2PJ037, Pall Corporation, Ann Arbor, MI) with Harvard impactors (Air Diagnostics and Engineering Inc., Harrison, ME). These impactors were installed upstream of a continuous-running exhaust fan (in most buildings) or near a downwind end door (in tom turkey buildings with natural ventilation), with a typical spacing of 0.6-1.0 m from fan face or end door and an installation height of 1.2-1.4 m. The sampling flow rate was controlled at approximately 20 LPM with venturi orifice developed in our group (Wang and Zhang, 1999). The accurate flow rate was acquired through calibration of venturi orifices in the lab (please refer to Appendix H), and used for calculating the actual volume of sampled air.

Each sampling lasted approximately 24 hours to cover a diurnal variation. An overloading of PM samplers was occasionally observed and normally occurred during the winter when PM concentrations were highest due to decreased ventilation rates. In those cases, a makeup field trip was conducted. To prevent the occurrence of overloading, time relays were used to run the sampling system intermittently. The selected sampling period was dependent on the dustiness of the visited building. In addition, for PM_{2.5} sampling, a pre-separator (PM₁₀ nozzle) was installed upstream of each PM_{2.5} impactor to first remove particles larger than 10 µm. After returning to campus, filters were post-conditioned and re-weighed to determine the collected PM mass, and then stored at -22 °C in a freezer until analysis. Two PM₁₀ and two PM_{2.5} filter samples were collected from each field trip. Two samples (a PM₁₀ and a PM_{2.5}) were subject to elemental analysis, and the other pair was used for soluble ion analysis.

4.3.2 Determination of inorganic elements and soluble ions in PM samples

4.3.2.1 Identification of inorganic elements with EDXRF

EDXRF (energy-dispersive X-ray fluorescence) tests were performed on a Kevex 770-EDX spectrometer (Fison Instruments, San Carlos, CA) at the Center for Microanalysis of Materials at the University of Illinois at Urbana-Champaign. A secondary excitation mode was employed. Both the incident and take-off angles were set at 45°. Three excitation conditions were selected as shown in Table 4.2. Teflon filters were held on 37 mm plastic holders. Sixteen filters were analyzed in a single batch, including 15 unknown samples and a quality control standard. Here, a filter with collected ambient aerosols was used as the quality control standard. The purpose was to track changes in peak counts among different test batches, and to correct them if necessary. An identification of inorganic elements included two steps: (1) an automatic identification by the instrument software; and (2) the element peaks were double-checked and manually corrected if necessary. The instrument software also calculated the count (area) of each element peak. However, no quantitative analysis was conducted based on the peak counts because of a lack of essential calibration standards.

Table 4.2. Excitation conditions applied on the Kevex 770 EDXRF analyzer.

#	Secondary fluorescor	Tube voltage	Tube current	Analysis time	Atmosphere	Elements Analyzed
1	Al	30 kV	2.0 mA	180s	vacuum	Light elements
2	Ge	30 kV	2.0 mA	400s	vacuum	Elements lighter than Ge
3	Gd	60 kV	2.0 mA	400s	vacuum	Heavy metals

4.3.2.2 Quantification of inorganic elements with ICP-AES

Based on the qualitative analysis results from EDXRF tests, we selected ICP-AES to quantify the contents of inorganic elements mainly for the following reasons:

- The availability of instrumentation. There are quite a few ICP-AES instruments available on campus. Other multi-element analysis instruments, such as PIXE, TXRF and NAA, are not available.
- Detection capability. The existing ICP-AES test protocols available on campus can quantify nearly all inorganic elements detected by EDXRF with reasonable sensitivity. A discussion on the sensitivity of the ICP-AES test protocol is presented later in the results and discussions section.

ICP-AES tests were conducted on a Varian VISTA-PRO CCD Simultaneous ICP-AES (Varian Inc., Palo Alto, CA) at the Illinois State Water Survey (Champaign, IL). Prior to ICP-AES tests, filter samples were digested in a 20 mL mixed acid solution of HCl and HNO₃ at approximately 160 °C on a hot plate. Multi-element standard solutions were used as the external reference standards for quantification. A spike, a replicate and a blank filter sample were prepared and analyzed every 15 to 20 test samples for quality assurance.

4.3.2.3 Quantification of soluble ions with IC and colorimeter

Extraction of soluble ions from filters followed the protocol specified in EPA Method IO-4.2 (USEPA, 1999a). A brief procedure is described as follows:

1. A filter was immersed into a 20mL 0.0001 M HClO₄ solution and then lifted over the extraction vial.
2. The filter was wet with 0.2 mL ACS grade ethanol (Cat. # AC615090020, Fisher Scientific Inc., Waltham, MA).
3. The filter was again immersed into the extraction solution and sonicated at the maximum intensity for 15 minutes;
4. The extract was filtered with a 0.45 μm pore-size Nylon filter to remove suspended particles. The filtrate was then transferred into a clean vial for subsequent analysis.

Anions (F^- , Cl^- , NO_3^- and SO_4^{2-}) were analyzed with a DIONEX DX-500 IC (Dionex Corporation, Sunnyvale, CA) at the Illinois State Water Survey. NH_4^+ was analyzed with an automated analyzer (Astoria analyzer 300, Astoria-Pacific Inc., Clackamas, OR). A quality assurance protocol was applied similar to that for ICP-AES tests.

4.3.3 Data analysis

For examining potential variations in PM chemical composition with animal building type, season and particle size, several multivariate data analysis tools were employed, including principle coordinate analysis (PCoA), analysis of similarity (ANOSIM), similarity percentage (SIMPER), principle component analysis (PCA), positive matrix factorization (PMF) and Mantel test. Some of them have been extensively used in ecology research to compare the composition of different biotic communities (Clarke, 1993) but have been seldom used in air quality research. An introduction to those tools would be described later in the results and discussions section.

ANOVA and paired t-tests were used to compare the content of a single chemical component between different cases. Prior to those tests, a Shapiro-Wilk test was used to test the normality. A log transformation was conducted if necessary. In case the normality of data was still poor after log transformation, a Kruskal-Wallis test (nonparametric ANOVA) was used to replace the ANOVA test. A significant level of 0.05 was selected for all the tests.

PCoA, ANOSIM and Mantel tests were performed in PAST, a free statistical program originally developed for paleontology research but becoming increasingly popular in other research areas. The SIMPER analysis was performed in PRIMER 6.0, a prevalent statistical package used for multivariate data analysis of ecological data. The PMF analysis was conducted with the EPA PMF 3.0.22. Other tests, such as PCA, ANOVA and paired t-test, were conducted in SPSS v17.0 and MATLAB.

4.4 Results and Discussions

4.4.1 Inorganic elements identified by EDXRF

The following inorganic elements were identified: Na, Mg, Al, Si, P, S, Cl, K, Ca, Ti, Cr, Mn, Fe, Co, Ni, Cu, Zn, Br, Sr, Sn and Ba. Among them Cr is an essential ingredient of animal feed additives (Kellems and Church, 1998) but can be toxic as well as Ni when inhaled by human and animals (Benson et al., 1989; Lee et al., 1989). No As, Cd, Hg or Pb was detected:

those metals are highly toxic and of major concern to food safety (WHO, 2007) and were reported to be occasionally found in animal feed (Nicholson et al., 1999) and animal waste (Day, 1988). The peak count of each identified element was recorded. $K\alpha$ peaks and $L\alpha$ were normally selected for peak counting except for Ca because of an overlap of $K\alpha(\text{Ca})$ with $K\beta(\text{K})$. An example of EDXRF spectra was shown in Figure 4.1.

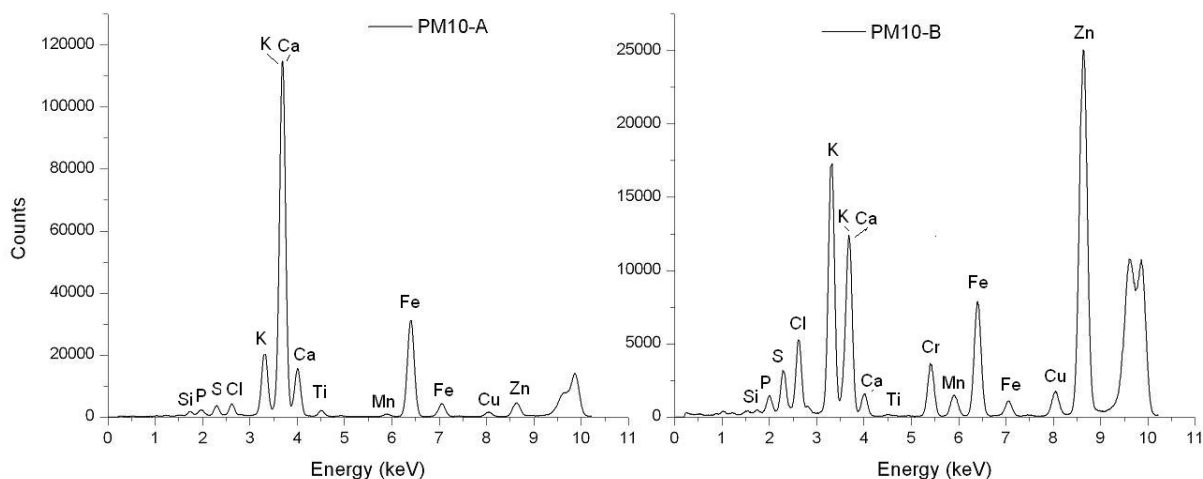


Figure 4.1. EDXRF spectra for two PM_{10} samples (excitation condition #2).

4.4.2 Issues with EDXRF- inappropriate for quantitative analysis.

Why was ICP-AES selected in this study instead of EDXRF? EDXRF has been widely used for quantification of inorganic elements in ambient aerosols (Chimidza et al., 2001; Dzubay et al., 1982; Johnson et al., 1984; Martuzevicius et al., 2004). In fact, it is cheaper and more popular than ICP-AES. However, a quantitative analysis of PM elemental composition with EDXRF is based on three assumptions:

- Thin layer assumption

Particles deposited on the filters are assumed to form a thin layer (Dzubay and Nelson, 1975). In such an ideal case, the incident X-rays can be irradiated on almost all collected particles and an attenuation of the emitted (fluorescent) X-rays, because of the scattering and absorption by deposited particles, can be minimized. The attenuation effect increases with the thickness of the particle layer, and is particularly significant for light elements because the low energy X-rays emitted from light elements are more easily adsorbed by the particle layer and filter. In reality, the filter itself can be a major source of X-ray attenuation (Davis et al., 1977).

Moreover, heavy particle loadings increase the spectral background, and consequently lower the signal-to-noise ratio. Accordingly, EDXRF analysis of ambient aerosols requires the mass loading of particles is less than $100 \mu\text{g}/\text{cm}^2$ filter area (USEPA, 1999a), and the best accuracy is achieved when the particle loading ranges from 10 to $50 \mu\text{g}/\text{cm}^2$ filter area (Watson et al., 1999). For 37 mm Telfo™ filters, the effective filter area for particle collection is about 5.7 cm^2 . This means the upper mass loading limit is 0.57 mg per filter. This limit may not be a main issue for ambient aerosol analysis because the concentration of ambient aerosols is normally low. However, it can be a major problem for PM from animal confinement buildings because of the high PM concentrations. Another problem caused by the heavy particle loading is that the instrumental dead time may exceed the allowable limit at the set value of the EDXRF tube current (3.3 mA) specified by the EPA Method IO-3.3. The unsatisfactory dead time means that too many fluorescent X-ray photons are generated from the particle matrix and may saturate the semiconductor detector of EDXRF. This would create an error for quantitative analysis. In this study, high volume PM₁₀ and PM_{2.5} samplers were selected. The collected PM mass normally exceeded 1.0 mg. A strong attenuation effect is thus likely. As shown in Figure 4.1 (right), the mass of a collected PM₁₀ sample was 8.57 mg, and the peaks of light elements (e.g., F, Na and Mg) disappeared because of a strong attenuation effect.

- Size assumption

Attenuation factors are affected by the size of particles (Criss, 1976). Larger particles lead to greater attenuation effects. In current EDXRF analysis, the average particle size was assumed from ambient aerosols (PM_{2.5}, PM₁₀, and PM_{2.5-10}, respectively) for calculating the associated attenuation factors used for data correction. However, the particle size distribution (PSD) of ambient aerosols is significantly different from that of PM from animal confinement buildings. Accordingly, using the attenuation factors (correction factors) derived from ambient aerosols may raise an uncertainty issue.

- Composition assumption

Attenuation factors are also affected by the chemical composition of particles (Criss, 1976) and differ with chemical element. In current EDXRF analysis, the attenuation factor of an element was calculated based on an assumed chemical composition typical for ambient aerosols (Dzubay and Nelson, 1975). Uncertainty analysis revealed that a deviation from the assumption

would have a great influence on the measurement result for light elements (Gutknecht et al., 2006). The chemical composition of PM from animal confinement buildings can be substantially different from ambient aerosols and consequently the validity of the composition assumption needs to be further testified.

A comparison was performed between the peak count generated from EDXRF and the mass of an element measured by ICP-AES. Here, the quantitative results from the ICP-AES test were employed as a reference to assess the performance of EDXRF. Remind that the quantification by EDXRF is based on the peak count of an element in a test sample relative to that in a thin film standard (e.g., XRF standards from Micromatter Co., Vancouver, Canada), which basically involves a single point calibration and assumes a linear relationship between the peak count and the mass of an element. Accordingly, the Pearson's correlation coefficient (r) can be used as an indicator for assessing the performance of EDXRF: the higher the correlation coefficient is, the better EDXRF performs. The comparison results showed that for light elements, e.g., Na, Mg and S, EDXRF generated a relatively poor linear relationship because of a strong adsorption of emitted X-rays by filter and deposited particles, and a strong interference from the background signals; while, for some heavy elements, e.g., Fe and Zn, EDXRF provided a better performance (linearity) (Figure 4.2). In summary, EDXRF cannot offer reasonable quantitative analysis results for light elements in our or similar cases with relatively heavy particulate load.

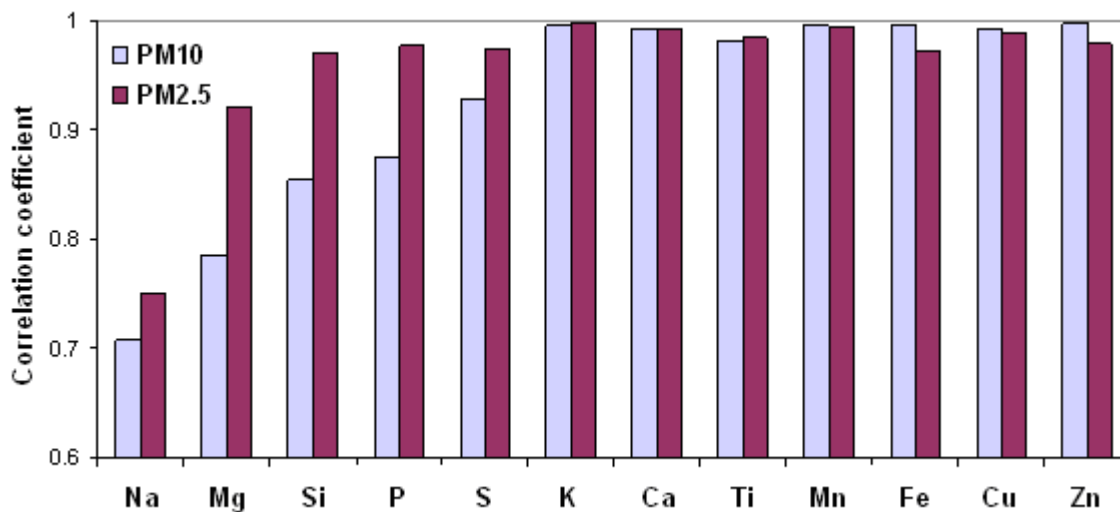


Figure 4.2. Correlation between EDXRF counts (from the 2nd excitation condition) and the mass of an element determined by ICP-AES.

4.4.3 Summary of quantitative analysis results by ICP-AES

The ICP-AES protocol selected for elemental analysis can simultaneously quantify thirty inorganic elements, including most elements detected by EDXRF. Cl and Br cannot be analyzed by the existing protocol, which is a limitation of this method. However, an advantage of the existing ICP-AES protocol is its capability to detect boron (B). The presence of B in PM from animal confinement buildings had been suggested by the presence of B in animal waste (Day, 1988) but were not detected by EDXRF since the element of B is too light. The detection limits of the ICP-AES test protocol in this study were examined to ensure that it has a comparable performance to the EPA Method IO-3.3 (EDXRF) and IO-3.4 (ICP-AES) (USEPA, 1999a). An estimation of the detection limits was based on the mass of collected PM₁₀ and PM_{2.5}. The results revealed that the test protocol selected in this study had a comparable or even better performance than the EPA Method IO-3.3 and 3.4 (data not shown here).

A total of nineteen inorganic elements were identified and quantified by ICP-AES, as summarized in Table 4.3 and 4.4. Consistent with the EDXRF test results, no As, Cd, Hg or Pb was detected by ICP-AES. Although EDXRF tests indicated the presence of Sn, its concentrations were all below the detection limit. Ca and K were found to be the most abundant inorganic elements, followed by P and S. Al, Ti and Si, three normally abundant crustal elements in ambient aerosols or soil dust, occurred at relatively low mass fractions. Most identified inorganic elements were present ubiquitously in all PM samples; while the occurrence frequency of Co, Cr and Ni was fairly low, especially Ni- it was detected in only six samples (6 of 115). Blank Teflon filters were found to occasionally contain trace contents of Ca, Cu and Ba, but much lower than those in PM samples. The content of impurities on blank filters was subtracted as a background.

No F⁻ was detected by IC. Blank filters contained a trace content of Cl⁻; however, the Cl⁻ content on blank filters was negligible compared to that in PM samples. The peak of PO₄³⁻ was observed on IC chromatograms but no quantification was done due to a lack of reference standard. The mass fraction of NH₄⁺ was found to be fairly low in both PM₁₀ and PM_{2.5} samples. Compared to the high concentrations of NH₃ (a few to tens of mg/m³) in animal confinement buildings (Radon et al., 2002; Zhu et al., 2000), this result suggests that the majority of emitted NH₃-N may exist in the gas phase and the formation of NH₄⁺-containing secondary inorganic

aerosols is insignificant in animal confinement buildings. A similar observation was recently reported by Li et al. (2009).

The average mass fraction of inorganic elements and soluble ions in PM samples from different types of animal confinement buildings are shown in Figure 4.3. The quantified inorganic elements and soluble ions only accounted for a small mass fraction of PM samples, typically less than 16%. Particularly, because the mass fraction of sulfur is contributed by soluble sulfate and non-soluble sulfate plus non-sulfate compounds (e.g., sulfide, sulfite and sulfur-containing organic compounds), they were considered separately in calculating the total mass fraction of identified components (Equation 4.1):

$$[S \text{ in non-soluble sulfate and non-sulfate compounds}] = [S] - [\text{SO}_4^{2-}] / 3 \quad (4.1)$$

Where, [X] refers to the mass fraction of specie X. The rest of PM mass may be composed of organic matter (OM), inorganic carbon (e.g., from limestone or dolomite in animal feed), water and other components (e.g., O in CuO and other oxides). The content of inorganic carbon may be significant, as suggested by the high content of Ca in PM samples. Regretfully, no analysis of inorganic carbon was conducted.

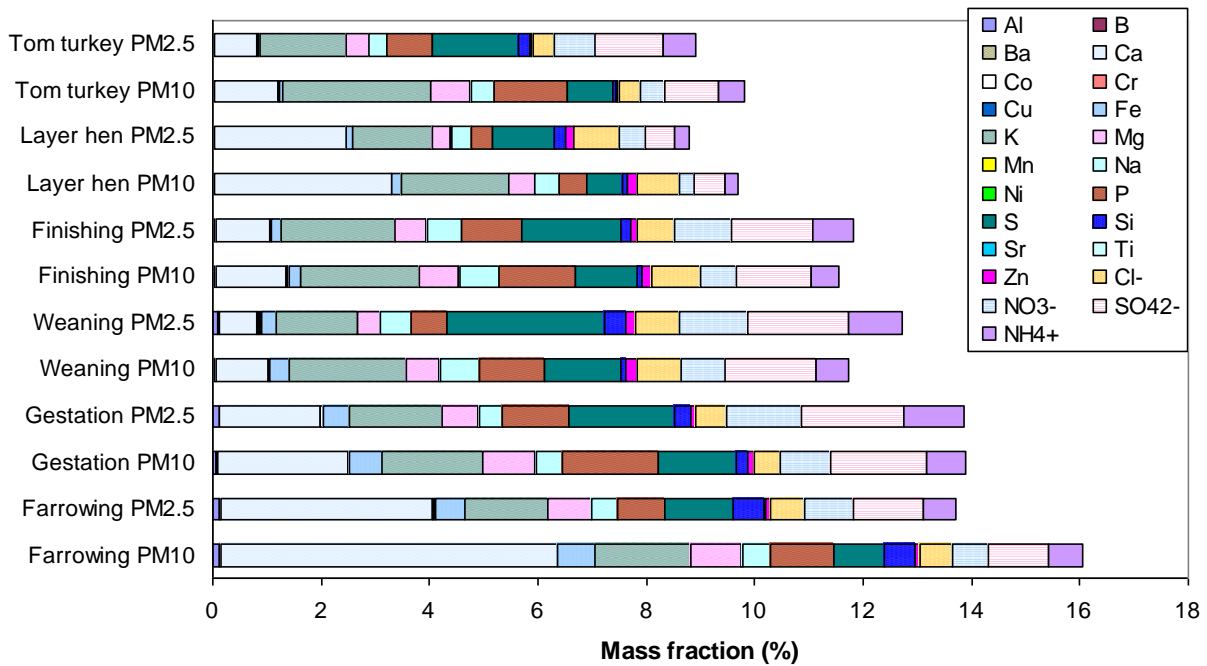


Figure 4.3. Average mass fraction of inorganic elements and soluble ions in PM samples.
 x. Here, S refers to sulfur in non-soluble sulfate and non-sulfate compounds only.

Table 4.3. Mass fraction of inorganic elements and soluble ions in PM₁₀ samples (in ng/mg dust).

Analyte	Farrowing		Gestation		Weaning		Finishing		Manure-belt layer hen		Tom turkey	
	Mean	SD	Mean	SD	Mean	SD	Mean	SD	Mean	SD	Mean	SD
Al	1212	607	707	567	301	182	300	178	286	260	356	349
B	103	99	65	83	140	94	292	240	11	19	26	18
Ba	112	117	88	23	27	13	33	10	13	8	15	7
Ca	62050	40623	24048	2816	9639	2286	12959	1998	32704	7940	11660	3322
Co	0	0	20	59	0	0	61	211	53	114	0	0
Cr	15	15	13	17	21	19	109	270	3	6	5	6
Cu	129	59	155	28	447	281	280	220	57	36	175	96
Fe	6978	6107	6133	2548	3434	2197	2050	713	1619	1993	574	297
K	17675	4029	18711	2334	21634	4961	21951	3683	19846	12532	27385	5479
Mg	9119	2501	9354	1125	6063	2205	7241	2370	4662	1578	7300	1764
Mn	286	91	369	45	275	87	268	40	201	133	255	99
Na	5208	1368	4697	1633	7244	2209	7336	1261	4457	1841	4032	1455
Ni	7	11	0	0	0	0	3	10	0	0	1	3
P	11782	3499	17880	2902	11937	2792	13871	3599	5237	2851	13715	4286
S	9161	2700	14415	3284	14028	8872	11435	4413	6561	3612	8244	2406
Si	5629	3470	1985	1351	1120	406	1084	527	793	672	787	361
Sr	66	24	40	12	19	6	30	7	64	49	21	8
Ti	54	38	36	21	14	9	16	9	9	10	16	11
Zn	771	254	1034	121	1978	1543	1599	1086	1715	1197	303	80
Cl ⁻	6259	2075	5009	935	7966	3179	9152	3434	7702	4164	3908	1247
NO ₃ ⁻	6502	5152	9316	5345	8109	4153	6414	2569	2899	2115	4737	1332
SO ₄ ²⁻	10958	5293	17631	3815	16945	6343	13785	3047	5683	3740	9774	3554
NH ₄ ⁺	6529	4772	7331	4067	5850	2620	5221	2156	2344	1288	4760	2445
Total mass fraction (%)	15.70	3.62	13.32	1.54	11.15	1.75	11.09	0.88	9.50	1.25	9.48	1.65

Table 4.4. Mass fraction of inorganic elements and soluble ions in PM_{2.5} samples (in ng/mg dust).

Analyte	Farrowing		Gestation		Weaning		Finishing		Manure-belt layer hen		Tom turkey	
	Mean	SD	Mean	SD	Mean	SD	Mean	SD	Mean	SD	Mean	SD
Al	1333	1045	1128	1399	941	2028	371	410	288	295	340	380
B	86	117	77	173	95	268	291	391	3	10	0	0
Ba	90	79	68	19	56	46	37	13	24	21	19	10
Ca	38991	24889	18626	1842	7099	4206	9882	1506	24294	8086	7809	2463
Co	428	1226	389	1166	218	329	0	0	0	0	0	0
Cr	15	26	31	51	177	295	76	118	35	61	11	24
Cu	146	146	151	121	356	297	220	172	64	54	130	63
Fe	5325	4517	4652	2070	2826	1535	1831	645	1135	928	508	441
K	15523	4655	17044	2435	15042	8356	20758	5096	14514	9022	15709	4546
Mg	7821	4215	6743	708	4014	2558	5879	1228	3560	844	4143	1204
Mn	224	93	276	57	187	101	220	42	159	82	162	59
Na	4632	1671	4242	1816	5617	3783	6376	1961	3742	1671	3300	1332
Ni	0	0	0	0	0	0	16	45	0	0	0	0
P	8748	3220	12367	1910	6582	3562	10913	2727	3790	1279	8465	2807
S	12503	10273	19432	10576	29143	24429	18495	10867	11506	8105	15851	10324
Si	5967	3964	2967	1841	3718	2961	1782	1039	2034	1935	2192	1146
Sr	51	18	45	41	19	11	25	5	52	44	15	6
Ti	51	41	37	24	15	19	18	13	32	67	15	10
Zn	871	494	931	153	2000	1152	1207	763	1400	846	500	279
Cl ⁻	6364	1987	5565	2232	8027	3514	6730	1158	8321	5424	3889	1812
NO ₃ ⁻	9054	6122	13749	8856	12455	9560	10623	5753	4801	3843	7406	3996
SO ₄ ²⁻	12930	7811	19055	9597	18589	13932	14899	8457	5593	5898	12723	7419
NH ₄ ⁺	5899	3450	11068	6996	9889	6611	7506	6098	2426	2743	6058	4682
Total mass fraction (%)	13.27	4.49	13.23	2.72	12.09	5.73	11.32	2.05	8.59	1.53	8.50	3.29

4.4.4 Variations in chemical composition with animal building type

In receptor modeling, the relative abundance of measured chemical species is of great significance. If PM samples from two different sources had the same or a very similar chemical composition in terms of relative abundance, it would be difficult to distinguish those two sources in chemical mass balance (CMB) and factor analysis (e.g., positive matrix factorization [PMF]) models. Conventional multivariate data analysis tools, such as PCA and Euclidean distance-based multidimensional scaling (MDS), cannot directly determine whether an observed difference between two samples is caused by a difference in relative abundance or in absolute abundance of chemical species, but rather investigate a combination effect of both factors. For instance, PM samples, with identical relative abundances of chemical species but differing in mass concentration, would scatter on a PCA plot. To address this issue, a correlation coefficient-based PCoA plot was implemented to depict variations in PM chemical composition with animal building type and other factors. Basically, a Pearson's correlation coefficient (r) was selected as a measure of the distance between samples (Equation 4.2).

$$d_{jk} = 1 - r_{jk} = 1 - \frac{n \sum_i x_{ji} x_{ki} - \sum_i x_{ji} \sum_i x_{ki}}{\sqrt{n \sum_i x_{ji}^2 - \left(\sum_i x_{ji} \right)^2} \sqrt{n \sum_i x_{ki}^2 - \left(\sum_i x_{ki} \right)^2}} \quad (4.2)$$

Where, d_{jk} is the correlation distance between the j^{th} and the k^{th} sample, r_{jk} is Pearson's correlation coefficient, x_{ji} is the content of the i^{th} specie in the j^{th} sample and x_{ki} is the content of the i^{th} specie in the k^{th} sample. When two PM samples are the same in terms of the relative abundance of chemical species, they will be assigned at the same location on a correlation distance-based PCoA plot.

The analysis results showed that the chemical composition of PM samples varied greatly with animal building type (Figure 4.4). Tom turkey, weaning and finishing buildings were closely clustered, indicating PM samples from those buildings may have a similar chemical composition. A similar but a less degree of clustering was found between farrowing, gestation and manure-belt layer hen buildings. Noticeably, those two clusters were clearly separated, suggesting a difference in PM chemical composition. PM_{10} and $PM_{2.5}$ samples from a cage-free

layer hen building were located fairly close to those from manure-belt layer hen buildings; while $PM_{2.5}$ samples from a broiler building were somehow isolated.

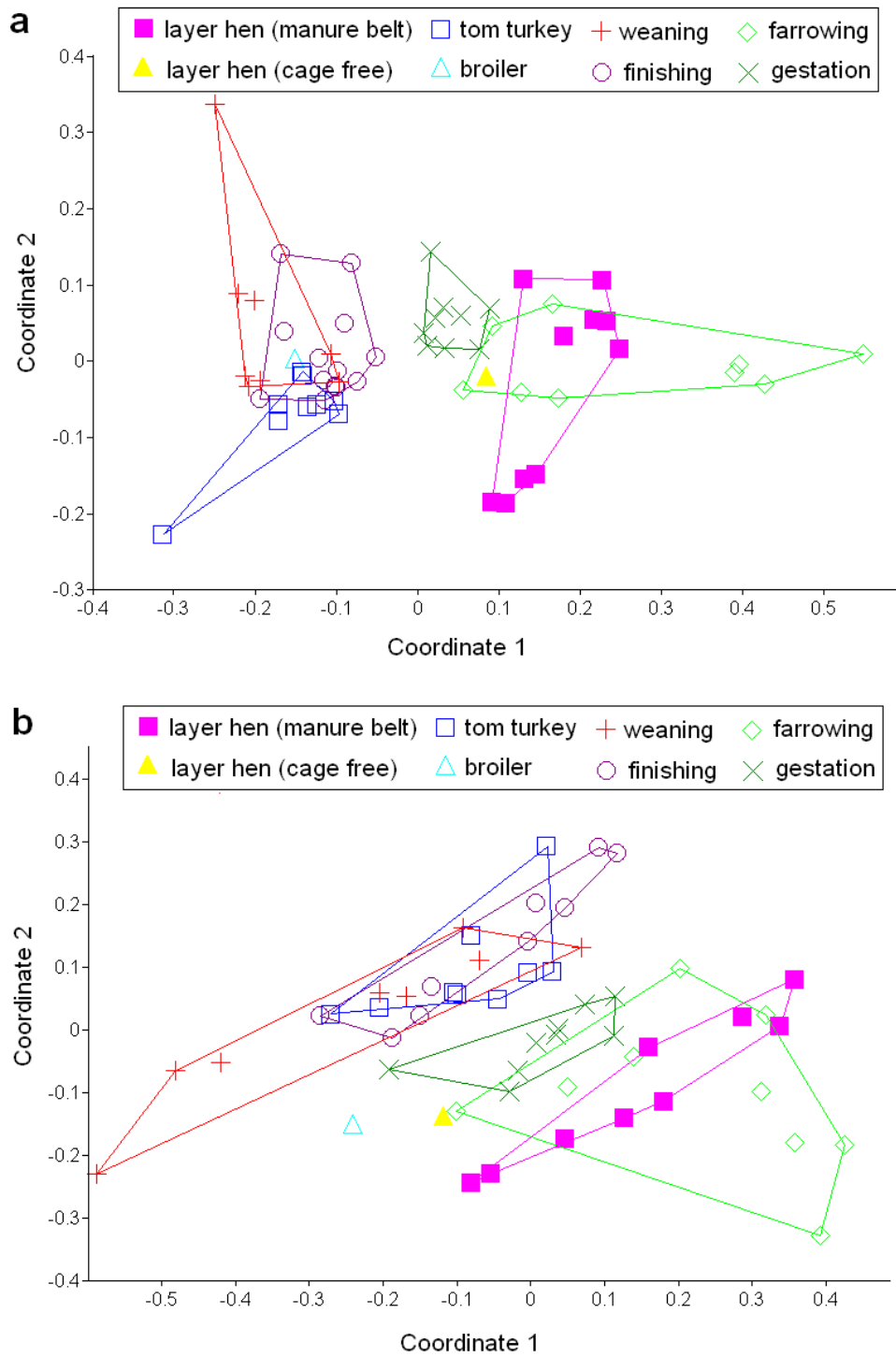


Figure 4.4. Correlation distance-based PCoA plot of PM samples from different types of animal buildings: (a) PM_{10} and (b) $PM_{2.5}$ samples.

The PCoA provides a convenient way to visualize differences in terms of the relative abundance of chemical species. Following that, a correlation distance-based ANOSIM test was employed to quantify and test the significance of observed differences (Table 4.5). The ANOSIM test measures the ratio (R) of distances between two groups to distances within individual groups (Clarke, 1993). In general, two groups are considered to be well separated when R is greater than 0.75, separated but with a slight overlap when R is greater than 0.5 but smaller than 0.75, separated but with a strong overlap when R is greater than 0.25 but smaller than 0.5, and hardly separable when R is smaller than 0.25 (Lin et al., 2003). A p value is also given by the test, as a measure of the significance of separation (difference) (significant when $p < 0.05$).

Table 4.5. Summary of ANOSIM test on PM₁₀ and PM_{2.5} samples from different type of animal confinement buildings^{x,y}.

PM ₁₀ : R global=0.634, p<0.001						
	Farrowing	Finishing	Gestation	Layer hen ^z	Tom turkey	Weaning
Farrowing		<0.001	<0.001	0.077	<0.001	<0.001
Finishing	***0.862		<0.001	<0.001	0.014	0.078
Gestation	**0.558	**0.715		<0.001	<0.001	<0.001
Layer hen	0.112	***0.981	***0.751		<0.001	<0.001
Tom turkey	***0.892	0.213	***0.966	***0.972		<0.001
Weaning	***0.876	0.127	***0.827	***0.958	*0.369	
PM _{2.5} : R global=0.426, p<0.001						
	Farrowing	Finishing	Gestation	Layer hen	Turkey	Weaning
Farrowing		<0.001	0.001	0.228	<0.001	<0.001
Finishing	**0.688		0.004	<0.001	0.245	0.130
Gestation	*0.409	*0.386		0.001	<0.001	0.002
Layer hen	0.040	*0.703	*0.463		<0.001	<0.001
Tom turkey	**0.735	0.035	*0.428	***0.781		0.058
Weaning	**0.692	0.098	*0.488	**0.681	0.159	

x. In the upright portion of the table are the p values and the R values are listed in the lower left portion.

y. R values are highlighted with ‘*’ if $0.50 \geq R > 0.25$, ‘**’ if $0.75 \geq R > 0.50$ and ‘***’ if $R > 0.75$.

z. Manure-belt layer hen building only.

The test results revealed that PM₁₀ samples from farrowing and manure-belt layer hen buildings were all well separated from those from weaning, finishing and tom turkey buildings; PM₁₀ samples from gestation buildings were well separated from those from manure-belt layer hen, tom turkey and weaning buildings, and were separated from but slightly overlapped with PM₁₀ samples from farrowing and finishing buildings; a separation but strong overlapping was identified between PM₁₀ samples from weaning and from tom turkey buildings. Comparatively, PM_{2.5} samples from different types of animal buildings had a more similar chemical composition

according to the global R value. The only ‘well separated’ groups were tom turkey and manure-belt layer hen buildings; PM_{2.5} samples from farrowing buildings were separated from but slightly overlapped with those from weaning, finishing and tom turkey buildings, and were separated from but strongly overlapped with those from gestation buildings; PM_{2.5} samples from manure-belt layer hen buildings were separated from but slightly overlapped with those from weaning and tom turkey buildings; PM_{2.5} samples from gestation buildings were separated from but strongly overlapped with those from all other five types of animal buildings. All observed separations (R>0.25) were of statistical significance based on the p value.

The implication of the R value to receptor modeling is not yet clear. Accordingly, it is hard to set an R threshold value such that above this value two types of animal buildings would be safely distinguishable in a receptor model. In ecology research, R=0.5 is often selected as an important cut value, i.e. two biotic communities are considered to be clearly different when R is greater than 0.5 (Lin et al., 2003). Similarly in this study, we selected R=0.5 as a tentative threshold value and conducted subsequent data analysis on cases with R greater than 0.5. However, R=0.5 may be insufficient for source distinguishing in receptor models.

Logically, the next step would be to determine which chemical species were correlated with the observed separations (differences). For this purpose, a SIMPER analysis was selected. The SIMPER analysis basically calculates the contribution percentage of each chemical species to the average Bray-Curtis dissimilarity (Equation 4.3) between two animal building types. Similar to Euclidean distance and Pearson’s correlation coefficient (r), the Bray-Curtis dissimilarity index (BC) can be used to measure ‘distance’ between samples.

$$BC_{jk} = \frac{\sum_{i=1}^s |x_{ij} - x_{ik}|}{\sum_{i=1}^s (x_{ij} + x_{ik})} \quad (4.3)$$

Where, BC_{ik} is the Bray-Curtis dissimilarity between the jth and kth samples, s is the number of chemical species, x_{ij} is the mass fraction of the ith specie in the jth sample, and x_{ik} is the abundance of the ith specie in the kth sample. The Bray-Curtis dissimilarity index has been widely employed in ecology research (Clarke, 1993) and is current the only option to the SIMPER analysis. The BC- and correlation distance-based PCoA plot and ANOSIM test actually produced very similar results (data not shown here). It would be ideal if a correlation distance-

based SIMPER analysis became available and were applied to this study. Anyhow, we expected that the BC-based SIMPER analysis would offer certain clues on sources of difference.

The SIMPER analysis results were shown in Table 4.6 and 4.7. It can be seen that differences in chemical composition between different types of animal buildings were mainly contributed by the contents of Ca, K, S, P, SO_4^{2-} , NO_3^- , NH_4^+ and Cl^- . Those chemical species were also abundant ones in PM_{10} and $\text{PM}_{2.5}$ samples. Among them, Ca was found to be the number one variation-contributor in most cases, suggesting that PM chemical composition may greatly be affected by the dose of, e.g., limestone or dolomite in animal diet. Particularly, Ca alone contributed to more than 40% differences in PM_{10} chemical composition between farrowing buildings and other building types. Another interesting observation was a ‘synchrony’ between different chemical species, e.g., in many cases, the sign (+ or -) of Ca, Ti, Mg and Si changed simultaneously. This implies that a certain correlation may exist between those chemical species. A detailed discussion on it would be described later in this chapter.

Table 4.6. Major chemical species in PM_{10} samples that contribute to variations in chemical composition among different types of animal confinement buildings.

Building type	Top ten contributing chemical species ^x	Cumulative contribution
Farrowing vs. Finishing	Ca(+), SO_4^{2-} (-), K(-), Fe(+), NO_3^- (+), Si(+), P(-), NH_4^+ (+), S(-), Cl^- (-)	91.9%
Farrowing vs. Gestation	Ca(+), SO_4^{2-} (-), NO_3^- (-), P(-), S(-), NH_4^+ (-), Fe(+), Si(+), K(-), Cl^+ (+)	94.0%
Farrowing vs. Tom turkey	Ca(+), K(-), Fe(+), SO_4^{2-} (+), Si(+), P(-), NH_4^+ (+), NO_3^- (+), S(+), Cl^+ (+)	93.8%
Farrowing vs. Weaning	Ca(+), SO_4^{2-} (-), K(-), S(-), NO_3^- (-), Fe(+), Si(+), NH_4^+ (+), P(-), Mg(+)	91.8%
Finishing vs. Gestation	Ca(-), S(-), NO_3^- (-), P(-), SO_4^{2-} (-), K(+), Cl^+ (+), Fe(-), NH_4^+ (-), Na(+)	89.7%
Finishing vs. Layer hen ^y	Ca(-), K(+), P(+), SO_4^{2-} (+), S(+), Cl^+ (+), NO_3^- (+), Mg (+), NH_4^+ (+), Na(+)	93.7%
Gestation vs. Layer hen	P(+), SO_4^{2-} (+), K(-), Ca(-), S(+), NO_3^- (+), NH_4^+ (+), Mg (+), Fe(+), Cl^+ (+)	93.8%
Gestation vs. Tom turkey	Ca(+), K(-), SO_4^{2-} (+), S(+), NO_3^- (+), Fe(+), P(+), NH_4^+ (+), Mg (+), Na(+)	93.2%
Gestation vs. Weaning	Ca(+), S(+), P(+), SO_4^{2-} (+), K(-), NO_3^- (+), NH_4^+ (+), Fe(+), Mg (+), Cl^- (-)	90.2%
Layer hen vs. Tom turkey	Ca(+), K(-), P(-), SO_4^{2-} (-), Cl^+ (+), S(-), Mg (-), NH_4^+ (-), NO_3^- (-), Na(+)	94.4%
Layer hen vs. Weaning	Ca(+), K(-), S(-), SO_4^{2-} (-), P(-), NO_3^- (-), Cl^- (-), NH_4^+ (-), Na(-), Fe(-)	93.4%

x. The symbol ‘+’ or ‘-’ in parenthesis represents a difference in abundance between two groups. For example, for farrowing versus finishing, Ca (+) indicates that PM samples from farrowing buildings have averagely higher Ca content than those from finishing buildings. Chemical species were listed in an order of contribution

y. Manure-belt layer hen building only.

Table 4.7. Major chemical species in PM_{2.5} samples that contribute to variations in chemical composition among different types of animal confinement buildings.

Building type	Top ten contributing chemical species	Cumulative contribution
Farrowing vs. Finishing	Ca(+), S(-), SO ₄ ²⁻ (-), K(-), NO ₃ ⁻ (-), NH ₄ ⁺ (-), Si(+), P(-), Fe(+), Mg ⁻ (+)	91.9%
Farrowing vs. Tom turkey	Ca(+), S(-), SO ₄ ²⁻ (+), K(-), NO ₃ ⁻ (+), Fe(+), Mg ⁻ (+), NH ₄ ⁺ (-), Si(+), P(+)	91.3%
Farrowing vs. Weaning	Ca(+), S(-), SO ₄ ²⁻ (-), K(+), NO ₃ ⁻ (-), NH ₄ ⁺ (-), Mg ⁻ (+), P(+), Si(+), Cl ⁻ (-)	90.3%
Finishing vs. Layer hen	Ca(-), SO ₄ ²⁻ (+), S(+), K(+), P(+), NO ₃ ⁻ (+), NH ₄ ⁺ (+), Cl ⁻ (-), Na(+), Mg(+)	93.7%
Layer hen vs. Tom turkey	Ca(+), S(-), SO ₄ ²⁻ (-), K(-), Cl ⁻ (+), P(-), NO ₃ ⁻ (-), NH ₄ ⁺ (-), Na(+), Si(-)	94.7%
Layer hen vs. Weaning	Ca(+), S(-), SO ₄ ²⁻ (-), K(-), NO ₃ ⁻ (-), NH ₄ ⁺ (-), Cl ⁻ (+), P(-), Na(-), Si(-)	92.6%

A pairwise ANOVA test was performed to compare the average mass fraction of each chemical species in PM samples from different types of animal buildings. Due to the relatively large database, this work was done with a MATLAB program. A Kruskal-Wallis test (nonparametric ANOVA) was used when zero mass fraction data were present, or when the normality of data was still poor after log transformation. We found that for PM₁₀ samples, 22.8% (84 of 368) of pairwise comparisons produced a significant difference; while for PM_{2.5} samples, the ratio was 9.8% (36 of 368). This again indicates that PM_{2.5} samples from different types of animal confinement building had a more similar chemical composition. The total mass fraction of identified inorganic elements and soluble ions was significantly higher in PM samples from swine buildings than those from poultry buildings ($p < 0.001$ for both PM₁₀ and PM_{2.5}), suggesting that PM samples from poultry buildings may contain higher contents of organic matter or other components.

What makes the chemical composition of PM samples vary with animal building type? We speculated that a major reason is a change in feed ingredients and manure characteristics with animal types. Turkeys and layer hens are clearly different from pigs, and thus require different feed diets and excrete manures of different composition. Even for pigs (swine), different growing stages (Figure 4.5) have different requirements of feed ingredients and accordingly may lead to different manure characteristics. For example, as reported by Nicholson et al. (1999), animal feeds in turkey and layer hen buildings have a content of Cu comparable to those in farrowing and gestation buildings but less than those in weaning and finishing buildings; a similar observation was made for manures. Noticeably, in this study PM samples from weaning and

finishing buildings had averagely a higher Cu content than those from the other four types of animal buildings (Table 4.3 and 4.4).

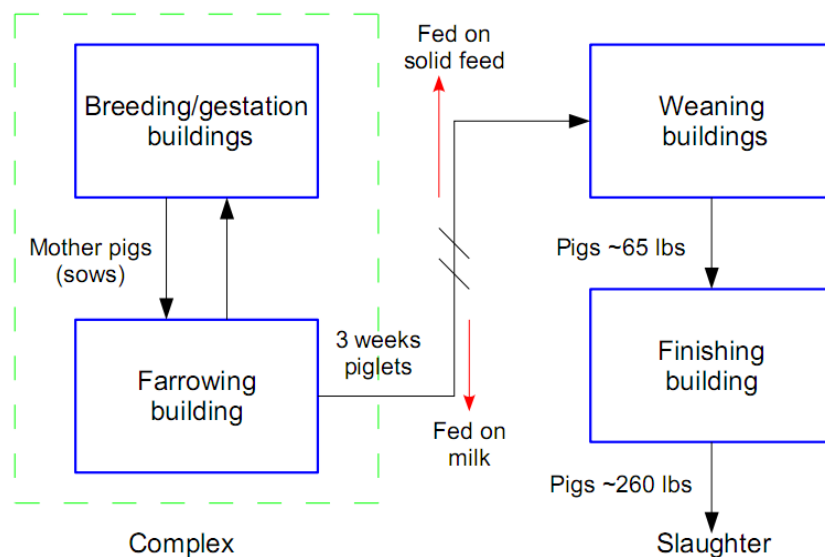


Figure 4.5. Schematic of swine production cycle used in the Midwest.

Another reason was considered to be differences in feeding system and manure management practice with animal building type. As an example, animal feeds in gestation and farrowing (including lactation and farrowing stages) buildings are fairly similar in feed ingredients (Brendemuhl and Myer, 2009). However, feeding systems are different: dry feeders in farrowing buildings and wet feeders in gestation buildings. A major difference between those two systems is that animal feed and water remain separate in a dry feeding system but are mixed in a wet feeding system. A mixing of feed and water reduces the aerosolization of feed particles. As a result, PM samples from gestation buildings may contain a less fraction of feed particles than those from farrowing buildings, thereby leading to a somewhat different PM chemical composition (Figure 4.4).

In reality, it is rare to have all six different types of animal confinement buildings in an area of interest. However, the presence of multiple animal building types can be still found in some areas, e.g., northwestern Iowa, where animal production is diverse and intensive. For the latter case, the results from this study demonstrate a possibility and potential limitations of using receptor modeling for PM source apportionment, with following observations and suggestions (it should be noted that here the observations were derived from limited sampling sites and visits and, thus, may not be apply to general cases):

- Receptor modeling may better apply to PM₁₀ since PM₁₀ samples from different types of animal confinement buildings were relatively more different in chemical composition.
- Weaning and finishing buildings may be considered to be the same type of sources.
- It can be difficult to distinguish tom turkey from weaning/ finishing buildings. Similarly, manure-belt layer hen and farrowing buildings can be hardly distinguishable.
- Manure-belt layer hen and weaning/ finishing buildings may be considered to be two different PM sources in receptor modeling. This is particularly of practical importance due to the large scale of layer hen and finishing pig industries.
- Manure-belt layer hen and tom turkey building may be distinguishable in receptor modeling, and so do with farrowing/ gestation and weaning/ finishing buildings.

4.4.5 Variation with season

A similar data analysis procedure was followed. No significant differences were identified among PM₁₀ samples from different seasons (Figure 4.6 and Table 4.8). Comparatively, PM_{2.5} samples from cold and mild season were similar but significantly different from those from hot seasons; however, the corresponding R values were both smaller than 0.25, indicating that the differences were barely distinguishable. We further investigated PM samples from each type of animal confinement buildings and did not find any significant differences among PM₁₀ samples from different seasons (data not shown here). In gestation and finishing buildings, a significant difference was observed between PM_{2.5} samples from hot and from cold and mild seasons; while in other buildings, no significant difference was identified. It is noteworthy that both gestation and finishing buildings visited in this study use a wet feeding system; while a dry feeding system is employed in other buildings. In summary, seasons had little effect on PM₁₀ chemical composition but had a slight effect on PM_{2.5} chemical composition.

Table 4.8. ANOSIM test on PM₁₀ and PM_{2.5} samples from different seasons.

PM ₁₀ : R global=0.0002, p=0.399				PM _{2.5} : R global=0.176, p<0.001			
	Cold	Mild	Hot		Cold	Mild	Hot
Cold		0.874	0.301	Cold		0.821	<0.001
Mild	-0.028		0.394	Mild	-0.032		0.003
Hot	0.009	0.001		Hot	0.210	0.217	

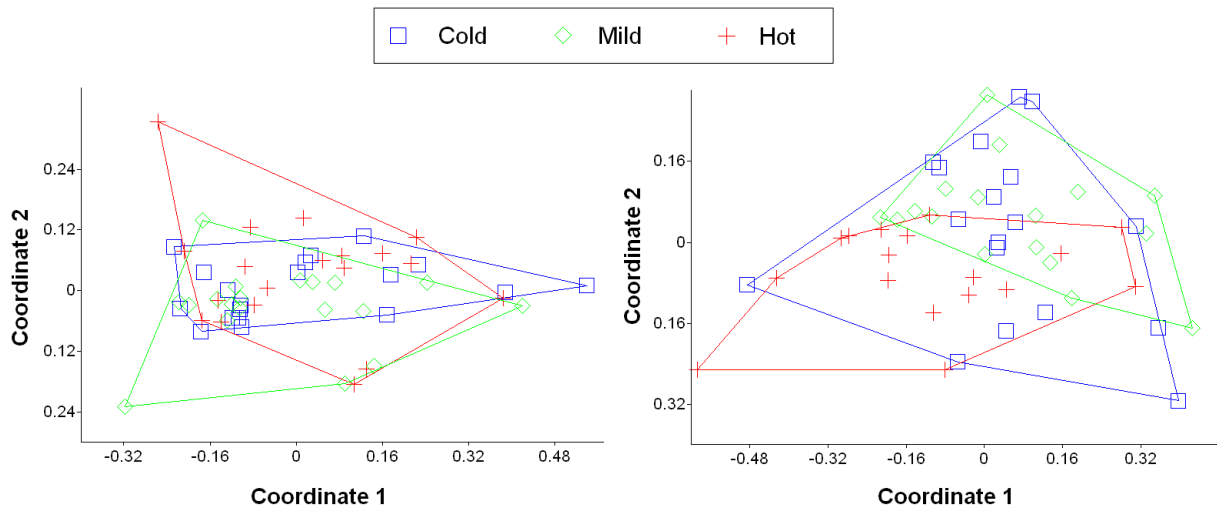


Figure 4.6. Correlation distance-based PCoA plot of PM samples from different seasons: (a) PM₁₀ and (b) PM_{2.5} samples.

As mentioned in Chapter 3, there is a strong correlation between PM concentrations and ambient temperatures. In general, PM concentrations in animal confinement buildings increase as the weather becomes colder, due to a decreased ventilation rate and an accumulation of PM inside buildings. Therefore, the conclusions drawn in the previous paragraph suggests that PM chemical composition (especially that of PM₁₀) may not change greatly with PM concentration in the same type of buildings.

Because of a large variation in PM₁₀ and PM_{2.5} concentrations with seasons (please refer to Table 3.10), using the air concentration ($\mu\text{g}/\text{m}^3$) of chemical species for summarizing PM chemical composition would lead to a large standard deviation. Accordingly, the mass fraction data were selected in this study for data presentation (Table 4.3 and 4.4).

4.4.6 Variations with particle size

No significant difference was found between PM₁₀ and PM_{2.5} samples collected in farrowing and manure-belt layer hen buildings (Figure 4.7 and Table 4.9); while, significant differences were identified in gestation, weaning, finishing and tom turkey buildings. However, only in tom turkey buildings, the chemical composition of PM₁₀ was clearly different from that of PM_{2.5}, according to the R value. The SIMPER analysis revealed that PM₁₀ samples from tom turkey buildings had higher contents of P, K, Ca, Na and Mg but fewer contents of S, SO_4^{2-} , NO_3^- and Si than PM_{2.5}. A difference in PM sources is a plausible explanation to such size-induced composition differences: coarse particles in animal buildings were considered to mainly

originate from animal feeds while fine particles were largely from fecal materials (Feddes et al., 1992; Heber et al., 1988a). However, little is known about how and to what degree the chemical composition of animal feeds differs from that of fecal materials in each type of animal buildings.

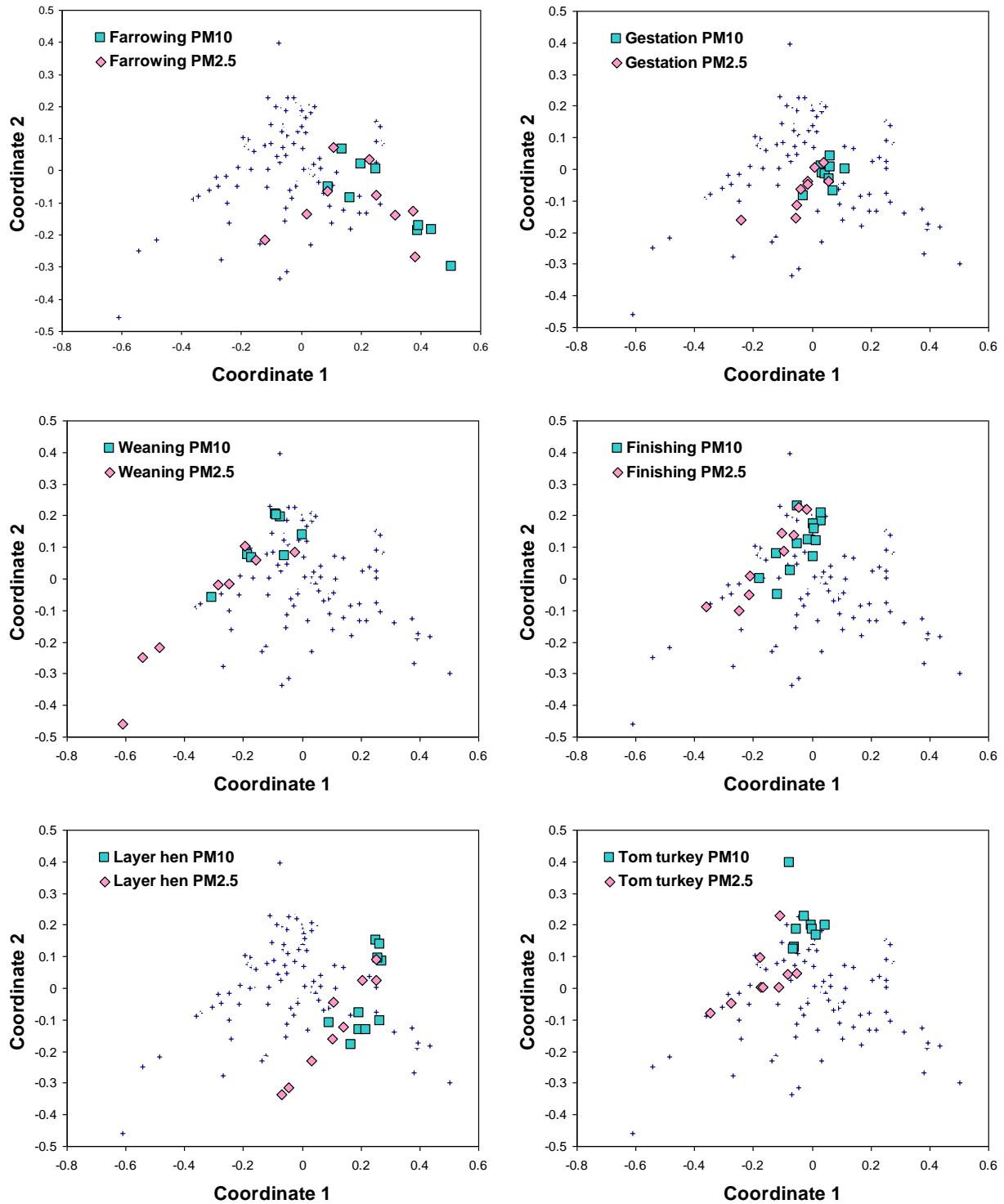


Figure 4.7. Correlation distance-based PCoA plot of PM₁₀ versus PM_{2.5} samples.

Table 4.9. Summary of ANOSIM test on PM samples from the same types of animal confinement buildings but differing in particle size (PM₁₀ versus PM_{2.5}).

Statistic	Overall	Farrowing	Gestation	Weaning	Finishing	Manure-belt layer hen	Tom turkey
R	0.130	-0.043	0.214	0.241	0.186	0.049	**0.561
p	<0.001	0.7153	0.009	0.025	0.028	0.189	<0.001

The Mantel test revealed a significant and fairly strong correlation ($r=0.723$, $p<0.001$) between the correlation distance matrix of PM₁₀ and that of PM_{2.5}, indicating that the chemical composition of PM₁₀ and PM_{2.5} samples varied in a similar pattern, ‘synchronously’ from one field trip to another. This is expectable since PM_{2.5} is a subfraction of PM₁₀.

4.4.7 Correlation between chemical species

The PCA results revealed that variations in PM chemical composition could hardly be explained by a few factors (Figure 4.8), implying that the sources of PM may be highly diverse in animal confinement buildings. The negative factor loadings generated from PCA created a great challenge to PM source identification. Alternatively, we used the EPA PMF3.0, another popular PM source apportionment tool, to analyze the dataset. However, as a measure of model fitting performance in PMF, the calculated Q values were much higher than the theoretical ones regardless of the selected number of factors, suggesting a poor fitting (data not shown here). In summary, factor analysis did not work well for PM samples in this study, possibly due to a significant difference in the chemical composition of animal feeds and manures among different types of animal confinement buildings.

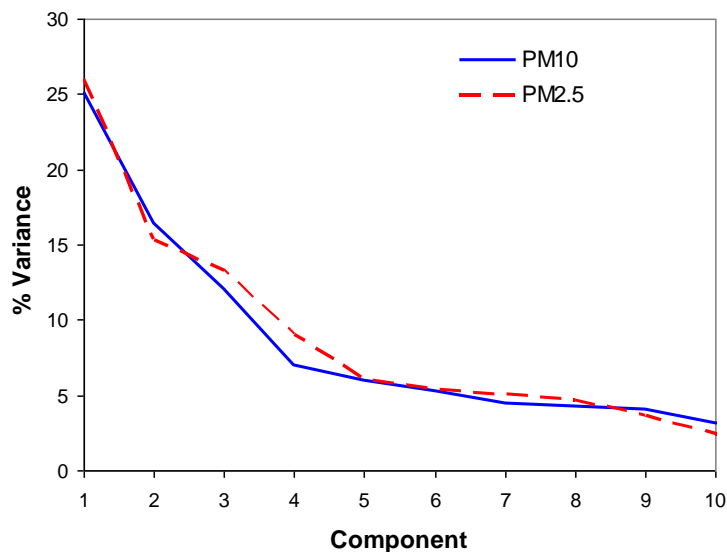


Figure 4.8. PCA scree plot for chemical composition of PM₁₀ and PM_{2.5} samples.

To address the limitations of factor analysis, a correlation distance-based PCoA was applied to chemical species in PM samples (Figure 4.9). Basically, if the variations of two species are highly correlated, they will likely originate from the same or similar sources. It can be seen from Figure 4.9 that SO_4^{2-} , S, NO_3^- and NH_4^+ , Cr and Zn were closely clustered, suggesting that most Zn, Cr and NH_4^+ may exist in the forms of sulfate and nitrate. Ca, Mg and Sr were clustered together and a possible source of them is dolomite as a feed additive. The grouping of Al, Si, Ti and Ba implies that they may originate from similar sources, e.g., soil dust since they are all typical crustal elements.

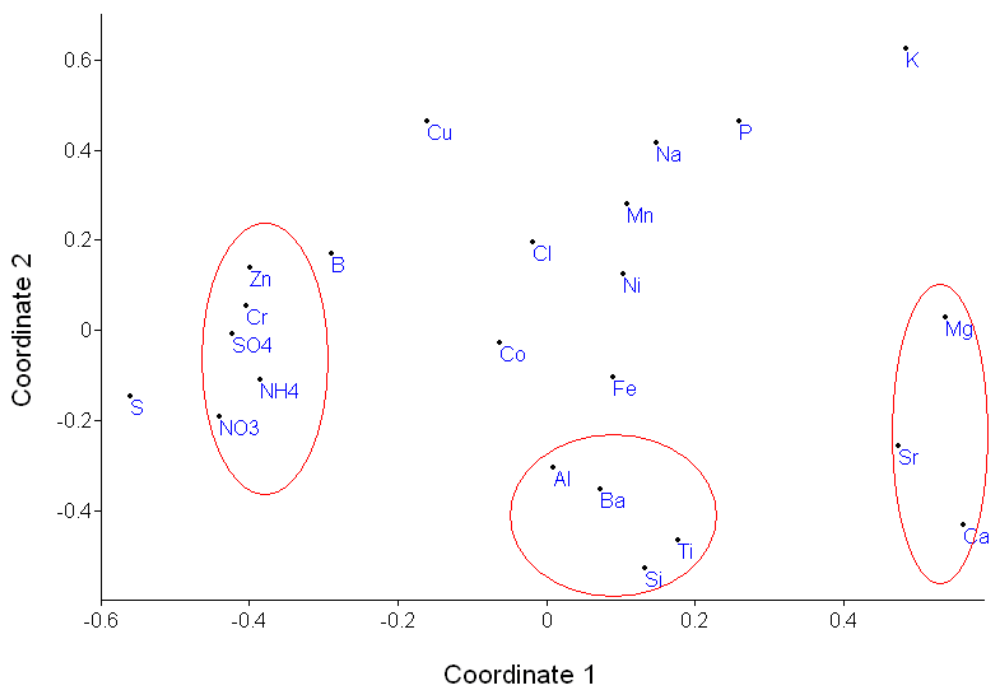


Figure 4.9. Correlation distance-based PCoA plot of chemical species in PM samples.

However, it should be noted that the PCoA did not exclude a possibility that Al, Si, Ti and Ba may come from animal feed additives, e.g., limestone or dolomite, as impurities. In reality, the source of Ca in animal feeds can be very diverse. Some Ca-containing ingredients, such as $\text{Ca}_3(\text{PO}_4)_2$, may contain fewer or higher contents of Al, Si, Ti and Ba than limestone. The presence of those ingredients would lead to a relatively poor correlation of Ca to Al, Si, Ti and Ba. This is an example showing a major limitation of correlation-based data analysis. In summary, the correlation distance-based PCoA plot can be a useful assisting tool for identification of potential PM sources but it alone can hardly offer definite conclusions.

4.5 Limitations and Recommendations

Potential issues associated with the present study are listed as follows:

- One of the biggest limitations is the limited sampling frequency, in terms of total sites and the number of field trips. This study should better be considered as a preliminary survey and more monitoring efforts should be made in the future.
- Although the presence of Cl and Br were detected by EDXRF tests, the ICP-AES test protocol used in this study could not quantify those two elements because of the use of HCl for sample digestion. An acid mixture of HNO₃ and HF would be recommended for future digestion, which may additionally improve the recovery efficiency of refractory elements such as Ti and Si.
- The IC system selected in this study has limited sensitivities to SO₄²⁻ and NO₃⁻. The concentrations of both ions were occasionally below the detection limits. Especially for PM_{2.5} samples with very low particle loading, the obtained extracts were too diluted for quantification of SO₄²⁻ and NO₃⁻.
- No OC/EC sampling and analysis were conducted. OC/EC has become a routine test for ambient aerosols and source PM's, and is usually included into receptor modeling. A lack of OC/EC data for PM from animal confinement buildings may cause certain data compatibility issues in receptor modeling when OC/EC data are available for the PM from other sources. Therefore, although there were obviously no EC sources in animal confinement buildings, it would be advantageous to monitor OC/EC in PM samples.
- No measurement of C, H, N and O was conducted. The quantified inorganic elements and soluble ions only accounted for small mass fractions of PM samples. The majority of PM mass may be contributed by organic matter. A measurement of C, H, N and O therefore can help in the reconstruction of the PM mass. In addition, there was no measurement on inorganic carbon (CO₃²⁻). Carbonate may contribute significantly to the mass of PM because of the use of limestone and/or dolomite as a supplement in animal diet.
- There could be a positive sampling artifact associated with NH₄⁺ analysis due to the adsorption of NH₃ gas on Teflon filters. It would be ideal to install a denuder prior to PM filters to pre-remove NH₃ gas.

4.6 Summary and Conclusions

4.6.1 Implication

Determination of inorganic elements and soluble ions in PM can provide critically useful data for receptor modeling. The CMB model requires a complete database of source chemical profiles. Consequently, an examination on PM from animal confinement buildings will be necessary if animal confinement buildings are perceived as potentially a major PM source. The PMF model does not require the input of source chemical profiles. However, knowledge of source chemical profiles is still of great importance because a source identification in PMF modeling primarily relies on a comparison of calculated factors to available source chemical profiles. This preliminary study offered essential PM source chemical profiles of animal confinement buildings, and hopefully will facilitate the application of receptor modeling to animal production-related air quality researches.

Investigation of the chemical composition of PM from animal confinement buildings can also provide valuable information for assessing the potential health effect of PM on human and animals. Most inorganic elements and soluble ions identified in this study are nontoxic. However, some of them, e.g., Ni and Cr, can become harmful at high airborne concentrations. This may raise certain concerns and needs further evaluation.

4.6.2 Summary of findings

In this chapter, we collected PM₁₀ and PM_{2.5} samples from six different types of animal confinement buildings and analyzed their chemical composition in terms of inorganic elements and soluble ions. Potential variations in PM chemical composition with animal building type, season and particle size were investigated through multivariate data analysis. The following observations and findings were obtained:

- The following inorganic elements and soluble ions were identified in PM from animal confinement buildings: B, Na, Mg, Al, Si, P, S, Cl, K, Ca, Ti, Cr, Mn, Fe, Co, Ni, Cu, Zn, Br, Sr, Sn, Ba, Cl⁻, SO₄²⁻, NO₃⁻, PO₄³⁻, and NH₄⁺.
- Ca and K were the most abundant inorganic elements, followed by S and P. Mg, Na, Cl⁻, SO₄²⁻, NO₃⁻ and NH₄⁺ were also of large quantity. The total mass fraction of identified chemical species was fairly low, typically less than 16%.

- PM chemical composition varied significantly with animal building type. PM samples from tom turkey, swine weaning and finishing buildings had similar chemical compositions. A similar observation was made for PM samples from manure-belt layer hen and farrowing buildings. A clear difference ($R > 0.5$) in PM chemical composition was found between manure-belt layer hen/ farrowing and tom turkey/ weaning/ finishing buildings. PM_{2.5} samples from different types of animal confinement buildings were more similar in chemical compositions than PM₁₀ samples.
- Differences in chemical composition with animal building type were mainly contributed by the contents of Ca, K, S, P, SO₄²⁻, NO₃⁻, NH₄⁺ and Cl⁻. Among them, Ca was the top one variable contributor. Variations with animal building type could be ascribed to (1) a change in feed ingredients and manure characteristics, and (2) a difference in feeding system and manure management practice with animal or animal building type.
- Seasons had no significant effect on PM₁₀ and a significant but weak effect on PM_{2.5} chemical composition. This suggests that the chemical composition of PM, especially PM₁₀ samples, does not change greatly with PM concentration.
- PM₁₀ samples from gestation, weaning, finishing and tom turkey buildings had significantly different chemical compositions than corresponding PM_{2.5} samples. This may be due to a difference in the sources of course versus fine particles.
- The sources of PM may be highly diverse in animal confinement buildings. A correlation distance-based PCoA plot can be a useful assisting tool for identifying potential PM sources.

4.6.3 Conclusions

Inorganic elements and soluble ions in PM₁₀ and PM_{2.5} samples collected from six different types of animal confinement buildings were quantified. Ca and K were the most abundant inorganic elements, followed by S and P. Mg, Na, Cl⁻, SO₄²⁻, NO₃⁻ and NH₄⁺ were also in abundance. The total mass fraction of identified chemical species was typically less than 16%. Future investigations should attempt to characterize the rest of PM mass.

Compared to the high concentrations of NH₃ gas (a few to tens of mg/m³) in animal confinement buildings reported in the literature, our result suggests that the majority of emitted

$\text{NH}_3\text{-N}$ exist in the gas phase and the formation of NH_4^+ -containing secondary aerosols is insignificant in animal confinement buildings.

PM chemical composition varied significantly with animal building type. PM samples from certain different types of animal confinement buildings, e.g., manure-belt layer hen and tom turkey, had substantially different chemical compositions, which indicates a possibility of applying receptor models to determining PM contributions by different animal building types. Compared to the PM_{10} samples, the $\text{PM}_{2.5}$ samples from different types of animal confinement buildings were more similar in terms of chemical composition. Seasons (hot, mild and cold) had no significant effect on PM_{10} and a weak but significant effect on $\text{PM}_{2.5}$ chemical compositions. This suggests an absence of seasonal variation (especially for PM_{10} samples), which is a positive finding for PM receptor modeling. To address the research need raised by NAS (2003), future efforts should be made to apply receptor models to animal production related air quality problems, and to compare receptor models with dispersion models to assess their respective advantages and limitations.

5. CHARACTERIZATION OF PARTICLE-BORNE ODORANTS FROM ANIMAL CONFINEMENT BUILDINGS

5.1 Introduction

Odor from animal facilities is a major nuisance to neighbor communities and may cause a number of environmental and health consequences (Schiffman, 1998; Schiffman et al., 1995; Schiffman et al., 2000; Thu et al., 1997). As more residence communities are being built near commercial animal operations, there has been a significant increase in complaints against the odors emanating from animal production (Bundy, 1992). Although currently there are no federal regulations regarding odor, some states and cities have implemented air quality standards for odors in the ambient air (Mahin, 2001). To address the upcoming challenge in odor control, it is essential to characterize the odorants from animal confinement buildings such that efficient and affordable mitigation strategies can be developed.

Odor can be analyzed by olfactometry, gas chromatography (GC), Fourier transform infrared spectroscopy (FTIR) and electronic nose. As a subjective method, olfactometry utilizes the human sense of smell and has been most extensively employed for determining odor levels and emission factors from animal facilities (Gallmann et al., 2001; Jerez et al., 2005; Lim et al., 2001; Sun et al., 2008; Zhu et al., 2000). However, the consistency and replicability of the olfactometry method are relatively poor - the measurement uncertainty can be up to 250 OU/m³ (van Kempen et al., 2002) or 50% (Lee and Zhang, 2008). Another limitation of olfactometry is that it can hardly identify the species of the major odorants. Accordingly, the use of gas chromatography-mass spectrometry (GC-MS) has become frequent in recent years (Cai et al., 2006; Rabaud et al., 2003; Wright et al., 2005), and more than 300 odorants have been identified in the air of animal facilities (Lo et al., 2008; Schiffman et al., 2001). These compounds include but not limited to NH₃, H₂S, aldehydes, ketones, alcohols, acids, aromatics, amides, amines, ethers, esters, hydrocarbons, phenols, nitrogen containing compounds (e.g., indole) and sulfur containing compounds (e.g., mercaptan). Many of them have relative high boiling points (>200°C) and thereby may be present in their condensed forms, that is, in the form of particles.

The role of particles in odor transport and amplification has been an intriguing topic for many years. Day et al. (1965) observed that in swine confinement buildings the majority of odors were carried by particles. Hammond et al (1979; 1981) reported that the removal of particles by

filtration resulted in a significant decrease in odor intensity at swine facilities. Burnett (1969) found a strong correlation between odor intensity and particle concentration in poultry buildings. However, an argument later made by Williams (1989) stated that the filtration of particles in broiler buildings did not significantly reduce the odor intensity. Despite of such a controversy, numerous odorants have been identified on particles collected from animal confinement buildings (Cai et al., 2006; Das et al., 2004; Hammond et al., 1979; Hammond et al., 1981; Hartung, 1985; Oehrl et al., 2001; Razote et al., 2004; Wang et al., 1998). Compared to airborne odors, particle-borne odors can be even more troublesome because particles can adhere to and then accumulate on the surface of objects (e.g., humans and vehicles) at and near animal facilities, thereby causing a persistent odor nuisance. In addition, the mitigation of particle-borne odors may require different technologies and management practices. An electrostatic precipitator, for example, may work effectively for particle-borne odors but less effectively for odors in the gas-phase. Therefore, it is of scientific and engineering importance to examine particle-borne odors from commercial animal confinement buildings.

Although many efforts have been made (Cai et al., 2006; Hammond et al., 1979; Hammond et al., 1981; Hartung, 1985; Lee and Zhang, 2008; Liao et al., 2001; Oehrl et al., 2001; Razote et al., 2004; Wang et al., 1998), two major limitations are associated with previous studies. First, most of them investigated only one or a few buildings and, thus, failed to consider potential variations in odorant composition with animal building type, season and particle size. It is known that, at least, swine buildings have noticeably different odor characteristics than poultry buildings. A pertinent central question is- What odorants cause that difference? Second, previous studies did not produce sufficient quantitative concentration data; instead, the contents of odorants were generally characterized by peak areas on a chromatogram. The lack of enough quantitative data creates a major obstacle for subsequent evaluations and discussions on particle-borne odors, e.g., the calculation of odor activity and receptor modeling. To fill the gap in knowledge resulted from these two limitations, a comprehensive and quantitative characterization of particle-borne odors is greatly needed.

In this study, we collected total suspended particulate matter (TSP) and PM₁₀ samples from eighteen commercial animal confinement buildings under three different seasons (hot, mild and cold, depending on ambient temperature). A total of 57 odorants were quantified with stable-isotope dilution GC/MS method. The specific research objectives were:

- To determine the most odor-contributing compounds under different animal building type, weather and particle size conditions;
- To develop a comprehensive odor intensity index for particle-borne odors and to use it for evaluation of odor contamination and for comparison.
- To investigate variations in odorant composition with animal building type, season and particle size;

5.2 Materials and Methods

5.2.1 PM sampling in animal confinement buildings

A total of twelve swine and six poultry confinement buildings were selected in Illinois and Indiana (Table 5.1). Each building was visited three times with each in cold (winter), mild (spring and fall) and hot (summer) seasons. For the purpose of comparison, we also collected PM samples in a cage-free layer hen and a chicken broiler building but only in hot seasons due to the budget constraints. All except for tom turkey buildings were mechanically ventilated. Detailed building information can be found in Table A.1.

Table 5.1. Summary of field sampling.

Animal type	Building Type	Location	# of buildings	# of visits ^{a,b}
Swine	Gestation	Illinois	3	9
	Farrowing	Illinois	3	9
	Weaning	Illinois	3	8
	Finishing	Illinois	3	15
Poultry	Manure-belt layer hen	Illinois and Indiana	3	11
	Tom turkey	Illinois	3	9
	Cage-free layer hen	Indiana	1	1
	Broiler	Kentucky	1	1
Total			20	63

a. A TSP and a PM₁₀ sample were collected from each visit.

b. For manure-belt layer hen and finishing buildings, we collected extra samples. For weaning buildings, one visit in summer had to be canceled because the farm was closed down.

A UIUC isokinetic TSP sampler and a Harvard impactor were used for TSP and PM₁₀ collection, respectively. Both samplers were installed upstream of a ventilation fan that ran continuously throughout the sampling period for approximately 24 hrs, except in tom turkey buildings PM samplers were set up near a downwind end door. The spacing of TSP inlet from the fan face was adjusted according to the air velocity to satisfy the requirements by isokinetic

sampling, but typically 0.2-0.6 m. A calm-air TSP sampling protocol (Zhang, 2005) was selected in tom turkey buildings with natural ventilation, with spacing from the end door of 0.6-1.0 m. Harvard impactor was installed with spacing typically of 0.6-1.0 m from the fan face or end door. The installation height of both TSP and Harvard samplers was normally 1.2-1.4 m. A flow rate of 20 liter per minute (LPM) was controlled with low pressure-drop venturi orifice developed by Wang and Zhang (1999). The accurate flow rate was determined through calibration of venturi orifices in the lab (please refer to Appendix H), and used for calculating the actual volume of sampled air. Both TSP and PM₁₀ samples were collected on pre-baked glass fiber filters (Type A/E, P/N 61652, Pall Corporation, Ann Arbor, MI). In addition to PM samples, feed samples were collected from feed bins or hoppers and kept in 40 mL pre-cleaned EPA vials with Teflon-lined cap.

Once a field sampling was done, the filter with particles was immediately transferred into a 50 mm sterile Petri dish sealed with parafilms and aluminum foils to minimize the loss in volatile and semi-volatile components. Upon arriving in the lab, the filter was quickly weighed, packed and then stored along with feed samples at -70°C.

5.2.2 Sample preparation and chemical analysis

A detailed description of methodology was presented by Lorjaroenphon and Cadwallader (2010). Briefly, the filter or feed was spiked with a stable-isotope labeled internal standard solution, and extracted in anhydrous diethyl ether mixed with odor-free water and NaSO₄. The extract was filtered, concentrated and then injected into a capillary column GC/MS (Agilent 6890 GC/5973 mass selective detector, Agilent Technologies Inc., Santa Clara, CA) for qualitative and quantitative analysis.

5.2.3 Data analysis

5.2.3.1 Data preparation

The mass of an odorant determined by GC/MS analysis was divided over the total particle mass of a given PM sample to calculate the odorant's mass fraction (in unit of ng/mg or ppm). By multiplying the mass fraction of the odorant by the mass concentration of the PM sample, the mass concentration of the odorant in air (in unit of mg/m³) was also determined.

To assess the odor potency carried by particles, the mass fraction and concentration of an odorant were normalized with its odor threshold. The same approach was previously employed for evaluating the odor intensity of gas-phase odorants (Lin and Blank, 2003; Zhou et al., 2002), where a dimensionless odor activity value (OAV) was calculated as the ratio of the concentration of an odorant to its odor threshold. Additionally, we defined a non-dimensionless particle odor activity value (OAV_p) as:

$$\text{OAV}_p = \frac{\text{mass fraction of a compound in PM}}{\text{odor threshold in air (mg/m}^3\text{)}} = \frac{\text{OAV}}{\text{PM concentration}} \quad (5.1)$$

This index was proposed to characterize the odor intensity of an odorant per unit concentration of particles or feed. Based on that, a comprehensive particle odor intensity index (COI_p) was defined as:

$$\text{COI}_p = \left(\sum_{i=1}^N \text{OAV}_{p,i} \right) / N \quad (5.2)$$

Where, OAV_{p,i} refers to the particle odor activity value of the *i*th odorous compound, and N is the number of quantified odorants. Similarly, a comprehensive odor intensity index (COI) was defined as:

$$\text{COI} = \left(\sum_{i=1}^N \text{OAV}_i \right) / N = \text{COI}_p \times \text{PM concentration} \quad (5.3)$$

Where, OAV_i refers to the odor activity value of the *i*th odorous compound.

The Simpson's diversity index (D) was used to characterize the evenness of odor or mass contributions by multiple odorants (Equation 5.4).

$$D = \sum_{i=1}^N p_i^2 \quad (5.4)$$

$$p_i = \text{OAV}_i / \left(\sum_{i=1}^N \text{OAV}_i \right) = \text{OAV}_{p,i} / \left(\sum_{i=1}^N \text{OAV}_{p,i} \right) \quad (5.5)$$

Where, *p_i* is the relative odor contribution or mass fraction of the *i*th odorants. According to the definition of the Simpson's diversity index, if D approaches 1, the odors will be predominately

contributed by a single odorant; if D approaches 0, then the odors will be evenly contributed by all quantified odorants.

5.2.3.2 Statistical analysis

Determination of the most odor-contributing compounds was carried out based on the calculated OAV_i or p_i . Higher values indicate greater contributions, and vice versa. For each animal building type, season or particle size, an average OVA_i or p_i was calculated for determination of major odorants.

For investigation of variations in odorant composition, a number of multivariate data analysis tools were employed, such as non-metric multidimensional scaling (MDS), principle coordinate analysis (PCoA), analysis of similarity (ANOSIM), similarity percentage (SIMPER) and Mantel test. Many of them have been extensively used in ecology and biology research for comparison among different biotic communities (Clarke, 1993) or nucleotide/protein sequences. Although their applications are currently limited in the area of air quality research, there is no question that these tools can offer a convenient way to examine variations in multi-contaminant air pollution among different scenarios. A brief introduction to those tools would be presented in the results and discussions section.

ANOVA and paired t-test were used for comparison of the mass fraction of odorants, COI, COI_p and D between different building types, seasons and particle sizes. Prior to ANOVA and t-test, the data of COI, COI_p and D were subject to a Shapiro-Wilk normality test. A log transformation was performed if the p value given by the test was smaller than 0.05. A Kruskal-Wallis test (nonparametric ANOVA) was employed when the normality of data was still poor even after log transformation.

Non-metric MDS, ANOSIM and SIMPER tests were conducted in PRIMER 6.0, a software package widely used for multivariate data analysis of ecological data. PCoA and Mantel tests were conducted in PAST, a free statistical program originally developed for paleontology research but later becoming popular in many other research areas. Other tests, including ANOVA and paired t-test, were performed in R and SPSS v17.0.

5.3 Results and Discussions

5.3.1 Summary of qualitative and quantitative analysis results

A total of 57 odorants were identified, belonging to five categories: aldehydes and ketones (carbonyls), alcohols, acids, phenols and nitrogen-containing compounds. Most compounds have been previously identified in particle and air samples from animal confinement buildings (Table 5.2). Two new odorants were found in this study- (E,Z)-2,6-nonadienal and trans-4,5-epoxy-(E)-2-decenal. Both have very low odor thresholds (Table 5.3), even more odorous than indole, a malodorous compound widely considered to be a major odor contributor and indicator at animal facilities (Williams, 1984; Yu et al., 1991). No propanol, butanol or aldehydes lighter than hexanal were identified although some previous studies reported the presence of butanal and pentanal in particle samples collected from animal facilities (Cai et al., 2006; Hammond et al., 1981; Razote et al., 2004). No sulfur-containing odorants were detected by GC/MS probably due to their extremely low contents in particles. Special detectors, e.g., flame photometric detector (FPD), may need to be used to minimize the interference of other compounds.

A total of 22 odorants existed ubiquitously in all collected TSP and PM₁₀ samples; while some odorants, e.g. (E)-2-hexenal, had fairly low occurrence frequency (Table 5.2). Overall, odorants were less diverse in feed samples than in particle samples. Two odorants, (E)-2-hexenal and (E,Z)-2,6-nonadienal, were only found in particle samples.

It can be seen from Table 5.3 that the identified 51 odorants originate from different substrates and/or microbial activities, have a great diversity in smell characteristics, and vary substantially in odor thresholds. Some odorants, e.g. vanillin, actually have a pleasant flavor but may feel less pleasant when mixed with other odorants in animal confinement buildings. Some odorants, e.g. (E,Z)-2,6-nonadienal, are highly odorous; while some others, e.g., ethanol, have only a light odor. The odor thresholds of identified odorants range from several ng/m³ to tens of mg/m³. Accordingly, their odor contributions were expected to differ greatly.

Most odorants are present in the form of liquid at room temperature (25°C) (Appendix I: Table I-1). Although some of them, e.g., skatole, exist as solid, none of them are gas at room temperature. At least 45 compounds have a boiling point less than 250°C (the boiling points of two compounds are unavailable) and, thus, can be classified as volatile organic compounds (VOC's) according to the definition of VOC (EUR-Lex, 2004; Health-Canada, 2007).

Table 5.2. Frequency of occurrence of the odorants identified in TSP, PM₁₀ and feed samples and comparison with references.

Compounds	ACS#	Frequency ^a (%)			References ^b											
		TSP	PM ₁₀	Feed	i	ii	iii	iv	v	vi	vii	viii	ix	x	xi	xii
Aldehydes and ketones																
hexanal	66-25-1	64	62	25	Y	Y	Y	Y			Y	Y		Y	Y	Y
2-methyl-2-pentenal	623-36-9	64	62	37	Y											
heptanal	111-71-7	64	61	17	Y			Y			Y	Y				Y
(E)-2-hexenal	6728-26-3	9	2	0	Y	Y	Y	Y								
octanal	124-13-0	64	53	17	Y		Y	Y				Y				Y
1-octen-3-one	4312-99-6	63	46	4		Y										
(E)-2-heptenal	18829-55-5	64	59	37	Y	Y		Y								
(E)-2-octenal	2548-87-0	64	61	36	Y			Y								
nonanal	124-19-6	64	62	34	Y		Y	Y			Y	Y				
decanal	112-31-2	30	19	11	Y	Y		Y				Y				Y
benzaldehyde	100-52-7	64	62	35	Y	Y		Y					Y		Y	Y
(E)-2-nonenal	18829-56-6	64	59	25	Y			Y			Y					
(E,Z)-2,6-nonadienal	557-48-2	10	5	0												
(E)-2-decenal	3913-81-3	60	52	36	Y			Y								
(E)-2-undecenal	53448-07-0	61	54	36	Y											
(E,E)-2,4-nonadienal	5910-87-2	58	48	22		Y	Y	Y			Y					
(E,E)-2,4-decadienal	25152-84-5	63	60	37	Y	Y					Y					
trans-4,5-epoxy-(E)-2-decenal	134454-31-2	15	16	7												
Alcohols																
ethanol	64-17-5	64	62	36	Y										Y	Y
1-pentanol	71-41-0	63	57	31	Y										Y	
1-hexanol	111-27-3	63	52	24	Y			Y				Y				
1-heptanol	111-70-6	46	26	7	Y		Y	Y								
2-ethyl-1-hexanol	104-76-7	64	59	31	Y		Y	Y								
1-octanol	111-87-5	64	59	25	Y		Y	Y								
2-furanmethanol	98-00-0	64	57	37	Y											
phenylmethanol	100-51-6	63	58	33			Y									

Table 5.2. (cont. 1)

Compounds	ACS#	Frequency (%)			References											
		TSP	PM ₁₀	Feed	i	ii	iii	iv	v	vi	vii	viii	ix	x	xi	xii
Acids																
acetic acid	64-19-7	64	62	37	Y	Y	Y	Y	Y	Y			Y		Y	Y
propanoic acid	79-09-4	64	62	37	Y	Y	Y	Y	Y	Y			Y		Y	Y
2-methylpropanoic acid	79-31-2	60	54	26	Y			Y	Y	Y			Y		Y	Y
2,2-dimethyl-propanoic acid	75-98-9	52	55	23	Y											
butanoic acid	107-92-6	60	58	33	Y	Y	Y	Y	Y	Y			Y		Y	Y
3-methylbutanoic acid	503-74-2	64	62	37	Y		Y	Y	Y	Y			Y		Y	Y
pentanoic acid	109-52-4	64	62	37	Y	Y	Y	Y	Y	Y					Y	Y
4-methylpentanoic acid	646-07-1	46	40	13	Y										Y	Y
hexanoic acid	142-62-1	64	62	37	Y	Y	Y		Y						Y	Y
2-ethylhexanoic acid	149-57-5	64	62	37	Y								Y			
heptanoic acid	111-14-8	64	62	37	Y	Y	Y		Y				Y		Y	Y
octanoic acid	124-07-2	64	62	37	Y	Y			Y						Y	Y
nonanoic acid	112-05-0	64	62	37	Y	Y			Y						Y	Y
decanoic acid	334-48-5	64	62	37	Y	Y										
undecanoic acid	112-37-8	64	62	21	Y	Y										
benzoic acid	65-85-0	64	62	37	Y	Y		Y				Y			Y	Y
dodecanoic acid	143-07-7	64	62	33	Y											
phenylacetic acid	103-82-2	64	62	37	Y	Y						Y				
tridecanoic acid	638-53-9	64	59	2		Y										
phenylpropanoic acid	501-52-0	64	60	32	Y							Y		Y		
Phenols																
guaiacol / 2-methoxyphenol	90-05-1	63	53	37	Y											
o-cresol / 2-methylphenol	95-48-7	33	21	8	Y								Y			
phenol	108-95-2	64	62	37	Y	Y	Y	Y	Y	Y	Y	Y	Y	Y	Y	
p-cresol / 4-methylphenol	106-44-5	64	62	28	Y		Y	Y	Y	Y	Y		Y		Y	
m-cresol / 3-methylphenol	108-39-4	37	29	3	Y										Y	Y
4-ethylphenol	123-07-9	64	62	14	Y		Y	Y		Y	Y		Y			Y
p-vinylguaiacol	7786-61-0	64	61	37	Y											
vanillin / 3-methoxy-4-hydroxybenzaldehyde	121-33-5	64	59	37	Y						Y					

Table 5.2. (cont. 2)

Compounds	ACS#	Frequency (%)			References											
		TSP	PM ₁₀	Feed	i	ii	iii	iv	v	vi	vii	viii	ix	x	xi	xii
Nitrogen containing compounds																
o-aminoacetophenone	551-93-9	64	62	37			Y							Y		
indole	120-72-9	64	61	29	Y		Y	Y	Y	Y				Y	Y	Y
3-methylindole / skatole	83-34-1	63	53	22	Y		Y	Y	Y	Y	Y	Y		Y		Y

a. The total number of sample was 64 for TSP, 62 for PM₁₀ and 37 for feed.

b. i- Schiffmann et al. (2001), ii- Hammond et al. (1981), iii- Cai et al. (2006), iv- Razote et al. (2004), v- Oehrl et al. (2001), vi- Hartung (1985), vii- Hammond et al. (1979), viii- Das et al. (2004), ix- Lo et al. (2008), x- Chmielowiec-Korzeniowska (2009), xi- Oneill and Phillips (1992), xii- Spoelstra (1980). Reference ii through viii are focused on particle-borne odors in animal confinement buildings; while the rest examined the odor occurred in the gas phase.

Table 5.3. Thresholds, sensory characteristics and sources of the odorants identified in this study.

Compounds	ACS#	Odor threshold in air ^{a, b, c} (mg/m ³)	Sensory characteristic ^d	Sources ^e
Aldehydes and ketones				
hexanal	66-25-1	0.0575 ¹ , 0.0184 ² , 0.028-0.067 ⁴ , 0.043 ⁵ , 0.03-0.053 ⁶	green ^{i,ii} , grass ^{i,ii} , resinous ⁱ , tallow ⁱⁱ , fat ⁱⁱ	Deamination of amino acids; bacterial conversion of simple carbohydrates ¹
2-methyl-2-pentenal	623-36-9	-	-	
heptanal	111-71-7	0.0229 ¹ , 0.342 ² , 0.006-0.26 ⁴ , 0.25 ⁶	oily ⁱ , fatty ^{i,ii} , resinous ⁱ , citrus ⁱⁱ , rancid ⁱⁱ	
(E)-2-hexenal	6728-26-3	0.132 ¹ , 0.034-0.63 ⁴	sweet ⁱ , fragrant ⁱ , green ⁱⁱ , leaf ⁱⁱ	
octanal	124-13-0	0.00724 ¹ , 0.00367 ² , 0.0078 ⁴ , 0.0058-0.0136 ⁶	fat ⁱⁱ , soap ⁱⁱ , lemon ⁱⁱ , green ⁱⁱ	
1-octen-3-one	4312-99-6	0.0001 ⁴ , 0.00007 ⁵ , 0.00003-0.00006 ⁶	mushroom ^{ii, iii} , metal ^{ii, iii}	
(E)-2-heptenal	18829-55-5	0.0631 ¹ , 0.0596 ² , 0.034-0.26 ⁴	soap ⁱⁱ , fat ⁱⁱ , almond ⁱⁱ	
(E)-2-octenal	2548-87-0	0.0107 ¹ , 0.047 ⁵	fat ^{ii,iii} , soap ⁱⁱⁱ , green ⁱⁱ , nut ⁱⁱ	
nonanal	124-19-6	0.0135 ¹ , 0.0268 ² , 0.0003-0.045 ⁴ , 0.0052-0.0121 ⁶	fat ⁱⁱ , citrus ⁱⁱ , green ⁱⁱ	
decanal	112-31-2	0.00589 ¹ , 0.000008 ² , 0.00025 ⁴ , 0.001 ⁶	soap ⁱⁱ , orange peel ⁱⁱ , tallow ⁱⁱ	
benzaldehyde	100-52-7	0.186 ¹ , 0.0000734 ² , 0.18-3400 ⁴	almond ^{i,ii} , aromatic ⁱ , burnt sugar ⁱⁱ	
(E)-2-nonenal	18829-56-6	0.000871 ¹ , 0.000459 ² , 0.0005-0.0036 ⁴ , 0.0001 ⁵ , 0.0001 ⁶	fat ^{ii,iii} , soap ⁱⁱⁱ , cucumber ⁱⁱ , green ⁱⁱ	
(E,Z)-2,6-nonadienal	557-48-2	0.0000741 ¹	cucumber ⁱⁱ , wax ⁱⁱ , green ⁱⁱ	
(E)-2-decenal	3913-81-3	0.00234 ¹	tallow ⁱⁱ , soap ⁱⁱⁱ	
(E)-2-undecenal	53448-07-0	-	fat ⁱⁱ , soap ^{ii,iii} , green ⁱⁱ	
(E,E)-2,4-nonadienal	5910-87-2	0.000204 ¹ , 0.00025-0.0004 ⁴ , 0.0004 ⁵ , 0.0004 ⁶	fat ^{ii,iii} , wax ⁱⁱ , green ⁱⁱ	
(E,E)-2,4-decadienal	25152-84-5	0.000219 ¹ , 0.000184, 0.0001 ⁵ , 0.00013 ⁶	oily ⁱ , fat ^{i,ii,iii} , rancid ⁱ , fried ^{ii,iii} , wax ⁱⁱ	
trans-4,5-epoxy-(E)-2-decenal	134454-31-2	0.0000015 ⁵ , 0.0000006-0.0000025 ⁶	green ^{ii, iii} , metal ^{ii, iii}	

Table 5.3. (cont. 1)

Compounds	ACS#	Odor threshold in air (mg/m ³)	Sensory characteristic	Sources
Alcohols				
ethanol	64-17-5	<u>55</u> ¹ , 0.913 ² , 0.64-1350 ⁴	sweet ⁱⁱ	Bacterial conversion of simple carbohydrates, e.g. anaerobic fermentation ¹ .
1-pentanol	71-41-0	<u>1.7</u> ¹ , 0.0419 ² , 0.4-35 ⁴	balsamic ⁱⁱ	
1-hexanol	111-27-3	<u>0.186</u> ¹ , 0.000088 ² , 0.04-1.93 ⁴	fragrant ⁱ , aromatic ⁱ , resin ⁱⁱ , flower ⁱⁱ , green ⁱⁱ	
1-heptanol	111-70-6	<u>0.120</u> ¹ , 2.37 ² , 0.05-2.4 ⁴	fragrant ⁱ , aromatic ⁱ , chemical ⁱⁱ , green ⁱⁱ	
2-ethyl-1-hexanol	104-76-7	<u>1.32</u> ¹ , 0.4 ⁴	rose ⁱⁱ , green ⁱⁱ	
1-octanol	111-87-5	<u>0.316</u> ¹ , 13.5 ²	oily ⁱ , fat ⁱ , aromatic ⁱ , chemical ⁱⁱ , metal ⁱⁱ , burnt ⁱⁱ	
2-furanmethanol	98-00-0	-	burnt ⁱⁱ	
phenylmethanol	100-51-6	-	sweet flower ⁱⁱ	
Acids				
acetic acid	64-19-7	<u>0.363</u> ¹ , 59.6 ² , 0.182 ³ , 0.025-10 ⁴ , 0.06 ⁶	sour ⁱⁱ	Bacterial conversion of structure carbohydrate ^{I,II} and proteins ^I
propanoic acid	79-09-4	<u>0.110</u> ¹ , 0.0848 ² , 0.003-0.89 ⁴	pungent ⁱⁱ , rancid ⁱⁱ , soy ⁱⁱ	Deamination of valine ^I
2-methylpropanoic acid	79-31-2	<u>0.0724</u> ¹ , 0.005-0.33 ⁴	rancid ⁱⁱ , butter ⁱⁱ , cheese ⁱⁱ	-
2,2-dimethyl-propanoic acid	75-98-9	-	-	-
butanoic acid	107-92-6	<u>0.0145</u> ¹ , 0.174 ² , 0.0004-42 ⁴	sickening ⁱ , rancid ^{i,ii} , cheese ⁱⁱ , sweat ⁱⁱ	Bacterial conversion of structure carbohydrate ^{I,II} and proteins ^I
3-methylbutanoic acid	503-74-2	<u>0.0105</u> ¹ , 0.0002-0.0069 ⁴ , 0.0015 ⁶	sickening ⁱ , rancid ⁱⁱ , acid ⁱⁱ , sweat ⁱⁱ	Deamination of isoleucine ^I
pentanoic acid	109-52-4	<u>0.0204</u> ¹ , 0.000029 ² , 0.0008-0.12 ⁴	sickening ⁱ , putrid ⁱⁱ , sweat ⁱⁱ	Bacterial conversion of structure carbohydrate ^{I,II}
4-methylpentanoic acid	646-07-1	<u>0.0759</u> ¹ , 0.037 ⁴	-	-
hexanoic acid	142-62-1	<u>0.0603</u> ¹ , 0.02-0.52 ⁴	sour ⁱ , vinegar ⁱ , sickening ⁱ , sweat ⁱⁱ	Bacterial conversion of structure carbohydrate ^{I,II}
2-ethylhexanoic acid	149-57-5	-	paint ⁱⁱ , varnish ⁱⁱ	-
heptanoic acid	111-14-8	<u>0.148</u> ¹ , 0.022-0.033 ⁴	unpleasant ⁱ , rancid ⁱ	Bacterial conversion of structure carbohydrate ^{I,II}
octanoic acid	124-07-2	<u>0.024</u> ¹ , 0.0003-0.6 (r) ⁴	sweat ⁱⁱ , cheese ⁱⁱ	
nonanoic acid	112-05-0	0.0016-0.12 (r) ⁴	unpleasant ⁱ , rancid ⁱ , green ⁱⁱ , fat ⁱⁱ	
decanoic acid	334-48-5	<u>0.0631</u> ¹ , 0.05 ⁴	rancid ⁱⁱ , fat ⁱⁱ	
undecanoic acid	112-37-8	<u>0.0126</u> ¹	oily ⁱⁱ	
benzoic acid	65-85-0	-	urine ⁱⁱ	Microbial degradation of tyrosine and phenylalanine ^I

Table 5.3. (cont. 2)

Compounds	ACS#	Odor threshold in air (mg/m ³)	Sensory characteristics	Sources
Acids				
dodecanoic acid	143-07-7	<u>0.0204</u> ¹	metal ⁱⁱ	Bacterial conversion of structure carbohydrate ^{i,ii}
phenylacetic acid	103-82-2	<u>0.00724</u> ¹ , 0.00003 ⁴	sickening ⁱ , urine ⁱ , honey ⁱⁱ , flower ⁱⁱ	Anaerobic oxidative degradation of phenylalanine ¹
tridecanoic acid	638-53-9	-	-	Bacterial conversion of structure carbohydrate ^{i,ii}
phenylpropanoic acid	501-52-0	-	balsamic ⁱⁱ	Reductive degradation of phenylalanine ^{i,ii} ; degradation of tyrosine ¹
Phenols				
guaiacol / 2-methoxyphenol	90-05-1	<u>0.00525</u> ¹ , 0.0037-0.64 ⁴	burnt ⁱ , smoke ^{i,ii} , medicine ^{i,ii} , sweet ⁱⁱ	-
o-cresol / 2-methylphenol	95-48-7	<u>0.00776</u> ¹ , 0.0004 ⁴	phenol ⁱⁱ	Microbial degradation of tyrosine ^{i,ii} ; liberation of phenols from their glucuronides ¹ .
phenol	108-95-2	<u>0.427</u> ¹ , 3.85 ² , 0.231 ³ , 0.022-4 ⁴	phenol ⁱⁱ	
p-cresol / 4-methylphenol	106-44-5	<u>0.00832</u> ¹ , 0.00005-0.024 ⁴ , 0.0000007-0.000001 ⁶	medicine ^{i,ii} , resin ⁱ , phenol ⁱⁱ , smoke ⁱⁱ	
m-cresol / 3-methylphenol	108-39-4	<u>0.00365</u> ¹ , 0.00268 ³ , 0.00022-0.035 ⁴	medicine ⁱ , disinfectant ⁱ , fecal ⁱⁱ , plastic ⁱⁱ	
4-ethylphenol	123-07-9	-	medicine ⁱ , phenol ⁱⁱ , spice ⁱⁱ	
p-vinylguaiacol	7786-61-0	-	clove ⁱⁱ , curry ⁱⁱ	Microbial degradation of tyrosine ^{i,ii} or p-coumaric acid ¹
vanillin / 3-methoxy-4-hydroxybenzaldehyde	121-33-5	0.0006-0.0012 ⁶	vanilla ^{i,ii} , sweet ⁱ	-
Nitrogen-containing compounds				
o-aminoacetophenone	551-93-9	-	foxy ⁱⁱ , sweet ⁱⁱ	-
indole	120-72-9	<u>0.000155</u> ¹ , 0.0006-0.0071 ⁴	mothball ^{i,ii} , sickening ⁱ , burnt ⁱⁱ	Microbial degradation of tryptophan ^{i,ii} or indole-3-carboxylic acid ¹
3-methylindole / skatole	83-34-1	<u>0.00309</u> ¹ , 0.00035-0.00078 ⁴	mothball ^{i,ii} , sickening ⁱ , fecal ⁱⁱ	

a. 1- Devos et al. (1990), 2- Fazzalari (1978), 3- AIHA (1989), 4- Van Gemert and Nettenbreijer (1977), 5- Lin and Blank (2003), 6 – Rychlik et al. (1998). A unit conversion was performed from ppmv to mg/m³ by assuming a standard condition of 25°C and 1 atm.

b. A symbol of (r) represents that the odor threshold is a reception threshold.

c. The odor thresholds selected for calculation are highlighted with underline. A total of 41 compounds were selected.

d. i- Dravnieks (1985), ii- Acree and Arn (2004), iii- Lin and Blank (2003).

e. I- Spoelstra (1980), II- Mackie et al. (1998).

Table 5.4. Summary of quantitative analysis results- mass fraction of odorants in particle and feed samples (in ppm).

Compound	Farrowing		Gestation		Weaning		Finishing		Manure-belt layer hen		Tom turkey	
	Mean	SD	Mean	SD	Mean	SD	Mean	SD	Mean	SD	Mean	SD
TSP												
hexanal	539	919	365	303	786	1194	855	791	399	277	255	210
2-methyl-2-pentenal	361	748	169	117	160	307	145	273	76	48	44	43
heptanal	380	695	221	235	71	51	135	164	66	52	55	59
(E)-2-hexenal	0	0	0	0	4	7	2	5	1	3	1	2
octanal	48	52	36	28	42	68	35	27	26	21	13	11
1-octen-3-one	13	12	8	6	14	24	14	13	6	3	3	3
(E)-2-heptenal	52	107	34	31	47	78	57	78	40	29	16	17
(E)-2-octenal	20	24	16	11	37	64	28	24	16	11	8	6
nonanal	313	337	196	175	170	229	267	278	343	300	124	118
decanal	12	27	7	14	9	16	5	10	6	6	0	1
benzaldehyde	107	224	46	33	88	36	75	61	50	38	45	37
(E)-2-nonenal	26	29	18	14	26	29	28	18	8	5	8	7
(E,Z)-2,6-nonadienal	0	0	0	0	0	0	0	0	0	0	0	0
(E)-2-decenal	4	3	5	3	37	66	17	26	10	8	5	4
(E)-2-undecenal	16	17	15	8	125	210	42	64	21	16	13	10
(E,E)-2,4-nonadienal	1	1	1	1	6	8	3	4	1	1	1	0
(E,E)-2,4-decadienal	5	3	5	3	32	47	21	26	12	11	5	4
trans-4,5-epoxy-(E)-2-decenal	0	1	1	2	1	1	9	22	3	4	0	1
ethanol	5918	7024	4103	2909	4975	8873	5464	5912	2300	1814	602	262
1-pentanol	103	221	59	67	50	65	94	102	45	31	33	26
1-hexanol	172	367	81	96	51	34	45	37	25	14	36	24
1-heptanol	6	8	11	17	12	20	12	13	5	6	5	7
2-ethyl-1-hexanol	3332	8414	1003	1295	2681	3514	1783	2567	115	166	294	288
1-octanol	208	267	138	134	152	275	154	146	133	103	64	54
2-furanmethanol	57	71	29	13	37	45	44	55	9	4	14	13
phenylmethanol	135	332	44	43	27	33	44	60	15	13	18	20
acetic acid	16877	9476	15576	7104	9403	12170	9875	7207	7759	6152	1095	546
propanoic acid	2433	4354	824	495	1242	1500	916	880	1768	4862	176	104
2-methylpropanoic acid	388	340	171	156	236	272	228	308	144	253	25	17
2,2-dimethyl-propanoic acid	649	854	452	720	16	12	138	277	61	71	2	2
butanoic acid	171	158	175	184	399	699	246	191	56	31	63	51

Table 5.4. (cont. 1)

Compound	Farrowing		Gestation		Weaning		Finishing		Manure-belt layer hen		Tom turkey	
	Mean	SD	Mean	SD	Mean	SD	Mean	SD	Mean	SD	Mean	SD
TSP												
3-methylbutanoic acid	569	533	645	523	469	609	367	298	113	71	89	74
pentanoic acid	146	131	177	148	281	426	200	151	39	24	16	9
4-methylpentanoic acid	80	90	82	98	77	110	32	28	26	27	16	21
hexanoic acid	95	58	117	60	134	131	183	141	130	53	49	37
2-ethylhexanoic acid	157	85	186	112	73	133	127	124	95	70	15	10
heptanoic acid	62	43	81	66	24	24	44	39	36	14	12	9
octanoic acid	191	166	131	118	65	46	135	132	96	44	42	32
nonanoic acid	219	144	236	188	75	79	152	152	438	169	90	67
decanoic acid	206	279	95	88	42	24	56	45	108	68	19	9
undecanoic acid	461	247	566	520	98	94	315	407	214	127	61	26
benzoic acid	670	560	1557	644	669	510	911	1339	73	38	34	19
dodecanoic acid	1430	810	1462	959	878	704	1057	677	820	551	242	75
phenylacetic acid	621	380	1431	611	1050	780	1081	1457	58	18	52	20
tridecanoic acid	786	652	1107	684	275	238	421	360	168	89	74	29
phenylpropanoic acid	314	191	366	162	207	200	230	333	32	17	13	8
guaiacol	1	1	3	2	4	2	5	3	1	0	2	2
o-cresol	0	1	1	1	0	0	0	1	0	0	0	0
phenol	13	10	22	10	31	27	36	58	6	2	5	3
p-cresol	139	139	290	149	264	234	273	370	8	3	5	7
m-cresol	11	15	25	13	0	0	1	2	0	0	0	0
4-ethylphenol	6	3	6	5	38	34	25	50	3	2	5	4
p-vinylguaiacol	6	4	12	6	37	51	19	17	8	5	27	13
o-aminoacetophenone	8	5	9	2	11	8	10	6	3	2	1	1
indole	6	4	9	4	16	7	21	21	3	1	6	2
skatole	5	4	5	3	13	14	9	8	1	0	0	0
vanillin	8	5	16	14	19	19	19	25	4	2	5	6

Table 5.4. (cont. 2)

Compound	Farrowing		Gestation		Weaning		Finishing		Manure-belt layer hen		Tom turkey	
	Mean	SD	Mean	SD	Mean	SD	Mean	SD	Mean	SD	Mean	SD
PM ₁₀												
hexanal	397	337	848	1295	475	323	765	548	515	387	249	208
2-methyl-2-pentenal	404	397	1311	2147	486	669	523	673	545	437	316	363
heptanal	281	253	526	889	104	101	149	146	89	61	59	69
(E)-2-hexenal	0	0	0	0	0	0	0	0	0	0	1	3
octanal	69	60	89	91	42	49	77	58	43	55	41	38
1-octen-3-one	11	11	8	11	12	13	28	26	11	12	7	8
(E)-2-heptenal	63	69	274	467	115	167	128	169	151	151	54	55
(E)-2-octenal	28	26	56	58	41	53	61	68	34	32	21	18
nonanal	338	247	311	315	200	184	374	367	412	497	284	250
decanal	2	5	26	57	12	27	8	23	8	14	1	2
benzaldehyde	71	88	165	287	108	62	75	63	83	62	105	135
(E)-2-nonenal	27	19	38	33	38	26	41	31	17	14	14	13
(E,Z)-2,6-nonadienal	0	0	0	0	0	0	1	2	0	0	0	1
(E)-2-decenal	7	10	25	28	27	38	25	27	19	23	9	9
(E)-2-undecenal	24	29	76	78	91	115	68	72	57	73	25	24
(E,E)-2,4-nonadienal	1	1	3	4	4	4	4	4	2	3	1	1
(E,E)-2,4-decadienal	10	15	30	39	24	22	30	36	19	21	9	10
trans-4,5-epoxy-(E)-2-decenal	10	24	1	4	5	15	6	10	12	15	0	0
ethanol	9207	6009	22891	22172	7923	3551	14892	13245	19905	24458	5395	5943
1-pentanol	80	78	263	478	63	59	118	85	98	92	12	11
1-hexanol	133	134	319	631	49	43	47	42	36	41	65	96
1-heptanol	6	8	9	15	7	9	11	14	1	2	7	16
2-ethyl-1-hexanol	2126	3933	4312	9409	4254	3763	3112	2862	753	1062	2062	2681
1-octanol	289	242	349	402	176	206	267	265	248	267	131	128
2-furanmethanol	95	124	80	65	159	338	74	61	48	35	104	252
phenylmethanol	211	435	186	351	84	86	75	80	103	125	212	520
acetic acid	52878	55288	43680	35156	20647	11724	35261	28495	66975	91614	8953	12103
propanoic acid	20528	38135	2083	1706	1490	952	2324	3516	16870	50060	11859	34173
2-methylpropanoic acid	6259	14215	347	393	213	97	425	637	2054	5107	1363	3888
2,2-dimethyl-propanoic acid	14602	40103	1691	1915	70	76	405	928	726	1098	151	389
butanoic acid	269	191	230	113	297	384	375	223	182	158	111	100

Table 5.4. (cont. 3)

Compound	Farrowing		Gestation		Weaning		Finishing		Manure-belt layer hen		Tom turkey	
	Mean	SD	Mean	SD	Mean	SD	Mean	SD	Mean	SD	Mean	SD
PM ₁₀												
3-methylbutanoic acid	768	782	653	490	360	200	486	354	371	335	153	139
pentanoic acid	284	301	190	100	195	155	248	149	130	137	29	23
4-methylpentanoic acid	109	188	127	142	58	86	78	75	131	183	47	75
hexanoic acid	228	151	320	211	170	110	315	150	341	241	91	90
2-ethylhexanoic acid	442	308	659	461	190	198	640	699	705	886	130	135
heptanoic acid	165	139	196	148	46	40	87	51	106	84	29	26
octanoic acid	364	258	254	186	121	72	198	161	260	259	71	42
nonanoic acid	639	769	585	410	187	172	317	231	1057	780	206	163
decanoic acid	383	314	178	118	85	46	93	72	291	235	48	24
undecanoic acid	691	450	975	622	184	141	896	1090	2295	5725	183	99
benzoic acid	627	269	2141	953	587	412	1113	869	169	151	72	87
dodecanoic acid	3802	2853	3057	1329	1454	1284	10829	29957	3330	3779	626	559
phenylacetic acid	564	167	1901	547	774	588	1250	741	177	187	128	129
tridecanoic acid	1350	786	1465	632	516	556	1663	2423	1176	2111	173	194
phenylpropanoic acid	442	309	418	391	153	130	302	353	103	155	29	31
guaiacol	1	1	23	49	13	14	7	4	1	1	2	1
o-cresol	1	2	4	8	2	3	0	0	0	0	1	1
phenol	22	25	44	18	44	41	61	106	22	15	11	15
p-cresol	124	75	392	121	240	208	306	357	13	10	5	4
m-cresol	9	11	35	20	6	13	2	3	0	1	0	1
4-ethylphenol	8	2	14	21	40	35	29	58	6	6	4	3
p-vinylguaiacol	9	11	37	18	55	52	31	15	11	8	15	7
o-aminoacetophenone	16	18	23	14	29	30	19	12	14	13	9	11
indole	6	2	14	4	25	21	21	14	5	4	7	2
skatole	6	6	7	4	15	10	17	19	1	1	1	0
vanillin	12	7	29	37	37	33	65	97	19	42	54	149

Table 5.4. (cont. 4)

Compound	Farrowing		Gestation		Weaning		Finishing		Manure-belt layer hen		Tom turkey	
	Mean	SD	Mean	SD	Mean	SD	Mean	SD	Mean	SD	Mean	SD
Feed												
hexanal	6	7	6	5	7	8	8	9	32	69	35	35
2-methyl-2-pentenal	93	56	96	31	86	35	101	44	86	26	99	59
heptanal	0	0	0	0	3	2	1	1	1	2	2	2
(E)-2-hexenal	0	0	0	0	0	0	0	0	0	0	0	0
octanal	2	1	4	3	1	2	2	3	2	3	3	4
1-octen-3-one	0	0	0	0	0	0	0	1	0	1	0	0
(E)-2-heptenal	39	42	37	17	21	10	52	36	44	22	51	42
(E)-2-octenal	4	2	4	1	3	2	5	2	8	4	8	2
nonanal	2	1	2	2	3	1	3	2	5	3	4	2
decanal	1	1	0	1	0	1	0	1	1	1	0	0
benzaldehyde	8	8	6	8	6	2	7	4	6	3	10	7
(E)-2-nonenal	1	2	1	1	1	1	1	2	3	2	3	2
(E,Z)-2,6-nonadienal	0	0	0	0	0	0	0	0	0	0	0	0
(E)-2-decenal	3	1	3	1	5	3	4	2	7	4	8	3
(E)-2-undecenal	10	5	10	5	14	10	13	5	23	13	28	11
(E,E)-2,4-nonadienal	0	0	0	0	0	0	0	0	1	1	1	0
(E,E)-2,4-decadienal	6	3	7	4	4	2	6	2	9	6	10	4
trans-4,5-epoxy-(E)-2-decenal	3	3	2	3	0	0	0	0	1	2	0	0
ethanol	1064	763	1299	950	1516	703	1396	591	1136	958	1131	434
1-pentanol	11	14	7	4	6	4	5	6	17	11	20	11
1-hexanol	7	7	2	3	6	4	1	2	15	24	13	4
1-heptanol	0	0	0	0	0	1	0	0	0	1	3	3
2-ethyl-1-hexanol	76	100	76	116	52	42	38	33	23	25	45	42
1-octanol	14	9	8	8	9	8	8	9	16	12	24	17
2-furanmethanol	14	6	23	19	17	15	14	11	9	7	9	6
phenylmethanol	24	23	25	34	8	6	10	9	9	4	13	9
acetic acid	1545	346	1649	743	2268	2003	1997	1371	3075	879	1958	109
propanoic acid	115	80	88	84	292	470	117	180	156	176	224	157
2-methylpropanoic acid	12	16	7	12	13	16	8	9	9	13	19	10
2,2-dimethyl-propanoic acid	114	76	54	21	3	6	1	1	18	29	2	3
butanoic acid	9	2	9	2	7	5	11	19	23	9	56	38

Table 5.4. (cont. 5)

Compound	Farrowing		Gestation		Weaning		Finishing		Manure-belt layer hen		Tom turkey	
	Mean	SD	Mean	SD	Mean	SD	Mean	SD	Mean	SD	Mean	SD
Feed												
3-methylbutanoic acid	5	1	8	4	20	37	10	19	13	5	28	24
pentanoic acid	6	3	6	2	4	1	3	2	11	5	34	11
4-methylpentanoic acid	1	1	5	10	10	14	12	31	4	6	7	6
hexanoic acid	20	4	23	5	17	5	24	23	37	29	44	12
2-ethylhexanoic acid	42	47	49	45	31	16	31	13	67	54	38	5
heptanoic acid	9	5	10	4	2	1	2	1	5	2	7	2
octanoic acid	16	8	18	8	6	2	5	2	11	5	18	5
nonanoic acid	19	12	23	13	3	1	2	1	7	6	9	6
decanoic acid	9	4	9	4	6	2	4	3	6	4	10	3
undecanoic acid	78	81	102	147	5	7	5	7	129	209	4	8
benzoic acid	13	4	23	12	118	174	55	86	7	3	9	3
dodecanoic acid	253	88	364	542	166	88	81	49	166	196	268	130
phenylacetic acid	44	32	41	13	127	194	100	189	24	13	28	19
tridecanoic acid	14	31	0	0	4	12	0	0	0	0	0	0
phenylpropanoic acid	2	3	4	4	24	37	11	18	4	2	9	9
guaiacol	1	0	2	2	4	2	2	1	1	1	1	0
o-cresol	0	0	0	0	0	0	0	0	0	0	0	0
phenol	3	1	4	3	6	6	5	6	2	0	2	0
p-cresol	1	1	2	1	1	2	1	1	0	0	1	1
m-cresol	0	0	0	1	0	1	0	0	0	0	0	0
4-ethylphenol	0	0	1	1	1	1	0	1	0	0	0	0
p-vinylguaiacol	16	1	38	28	45	36	33	44	17	20	7	2
o-aminoacetophenone	2	1	2	0	1	0	1	0	1	0	1	0
indole	1	1	0	1	2	3	2	2	1	0	1	1
skatole	0	0	0	0	0	0	0	0	0	0	0	0
vanillin	23	40	6	2	30	52	11	14	7	6	3	1

A summary of quantitative results was shown in Table 5.4. The total mass fraction of identified odorants was $2.4\pm 2.0\%$ in TSP, $8.2\pm 10.0\%$ in PM_{10} and $0.46\pm 0.20\%$ in feed samples. Particularly in PM_{10} samples, the mass fraction of identified VOC's could be up to 46%. This implies that a tapered element oscillating microbalance (TEOM), with a mass sensor generally working at $50^{\circ}C$, may significantly under-estimate PM_{10} concentration from animal facilities. The top six abundant odorants were listed in Table 5.5, and differed with animal building type and particle size. Acetic acid and ethanol were found to be overall the most abundant odorants in particle and feed samples, accounting for over 55% of the total mass of all identified odorants. The high abundance of acetic acid in particles was also reported by Razote et al. (2004) and Oehrl et al. (2001).

Table 5.5. Most abundant odorants in particle and feed samples.

Building type	Sample	Top six abundant compounds
farrowing	TSP	acetic acid, ethanol, 2-ethyl-hexanol, propanoic acid, dodecanoic acid, tridecanoic acid
	PM_{10}	acetic acid, propanoic acid, 2,2-dimethyl-propanoic acid, ethanol, 2-methylpropanoic acid, dodecanoic acid
	Feed	acetic acid, ethanol, dodecanoic acid, propanoic acid, 2,2-dimethyl-propanoic acid, 2-methyl-2-pentenal
gestation	TSP	acetic acid, ethanol, benzoic acid, dodecanoic acid, phenylacetic acid, tridecanoic acid
	PM_{10}	acetic acid, ethanol, 2-ethyl-1-hexanol, dodecanoic acid, benzoic acid, propanoic acid
	Feed	acetic acid, ethanol, dodecanoic acid, undecanoic acid, 2-methyl-2-pentenal, propanoic acid
weaning	TSP	acetic acid, ethanol, 2-ethyl-1-hexanol, propanoic acid, phenylacetic acid, dodecanoic acid
	PM_{10}	acetic acid, ethanol, 2-ethyl-1-hexanol, propanoic acid, dodecanoic acid, phenylacetic acid
	Feed	acetic acid, ethanol, propanoic acid, dodecanoic acid, phenylacetic acid, benzoic acid
finishing	TSP	acetic acid, ethanol, 2-ethyl-1-hexanol, dodecanoic acid, hexanal, propanoic acid
	PM_{10}	acetic acid, ethanol, dodecanoic acid, propanoic acid, 2-ethyl-1-hexanol, tridecanoic acid
	Feed	acetic acid, ethanol, propanoic acid, 2-methyl-2-pentenal, phenylacetic acid, dodecanoic acid
manure-belt layer hen	TSP	acetic acid, ethanol, dodecanoic acid, nonanoic acid, hexanal, nonanal
	PM_{10}	acetic acid, ethanol, dodecanoic acid, undecanoic acid, propanoic acid, tridecanoic acid
	Feed	acetic acid, ethanol, dodecanoic acid, propanoic acid, undecanoic acid, 2-methyl-2-pentenal
tom turkey	TSP	acetic acid, ethanol, 2-ethyl-1-hexanol, hexanal, dodecanoic acid, propanoic acid
	PM_{10}	acetic acid, ethanol, propanoic acid, 2-ethyl-1-hexanol, 2-methylpropanoic acid, dodecanoic acid
	Feed	acetic acid, ethanol, dodecanoic acid, propanoic acid, 2-methyl-2-pentenal, butanoic acid

However, despite of their high concentrations, both acetic acid and ethanol are lightly odorous; while some compounds, e.g., indole and skatole, although occurring at much lower

concentrations, may be of even greater importance due to their low odor thresholds and malodor. A more appropriate assessment should therefore be based on particle odor threshold values (OAV_P 's). A practical difficulty in OAV_P calculation is that the reported odor thresholds differed greatly with literature (Table 5.3). To be consistent, only the thresholds compiled by Devos et al. (1990) were selected, which cover 41 compounds identified in this study. Failing to consider the rest of 16 compounds would inevitably create some uncertainties. However, the current results were still fairly informative since most identified malodorous compounds had been included in OAV_P calculation.

Based on the calculation results, the major odor-contributing compounds were determined (Table 5.6), and differed with animal building type and particle size. As the second most abundant compound, ethanol was not among the top odor contributors in any animal building types. Acetic acid, although most abundant, was less odor-contributing than compounds such as phenylacetic acid, dodecanoic acid and much less abundant (E,E)-2,4-decadienal. Similar to previous studies (Williams, 1984; Yu et al., 1991; Zahn et al., 1997; Zahn et al., 2001) on manure and air, indole and volatile fatty acids, such as acetic acid and 3-methylbutanoic acid (isovaleric acid), were found to be the major odor-contributors; while additionally, we found that long carbon-chain fatty acids, such as dodecanoic acid and undecanoic acid, could be equally or even more contributing to particle-borne odors, as previously suggested by Zhu (2000).

Four most odor-contributing compounds (phenylacetic acid, dodecanoic acid, (E,E)-2,4-decadienal, undecanoic acid) all have fairly high boiling points ($>245^\circ\text{C}$). Because of the non-volatility of those compounds, they may mainly exist in the particle phase or become accumulated on the surface of particles, thereby generating significant odors. Besides dodecanoic acid and undecanoic acid, another abundant non-volatile acid was tridecanoic acid. Although its odor threshold is unavailable, tridecanoic acid may be another top odor contributor assuming its odor threshold is comparable to chemically similar dodecanoic acid. In contrast to non-volatile acids, skatole and phenol, previously considered to be major odorants in the air of animal facilities studies (Williams, 1984; Yu et al., 1991; Zahn et al., 1997; Zahn et al., 2001), were found to be of less contribution than expected. The relative odor contribution (p_i) of skatole was averagely 0.33% in TSP, 0.25% in PM_{10} and 0.072% in feed samples; for phenol, the corresponding p_i values phenol were 0.009%, 0.008% and 0.011%, respectively..

Table 5.6. Top odor-contributing compounds in particle and feed samples.

Building type	Sample	Top six odor contributor / their relative odor contribution (%)
farrowing	TSP	phenylacetic acid, dodecanoic acid, 3-methylbutanoic acid, acetic acid, indole, undecanoic acid / 61.4%
	PM ₁₀	propanoic acid, dodecanoic acid, acetic acid, 2-methylpropanoic acid, phenylacetic acid, 3-methylbutanoic acid / 69.9%
	Feed	(E,E)-2,4-decadienal, dodecanoic acid, undecanoic acid, phenylacetic acid, indole, acetic acid / 86.6%
gestation	TSP	phenylacetic acid, (E,E)-2,4-decadienal, dodecanoic acid, indole, 3-methylbutanoic acid, undecanoic acid / 73.0%
	PM ₁₀	phenylacetic acid, dodecanoic acid, (E,E)-2,4-decadienal, acetic acid, indole, undecanoic acid / 69.3%
	Feed	(E,E)-2,4-decadienal, dodecanoic acid, undecanoic acid, phenylacetic acid, acetic acid, indole / 88.1%
weaning	TSP	phenylacetic acid, (E,E)-2,4-decadienal, indole, 3-methylbutanoic acid, dodecanoic acid, p-cresol / 69.4%
	PM ₁₀	indole, (E,E)-2,4-decadienal, phenylacetic acid, dodecanoic acid, acetic acid, (E)-2-nonenal / 70.9%
	Feed	(E,E)-2,4-decadienal, phenylacetic acid, indole, dodecanoic acid, acetic acid, propanoic acid / 85.6%
finishing	TSP	(E,E)-2,4-decadienal, indole, phenylacetic acid, dodecanoic acid, (E)-2-nonenal, 3-methylbutanoic acid / 66.5%
	PM ₁₀	dodecanoic acid, (E,E)-2,4-decadienal, phenylacetic acid, acetic acid, indole, undecanoic acid / 81.0%
	Feed	(E,E)-2,4-decadienal, phenylacetic acid, indole, acetic acid, dodecanoic acid, (E)-2-decenal / 86.1%
manure-belt layer hen	TSP	(E,E)-2,4-decadienal, dodecanoic acid, nonanal, indole, undecanoic acid, acetic acid / 68.4%
	PM ₁₀	undecanoic acid, dodecanoic acid, acetic acid, (E,E)-2,4-decadienal, nonanal, 3-methylbutanoic acid / 76.0%
	Feed	(E,E)-2,4-decadienal, undecanoic acid, acetic acid, dodecanoic acid, indole, phenylacetic acid / 79.9%
tom turkey	TSP	indole, (E,E)-2,4-decadienal, dodecanoic acid, nonanal, (E)-2-nonenal, 3-methylbutanoic acid / 67.4%
	PM ₁₀	propanoic acid, indole, (E,E)-2,4-decadienal, dodecanoic acid, acetic acid, nonanal / 66.1%
	Feed	(E,E)-2,4-decadienal, dodecanoic acid, indole, acetic acid, butanoic acid, phenylacetic acid / 77.6%

5.3.2 Variation with animal building type

Two sets of data were used for investigating the variations in odorant composition: mass fraction (ng/mg) and particle odor activity value (OAV_P, m³/mg) of odorants. The dataset of OAV_P was selected because they may better represent the composition of odors. However, this dataset did not include all 51 compounds. To overcome such a limitation, the dataset of mass fraction was also selected and expected to produce results complimentary to those from the OAV_P dataset.

A basic procedure of data analysis was as follows:

- One-way ANOVA/ Tukey’s test was used for comparing the total mass fraction (or COI and COI_P) of identified odorants and the Simpson’s diversity index (D) among different animal building types.
- Non-metric MDS was used to illustrate the clustering pattern of particle samples according to their corresponding animal building types.
- An ANOSIM test was then performed to determine whether and how distantly the observed clusters were separated from each other.
- Next, a SIMPER analysis was conducted to identify the odorants most contributing to separation between clusters and to determine the relative contribution of each odorant.

5.3.2.1 Variation in mass fraction-based odorant composition of TSP samples

One-way ANOVA test

Table 5.7 listed the total mass fraction of identified odorants and the Simpson’s diversity index (D) in different types of animal confinement buildings. The 51 identified odorants accounted for 0.22~ 12.8% mass of TSP samples; and the total mass fractions of these odorants were apparently greater in swine buildings than in manure-belt layer hen and tom turkey buildings. The calculated Simpson’s index values ranged from 0.075 to 0.38 and were minimal for TSP samples from tom turkey buildings.

Table 5.7. Total mass fraction and Simpson’s diversity index of odorants in TSP samples from different types of animal confinement buildings.

	Statistic	Farrowing	Gestation	Weaning	Finishing	Layer hen ^a	Tom turkey
Total mass fraction of identified odorants	Mean	0.0386	0.0324	0.0258	0.0265	0.0160	0.0039
	SD	0.0325	0.0092	0.0200	0.0159	0.0115	0.0014
Simpson’s diversity index (D)	Mean	0.2840	0.2603	0.2332	0.2191	0.2849	0.1403
	SD	0.0949	0.0871	0.1529	0.0689	0.0980	0.0473

a. manure-belt layer hen buildings only.

Prior to ANOVA test, a log transformation of the total mass fraction data was carried out and successfully improved the data’s normality. The ANOVA test revealed that TSP samples collected from tome turkey buildings had significantly lower contents of identified odorants than those from manure-belt layer hen and all four types of swine buildings (all p<0.001); while samples from farrowing and gestation buildings had significantly higher odorant contents than

those from manure belt layer hen buildings (both $p < 0.025$) as illustrated in Figure 5.1a. Similarly, a log transformation was conducted for the Simpson's index data. The ANOVA test revealed that the mass of identified odorants was more evenly distributed in TSP samples from tom turkey buildings than those from farrowing, gestation and manure belt layer hen buildings (all $p < 0.025$) (Figure 5.1b).

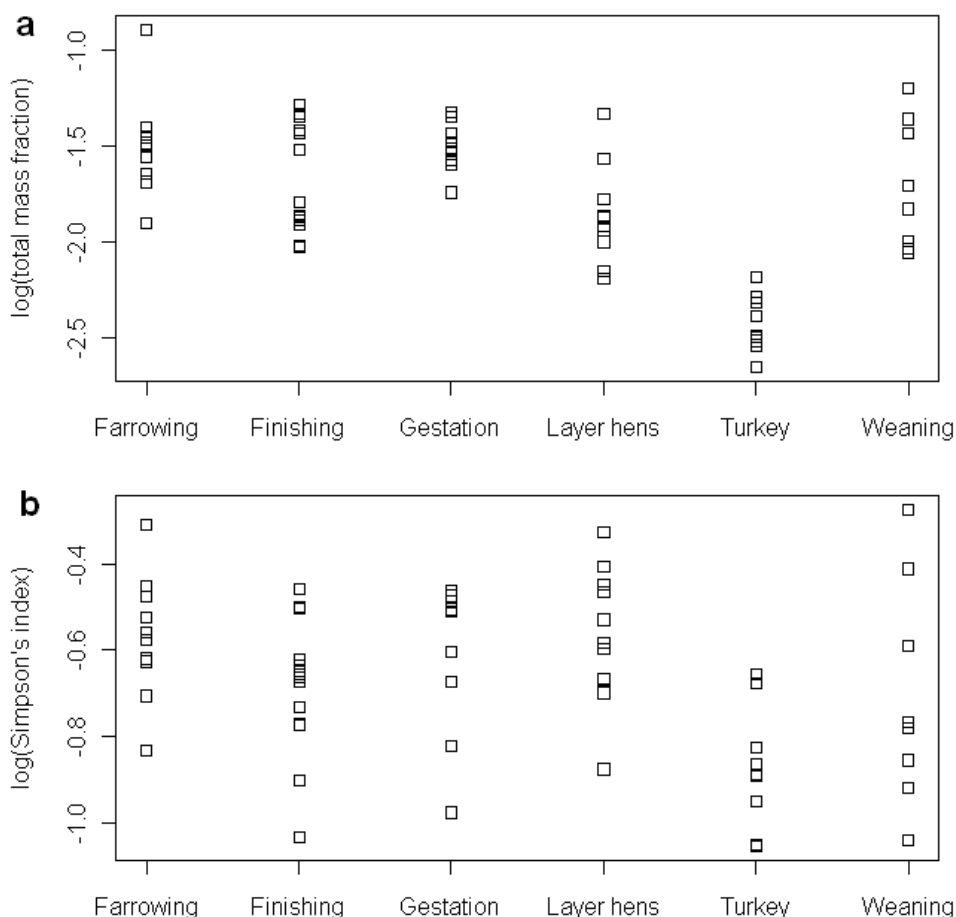


Figure 5.1. Effect of animal building type on (a) total mass fraction and (b) Simpson's diversity index of odorants in TSP samples.

Non-metric MDS analysis

A difference in odorant composition between two samples can be quantified with a variety of distances or dissimilarity indices, e.g., Euclidean distance. A pair-wise comparison among multiple samples therefore would generate a distance or dissimilarity matrix. Non-metric MDS is basically a tool to visualize the matrix by assigning the location of each sample in a 3-D space or on a 2-D plane based on the rank order of distance. On a 2-D non-metric MDS plot, samples will cluster together if they have similar odorant compositions; however, distances between samples

have been rescaled and are not proportional to the original distance. Compared to PCA, non-metric MDS has several advantages:

- A number of distance or dissimilarity indices are available for non-metric MDS, thereby making it more flexible.
- PCA assumes that the observed samples are linear combinations of principal components and therefore is less suitable for cases when many zero data are present. Non-metric MDS does not have such a limitation.
- Samples on a non-metric MDS plot are more evenly distributed since the location of samples is determined according to the rank order of distance, thereby offering a better data visualization than PCA.

In this study, non-metric MDS analysis was performed on the basis of Bray-Curtis dissimilarity index, defined as:

$$BC_{jk} = \frac{\sum_{i=1}^s |x_{ij} - x_{ik}|}{\sum_{i=1}^s (x_{ij} + x_{ik})} \quad (5.6)$$

Where, BC_{ik} is the Bray-Curtis dissimilarity between the j^{th} and k^{th} samples, s is the number of species (odorants), x_{ij} is the abundance (mass fraction or OAV_P) of the i^{th} compounds in the j^{th} sample, and x_{ik} is the abundance of the i^{th} compounds in the k^{th} sample. The Bray-Curtis dissimilarity index has been extensively used in ecology to measure a difference between two biotic communities, or a discrepancy in abiotic (physical and chemical) parameters between two habitats (Clarke, 1993). The Bray-Curtis dissimilarity index is currently the only option to the SIMPER test. To be consistent, this index was also selected for non-metric MDS analysis and ANOSIM test.

The mass fraction-based odorant composition of TSP samples was found to vary greatly with animal building type (Figure 5.2). TSP samples collected from the same type of animal confinement buildings clustered together. Samples were less closely clustered for samples from finishing and weaning buildings, indicating a large variation in odorant composition within these two building types. As a measure of the closeness of clustering, a multivariate dispersion index (MVDISP) was calculated with PRIMER 6.0 to be 0.82 for farrowing, 0.77 for gestation, 1.59

for weaning, 1.10 for finishing, 0.951 for manure-belt layer hen, and 0.789 for tom-turkey buildings.

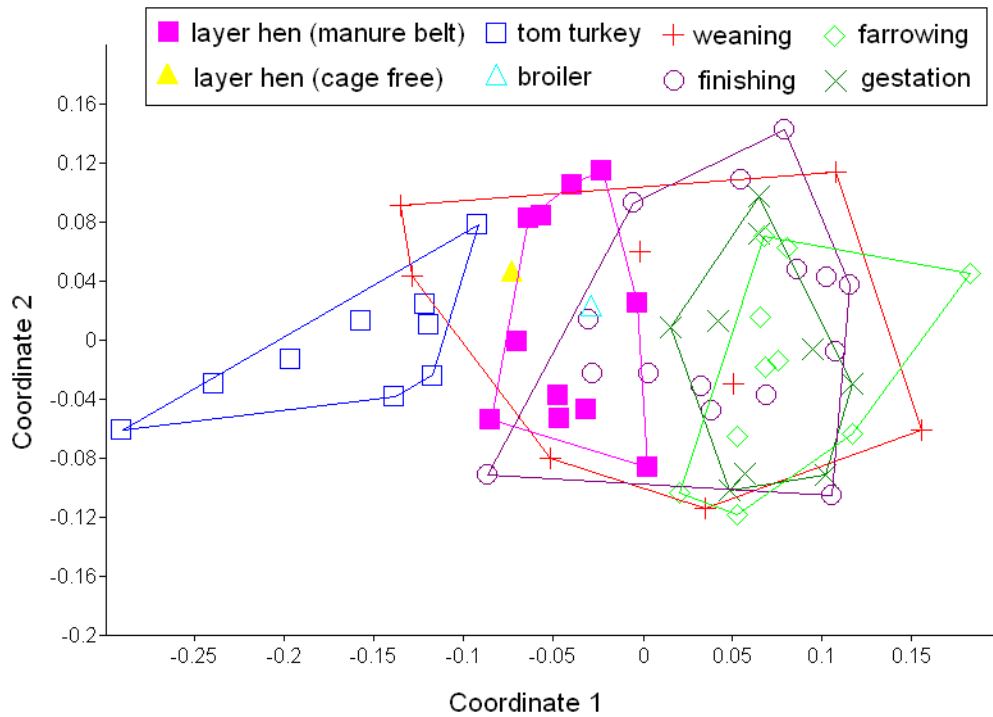


Figure 5.2. Non-metric MDS plot of TSP samples from different types of animal confinement buildings based on mass fraction of odorants.

Tom turkey buildings were clearly separated from farrowing, gestation and finishing buildings, but slightly overlapped with finishing buildings. Manure-belt layer hen buildings had a significant overlap with finishing and weaning buildings but were noticeably separated from farrowing and gestation buildings. Interestingly, TSP samples from cage-free layer hen and broiler buildings were clustered closely to those from manure-belt layer hen buildings, implying that TSP samples collected from those three types of animal confinement buildings may have a similar odorant composition (mass fraction based). Comparatively, no clear difference was found among four types of swine buildings. Particularly, TSP samples from farrowing and gestation buildings were closely clustered and indistinguishable.

ANOSIM test

To measure the degree of separation, an ANOSIM test was selected. ANOSIM basically measures the ratio of distances between two clusters to distances within individual clusters. A statistic R is generated as:

$$R = \frac{4(r_b - r_w)}{N(N-1)} \quad (5.7)$$

Where, r_b is the mean rank of distances between two clusters, r_w is the mean rank of distances within individual clusters, and N is the number of samples. Two clusters are considered to be well separated when R is greater than 0.75, separated but slightly overlapped when R is greater than 0.5 but smaller than 0.75, separated but strongly overlapped when R is greater than 0.25 but smaller than 0.5, and inseparable when R is smaller than 0.25 (Lin et al., 2003). The significance of the statistic R is determined through a permutation test ($N=9,999$ in this study). This test randomly selects a number of samples for R calculation, and then computes a p value defined as the fraction of generated R values equal to or less than zero. The separation (difference) between two clusters is considered to be significant when the p value is less than 0.05.

The ANOSIM test results (Table 5.8) showed that tom turkey buildings were well separated from gestation and farrowing buildings, and separated from but slightly overlapped with manure-belt layer hen, weaning and finishing buildings; manure-belt layer hen buildings were separated from but slightly overlapped with weaning, gestation and farrowing buildings, and separated from but strongly overlapped with finishing buildings. Again, no clear separation ($R>0.5$) was found among four types of swine buildings- a separation was present between weaning and gestation buildings but with a strong overlapping. All identified separations ($R>0.25$) were significant according to their corresponding p values.

Table 5.8. Summary of ANOSIM test on TSP samples from different types of animal confinement buildings based on mass fraction of odorants ($R_{\text{global}}=0.416$, $p<0.001$)^{a,b}.

	Weaning	Tom turkey	Layer hen	Gestation	Finishing	Farrowing
Weaning		<0.001	<0.001	0.003	0.160	0.007
Tom turkey	**0.518		<0.001	<0.001	<0.001	<0.001
Layer hen ^c	**0.526	**0.535		<0.001	<0.001	<0.001
Gestation	*0.332	***0.923	**0.569		0.078	0.463
Finishing	0.085	**0.686	*0.391	0.114		0.353
Farrowing	0.241	***0.928	**0.535	-0.004	0.018	

a. In the upright portion of the table are the p values and the R values are listed in the lower left portion.

b. R values are highlighted with '*' if $0.50 \geq R > 0.25$, '**' if $0.75 \geq R > 0.50$ and '***' if $R > 0.75$.

c. Manure-belt layer hen building only.

What is the practical implication of an R value? The R value is a measure of difference between two clusters. High R values indicate that two clusters are considerably distinct from each other. Assuming a cluster represents multiple pollution sources but of the same type (e.g. the same type of animal confinement buildings) or multiple samples from a single source (e.g.,

TSP samples collected on different days from a swine building), high R values indicate that this type of pollution sources or this source have distinctly different chemical profiles than other sources. This is particularly important for receptor modeling, either chemical mass balance (CMB) or factor analysis such as positive matrix factorization (PMF). Suppose that the PMF model is being used in a region where turkey and farrowing buildings coexist. Their substantially different odorant compositions would help distinguish and identify potential PM sources.

SIMPER analysis

Once a difference between two animal building types is identified, the next task is to determine which odorants and how much they contribute to that difference. This task was done with the SIMPER analysis, which calculates the contribution percentage of each odorants to the average Bray-Curtis dissimilarity between two animal building types. To be concise, only those with the R value greater than 0.5 were subject to the SIMPER analysis.

The results (Table 5.9) revealed that variations in odorant composition with animal building type were mainly contributed by the contents of ethanol, 2-ethyl-1-hexanol, acetic acid, propanoic acid, 3-methylbutanoic acid, 2,2-dimethyl-propanoic acid, nonanoic acid, dodecanoic acid, undecanoic acid, tridecanoic acid, benzoic acid, phenylacetic acid, p-cresol, hexanal and nonanal. Many of them, such as acetic acid and ethanol, were also among the most abundant odorants in TSP samples (Table 5.5). The cumulative contributions of top ten contributing compounds were all greater than 83%, indicating that these compounds predominantly account for variations among different animal building types.

The results also revealed that separations between tom turkey and all four types of swine buildings were primarily related to the significantly lower contents of identified odorants in TSP samples from tom turkey buildings (Table 5.7). The top ten contributing odorants all occurred at lower mass fractions in TSP samples from tom turkey buildings than from swine buildings. Manure-belt layer hen buildings were separated from farrowing, gestation and weaning buildings for possibly a similar reason; however, TSP samples from manure-belt layer hen buildings were found to have higher propanoic acid mass fractions than samples from gestation and weaning building. Although the total mass fraction of identified odorants was much lower in TSP samples from tom turkey buildings, TSP samples from tom turkey buildings had averagely two times higher mass fraction of 2-ethyl-1-hexanol than those from manure-belt layer hen buildings.

Accordingly, 2-ethyl-1-hexanol may be selected as a characteristic TSP-borne odorant for tom turkey buildings to distinguish from manure-belt layer hen buildings.

Table 5.9. Major odorants in TSP samples that contribute to variations in mass fraction-based odorant composition among different animal building types.

Building type	Top ten contributing compounds ^a	Cumulative contribution
Weaning vs. tom turkey	acetic acid (+), ethanol (+), 2-ethyl-1-hexanol (+), phenylacetic acid (+), hexanal (+), propanoic acid (+), benzoic acid (+), dodecanoic acid (+), 3-methylbutanoic acid (+), p-cresol (+)	84.6%
Weaning vs. layer hen ^b	acetic acid (+), ethanol (+), 2-ethyl-1-hexanol (+), propanoic acid (-), phenylacetic acid (+), hexanal (+), dodecanoic acid (+), benzoic acid (+), nonanoic acid (-), nonanal (-)	83.6%
Tom turkey vs. layer hen	acetic acid (-), ethanol (-), propanoic acid (-), dodecanoic acid (-), nonanoic acid (-), nonanal (-), hexanal (-), 2-ethyl-1-hexanol (+), undecanoic acid (-), 1-octanol (-)	88.1%
Tom turkey vs. gestation	acetic acid (-), ethanol (-), benzoic acid (-), phenylacetic acid (-), dodecanoic acid (-), tridecanoic acid (-), 2-ethyl-1-hexanol (-), propanoic acid (-), 3-methylbutanoic acid (-), undecanoic acid (-)	87.5%
Tom turkey vs. finishing	acetic acid (-), ethanol (-), 2-ethyl-1-hexanol (-), dodecanoic acid (-), phenylacetic acid (-), benzoic acid (-), propanoic acid (-), hexanal (-), 3-methylbutanoic acid (-), tridecanoic acid (-)	84.7%
Tom turkey vs. farrowing	acetic acid (-), ethanol (-), 2-ethyl-1-hexanol (-), propanoic acid (-), dodecanoic acid (-), tridecanoic acid (-), 2,2-dimethyl-propanoic acid (-), benzoic acid (-), 3-methylbutanoic acid (-), phenylacetic acid (-)	86.6%
Layer hen vs. gestation	acetic acid (-), ethanol (-), benzoic acid (-), propanoic acid (+), phenylacetic acid (-), tridecanoic acid (-), 2-ethyl-1-hexanol (-), 3-methylbutanoic acid (-), undecanoic acid (-)	84.7%
Layer hen vs. farrowing	acetic acid (-), ethanol (-), propanoic acid (-), 2-ethyl-1-hexanol (-), dodecanoic acid (-), tridecanoic acid (-), 2,2-dimethyl-propanoic acid (-), benzoic acid, phenylacetic acid (-), 3-methylbutanoic acid (-)	83.4%

a. The symbol '+' or '-' in parenthesis represents a difference in abundance between two groups. For example, for weaning versus tom turkey, acetic acid (+) indicates that TSP samples from weaning buildings have averagely higher acetic acid content than those from tom turkey buildings.

b. Manure-belt layer hen building only.

Since the total mass fraction of identified odorants had a significant implication on observed clustering patterns, a question is- why not further normalize the data by dividing the mass fraction of each odorant over the total mass fraction of all identified odorants. The reasons are:

- The mass fraction data were already a result of normalization- by dividing the mass concentration of each odorant over the TSP concentration.
- Receptor modeling relies on the data of mass fraction. A further normalization of the fraction data is unnecessary and meaningless in this regard.
- Adding or removing one or a few odorants may greatly change the normalization results, thereby making them hardly useful.

5.3.2.2 Variation in OAV_P-based odorant composition of TSP samples

One-way ANOVA test

Table 5.10 listed the COI_P, COI and the Simpson's diversity index (D) in different types of animal confinement buildings. It can be seen that the COI_P's of TSP samples were averagely higher in swine buildings than in manure-belt layer hen and tom turkey buildings; the average COI was higher in tom turkey, weaning and finishing buildings but lower in farrowing and gestation buildings; the Simpson's index values ranged from 0.074 to 0.38 and were minimal for samples from farrowing buildings and maximal for samples from weaning buildings. Noticeably, the standard deviations of COI_P's were smaller than those of COI's. This implies that the odor strength per mass of TSP particles is relatively constant in the same type of animal confinement buildings, and a significant variation in odor levels, if observed, may be mainly caused by different TSP mass concentrations.

Table 5.10. Total mass fraction and Simpson's diversity index of odorants in TSP samples from different types of animal confinement buildings.

	Statistic	Farrowing	Gestation	Weaning	Finishing	Layer hen ^a	Tom turkey
COI _P (m ³ /g)	Mean	0.0133	0.0160	0.0180	0.0154	0.0060	0.0037
	SD	0.0059	0.0034	0.0083	0.0048	0.0014	0.0012
COI	Mean	0.0117	0.0111	0.0237	0.0276	0.0168	0.0232
	SD	0.0068	0.0046	0.0132	0.0150	0.0136	0.0252
Simpson's index (D)	Mean	0.1148	0.1681	0.1974	0.1559	0.1400	0.1388
	SD	0.0289	0.0646	0.0802	0.0640	0.0344	0.0284

a. manure-belt layer hen buildings only.

The data of COI_P's and COI's were log-transformed and then subject to the ANOVA test. The results showed that TSP samples from tom turkey buildings had a significantly lower COI_P than those from manure-belt layer hen buildings ($p < 0.017$); while, TSP samples from manure-belt layer hen buildings had a significantly lower mean COI_P than those from all four types of swine buildings (all $p < 0.003$). However, no significant difference in COI_P was observed among TSP samples from different types of swine buildings (Figure 5.3a). This implies that at the same mass or mass concentrations, TSP particles (total particles) from swine buildings can be more odorous than those from manure-belt layer hen and tom turkey buildings; TSP particles from tom turkey buildings may be least odorous.

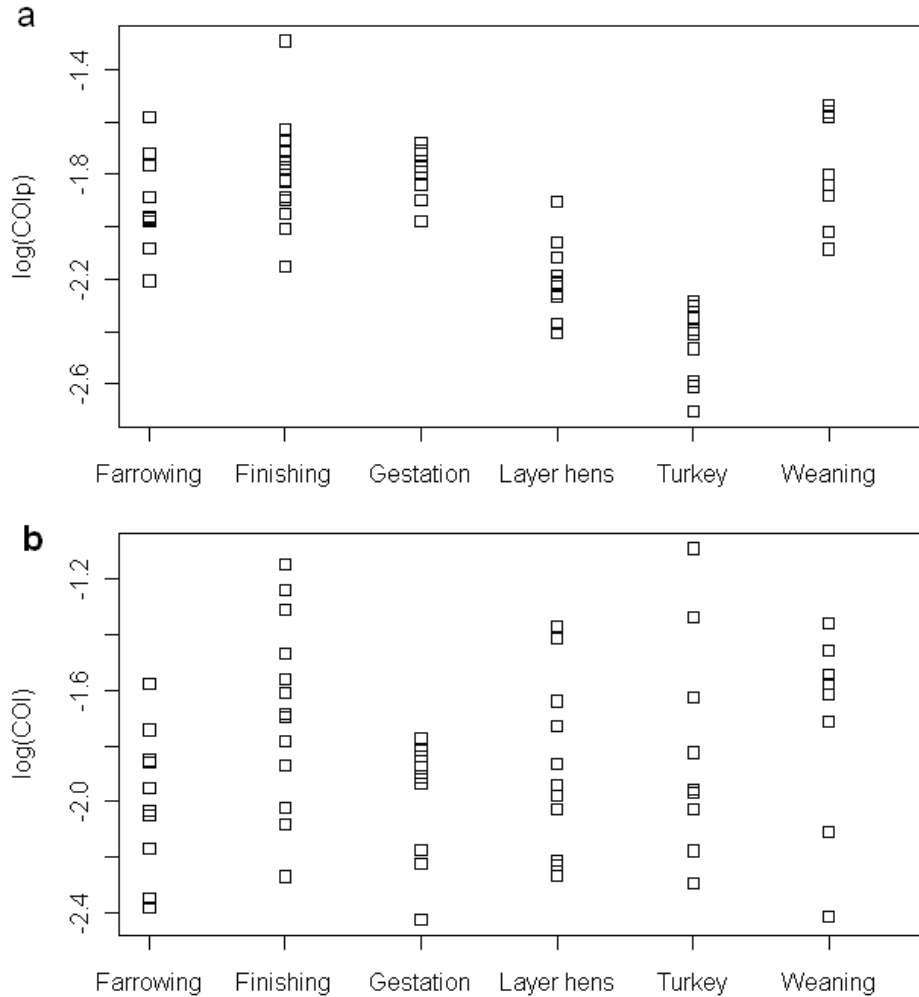


Figure 5.3. Effect of animal building type on (a) COI_p and (b) COI of TSP samples.

Comparatively, no significant difference in COI was identified among TSP samples from different types of animal confinement buildings (Figure 5.3b). This phenomenon can be explained by (1) COI equals to the product of COI_p and PM mass concentration, and (2) tom turkey and manure-belt layer hen buildings had higher TSP concentrations than swine buildings, which compensated for the lower COI_p values in visited poultry buildings. No significant difference in the Simpson's diversity index was found among different types of animal confinement buildings (Figure 5.4), suggesting a similar pattern in terms of the evenness of odor contribution by multiple odorants in TSP samples.

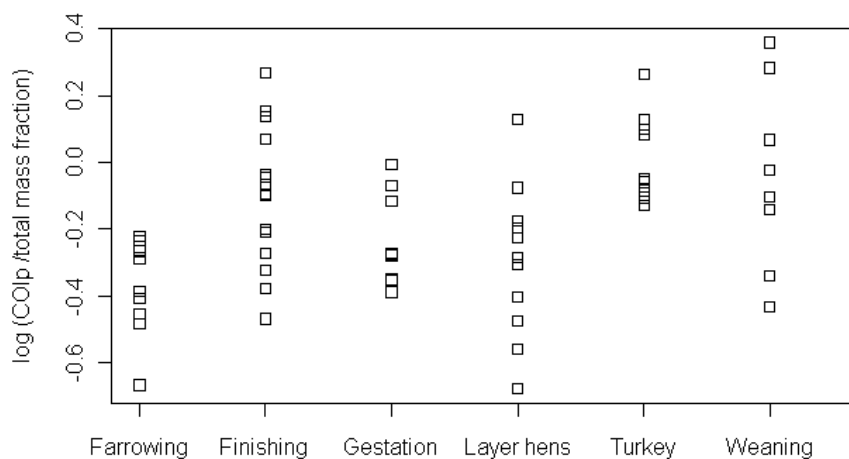


Figure 5.5. Effect of animal building type on odor strength per mass of odorants in TSP samples.

Non-metric MDS analysis

The OAV_p-based odorant composition of TSP samples varied greatly with animal building type (Figure 5.6). Similar to Figure 5.2, TSP samples from the same type of animal confinement buildings clustered together. No distinct difference was identified among different types of swine buildings. Tom turkey buildings were noticeably separated from all four types of swine buildings but slightly overlapped with manure-belt layer hen buildings. Manure-belt layer hen buildings were also separated from all four types of swine buildings but to a less degree. The TSP sample collected from the cage-free layer hen building was again clustered close to samples from manure-belt layer hens building, implying a similar OAV_p-based odorant composition.

However, the TSP sample from the broiler building was located distantly from samples from manure-belt layer hen buildings. By reviewing the raw data sheets, we found that TSP sample from this broiler building had no (E,E)-2,4-decadienal but had an unusually high content of 3-methylbutanoic acid. Both compounds occurred at low mass fractions (Table 5.4); consequently, they would not significantly affect the location of TSP samples on Figure 5.2 since the plot was based on the mass fraction of odorants. However, both (E,E)-2,4-decadienal and 3-methylbutanoic acid have low odor thresholds (Table 5.3) and were identified to be major odor-contributors in TSP samples (Table 5.6). Accordingly, the isolation of this broiler building from manure-belt layer hen buildings on Figure 5.6 may be explained by the ‘unusual’ mass fractions of (E,E)-2,4-decadienal and 3-methylbutanoic acid in the broiler building TSP sample. This is an example showing the essentialness of normalizing odorant contents with their odor thresholds.

Without normalization, we may fail to identify patterns induced by less abundant but strong odorants.

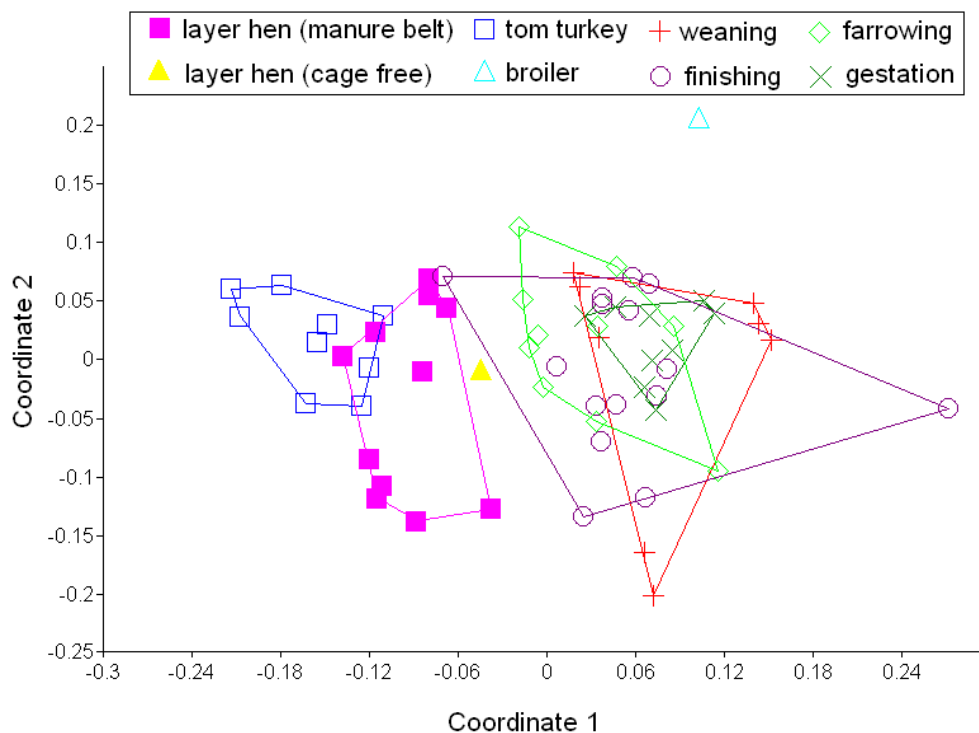


Figure 5.6. Non-metric MDS plot of TSP samples from different types of animal confinement buildings based on OAV_p of odorants.

The multivariate dispersion index (MVDISP) was determined to be 0.99 for farrowing, 0.67 for gestation, 1.39 for weaning, 1.12 for finishing, 1.01 for manure-belt layer hen and 0.66 for tom-turkey buildings. Similar to Figure 5.2, a relatively large variation in OAV_p-based odorant composition was found within weaning and finishing buildings; while gestation and turkey buildings were both associated with a relatively small variation.

ANOSIM test

The ANOSIM test results (Table 5.11) confirmed our observations from Figure 5.6. Tom turkey buildings were well separated from all four types of swine buildings, and separated from but strongly overlapped with manure-belt layer hen buildings; manure-belt layer hen buildings were well separated from gestation and weaning buildings but slightly overlapped with farrowing and finishing buildings; no clear difference ($R > 0.5$) was found among four types of swine buildings; however, a weak separation but strong overlapping was present between weaning and farrowing buildings. All identified separations ($R > 0.25$) were significant ($P < 0.05$). Compared to

mass fraction-based odorant compositions ($R_{\text{global}} = 0.416$), OAV_P based odorant compositions generated a better separation pattern ($R_{\text{global}} = 0.495$).

Table 5.11. Summary of ANOSIM test on TSP samples from different types of animal confinement buildings based on OAV_P of odorants ($R_{\text{global}} = 0.495$, $p < 0.001$)^{a,b}.

	Weaning	Turkey	Layer hen	Gestation	Finishing	Farrowing
Weaning		<0.001	<0.001	0.012	0.314	0.002
Turkey	***0.794		<0.001	<0.001	<0.001	<0.001
Layer hen ^c	***0.751	*0.473		<0.001	<0.001	<0.001
Gestation	0.205	***0.999	***0.831		0.093	0.031
Finishing	0.033	***0.787	**0.610	0.115		0.041
Farrowing	*0.319	***0.938	**0.512	0.177	0.133	

a. In the upright portion of the table are the p values and the R values are listed in the lower left portion.

b. R values are highlighted with '*' if $0.50 \geq R > 0.25$, '**' if $0.75 \geq R > 0.50$ and '***' if $R > 0.75$.

c. Manure-belt layer hen building only.

SIMPER analysis

The SIMPER analysis results (Table 5.12) revealed that variations in OAV_P -based odorant composition with animal building type were mainly contributed by the contents of acetic acid, propanoic acid, butanoic acid, 3-methylbutanoic acid, undecanoic acid, dodecanoic acid, phenylacetic acid, (E,E)-2,4-decadienal, (E,E)-2,4-nonadienal, (E)-2-nonenal, indole and p-cresol. Many of them were also among the most odor-contributing compounds in Table 5.6. The cumulative contributions of top ten variation-contributing compounds were all greater than 78.0%, indicating a predominant role of those compounds in explaining variations among different type of animal confinement buildings. The results also revealed that differences between tom-turkey and four types of swine buildings were mainly resulted from lower contents of major odor-contributing compounds in TSP samples from tom turkey buildings. A similar observation was made between manure-belt layer hen and four types of swine buildings. However, a higher content of nonanal was found in manure-belt layer hen buildings than in swine buildings, suggesting that nonanal may be selected as a characteristic odorant for TSP samples from manure-belt layer hen buildings.

Table 5.12. Major compounds in TSP samples that contribute to variations in OAVP-based odorant composition among different animal building types.

Building type	Top ten contributing compounds ^a	Cumulative contribution
Weaning vs. tom turkey	phenylacetic acid (+), (E,E)-2,4-decadienal (+), indole (+), p-cresol (+), 3-methylbutanoic acid (+), dodecanoic acid (+), butanoic acid (+), (E,E)-2,4-nonadienal (+), (E)-2-nonenal (+), acetic acid (+)	84.5%
Weaning vs. layer hen ^b	phenylacetic acid (+), (E,E)-2,4-decadienal (+), indole (+), p-cresol (+), dodecanoic acid (+), 3-methylbutanoic acid (+), nonanal (-), butanoic acid (+), acetic acid (+), (E,E)-2,4-nonadienal (+)	81.4%
Tom turkey vs. gestation	phenylacetic acid (-), dodecanoic acid (-), 3-methylbutanoic acid (-), acetic acid (-), undecanoic acid (-), p-cresol (-), indole (-), (E,E)-2,4-decadienal (+), (E)-2-nonenal (-), nonanal (-)	86.7%
Tom turkey vs. finishing	phenylacetic acid (-), indole (-), (E,E)-2,4-decadienal (-), dodecanoic acid (-), 3-methylbutanoic acid (-), p-cresol (-), acetic acid (-), (E)-2-nonenal (-), undecanoic acid (-), nonanal (-)	82.3%
Tom turkey vs. farrowing	phenylacetic acid (-), dodecanoic acid (-), 3-methylbutanoic acid (-), acetic acid (-), undecanoic acid (-), indole (-), (E)-2-nonenal (-), nonanal (-), (E,E)-2,4-decadienal (+), propanoic acid (-)	78.5%
Layer hen vs. gestation	phenylacetic acid (-), 3-methylbutanoic acid (-), dodecanoic acid (-), indole (-), (E,E)-2,4-decadienal (+), p-cresol (-), undecanoic acid (-), acetic acid (-), nonanal (+), propanoic acid (+)	86.1%
Layer hen vs. finishing	phenylacetic acid (-), indole (-), (E,E)-2,4-decadienal (-), dodecanoic acid (-), 3-methylbutanoic acid (-), p-cresol (-), nonanal (+), (E)-2-nonenal (-), undecanoic acid (-), acetic acid (-)	81.9%
Layer hen vs. farrowing	phenylacetic acid (-), 3-methylbutanoic acid (-), (E,E)-2,4-decadienal (+), dodecanoic acid (-), acetic acid (-), nonanal (+), indole (-), propanoic acid (-), undecanoic acid (-), (E)-2-nonenal (-)	78.7%

a. The symbol '+' or '-' in parenthesis represents a difference in abundance between two groups. For example, for weaning versus tom turkey, acetic acid (-) indicates that TSP samples from weaning buildings have averagely lower acetic acid content than those from tom turkey buildings.

b. Manure-belt layer hen building only.

5.3.2.3 Variation in mass fraction-based odorant composition of PM₁₀ samples

One-way ANOVA test

The total mass fraction of identified odorants in PM₁₀ samples from different types of animal confinement buildings and the corresponding Simpson's diversity index (D) were summarized in Table 5.13. The total mass fractions of identified compounds ranged from 0.67 to 46.9% and were higher in farrowing and manure-belt layer buildings and lower in weaning and tom turkey buildings. The calculated Simpson's index values ranged from 0.100 to 0.564, and, similar to the case of TSP samples, were minimal for PM₁₀ samples from tom turkey buildings.

Table 5.13. Total mass fraction and Simpson’s diversity index of odorants in PM₁₀ samples from different types of animal confinement buildings.

	Statistic	Farrowing	Gestation	Weaning	Finishing	Layer hen ^a	Tom turkey
Total mass fraction of identified odorants	Mean	0.1195	0.0940	0.0428	0.0788	0.1208	0.0337
	SD	0.1425	0.0640	0.0186	0.0647	0.1610	0.0602
Simpson’s diversity index (D)	Mean	0.3223	0.2962	0.2971	0.2851	0.3630	0.2584
	SD	0.0394	0.0794	0.1004	0.1122	0.0981	0.1107

a. manure-belt layer hen buildings only.

The total mass fraction data were log transformed and then subjected to one-way ANOVA test; while, a log transformation was found to be unnecessary for the data of the Simpson’s diversity index. The ANOVA test results showed that the total mass fraction of identified odorants was significantly lower in PM₁₀ samples from tom turkey buildings than in those from farrowing, gestation, finishing and manure-belt layer hen buildings (all $p < 0.018$); while, no significant difference in the Simpson’s diversity index was found among different types of animal confinement buildings.

Non-metric MDS analysis

The mass fraction-based odorant composition of PM₁₀ samples varied greatly with animal building type (Figure 5.7). Similar to the case of TSP samples (Figure 5.2), PM₁₀ samples from the same type of animal confinement buildings clustered together; gestation and farrowing buildings again were very closely clustered and hardly distinguishable; broiler and cage-free layer hen buildings was clustered close to manure-belt layer hens buildings, indicating a similar odorant composition. However, an overall stronger overlap was found among PM₁₀ than TSP samples from different types of animal confinement buildings. For instance, in Figure 5.7 tom turkey building showed a noticeable overlap with finishing buildings; while in Figure 5.2, those two types of building were clearly separated. The stronger overlap indicated that PM₁₀ samples from different types of animal confinement buildings had a more similar mass fraction-based odorant composition than TSP samples. Considering that larger particles in TSP samples will quickly settle down after discharged into the ambient air and only smaller particles, such as PM₁₀, will be able to transport a relatively long distance, it is speculated that although distinctly different odors may be sensed in or near different types of animal confinement buildings, such a difference may become less distinguishable when particle-borne odors reach neighboring communities.

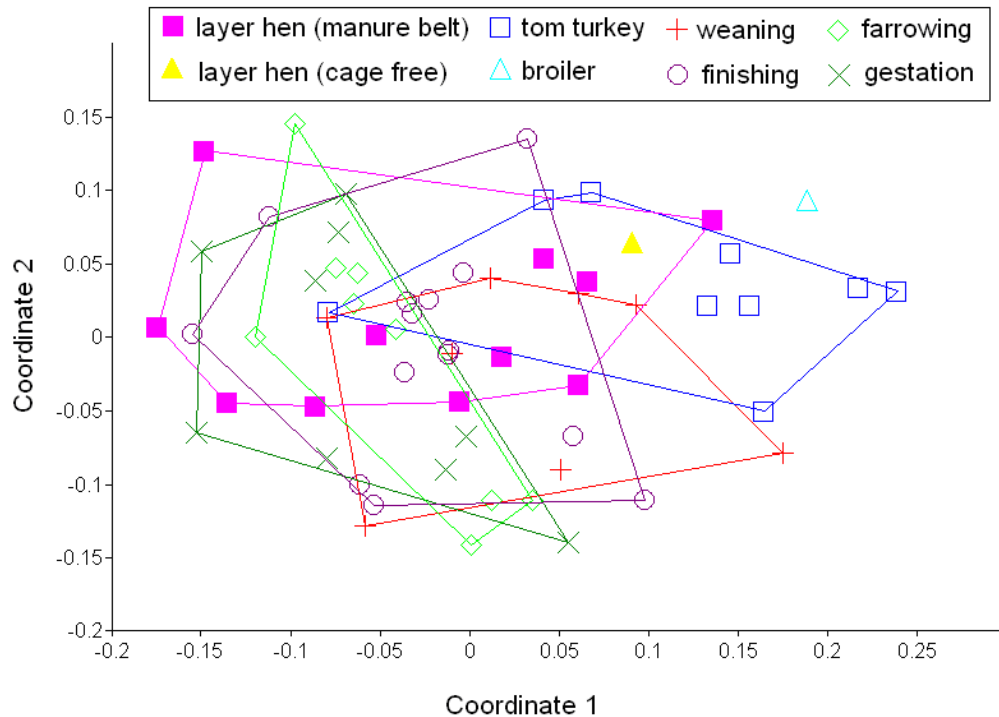


Figure 5.7. Non-metric MDS plot of PM₁₀ samples from different types of animal confinement buildings based on mass fraction of odorants.

The MVDISP was calculated to be 0.90 for farrowing, 0.80 or gestation, 0.70 for weaning, 1.02 for finishing, 1.28 for manure-belt layer hen and 1.05 for tom turkey buildings. Compared to the case of TSP samples, there was overall no significant difference.

ANOSIM test

The ANOSIM test results (Table 5.14) confirmed that the mass fraction-based odorant composition of PM₁₀ samples was more similar among different types of animal confinement buildings (R_{global} of PM₁₀ samples = 0.267 vs. R_{global} of TSP samples = 0.416). PM₁₀ samples from tom turkey buildings were found to be separated but slightly overlapped with samples from farrowing, gestation and finishing buildings, and separated but strongly overlapped with samples from weaning buildings. A separation but with a strong overlap was identified between gestation and weaning and between manure-belt layer hen and farrowing buildings. Because the total mass fraction of identified odorants in PM₁₀ samples was comparable between manure-belt layer hen and farrowing buildings (Table 5.13), a difference in odorant composition between those two types of buildings may mainly be explained by the relative abundance instead of the absolute abundance of odorants.

Table 5.14. Summary of ANOSIM test on PM₁₀ samples from different types of animal confinement buildings based on mass fraction of odorants (R global= 0.267, p<0.001)^{a,b}.

	Weaning	Turkey	Layer hen ^c	Gestation	Finishing	Farrowing
Weaning		0.005	0.023	0.012	0.285	0.012
Turkey	*0.349		0.010	<0.001	<0.001	<0.001
Layer hen	0.192	0.242		0.005	0.035	0.002
Gestation	*0.259	**0.700	0.235		0.273	0.020
Finishing	0.043	**0.526	0.116	0.037		0.130
Farrowing	0.238	**0.711	*0.263	0.239	0.085	

a. In the upright portion of the table are the p values and the R values are listed in the lower left portion.

b. R values are highlighted with ‘*’ if 0.50>=R>0.25, ‘**’ if 0.75>=R>0.50 and ‘***’ if R>0.75.

c. Manure-belt layer hen building only.

SIMPER analysis

The SIMPER analysis results (Table 5.15) revealed that differences between tom turkey and farrowing/ gestation/ finishing buildings were predominantly contributed by the contents of ethanol, 2-ethyl-1-hexanol, acetic acid, propanoic acid, 2-methyl-propanoic acid, 2,2-dimethyl-propanoic acid, dodecanoic acid, tridecanoic acid, benzoic acid and phenylacetic acid. Most of them occurred at lower mass fractions in PM₁₀ samples from tom turkey buildings. Noticeably, the mass fraction of propanoic acid was higher in tom turkey than in gestation and finishing buildings, suggesting that propanoic acid may be selected as a characteristic PM₁₀-borne odorant from tom turkey buildings.

Table 5.15. Major compounds in PM₁₀ samples that contribute to variations in mass fraction-based odorant composition among different animal building types.

Building type	Top ten contributing compounds ^a	Cumulative contribution
Tom turkey vs. farrowing	acetic acid (-), propanoic acid (-), ethanol (-), dodecanoic acid (-), 2,2-dimethyl-propanoic acid (-), 2-ethyl-1-hexanol (-), 2-methylpropanoic acid (-), tridecanoic acid (-), 3-methylbutanoic acid (-), benzoic acid (-)	90.9%
Tom turkey vs. gestation	acetic acid (-), ethanol (-), propanoic acid (+), 2-ethyl-1-hexanol (-), dodecanoic acid (-), benzoic acid (-), phenylacetic acid (-), 2,2-dimethyl-propanoic acid (-), tridecanoic acid (-), undecanoic acid (-)	89.2%
Tom turkey vs. finishing	acetic acid (-), ethanol (-), propanoic acid (+), dodecanoic acid (-), 2-ethyl-1-hexanol (-), benzoic acid (-), phenylacetic acid (-), tridecanoic acid (-), undecanoic acid (-), 2-methylpropanoic acid (+)	89.4%

a. The symbol ‘+’ or ‘-’ in parenthesis represents a difference in abundance between two groups. For example, for weaning versus tom turkey, acetic acid (-) indicates that TSP samples from weaning buildings have averagely lower acetic acid content than those from tom turkey buildings.

5.3.2.4 Variation in OAV_P-based odorant composition of PM₁₀ samples

One-way ANOVA test

Table 5.16 summarized the COI_P, COI and Simpson's diversity index (D) in different types of animal confinement buildings. Similar to the case of TSP samples, the COI_P's of PM₁₀ samples were averagely higher in swine buildings than in tom turkey buildings. The mean COI was highest in finishing buildings and lowest in gestation buildings, which may be mainly because of a difference in PM₁₀ concentrations. The mean Simpson's index was highest in farrowing buildings and lowest in gestation buildings, indicating different odorant compositions in those two types of buildings.

Table 5.16. Total mass fraction and Simpson's diversity index of odorants in PM₁₀ samples from different types of animal confinement buildings.

	Statistic	Farrowing	Gestation	Weaning	Finishing	Layer hen ^a	Tom turkey
COI _P (m ³ /g)	Mean	0.0264	0.0295	0.0189	0.0257	0.0254	0.0098
	SD	0.0164	0.0099	0.0077	0.0075	0.0284	0.0112
COI	Mean	0.0087	0.0058	0.0065	0.0124	0.0102	0.0095
	SD	0.0037	0.0028	0.0053	0.0099	0.0065	0.0066
Simpson's index (D)	Mean	0.1726	0.1378	0.1416	0.1526	0.1587	0.1447
	SD	0.0913	0.0354	0.0440	0.0505	0.0284	0.0874

a. manure-belt layer hen buildings only.

A log transformation was conducted on the COI_P and COI data, which were then subject to the one-way ANOVA test. The results showed that the mean COI_P of PM₁₀ samples from tom turkey buildings was significant lower than the samples from farrowing, gestation and finishing buildings (all $p < 0.007$); while, no significant difference in COI was identified among different types of animal confinement buildings. A Mann-Whitney test was used for testing the data of the Simpson's diversity index because the normality of the data was still poor even after log transformation; yet no significant difference was found among different types of animal confinement buildings.

We also examined the ratio of COI_P to the total mass fraction of the odorants included in COI_P calculation. The calculated ratios were log transformed prior to the ANOVA test (Figure 5.8). The test results revealed that this ratio was significantly lower in manure-belt layer hen buildings than in tom turkey, weaning and finishing buildings (all $p < 0.049$), and was significantly higher in finishing buildings than in farrowing buildings ($p = 0.048$). A similar observation was made for TSP samples (Figure 5.5): this ratio was relatively high in weaning,

finishing and tom turkey buildings. This suggests that the odorant part in TSP and PM₁₀ samples from these buildings may contain more malodorous compounds in terms of relative abundance.

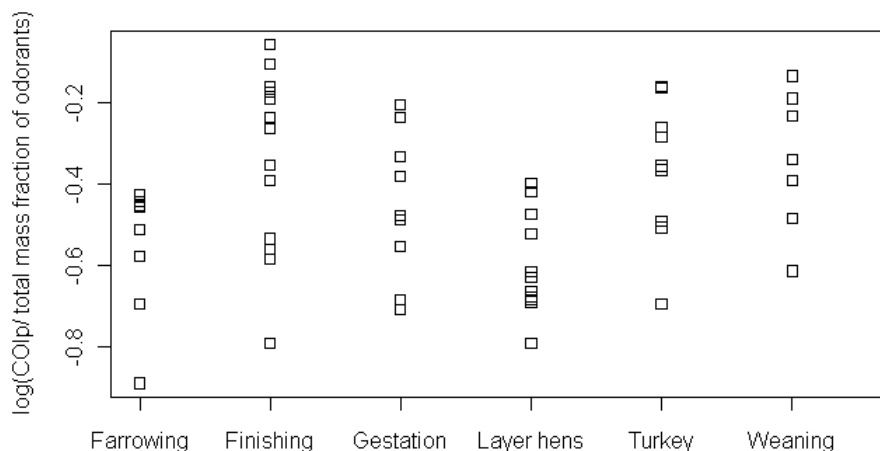


Figure 5.8. Effect of animal building type on odor strength per mass of odorants in PM₁₀ samples.

Non-metric MDS analysis

PM₁₀ samples from different types of animal confinement buildings had different OAV_P-based odorant compositions (Figure 5.9). PM₁₀ samples from four types of swine buildings were closely clustered. Manure-belt layer hen buildings had a significant overlapping with tom turkey and swine buildings; while a less degree of overlapping was observed between tom turkey and swine buildings. The cage-free layer hen building was clustered close to manure-belt layer hen buildings, indicating they share a similar odorant composition; while, the broiler building was somehow more different than manure-belt layer hen buildings in terms of OAV_P-based odorant composition.

The MVDISP was calculated to be 0.98 for farrowing, 0.49 for gestation, 0.92 for weaning, 1.06 for finishing, 1.34 for manure-belt layer hen and 0.93 for tom turkey buildings. A remarkably small variation in OAV_P-based odorant composition was found for PM₁₀ samples from gestation buildings.

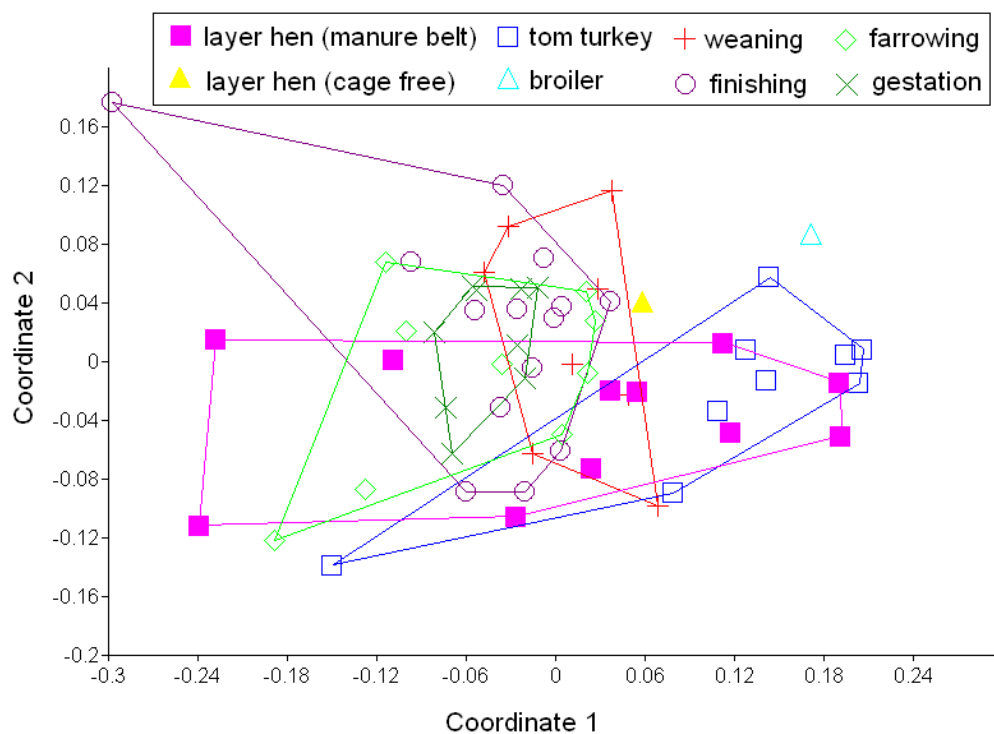


Figure 5.9. Non-metric MDS plot of PM₁₀ samples from different types of animal confinement buildings based on OAV_P of odorants.

ANOSIM test

The ANOSIM test results (Table 5.17) revealed that tom turkey buildings were well separated from gestation buildings, and separated but slightly overlapped with farrowing, weaning and finishing buildings; manure-belt layer hen buildings were separated from but heavily overlapped with gestation and finishing buildings; a poor separation but strong overlapping was also observed between weaning and gestation, between weaning and farrowing and between farrowing and gestation buildings. Compared to mass fraction-based odorant compositions ($R_{\text{global}}=0.267$), OAV_P-based odorant compositions again produced a slightly better separation pattern ($R_{\text{global}}=0.291$); however, it was still much poorer than that for TSP samples ($R_{\text{global}}=0.495$). This confirmed our observation that PM₁₀ samples from different types of animal confinement buildings (visited in this study) were more similar in odorant composition than corresponding TSP samples.

Table 5.17. Summary of ANOSIM test on PM₁₀ samples from different types of animal confinement buildings based on OAV_P of odorants (R global=0.291, p<0.001)^{a,b}.

	Weaning	Turkey	Layer hen ^c	Gestation	Finishing	Farrowing
Weaning		0.000	0.011	0.003	0.662	0.001
Turkey	**0.506		0.047	0.000	0.000	0.000
Layer hen	0.227	0.134		0.001	0.000	0.075
Gestation	*0.346	***0.785	*0.369		0.851	0.000
Finishing	-0.048	**0.606	*0.324	-0.075		0.045
Farrowing	*0.297	**0.545	0.110	*0.316	0.147	

a. In the upright portion of the table are the p values and the R values are listed in the lower left portion.

b. R values are highlighted with ‘*’ if 0.50>=R>0.25, ‘**’ if 0.75>=R>0.50 and ‘***’ if R>0.75.

c. Manure-belt layer hen building only.

SIMPER analysis

The SIMPER analysis results (Table 5.18) revealed that variations in the OAV_P-based odorant composition of PM₁₀ samples were mainly contributed by the contents of acetic acid, propanoic acid, 2-methylpropanoic acid, 3-methylbutanoic acid, dodecanoic acid, undecanoic acid, phenylacetic acid, (E,E)-2,4-decadienal, (E)-2-nonenal, nonanal, p-cresol and indole. Many of them were also the major odor contributors in PM₁₀ samples (Table 5.6). PM₁₀ samples from tom turkey buildings had averagely lower contents of major odor-contributing compounds than samples from swine buildings. Despite of the lower content of total odorants in PM₁₀ samples, propanoic acid was again found to occur at higher levels in tom turkey buildings than in gestation, weaning and gestation buildings.

Table 5.18. Major compounds in PM₁₀ samples that contribute to variations in OAV_P-based odorant composition among different animal building types.

Building type	Top ten contributing compounds ^a	Cumulative contribution
Tom turkey vs. farrowing	dodecanoic acid (-), propanoic acid (-), acetic acid (-), phenylacetic acid (-), 3-methylbutanoic acid (-), 2-methylpropanoic acid (-), (E,E)-2,4-decadienal (-), undecanoic acid (-), (E)-2-nonenal (-), nonanal (-).	83.8%
Tom turkey vs. gestation	phenylacetic acid (-), dodecanoic acid (-), (E,E)-2,4-decadienal (-), acetic acid (-), propanoic acid (+), undecanoic acid (-), indole (-), p-cresol (-), 3-methylbutanoic acid (-), (E)-2-nonenal (-), nonanal (-).	85.8%
Tom turkey vs. weaning	indole (-), (E,E)-2,4-decadienal (-), phenylacetic acid (-), propanoic acid (+), acetic acid (-), dodecanoic acid (-), (E)-2-nonenal (-), p-cresol (-), 3-methylbutanoic acid (-), nonanal (+).	80.8%
Tom turkey vs. finishing	dodecanoic acid (-), phenylacetic acid (-), (E,E)-2,4-decadienal (-), indole (-), acetic acid (-), propanoic acid (+), undecanoic acid (-), p-cresol (-), 3-methylbutanoic acid (-), (E)-2-nonenal (-).	84.0%

a. The symbol ‘+’ or ‘-’ in parenthesis represents a difference in abundance between two groups. For example, for weaning versus tom turkey, acetic acid (-) indicates that TSP samples from weaning buildings have averagely lower acetic acid content than those from tom turkey buildings.

5.3.2.5 Variation in relative abundance of odorants

Certain limitations were associated with previous analysis that relies on the Bray-Curtis dissimilarity index. Generally, a difference between two samples is a result of combination of differences in absolute and in relative abundance of each odorant. The Bray-Curtis dissimilarity index, regrettably, cannot distinguish the respective contributions of absolute and relative abundance, and rather evaluates an integrated effect of both factors. In this study, the absolute abundances of identified compounds differed greatly with animal building type and thereby might override the effect of relative abundance in previous analysis. This creates certain difficulties in determining the fingerprint or characteristic odorants for each type of animal confinement buildings.

To overcome such difficulties, a correlation distance-based PCoA plot was used to illustrate variations in terms of the relative abundances of odorants among different types of animal confinement buildings. Basically, Pearson's correlation coefficient (r) was selected as a measure of distance between two samples (Equation 5.8).

$$d_{jk} = 1 - r_{jk} = 1 - \frac{n \sum_i x_{ji} x_{ki} - \sum_i x_{ji} \sum_i x_{ki}}{\sqrt{n \sum_i x_{ji}^2 - \left(\sum_i x_{ji} \right)^2} \sqrt{n \sum_i x_{ki}^2 - \left(\sum_i x_{ki} \right)^2}} \quad (5.8)$$

Where, d_{jk} is the correlation distance between the j^{th} and the k^{th} sample, r_{jk} is Pearson's correlation coefficient, x_{ji} is the content of the i^{th} specie in the j^{th} sample and x_{ki} is the content of the i^{th} specie in the k^{th} sample. If two samples were identical in terms of the relative abundance of compounds but differed in their absolute amounts (an analogous case is two similar figures), the correlation distance would be equal to 0 and on the PCoA plot these two samples would appear at the same point.

The PCoA plots (Figure 5.10) showed that the odorant composition of TSP and PM₁₀ samples, both mass fraction- and OAV_P-based, differed with animal building type. Such a difference was explained by variations in the relative abundance of odorants (relative to other compounds). An overall better separation pattern was found for TSP samples. This again confirmed our previous observation that PM₁₀ samples from different types of animal confinement buildings had more similar odorant compositions than TSP samples.

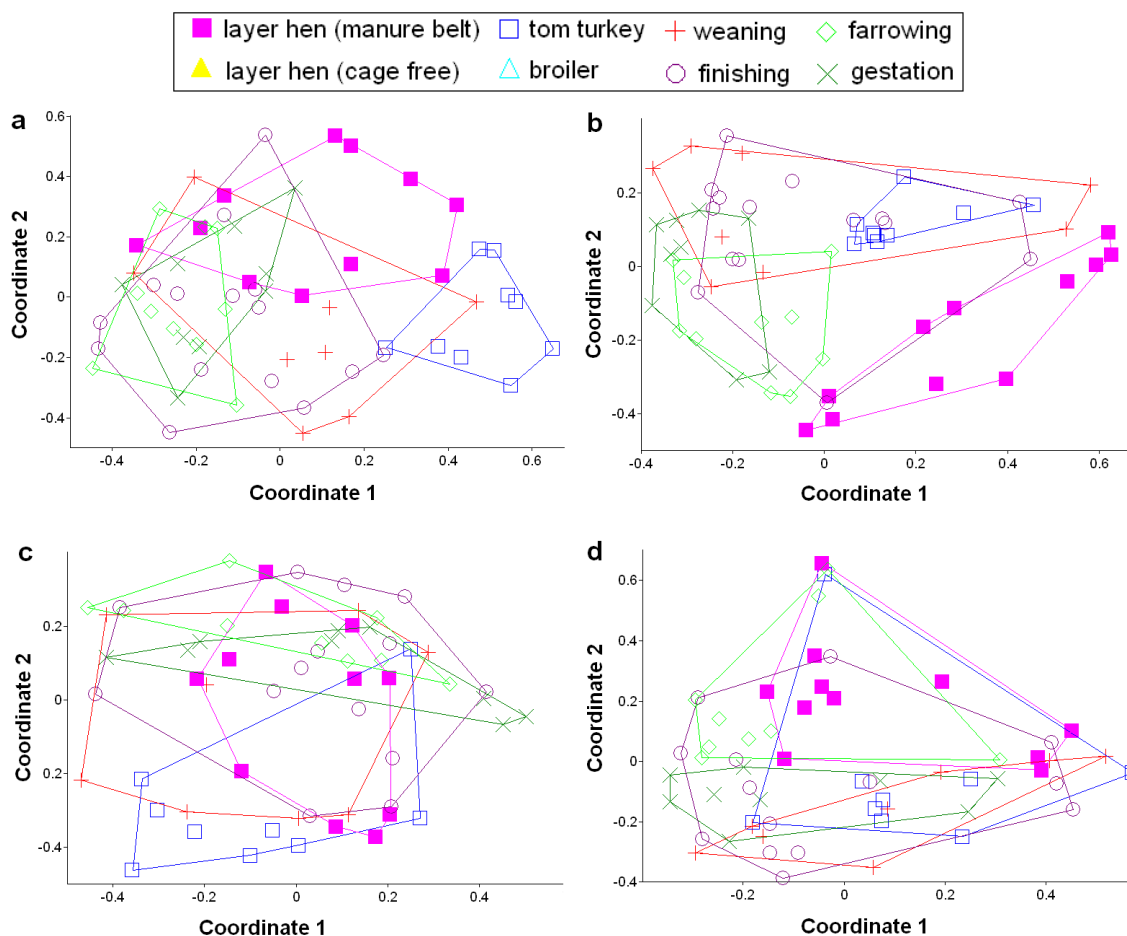


Figure 5.10. Correlation distance-based PCoA plot of particle samples from different types of animal confinement buildings: (a) TSP samples, mass fraction; (b) TSP samples, OVA_P; (c) PM₁₀ samples, mass fraction; (d) PM₁₀ samples, OVA_P.

An ANOSIM test was conducted based on the distance of correlation coefficient, and the results were summarized in Table 5.19. Overall, particle samples especially TSP samples from tom turkey buildings had very different odorant composition than those from farrowing and gestation buildings. This is consistent with our previous observation from the Bray-Curtis dissimilarity index-based data analysis.

Table 5.19. Summary of ANOSIM test on particle samples from different types of animal confinement buildings-based on correlation coefficient^{a,b}.

Mass fraction-based odorant composition of TSP samples (R _{global} =0.355, p<0.001)						
	Weaning	Turkey	Layer hen ^c	Gestation	Finishing	Farrowing
Weaning		<0.001	<0.001	0.033	0.139	0.011
Turkey	*0.400		<0.001	<0.001	<0.001	<0.001
Layer hen	*0.407	**0.503		0.001	<0.001	0.001
Gestation	0.200	***0.788	*0.332		0.049	0.439
Finishing	0.094	**0.599	*0.354	0.134		0.231
Farrowing	0.245	***0.852	*0.375	0.000	0.045	

Table 5.19. (cont.)

OAV _p -based odorant composition of TSP samples (R global =0.373, p<0.001)						
	Weaning	Turkey	Layer hen	Gestation	Finishing	Farrowing
Weaning		<0.001	0.001	0.015	0.405	0.002
Turkey	*0.424		<0.001	<0.001	<0.001	0.017
Layer hen	*0.456	*0.486		<0.001	<0.001	<0.001
Gestation	0.198	***0.979	**0.733		0.031	0.070
Finishing	0.001	0.204	*0.457	0.184		0.001
Farrowing	*0.288	***0.844	*0.431	0.125	*0.279	
Mass fraction-based odorant composition of PM ₁₀ samples (R global=0.165, p<0.001)						
	Weaning	Turkey	Layer hen	Gestation	Finishing	Farrowing
Weaning		0.047	0.023	0.011	0.218	0.047
Turkey	0.165		0.074	<0.001	0.007	<0.001
Layer hen	0.196	0.118		0.071	0.364	0.018
Gestation	*0.261	*0.452	0.122		0.494	0.016
Finishing	0.061	0.230	0.015	-0.007		0.368
Farrowing	0.165	**0.592	0.193	0.247	0.019	
OAV _p -based odorant composition of PM ₁₀ samples (R global=0.161, p<0.001)						
	Weaning	Turkey	Layer hen	Gestation	Finishing	Farrowing
Weaning		0.295	<0.001	0.013	0.808	<0.001
Turkey	0.024		0.006	<0.001	0.221	0.003
Layer hen	*0.357	0.224		<0.001	0.008	0.196
Gestation	*0.304	*0.446	*0.420		0.943	0.002
Finishing	-0.071	0.051	0.204	-0.094		0.097
Farrowing	*0.358	*0.301	0.054	*0.267	0.106	

- a. In the upright portion of the table are the p values and the R values are listed in the lower left portion.
 b. R values are highlighted with '*' if 0.50>=R>0.25, '**' if 0.75>=R>0.50 and '***' if R>0.75.
 c. Manure-belt layer hen building only.

A substantial difference in the relative abundance of compounds among different types of pollution sources is of particular importance for receptor modeling. Take chemical mass balance (CMB) model as an example (Equation 5.8).

$$\begin{bmatrix} C_1 \\ C_2 \\ C_3 \\ \vdots \\ C_i \end{bmatrix} = \begin{bmatrix} f_{1,1} & f_{2,1} & f_{3,1} & \dots & f_{i,1} \\ f_{1,2} & f_{2,2} & f_{3,2} & \dots & f_{i,2} \\ f_{1,3} & f_{2,3} & f_{3,3} & \dots & f_{i,3} \\ \vdots & \vdots & \vdots & \ddots & \vdots \\ f_{1,j} & f_{2,j} & f_{3,j} & \dots & f_{i,j} \end{bmatrix} \begin{bmatrix} S_1 \\ S_2 \\ S_3 \\ \vdots \\ S_j \end{bmatrix} \quad (5.8)$$

Where, C_i is the concentration of the ith species at the receptor site, f_{i,j} is the fraction of the ith species from the jth source, and S_j is the contribution of the jth source to a pollution at the receptor site. If two sources have similar chemical profiles in terms of relative abundance, it will be difficult to solve the CMB equations, thereby creating a great challenge to PM source

apportionment. For example, as suggested by this study, it can be difficult to distinguish weaning and finishing buildings in odors-based receptor models.

The observed difference in relative abundance presented a possibility of using the mass ratio of two odorants as a fingerprint for each type of animal confinement buildings. Unfortunately, there was no convenient tool, similar to SIMPER, to determine the fingerprint/ characteristic odorants or their ratios. This is a limitation of the correlation distance-based data analysis.

5.3.2.6 Determination of characteristic odorants or odorant ratios for each type of animal confinement buildings

In this study, a fingerprint or characteristic odorant was defined to satisfy the following requirements:

- It occurs ubiquitously and exclusively in TSP or PM₁₀ samples from the targeted type of animal confinement buildings, so that it can be selected as a tracer compound.
- Or, it occurs ubiquitously in TSP or PM₁₀ samples from the targeted type of animal confinement buildings, and its average mass fraction is significantly ($p < 0.05$) and at least two times higher than in any other types of animal confinement buildings.

A characteristic odorant ratio was expected to satisfy the following requirements:

- Both compounds must be ubiquitously present in TSP or PM₁₀ samples from the targeted type of animal confinement buildings.
- And, the average ratio must be significantly ($p < 0.05$) and at least two times higher in the targeted type of animal confinement buildings than any other types of buildings.

A MATLAB program was developed to assist to determine the characteristic odorants or odorant ratios. It first selected the odorants that ubiquitously existed in the targeted type of animal confinement buildings, calculated their average mass fractions and pair-wise mass ratios, and then compared the calculation results with those from other types of animal confinement buildings. Particularly, if the average concentration of an odorant was zero in all other types of animal confinement buildings, this odorant would be taken as a tracer odorant.

Table 5.20 listed parts of identified characteristic odorants or ratios. No tracer odorant was found, indicating the ubiquitous existence of 51 compounds in all types of animal confinement

buildings. No characteristic odorant or ratio was found for TSP or PM₁₀ samples from finishing buildings, or for PM₁₀ samples from manure-belt layer hen buildings.

Table 5.20. Characteristic odorants or ratios for each type of animal confinement buildings.

Animal building type	Size	Fingerprint odorants or ratios	Mean value
Farrowing	TSP	[2-methyl-2-pentenal]/[p-vinylguaiacol]	29.0
	PM ₁₀	[pentanoic acid]/[p-vinylguaiacol]	29.1
Gestation	TSP	m-cresol	25 ng/mg
	PM ₁₀	m-cresol	35 ng/mg
Weaning	TSP	[4-ethylphenol]/[octanoic acid]	1.2
	PM ₁₀	[4-ethylphenol]/[nonanoic acid]	0.21
Finishing	TSP	n/a	n/a
	PM ₁₀	n/a	n/a
Manure-belt layer hen	TSP	[nonanal]/[2-ethyl-1-hexanol]	6.9
	PM ₁₀	n/a	n/a
Tom turkey	TSP	[p-vinylguaiacol]/ [benzoic acid]	1.0
	PM ₁₀	[p-vinylguaiacol]/[p-cresol]	3.2

Previous ANISOM tests revealed that particle samples from finishing and weaning buildings were very similar in odorant composition. A similar observation was made for farrowing and gestation buildings. In reality, finishing and weaning buildings share many similar features, such as feed, animal, ventilation and manure management. There has been a trend to host weaning and finishing stages in a single building. Actually, one of the weaning buildings visited in this study (Site G) was also occasionally used for finishing. The similarity between finishing and weaning buildings may explain why similar odorant compositions were present in these two types of animal confinement buildings. An analogous explanation may apply to the case of farrowing and gestation buildings since they both house mother pigs in small crates. The influence of newborn piglets in farrowing buildings is negligible because of their low body mass and relatively small amount of excrements.

The similarity between weaning and finishing and between farrowing and gestation buildings raised certain difficulties in determining characteristic odorants or ratios for individual types of swine buildings. To address this issue, the visited animal confinement buildings were reclassified into four categories: farrowing-gestation, weaning-finishing, tom turkey and manure-belt layer hen buildings, and furthermore into swine, tom turkey and manure-belt layer hen buildings. The MATLAB calculation results revealed that benzoic acid, phenylacetic acid, phenylpropanoic acid, p-cresol and 3-methylindole (skatole) could be selected as the characteristic particle-borne odorants for swine buildings; while 4-ethylphenol and m-cresol were characteristic for weaning-finishing and farrowing-gestation buildings, respectively.

5.3.3 Variation with season

5.3.3.1 Variation in odorant composition of TSP samples

Table 5.21 summarized the total mass fraction of odorants, the Simpson's diversity index (D), COI_p and COI in different seasons (cold, mild and hot). Both the total mass fraction of odorants and COI_p increased as the weather getting hotter; while the average COI increased as the weather getting colder. Comparatively, no clear variation pattern was found for the Simpson's diversity index (D) either for mass fraction- or for OAV_p-based odorant composition.

A paired t-test was performed to determine the statistical significance of the effect of seasons. Prior to the test, unpaired data was removed; for animal confinement buildings with multiple visits in the same season, the average data were selected for comparison. The test resulted revealed that seasons did not have a significant effect on the total mass fraction of odorants, COI_p and the Simpson's diversity index (D). However, a significant difference in COI was found between hot and cold (p=0.045) and between hot and mild seasons (p=0.007). This could be explained by a significant influence of seasons on TSP mass concentrations, as revealed previously in Chapter three.

Table 5.21. Summary of total mass fraction of odorants, COI_p, COI and the Simpson's diversity index of TSP samples from different seasons.

	Weather	Cold		Mild		Hot	
	Statistic	Mean	SD	Mean	SD	Mean	SD
Mass fraction-based composition	Total mass fraction	0.0211	0.0141	0.0200	0.0131	0.0298	0.0277
	Simpson's index (D)	0.2409	0.1127	0.2338	0.1091	0.2335	0.0833
OAV _p -based composition	COI _p (m ³ /g)	0.0116	0.0069	0.0129	0.0109	0.0136	0.0760
	Simpson's index (D)	0.1528	0.0491	0.1458	0.0604	0.1656	0.0760
	COI	0.0139	0.0069	0.0088	0.0061	0.0046	0.0028

Non-metric MDS (based on the Bray-Curtis dissimilarity index) plots were used to illustrate the variation in odorant composition with season (Figure 5.11). Noticeably, TSP samples from mild seasons (spring and fall) were located between samples from cold and hot seasons, indicating a gradual seasonal change in odorant composition.

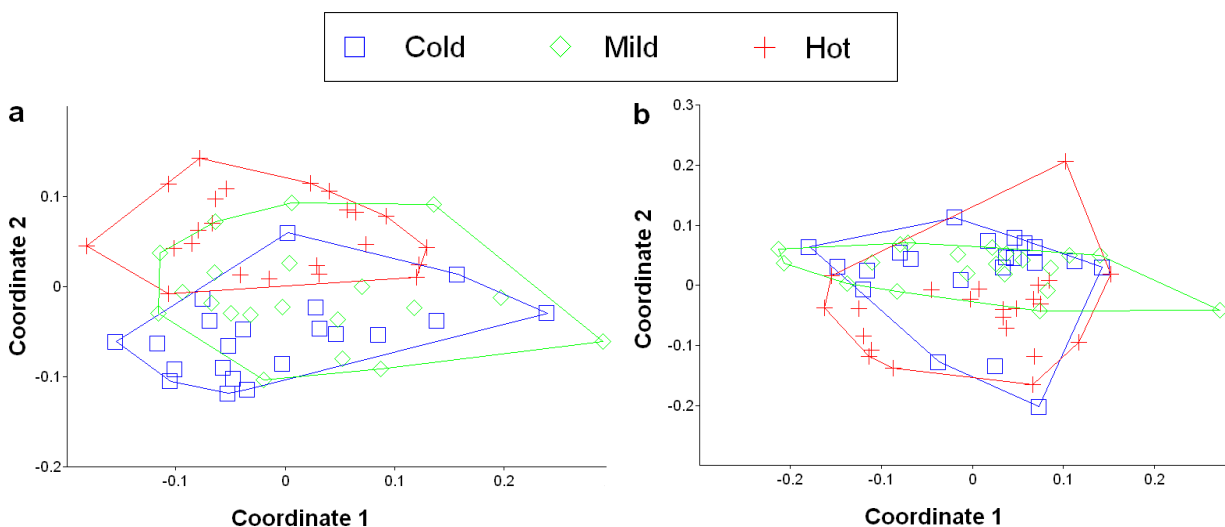


Figure 5.11. Non-metric MDS plot of TSP samples collected in different seasons- (a) mass fraction-based and (b) OVA_P based odorant composition.

The ANOSIM tests (Table 5.22) confirmed the presence of a separation between TSP samples from hot and from cold seasons in terms of mass fraction-based odorant composition. Although such a separation was relatively weak with strong overlapping, it was of statistical significance according to the p value. Comparatively, no noticeable separation ($R > 0.25$) was identified in terms of OVA_P-based odorant composition, suggesting that a seasonal change in TSP-borne odorant composition may be mainly contributed by odorants with light odors.

Table 5.22. Summary of ANOSIM test on TSP samples from different seasons^{a,b}.

Mass fraction-based odorant composition				OAV _P -based odorant composition			
R global=0.178, p<0.001				R global=0.120, p<0.001			
	Cold	Mild	Hot		Cold	Mild	Hot
Cold		0.201	<0.001	Cold		0.519	<0.001
Mild	0.025		0.002	Mild	-0.009		0.001
Hot	*0.333	0.159		Hot	0.197	0.155	

a. In the upright portion of the table are the p values and the R values are listed in the lower left portion.

b. R values are highlighted with ‘*’ if $0.50 \geq R > 0.25$, ‘**’ if $0.75 \geq R > 0.50$ and ‘***’ if $R > 0.75$.

The SIMPER analysis revealed that the difference in mass fraction-based odorant composition between hot and cold seasons was mainly contributed by the higher contents of hexanal, heptanal, nonanal, ethanol, 1-octanol and 2-ethyl-1-hexanol but the lower contents of acetic acid, propanoic acid and 3-methylbutanoic acid in TSP samples from hot seasons. A change in the contents of those odorants in particle samples may be related to variations in bacterial communities with season as recently observed by Nehme et al. (2008) in swine confinement buildings.

5.3.3.2 Variation in odorant composition of PM₁₀ samples.

As shown in Table 5.23, the Simpson's diversity index for mass fraction-based odorant composition increased but COI decreased as the weather getting hotter; while, no obvious seasonal variation was identified in the total mass fraction of odorants, COI_P or the Simpson's diversity index for OVA_P-based odorant composition.

Table 5.23. Summary of total mass fraction of odorants, COI_P, COI and the Simpson's diversity index of PM₁₀ samples from different seasons.

	Weather	Cold		Mild		Hot	
	Statistic	Mean	SD	Mean	SD	Mean	SD
Mass fraction-based composition	Total mass fraction	0.0867	0.1244	0.0584	0.0598	0.0983	0.1045
	Simpson's index (D)	0.2853	0.0902	0.2925	0.0853	0.3567	0.1358
OAV _P -based composition	COI _P (m ³ /g)	0.0249	0.0210	0.0252	0.0358	0.0247	0.0153
	Simpson's index (D)	0.1858	0.0776	0.1493	0.1213	0.1467	0.0622
	COI	0.0139	0.0069	0.0088	0.0061	0.0046	0.0028

The paired t-test results revealed that seasons did have a significant impact on COI (all $p < 0.007$ from pairwise comparison) but did not have a significant effect on others. The elevated level of COI in cold seasons may be related to higher PM₁₀ mass concentrations due to reduced ventilation rates.

Non-metric MDS plots (Figure 5.12) showed that seasons had certain effects on the odorant composition of PM₁₀ samples but the effects were fairly weak, especially on OVA_P-based odorant composition. This observation was confirmed by the following ANOSIM test (Table 5.24). For mass fraction-based odorant composition, a significant separation but with strong overlapping was found between PM₁₀ samples from hot and those from cold seasons; while, similar to the case of TSP samples, for OVA_P-based odorant composition, no noticeable separation ($R > 0.25$) was identified between PM₁₀ samples from different seasons.

The presence of the effect of seasons could also be identified by a comparison of the R values between cold and mild, between mild and hot and between cold and hot seasons (Table 5.22 and 5.24). Noticeably, the R values between cold and hot seasons were unexceptionally higher than those between cold and mild and between mild and hot seasons, suggesting a gradual change in odorant composition in an order from cold, mild to hot seasons.

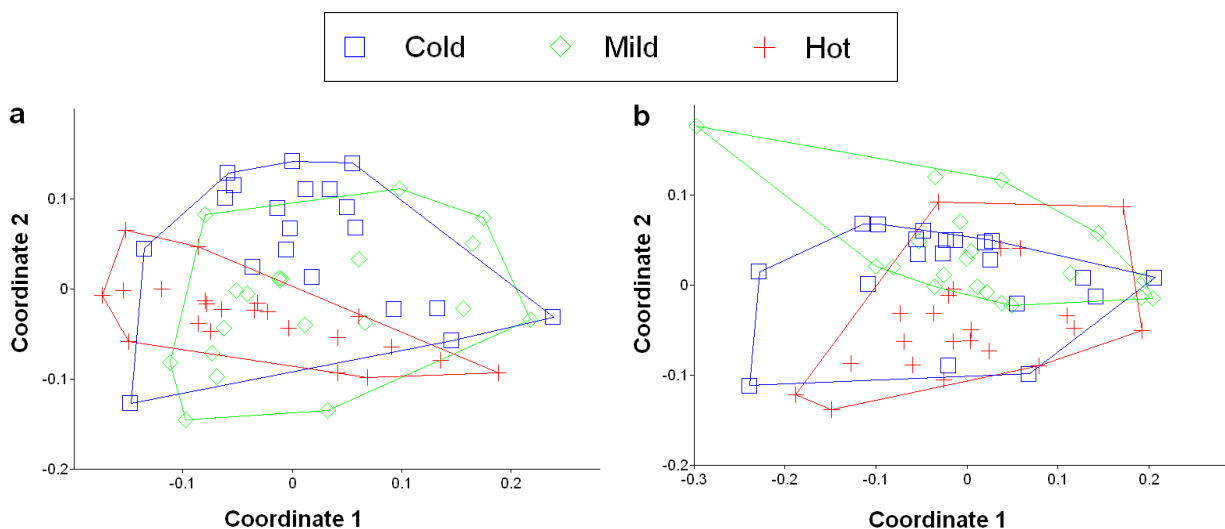


Figure 5.12. Non-metric MDS plot of PM₁₀ samples collected in different seasons- (a) mass fraction-based and (b) OVA_P based odorant composition.

Table 5.24. Summary of ANOSIM test on PM₁₀ samples from different seasons.

Mass fraction-based odorant composition				OAV _P -based odorant composition			
R global=0.171, p<0.001				R global=0.120, p<0.001			
	Cold	Mild	Hot		Cold	Mild	Hot
Cold		0.015	<0.001	Cold		0.179	<0.001
Mild	0.096		0.011	Mild	0.022		0.004
Hot	*0.309	0.096		Hot	0.169	0.116	

a. In the upright portion of the table are the p values and the R values are listed in the lower left portion.

b. R values are highlighted with ‘*’ if 0.50>=R>0.25, ‘***’ if 0.75>=R>0.50 and ‘****’ if R>0.75.

The SIMPER analysis revealed that the difference in mass fraction-based odorant composition between hot and cold seasons was primarily contributed by a decrease in the contents of hexanal, heptanal, octanal, nonanal, 1-octanol, nonanoic acid and dodecanoic acid and an increase in the contents of propanoic acid, 2,2-dimethyl-propanoic acid and 3-methylbutanoic acid in PM₁₀ samples collected in cold seasons. By combining them with the corresponding results for TSP samples, we found that in general particle samples from hot seasons had fewer contents of short-chain fatty acids but higher contents of aldehydes, short-chain alcohols and long-chain fatty acids.

5.3.4 Difference between TSP, PM₁₀ and feed samples

5.3.4.1 Difference in total mass fraction of odorants, COI_P, COI and Simpson’s diversity index

As shown in Table 5.25, the total mass fraction of odorants and COI_P were highest in PM₁₀ samples and lowest in feed samples. Feed samples had the highest Simpson’s diversity index for both mass fraction- and OAV_P-based compositions. The mean COI was higher for TSP samples

than for PM₁₀ samples, which is reasonable since PM₁₀ is only a subfraction (fine particle fraction) of TSP.

Table 5.25. Summary of total mass fraction of odorants, Simpson’s diversity index, COI_P and COI for TSP, PM₁₀ and feed samples.

	Statistics	TSP		PM ₁₀		Feed	
		Mean	SD	Mean	SD	Mean	SD
Mass fraction-based composition	Total mass fraction	0.0239	0.0201	0.0817	0.0999	0.0046	0.0020
	Simpson’s index (D)	0.2360	0.1003	0.3130	0.1109	0.3560	0.1008
OAV _P -based composition	COI _P (m ³ /g)	0.0127	0.0083	0.0249	0.0249	0.0020	0.0009
	Simpson’s index (D)	0.1552	0.0629	0.1672	0.0901	0.2553	0.0731
	COI	0.0193	0.0164	0.0091	0.0066	-	-

The significance of observed differences between TSP, PM₁₀ and feed samples was examined by one-way ANOVA test. Prior to the test, the original data, with a poor normality, were log transformed. The ANOVA test results revealed that the mean total mass fraction of identified odorants and mean COI_P were both significantly higher for PM₁₀ samples than for TSP samples (both p<0.001), and again significantly higher for TSP samples than for feed samples (both p<0.001) (Figure 5.13a and 5.13c). This indicates that PM₁₀ samples are averagely more odorous than TSP and feed samples at the same mass or mass concentrations. For mass fraction-based odorant composition, the mean Simpson’s diversity index was significantly higher for PM₁₀ and feed samples than for TSP samples (both p<0.001); while no significant difference was found between PM₁₀ and feed samples (Figure 5.13b). This result implies that the mass of identified odorants are more evenly distributed in TSP samples. For OAV_P-based odorant composition, the mean Simpson’s diversity index was significantly higher in feed samples than in TSP and PM₁₀ samples (both p<0.001) (Figure 5.13d), suggesting that the odors of feed samples are more predominantly contributed by a few odorants. The ANOVA test also revealed a significantly higher COI (mean value) for TSP samples than for PM₁₀ samples (p<0.001).

We calculated the ratio of COI_P for PM₁₀ sample to that for TSP sample (COI_{P-PM10}/COI_{P-TSP}) from the same visit (Table 5.26), and examined potential changes in this ratio with animal building type and season. PM₁₀ samples were found to have averagely 1.73 times higher COI_P’s than TSP samples and this ratio varied with animal building type and season. However, no significant difference was found from the one-way ANOVA test. A similar ratio (COI_{PM10}/COI_{TSP}) was calculated for COI (Table 5.26) and the results showed that particles smaller than 10 μm (PM₁₀) may contribute around half of the odor strength of TSP samples. This

ratio also varied with animal building type and season; however, similar to the case of COI_P , PM_{10}/COI_{P-TSP} , no significant difference was identified from statistical analysis.

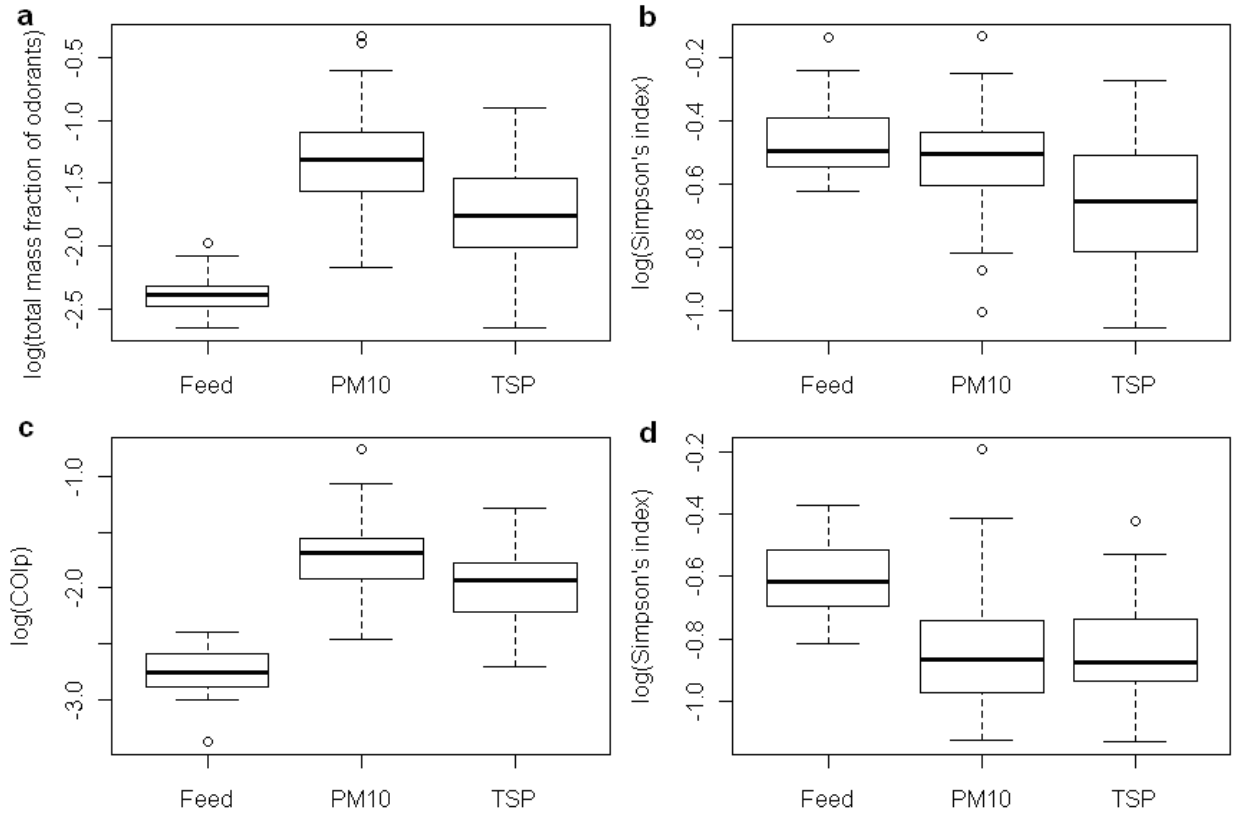


Figure 5.13. Comparison among TSP, PM_{10} and feed samples in terms of (a) total mass fraction of identified odorants, (b) Simpson's index for mass fraction-based odorant composition, (c) COI_P , and (d) Simpson's index for OAV_P -based odorant composition.

Table 5.26. A comparison of COI and COI_P between TSP and PM_{10} samples- effects of animal building type and season.

PM ₁₀ vs. TSP; effect of season							
Ratio of	Statistic	Overall	Cold	Mild	Hot		
COI_P	Mean	1.728	1.611	1.708	1.860		
	SD	0.776	0.581	0.828	0.896		
COI	Mean	0.478	0.519	0.469	0.446		
	SD	0.214	0.209	0.253	0.176		
PM ₁₀ vs. TSP; effect of animal building type							
Ratio of	Statistic	Farrowing	Gestation	Weaning	Finishing	Layer hen	Tom turkey
COI_P	Mean	1.727	1.931	1.194	1.793	1.777	1.858
	SD	0.848	0.814	0.543	0.751	0.897	0.768
COI	Mean	0.544	0.530	0.297	0.441	0.514	0.541
	SD	0.159	0.181	0.164	0.254	0.265	0.197

We also compared the ratio of COI_P to the total mass fraction of odorants used for COI_P calculation, and found that this ratio was significantly higher for TSP samples than for PM_{10}

samples ($p < 0.001$). This suggests that although TSP samples had lower odorant contents, the odorant part in TSP samples may contain more (in terms of relative abundance) strong odorants.

5.3.4.2 Difference in odorant composition

The non-metric MDS analysis revealed a noticeable difference between TSP, PM₁₀ and feed samples in both mass fraction- and OAV_p-based odorant compositions (Figure 5.14a and 5.14c). PM₁₀ samples were more separated from feed samples than TSP samples. Such a difference may be explained by a difference in the absolute abundance of identified odorants. As an indicator of absolute abundance, the total mass fraction of identified odorants differed greatly between TSP, PM₁₀ and feed samples (Table 5.25).

To examine a variation in the relative abundance of identified odorants, a correlation distance-based PCoA was applied. The results showed that in terms of mass fraction-based odorant composition, there was no significant difference between TSP, PM₁₀ and feed samples (Figure 5.14b); while in terms of OAV_p-based odorant composition, a certain difference was present between feed and TSP/ PM₁₀ samples (Figure 5.14d). Remind that a Pearson's correlation coefficient between two arrays (X and Y) was relatively sensitive to the edge points of (x, y) that in this case were corresponding to the most abundant and the least abundant odorants; while, the abundances of the least abundant odorants were often close or equal to zero. Accordingly, the distance between two samples on the correlation distance-based PCoA plot was greatly affected by the most abundant odorants; herein, the abundance of an odorant was measured by its mass fraction or OVA_p. Therefore, a comparison of Figure 5.14b to 5.14c actually showed that the relative abundances of the most mass-contributing odorants were similar between TSP, PM₁₀ and feed samples; however, the relative abundances of the most odor-contributing odorants were somehow different between feed and TSP/ PM₁₀ samples. The subsequent ANOSIM test also confirmed these observations (Table 5.27).

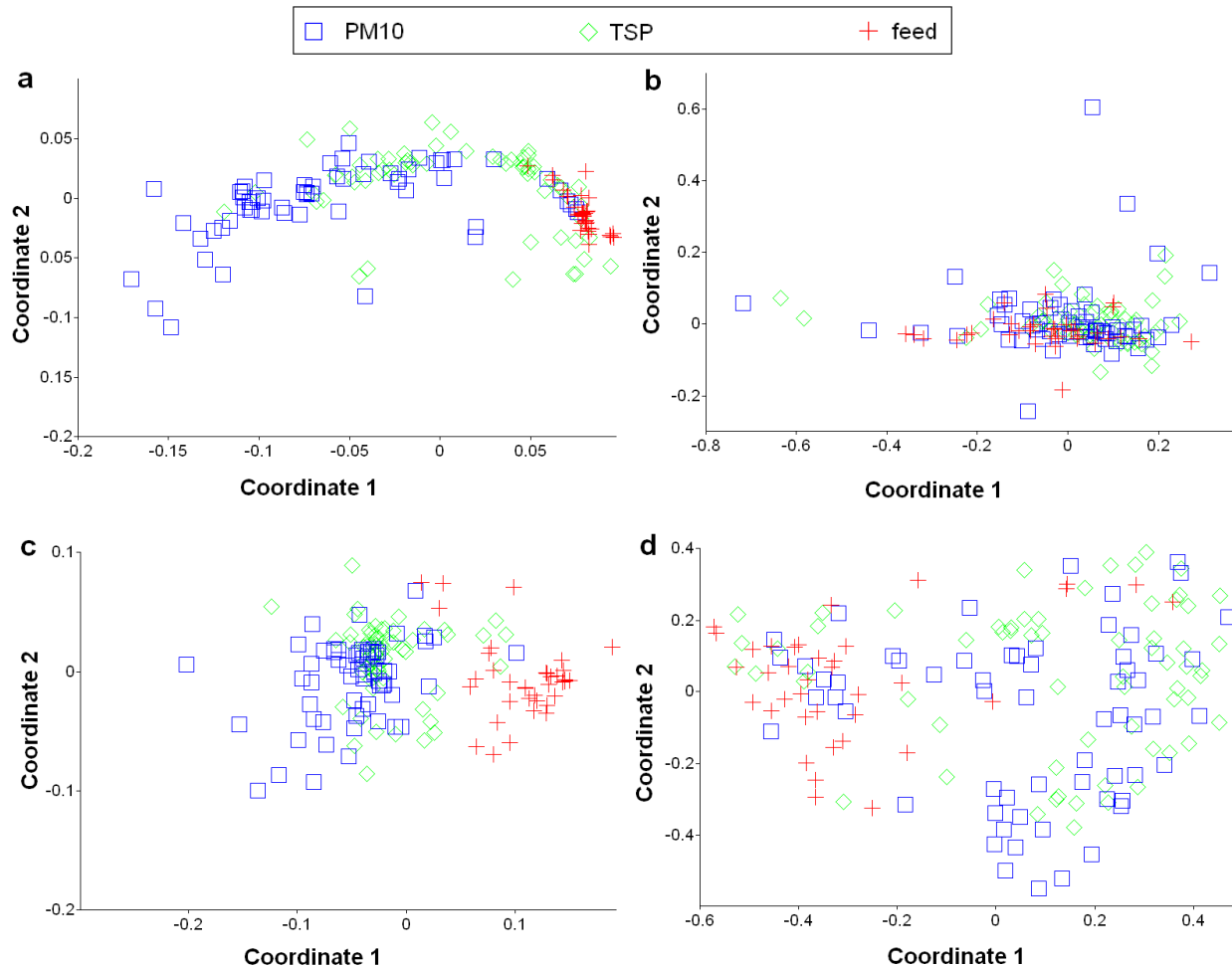


Figure 5.14. Bray-Curtis dissimilarity-based non-metric MDS and correlation distance-based PCoA plots of TSP, PM₁₀ and feed samples- (a) Non-metric MDS plot based on mass fraction of odorants, (b) PCoA plot based on mass fraction of odorants, (c) Non-metric MDS plot based on OAV_P of odorants; (d) PCoA plot based on OAV_P of odorants.

Table 5.27. Summary of ANOSIM tests on TSP, PM₁₀ and feed samples^a.

Bray-Curtis dissimilarity, mass fraction of odorants (R global=0.417, p<0.001)				Correlation coefficient, mass fraction of odorants (R global=0.036, p=0.028)			
	TSP	PM ₁₀	Feed		TSP	PM ₁₀	Feed
TSP		<0.001	<0.001	TSP		0.024	0.023
PM ₁₀	0.177		<0.001	PM ₁₀	0.020		0.318
Feed	*0.458	**0.738		Feed	0.082	0.013	
Bray-Curtis dissimilarity, OAV _P of odorants (R global=0.447, p<0.001)				Correlation coefficient, OAV _P of odorants (R global=0.166, p<0.001)			
	TSP	PM ₁₀	Feed		TSP	PM ₁₀	Feed
TSP		<0.001	<0.001	TSP		0.025	<0.001
PM ₁₀	0.074		<0.001	PM ₁₀	0.028		<0.001
Feed	**0.692	***0.783		Feed	*0.310	0.225	

a. In the upright portion of the table are the p values and the R values are listed in the lower left portion.

b. R values are highlighted with ‘*’ if 0.50>=R>0.25, ‘**’ if 0.75>=R>0.50 and ‘***’ if R>0.75.

An issue associated with discussions in the previous paragraph is that they failed to consider the potential interference of animal building type. For example, TSP samples from tom turkey buildings might be overlapped with feed samples from swine buildings, thereby leading to a poor separation of TSP from feed samples. To address this issue, we further investigated differences between TSP, PM₁₀ and feed samples from the same type of animal confinement buildings. The non-metric MDS and the following ANOSIM test showed that, in terms of both mass fraction- and OAV_P-based odorant compositions, a noticeable separation ($R > 0.25$) was present between feed and TSP/ PM₁₀ samples for all types of animal confinement buildings, and overall PM₁₀ samples were more separated from feed samples than TSP samples (data not shown here). The PCoA analysis and the subsequent ANOSIM test revealed that, in terms of mass fraction-based odorant composition, a noticeable separation ($R > 0.25$) between feed and TSP/ PM₁₀ samples was present for farrowing, weaning and finishing buildings; while, in terms of OAV_P-based odorant composition, a noticeable separation ($R > 0.25$) between feed and TSP/ PM₁₀ samples was found for farrowing, gestation, finishing and manure-belt layer hen buildings; however, in all cases, no significant difference was observed between TSP and PM₁₀ samples (data not shown here).

In this study, feed samples were collected from feed bins or hoppers. However, a contamination by odorants from other sources may be inevitable because of the adsorption of odorants on the surface of feed particles. Some malodorous odorants, such as *p*-cresol and indole, were detected in feed samples; however, they were unlikely originate from feed materials but from anaerobic degradation of organic substrates by bacteria in gastrointestinal tracts and/or manure pits (Mackie et al., 1998). In fact, even if those odorants were included in comparison, a significant difference between feed and TSP/ PM₁₀ samples would still be identified. This implies that particle-borne odorants may primarily originate from sources other than feed. Such a conclusion is also suggested by a previous observation that the total mass fractions of identified odorants were much higher in TSP and PM₁₀ samples than in feed samples (Table 5.25).

Although the absolute abundance (mass fraction) of odorants differed greatly (Table 5.4), the relative abundance of odorants was similar between TSP and PM₁₀ samples. This finding seemed to somehow contradict with that the odorant part in TSP samples contained more (in terms of relative abundance) strong odorants. Such a ‘contradiction’ might be resulted from different statistical methods applied.

The SIMPER test was performed. However, because of a significant difference in terms of the absolute abundance of odorants between TSP, PM₁₀ and feed samples, almost all identified odorants were averagely at least two times more concentrated in PM₁₀ samples than in TSP samples, and again at least two times more concentrated in TSP samples than in feed samples. For obvious reasons, these odorants should not be selected as the characteristic odorants. To surmount this difficulty, we switched our targets to odorant ratios since they only relied on the relative abundance of odorants. A MATLAB program was developed, which basically follows the same criteria, algorithms and procedures as mentioned in Section 5.3.2.6. The calculation results revealed that [hexanal]/ [2-ethyl-hexanoic acid] could be selected as a characteristic ratio for TSP samples. Although no characteristic ratios were identified for PM₁₀ and feed samples, a ratio of [p-cresol]/[2-methyl-2-pentenal] could be used to distinguish feed samples (much lower) from TSP and PM₁₀ samples (much higher).

5.3.4.3 Correlation between the variation of PM₁₀ samples and that of TSP samples

It was found from previous sections that the odorant composition of TSP and PM₁₀ samples varied with animal building type and, to a less degree, with season. Here a question is- Do TSP and PM₁₀ samples vary in a similar pattern? Reminding that the variation of TSP or PM₁₀ samples was mathematically described by a distance matrix where the distance was either the Bray-Curtis dissimilarity index or correlation distance between samples, this question therefore could be simplified as the degree of correlation between the distance matrix for TSP and that for PM₁₀ samples. The evaluation was done using a Mantel test.

We only compared the matrices made of the Bray-Curtis dissimilarity index. The test results showed that for mass fraction-based odorant composition, a weak but significant correlation existed between TSP and PM₁₀ samples ($r=0.373$, $p<0.001$); for OAV_P-based odorant composition, a still weak but slightly stronger correlation was identified ($r=0.457$, $p<0.001$). Considering that PM₁₀ is a subfraction of TSP, it is not surprising to find a correlation between TSP and PM₁₀ samples.

5.3.5 Correlation between compounds- implication to origins of odorants

In general, if the variations of two odorants are strongly correlated, they will likely originate from similar sources or metabolic pathways. Therefore, it was expected that a correlation

distance-based PCoA analysis would offer certain clues for determination of the sources of individual odorants.

Two PCoA plots were derived: one for TSP and one for PM₁₀ samples (Figure 5.15). It can be seen that all identified odorants, except for nitrogen-containing compounds, were clustered according to their chemical categories. Alcohols and aldehydes/ ketones were closely clustered, suggesting their similar origins. According to Spoelstra (1980), they may be produced from bacterial conversion of simple carbohydrates. Phenols were fairly closely clustered on this plot. Most of them, including phenol, o-cresol, p-cresol, m-cresol, 4-ethylphenol and p-vinylguaiacol, were considered to have similar biological origins, e.g., bacterial degradation of tyrosine (Mackie et al., 1998; Spoelstra, 1980). Comparatively, acids have relatively diverse biological origins, which, however, could be roughly classified into two major categories: deamination of amino acids and bacterial conversion of structure carbohydrates. Correspondingly, a relatively large variation was observed within the category of acids on the PCoA plot. A particularly interesting observation was made for phenylpropanoic acid, phenylacetic acid, and benzoic acid. The first one was considered to be produced from anaerobic reductive degradation of phenylalanine; while the last two was believed to originate from anaerobic oxidative degradation of phenylalanine. On the PCoA plot, benzoic acid and phenylacetic acid were positioned closest to each other; while phenylpropanoic acid was somehow separated from those two odorants, probably due to a difference in metabolic pathways. This is a good example showing that the correlation distance-based PCoA plot can be a useful assisting tool in determining the potential origins of odorants or other pollutants.

Because only limited information is available on the origins of odorants, no further discussions were carried out with the PCoA plot. However, it should be noted that the PCoA plot may oversimplify relationships between odorants, e.g., competition, inhibition and substrate/ products, and fail to consider possible changes in odorant composition during a series of physical, chemical and biological processes (e.g., evaporation of odorants during transport). Therefore, PCoA plots should only be used as a supporting tool.

A Mantel test was performed to determine whether the clustering of odorants in TSP samples was similar to that in PM₁₀ samples. The test results revealed a significant correlation ($r=0.529$, $p<0.001$). The similar pattern between TSP and PM₁₀ samples suggests that the

clustering of odorants according to their chemical categories and possible origins is not likely accidental but deterministic.

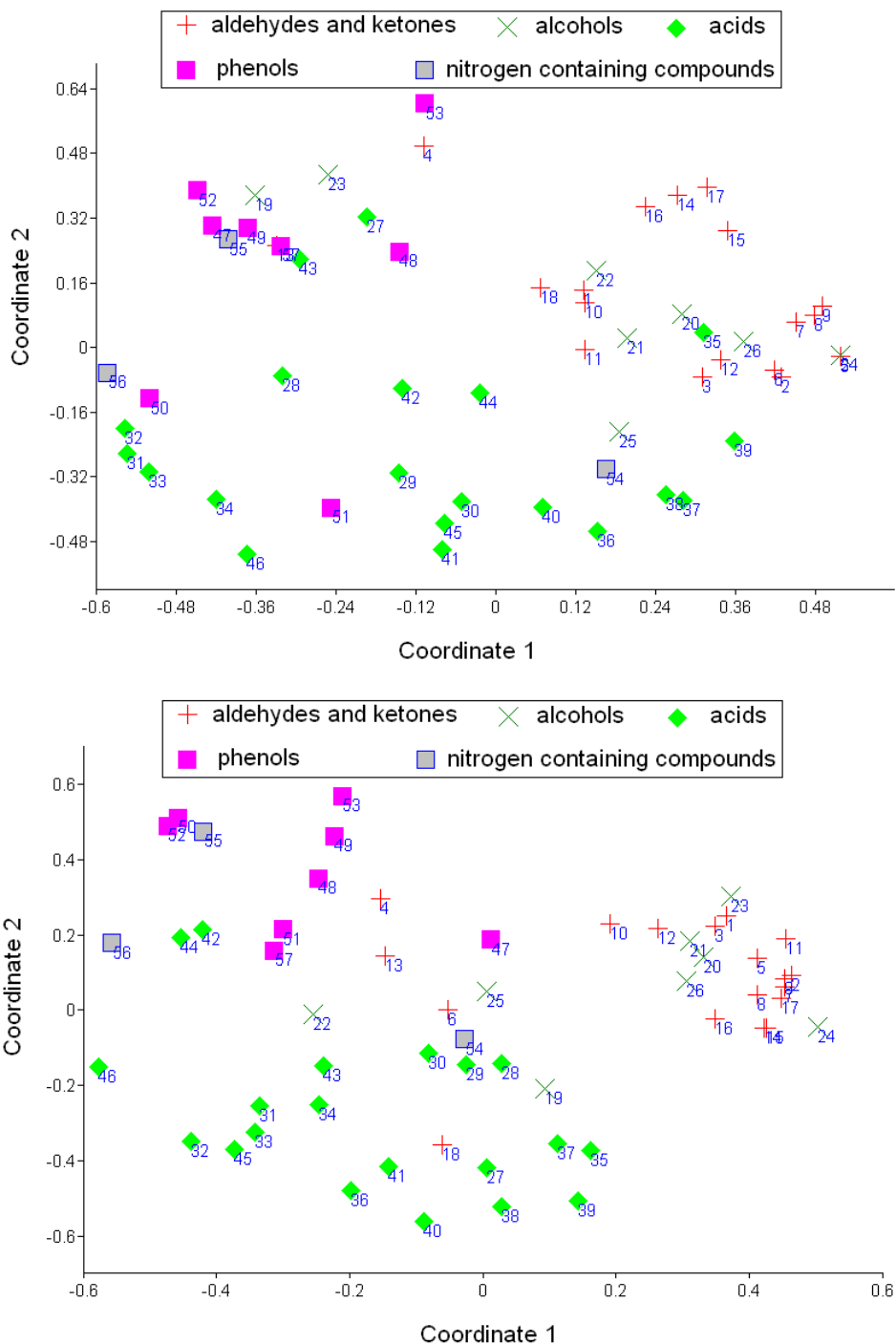


Figure 5.15. PCoA plots of identified odorants in (a) TSP and (b) PM₁₀ samples.

5.3.6 Comparison with odorants in gas phase.

In this study, we did not simultaneously measure the concentration of odorants in the gas phase. Consequently, there was no direct comparison between particle-borne and gas-phase odorants. All the quantitative data of the gas-phase odorants were cited from previous studies conducted by other researchers, as briefly summarized in Table 5.28. It can be seen that particle-borne odorants actually occur at much lower concentrations than those in the gas-phase. A similar observation was made by Hammond (1981) who reported that the concentrations of p-cresol and butanoic acid in the gas phase were four to five times higher than those on particles. Accordingly, it is unlikely that particles can be a major carrier of odors from animal facilities; instead, the majority of odorants may exist in the gas phase. However, this does exclude a possibility that some non-volatile odorants may occur at higher concentrations in the particle phase than in the gas phase. In addition, because of the adhesion and accumulation of particles on the surface of objects, particles may play a different but important role in propagating odors into neighboring communities. An investigation of particle-borne odors, therefore, would be still of great importance and interest, especially for studying the transport of odors in environments.

Table 5.28. An incomplete comparison of odorant concentrations in gas and particle phase.

Item to be compared	Concentration in particle phase-this study	Concentration in gas phase	Building type	Reference and notes
Total identified odorants	TSP: 0.005~0.069mg/m ³ ; mean- 0.028 mg/m ³ PM ₁₀ : 0.003~0.046 mg/m ³ ; mean- 0.019 mg/m ³	0.60 mg/m ³	swine	Schiffman et al. (2001)
		11.72 mg/m ³	swine	Hartung and Phillips (1994); including CH ₄ , H ₂ S, NH ₃ and methylamines
		2.52 mg/m ³	swine finishing	Chmielowiec-Korzeniowska (2009); including sulfur containing compounds
Propanoic acid	TSP: 0.075~17.9 µg/m ³ ; mean- 1.38 µg/m ³ PM ₁₀ : 0.043~10.9 µg/m ³ ; mean- 0.84 µg/m ³	43.7 µg/m ³	broiler	Trabue et al. (2010)
		91.0 µg/m ³	swine farrowing	Cai et al. (2010)
Indole	TSP: 0.001~0.131 µg/m ³ ; mean- 0.020 µg/m ³ PM ₁₀ : 0.~0.037 µg/m ³ ; mean- 0.006 µg/m ³	18.8 µg/m ³	broiler	Trabue et al. (2010)
		35.7 µg/m ³	swine finishing	Chmielowiec-Korzeniowska (2009)
		1.18 µg/m ³	swine farrowing	Cai et al. (2010)

5.3.7 Potential issues and limitations associated with this study

5.3.7.1 Applicability of odor thresholds in air to particles

In this study, the OVA and OVA_P of an odorant were calculated by normalizing the concentration/ mass fraction of the odorant with its odor thresholds in air. However, the

applicability of odor thresholds in air to particles is questionable. The perception of particle-borne odors by human may occur mainly through two ways.

First, volatile and semi-volatile odorants are released from particles (desorption or evaporation, depending on the state of particles- solid or liquid), transported in the air (dispersion), and then inhaled and detected by human nose. In this case, the concentration of an odorant in air would be greatly dependent on the gas/ particle partitioning coefficient (K_p) of this compound, where K_p refers to the ratio of the mass concentration of a compound in the gas phase to that in particles. Some particle-borne odorants, although with very low odor thresholds in air, may become less significant in terms of odor nuisance because of their low K_p values. An analogous example was given in Table 5.29. Butanoic acid is believed to be much more odorous than hexanal in air; however, hexanal actually has a lower odor threshold than butanoic acid when dissolved in water, because of its relatively high Henry's law constant ($K_{H,cp}$: hexanal- 0.526 kg-bar/mol vs. butanoic acid- 0.0005 kg-bar/mol) (NIST, 2010). Therefore, the odor threshold in air may not correctly reflect the odor potency of particle-borne odorants.

Table 5.29. Comparison of odor thresholds of several compounds in air and in water^a.

Odorous compound	In air (ppm)	in water (ppb)
Phenol	0.11	5900
Hexanal	0.0138	4.5-5
Butanoic acid	0.00389	240
Indole	0.0000316	140

a. Compiled from van Germert and Nettenbreijer (1977) and Devos et al. (1990)

Second, particles were inhaled, retained in human nose and then detected by olfactory cells. In this case, the odorants carried on particles may undergo substantially different diffusion, inception and detection processes than gas-phase odors. Accordingly, human's sensory thresholds of particle-borne odors and gas-phase odors could be significantly different. Regretfully, by far there are few studies on the odor threshold of particle-borne odorants. Moreover, the odor threshold of a compound on particles may be closely related to the physical characteristics and chemical composition of particles, thus creating an additional difficulty.

5.3.7.2 Nonlinearity of odor perception

The calculation of OVA and OVA_p is based on an assumption that the odor intensity of an odorant sensed by humans is linearly proportional to its concentration. However, this is not correct (Rosen et al., 1962); rather, the intensity of odor sensation versus the concentration of

odorants follows a nonlinear psychophysical law (e.g. the Weber-Fechner law). Therefore, the calculated OVA and OVA_P cannot properly represent the odor intensity perceived by humans.

Nonlinear relationships, such as subtraction, addition and synergism, also occur for mixed odorants (Rosen et al., 1962). This can be another major reason why there exists a poor correlation between the olfactory odor intensity and the odorant concentrations quantified by GC/MS (Zahn et al., 2001; Zhang et al., 2010). In this study, the calculation of COI and COI_P assumed no interactions between different odorants and, thereby, may greatly misrepresent the real odor intensity. However, the use of COI and COI_P enables a convenient comparison between different odor pollution scenarios. In this regard, previous discussions based on COI and COI_P would still be valuable and informative.

5.3.7.3 Positive and negative sampling artifacts

In this study, we assumed that there were no sampling artifacts associated with particle-borne odorants. However, both positive and negative artifacts may exist. The occurrence of positive artifacts might be caused by the adsorption of gas-phase odorants on glass fiber filters, thereby leading to an overestimation of the mass of particle-borne odorants. The influence of positive artifacts can be greater on PM₁₀ samples than TSP samples, as suggested by Equation 5.10 (Mader and Pankow, 2001).

$$\frac{c_{p,\text{meas}}}{c_p} = \left(1 + \frac{V_{\text{min},f}}{K_p \times \text{PM} \times V} \right) \quad (5.10)$$

Where, $c_{p,\text{meas}}$ is the measured concentration of a particle-borne odorants, c_p is the true concentration of this particle-borne odorant, $V_{\text{min},f}$ is the minimum volume of air required to saturate the adsorption of this odorant on filters, K_p is the gas/ particle partitioning coefficient, PM is the concentration of particles, and V is the volume of sampled air. Because the concentration of TSP is always greater than that of PM₁₀, the measurement error induced by positive sampling artifact is smaller for TSP. A mathematical discussion on potential positive artifacts was not conducted due to lack of essential K_p and $V_{\text{min},f}$ data.

Certain protocols were developed to determine whether positive artifacts occurred. For example, if an odorant was not detected in a PM₁₀ sample but detected in the corresponding TSP

sample, this odorant was considered to be exempt from positive artifacts, as illustrated in Equation (5.11).

$$\begin{aligned}c_{PM_{10},meas} &= c_{PM_{10}} + c_{f,PM_{10}} \\c_{TSP,meas} &= c_{TSP} + c_{f,TSP}\end{aligned}\tag{5.11}$$

Where, $c_{PM_{10},meas}$ is the measured concentration of an odorant in a PM_{10} sample, $c_{PM_{10}}$ is the true concentration of this odorant in the PM_{10} sample, $c_{f,PM_{10}}$ is the concentration of the odorant adsorbed on PM_{10} filter, $c_{TSP,meas}$ is the measured concentration of the odorant in a TSP sample, c_{TSP} is the true concentration in the TSP sample, and $c_{f,TSP}$ is the concentration of the odorant adsorbed on TSP filter. Because the volume of sampled air was equal for TSP and PM_{10} sample collection, $c_{f,PM_{10}}$ were equal to $c_{f,TSP}$. Accordingly, if $c_{PM_{10},meas}=0$, then $c_{f,TSP}=c_{f,TSP}=0$, indicating there are no positive artifacts. Through this approach, a total of 34 odorants were found to be likely exempt from positive artifacts. However, for the rest of odorants, the presence of positive artifacts was suggested from a comparison of the odorant concentration in PM_{10} to that in TSP samples (details not shown here). In summary, positive artifacts can be a great issue associated with quantitative analysis of particle-borne odorants. In some early works (Day et al., 1965; Hammond et al., 1979), particles were considered to a major carrier of odors based on an experimental observation that removal of particles with filters greatly reduced the odor intensity. However, a decrease in odors could be contributed by an adsorption of gas-phase odorants on filters. An accurate assessment of particle-borne odors would require an improved experiment design to minimize the interference from positive artifacts.

A possible solution is to use Teflon filters, which are generally considered to adsorb less VOC's than glass fiber and quartz fiber filters (Turpin et al., 1994). However, under high humidity conditions (e.g., in animal confinement buildings), the VOC's adsorption capacity of Teflon filters could be comparable to that of quartz fiber filters (Mader and Pankow, 2001). Because of the high concentrations of gas-phase organic compounds in animal confinement buildings, using Teflon filters alone may not be sufficient to overcome positive sampling artifacts. The use of denuder may be necessary to pre-remove gas-phase organic compounds from the airstream. However, the availability of appropriate solvents and the limited capacity of denuder can be major challenges, because of the great diversity and high concentrations of gas-phase odorants in animal confinement buildings.

Negative sampling artifacts were induced by the evaporation of particle-borne odorants after collected on filters. There was no solid evidence to support the occurrence of negative artifacts. However, the strong odors of collected particles could be sensed even in animal confinement buildings, indicating an undergoing evaporation of particle-borne odorants driven by the gas/particle partitioning equilibrium. To eliminate the potential influence of negative artifacts, a sampling setup shown in Figure 5.16 was recommended. Briefly, a denuder is used to remove odorants in the gas-phase so as to minimize potential positive artifacts; next, particles were collected on a Teflon filter; the evaporated odorants were then collected onto a quartz fiber filter (back filter). The concentration of odorants in the gas phase can be determined with the denuder extract; while particle-borne odorants can be quantified by combining the odorants in particles with those on the back filter.

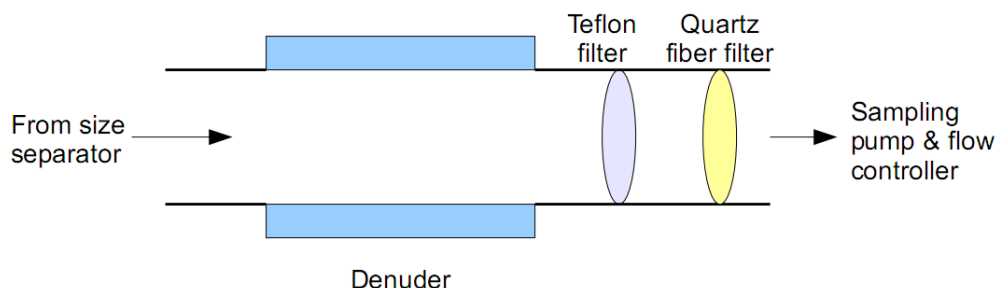


Figure 5.16. Proposed sample setup for collection of particle-borne odors

It was speculated that the sampling artifacts of gas-phase odorants using canisters or adsorption tubes may be relatively insignificant in animal confinement buildings because the odorant concentrations on particles are generally much lower than those in the gas phase.

5.4 Chapter Summary and Conclusions

5.4.1 Summary of observations

Particles were considered to a major carrier of odors from animal confinement buildings. Over 300 odorants have been identified in particle samples. However, previous studies produced only limited quantitative data and omitted to consider potential variations with animal building type, season and particle size. The overall goal of this chapter is to address these current limitations. In this chapter, TSP, PM₁₀ and feed samples were collected from eighteen animal confinement buildings. A total of 57 odorants were identified and quantified with GC/MS. These compounds belong to five chemical categories: aldehydes and ketones (carbonyls), alcohols,

acids, phenols and nitrogen-containing compounds. The main research objectives were: (1) to determine the most abundant and most odor-contributing odorants; (2) to develop a comprehensive odor intensity index for particle-borne odors; (3) to examine variations in odorant composition with animal building type, season and particle size. The following observations were derived from this chapter:

- Two new odorants were identified- (E,Z)-2,6,-nonadienal and trans-4,5-epoxy-(E)-2-decenal. No propanol, butanol, butanal or pentanal was detected. Most identified odorants are VOC's with a boiling point less than 250°C. The odor thresholds of identified odorants ranged from a few ng/m³ to tens of mg/m³.
- A total of 22 odorants existed in all TSP and PM₁₀ samples; while some odorants had a very low occurrence frequency. Odorants in feed samples were less diverse. The total mass fraction of identified odorants was 2.4±2.0% in TSP, 8.2±10.0% in PM₁₀ and 0.46±0.20% in feed samples. Due to the high content of VOC's, TEOM may significantly underestimate PM₁₀ mass concentrations.
- Acetic acid and ethanol were the most abundant odorants in particle and feed samples. However, both odorants are only lightly odorous. Other abundant odorants included propanoic acid, 2-methylpropanoic acid, 2,2-dimethyl-propanoic acid, dodecanoic acid and 2-ethyl-1-hexanol.
- Phenylacetic acid and (E,E)-2,4-decadienal were two of the most odor-contributing odorants. Other top odor-contributors included indole, dodecanoic acid, acetic acid and undecanoic acid. Skatole and phenol were of less importance than previously considered in literature.
- The total mass fraction of identified odorants was lowest in TSP samples from tom turkey buildings and 2nd lowest in TSP samples from manure-belt layer hen buildings. TSP samples from tom turkey buildings had the lowest COI_p, followed by those from manure-belt layer hen buildings. However, TSP samples from tom turkey buildings had relatively high COI because of high TSP mass concentrations.
- For TSP samples, a great similarity in terms of odorant composition was present between farrowing and gestation, and between weaning and finishing buildings; while, a clear

difference ($R>0.5$) was found between manure-belt layer hen and farrowing/ gestation/ weaning, and between tom turkey and all other types of animal confinement buildings. Variations in mass fraction-based odorant composition with animal building type were mainly contributed by the contents of ethanol, 2-ethyl-1-hexanol, acetic acid, propanoic acid, 3-methylbutanoic acid, 2,2-dimethyl-propanoic acid, nonanoic acid, dodecanoic acid, undecanoic acid, tridecanoic acid, benzoic acid, phenylacetic acid, p-cresol, hexanal and nonanal. Variations in OAV_p-based odorant composition were mainly contributed by the contents of acetic acid, propanoic acid, butanoic acid, 3-methylbutanoic acid, undecanoic acid, dodecanoic acid, phenylacetic acid, (E,E)-2,4-decadienal, (E,E)-2,4-nonadienal, (E)-2-nonenal, indole and p-cresol.

- The total mass fraction of identified compounds was lowest in PM₁₀ samples from tom turkey buildings. PM₁₀ samples from tom turkey buildings also had the lowest COI_p. No significant difference in COI was observed among different animal building types.
- PM₁₀ samples from different types of animal confinement buildings were more similar in odorant composition than TSP samples. In terms of mass fraction-based odorant composition, a clear difference ($R>0.5$) existed between farrowing/ gestation and tom turkey buildings; while, in terms of OAV_p-based odorant composition, a clear difference ($R>0.5$) was present between tom turkey and all four types of swine buildings. Variations in mass fraction-based odorant composition were mainly contributed by the contents of ethanol, 2-ethyl-1-hexanol, acetic acid, propanoic acid, 2-methylpropanoic acid, 2,2-dimethyl-propanoic acid, dodecanoic acid, tridecanoic acid, benzoic acid and phenylacetic acid. Variations in OAV_p-based odorant composition were primarily contributed by the contents of acetic acid, propanoic acid, 2-methylpropanoic acid, 3-methylbutanoic acid, undecanoic acid, dodecanoic acid, phenylacetic acid, (E,E)-2,4-decadienal, (E)-2-nonenal, nonanal, indole and p-cresol.
- A correlation distance-based PCoA was used to examine differences in the relative abundance of identified odorants. The results indicated a weak but significant variation with animal building type. The biggest difference was found between farrowing/gestation and turkey buildings. PM₁₀ samples from different types of animal confinement buildings

were more similar than TSP samples. Because of a great similarity among different types of swine buildings, it would be difficult to distinguish them in receptor modeling.

- Characteristic odorants or odorant ratios were identified. Benzoic acid, phenylacetic acid, phenylpropanoic acid, p-cresol and 3-methylindole were found to be characteristic for swine buildings; while 4-ethyl-phenol and m-cresol were characteristic for weaning/ finishing and farrowing/ gestation buildings, respectively.
- Seasons did not have a significant effect on the total mass fraction of identified odorants, COI_p and the Simpson's diversity index for either TSP or PM₁₀ samples. However, significantly higher COI values were observed in cold than in hot seasons because of elevated particle concentrations.
- There was a gradual change in odorant composition from hot to mild to cold seasons. Generally, particle samples from hot seasons had fewer contents of shorn-chain fatty acids but greater contents of aldehydes, short-chain alcohols and long-chain fatty acids.
- Compared to TSP and PM₁₀ samples, feed samples were lower in the total mass fraction of identified odorants and COI_p. A clear difference ($R > 0.5$) in odorant composition existed between feed and TSP/ PM₁₀ samples; while TSP and PM₁₀ samples were relatively similar in terms of odorant composition.
- Both the total mass fraction of identified odorants and COI_p were higher for PM₁₀ samples than for TSP samples. Based on the ratio of COI, PM₁₀ samples were found to contribute around half of the odor strength of TSP samples.
- The correlation distance-based PCoA can be a useful assisting tool for identifying the potential origins of odorants or other pollutants.
- The majority of odorants may exist in the gas phase rather than on particles. The odor thresholds in air are not readily applied to particle-borne odors. Also, certain limitations were associated with OAV, OAV_p, COI and COI_p because of the nonlinearity of odor perception. Sampling artifacts can be a major challenge to the investigation of particle-borne odors. An appropriate sampling protocol needs to be developed.

5.4.2 Conclusions

Particle-borne odors carried on TSP and PM₁₀ samples from six different types of animal confinement buildings were investigated. A total of 57 odorants were identified and quantified. Although acetic acid and ethanol were the most abundant odorants, phenylacetic acid and (E,E)-2,4-decadienal were found to be more odor-contributing, because of their low odor thresholds. Skatole and phenol were of less importance than previously reported in the literature. The total mass fraction of identified odorants was significantly higher in PM₁₀ (up to 46%) than in TSP and feed samples. Because of highly volatile contents in PM₁₀, TEOM may significantly underestimate PM₁₀ mass concentrations.

The odorant composition of TSP and PM₁₀ samples varied significantly with animal building type. Compared to the TSP samples, the PM₁₀ samples from different types of animal confinement buildings were more similar in both mass fraction- and OAV_P-based odorant compositions. The odorant compositions of the TSP and PM₁₀ samples were also significantly affected by seasons: a gradual change in odorant composition was present from hot to mild to cold seasons. As a measure of odor intensity, the COI values were highest during the winter (cold seasons).

TSP and PM₁₀ samples were found to have significantly different odorant compositions and significantly higher odorant contents than feed samples, suggesting that the majority of particle-borne odorants may originate from sources other than feed. Based on the ratio of COI, PM₁₀ samples contributed on average 50% of the odor strength of TSP samples, indicating a key role of fine particles in the propagation of odors. Although PM was identified as an odor carrier, the majority of odorants may exist in the gas phase rather than on particles.

6. ASSESSMENT OF AIRBORNE ENDOTOXIN AND (1→3)-BETA-D-GLUCAN IN SWINE AND POULTRY CONFINEMENT BUILDINGS

6.1 Introduction

The adverse health effects of PM produced in animal confinement buildings have been recognized for many years (Donham et al., 1977; Lincoln et al., 1974; Martin and Willough, 1972). PM exposure has been associated with the occurrence of infectious diseases, respiratory diseases (Donham et al., 1989; Douwes et al., 2003; Heederik et al., 2007; Kirkhorn and Garry, 2000; Schenker et al., 1998) and even cancer (Olsen et al., 1988) among animal farm workers. In addition, PM emission from animal confinement buildings may create certain health issues in neighboring communities (Bullers, 2005; Thu, 2002).

A number of toxic, allergenic, pathogenic and carcinogenic components have been identified in PM collected from animal confinement buildings (Douwes et al., 2003; Schenker et al., 1998). Among them, bacterial endotoxin (lipopolysaccharide, LPS) has been linked to a variety of acute and chronic respiratory symptoms such as fever, shivering, pulmonary inflammation, non-allergic asthma, airway obstruction and decreased lung function (Douwes et al., 2003; Heederik et al., 2007; Kirkhorn and Garry, 2000; Rylander, 2002). Endotoxin is a cell envelope component released by Gram-negative bacteria. Airborne endotoxin has been found to be a better predictor than the total counts of viable airborne bacteria in epidemiological research (Donham et al., 1989). Based on the results from dose-response studies, Donham et al. (2000; 1995) recommended an exposure limit of total endotoxin of 100 EU/m³ for swine buildings, and 614 EU/m³ for poultry buildings. Numerous studies have been performed regarding the concentration of airborne endotoxin in animal confinement buildings (Attwood et al., 1987; Chang et al., 2001; Clark et al., 1983; Donham et al., 1989; Jones et al., 1984; Preller et al., 1995a; Radon et al., 2002; Reynolds and Milton, 1993; Reynolds et al., 1996; Seedorf et al., 1998; Thorne et al., 1997). In many cases, the measured concentrations exceeded the Donham's recommended exposure limits (Attwood et al., 1987; Clark et al., 1983; Donham et al., 1989; Preller et al., 1995a; Radon et al., 2002; Reynolds and Milton, 1993; Reynolds et al., 1996; Seedorf et al., 1998; Thorne et al., 1997). Airborne endotoxin is not only detrimental to workers staying inside buildings, but after being discharged into the atmosphere, may create certain health effects on

people living in neighboring communities. Elevated airborne endotoxin concentrations in the ambient air were observed in the regions where animal production is intensive, in comparison to the urban area (Schulze et al., 2006).

In contrast to endotoxin, (1→3)-β-D-glucan is a major component of the fungal cell wall. It is also contained in the cell wall of some bacteria and most plants (Rylander, 1999). Airborne (1→3)-β-D-glucan has also been found to be related to atopy and respiratory symptoms, including non-allergic asthma, airway inflammation and decreased lung function (Thorn et al., 1998; Wan and Li, 1999). A potential synergistic effect may exist between (1→3)-β-D-glucan and endotoxin on facilitating the secretion of pro-inflammatory cytokines in rats and mice (Engstad et al., 2002). Currently, there is no official or recommended exposure limit available for airborne (1→3)-β-D-glucan due to lack of essential dose-response data. (1→3)-β-D-glucan is frequently used as a surrogate for fungal exposure because a direct and accurate measurement of fungus is normally difficult (Iossifova, 2006). To date, only a few efforts have been made to determine the concentration of airborne (1→3)-β-D-glucan in animal confinement buildings (Douwes et al., 1996; Rylander and Carneiro, 2006; Sander et al., 2008). The existing data are very limited and a systematic investigation is needed. This lack of data was a major motivation of our study.

Besides a lack of exposure data, another motivation is raised by a hypothesis that airborne endotoxin and (1→3)-β-D-glucan may exhibit different seasonal variation patterns. As a supporting example, Duchane et al. (2000) reported a different seasonal effect on viable bacterial concentrations than that on viable fungal concentrations in swine confinement buildings. Specifically, they found that viable bacterial concentrations were significantly higher in winter than in summer while viable fungal concentrations were usually lower in winter. Therefore, it would be interesting to simultaneously investigate potential seasonal variations in airborne endotoxin and (1→3)-β-D-glucan concentrations because of their different biological origins.

Accordingly, in this study we collected TSP samples from six different types of animal confinement buildings, and measured particle-borne endotoxin and (1→3)-β-D-glucan concentrations with kinetic chromogenic LAL (*Limulus amoebocyte lysate*) assays. The main objectives of this chapter were (1) to examine variations in airborne endotoxin and (1→3)-β-D-glucan concentrations with animal building type, season, and other environmental and

operational factors, (2) to compare a variation in airborne endotoxin concentrations to that in (1→3)-β-D-glucan concentrations, and (3) to investigate a potential relationship between airborne endotoxin/ (1→3)-β-D-glucan concentrations and TSP concentrations.

6.2 Approaches

6.2.1 Particle sampling

We selected a total of eighteen swine and poultry confinement buildings mostly in Illinois (Table 6.1), and visited each building three times in different seasons: winter, spring or fall, and summer. Detailed descriptions about sampling sites can be found in Appendix A and B. Additional PM samples came from a cage-free layer hen and a broiler building, but only a single summer visit to each was conducted.

Table 6.1. Summary of field sampling.

Animal type	Building Type	Location	# of buildings	# of visits ^x
Swine	Gestation	Illinois	3	9
	Farrowing	Illinois	3	9
	Weaning	Illinois	3	^y 8
	Finishing	Illinois	3	9
Poultry	Manure-belt layer hen	Illinois and Indiana	3	9
	Tom turkey	Illinois	3	9
	Cage-free layer hen	Indiana	1	^z 1
	Broiler	Kentucky	1	^z 1
Total			20	53

x. Only one TSP sample was collected from each field trip.

y. One farm was closed down before our last visit, thus the summer season samples were not taken.

z. Summer season only.

TSP samples were collected on glass fiber filters (Type A/E, P/N 61652, Pall Corporation, Ann Arbor, MI) with UIUC TSP isokinetic samplers. Filters were autoclaved and conditioned prior to sampling. TSP samplers and polycarbonate filter cassettes were also sterilized (Please refer to Appendix C for detailed information). TSP samplers were installed upstream of a continuous-running exhaust fan and the height of sampler inlets was typically 1.2-1.4 m, with spacing from the fan face adjusted to match the isokinetic sampler velocity requirements, but typically 0.2-0.6 m. Natural ventilation was primarily employed in the tom turkey buildings, thus a calm-air PM sampling protocol was selected (Zhang, 2005), and TSP samplers were installed near a downwind end door if no exhaust fan was available. The sampling period was approximately 24 hours, and recorded to the nearest minute. Low-pressure-drop venturi orifices

(Wang and Zhang, 1999) were used to control the sampling airflow rate at approximately 20 LPM. The accurate flow rate was acquired through a calibration of venturi orifices in the lab (Please refer to Appendix H), and used for calculating the actual volume of sampled air. TSP concentrations were determined gravimetrically, following a general procedure that basically involves pre-conditioning and pre-weighing of blank filters, and post-conditioning and post-weighing of filters with collected particles. After post-weighing, particle filters were transferred into sterile Petri dishes, sealed and then stored at -20 °C in a freezer until extraction.

6.2.2 Analysis of endotoxin

Because endotoxin analysis with a kinetic chromogenic LAL assay relies on the activity of enzyme, many experimental factors can affect the potency of endotoxin and consequently may alter the analysis results. No standard protocol for airborne endotoxin analysis is currently available (Spaan et al., 2008). In this study, an experimental protocol was developed based on previous studies on the affecting factors (Douwes et al., 1995; Spaan et al., 2007; Spaan et al., 2008; Thorne et al., 2003). A brief procedure was as follows:

- A filter was extracted in a 10 mL 0.05% Tween20 solution. The extraction was performed in a water bath shaker for 120 minutes at maximum agitation rate and at room temperature. The extract was then centrifuged at 1,000 G for 15 minutes.
- A 1.0 mL supernatant was collected and diluted with pyrogen-free water. The dilution ratio was dependent on the mass of PM but no less than 50 so as to eliminate the interference from Tween-20 (Spaan et al., 2008). A pH adjustment was performed by addition of a 0.01M KOH or 0.01M HCl solution if a measured pH value was beyond the optimal pH range of 6.8.
- Endotoxin levels in the diluted extracts were quantified with Kinetic-QCL[®] assay (Cat. # 50-650U, Lonza Group Ltd, Basel, Switzerland). The analysis was performed on an incubating microplate reader (BioTek ELx808, BioTek Instrument Inc., Winooski, VT) at 37°C and 405 nm. The stock endotoxin standard (potency: 1 ng= 11 EU) was diluted in series into 50, 5, 0.5, 0.05 and 0.005 EU/mL to build a calibration curve. For each test sample, possible inhibition or enhancement was checked with positive product control (PPC). A further dilution or pH adjustment would be performed if the recovery efficiency

was less than 50% or over 200%. The test of a sample was repeated if the coefficient of variation (CV) between duplicate test samples exceeded 10%.

- The level of airborne endotoxin was presented in units of EU/m³ air (airborne concentration) and EU/mg PM (content in particles).

6.2.3 Analysis of (1→3)-β-D-glucans

Similar to the case of airborne endotoxin, there is currently no standard protocol available for airborne (1→3)-β-D-glucan analysis. The experimental protocol in this study basically followed the protocol proposed by Rylander and Carvlheriro (2006). Because a similar kinetic chromogenic LAL assay was selected for (1→3)-β-D-glucan analysis, the experimental procedure was analogous to that for airborne endotoxin.

- A 1.0 mL 3M NaOH solution was added into the remaining 9 mL extract after 1.0 mL supernatant was collected for endotoxin analysis. The mixture was vortexed and then agitated in a water bath shaker for 10 minutes with ice cooling. The extract was centrifuged at 1,000 G for 15 minutes.
- A 1.0 mL supernatant was collected and diluted in series with reagent-grade water. The dilution ratio was dependent on the mass of PM. An adjustment of pH values to 6.8 was performed by addition of a 0.01M HCl solution but generally unnecessary due to the high dilution ratio (>1,000) and the use of buffer solution in test.
- A Glucate[®] Kit (Cat. # GT002, Associates of Cape Cod Incorporated, East Falmouth, MA) was used for determination of the (1→3)-β-D-glucan levels in the diluted extracts. A kinetic time-of-onset assay was selected. The analysis was also performed on the incubating microplate reader at 37°C and 405 nm. The stock standard was diluted with reagent-grade water into 100, 50, 25, 12.5, 6.25 and 3.125 pg/mL to build a calibration curve. Similar to the case of endotoxin analysis, potential inhibition or enhancement was checked with PPC but only on parts of samples. The test of a sample was repeated if the CV between duplicate test samples exceeded 10%.
- The level of airborne (1→3)-β-D-glucan was expressed in units of ng/m³ air (airborne concentration) and ng/mg PM (content in particles).

6.2.4 Statistical analysis

All statistical analyses were conducted in SPSS v17.0. The normality of measured concentration data was tested by the Shapiro-Wilk test. A log transformation was performed if the p value given by the Shapiro-Wilk test was smaller than 0.05. One-way ANOVA/ Tukey's test was used with animal building type as the factor and a Kruskal-Wallis test (nonparametric ANOVA) was selected when the normality of data remained poor even after log transformation. Paired t-tests were employed to compare the levels of airborne endotoxin or (1→3)-β-D-glucan in different seasons. Pearson's correlation coefficient and its related p value were used to examine the relationship of airborne endotoxin/ (1→3)-β-D-glucan levels to TSP concentrations and other parameters. A significance level of 0.05 was chosen for the tests mentioned above.

6.3 Results and Discussions

6.3.1 Summary of quantitative results

Besides PM samples, autoclaved blank filters were also subject to analysis and the endotoxin and (1→3)-β-D-glucan contents were found to be negligible. Thus, all values reported were as-measured and not adjusted for background correction.

6.3.1.1 Airborne endotoxin

A great variation in airborne endotoxin concentrations was observed within the same type of animal confinement buildings (Table 6.2). The endotoxin contents in particles (EU/mg PM) also varied greatly; however, the mean content values were more similar among different animal building types. The lowest endotoxin concentration, 98 EU/m³, occurred in a farrowing building in summer; while the highest concentration, 23,157 EU/m³, was detected in a tom turkey building in winter. Tom turkey buildings had overall the highest airborne endotoxin concentrations, followed by manure-belt layer hen buildings. As reported in Chapter 3, these two types of poultry buildings were also associated with higher TSP concentrations. Although the sampled farrowing buildings had overall the lowest airborne endotoxin concentration, the endotoxin content in particles was slightly higher in farrowing buildings than in manure-belt layer hen buildings (mean values of 735 EU/mg vs. 672 EU/mg, respectively). This suggests that TSP concentrations may be a major determining factor on airborne endotoxin contaminations in animal confinement buildings.

Table 6.2. Summary of measured airborne endotoxin concentrations^x.

	Endotoxin content in particles (EU/mg PM)				Airborne endotoxin concentration (EU/m ³)				
	Mean	SD	GM ^{y,z}	GSD ^y	Mean	SD	GM ^{y,z}	GSD ^y	Range
Farrowing (n=9)	735	857	^a 439	2.79	508	617	^c 334	2.47	98- 2099
Gestation (n=9)	1027	1007	^a 622	2.96	510	317	^{bc} 419	1.98	164- 991
Weaning (n=8)	1176	840	^a 875	2.38	1971	2816	^{abc} 1017	3.30	217- 8702
Finishing (n=9)	1204	872	^a 929	2.17	1508	978	^{ab} 1285	1.51	693- 3588
Manure-belt layer hen (n=9)	672	1333	^a 287	3.01	2008	4092	^{bc} 607	4.17	148- 12661
Tom turkey (n=9)	1154	949	^a 780	2.89	5460	7377	^a 3044	3.09	593- 23157

x. The content of endotoxin in TSP particles was 159 EU/mg in the cage-free layer hen and 625 EU/mg in the broiler building; airborne endotoxin concentration was 356 EU/m³ and 1368 EU/m³, respectively. It must be noted that only a single visit to these buildings was conducted, thus the data should not be applied to general cases.

y. The Shapiro-Wilk test revealed that the measured concentration data were not normally distributed but rather followed a lognormal distribution. Accordingly, GM (geometric mean) and GSD (geometric standard deviation) are also presented.

z. Within a column, values labeled with the same letter were not significantly different (p>0.05).

As previously mentioned, the UIUC isokinetic samplers were used for collection of TSP samples. Theoretically this sampler has 100% collection efficiency for all-size particles (Zhang, 2005). According to a recent study by Lee (2009), particles in and from animal confinement buildings were substantially larger than ambient aerosols but mostly smaller than 100 µm, the cut size of inhalable PM samplers. Therefore, the measurement results could be considered to roughly represent the concentration of inhalable endotoxins.

We compared our measurement results to the exposure limits proposed by Donham et al. (2000; 1995) and found that the percentage of TSP samples exceeding the exposure limits was 100% in the weaning, gestation and finishing buildings sampled, 89% (8/ 9) in the farrowing and tom turkey buildings sampled, and 33% (3/ 9) in the manure-belt layer hen buildings sampled. The sample collected from the TSP broiler building exceeded the proposed exposure limit while that from the cage-free layer hen building was lower than the exposure limit.

The measurement results were also compared to those reported in the literature, as summarized in Table 6.3. Airborne endotoxin concentrations are presented in unit of EU/m³ or ng/m³, and in general 1.0 ng endotoxin approximately equals to 10-15 EU. It can be seen that our

measurement results were of a similar order of magnitude to those from previous studies. It should be noted that different samplers, filters and analysis methods may lead to substantially different results. For example, endpoint chromogenic LAL assays were found to generate higher endotoxin concentrations than KLARE assays in swine buildings (Thorne et al., 1997). Regardless of possible differences in sampling and analysis protocols, many reported airborne endotoxin concentrations in the literature exceeded the exposure limits proposed by Donham et al. (2000; 1995) and the TLV/TWA (4.5 ng/m^3 , $\sim 50 \text{ EU/m}^3$) issued by the Dutch Health Council in the Netherlands (Schenker et al., 1998). Most lower-than-threshold values in Table 6.3 came from a study by Chang et al. (2001). The swine buildings they visited were open-style and, thus, low endotoxin concentrations were expected due to the dilution by ambient air from natural ventilation. As a comparison to animal buildings, urban areas have much lower airborne endotoxin concentrations, with geometric means typically less than 0.5 EU/m^3 (Madsen, 2006).

Table 6.3. Comparison of airborne endotoxin concentrations in swine and poultry buildings.

Building type	Farm sites	Particle size	Mean endotoxin concentration	Method	Reference
Swine	Illinois	TSP	1122 EU/m ³ (n=35)	Kinetic chromogenic LAL assay	This study
Farrowing			508 EU/m ³ (n=9)		
Gestation			510 EU/m ³ (n=9)		
Weaning			1971 EU/m ³ (n=8)		
Finishing			1508 EU/m ³ (n=9)		
Swine	n/a	Total	120 ng/m ³ (n=8)	Gel clot LAL assay	Clark et al. (1983)
Farrowing and nursery	The Netherlands	Total	128 ng/m ³ (n=96)	Chromogenic LAL assay	Attwood et al. (1987)
Finishing			120 ng/m ³ (n=70)		
Swine	Sweden	Total	240 ng/m ³ (n=30)	n/a	Donham et al. (1989)
Swine	The Netherlands	Inhalable	112 ng/m ³ (n=161)	n/a	Preller et al. (1995a)
Swine	Iowa (Time 1)	Total	202.7 EU/m ³ (n=151)	Endpoint chromogenic LAL assay	Reynolds et al. (1996)
	Iowa (Time 2)		176.1 EU/m ³ (n=151)		
Swine	Iowa	Total	8290 EU/m ³	KLARE assay; endpoint assay	Thorne et al. (1997)
Sows	North Europe	Inhalable	83.5 ng/m ³ (n=44)	Kinetic turbidimetric LAL assay	Seedorf et al. (1998)
Weaning			172.0 ng/m ³ (n=27)		
Fattening			122.1 ng/m ³ (n=39)		
Breeding	Taiwan	Total	36.8 EU/m ³ (n=12)	KLARE assay	Chang et al. (2001)
Farrowing			82.1 EU/m ³ (n=12)		
Nursery			298 EU/m ³ (n=12)		
Growing			145 EU/m ³ (n=12)		
Finishing			136 EU/m ³ (n=12)		
Swine	Denmark	Total	58.0 ng/m ³ (n=40)	Kinetic chromogenic LAL assay	Radon et al. (2002)
	Germany		76.3 ng/m ³ (n=100)		

Table 6.3. (cont.)

Animal type	Farm sites	Particle size	Mean endotoxin concentration	Method	Reference
Swine	Canada	Inhalable	summer: 6553 EU/m ³ winter: 25690 EU/m ³	Chromogenic LAL assay	Bonlokke et al. (2009)
Swine- hoop	Iowa	Inhalable	3520 EU/m ³ (GM ^x)	Kinetic chromogenic LAL assay	Thorne et al. (2009)
Swine- confinement			3100 EU/m ³ (GM ^x)		
Manure-belt layer hen	Illinois and Indiana	TSP	2008 EU/m ³ (n=9)	Kinetic chromogenic LAL assay	This study
Tom turkey	Illinois		5460 EU/m ³ (n=9)		
Cage-free layer hen	Indiana		356 EU/m ³ (n=1)		
Broiler	Kentucky		1368 EU/m ³ (n=1)		
Poultry	n/a	Total	310 ng/m ³ (n=7)	Gel clot LAL assay	Clark et al. (1983)
Broiler	North Carolina	Total	40 ng/m ³ (n=3)	Gel clot LAL assay	Jones et al. (1984)
Broiler	n/a	Inhalable	3132 EU/m ³	KLARE assay	Reynolds and Milton (1993)
Chicken brooder			4593 EU/m ³	Endpoint assay	
		Inhalable	1274 EU/m ³	KLARE assay	
1164 EU/m ³	Endpoint assay				
Poultry	Iowa	Total	1340 EU/m ³	KLARE assay; endpoint assay	Thorne et al. (1997)
Layer hen	North Europe	Inhalable	600.0 ng/m ³ (n=43)	Kinetic turbidimetric LAL assay	Seedorf et al. (1998)
Broiler			785.0 ng/m ³ (n=21)		
Poultry	Switzerland	Total	257.6 ng/m ³ (n=36)	Kinetic chromogenic LAL assay	Radon et al. (2002)
Poultry	Sweden	n/a	410 ng/m ³ (n=39)	Kinetic chromogenic LAL assay	Rylander and Carvalho (2006)
Poultry	Canada	Total	Floor ^y : 7484 EU/m ³ (n=80)	Endpoint LAL assay	Kirychuk et al. (2006)
			Cage ^y : 9544 EU/m ³ (n=80)		
Broiler	Switzerland	Total	Catcher ^z : 6198 EU/m ³ (n=19)	Kinetic chromogenic LAL assay	Oppliger et al. (2008)

x. Only geometric mean was available.

y. Floor refers to floor-housed poultry operations, including broiler breeding, broiler roaster and turkey. Cage refers to cage-housed poultry operations, including egg/pullet operations.

z. Personal exposure when catching mature birds.

It should be noted that in this study TSP samplers were installed near exhaust fans (most buildings) or end doors (tom turkey buildings), which are considered representative of emissions from the buildings. Because of a heterogeneous spatial distribution of TSP concentrations (Jerez, 2007; Wang, 2000), the measured airborne endotoxin concentrations can be greatly different than indoor average concentrations and those determined with personal samplers. Accordingly to Jerez (2007), TSP concentrations near exhaust fans were lower than the indoor average

concentration in a tunnel ventilated finishing building. The measurement results given by this study, therefore, may underestimate the real personal exposure.

Endotoxin is normally embedded into the outer membrane of Gram-negative bacterial cells, and is released and becomes biologically active when bacterial cells are lysed or at the multiplication stage (Todar, 2008). Previous studies have revealed the ubiquitous presence of Gram-negative bacteria in PM from animal confinement buildings. Martin et al. (1996) investigated bacterial flora of deposited dust (from the settlement of suspended PM) in a swine finishing building. Four Gram-negative bacterial genera were identified, including *Acinetobacter*, *Enterobacter*, *Pasteurella* and *Vibro*. Predicala et al. (2002) collected airborne bacterial and fungal samples in a swine finishing building in Kansas and reported the presence of genera *Pseudomonas*, *Vibro* and Gram-negative Bacilli. Both studies used culture based methods, with which only culturable bacterial and fungal species can be identified. To overcome this difficulty, Nehme et al. (2008) recently used culture-independent molecular methods- 16S rDNA gene clone library- for determination of bacterial diversity and species in PM samples from eight swine confinement buildings in Canada, and found that the airborne Gram-negative bacteria mainly belonged to genera *Moraxella*, *Bacteroides* and *Pseudomonas*. However, Gram-negative bacteria may only account for a small fraction of the total airborne bacteria in animal confinement buildings. A recent study (P. Hong et al., unpublished data, 2010. Urbana IL: University of Illinois at Urbana-Champaign) revealed that proteobacteria, cyanobacteria and spirochaetes, three major phylums of Gram-negative bacteria, together only accounted for less than 10% of all 16S rDNA sequences (6,000 sequences per particle sample) extracted and PCR-amplified from TSP samples collected in the current study; while the majority of airborne bacterial populations seemed to be contributed by phylums Firmicutes and Bacterioidetes. Both are typical Gram-positive bacteria.

6.3.1.2 Airborne (1→3)-β-D-glucan

Similar to the case of endotoxin, a large variation in airborne (1→3)-β-D-glucan concentrations was found among different types of and within the same type of animal confinement buildings (Table 6.4), and so did the (1→3)-β-D-glucan contents in particles (ng/mg PM). Again, tom turkey buildings were found to have overall the highest airborne (1→3)-β-D-glucan concentration, followed by manure-belt layer hen buildings. The highest (1→3)-β-D-

glucan concentration, 537.9 ng/m³, occurred in a tom turkey building in winter; while the lowest concentration, 2.4 ng/m³, was detected in a farrowing building but in winter. The average (1→3)-β-D-glucan level in particles was highest in manure-belt layer hen buildings and lowest in weaning buildings. Compared to airborne (1→3)-β-D-glucan concentrations, the contents of (1→3)-β-D-glucan in particles (ng/mg PM) were relatively more similar among different animal building types.

Table 6.4. Summary of airborne (1→3)-β-D-glucan concentrations^x.

	(1→3)-β-D-glucan content in PM (ng/mg PM)				Airborne (1→3)-β-D-glucan concentration (ng/m ³)				
	Mean	SD	GM ^y	GSD	Mean	SD	GM ^y	GSD	Range
Farrowing (n=9)	25.2	21.4	^a 15.6	3.24	21.2	20.2	^b 12.5	3.50	2.4- 50.7
Gestation (n=9)	34.3	19.4	^a 26.6	2.41	25.2	20.2	^{ab} 17.2	2.71	3.7-50.8
Weaning (n=8)	20.0	16.5	^a 14.0	2.59	34.9	48.4	^{ab} 16.3	3.58	3.8-140.1
Finishing (n=9)	31.9	49.1	^a 17.6	2.80	32.7	22.0	^{ab} 24.3	2.62	3.9-65.0
Manure-belt layer hen (n=8) ^z	56.1	50.0	^a 35.4	3.07	106.7	98.3	^a 63.8	3.32	11.4-272.4
Tom turkey (n=9)	28.0	27.5	^a 16.3	3.47	121.0	173.4	^a 63.5	3.26	10.0-537.9

x. The Shapiro-Wilk test revealed that the measured concentration data were not normally distributed but rather followed a lognormal distribution. The content of (1→3)-β-D-glucan in TSP particles was 10.4 ng/mg in the cage-free layer hen and 18.6 ng/mg in the broiler building; airborne (1→3)-β-D-glucan concentration was 11.0 ng/m³ and 40.7 ng/m³, respectively. Only a single visit was performed to these buildings, thus the data should not be generalized.

y. Within a column, values labeled with the same letter were not significantly different (p>0.05).

z. One TSP sample was lost during centrifuging.

There are no issued or proposed exposure limits currently available for airborne (1→3)-β-D-glucan exposure. Therefore, it is unknown whether the measured (1→3)-β-D-glucan concentrations exceeded a harmful level. In fact, the potential health effect of airborne (1→3)-β-D-glucan is not entirely clear. Although most previous studies stated that airborne (1→3)-β-D-glucan pose an adverse effect on human and animal health (Douwes, 2005; Thorn et al., 1998; Wan and Li, 1999), some researchers suggested that early exposure to low levels of (1→3)-β-D-glucan may have a protective effect against the development of atopy and allergic asthma (Gehring et al., 2007; Iossifova et al., 2007). Either way, the measurement of airborne (1→3)-β-D-glucan in animal confinement buildings would offer valuable information.

A comparison to the literature showed that this study produced overall lower airborne (1→3)-β-D-glucan concentrations (Table 6.5). This may be mainly ascribed to a difference in sampling sites. Most existing data came from Europe where animal buildings are generally smaller than their counterparts in the United States; the ventilation, feeding and manure handling systems are generally also different. Another possible explanation is a difference in analytical methods: no kinetic chromogenic LAL assay was employed in previous similar studies. In addition, different samplers and sampling points may also make a difference due to different collection efficiencies and the heterogeneous spatial distribution of TSP in animal buildings (Jerez, 2007; Wang, 2000).

Table 6.5. Comparison of airborne (1→3)-β-D-glucan concentration in animal buildings.

Animal type	Farm sites	Particle size	Mean (1→3)-β-D-glucan concentration	Method	Reference
Swine	Illinois	TSP	28.5 ng/m ³ (n=35)	Kinetic chromogenic LAL assay	This study
Farrowing			21.2 ng/m ³ (n=9)		
Gestation			25.2 ng/m ³ (n=9)		
Weaning			34.9 ng/m ³ (n=8)		
Finishing			32.7 ng/m ³ (n=9)		
Swine	n/a	Inhalable	Geometric: 4300 ng/m ³ (n=5)	EIA assay	Douwas et al. (1996)
Swine	Germany	n/a	2-972 ng/m ³ (n=12)	mAb-EIA assay	Sander et al. (2008)
Manure-belt layer hen	Illinois and Indiana	TSP	98.3 ng/m ³ (n=8)	Kinetic chromogenic LAL assay	This study
Tom turkey	Illinois		121.0 ng/m ³ (n=9)		
Cage-free layer hen	Indiana		11.0 ng/m ³ (n=1)		
Broiler	Kentucky		40.7 ng/m ³ (n=1)		
Poultry	Sweden	Total	270 ng/m ³ (n=39)	Endpoint LAL assay	Rylander and Carvalho (2006)
Poultry	Germany	n/a	33-410 ng/m ³ (n=9)	mAb-EIA assay	Sander et al. (2008)

Fungi are a major source of airborne (1→3)-β-D-glucan. In animal confinement buildings, animal feeds, manures and bedding materials (e.g. wood shavings) provide abundant substrates and nutrients; in addition, the indoor temperature and humidity are normally high, which is suitable for the growth of many fungal species. Martin et al. (1996) reported the presence of fungal genera *Absidia*, *Alternaria*, *Cladosporium*, *Penicillium*, *Rhizopus*, and *Scopulariopsis* in deposited dusts collected from a finishing building. Seedorf et al. (1998) identified fungal genera *Aspergillus*, *Penicillium*, and *Mucor* in animal buildings in North Europe. Predicala et al. (2002) found the existence of fungal genus *Penicillium* in the air of a finishing building. All those

studies investigated only culturable fungal species; however, the majority of airborne fungal spores may be non-culturable (Rylander and Etzel, 1999). Even so, the concentrations of culturable airborne fungi in animal confinement buildings could be up to 10,000 CFU/m³ (Seedorf et al., 1998), much higher than 100 CFU/m³, a concentration believed to be potentially harmful to immunosuppressed people (ACGIH, 1989). Therefore, it is of importance to further examine the fungal exposure in animal confinement buildings. Future efforts may better focus on fungal biomarkers, such as (1→3)-β-D-glucan, ergosterol and cholesterol, and on cultural-independent molecular biology techniques, such as 18s rDNA qPCR and DNA sequencing.

6.3.2 Effect of animal building type

Variations in endotoxin and (1→3)-β-D-glucan levels with animal building type were illustrated in Figure 6.1. The measured data were log transformed and then subject to one-way ANOVA/ Tukey's test with animal building type as the factor. The test results revealed that the average airborne endotoxin concentrations were significantly higher in tom turkey buildings than in farrowing, gestation and manure-belt layer hen buildings (all $p < 0.045$), and significantly higher in finishing buildings than in farrowing buildings ($p = 0.049$); however, no significant difference in endotoxin contents in particles was found among different types of animal confinement buildings. Poultry buildings (including cage-free layer hen and broiler buildings) had significantly higher airborne endotoxin concentrations than swine buildings ($p = 0.039$), but no significant difference in endotoxin contents in particles was present.

The average airborne (1→3)-β-D-glucan concentrations were significantly lower in farrowing buildings than in manure-belt layer hen and tom turkey buildings (both $p < 0.047$); however, again no significant difference in (1→3)-β-D-glucan contents in particles was identified among different types of animal confinement buildings. Similar to the case of endotoxin, poultry buildings had significantly higher airborne (1→3)-β-D-glucan concentrations than swine buildings ($p < 0.001$), but there was no significant difference in (1→3)-β-D-glucan contents in particles.

Since there was no significant variation in endotoxin or (1→3)-β-D-glucan contents in particles with animal building types, the observed differences in airborne endotoxin and (1→3)-β-D-glucan concentrations may primarily be attributed to different TSP mass concentrations. A discussion on the effect of animal building type on TSP concentrations can be found in Chapter 3.

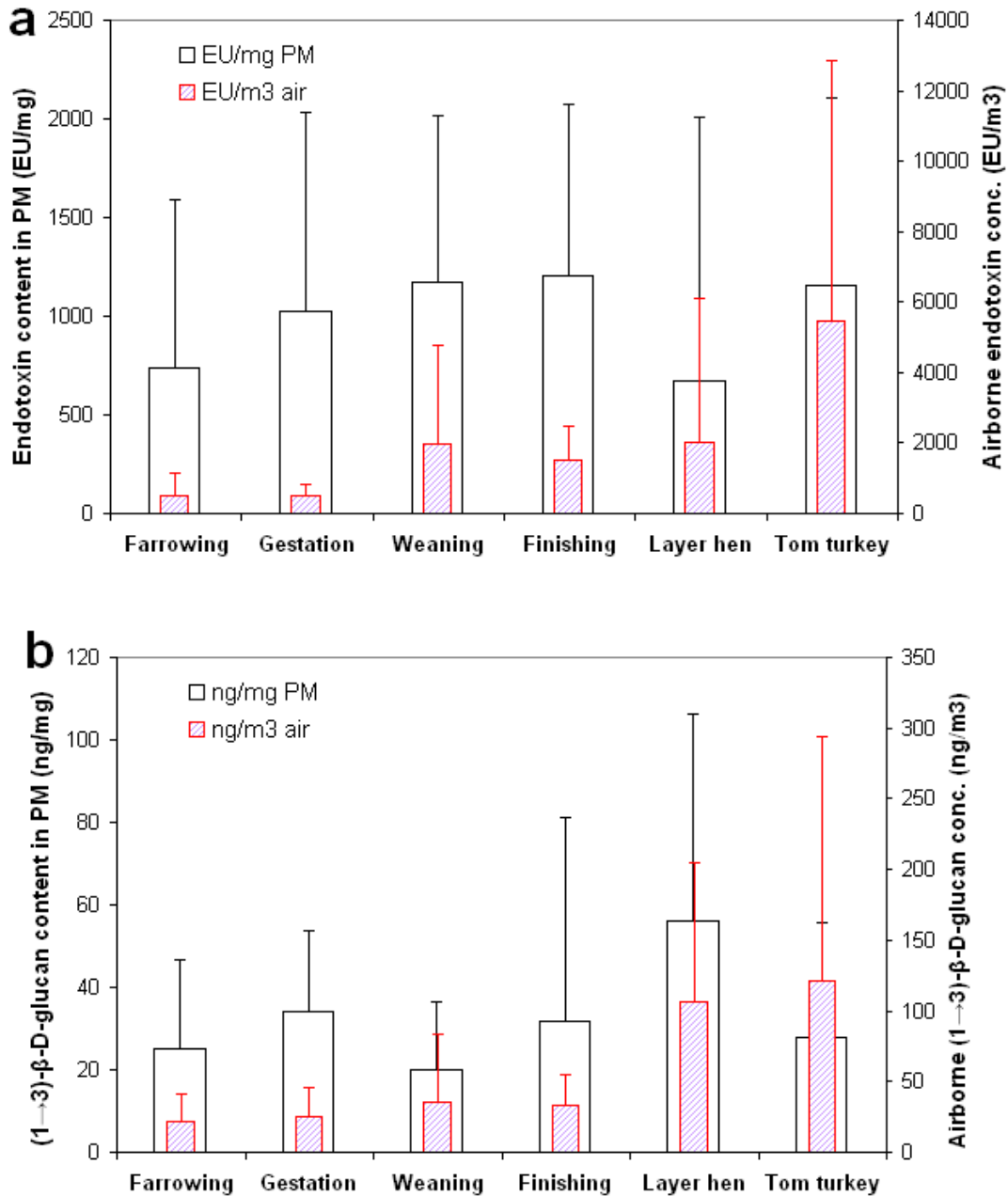


Figure 6.1. Variations in (a) endotoxin and (b) (1→3)-β-D-glucan levels with animal building type.

6.3.3 Seasonal variation

Variations in endotoxin and (1→3)-β-D-glucan levels with season were illustrated in Figure 6.2. Paired t-test was used to examine the effect of seasons on endotoxin and (1→3)-β-D-glucan levels. Standing in a sharp contrast to the case of TSP concentrations (Table 3.18), the test results

(Table 6.6) showed that there was no significant seasonal effect on airborne endotoxin and (1→3)-β-D-glucan concentrations. Although the identified differences were statistically insignificant, both endotoxin and (1→3)-β-D-glucan attained their highest airborne concentrations in spring or fall, and were slightly more concentrated in winter than in summer. Comparatively, the test results revealed a great effect of seasons on the contents of endotoxin and (1→3)-β-D-glucan in particles, which increased as the weather getting warmer. Noticeably, TSP samples from summer had significantly higher endotoxin and (1→3)-β-D-glucan contents in particles than those from winter. Reminding that airborne endotoxin/ (1→3)-β-D-glucan concentrations are the product of TSP concentrations multiplied by the endotoxin/ (1→3)-β-D-glucan contents in TSP particles, the seasonal variation of airborne endotoxin/ (1→3)-β-D-glucan concentrations would therefore be determined by a combination of the effects of seasons on the latter two factors.

As discussed in Chapter 3, seasons had a significant effect on TSP concentrations that normally increased as weather became colder. In contrast, as revealed by this study, the contents of endotoxin and (1→3)-β-D-glucan in TSP particles varied in a very opposite manner. Therefore, it is not surprising to see that a combination of both factors could result in an insignificant seasonal change in airborne endotoxin and (1→3)-β-D-glucan concentrations. In fact, the lack of significant seasonal variation in airborne endotoxin concentrations was previously observed by Seedorf et al. (1998). However, different observations were also reported (Bonlokke et al., 2009; Preller et al., 1995b; Schierl et al., 2007). In the first two papers, airborne endotoxin concentrations were found to be significantly higher in winter than in summer and there were no data available for spring or fall. In the last paper, the authors observed that airborne endotoxin concentrations were highest in winter, followed by summer, and usually lowest in spring. Such controversies suggest a complexity in the seasonal effect on airborne endotoxin contaminations and a necessity to further examine the seasonal variation of endotoxin exposure. Comparatively, few studies have been done regarding the effect of seasons on airborne (1→3)-β-D-glucan. This study revealed airborne (1→3)-β-D-glucan may exhibit a similar seasonal variation to airborne endotoxin.

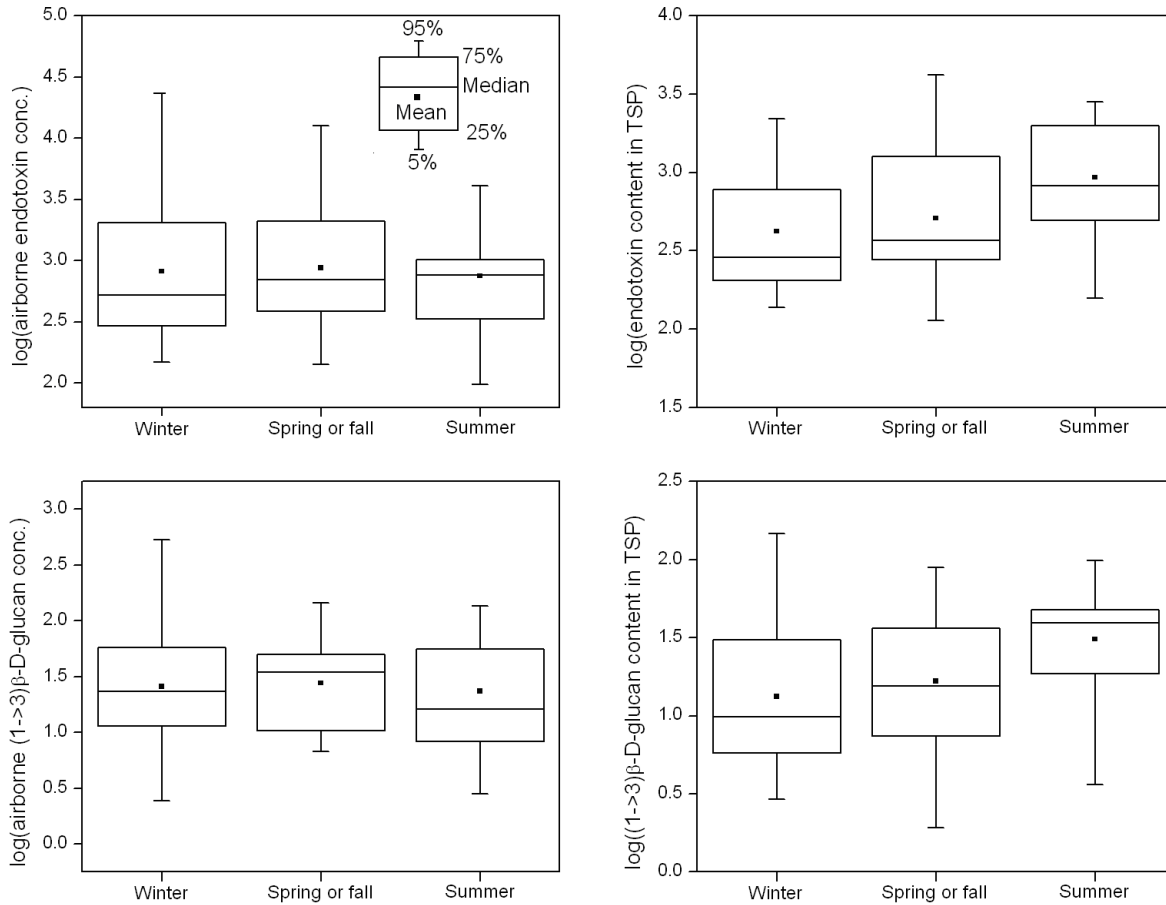


Figure 6.2. Effect of seasons on endotoxin and (1→3)-β-D-glucan levels.

Table 6.6. Paired t-test on endotoxin and (1→3)-β-D-glucan levels in different seasons.

Seasons	statistic	Endotoxin content in particles	Airborne endotoxin concentration	(1→3)-β-D-glucan content in particles	Airborne (1→3)-β-D-glucan concentration
Winter vs. Spring or Fall	Δ^x	-0.089	-0.023	-0.111	-0.039
	P^y	0.364	0.446	0.122	0.322
Winter vs. Summer	Δ	-0.420	0.016	-0.431	0.036
	P	<0.001	0.382	0.006	0.405
Spring or Fall vs. Summer	Δ	-0.331	0.038	-0.319	0.075
	P	0.059	0.393	0.067	0.373

x. Data had been log transformed prior to paired t-test. Thus, the Δ value here represented a difference in log transformed data.

y. The p value was highlighted in bold fonts when smaller than 0.05.

To address uncertainties associated with the classification of seasons, the endotoxin and (1→3)-β-D-glucan levels were correlated to daily average ambient temperature (Figure 6.3 and Table 6.7). The results showed a weak but significant correlation of daily average ambient temperatures to endotoxin and to (1→3)-β-D-glucan contents in particles; while no correlation to airborne concentrations was noted.

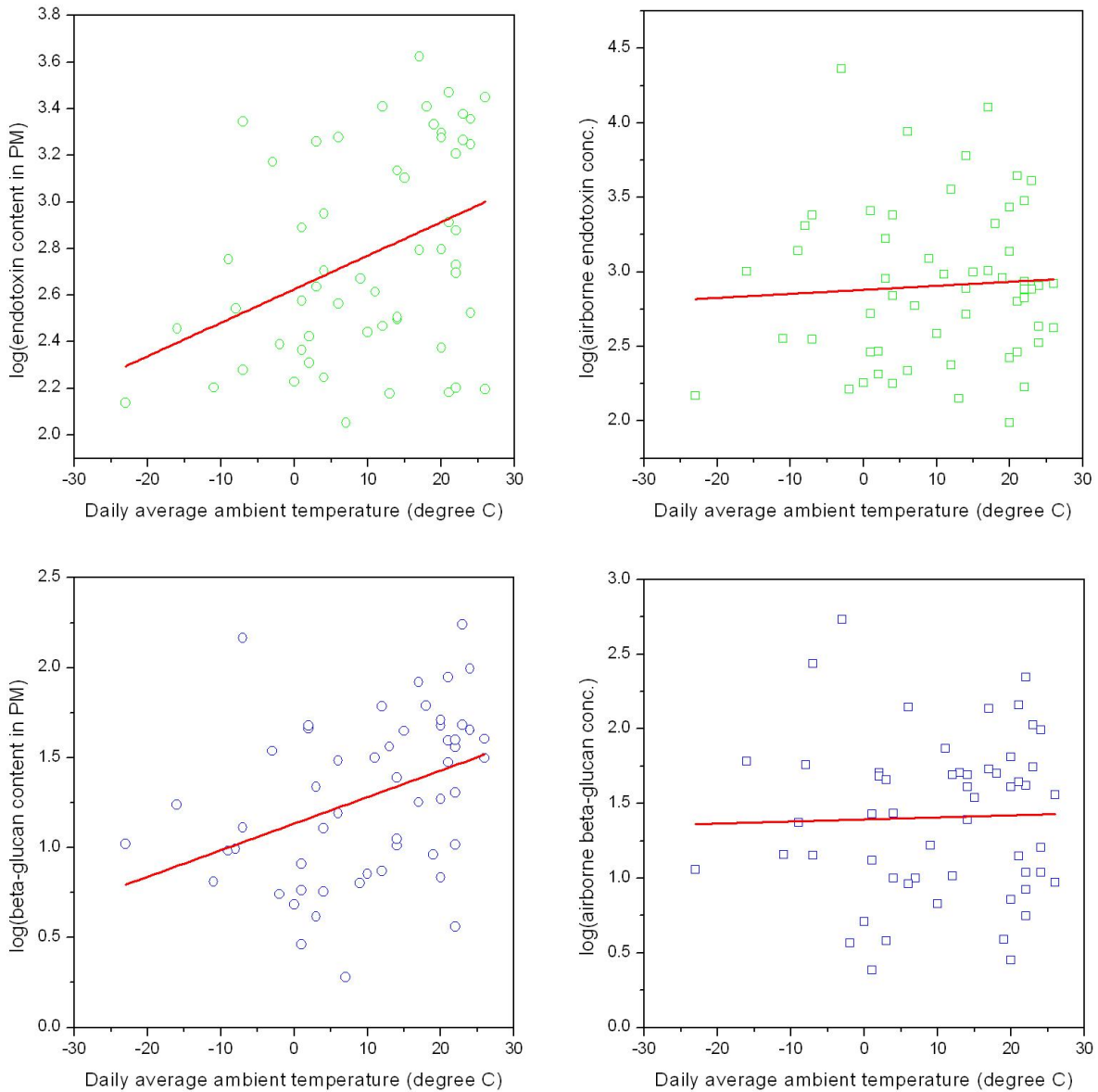


Figure 6.3. Effect of ambient temperature on endotoxin and (1→3)-β-D-glucan levels.

Table 6.7. Correlation of ambient temperature to endotoxin and (1→3)-β-D-glucan levels.

Statistic	Daily average ambient temperature versus			
	Endotoxin content in particles	Airborne endotoxin concentration	(1→3)-β-D-glucan content in particles	Airborne (1→3)-β-D-glucan concentration
r	0.383	0.061	0.390	0.031
P	0.004	0.654	0.003	0.821

Why is there a correlation between the daily average ambient temperature and the contents of endotoxin and (1→3)-β-D-glucan in particles? A possible explanation is that higher ambient temperatures may facilitate the growth and propagation of bacteria and fungi, thereby leading to

higher bacterial and fungal populations in unit mass of particles. In an animal confinement building, the thermal conditions, including temperature and humidity, were controlled within a certain range so as to offer a healthy and optimal environment for animal growth. Relevant engineering solutions include but not limited to changes in ventilation rates, the use of additional heaters and evaporation cooling. However, there is inevitably still a seasonal variation of thermal conditions in animal confinement buildings, especially the compartments normally of less concern, e.g. manure pits where the air temperature would be greatly affected by ambient seasons. In general, the indoor air temperature was warmest in summer and coolest in winter (Figure 6.4). Therefore, it is not unexpected that the contents of endotoxin and (1→3)-β-D-glucan would attain their maximum in summer. In addition, as a potential source of fungi and bacteria, animal feed is generally stored in feed bins outside an animal confinement building. Low ambient temperatures during the winter may inhibit the growth of fungi and bacteria on feed, thereby lowering the contents of endotoxin and (1→3)-β-D-glucan in TSP particles.

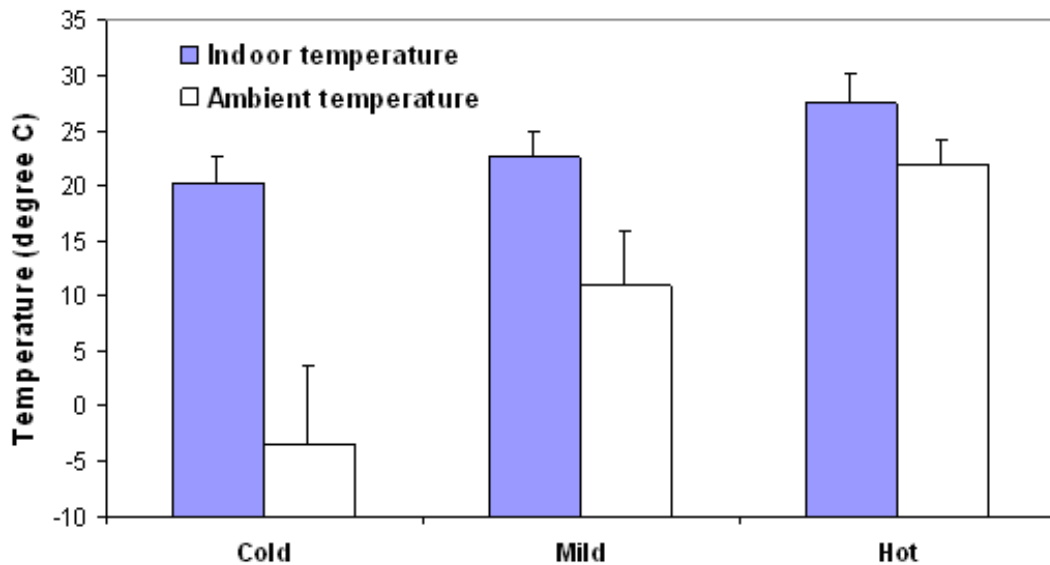


Figure 6.4. Indoor and ambient temperature in different seasons.

We also investigated other environmental and operational factors, such as feeding systems (dry versus wet), indoor air humidity, and animal density. However, no significant effects were identified (data not shown here) on endotoxin and (1→3)-β-D-glucan levels.

6.3.4 Correlation with TSP concentration

Because of the detrimental health effects of airborne endotoxin and (1→3)-β-D-glucan, it is of practical importance to develop effective and affordable mitigation strategies to reduce their concentrations and emissions. Regretfully, there are currently no specific control strategies for airborne endotoxin and (1→3)-β-D-glucan but a number of techniques available for PM reduction, as summarized in Section 2.3.6. To examine the potential effectiveness of those techniques on endotoxin and (1→3)-β-D-glucan, we correlated TSP to airborne endotoxin and (1→3)-β-D-glucan concentrations (Table 6.8), and found a significant and strong correlation. However, it can be seen from Figure 6.5 that such a strong correlation may be mainly attributed to the rightmost data point that is somehow isolated from the majority. After removing this data point, a significant correlation was still observed; however, the correlation coefficient (r) dropped to 0.423 for airborne endotoxin and 0.366 for (1→3)-β-D-glucan, indicating a weak correlation. In conclusion, dust control techniques may also apply to airborne endotoxin and (1→3)-β-D-glucan; however, a large uncertainty is associated with the removal efficiency that may vary greatly with animal building type, season, and other factors.

Table 6.8. Correlation of TSP to airborne endotoxin and (1→3)-β-D-glucan concentrations.

Statistic	TSP concentration versus	
	Airborne endotoxin concentration	Airborne (1→3)-β-D-glucan concentration
r	0.784	0.760
P	<0.001	<0.001

An additional effort was made to correlate airborne endotoxin to airborne (1→3)-β-D-glucan concentrations. A significant and strong correlation was observed (r=0.709, p<0.001). However, similar to the case of TSP versus endotoxin/ (1→3)-β-D-glucan concentrations, such a strong correlation may be primarily due to the existence of an isolated edge point. Upon removing the edge point, no significant correlation was identified between airborne endotoxin and airborne (1→3)-β-D-glucan concentrations (r=0.225, p=0.102), suggesting a potential difference in their variation patterns.

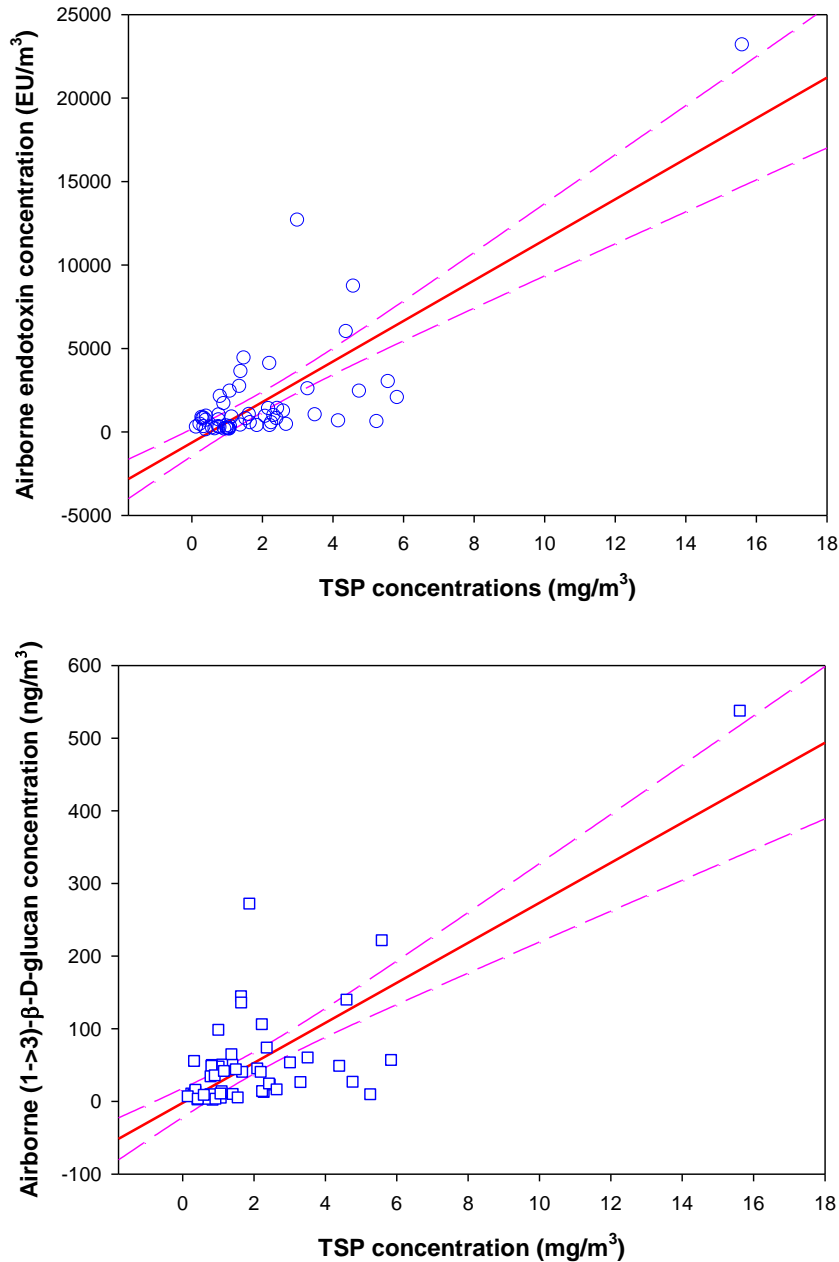


Figure 6.5. Airborne endotoxin/ (1→3)-β-D-glucan concentration versus TSP concentration.

6.3.5 Issues and limitations associated with this study

- Kinetic chromogenic LAL assays were used to determine the airborne endotoxin concentrations. However, as revealed by Reynolds et al. (2005), LAL assays are more suitable for comparing airborne endotoxin concentrations within similar environments, e.g., in the same type of animal confinement buildings, but are less suitable for a comparison between heterogeneous environments, e.g., between swine and poultry

buildings. Numerous environmental and experimental factors may change the measurement results, which makes an accurate quantification of endotoxin very difficult. GS/MS analysis on 3-hydroxylated fatty acids (3-OH FAs) (Laitinen et al., 2001; Liu et al., 2000; Mielniczuk et al., 1993) may be a better choice for future similar studies.

- A GlucateLL[®] Kit and a kinetic time-of-onset assay were used for quantification of (1→3)-β-D-glucan. However, this method has a very limited detection range (3.125- 100 ng/mL), leading to a great difficulty in sample dilution and analysis. An alternative method is to use GC/MS to quantify the concentration of ergosterol in PM samples. Ergosterol has been widely used a surrogate for fungal biomass (Lau et al., 2006; Robine et al., 2005). It is expected that a wet chemistry coupled with GC/MS method would offer improved linearity and reproducibility.
- In this study, TSP samples were collected on autoclaved glass fiber filters. However, autoclave may not be able to entirely eliminate endotoxin and (1→3)-β-D-glucan on blank filters because both compounds are heat-tolerant. Pre-baked quartz fiber filters may be a better option as the high baking temperature (around 600°C) can completely remove all organic matter.

6.4 Chapter Summary and Conclusions

6.4.1 Summary of observations

Airborne endotoxin and (1→3)-β-D-glucan have been associated with the occurrence of respiratory symptoms among animal farm workers, and potentially in neighboring communities. While efforts have been made to determine their concentrations at animal facilities, limited data have been available to date. To address this issue, this study monitored the airborne endotoxin and (1→3)-β-D-glucan concentrations in TSP samples from six different types of animal confinement buildings. The measurement results are expected to be useful for occupational exposure assessment and for evaluation of endotoxin and (1→3)-β-D-glucan emissions from animal confinement buildings, thus offering essential baseline data for the development of relevant regulations and control strategies. The key observations and findings from this chapter are listed as follows:

- The mean airborne endotoxin concentration in TSP samples was 508 ± 617 EU/m³ in farrowing, 510 ± 317 EU/m³ in gestation, 1971 ± 2816 EU/m³ in weaning, 978 ± 1285 EU/m³ in finishing, 2008 ± 4091 EU/m³ in manure-belt layer hen and 7377 ± 3044 EU/m³ in tom turkey buildings.
- The mean airborne endotoxin concentrations were significantly higher in tom turkey buildings than in farrowing, gestation and manure-belt layer hen buildings, and were significantly higher in finishing buildings than in farrowing buildings, and were significantly higher in poultry buildings than in swine buildings.
- The mean airborne (1→3)-β-D-glucan concentration in TSP samples was 21.2 ± 20.2 ng/m³ in farrowing, 25.2 ± 20.2 ng/m³ in gestation, 34.9 ± 48.4 ng/m³ in weaning, 32.7 ± 22.0 ng/m³ in finishing, 106.7 ± 98.3 ng/m³ in manure-belt layer hen and 121.0 ± 173.4 ng/m³ in tom turkey buildings.
- The mean airborne (1→3)-β-D-glucan concentrations were significantly higher in tom turkey and manure-belt layer hen buildings than in farrowing buildings, and were significantly higher in poultry buildings than in swine buildings.
- No significant difference in the content of endotoxin or (1→3)-β-D-glucan in TSP particles was observed among different animal building types.
- Season had no significant effect on airborne endotoxin or (1→3)-β-D-glucan concentrations but had a significant effect on the contents of endotoxin and (1→3)-β-D-glucan in particles, which in this study increased as the weather became warmer. A weak but significant correlation was present between the daily average ambient temperature and the endotoxin/ (1→3)-β-D-glucan content in particles.
- Feeding system, indoor air humidity and animal density had no significant effect on endotoxin and (1→3)-β-D-glucan levels.
- A significant correlation was present between TSP and airborne endotoxin/ (1→3)-β-D-glucan concentrations, suggesting a possibility of applying existing dust control strategies to these two bioactive agents.

6.4.2 Conclusions

Airborne endotoxin and (1→3)-β-D-glucan levels in TSP samples from six different types of animal confinement buildings were monitored with kinetic chromogenic LAL assays. Most measured airborne endotoxin concentrations exceeded the exposure limit proposed by Donham et al. (1995; 2000) and the threshold issued by the Dutch Health Council in the Netherlands, which may raise a health concern for farm workers as well as animals grown in confined environments.

The present study revealed that airborne endotoxin and (1→3)-β-D-glucan levels were influenced by animal building type and season. Specifically, animal building types had a significant effect on airborne endotoxin and (1→3)-β-D-glucan concentrations but had no significant effect on the contents of endotoxin and (1→3)-β-D-glucan in TSP particles. By contrast, seasons had no significant effect on the airborne concentrations of endotoxin and (1→3)-β-D-glucan but a significant effect on their contents in particles, which in this study increased with ambient temperature. Elevated indoor temperatures during the summer were considered to facilitate the growth and propagation of bacteria and fungi, thus leading to higher microbial contents in particles.

A significant and positive correlation was identified between TSP and airborne endotoxin/(1→3)-β-D-glucan concentrations, suggesting a possibility of applying dust control strategies for the mitigation of airborne endotoxins and (1→3)-β-D-glucans. Future studies are desirable to examine the size distribution of airborne endotoxin and (1→3)-β-D-glucan so as to offer essential data for assessing the performance of existing dust control strategies and for developing effective and affordable mitigation techniques specifically for airborne endotoxins and (1→3)-β-D-glucans.

7. CONCLUSIONS AND RECOMMENDATIONS

This dissertation is aimed at addressing a current difficulty in agricultural air quality research, i.e. lack of a comprehensive understanding of the physical, chemical and biological characteristics of PM from animal confinement buildings. TSP, PM₁₀ and PM_{2.5} samples were collected from a total of 18 animal confinement buildings in three different seasons, and were characterized in terms of mass concentration, inorganic elements, soluble ions, particle-borne odorants, airborne endotoxins and (1→3)-β-D-glucans. Essential data analyses were performed. The major observations and conclusions drawn from this dissertation, and the recommendations for future similar studies were summarized and are presented in this chapter.

7.1 Conclusions

- PM concentrations were significantly affected by animal building type, season (ambient temperature) and feeding system; while animal density had no significant effect. Specifically, higher PM concentrations occurred in poultry buildings than swine buildings; PM concentrations increased as ambient temperature decreased; and wet feeding systems were associated with lower TSP and PM₁₀ concentrations than dry feeding systems. A generalized linear model was established for estimating PM₁₀ concentrations in swine buildings with animal building type, daily average ambient temperature, specific fan area, animal density, and TSP concentration as predictors. The coefficient of determination (R^2) of the proposed model was 0.907.
- Some previous studies reported that FRM/FEM PM samplers oversample PM₁₀ and PM_{2.5} from agricultural sources, and accordingly proposed an indirect method that calculates PM₁₀ and PM_{2.5} concentrations from TSP concentrations and the PSD of TSP. The conclusion and the proposed calculation method were established based on several assumptions. The present study shows that when different assumptions are employed, substantially different conclusions and calculation results could be obtained. The PM₁₀ and PM_{2.5} concentrations derived from different particle size analyzers could be substantially different. Among the four analyzers under investigation, Aerosizer DSP produced the most comparable PM₁₀ concentrations to the gravimetric method.

- The inorganic elements and soluble ions in PM₁₀ and PM_{2.5} samples were quantified. Ca and K were the most abundant inorganic elements, followed by S and P. Mg, Na, Cl⁻, SO₄²⁻, NO₃⁻ and NH₄⁺ were also in abundance. The total mass fraction of identified chemical species was typically less than 16%. Compared to the concentrations of NH₃ gas (a few to tens of mg/m³) reported in the literature, this study suggests that the majority of emitted NH₃-N exists in the gas phase and the formation of NH₄⁺-containing secondary aerosols is insignificant in animal confinement buildings.
- The PM chemical composition varied significantly with animal building type. PM samples from certain different types of animal confinement buildings, e.g., manure-belt layer hen and tom turkey, had substantially different chemical compositions, indicating a possibility of applying receptor models to determining PM contributions by different animal building types. Compared to the PM₁₀ samples, the PM_{2.5} samples from different types of animal confinement buildings were more similar in terms of chemical composition. Seasons had no significant effect on PM₁₀ and a weak but significant effect on PM_{2.5} chemical compositions. The absence of strong seasonal variations in PM₁₀ chemical composition is a good news for applying receptor models for animal facilities involved PM source apportionment.
- Particle-borne odors carried on TSP and PM₁₀ samples from six different types of animal confinement buildings were investigated. A total of 57 odorants were identified and quantified. Acetic acid and ethanol were the most abundant odorants; phenylacetic acid and (E,E)-2,4-decadienal were found to be more odor-contributing, because of their low odor thresholds. Skatole and phenol were of less importance than previously reported in the literature. The total mass fraction of identified odorants was significantly higher in PM₁₀ (up to 46%) than in TSP and feed samples. Because of highly volatile contents in PM₁₀, TEOM may significantly underestimate PM₁₀ mass concentrations.
- The odorant composition of the TSP and PM₁₀ samples varied significantly with animal building type. Compared to the TSP samples, the PM₁₀ samples from different types of animal confinement buildings were more similar in both mass fraction- and OAV_P-based odorant compositions. The odorant composition of PM samples was also significantly affected by seasons. A gradual change in odorant composition was observed from hot to

mild to cold seasons. As a measure of odor intensity, the highest COI values occurred in cold seasons.

- The TSP and PM₁₀ samples had significantly different odorant compositions and significantly higher odorant contents than feed samples, suggesting that the majority of particle-borne odorants may originate from sources other than feed. Based on the ratio of COI, PM₁₀ samples contributed almost half of the odor strength of the TSP samples, indicating a key role of fine particles in the propagation of odors. Although PM was identified as an odor carrier, the majority of odorants may still exist in the gas phase rather than on particles.
- The airborne endotoxin and (1→3)-β-D-glucan levels in TSP samples were determined with kinetic chromogenic LAL assays. Most measured airborne endotoxin concentrations exceeded the exposure limit proposed by Donham et al. (1995; 2000) and the threshold issued by the Dutch Health Council in the Netherlands. This may raise a health concern for farm workers as well as animals grown in confined environments.
- The present study revealed that airborne endotoxin and (1→3)-β-D-glucan levels were influenced by animal building type and season. Specifically, animal building type had a significant effect on airborne endotoxin and (1→3)-β-D-glucan concentrations but had no significant effect on the contents of endotoxin and (1→3)-β-D-glucan in TSP particles. By contrast, seasons had no significant effect on the airborne concentrations of endotoxin and (1→3)-β-D-glucan but a significant effect on their contents in particles, which in this study increased with ambient temperature. Elevated indoor temperatures during the summer were considered to facilitate the growth and propagation of bacteria and fungi, thus leading to higher microbial contents in particles.
- A significant and positive correlation was identified between TSP and airborne endotoxin/ (1→3)-β-D-glucan concentrations, suggesting a possibility of applying dust control strategies for airborne endotoxins and (1→3)-β-D-glucans.

7.2 Recommendations

- Future studies should consider increasing the number of sampling sites and field trips to improve the data representativeness, or focusing on one to a few animal confinement buildings and carrying out long-term continuous monitoring.
- Chicken broiler buildings should be included in the sampling effort, considering the large scale and potential environmental effects of the broiler industry.
- FRM/FEM PM₁₀ and PM_{2.5} samples are recommended for future similar studies. Particularly, a VSCCTM cyclone-based sampler should be used for PM_{2.5} sampling because of its better tolerance to high dust loading.
- The use of Teflon filters or Teflon-coated glass fiber filters are recommended for PM mass measurement to reduce potential sampling artifacts.
- There is a great need to develop a protocol or guideline to standardize PM sampling operations in animal buildings, e.g., the selection of sampling points.
- A microbalance with readability of 1 µg or 0.1 µg is recommended for PM mass measurement.
- More information should be recorded, such as animal activity, room lighting, cleanliness, diurnal variations in indoor and outdoor temperature and humidity, wind speed, precipitation and solar irradiation. Also, it would be advantageous to measure the ventilation rate, monitor upwind and downwind PM, and collect manure and soil samples for essential comparison.
- A mixed acid of HNO₃ and HF and a microwave digestion method are recommended for future ICP analysis to improve the recovery efficiency of inorganic elements, especially refractory elements such as Si, Ti and Zn.
- A more sensitive IC system is recommended for quantification of SO₄²⁻ and NO₃⁻.
- A measurement of OC/EC is recommended for PM chemical speciation. If no OC/EC measurement is available, at least parts of the PM samples should be sent for C, H and N analysis. This may help in the reconstruction of the PM mass. For similar reasons, it would be better to measure inorganic carbon (CO₃²⁻).

- Nylon filters are recommended for collecting PM samples for ion analysis. A denuder is suggested to be installed upstream of the Nylon filter to minimize potential positive sampling artifacts due to the adsorption of NH_3 gas on the filters.
- To address the research need raised by NAS (2003), future efforts should be made to apply receptor models to animal production related air quality problems, and to compare receptor models with dispersion models to assess their respective advantages and limitations.
- Future characterizations of particle-borne odors should include sulfur-containing compounds since they are major contributors to animal-related odors.
- Odorants carried on $\text{PM}_{2.5}$ samples should better be investigated.
- A sampling system illustrated in Figure 5.17 is recommended for collecting PM samples for odor analysis.
- It would be of great interest to simultaneously measure the concentrations of gas-phase and particle-borne odorants and conduct a direct comparison.
- For airborne endotoxin and (1→3)- β -D-glucan measurement, it was found to be better to use the same type of filters for sample collection. Quartz fiber filters are recommended.
- Due to the limitation of LAL assays, a wet chemistry coupled with GC/MS method is recommended for assessing the level of endotoxin and (1→3)- β -D-glucan contamination.
- Future studies are desired to examine the size distribution of airborne endotoxins and (1→3)- β -D-glucans so as to offer essential data for assessing the performance of existing dust control strategies, and for developing effective and affordable mitigation techniques specifically for airborne endotoxins and (1→3)- β -D-glucans.

REFERENCES

- ACGIH. 1985. Particle size-selective sampling in the workplace: Report of the ACGIH technical committee on air sampling procedure. Publication No. 830. Cincinnati, OH: American Conference of Industrial Hygienists.
- ACGIH. 1989. Step Two: On-site investigation. Committee on Bioaerosols, eds. In *Guidelines for the Assessment of Bioaerosols in the Indoor Environment*. Cincinnati, OH: American Conference of Industrial Hygienists.
- ACGIH. 2000. *Threshold Limit Values for Chemical Substances and Physical Agents and Biological Exposure Indices*. Cincinnati, OH: American Conference of Governmental Industrial Hygienists.
- Acree, T. and H. Arn. 2004. Flavornet. Available at: <http://www.favornet.org/favor-net.html>. Assessed 12 March 2010.
- AIHA. 1989. *Odor Thresholds for Chemicals with Established Occupational Health Standards*. Fairfax, VA: American Industrial Hygiene Association.
- Almuhanna, E. A. 2007. Dust control in livestock buildings with electrostatically-charged water spray. PhD diss. Manhattan, Kansas: Kansas State University, Department of Biological and Agricultural Engineering.
- Anderson, W. B., R. M. Slawson, and C. I. Mayfield. 2002. A review of drinking-water-associated endotoxin, including potential routes of human exposure. *Canadian Journal of Microbiology*. 48(7): 567-587.
- Anderson, W. B., C. I. Mayfield, D. G. Dixon, and P. M. Huck. 2003. Endotoxin inactivation by selected drinking water treatment oxidants. *Water Research*. 37(19): 4553-4560.
- Aneja, V. P., P. A. Roelle, G. C. Murray, J. Southerland, J. W. Erisman, D. Fowler, W. A. H. Asman, and N. Patni. 2001. Atmospheric nitrogen compounds ii: Emissions, transport, transformation, deposition and assessment. *Atmospheric Environment*. 35(11): 1903-1911.
- Armand-Lefevre, L., R. Ruimy, and A. Andreumont. 2005. Clonal comparison of *Staphylococcus aureus* isolates from healthy pig farmers, human controls, and pigs. *Emerging Infectious Diseases*. 11(5): 711-714.
- Arogo, J., P. W. Westerman, and A. J. Heber. 2003. A review of ammonia emissions from confined swine feeding operations. *Transactions of the ASAE*. 46(3): 805-817.
- Artaxo, P., J. V. Martins, M. A. Yamasoe, A. S. Procopio, T. M. Pauliquevis, M. O. Andreae, P. Guyon, L. V. Gatti, and A. M. C. Leal. 2002. Physical and chemical properties of aerosols in the wet and dry seasons in Rondonia, Amazonia. *Journal of Geophysical Research-Atmospheres*. 107(D20): -.

- Attwood, P., R. Brouwer, P. Ruigewaard, P. Versloot, R. Dewit, D. Heederik, and J. S. M. Boleij. 1987. A study of the relationship between airborne contaminants and environmental-factors in Dutch swine confinement buildings. *American Industrial Hygiene Association Journal*. 48(8): 745-751.
- Babich, P., M. Davey, G. Allen, and P. Koutrakis. 2000. Method comparisons for particulate nitrate, elemental carbon, and PM_{2.5} mass in seven US cities. *Journal of the Air & Waste Management Association*. 50(7): 1095-1105.
- Bah, A. R., O. Kravchuk, and G. Kirchhof. 2009. Fitting performance of particle-size distribution models on data derived by conventional and laser diffraction techniques. *Soil Science Society of America Journal*. 73(4): 1101-1107.
- Banhazi, T. M., J. Seedorf, M. Laffrique, and D. L. Rutley. 2008. Identification of the risk factors for high airborne particle concentrations in broiler buildings using statistical modeling. *Biosystems Engineering*. 101(1): 100-110.
- Barthelmie, R. J., and S. C. Pryor. 1998. Implications of ammonia emissions for fine aerosol formation and visibility impairment - a case study from the lower Fraser valley, British Columbia. *Atmospheric Environment*. 32(3): 345-352.
- Battye, R., W. Battye, C. Overcash, and S. Fudge. 1994. Development and selection of ammonia emission factors- project summary. EPA/600/SR-94/190. Research Triangle Park, NC: United States Environmental Protection Agency.
- Benson, J. M., D. G. Burt, Y. S. Cheng, F. F. Hahn, P. J. Haley, R. F. Henderson, C. H. Hobbs, J. A. Pickrell, and J. K. Dunnick. 1989. Biochemical responses of rat and mouse lung to inhaled nickel compounds. *Toxicology*. 57(3): 255-266.
- Berges, M. G. M., and P. J. Crutzen. 1996. Estimates of global N₂O emissions from cattle, pig and chicken manure, including a discussion of CH₄ emissions. *Journal of Atmospheric Chemistry*. 24(3): 241-269.
- Berti, W. R., and L. W. Jacobs. 1996. Chemistry and phytotoxicity of soil trace elements from repeated sewage sludge applications. *Journal of Environmental Quality*. 25(5): 1025-1032.
- Biegalski, S. R., and S. Landsberger. 1995. Improved detection limits for trace-elements on aerosol filters using Compton suppression counting and epithermal irradiation techniques. *Journal of Radioanalytical and Nuclear Chemistry-Articles*. 192(2): 195-204.
- Bingham, F. T. 1979. Bioavailability of Cd to food crops in relation to heavy-metal content of sludge-amended soil. *Environmental Health Perspectives*. 28(FEB): 39-43.
- Binkowski, F. S. 1999. Chapter 10: Aerosols in Models-3 CMAQ. In *Science Algorithms of the EPA Model-3 Community Multiscale Air Quality (CMAQ) Modeling System*. Byun, D.W. and Ching, J.K.S, ed. Cincinnati, OH: United States Environmental Protection Agency.

- Blanes-Vidal, V., M. N. Hansen, S. Pedersen, and H. B. Rom. 2008. Emissions of ammonia, methane and nitrous oxide from pig houses and slurry: Effects of rooting material, animal activity and ventilation flow. *Agriculture Ecosystems & Environment*. 124(3-4): 237-244.
- Blunden, J., V. P. Aneja, and P. W. Westerman. 2008. Measurement and analysis of ammonia and hydrogen sulfide emissions from a mechanically ventilated swine confinement building in North Carolina. *Atmospheric Environment*. 42(14): 3315-3331.
- Bonlokke, J. H., A. Meriaux, C. Duchaine, S. Godbout, and Y. Cormier. 2009. Seasonal variations in work-related health effects in swine farm workers. *Annals of Agricultural and Environmental Medicine*. 16(1): 43-52.
- Bottcher, R. W. 2001. An environmental nuisance: Odor concentrated and transported by dust. *Chemical Senses*. 26(3): 327-331.
- Bottcher, R. W., K. M. Keener, R. D. Munilla, G. L. van Wicklen, and K. E. Parbst. 1999. Field evaluation of a wet pad scrubber for controlling dust and odor emissions. In *ASAE/CSAE-SCGR Annual International Meeting*, 7-. Toronto, Ontario, Canada: American Society of Agricultural Engineers.
- Brendemuhl, J., and B. Myer. 2009. Types of swine diets. Gainesville, FL: University of Florida, IFAS Extension
- Brunekreef, B., and S. T. Holgate. 2002. Air pollution and health. *Lancet*. 360(9341): 1233-1242.
- Bullers, S. 2005. Environmental stressors, perceived control, and health: The case of residents near large-scale hog farms in eastern North Carolina. *Human Ecology*. 33(1): 1-16.
- Bundy, D. S. 1992. Odor issues with wastes. In *National Livestock, Poultry and Aquaculture Waste Management*. ASAE Publication No. 03-92, 288-292. St. Joseph, Michigan: American Society of Agricultural Engineers.
- Bunton, B., P. O'Shaughnessy, S. Fitzsimmons, J. Gering, S. Hoff, M. Lyngbye, P. S. Thorne, J. Wasson, and M. Werner. 2007. Monitoring and modeling of emissions from concentrated animal feeding operations: Overview of methods. *Environmental Health Perspectives*. 115(2): 303-307.
- Burnett, W. E. 1969. Odor transport by particulate matter in high density poultry houses. *Poultry Science*. 48(1): 182-185.
- Burns, R., H. Li, L. Moody¹, H. Xin, R. Gates, D. Overhults, and D. Earnest. 2008. Quantification of particulate emissions from broiler houses in the southeastern United States. In *The 8th International Livestock Symposium (ILES VIII)*. Iguassu Falls, Brazil: American Society of Agricultural and Biological Engineers.
- Buser, M. D. 2004. Errors associated with particulate matter measurements on rural sources: Appropriate basis for regulating cotton gins. PhD Diss. College Station, TX: Texas A&M University, Department of Agricultural and Biological Engineering.

- Buser, M. D., C. B. Parnell, B. W. Shaw, and E. Lacey. 2007a. Particulate matter sampler errors due to the interaction of particle size and sampler performance characteristics: Ambient PM₁₀ samplers. *Transactions of the ASABE*. 50(1): 229-240.
- Buser, M. D., C. B. Parnell, B. W. Shaw, and R. E. Lacey. 2007b. Particulate matter sampler errors due to the interaction of particle size and sampler performance characteristics: Ambient PM_{2.5} samplers. *Transactions of the ASABE*. 50(1): 241-254.
- Buser, M. D., C. B. Parnell, B. W. Shaw, and R. E. Lacey. 2007c. Particulate matter sampler errors due to the interaction of particle size and sampler performance characteristics: Background and theory. *Transactions of the ASABE*. 50(1): 221-228.
- Buser, M. D., J. D. Wanjura, D. P. Whitelock, S. C. Capareda, B. W. Shaw, and R. E. Lacey. 2008. Estimating FRM PM₁₀ sampler performance characteristics using particle size analysis and collocated tsp and PM₁₀ samplers: Cotton gins. *Transactions of the ASABE*. 51(2): 695-702.
- Butera, M., J. H. Smith, W. D. Morrison, R. R. Hacker, F. A. Kains, and J. R. Ogilvie. 1991. Concentration of respirable dust and bioaerosols and identification of certain microbial types in a hog-growing facility. *Canadian Journal of Animal Science*. 71(2): 271-277.
- Cai, L. S., J. A. Koziel, Y. C. Lo, and S. J. Hoff. 2006. Characterization of volatile organic compounds and odorants associated with swine barn particulate matter using solid-phase microextraction and gas chromatography-mass spectrometry-olfactometry. *Journal of Chromatography A*. 1102(1-2): 60-72.
- Cai, L. S., S. C. Zhang, J. A. Koziel, G. Sun, K. Y. Heathcote, S. J. Hoff, D. B. Parker, E. A. Caraway, L. D. Jacobson, N. Akdeniz, B. P. Hetchler, E. L. Cortus, S. D. Bereznicki, and A. J. Heber. 2010. Odor and odorous chemical emissions from animal buildings: Part 3-chemical emissions. ASABE Publication No. 711p0510cd. In *the International Symposium on Air Quality and Manure Management for Agriculture*. Dallas, TX: American Society of Agricultural and Biological Engineers.
- Cambra-Lopez, M., A. J. A. Aarnink, Y. Zhao, S. Calvet, and A. G. Torres. 2010. Airborne particulate matter from livestock production systems: A review of an air pollution problem. *Environmental Pollution*. 158(1): 1-17.
- Cao, Z. D., L. J. Wang, Z. F. Liu, Q. F. Li, and D. B. Beasley. 2009. Particle size distribution of particulate matter emitted from a layer operation in southeast U.S.. ASABE Paper No. 090025. St. Joseph, MI: American Society of Agricultural and Biological Engineers.
- CEN. 2000. 14031: Workplace atmosphere- determination of airborne endotoxin. Brussels, Belgium: European Committee for Standardization.
- CEN. 2003. Air quality: Determination of odor concentration by dynamic olfactometry; European Standard-EN13725. Brussels, Belgium: European Committee for Standardization.

- CFR. 1987. Subpart D- procedures for testing performance characteristics of methods for PM₁₀. CFR 40: Part 53 of the Code of Federal Regulations.
- CFR. 1997. Subpart F- procedures for testing performance characteristics of class ii equivalent methods for PM_{2.5}. CFR 40: Part 53 of the Code of Federal Regulations.
- CFR. 2001a. Appendix J- Reference method for the determination of particulate matter as PM₁₀ in the atmosphere. CFR 40: Part 50 of the Code of Federal Regulations.
- CFR. 2001b. Ambient air monitoring reference and equivalent methods. CFR 40: Part 53 of the Code of Federal Regulations.
- CFR. 2001c. Appendix L- Reference method for the determination of particulate matter as PM_{2.5} in the atmosphere. CFR 40: Part 50 of the Code of Federal Regulations.
- CFR. 2005. Appendix W- Revision to the guideline on air quality models: Adoption of a preferred general purpose (flat and complex terrain) dispersion model and other revisions; final rule. CFR 40: Part 51 of the Code of Federal Regulations.
- Chai, M., M. Lu, T. Keener, S. J. Khang, C. Chaiwatpongsakorn, and J. Tisch. 2009. Using an improved electrostatic precipitator for poultry dust removal. *Journal of Electrostatics*. 67(6): 870-865.
- Chang, C. W., H. Chung, C. F. Huang, and H. J. J. Su. 2001. Exposure assessment to airborne endotoxin, dust, ammonia, hydrogen sulfide and carbon dioxide in open style swine houses. *Annals of Occupational Hygiene*. 45(6): 457-465.
- Chao, C. Y., and E. C. Cheng. 2002. Source apportionment of indoor PM_{2.5} and PM₁₀ in homes. *Indoor and Built Environment*. 11(1): 27-37.
- Chapin, A., A. Rule, K. Gibson, T. Buckley, and K. Schwab. 2005. Airborne multidrug-resistant bacteria isolated from a concentrated swine feeding operation. *Environmental Health Perspectives*. 113(2): 137-142.
- Charron, A., R. M. Harrison, S. Moorcroft, and J. Booker. 2004. Quantitative interpretation of divergence between PM_{2.5} and PM₁₀ mass measurement by TEOM and gravimetric (Partisol) instruments. *Atmospheric Environment*. 38(3): 415-423.
- Chen, Y., Y. Zhang, and E. M. Barber. 1995. A new mathematical model of particle size distribution for swine building dust. *ASHRAE Transactions*. 101(2): 1169-1178.
- Chiba, L. I., E. R. Peo, A. J. Lewis, M. C. Brumm, R. D. Fritschen, and J. D. Crenshaw. 1985. Effect of dietary-fat on pig performance and dust levels in modified-open-front and environmentally regulated confinement buildings. *Journal of Animal Science*. 61(4): 763-781.
- Chimidza, S., A. Viksna, and E. S. Lindgren. 2001. EDXRF and TXRF analysis of aerosol particles and the mobile fraction of soil in Botswana. *X-Ray Spectrometry*. 30(5): 301-307.

- Chmielowiec-Korzeniowska, A. 2009. The concentration of volatile organic compounds (VOCs) in pig farm air. *Annals of Agricultural and Environmental Medicine*. 16(2): 249-256.
- Choi, M. S., D. S. Lee, J. C. Choi, H. J. Cha, and H. I. Yi. 2006. Pu²³⁹⁺²⁴⁰ concentration and isotope ratio (Pu-240/Pu-239) in aerosols during high dust (yellow sand) period, Korea. *Science of the Total Environment*. 370(1): 262-270.
- Chow, J. C., and J. G. Watson. 1999. Ion chromatography in elemental analysis of airborne particles. In *Elemental Analysis of Airborne Particles*. S. Landsberger and M. Creatchman, eds. Amsterdam, The Netherlands: Gordon and Breach Science Publishers.
- Clark, S., R. Rylander, and L. Larsson. 1983. Airborne bacteria, endotoxin and fungi in dust in poultry and swine confinement buildings. *American Industrial Hygiene Association Journal*. 44(7): 537-541.
- Clarke, K. R. 1993. Nonparametric multivariate analyses of changes in community structure. *Australian Journal of Ecology*. 18(1): 117-143.
- Cohen, D. D. 1999. Accelerator based ion beam techniques for trace element aerosol analysis. In *Elemental Analysis of Airborne Particles*. S. Landsberger and M. Creatchman, eds. Amsterdam, The Netherlands: Gordon and Breach Science Publishers.
- Costa, A., and M. Guarino. 2009. Definition of yearly emission factor of dust and greenhouse gases through continuous measurements in swine husbandry. *Atmospheric Environment*. 43(8): 1548-1556.
- Costa, A., M. Guardino, M. Porro, and P. Navarotto. 2007. Evaluation of PM₁₀ emission from farrowing and fattening swine rooms by continuous on-line measurements. *Rivista di Ingegneria Agraria*. 38(1): 59-64.
- Coulter, C. T. 2004. EPA-CMB8.2 users manual. USEPA Technical Report No. EPA-452/R-04-011. Research Triangle Park, NC: United States Environmental Protection Agency.
- Cox, C. S., and C. M. Wathes. 1995. *Bioaerosols Handbook*. Boca Raton, FL: Lewis Publishers/CRC Press.
- Criss, J. W. 1976. Particle-size and composition effects in X-ray-fluorescence analysis of pollution samples. *Analytical Chemistry*. 48(1): 179-186.
- Curtis, S. E., J. G. Drummond, D. J. Grunloh, P. B. Lynch, and A. H. Jensen. 1975. Relative and qualitative aspects of aerial bacteria and dust in swine houses. *Journal of Animal Science*. 41(5): 1512-1520.
- Cyrys, J., M. Stolzel, J. Heinrich, W. G. Kreyling, N. Menzel, K. Wittmaack, T. Tuch, and H. E. Wichmann. 2003. Elemental composition and sources of fine and ultrafine ambient particles in Erfurt, Germany. *Science of the Total Environment*. 305(1-3): 143-156.

- Das, K. C., J. R. Kastner, and S. M. Hassan. 2004. Potential of particulate matter as a pathway for odor dispersion. ASABE Paper No. 044125. St. Joseph, MI: American Society of Agricultural and Biological Engineers.
- Davies, C. N. 1968. Entry of aerosols into sampling tubes and heads. *Journal of Physics D-Applied Physics*. 1(7): 921-&.
- Davis, D. W., R. L. Reynolds, G. C. Tsou, and L. Zafonte. 1977. Filter attenuation corrections for X-ray-fluorescence analysis of atmospheric aerosols. *Analytical Chemistry*. 49(13): 1990-1993.
- Day, D. L. 1988. *Livestock Manure Management: Text & Reference Book*. Urbana IL: Agricultural Engineering Department, University of Illinois at Urbana-Champaign.
- Day, D. L., E. L. Hansen, and S. Anderson. 1965. Gases and odors in confinement swine buildings. *Transactions of the ASAE*. 8: 118-121.
- Defelippe, J., M. D. E. Silva, F. M. B. Maciel, A. D. Soares, and N. F. Mendes. 1993. Infection prevention in patients with severe multiple trauma with the immunomodulator beta-1-3 polyglucose (glucan). *Surgery Gynecology & Obstetrics*. 177(4): 383-388.
- Demokritou, P., S. J. Lee, S. T. Ferguson, and P. Koutrakis. 2004. A compact multistage (cascade) impactor for the characterization of atmospheric aerosols. *Journal of Aerosol Science*. 35(3): 281-299.
- Dentener, F. J., and P. J. Crutzen. 1994. A 3-dimensional model of the global ammonia cycle. *Journal of Atmospheric Chemistry*. 19(4): 331-369.
- Devos, M., F. Patte, J. Rouault, P. Laffort, and L. J. Van Gemert. 1990. *Standardized Human Olfactory Thresholds*. New York, USA: Oxford University Press.
- Dlugokencky, E. J., L. P. Steele, P. M. Lang, and K. A. Masarie. 1994. The growth-rate and distribution of atmospheric methane. *Journal of Geophysical Research-Atmospheres*. 99(D8): 17021-17043.
- Donham, K., P. Haglind, Y. Peterson, R. Rylander, and L. Belin. 1989. Environmental and health studies of farm-workers in Swedish swine confinement buildings. *British Journal of Industrial Medicine*. 46(1): 31-37.
- Donham, K. J. 1986. Hazardous agents in agricultural dusts and methods of evaluation. *American Journal of Industrial Medicine*. 10(3): 205-220.
- Donham, K. J. 1990. Health-effects from work in swine confinement buildings. *American Journal of Industrial Medicine*. 17(1): 17-25.
- Donham, K. J., D. C. Zavala, and J. A. Merchant. 1984a. Respiratory symptoms and lung-function among workers in swine confinement buildings - a cross-sectional epidemiological-study. *Archives of Environmental Health*. 39(2): 96-101.

- Donham, K. J., D. C. Zavala, and J. Merchant. 1984b. Acute effects of the work-environment on pulmonary functions of swine confinement workers. *American Journal of Industrial Medicine*. 5(5): 367-375.
- Donham, K. J., D. Cumro, and S. Reynolds. 2002. Synergistic effects of dust and ammonia on the occupational health effects of poultry workers. *Journal of Agromedicine*. 8(2): 57-76.
- Donham, K. J., M. Rubino, T. D. Thedell, and J. Kammermeyer. 1977. Potential health-hazards to agricultural-workers in swine confinement buildings. *Journal of Occupational and Environmental Medicine*. 19(6): 383-387.
- Donham, K. J., P. Haglind, Y. Peterson, and R. Rylander. 1986a. Environmental and health studies in swine confinement buildings. *American Journal of Industrial Medicine*. 10(3): 289-293.
- Donham, K. J., D. Cumro, S. J. Reynolds, and J. A. Merchant. 2000. Dose-response relationships between occupational aerosol exposures and cross-shift declines of lung function in poultry workers: Recommendations for exposure limits. *Journal of Occupational and Environmental Medicine*. 42(3): 260-269.
- Donham, K. J., L. J. Scallon, W. Popendorf, M. W. Treuhaft, and R. C. Roberts. 1986b. Characterization of dusts collected from swine confinement buildings. *American Industrial Hygiene Association Journal*. 47(7): 404-410.
- Donham, K. J., S. J. Reynolds, P. Whitten, J. A. Merchant, L. Burmeister, and W. J. Popendorf. 1995. Respiratory dysfunction in swine production facility workers- dose-response relationships of environmental exposures and pulmonary-function. *American Journal of Industrial Medicine*. 27(3): 405-418.
- Donham, K. J., S. Wing, D. Osterberg, J. L. Flora, C. Hodne, K. M. Thu, and P. S. Thorne. 2007. Community health and socioeconomic issues surrounding concentrated feeding operations. *Environmental Health Perspectives*. 115(2): 317-320.
- Douwes, J. 2005. (1-> 3)-beta-d-glucans and respiratory health: A review of the scientific evidence. *Indoor Air*. 15(3): 160-169.
- Douwes, J., P. Thorne, N. Pearce, and D. Heederik. 2003. Bioaerosol health effects and exposure assessment: Progress and prospects. *Annals of Occupational Hygiene*. 47(3): 187-200.
- Douwes, J., P. Versloot, A. Hollander, D. Heederik, and G. Doekes. 1995. Influence of various dust sampling and extraction methods on the measurement of airborne endotoxin. *Applied and Environmental Microbiology*. 61(5): 1763-1769.
- Douwes, J., G. Doekes, R. Montijn, D. Heederik, and B. Brunekreef. 1996. Measurement of beta(1->3)-glucans in occupational and home environments with an inhibition enzyme immunoassay. *Applied and Environmental Microbiology*. 62(9): 3176-3182.

- Douwes, J., A. Zuidhof, G. Doekes, S. van der Zee, I. Wouters, H. M. Boezen, and B. Brunekreef. 2000. (1-> 3)-beta-d-glucan and endotoxin in house dust and peak flow variability in children. *American Journal of Respiratory and Critical Care Medicine*. 162(4): 1348-1354.
- Dravnieks, A. 1985. *Atlas of Odor Character Profiles*. Philadelphia, PA: American Society for Testing and Materials.
- Duchaine, C., Y. Grimard, and Y. Cormier. 2000. Influence of building maintenance, environmental factors, and seasons on airborne contaminants of swine confinement buildings. *American Industrial Hygiene Association Journal*. 61(1): 56-63.
- Duchaine, C., P. S. Thorne, A. Meriaux, Y. Grimard, P. Whitten, and Y. Cormier. 2001. Comparison of endotoxin exposure assessment by bioaerosol impinger and filter-sampling methods. *Applied and Environmental Microbiology*. 67(6): 2775-2780.
- Dzubay, T. G., and R. O. Nelson. 1975. Self absorption corrections for x-ray fluorescence analysis of aerosols. In *Advances in X-ray Analysis*, 619-631 New York: Plenum Publishing Corporation.
- El-Zanan, H. S., D. H. Lowenthal, B. Zielinska, J. C. Chow, and N. Kumar. 2005. Determination of the organic aerosol mass to organic carbon ratio in IMPROVE samples. *Chemosphere*. 60(4): 485-496.
- Engstad, C. S., R. E. Engstad, J. O. Olsen, and B. Osterud. 2002. The effect of soluble beta-1,3-glucan and lipopolysaccharide on cytokine production and coagulation activation in whole blood. *International Immunopharmacology*. 2(11): 1585-1597.
- Espinosa, A. J. F., M. T. Rodriguez, F. J. B. de la Rosa, and J. C. J. Sanchez. 2002. A chemical speciation of trace metals for fine urban particles. *Atmospheric Environment*. 36(5): 773-780.
- Etzler, F. M., and M. S. Sanderson. 1995. Particle size analysis: A comparative study of various methods. *Particle & Particle Systems Characterization*. 12(5): 217-224.
- EUR-Lex. 2004. Directive 2004/42/ce of the European parliament and of the council: EUR-Lex. Available at: http://eur-lex.europa.eu/smartapi/cgi/sga_doc?smartapi!cele-xapi!prod!CELEXnumdoc&numdoc=32004L0042&model=guichett&lg=en. Assessed 10 August 2010.
- Faulkner, W. B., J. J. Powell, J. M. Lange, B. W. Shaw, R. E. Lacey, and C. B. Parnell. 2007. Comparison of dispersion models for ammonia emissions from a ground-level area source. *Transactions of the ASABE*. 50(6): 2189-2197.
- Favez, O., H. Cachier, J. Sciare, and Y. Le Moullec. 2007. Characterization and contribution to PM_{2.5} of semi-volatile aerosols in Paris (France). *Atmospheric Environment*. 41(36): 7969-7976.
- Fazzalari, F. A. 1978. *Compilation of Odor and Taste Threshold Values Data*. Philadelphia, PA: American Society for Testing and Materials.

- FDA. 2003. Class II special controls guidance document: Endotoxin assay. Rockville, MD: United States Food and Drug Administration.
- Feddes, J. J. R., H. Cook, and M. J. Zuidhof. 1992. Characterization of airborne dust particles in turkey housing. *Canadian Agricultural Engineering*. 34(3): 273-280.
- Fogelmark, B., H. Goto, K. Yuasa, B. Marchat, and R. Rylander. 1992. Acute pulmonary toxicity of inhaled beta-1,3-glucan and endotoxin. *Agents and Actions*. 35(1-2): 50-56.
- FR. 1987. Revisions to the national ambient air quality standards for particulate matter: 40 CFR part 51 and 52., 24634-24669. Federal Register, ed. 52.
- Gallmann, E., G. Brose, E. Hartung, and T. Jungbluth. 2001. Influence of different pig housing systems on odor emissions. *Water Science and Technology*. 44(9): 237-244.
- Gast, R. M., and D. S. Bundy. 1986. Control of feed dusts by adding oils. ASAE Paper No. 864039. St. Joseph, MI.: American Society of Agricultural Engineers.
- Gates, R. S., H. Xin, K. D. Casey, Y. Liang, and E. F. Wheeler. 2005. Method for measuring ammonia emissions from poultry houses. *Journal of Applied Poultry Research*. 14(3): 622-634.
- Gay, S. W., D. R. Schmidt, C. J. Clanton, K. A. Janni, L. D. Jacobson, and S. Weisberg. 2003. Odor, total reduced sulfur, and ammonia emissions from animal housing facilities and manure storage units in Minnesota. *Applied Engineering in Agriculture*. 19(3): 347-360.
- Gehrig, R., C. Hueglin, B. Schwarzenbach, T. Seitz, and B. Buchmann. 2005. A new method to link PM₁₀ concentrations from automatic monitors to the manual gravimetric reference method according to en12341. *Atmospheric Environment*. 39(12): 2213-2223.
- Gehring, U., J. Heinrich, G. Hoek, M. Giovannangelo, E. Nordling, T. Bellander, J. Gerritsen, J. C. de Jongste, H. A. Smit, H. E. Wichmann, M. Wickman, and B. Brunekreef. 2007. Bacteria and mould components in house dust and children's allergic sensitisation. *European Respiratory Journal*. 29(6): 1144-1153.
- Gilchrist, M. J., C. Greko, D. B. Wallinga, G. W. Beran, D. G. Riley, and P. S. Thorne. 2007. The potential role of concentrated animal feeding operations in infectious disease epidemics and antibiotic resistance. *Environmental Health Perspectives*. 115(2): 313-316.
- Gladding, T., J. Thorn, and D. Stott. 2003. Organic dust exposure and work-related effects among recycling workers. *American Journal of Industrial Medicine*. 43(6): 584-591.
- Gomes, A. M., J. P. Sarrette, L. Madon and A. Almi. 1996. Continuous emission monitoring of metal aerosol concentrations in atmospheric air. *Spectrochimica Acta Part B-Atomic Spectroscopy*. 51(13): 1695-1705.

- Green, D., G. Fuller, and B. Barratt. 2001. Evaluation of TEOM (tm) 'correction factors' for assessing the EU stage 1 limit values for PM₁₀. *Atmospheric Environment*. 35(14): 2589-2593.
- Grohse, P. M. 1999. Trace element analysis of airborne particles by atomic absorption spectroscopy, inductively coupled plasma- atomic emission spectroscopy, and inductively coupled plasma- mass spectrometry. In *Elemental Analysis of Airborne Particles*. S. Landsberger and M. Creatchman, eds. Amsterdam, The Netherlands: Gordon and Breach Science Publishers.
- Guo, H., L. D. Jacobson, D. R. Schmidt, and R. E. Nicolai. 2001. Calibrating INPUFF-2 model by resident-panelists for long-distance odor dispersion from animal production sites. *Applied Engineering in Agriculture*. 17(6): 859-868.
- Gutknecht, W. F., J. B. Flanagan, and A. McWilliams. 2006. Harmonization of interlaboratory X-ray fluorescence measurement uncertainties. Research Triangle Park, NC: RTI International
- Haeussermann, A., A. Costa, J. M. Aerts, E. Hartung, T. Jungbluth, M. Guarino, and D. Berckmans. 2008. Development of a dynamic model to predict PM₁₀ emissions from swine houses. *Journal of Environmental Quality*. 37(2): 557-564.
- Hammond, E. G., C. Fedler, and G. Junk. 1979. Identification of dust-born odors in swine confinement facilities. *Transactions of the ASAE*. 22(5): 1186-&.
- Hammond, E. G., C. Fedler, and R. J. Smith. 1981. Analysis of particle-borne swine house odors. *Agriculture and Environment*. 6(4): 395-401.
- Hamscher, G., H. T. Pawelzick, S. Sczesny, H. Nau, and J. Hartung. 2003. Antibiotics in dust originating from a pig-fattening farm: A new source of health hazard for farmers? *Environmental Health Perspectives*. 111(13): 1590-1594.
- Hanna, S. R., B. A. Egan, and J. Purdum. 2001. Evaluation of the ADMS, AERMOD, and ISC3 dispersion models with the Optex, Duke forest, Kincaid, Indianapolis and Lovett field datasets. *International Journal of Environment and Pollution*. 16(1-6): 301-314.
- Harper, L. A., T. K. Flesch, J. M. Powell, W. K. Coblenz, W. E. Jokela, and N. P. Martin. 2009. Ammonia emissions from dairy production in Wisconsin. *Journal of Dairy Science*. 92(5): 2326-2337.
- Hartung, J. 1985. Gas-chromatographic analysis of volatile fatty-acids and phenolic indolic compounds in pig house dust after ethanolic extraction. *Environmental Technology Letters*. 6(1): 21-30.
- Hartung, J., and V. R. Phillips. 1994. Control of gaseous emissions from livestock buildings and manure stores. *Journal of Agricultural Engineering Research*. 57(3): 173-189.

- Hayes, E. T., T. P. Curran, and V. A. Dodd. 2006. A dispersion modeling approach to determine the odor impact of intensive poultry production units in Ireland. *Bioresource Technology*. 97(15): 1773-1779.
- Hazama, S., S. Watanabe, M. Ohashi, M. Yagi, M. Suzuki, K. Matsuda, T. Yamamoto, Y. Suga, T. Suga, S. Nakazawa, and M. Oka. 2009. Efficacy of orally administered superfine dispersed lentinan (beta-1,3-glucan) for the treatment of advanced colorectal cancer. *Anticancer Research*. 29(7): 2611-2617.
- Health-Canada. 2007. Indoor air quality in office buildings: A technical guide: Health Canada. Available at: http://www.hc-sc.gc.ca/ewh-semt/pubs/air/office_building-immeubles_bureaux/organic-organiques-eng.php. Assessed 10 August 2010.
- Heber, A. J., M. Stroik, J. M. Faubion, and L. H. Willard. 1988a. Size distribution and identification of aerial dust particles in swine finishing buildings. *Transactions of the ASAE*. 31(3): 882-887.
- Heber, A. J., M. Stroik, J. L. Nelssen, and D. A. Nichols. 1988b. Influence of environmental-factors on concentrations and inorganic content of aerial dust in swine finishing buildings. *Transactions of the ASAE*. 31(3): 875-881.
- Heber, A. J., T. T. Lim, J. Q. Ni, P. C. Tao, A. M. Schmidt, J. A. Koziel, S. J. Hoff, L. D. Jacobson, Y. H. Zhang, and G. B. Baughman. 2006. Quality-assured measurements of animal building emissions: Particulate matter concentrations. *Journal of the Air & Waste Management Association*. 56(12): 1642-1648.
- Heber, A. J., W. W. Bogan, J. Q. Ni, T. T. Lim, J. C. Ramirez-Dorransoro, E. L. Cortus, C. A. Diehl, S. M. Hanni, C. Xiao, K. D. Casey, C. A. Gooch, L. D. Jacobson, J. A. Koziel, F. M. Mitloehner, P. M. Ndegwa, W. P. Robarge, L. Wang, and R. Zhang. 2008. The national air emission monitoring study: Overviews of barn sources. In *The 8th International Livestock Symposium (ILES VIII)*. Iguassu Falls, Brazil: American Society of Agricultural and Biological Engineers.
- Heederik, D., T. Sigsgaard, P. S. Thorne, J. N. Kline, R. Avery, J. H. Bonlokke, E. A. Chrischilles, J. A. Dosman, C. Duchaine, S. R. Kirkhorn, K. Kulhankova, and J. A. Merchant. 2007. Health effects of airborne exposures from concentrated animal feeding operations. *Environmental Health Perspectives*. 115(2): 298-302.
- Hering, S. V., and M. R. Stolzenburg. 1995. Online determination of particle-size and density in the nanometer-size range. *Aerosol Science and Technology*. 23(2): 155-173.
- Hinds, W. C. 1982. *Aerosol Technology: Properties, Behavior, and Measurement of Airborne Particles*. New York, NY: John Wiley and Sons, Inc.
- Hiranuma, N., S. D. Brooks, B. W. Auvermann, and R. Littleton. 2008. Using environmental scanning electron microscopy to determine the hygroscopic properties of agricultural aerosols. *Atmospheric Environment*. 42(9): 1983-1994.

- Hirst, J. M. 1995. Bioaerosols: Introduction, Retrospect and Prospect. In *Bioaerosols Handbook*. C.S. Cox and C.M. Wathes, eds. Boca Raton, FL: CRC Press.
- Hoff, S., B. C. Zelle, M. A. Huebner, and A. K. Gralapp. 2005. NH₃, H₂S, CO₂, PM and odor animal emission data from the six-state (APECAB) project: swine deep-pit finishing building. In *Proc. 98th Annual Conference and Exhibition*, AWMA Paper No. 05A648. Minneapolis, MN: Air & Waste Management Association.
- Holmes, N. S., and L. Morawska. 2006. A review of dispersion modeling and its application to the dispersion of particles: An overview of different dispersion models available. *Atmospheric Environment*. 40(30): 5902-5928.
- Hopke, P. K. 1999. An introduction to source receptor modeling. In *Elemental Analysis of Airborne Particles*. S. Landsberger and M. Creatchman, eds. Amsterdam, The Netherlands: Gordon and Breach Science Publishers.
- Hsieh, L. Y., S. C. Kuo, C. L. Chen, and Y. I. Tsai. 2007. Origin of low-molecular-weight dicarboxylic acids and their concentration and size distribution variation in suburban aerosol. *Atmospheric Environment*. 41(31): 6648-6661.
- Hudon, G., C. Guy, and J. Hermia. 2000. Measurement of odor intensity by an electronic nose. *Journal of the Air & Waste Management Association*. 50(10): 1750-1758.
- Iossifova, Y. Y. 2006. (1→3)-β-d-glucans in indoor environments- laboratory analysis and wheeze in infants. PhD diss. Cincinnati, Ohio: University of Cincinnati, Department of Environmental Health.
- Iossifova, Y. Y., T. Reponen, D. I. Bernstein, L. Levin, H. Kalra, P. Campo, M. Villareal, J. Lockey, G. K. K. Hershey, and G. LeMasters. 2007. House dust (1-3)-beta-d-glucan and wheezing in infants. *Allergy*. 62(5): 504-513.
- IPCC. 1995. Climate change 1994: Radiative forcing of climate change and an evaluation of the IPCC IS92 emission scenarios. Cambridge, UK: Cambridge University Press.
- IUPAC. 1997. Isokinetic sampling (in atmospheric chemistry): International Union of Pure and Applied Chemistry. Available at: <http://www.iupac.org/goldbook/I03286.pdf>. Assessed 5 August 2009.
- Jacobson, L. D., B. P. Hetchler, V. J. Johnson, R. E. Nicolai, and D. R. Schmidt. 2005. Seasonal variations in NH₃, H₂S and PM₁₀ emissions from pig and poultry buildings from a multi-state project. In *Symposium on the State of the Science of Animal Manure and Waste Management*. San Antonio, Texas: American Society of Agricultural Engineers.

- Jacobson, L. D., B. P. Hetchler, V. J. Johnsen, R. E. Nicolai, D. R. Schmidt, P. R. Goodrich, A. J. Heber, J. Q. Ni, T. T. Lim, P. C. Tao, S. J. Hoff, D. S. Bundy, M. A. Huebner, B. C. Zelle, Y. Zhang, J. McClure, M. Roberts, J. A. Koziel, B. H. Baek, A. Balota, J. P. Spinhirne, J. M. Sweeten, D. B. Beasley, G. R. Baughman, and R. Munilla. 2004. Preliminary NH₃, H₂S, and PM₁₀ data from pig and poultry buildings from six-state project. ASAE Paper No. 044156. St. Joseph, MI: American Society of Agricultural Engineers.
- Jerez, S. B. 2007. Airborne pollutant spatial distribution, emission, and ventilation effectiveness for mechanically ventilated livestock buildings. PhD diss. Urbana, Illinois: University of Illinois at Urbana-Champaign, Department of Agricultural and Biological Engineering.
- Jerez, S. B., Y. Zhang, J. W. McClure, A. J. Heber, J. A. Koziel, S. J. Hoff, L. D. Jacobson, and D. Beasley. 2005. Aerial pollutant concentration and emission rate measurements from a swine farrowing building in Illinois. In *Proc. 98th Annual Conference and Exhibition*, AWMA Paper No. 1026. Minneapolis, MN: Air & Waste Management Association.
- Jerez, S. B., Y. H. Zhang, J. W. McClure, L. Jacobson, A. Heber, S. Hoff, J. Koziel, and D. Beasley. 2006. Comparison of measured total suspended particulate matter concentrations using tapered element oscillating microbalance and a total suspended particulate sampler. *Journal of the Air & Waste Management Association*. 56(3): 261-270.
- Jones, W., K. Moring, S. A. Olenchok, T. Williams, and J. Hickey. 1984. Environmental-study of poultry confinement buildings. *American Industrial Hygiene Association Journal*. 45(11): 760-766.
- Jorquera, H., and B. Rappengluck. 2004. Receptor modeling of ambient voc at Santiago, Chile. *Atmospheric Environment*. 38(25): 4243-4263.
- Junge, C. E. 1963. *Air Chemistry and Radioactivity*. New York: Academic Press.
- Juntto, S., and P. Paatero. 1994. Analysis of daily precipitation data by positive matrix factorization. *Environmetrics*. 5(2): 127-144.
- Kellems, R. O., and D. C. Church. 1998. *Livestock Feeds and Feeding, the Fourth Edition*. Upper Saddle River, NJ: Prentice Hall.
- Kenny, L. C., and R. A. Gussman. 1997. Characterization and modeling of a family of cyclone aerosol pre separators. *Journal of Aerosol Science*. 28(4): 677-688.
- Kenny, L. C., R. Gussmann, and M. Meyer. 2000. Development of a sharp-cut cyclone for ambient aerosol monitoring applications. *Aerosol Science and Technology*. 32(4): 338-358.
- Kenny, L. C., T. Merrifield, D. Mark, R. Gussman, and A. Thorpe. 2004. The development and designation testing of a new USEPA-approved fine particle inlet: A study of the USEPA designation process. *Aerosol Science and Technology*. 38: 15-22.

- Kim, K. Y., H. J. Ko, Y. S. Kim, and C. N. Kim. 2008a. Assessment of Korean farmer's exposure level to dust in pig buildings. *Annals of Agricultural and Environmental Medicine*. 15(1): 51-58.
- Kim, K. Y., H. J. Ko, H. T. Kim, Y. S. Kim, Y. M. Roh, C. M. Lee, and C. N. Kim. 2008b. Quantification of ammonia and hydrogen sulfide emitted from pig buildings in Korea. *Journal of Environmental Management*. 88(2): 195-202.
- Kirkhorn, S. R., and V. F. Garry. 2000. Agricultural lung diseases. *Environmental Health Perspectives*. 108: 705-712.
- Kiryuchuk, S. P., J. A. Dosman, S. J. Reynolds, P. Willson, A. Senthilselvan, J. J. R. Feddes, H. L. Classen, and W. Guenter. 2006. Total dust and endotoxin in poultry operations: Comparison between cage and floor housing and respiratory effects in workers. *Journal of Occupational and Environmental Medicine*. 48(7): 741-748.
- Knutson, E. O., and P. J. Lioy. 1989. Measurement and presentation of aerosol size distributions. In *Air Sampling Instruments for Evaluation of Atmospheric Contaminants, 7th Edition*, 59-72. S. V. Hering, ed. Cincinnati, OH: American Conference of Governmental Industrial Hygienists.
- Koerkamp, P. W. G. G., J. H. M. Metz, G. H. Uenk, V. R. Phillips, M. R. Holden, R. W. Sneath, J. L. Short, R. P. White, J. Hartung, J. Seedorf, M. Schroder, K. H. Linkert, S. Pedersen, H. Takai, J. O. Johnsen, and C. M. Wathes. 1998. Concentrations and emissions of ammonia in livestock buildings in northern Europe. *Journal of Agricultural Engineering Research*. 70(1): 79-95.
- Koon, J., J. R. Howes, W. Grub, and C. A. Rollo. 1963. Poultry dust: Origin and composition. *Agricultural Engineering*. 44(11): 608-609.
- Koziel, J. A., B. H. Baek, C. L. Bayley, K. J. Bush, J. P. Spinhirne, A. Balota, D. B. Parker, J. M. Sweeten, L. D. Jacobson, A. J. Heber, J. Q. Ni, S. J. Hoff, Y. Zhang, and D. B. Beasley. 2005. Aerial pollutant emissions from confined animal buildings: Swine finisher buildings in Texas. In *Proc. 98th Annual Conference and Exhibition*, AWMA Paper No. 1043. Minneapolis, MN: Air & Waste Management Association.
- Lacey, R. E., J. S. Redwine, and C. B. Parnell. 2003. Particulate matter and ammonia emission factors for tunnel-ventilated broiler production houses in the southern US. *Transactions of the ASAE*. 46(4): 1203-1214.
- Laitinen, S., J. Kangas, K. Husman, and P. Susitaival. 2001. Evaluation of exposure to airborne bacterial endotoxins and peptidoglycans in selected work environments. *Annals of Agricultural and Environmental Medicine*. 8(2): 213-219.
- Lammel, G., F. Schneider, E. Bruggemann, T. Gnauk, A. Rohrl, and P. Wieser. 2004. Aerosols emitted from a livestock farm in southern Germany. *Water Air and Soil Pollution*. 154(1-4): 313-330.

- Landsberger, S. 1999. Trace element determination of airborne particles by neutron activation analysis. In *Elemental Analysis of Airborne Particles*. S. Landsberger and M. Creatchman, eds. Amsterdam, The Netherlands: Gordon and Breach Science Publishers.
- Lavado, R. S., C. A. Porcelli, and R. Alvarez. 2001. Nutrient and heavy metal concentration and distribution in corn, soybean and wheat as affected by different tillage systems in the argentine pampas. *Soil & Tillage Research*. 62(1-2): 55-60.
- Lau, A. P. S., A. K. Y. Lee, C. K. Chan, and M. Fang. 2006. Ergosterol as a biomarker for the quantification of the fungal biomass in atmospheric aerosols. *Atmospheric Environment*. 40(2): 249-259.
- Lee, A. K. Y., C. K. Chan, M. Fang, and A. P. S. Lau. 2004. The 3-hydroxy fatty acids as biomarkers for quantification and characterization of endotoxins and gram-negative bacteria in atmospheric aerosols in Hong Kong. *Atmospheric Environment*. 38(37): 6307-6317.
- Lee, J. 2009. Characterization and concentrations of particulate matters emitted from confinement animal buildings. PhD diss. Urbana, Illinois: University of Illinois at Urbana-Champaign, Department of Agricultural and Biological Engineering.
- Lee, J., and Y. H. Zhang. 2008. Evaluation of gas emissions from animal building dusts using a cylindrical convective chamber. *Biosystems Engineering*. 99(3): 403-411.
- Lee, J., Y. Zhang, X. Wang, X. Yang, J. Su, B. W. Shaw, G. Riskowski, and B. Faulkner. 2008. Measurement of particle size distributions in swine buildings. In *The 8th International Livestock Symposium (ILES VIII)*. Iguassu Falls, Brazil: American Society of Agricultural and Biological Engineers.
- Lee, J. H., P. K. Hopke, T. M. Holsen, D. W. Lee, P. A. Jaques, C. Sioutas, and J. R. L. Ambs. 2005. Performance evaluation of continuous PM_{2.5} mass concentration monitors. *Journal of Aerosol Science*. 36(1): 95-109.
- Lee, K. P., C. E. Ulrich, R. G. Geil and H. J. Trochimowicz. 1989. Inhalation toxicity of chromium dioxide dust to rats after 2 years exposure. *Science of the Total Environment*. 86(1-2): 83-108.
- Lee, S. J., and A. C. Noble. 2003. Characterization of odor-active compounds in Californian chardonnay wines using GC-olfactometry and GC-mass spectrometry. *Journal of Agricultural and Food Chemistry*. 51(27): 8036-8044.
- Levy, S. B. 1998. The challenge of antibiotic resistance. *Scientific American*. 278(3): 46-53.
- Li, Q. F., L. J. Wang, Z. F. Liu, D. B. Beasley, and R. K. M. Jayanty. 2009. Chemical characterization of particulate matter emitted from animal feeding operations. ASABE Paper No. 095948. St. Joseph, MI: American Society of Agricultural and Biological Engineers.

- Liao, C. M., J. W. Chen, M. Y. Huang, J. S. Chen, and T. J. Chang. 2001. An inhalation dose model for assessing dust-borne VOC-odor exposure from feeding in swine buildings. *Transactions of the ASAE*. 44(6): 1813-1824.
- Lim, T. T., A. J. Heber, J. Q. Ni, A. L. Sutton, and D. T. Kelly. 2001. Characteristics and emission rates of odor from commercial swine nurseries. *Transactions of the ASAE*. 44(5): 1275-1282.
- Lim, T. T., A. J. Heber, J. Q. Ni, J. X. Gallien, and H. Xin. 2003. Air quality measurements at a laying hen house: Particulate matter concentrations and emissions. In *Proc. Air Pollution from Agricultural Operations III*, 249-256. St. Joseph, MI: American Society of Agricultural and Biological Engineers.
- Lim, T. T., A. J. Heber, J. Q. Ni, D. C. Kendall, and B. T. Richert. 2004. Effects of manure removal strategies on odor and gas emissions from swine finishing. *Transactions of the ASAE*. 47(6): 2041-2050.
- Lin, H. J., K. T. Shao, W. L. Chiou, C. J. W. Maa, H. L. Hsieh, W. L. Wu, L. L. Severinghaus, and Y. T. Wang. 2003. Biotic communities of freshwater marshes and mangroves in relation to saltwater incursions: Implications for wetland regulation. *Biodiversity and Conservation*. 12(4): 647-665.
- Lin, J. J. 2002. Characterization of the major chemical species in PM_{2.5} in the Kaohsiung city, Taiwan. *Atmospheric Environment*. 36(12): 1911-1920.
- Lin, J. M., and I. Blank. 2003. Odorants generated by thermally induced degradation of phospholipids. *Journal of Agricultural and Food Chemistry*. 51(15): 4364-4369.
- Lincoln, T. A., N. E. Bolton, and A. S. Garrett. 1974. Occupational allergy to animal dander and sera. *Journal of Occupational and Environmental Medicine*. 16(7): 465-469.
- Liu, A. H., and D. Y. M. Leung. 2000. Modulating the early allergic response with endotoxin. *Clinical and Experimental Allergy*. 30(11): 1535-1539.
- Liu, H. Y., A. Probst, and B. H. Liao. 2005. Metal contamination of soils and crops affected by the Chenzhou lead/zinc mine spill (Hunan, China). *Science of the Total Environment*. 339(1-3): 153-166.
- Liu, L. J. S., M. Kraemer, A. Fox, C. E. Feigley, A. Featherstone, A. Saraf, and L. Larsson. 2000. Investigation of the concentration of bacteria and their cell envelope components in indoor air in two elementary schools. *Journal of the Air & Waste Management Association*. 50(11): 1957-1967.
- Liu, Y., and F. Liu. 1994. On the description of aerosol particle size distribution. *Atmospheric Research*. 31((1-3)): 187-198.

- Lo, Y. C. M., J. A. Koziel, L. S. Cai, S. J. Hoff, W. S. Jenks, and H. W. Xin. 2008. Simultaneous chemical and sensory characterization of volatile organic compounds and semi-volatile organic compounds emitted from swine manure using solid phase microextraction and multidimensional gas chromatography-mass spectrometry-olfactometry. *Journal of Environmental Quality*. 37(2): 521-534.
- Lorjaroenphon, Y., and K. R. Cadwallader. 2010. Characteristics of flavor compounds in dust collected in animal confinement facilities. In preparation.
- Machida, T., T. Nakazawa, Y. Fujii, S. Aoki, and O. Watanabe. 1995. Increase in the atmospheric nitrous-oxide concentration during the last 250 years. *Geophysical Research Letters*. 22(21): 2921-2924.
- Mackie, R. I., P. G. Stroot, and V. H. Varel. 1998. Biochemical identification and biological origin of key odor components in livestock waste. *Journal of Animal Science*. 76(5): 1331-1342.
- Mader, B. T., and J. F. Pankow. 2001. Gas/solid partitioning of semivolatile organic compounds (SOCs) to air filters. 3. An analysis of gas adsorption artifacts in measurements of atmospheric SOC and organic carbon (OC) when using Teflon membrane filters and quartz fiber filters. *Environmental Science & Technology*. 35(17): 3422-3432.
- Madsen, A. M. 2006. Airborne endotoxin in different background environments and seasons. *Annals of Agricultural and Environmental Medicine*. 13(1): 81-86.
- Mahin, T. D. 2001. Comparison of different approaches used to regulate odors around the world. *Water Science and Technology*. 44(9): 87-102.
- Marenco, F., P. Bonasoni, F. Calzolari, M. Ceriani, M. Chiari, P. Cristofanelli, A. D'Alessandro, P. Fermo, F. Lucarelli, F. Mazzei, S. Nava, A. Piazzalunga, P. Prati, G. Valli, and R. Vecchi. 2006. Characterization of atmospheric aerosols at Monte Cimone, Italy, during summer 2004: Source apportionment and transport mechanisms. *Journal of Geophysical Research-Atmospheres*. 111(D24): -.
- Martin, R. S., P. J. Silva, K. Moore, M. Erupe, and V. S. Doshi. 2008. Particle composition and size distributions in and around a deep-pit swine operation, Ames, Ia. *Journal of Atmospheric Chemistry*. 59(2): 135-150.
- Martin, S. W., and R. A. Willough. 1972. Organic dusts, sulfur-dioxide, and respiratory tract of swine. *Archives of Environmental Health*. 25(3): 158-&.
- Martin, W. T., Y. H. Zhang, P. Willson, T. P. Archer, C. Kinahan, and E. M. Barber. 1996. Bacterial and fungal flora of dust deposits in a pig building. *Occupational and Environmental Medicine*. 53(7): 484-487.
- Martinec, M., E. Hartung, T. Jungbluth, F. Schneider, and P. H. Wieser. 2001. Reduction of gas, odor and dust emissions from swine operations with biofilters. ASAE Paper No. 014079. St. Joseph, MI.: American Society of Agricultural Engineers.

- Martuzevicius, D., S. A. Grinshpun, T. Reponen, R. L. Gorny, R. Shukla, J. Lockey, S. H. Hu, R. McDonald, P. Biswas, L. Kliucininkas, and G. LeMasters. 2004. Spatial and temporal variations of PM_{2.5} concentration and composition throughout an urban area with high freeway density - the greater Cincinnati study. *Atmospheric Environment*. 38(8): 1091-1105.
- Matthias, V., A. Aulinger, and M. Quante. 2009. CMAQ simulations of the benzo(a)pyrene distribution over Europe for 2000 and 2001. *Atmospheric Environment*. 43(26): 4078-4086.
- Mazin, I. P., and A. K. Khrgian. 1989. *Clouds and cloudy atmosphere handbook*. Leningrad, USSR: Gidrometeoizdat.
- McClure, J. W. 2009. Determination of particulate emissions from confined animal housing. Ph.D. diss. Urbana, Illinois: University of Illinois at Urbana-Champaign, Department of Agricultural and Biological Engineering.
- McMurry, P. H. 2000. A review of atmospheric aerosol measurements. *Atmospheric Environment*. 34(12-14): 1959-1999.
- Michel, O., A. M. Nagy, M. Schroeven, J. Duchateau, J. Neve, P. Fondu, and R. Sergysels. 1997. Dose-response relationship to inhaled endotoxin in normal subjects. *American Journal of Respiratory and Critical Care Medicine*. 156(4): 1157-1164.
- Mielniczuk, Z., E. Mielniczuk, and L. Larsson. 1993. Gas-chromatography mass-spectrometry methods for analysis of 2-hydroxylated and 3-hydroxylated fatty-acids - application for endotoxin measurement. *Journal of Microbiological Methods*. 17(2): 91-102.
- Milby, T. H., and R. C. Baselt. 1999. Hydrogen sulfide poisoning: Clarification of some controversial issues. *American Journal of Industrial Medicine*. 35(2): 192-195.
- Miller, B. V., and R. W. Lines. 1988. Recent advances in particle size measurement: A critical review. *Critical Reviews in Analytical Chemistry*. 20(2): 75-166.
- Milton, D. K., H. A. Feldman, D. S. Neuberg, R. J. Bruckner, and I. A. Greaves. 1992. Environmental endotoxin measurement - the kinetic limulus assay with resistant-parallel-line estimation. *Environmental Research*. 57(2): 212-230.
- Misselbrook, T. H., T. J. Van der Weerden, B. F. Pain, S. C. Jarvis, B. J. Chambers, K. A. Smith, V. R. Phillips, and T. G. M. Demmers. 2000. Ammonia emission factors for UK agriculture. *Atmospheric Environment*. 34(6): 871-880.
- Mosquera, J., G. J. Monteny, and J. W. Erisman. 2005. Overview and assessment of techniques to measure ammonia emissions from animal houses: The case of the Netherlands. *Environmental Pollution*. 135(3): 381-388.
- Myers, K. P., C. W. Olsen, S. F. Setterquist, A. W. Capuano, K. J. Donham, E. L. Thacker, J. A. Merchant, and G. C. Gray. 2006. Are swine workers in the United States at increased risk of infection with zoonotic influenza virus? *Clinical Infectious Diseases*. 42(1): 14-20.

- NAS. 2003. Air emissions from animal feeding operations, current knowledge, future needs. Washington, DC: The National Academies Press.
- Nehme, B., V. Letourneau, R. J. Forster, M. Veillette, and C. Duchaine. 2008. Culture-independent approach of the bacterial bioaerosol diversity in the standard swine confinement buildings, and assessment of the seasonal effect. *Environmental Microbiology*. 10(3): 665-675.
- Ngwabie, N. M., K. H. Jeppsson, S. Nimmermark, C. Swensson, and G. Gustafsson. 2009. Multi-location measurements of greenhouse gases and emission rates of methane and ammonia from a naturally-ventilated barn for dairy cows. *Biosystems Engineering*. 103(1): 68-77.
- Ni, J. Q., A. J. Heber, T. T. Lim, P. C. Tao, and A. M. Schmidt. 2008. Methane and carbon dioxide emission from two pig finishing barns. *Journal of Environmental Quality*. 37(6): 2001-2011.
- Ni, J. Q., A. J. Heber, C. A. Diehl, T. T. Lim, R. K. Duggirala, and B. L. Haymore. 2002a. Summertime concentrations and emissions of hydrogen sulfide at a mechanically ventilated swine finishing building. *Transactions of the ASAE*. 45(1): 193-199.
- Ni, J. Q., A. J. Heber, T. T. Lim, C. A. Diehl, R. K. Duggirala, and B. L. Haymore. 2002b. Hydrogen sulfide emission from two large pig-finishing buildings with long-term high-frequency measurements. *Journal of Agricultural Science*. 138: 227-236.
- Ni, J. Q., A. J. Heber, T. T. Lim, C. A. Diehl, R. K. Duggirala, B. L. Haymore, and A. L. Sutton. 2000. Ammonia emission from a large mechanically-ventilated swine building during warm weather. *Journal of Environmental Quality*. 29(3): 751-758.
- Nicholson, F. A., B. J. Chambers, J. R. Williams, and R. J. Unwin. 1999. Heavy metal contents of livestock feeds and animal manures in England and Wales. *Bioresource Technology*. 70(1): 23-31.
- Nicolas, J. F., N. Galindo, E. Yubero, C. Pastor, R. Esclapez, and J. Crespo. 2009. Aerosol inorganic ions in a semiarid region on the southeastern Spanish Mediterranean coast. *Water Air and Soil Pollution*. 201(1-4): 149-159.
- NIST. 2010. NIST Chemistry Webbook: National Institute of Standards and Technology Available at: <http://webbook.nist.gov/chemistry>. Assessed 20 March 2010.
- Noble, C. A., R. W. Vanderpool, T. M. Peters, F. F. McElroy, D. B. Gemmill, and R. W. Wiener. 2001. Federal reference and equivalent methods for measuring fine particulate matter. *Aerosol Science and Technology*. 34(5): 457-464.
- Nukiyama, S., and Y. Tanasawa. 1939. Experiments on the atomization of liquids in an air stream. Report 3: On the droplet-size distribution in an atomized jet. *Transaction of the Japan Society of Mechanical Engineers*. 5: 62-65.

- Odman, M. T., Y. T. Hu, A. G. Russell, A. Hanedar, J. W. Boylan, and P. F. Brewer. 2009. Quantifying the sources of ozone, fine particulate matter, and regional haze in the southeastern United States. *Journal of Environmental Management*. 90(10): 3155-3168.
- Oehrl, L. L., K. M. Keener, R. W. Bottcher, R. D. Munilla, and K. M. Connelly. 2001. Characterization of odor components from swine housing dust using gas chromatography. *Applied Engineering in Agriculture*. 17(5): 659-661.
- Olsen, J. H., L. Dragsted, and H. Autrup. 1988. Cancer risk and occupational exposure to aflatoxins in Denmark. *British Journal of Cancer*. 58(3): 392-396.
- O'Neill, D. H., and V. R. Phillips. 1992. A review of the control of odor nuisance from livestock buildings .3. Properties of the odorous substances which have been identified in livestock wastes or in the air around them. *Journal of Agricultural Engineering Research*. 53(1): 23-50.
- Oppliger, A., N. Charriere, P. O. Droz, and T. Rinsoz. 2008. Exposure to bioaerosols in poultry houses at different stages of fattening; use of real-time PCR for airborne bacterial quantification. *Annals of Occupational Hygiene*. 52(5): 405-412.
- Osada, T., H. B. Rom, and P. Dahl. 1998. Continuous measurement of nitrous oxide and methane emission in pig units by infrared photoacoustic detection. *Transactions of the ASAE*. 41(4): 1109-1114.
- Paloposki, T. 1991. The physically relevant parameter space of the Nukiyama-Tanasawa distribution function. *Particle & Particle Systems Characterization*. 8(4): 287-293.
- Park, S. S., and Y. J. Kim. 2005. Source contributions to fine particulate matter in an urban atmosphere. *Chemosphere*. 59(2): 217-226.
- Patashnick, H., and E. G. Rupprecht. 1991. Continuous PM₁₀ measurements using the tapered element oscillating microbalance. *Journal of the Air & Waste Management Association*. 41(8): 1079-1083.
- Patashnick, H., G. Rupprecht, J. L. Ambs, and M. B. Meyer. 2001. Development of a reference standard for particulate matter mass in ambient air. *Aerosol Science and Technology*. 34(1): 42-45.
- Pathak, R. K., W. S. Wu, and T. Wang. 2009. Summertime PM_{2.5} ionic species in four major cities of China: Nitrate formation in an ammonia-deficient atmosphere. *Atmospheric Chemistry and Physics*. 9(5): 1711-1722.
- Patnaik, P. 2003. *Handbook of Inorganic Chemicals*. New York City, NY: McGraw-Hill Professional.
- Peters, T. M., R. W. Vanderpool, and R. W. Wiener. 2001. Design and calibration of the EPA PM_{2.5} well impactor ninety-six (WINS). *Aerosol Science and Technology*. 34(5): 389-397.

- Predicala, B. Z., and R. G. Maghirang. 2002. Measurement of particulate emissions from mechanically ventilated swine barns. AASE Paper No. 024209. St. Joseph, MI: American society of agricultural engineers
- Predicala, B. Z., R. G. Maghirang, S. B. Jerez, J. E. Urban, and R. D. Goodband. 2001. Dust and bioaerosol concentrations in two swine-finishing buildings in Kansas. *Transactions of the ASAE*. 44(5): 1291-1298.
- Predicala, B. Z., J. E. Urban, R. G. Maghirang, S. B. Jerez, and R. D. Goodband. 2002. Assessment of bioaerosols in swine barns by filtration and impaction. *Current Microbiology*. 44(2): 136-140.
- Preller, L., D. Heederik, J. S. M. Boleij, P. F. J. Vogelzang, and M. J. M. Tielen. 1995a. Lung-function and chronic respiratory symptoms of pig farmers - focus on exposure to endotoxins and ammonia and use of disinfectants. *Occupational and Environmental Medicine*. 52(10): 654-660.
- Preller, L., D. Heederik, H. Kromhout, J. S. M. Boleij, and M. J. M. Tielen. 1995b. Determinants of dust and endotoxin exposure of pig farmers - development of a control strategy using empirical modeling. *Annals of Occupational Hygiene*. 39(5): 545-557.
- Rabaud, N. E., S. E. Ebeler, L. L. Ashbaugh, and R. G. Flocchini. 2003. Characterization and quantification of odorous and non-odorous volatile organic compounds near a commercial dairy in California. *Atmospheric Environment*. 37(7): 933-940.
- Radon, K., B. Danuser, M. Iversen, E. Monso, C. Weber, J. Hartung, K. J. Donham, U. Palmgren, and D. Nowak. 2002. Air contaminants in different European farming environments. *Annals of Agricultural and Environmental Medicine*. 9(1): 41-48.
- Razote, E. B., R. G. Maghirang, L. M. Seitz, and I. J. Jeon. 2004. Characterization of volatile organic compounds on airborne dust in a swine finishing barn. *Transactions of the ASAE*. 47(4): 1231-1238.
- Redwine, J. S., R. E. Lacey, S. Mukhtar, and J. B. Carey. 2002. Concentration and emissions of ammonia and particulate matter in tunnel-ventilated broiler houses under summer conditions in Texas. *Transactions of the ASAE*. 45(4): 1101-1109.
- Renard, J. J., S. E. Calidonna, and M. V. Henley. 2004. Fate of ammonia in the atmosphere - a review for applicability to hazardous releases. *Journal of Hazardous Materials*. 108(1-2): 29-60.
- Reponen, T., A. Nevalainen, M. Jantunen, M. Pellikka, and P. Kalliokoski. 1992. Normal range criteria for indoor air bacteria and fungal spores in a subarctic climate. *Indoor Air*. 2(1): 26-31.
- Reynolds, S. J., and D. K. Milton. 1993. Comparison of methods for analysis of airborne endotoxin. *Applied Occupational and Environmental Hygiene*. 8(9): 761-767.

- Reynolds, S. J., K. J. Donham, P. Whitten, J. A. Merchant, L. F. Burmeister, and W. J. Pependorf. 1996. Longitudinal evaluation of dose-response relationships for environmental exposures and pulmonary function in swine production workers. *American Journal of Industrial Medicine*. 29(1): 33-40.
- Reynolds, S. J., P. S. Thorne, K. J. Donham, E. A. Croteau, K. M. Kelly, D. Lewis, M. Whitmer, D. J. J. Heederik, J. Douwes, I. Connaughton, S. Koch, P. Malmberg, B. M. Larsson, and D. K. Milton. 2002. Comparison of endotoxin assays using agricultural dusts. *AIHAJ*. 63(4): 430-438.
- Reynolds, S. J., D. K. Milton, D. Heederik, P. S. Thorne, K. J. Donham, E. A. Croteau, K. M. Kelly, J. Douwes, D. Lewis, M. Whitmer, I. Connaughton, S. Koch, P. Malmberg, B. M. Larsson, J. Deddens, A. Saraf, and L. Larsson. 2005. Interlaboratory evaluation of endotoxin analyses in agricultural dusts - comparison of LAL assay and mass spectrometry. *Journal of Environmental Monitoring*. 7(12): 1371-1377.
- Robbiano, L., D. Baroni, R. Carrozzino, E. Mereto, and G. Brambilla. 2004. DNA damage and micronuclei induced in rat and human kidney cells by six chemicals carcinogenic to the rat kidney. *Toxicology*. 204(2-3): 187-195.
- Robine, E., I. Lacaze, S. Moularat, S. Ritoux, and M. Boissier. 2005. Characterisation of exposure to airborne fungi: Measurement of ergosterol. *Journal of Microbiological Methods*. 63(2): 185-192.
- Robertson, J. H., and W. R. Frieben. 1984. Microbial validation of vent filters. *Biotechnology and Bioengineering*. 26(8): 828-835.
- Ronald, M. 1995. *A review of the Literature on the Nature and Control of Odors from Pork Production Facilities*. Des Moines, IA: National Pork Producers Council.
- Rosen, A. A., J. B. Peter, and F. M. Middleton. 1962. Odor thresholds of mixed organic chemicals. *Journal Water Pollution Control Federation*. 34(1): 7-14.
- Rosin, P., and E. Rammler. 1933. The laws governing the fineness of powdered coal. *Journal of the Institute of Fuel*. 7: 29-36.
- Roumeliotis, T. S., and B. J. Van Heyst. 2007. Size fractionated particulate matter emissions from a broiler house in southern Ontario, Canada. *Science of the Total Environment*. 383(1-3): 174-182.
- Roumeliotis, T. S., and B. J. Van Heyst. 2008. Summary of ammonia and particulate matter emission factors for poultry operations. *Journal of Applied Poultry Research*. 17(2): 305-314.
- Rule, A. M., A. R. Chapin, S. A. McCarthy, K. E. Gibson, K. J. Schwab, and T. J. Buckley. 2005. Assessment of an aerosol treatment to improve air quality in a swine concentrated animal feeding operation (CAFO). *Environmental Science & Technology*. 39(24): 9649-9655.

- Rychlik, M., P. Schieberle, and W. Grosch. 1998. *Compilation of Odor Thresholds, Odor Qualities and Retention Indices of Key Food Odorants*. Garching, Germany: Deutsche Forschungsanstalt für Lebensmittelchemie and Institut für Lebensmittelchemie der Technischen Universität München.
- Rylander, R. 1999. Indoor air-related effects and airborne (1 → 3)-beta-D-glucan. *Environmental Health Perspectives*. 107: 501-503.
- Rylander, R. 2002. Endotoxin in the environment - exposure and effects. *Journal of Endotoxin Research*. 8(4): 241-252.
- Rylander, R., and R. Etzel. 1999. Introduction and summary: Workshop on children's health and indoor mold exposure. *Environmental Health Perspectives*. 107: 465-468.
- Rylander, R., and M. F. Carneiro. 2006. Airways inflammation among workers in poultry houses. *International Archives of Occupational and Environmental Health*. 79(6): 487-490.
- Sander, I., C. Fleischer, G. Borowitzki, T. Bruning, and M. Raulf-Heimsoth. 2008. Development of a two-site enzyme immunoassay based on monoclonal antibodies to measure airborne exposure to (1 → 3)-beta-d-glucan. *Journal of Immunological Methods*. 337(1): 55-62.
- Sapkota, A. R., K. K. Ojo, M. C. Roberts, and K. J. Schwab. 2006. Antibiotic resistance genes in multidrug-resistant enterococcus spp. and streptococcus spp. recovered from the indoor air of a large-scale swine-feeding operation. *Letters in Applied Microbiology*. 43(5): 534-540.
- Saraf, A., J. H. Park, D. K. Milton, and L. Larsson. 1999. Use of quadrupole GC-MS and ion trap GC-MS-MS for determining 3-hydroxy fatty acids in settled house dust: Relation to endotoxin activity. *Journal of Environmental Monitoring*. 1(2): 163-168.
- Schenker, M. B., D. Christiani, Y. Cormier, H. Dimich-Ward, G. Doekes, J. Dosman, J. Douwes, K. Dowling, D. Enarson, F. Green, D. Heederik, K. Husman, S. Kennedy, G. Kullman, Y. Lacasse, B. Lawson, P. Malmberg, J. May, S. McCurdy, J. Merchant, J. Myers, M. Nieuwenhuijsen, S. Olenchock, C. Saiki, D. Schwartz, J. Seiber, P. Thorne, G. Wagner, N. White, X. P. Xu, M. Chan-Yeung, and A. E. O. Hlth. 1998. Respiratory health hazards in agriculture. *American Journal of Respiratory and Critical Care Medicine*. 158(5): S1-S76.
- Schierl, R., A. Heise, U. Egger, F. Schneider, R. Eichelser, S. Nesper, and D. Nowak. 2007. Endotoxin concentration in modern animal houses in southern Bavaria. *Annals of Agricultural and Environmental Medicine*. 14(1): 129-136.
- Schiffman, S. S. 1998. Livestock odors: Implications for human health and well-being. *Journal of Animal Science*. 76(5): 1343-1355.
- Schiffman, S. S., J. L. Bennett, and J. H. Raymer. 2001. Quantification of odors and odorants from swine operations in North Carolina. *Agricultural and Forest Meteorology*. 108(3): 213-340.

- Schiffman, S. S., E. A. S. Miller, M. S. Suggs, and B. G. Graham. 1995. The effect of environmental odors emanating from commercial swine operations on the mood of nearby residents. *Brain Research Bulletin*. 37(4): 369-375.
- Schiffman, S. S., J. M. Walker, P. Dalton, T. S. Lorig, J. H. Raymer, D. Shusterman, and C. M. Williams. 2000. Potential health effects of odor from animal operations, wastewater treatment, and recycling of byproducts. *Journal of Agromedicine*. 7(1): 7-81.
- Schiffman, S. S., J. T. Walker, P. Dalton, T. S. Lorig, J. H. Raymer, D. Shusterman, and C. M. Williams. 2002. Potential health effects of odor from animal operations, wastewater treatment, and recycling of byproducts. *Journal of Agromedicine*. 7(1): 7-81.
- Schmidt, D. R., L. D. Jacobson, and K. A. Janni. 2002. Continuous monitoring of ammonia, hydrogen sulfide and dust emissions from swine, dairy and poultry barns. ASABE meeting Paper No. 024060. St. Joseph, MI: American Society of Agricultural and Biological Engineers.
- Schnelle, K. B., and P. R. Dey. 2000. *Atmospheric Dispersion Modeling Compliance Guide*. Now York: McGraw-Hill.
- Schulze, A., R. van Strien, V. Ehrenstein, R. Schierl, H. Kuchenhoff, and K. Radon. 2006. Ambient endotoxin level in an area with intensive livestock production. *Annals of Agricultural and Environmental Medicine*. 13(1): 87-91.
- Seedorf, J. 2004. An emission inventory of livestock-related bioaerosols for lower Saxony, Germany. *Atmospheric Environment*. 38(38): 6565-6581.
- Seedorf, J., J. Hartung, M. Schroder, K. H. Linkert, V. R. Phillips, M. R. Holden, R. W. Sneath, J. L. Short, R. P. White, S. Pedersen, H. Takai, J. O. Johnsen, J. H. M. Metz, P. W. G. G. Koerkamp, G. H. Uenk, and C. M. Wathes. 1998. Concentrations and emissions of airborne endotoxins and microorganisms in livestock buildings in northern Europe. *Journal of Agricultural Engineering Research*. 70(1): 97-109.
- Seinfeld, J. H., and S. N. Pandis. 1998. *Atmospheric Chemistry and Physics: From Air Pollution to Climate Change*. Singapore: John Wiley & Sons. Inc..
- Senthilselvan, A., Y. Zhang, J. A. Dosman, E. M. Barber, L. E. Holfeld, S. P. Kirychuk, Y. Cormier, T. S. Hurst, and C. S. Rhodes. 1997. Positive human health effects of dust suppression with canola oil in swine barns. *American Journal of Respiratory and Critical Care Medicine*. 156(2): 410-417.
- Sigsgaard, T., P. Malmros, L. Nersting, and C. Petersen. 1994. Respiratory disorders and atopy in Danish refuse workers. *American Journal of Respiratory and Critical Care Medicine*. 149(6): 1407-1412.
- Sillanpaa, M., A. Frey, R. Hillamo, A. S. Pennanen, and R. O. Salonen. 2005. Organic, elemental and inorganic carbon in particulate matter of six urban environments in Europe. *Atmospheric Chemistry and Physics*. 5: 2869-2879.

- Skoog, D. A., F. J. Holler, and T. A. Nieman. 1998. *Principles of Instrumental Analysis, 5th edition*. Toronto, Canada: Books/Cole.
- Smith, R. J. 1995. A Gaussian model for estimating odor emissions from area sources. *Mathematical and Computer Modeling*. 21(9): 23-29.
- Smith, W. B., R. R. J. Wilson, and D. B. Harris. 1979. A five-stage cyclone system for in situ sampling. *Environmental Science & Technology*. 13(11): 1387-1392.
- Sneath, R. W. 1996. Measuring losses of methane and nitrous oxide from livestock buildings. In: *Methane and Nitrous Oxide Emissions — Agriculture's Contribution. Symposium*. London, UK: Society of Chemical Industry.
- Snell, H. G. J., F. Seipelt, and H. F. A. Van den Weghe. 2003. Ventilation rates and gaseous emissions from naturally ventilated dairy houses. *Biosystems Engineering*. 86(1): 67-73.
- Spaan, S., D. J. J. Heederik, P. S. Thorne, and I. M. Wouters. 2007. Optimization of airborne endotoxin exposure assessment: Effects of filter type, transport conditions, extraction solutions, and storage of samples and extracts. *Applied and Environmental Microbiology*. 73(19): 6134-6143.
- Spaan, S., G. Doekes, D. Heederik, P. S. Thorne, and I. A. Wouters. 2008. Effect of extraction and assay media on analysis of airborne endotoxin. *Applied and Environmental Microbiology*. 74(12): 3804-3811.
- Spoelstra, S. F. 1980. Origin of objectionable odorous components in piggery wastes and the possibility of applying indicator components for studying odor development. *Agriculture and Environment*. 5(3): 241-260.
- Squire, R. A. 1981. Ranking animal carcinogens - a proposed regulatory approach. *Science*. 214(4523): 877-880.
- Stephenson, D. J., D. R. Lillquist, F. D. DeRosso, D. D. Greene, and G. White. 2004. Side-by-side comparison of three sampling methods for aerosolized endotoxin in a wastewater treatment facility. *Journal of Environmental Health*. 67(4): 16-19.
- Sun, G., H. Q. Guo, J. Peterson, B. Predicala, and C. Lague. 2008. Diurnal odor, ammonia, hydrogen sulfide, and carbon dioxide emission profiles of confined swine grower/finisher rooms. *Journal of the Air & Waste Management Association*. 58(11): 1434-1448.
- Svennerstedt, B. 1999. Drainage properties and ammonia emissions in slatted floor systems for animal buildings. *Journal of Agricultural Engineering Research*. 72(1): 19-25.
- Takai, H., L. D. Jacobson, and S. Pedersen. 1996. Reduction of dust concentration and exposure in pig buildings by adding animal fat in feed. *Journal of Agricultural Engineering Research*. 63(2): 113-120.

- Takai, H., S. Pedersen, J. O. Johnsen, J. H. M. Metz, P. W. G. G. Koerkamp, G. H. Uenk, V. R. Phillips, M. R. Holden, R. W. Sneath, J. L. Short, R. P. White, J. Hartung, J. Seedorf, M. Schroder, K. H. Linkert, and C. M. Wathes. 1998. Concentrations and emissions of airborne dust in livestock buildings in northern Europe. *Journal of Agricultural Engineering Research*. 70(1): 59-77.
- Tan, Z. C., and Y. H. Zhang. 2004. A review of effects and control methods of particulate matter in animal indoor environments. *Journal of the Air & Waste Management Association*. 54(7): 845-854.
- Thorn, J., L. Beijer, and R. Rylander. 1998. Airways inflammation and glucan exposure among household waste collectors. *American Journal of Industrial Medicine*. 33(5): 463-470.
- Thorne, P. S., K. H. Bartlett, J. Phipps, and K. Kulhankova. 2003. Evaluation of five extraction protocols for quantification of endotoxin in metalworking fluid aerosol. *Annals of Occupational Hygiene*. 47(1): 31-36.
- Thorne, P. S., A. C. Ansley, and S. S. Perry. 2009. Concentrations of bioaerosols, odors, and hydrogen sulfide inside and downwind from two types of swine livestock operations. *Journal of Occupational and Environmental Hygiene*. 6(4): 211-220.
- Thorne, P. S., S. J. Reynolds, D. K. Milton, P. D. Bloebaum, X. J. Zhang, P. Whitten, and L. F. Burmeister. 1997. Field evaluation of endotoxin air sampling assay methods. *American Industrial Hygiene Association Journal*. 58(11): 792-799.
- Thu, K., K. Donham, R. Ziegenhorn, S. Reynolds, P. Subramanian, P. Whitten, J. Stookesberry, and P. S. Thorne. 1997. A control study of the physical and mental health of residents living near a large-scale swine operation. *Journal of Agricultural Safety and Health*. 3(1): 13-26.
- Thu, K. M. 2002. Public health concerns for neighbors of large-scale swine production. *Journal of Agricultural Safety and Health*. 8(2): 175-184.
- Tirabassi, T., and U. Rizza. 1993. Flux parameterization for atmospheric-diffusion models in an industrialized area. *Nuovo Cimento Della Societa Italiana Di Fisica C-Geophysics and Space Physics*. 16(2): 187-194.
- Todar, K. 2008. *Todar's Online Textbook of Bacteriology*. Madison, WI. Available at: <http://www.textbookofbacteriology.net>. Assessed 27 Apr 2010.
- Trabue, S., K. Scoggin, H. Li, R. Burns, H. W. Xin, and J. Hatfield. 2010. Speciation of volatile organic compounds from poultry production. *Atmospheric Environment*. 44(29): 3538-3546.
- Tsapakis, M., E. Lagoudaki, E. G. Stephanou, I. G. Kavouras, P. Koutrakis, P. Oyola, and D. von Baer. 2002. The composition and sources of PM_{2.5} organic aerosol in two urban areas of Chile. *Atmospheric Environment*. 36(23): 3851-3863.
- Turner, N. W., S. Subrahmanyam, and S. A. Piletsky. 2009. Analytical methods for determination of mycotoxins: A review. *Analytica Chimica Acta*. 632(2): 168-180.

- Turner, W. A., B. A. Olson, and G. A. Allen. 2000. Calibration of sharp cut impactors for indoor and outdoor particle sampling. *Journal of the Air & Waste Management Association*. 50(4): 484-487.
- Turpin, B. J., J. J. Huntzicker, and S. V. Hering. 1994. Investigation of organic aerosol sampling artifacts in the Los Angeles basin. *Atmospheric Environment*. 28(19): 3061-3071.
- UCS. 2001. Hogging it! Estimates of antimicrobial abuse in livestock. Cambridge, MA: Union of Concerned Scientists. Available: http://www.ucsusa.org/food_and_agriculture/science_and_impacts/impacts_industrial_agriculture/hogging-it-estimates-of.html. Assessed 15 August 2009.
- UGA. 2009. Glossary- a guide for prescribed fire in southern forests. Athens, GA: The Bugwood Network. Available at: <http://www.bugwood.org/pfire/glossary.html>. Assessed 2 September 2009.
- Ullman, J. L., S. Mukhtar, R. E. Lacey, and J. B. Carey. 2004. A review of literature concerning odors, ammonia, and dust from broiler production facilities: 4. remedial management practices. *Journal of Applied Poultry Research*. 13(3): 521-531.
- USDA. 2009. Livestock and Animal National Statistics. National Agricultural Statistics Database. Washington, D.C.: USDA National Agricultural Statistics Service.
- USEPA. 1995. User's guide for the industrial source complex (ISC3) dispersion models. Volume I - user instructions. EPA technical report No. EPA-454/b-95-003A. Cincinnati, OH: United States Environmental Protection Agency.
- USEPA. 1999a. Compendium of methods for the determination of inorganic compounds in ambient air. EPA technical report No. EPA/625/R-96/010A. Washington, DC: United States Environmental Protection Agency.
- USEPA. 1999b. Particulate matter (PM_{2.5}) speciation guidance, final draft. Research Triangle Park, NC: United States Environmental Protection Agency.
- USEPA. 2003. Comparison of regulatory design concentrations: AERMOD vs ISCST3, CTDMPPLUS, ISC-PRIME. EPA technical report No. EPA-454/R-03-002. Cincinnati, OH: United States Environmental Protection Agency.
- USEPA. 2004a. User's guide for the AMS/EPA regulatory model- AERMOD. EPA technical report No. EPA-454/B-03-001. Cincinnati, OH: United States Environmental Protection Agency.
- USEPA. 2004b. Chapter 4. Air quality model. Cincinnati, OH: United States Environmental Protection Agency. Available at: http://www.epa.gov/ies/pdf/handbook/Chapter_4_45-53.pdf. Assessed 2 September 2009.

- USEPA. 2006. Notice of EPA re-designation of certain equivalent methods for PM_{2.5}. Cincinnati, OH: United States Environmental Protection Agency. Available at <http://www.epa.gov/ttn/amtic/files/ambient/criteria/redesgvsc.pdf>. Assessed 2 September 2009.
- USEPA. 2008. EPA positive matrix factorization (PMF) 3.0 fundamentals & user guide. EPA technical report No. EPA 600/R-08/108. Washington, DC: United States Environmental Protection Agency.
- USEPA. 2009a. Particulate matter emissions. Cincinnati, OH: United States Environmental Protection Agency. Available at: <http://cfpub.epa.gov/eroe/index.cfm?fuseaction=detail.viewpdf&ch=46&lshowind=0&subtop=341&lv=list.listbychapter&r=209839>. Assessed 2 September 2009.
- USEPA. 2009b. FIP rule definitions. Cincinnati, OH: United States Environmental Protection Agency. Available at: <http://www.epa.gov/region/air/phoenixpm/fip/define.html>. Assessed 25 July 2007.
- USEPA. 2009c. List of designated reference and equivalent methods. Research Triangle Park, NC: United States Environmental Protection Agency. Available at: <http://www.epa.gov/ttn/amtic/criteria.html>. Assessed 5 April 2006.
- van Gemert, L. J., and A. H. Nettenbreijer. 1977. *Compilation of Odor Threshold Values in Air and Water*. Voorburg, Netherlands: National Institute for Water supply.
- van Kempen, T. A. T. G., W. J. Powers, and A. L. Sutton. 2002. Technical note: Fourier transform infrared (FTIR) spectroscopy as an optical nose for predicting odor sensation. *Journal of Animal Science*. 80(6): 1524-1527.
- Vanderpool, R. W., T. M. Peters, S. Natarajan, D. B. Gemmill, and R. W. Wiener. 2001a. Evaluation of the loading characteristics of the EPA WINS PM_{2.5} separator. *Aerosol Science and Technology*. 34(5): 444-456.
- Vanderpool, R. W., T. M. Peters, S. Natarajan, M. P. Tolocka, D. B. Gemmill, and R. W. Wiener. 2001b. Sensitivity analysis of the USEPA WINS PM_{2.5} separator. *Aerosol Science and Technology*. 34(5): 465-476.
- Var, F., Y. Narita, and S. Tanaka. 2000. The concentration, trend and seasonal variation of metals in the atmosphere in 16 Japanese cities shown by the results of national air surveillance network (NASN) from 1974 to 1996. *Atmospheric Environment*. 34(17): 2755-2770.
- Von Ehrenstein, O. S., E. Von Mutius, S. Illi, L. Baumann, O. Bohm, and R. Von Kries. 2000. Reduced risk of hay fever and asthma among children of farmers. *Clinical and Experimental Allergy*. 30(2): 187-193.
- Von Essen, S., and K. Donham. 1999. Illness and injury in animal confinement workers. *Occupational Medicine-State of the Art Reviews*. 14(2): 337-350.

- Voss, A., F. Loeffen, J. Bakker, C. Klaassen, and M. Wulf. 2005. Methicillin-resistant *Staphylococcus aureus* in pig farming. *Emerging Infectious Diseases*. 11(12): 1965-1966.
- Wan, G. H., and C. S. Li. 1999. Indoor endotoxin and glucan in association with airway inflammation and systemic symptoms. *Archives of Environmental Health*. 54(3): 172-179.
- Wang, L. J., J. D. Wanjura, C. B. Parnell, R. E. Lacey, and B. W. Shaw. 2005a. Performance characteristics of a low-volume PM₁₀ sampler. *Transactions of the ASAE*. 48(2): 739-748.
- Wang, L. J., D. B. Parker, C. B. Parnell, R. E. Lacey, and B. W. Shaw. 2006. Comparison of CALPUFF and ISCST3 models for predicting downwind odor and source emission rates. *Atmospheric Environment*. 40(25): 4663-4669.
- Wang, L. J., C. B. Parnell, B. W. Shaw, R. E. Lacey, A. D. Buser, L. B. Goodrich, and S. C. Capareda. 2005b. Correcting PM₁₀ over-sampling problems for agricultural particulate matter emissions: Preliminary study. *Transactions of the ASAE*. 48(2): 749-755.
- Wang, X., P. G. Stroot, Y. Zhang, and G. L. Riskowski. 1998. Odor carrying characteristics of dust from swine facilities. ASAE Paper No. 98-4068. St. Joseph, MI: American Society of Agricultural Engineers.
- Wang, X. L. 2000. Measurement and modeling of spatial distribution of particulate matter in indoor environments. PhD diss. Urbana, Illinois: University of Illinois at Urbana-Champaign, Department of Agricultural Engineering.
- Wang, X. L., and Y. H. Zhang. 1999. Development of a critical airflow venturi for air sampling. *Journal of Agricultural Engineering Research*. 73(3): 257-264.
- Wang, Z. H., L. Z. Zhang, Y. L. Zhang, Z. Zhao, and S. M. Zhang. 2008. Morphology of single inhalable particle in the air polluted city of Shijiazhuang, China. *Journal of Environmental Sciences-China*. 20(4): 429-435.
- Wanjura, J. D., M. D. Buser, C. B. Parnell, B. W. Shaw, and R. E. Lacey. 2005. A simulated approach to estimating PM₁₀ and PM_{2.5} concentrations downwind from cotton gins. *Transactions of the ASAE*. 48(5): 1919-1925.
- Watson, J. G., T. Zhu, J. C. Chow, J. Engelbrecht, E. M. Fujita, and W. E. Wilson. 2002. Receptor modeling application framework for particle source apportionment. *Chemosphere*. 49(9): 1093-1136.
- Watson, J. G., J. C. Chow, and C. A. Frazier. 1999. X-ray fluorescence analysis of ambient air samples. In *Elemental Analysis of Airborne Particles*. S. Landsberger and M. Creatchman, eds. Amsterdam, The Netherlands Gordon and Breach Science Publishers.
- Wei, B., K. Y. Wang, X. R. Dai, Z. Y. Li, and H. J. Luo. 2010. Evaluation of indoor environmental conditions of micro-fermentation deep litter pig building in southeast China. ASABE Paper No. 1009679. St. Joseph, MI: American Society of Agricultural and Biological Engineers.

- Wei, F., E. Teng, G. Wu, W. Hu, W. E. Wilson, R. S. Chapman, J. C. Pau, and J. Zhang. 1999. Ambient concentrations and elemental compositions of PM₁₀ and PM_{2.5} in four Chinese cities. *Environmental Science & Technology*. 33(23): 4188-4193.
- Weibull, W. 1951. A statistical distribution function of wide applicability. *Journal of Applied Mechanics- Transaction of ASME*. 18(3): 293-297.
- Wheeler, P. A., I. Stewart, P. Dumitrean, and B. Donovan. 2001. Health Effects of Composting: A Study of Three Compost Sites and Review of Past Data. R & D Technical Report P1-315/TR. Bristol, United Kingdom: Environmental Agency.
- WHO. 2007. Animal Feed Impact on Food Safety. Rome, Italy: World Health Organization.
- Williams, A. G. 1984. Indicators of piggery slurry odor offensiveness. *Agricultural Wastes*. 10(1): 15-36.
- Williams, A. G. 1989. Dust and odor relationships in broiler house air. *Journal of Agricultural Engineering Research*. 44(3): 175-190.
- Williams, K. L. 2007. *Endotoxins: Pyrogens, LAL testing and Depyrogenation, 3rd Edition*. Boca Raton, FL: CRC Press.
- Williams, R., J. Suggs, C. Rodes, P. Lawless, R. Zweidinger, R. Kwok, J. Creason, and L. Sheldon. 2000. Comparison of PM_{2.5} and PM_{2.5} monitors. *Journal of Exposure Analysis and Environmental Epidemiology*. 10(5): 497-505.
- Wilson, W. E., J. C. Chow, C. Claiborn, F. S. Wei, J. Engelbrecht, and J. G. Watson. 2002. Monitoring of particulate matter outdoors. *Chemosphere*. 49(9): 1009-1043.
- Wouters, I. M., S. Spaan, J. Douwes, G. Doekes, and D. Heederik. 2006. Overview of personal occupational exposure levels to inhalable dust, endotoxin, beta(1 -> 3)-glucan and fungal extracellular polysaccharides in the waste management chain. *Annals of Occupational Hygiene*. 50(1): 39-53.
- Wright, D. W., D. K. Eaton, L. T. Nielsen, F. W. Kuhrt, J. A. Koziel, J. P. Spinhirne, and D. B. Parker. 2005. Multidimensional gas chromatography-olfactometry for the identification and prioritization of malodors from confined animal feeding operations. *Journal of Agricultural and Food Chemistry*. 53(22): 8663-8672.
- Yu, J. C., C. E. Isaac, R. N. Coleman, J. J. R. Feddes, and B. S. West. 1991. Odorous compounds from treated pig manure. *Canadian Agricultural Engineering*. 33(1): 131-136.
- Yue, W. S., Y. Li, X. L. Li, X. H. Yu, B. Deng, J. F. Liu, T. M. Wan, G. L. Zhang, Y. Y. Huang, W. He, and W. Hua. 2004. Source identification of PM₁₀, collected at a heavy-traffic roadside, by analyzing individual particles using synchrotron radiation. *Journal of Synchrotron Radiation*. 11: 428-431.

- Zahn, J. A., A. A. DiSpirito, Y. S. Do, B. E. Brooks, E. E. Cooper, and J. L. Hatfield. 2001. Correlation of human olfactory responses to airborne concentrations of malodorous volatile organic compounds emitted from swine effluent. *Journal of Environmental Quality*. 30(2): 624-634.
- Zahn, J. A., J. L. Hatfield, Y. S. Do, A. A. DiSpirito, D. A. Laird, and R. L. Pfeiffer. 1997. Characterization of volatile organic emissions and wastes from a swine production facility. *Journal of Environmental Quality*. 26(6): 1687-1696.
- Zhang, S., L. Cai, J. A. Koziel, S. J. Hoff, K. Heathcote, L. Jacobson, N. Akdeniz, B. Hetchler, D. B. Parker, E. Caraway, A. J. Heber, and S. Bereznicki. 2010. Odor and odorous chemical emissions from animal buildings: Part 5- correlations between odor intensities and chemical concentrations (GC-MS/O). ASABE Publication No. 711p0510cd. In *International Symposium on Air Quality and Manure Management for Agriculture*. Dallas, TX: American Society of Agricultural and Biological Engineers.
- Zhang, Y. 2005. *Indoor Air Quality Engineering*. Boca Raton, FL: CRC Press.
- Zhang, Y., Z. Tan, and X. Wang. 2005. Aerodynamic deduster technologies for removing dust and ammonia in air streams. In *Proc. 7th International Symposium- Livestock Environment VII*, 230-238. Beijing, China: American Society of Agricultural Engineers.
- Zhang, Y., A. Tanaka, E. M. Barber, and J. J. R. Feddes. 1996. Effects of frequency and quantity of sprinkling canola oil on dust reduction in swine buildings. *Transactions of the ASAE*. 39(3): 1077-1081.
- Zhang, Y., J. A. Polakow, X. Wang, G. L. Riskowski, Y. Sun, and S. E. Ford. 2001. An aerodynamic deduster to reduce dust and gas emissions from ventilated livestock facilities. In *Proc. 6th International Symposium- Livestock Environment VI*, 596-603. Louisville, KY: American Society of Agricultural Engineers.
- Zhao, Y., A. J. A. Aarninka, P. Hofschreudera, and P. W. G. GrootKoerkamp. 2009. Evaluation of an impaction and a cyclone pre-separator for sampling high PM₁₀ and PM_{2.5} concentrations in livestock houses *Journal of Aerosol Science*. 40(10): 868-878.
- Zhou, Q. X., C. L. Wintersteen, and K. R. Cadwallader. 2002. Identification and quantification of aroma-active components that contribute to the distinct malty flavor of buckwheat honey. *Journal of Agricultural and Food Chemistry*. 50(7): 2016-2021.
- Zhu, J. 2000. A review of microbiology in swine manure odor control. *Agriculture Ecosystems & Environment*. 78(2): 93-106.
- Zhu, J., L. Jacobson, D. Schmidt, and R. Nicolai. 2000. Daily variations in odor and gas emissions from animal facilities. *Applied Engineering in Agriculture*. 16(2): 153-158.
- Zock, J. P., A. Hollander, D. Heederik, and J. Douwes. 1998. Acute lung function changes and low endotoxin exposures in the potato processing industry. *American Journal of Industrial Medicine*. 33(4): 384-391.

APPENDIX A. FARM INFORMATION OF SAMPLING SITES

Table A.1. Basic information of sampling sites.

Site	Animal type	Room size /m			Floor type	Manure storage	Feeding system	Ventilation fans ^a	Nearest weather station (distance to farm /miles)
		L	W	H					
A	farrowing	15	6	2.4	partially slatted	shallow pit	dry feed	0.3m ×1; 0.6m ×1; 0.9m ×1	Pittsfield, IL (13.6)
B		18	8	2.4				0.3m ×1; 0.6m ×1; 0.9m ×1	Pittsfield, IL (10.4)
C		15	13	2.4				0.9m ×3; 0.6m ×2	Quincy, IL (36.3)
D	gestation	185	28.6	2.5	fully slatted	deep pit	wet feed	1.2m ×16; <u>0.5m ×30</u>	Pittsfield, IL (13.6)
E		150	28.6	2.5				1.2m ×14	Pittsfield, IL (10.4)
F		168	25.8	2.5				1.2m ×18	Quincy, IL (36.3)
G	weaning	95	16	2.4	partially slatted	shallow pit	dry feed	1.2m ×7; 0.9m ×6	Bloomington, IL (14.2)
H		18	12	2.7				0.9m ×2; 0.6m ×2; <u>0.3m ×2</u>	Salem, IL (29.4)
I		18.2	12.2	2.4				0.6m ×2; <u>0.23m ×2</u>	Jacksonville, IL (25.6)
J	finishing	65	12	2.4	fully slatted	deep pit	wet feed	1.2m ×4; 0.9m ×1; <u>0.4m ×4</u>	Lincoln, IL (17.5)
K		56	24	2.2				1.2m ×2; 0.6m ×22	Bloomington, IL (11.7)
L		67	16	2.5				1.2m ×2; 0.9m ×1; <u>0.4m ×8</u>	Bloomington, IL (13)
M	tom turkey	91	18	3.6	wood shaving bedding	bedding	dry feed	0.6m ×2	Pontiac, IL (17.8)
N		76	24.3	3.6				natural ventilation	Lacon, IL (20.3)
O		120	20	3.6				natural ventilation	Peoria, IL (17.4)
P	layer hens	140	21	12	concrete	manure belt	dry feed	1.4m ×88; 1.2m ×4	Warsaw, IN (19.4)
Q		180	28	12				1.4m ×154	Rantoul, IL (17)
R		108	18	6.0				1.2m ×26	Freeport, IL (13.8)
S	chicken broiler	152	12	2.4	wood shaving bedding	bedding	Dry feed	1.3m ×1; 1.2m ×8; 0.9m ×1	Bowling Green, KY (32.5)
T	layer hens	128	12	2.4	plastic slat	first floor		0.9m ×10	Warsaw, IN (19.4)

a. Fans highlighted with underline are pit fans.

Table A.2. Distance Matrix of sampling sites^a (km).

Sites	A	B	C	D	E	F	G	H	I	J	K	L	M	N	O	P	Q	R	S	T
A	0	36	62	0.2	36	62	207	175	85	180	183	182	251	206	159	478	273	306	553	478
B	36	0	80	36	0.1	80	191	139	81	165	168	167	238	200	151	459	256	319	517	459
C	62	80	0	62	81	0.1	171	190	49	143	146	147	209	157	115	440	235	244	571	440
D	0.2	36	62	0	36	62	207	174	85	179	182	182	251	206	159	478	273	306	553	478
E	36	0.1	81	36	0	81	191	139	81	165	168	168	238	200	152	459	256	320	517	459
F	62	80	0.1	62	81	0	171	190	49	143	146	147	209	157	115	440	235	244	571	440
G	207	191	171	207	191	171	0	153	125	28	25	25	50	57	61	271	66	236	469	271
H	175	139	190	174	139	190	153	0	150	146	147	145	200	199	164	373	198	370	382	373
I	85	81	49	85	81	49	125	150	0	97	100	101	167	121	74	396	191	244	528	396
J	180	165	143	179	165	143	28	146	97	0	3	4	73	53	36	299	93	229	483	299
K	183	168	146	182	168	146	25	147	100	3	0	3	70	52	37	296	91	229	482	296
L	182	167	147	182	168	147	25	145	101	4	3	0	71	55	39	296	90	232	479	296
M	251	238	209	251	238	209	50	200	167	73	70	71	0	60	94	232	34	217	487	232
N	206	200	157	206	200	157	57	199	121	53	52	55	60	0	48	289	94	179	527	289
O	159	151	115	159	152	115	61	164	74	36	37	39	94	48	0	325	121	206	515	325
P	478	459	440	478	459	440	271	373	396	299	296	296	232	289	325	0	205	379	471	0.1
Q	273	256	235	273	256	235	66	198	191	93	91	90	34	94	121	205	0	248	460	205
R	306	319	244	306	320	244	236	370	244	229	229	232	217	179	206	379	248	0	703	379
S	553	517	571	553	517	571	469	382	528	483	482	479	487	527	515	471	460	703	0	471
T	478	459	440	478	459	440	271	373	396	299	296	296	232	289	325	0.1	205	379	471	0

a. A distance matrix is calculated for analysis of potential geographic patterns.

Table A.3. Basic information of sampling sites.

Field trip #	1	2	3	4	5		
Date ^a	10/4/2007	10/22/2007	10/23/2007	12/4/2007	12/5/2007		
Sites	L	A	A	B	E		
Season ^b	Hot	Mild	Mild	Cold	Cold		
# of animals	2700	26	2400	28	2000		
Average weight (kg)	20	200	200	200	200		
Animal density (kg/m ³)	20.1	24.1	36.2	16.2	37.2		
Feed	corn and soybean pellet	corn and soybean ground					
Cleaning cycle	6 months	3 weeks	6 months	3 weeks	6 months		
Fans running continuously ^c	1.2m ×2; 0.9m ×1; 0.4m ×8	0.3m ×1; 0.6m ×1;	1.2m ×4; 0.5m ×30	0.3m×1	none		
Fans running intermittently ^c	none	0.9m×1	1.2m×8	0.6m×1	1.2m×4		
Measured environmental data ^d	Outside	Temperature /°C	33	21	21	19	18
		Humidity /%	50	57	56	73	55
	Inside	Temperature /°C	33	16	15	4	2
		Humidity /%	45	43	48	55	55
Meteorological data from the nearest weather station	Temperature /°C	Mean	21	13	10	0	2
		Max	30	19	15	3	7
		Min	13	8	6	-2	-2
	Humidity /%	Mean	67	75	63	70	76
		Max	86	100	87	81	93
		Min	49	52	81	56	61
Pressure /inch Hg	30.05	29.95	30.02	29.98	29.93		

a. The day when a sampling started.

b. Seasons were roughly classified into ‘cold’, ‘mild’ and ‘hot’ based on the mean outside temperature (T_{mean}) during the sampling period: cold- $T_{\text{mean}} < 5^{\circ}\text{C}$, mild- $5^{\circ}\text{C} \leq T_{\text{mean}} < 20^{\circ}\text{C}$, and hot- $T_{\text{mean}} \geq 20^{\circ}\text{C}$. Although there were a few exceptions, the principle was to ensure significant temperature differences were present between hot, cold and mild seasons for each sampling site.

c. Information of fan operations was learned via conversation with farm managers and workers, but should not used for estimation of ventilation rates because of the inaccuracy.

d. Temperature and humidity were measured at around two o’clock in afternoon each day. Therefore, the temperature data in this table may represent be the maximum daytime temperature.

Table A.3. (cont. 1)

Field trip #		6	7	8	9	10	
Date		12/18/2007	12/19/2007	1/9/2008	1/10/2008	1/24/2008	
Sites		A	D	C	F	J	
Season		Cold	Cold	Cold	Cold	Cold	
# of animals		26	2400	52	2050	1800	
Average weight (kg)		150	150	200	200	8	
Animal density (kg/m ³)		18.1	27.1	22.2	37.8	7.7	
Feed		corn and soybean ground	corn and soybean pellet				
Cleaning cycle		6 months	6 months	manure: 4h; floor: 1d	manure:6h; floor: 1d	manure: 2d; floor: 1d	
Fans running continuously		0.4m ×8	none	1.4m ×12	1.4m ×24	1.2m ×4	
Fans running intermittently		0.9m ×1	0.6m ×22	1.4m ×20	1.4m ×20	none	
Measured environmental data	Outside	Temperature /°C	21	20	20	20	19
		Humidity /%	73	67	51	67	55
	Inside	Temperature /°C	6	5	8	6	-9
		Humidity /%	55	72	64	69	48
Meteorological data from the nearest weather station	Temperature /°C	Mean	1	-2	1	2	-16
		Max	6	3	5	5	-12
		Min	-4	-7	-3	0	-20
	Humidity /%	Mean	84	87	76	87	69
		Max	100	100	89	97	85
		Min	61	65	51	79	48
	Pressure /inch Hg		30.09	30.06	30.08	29.65	30.35

Table A.3. (cont. 2)

Field trip #		11	12	13	14	15	
Date		2/5/2008	2/12/2008	2/19/2008	2/27/2008	3/6/2008	
Sites		L	K	P	Q	R	
Season		Cold	Cold	Cold	Cold	Cold	
# of animals		2500	2500	262300	449800	75600	
Average weight (kg)		100	30	1.44	1.44	1.53	
Animal density (kg/m ³)		93.3	25.4	10.7	10.7	9.9	
Feed		corn and soybean ground	corn, soybean, DDGS, ground				
Cleaning cycle		6 months	6 months	manure: 4h; floor: 1d	manure:6h; floor: 1d	manure: 2d; floor: 1d	
Fans running continuously		0.4m ×8	none	1.4m ×12	1.4m ×24	1.2m ×4	
Fans running intermittently		0.9m ×1	0.6m ×22	1.4m ×20	1.4m ×20	none	
Measured environmental data	Outside	Temperature /°C	15	19	23	19	20
		Humidity /%	74	56	78	80	79
	Inside	Temperature /°C	5	-1.5	-3	-1	1
		Humidity /%	78	68	63	58	60
Meteorological data from the nearest weather station	Temperature /°C	Mean	3	-9	-11	-6	-7
		Max	6	-8	-9	-5	-2
		Min	0	-11	-13	-7	-12
	Humidity /%	Mean	100	85	70	75	75
		Max	100	93	73	86	86
		Min	100	77	58	54	54
	Pressure /inch Hg		29.83	29.96	29.89	30.03	30.05

Table A.3. (cont. 3)

Field trip #		16	17	18	19	20	
Date		3/13/2008	3/19/2008	3/27/2008	4/3/2008	4/10/2008	
Sites		J	K	M	L	R	
Season		Mild	Mild	Mild	Mild	Mild	
# of animals		1700	2500	4500	2700	74000	
Average weight (kg)		32	50	20	5	1.6	
Animal density (kg/m ³)		29.1	42.3	15.3	5.0	10.2	
Feed		corn and soybean pellet	corn and soybean ground	corn and soybean ground	corn and soybean pellet	corn, soybean, DDGS, ground	
Cleaning cycle		6 months	6 months	2 years	6 months	manure: 2d; floor: 1d	
Fans running continuously		0.9m ×1; 0.4m ×4	0.6m ×8	0.6m ×2	0.9m ×1; 0.4m ×8	1.2m ×8	
Fans running intermittently		none	0.6m ×4	none	none	none	
Measured environmental data	Outside	Temperature /°C	21	17	21	23	22
		Humidity /%	54	51	74	55	68
	Inside	Temperature /°C	16	16	10	11	11
		Humidity /%	49	37	68	47	73
Meteorological data from the nearest weather station	Temperature /°C	Mean	9	4	4	6	4
		Max	16	7	7	12	6
		Min	2	-1	2	-1	3
	Humidity /%	Mean	59	85	76	80	84
		Max	93	100	100	100	93
		Min	34	56	61	49	81
	Pressure /inch Hg		29.7	29.88	29.99	29.97	29.83

Table A.3. (cont. 4)

Field trip #		21	22	23	24	25	
Date		4/17/2008	4/23/2008	5/7/2008	5/8/2008	5/21/2008	
Sites		P	Q	B	E	C	
Season		Mild	Mild	Mild	Mild	Mild	
# of animals		261000	449800	28	2064	52	
Average weight (kg)		1.45	1.44	180	160	200	
Animal density (kg/m ³)		10.7	10.7	14.6	30.8	22.2	
Feed		corn and soybean ground					
Cleaning cycle		manure: 4h; floor: 1d	manure:6h; floor: 1d	3 weeks	6 months	3 weeks	
Fans running continuously		1.4m ×24	1.4m ×32	0.6m ×1; 0.3m ×1;	1.2m ×4	0.6m ×2	
Fans running intermittently		1.4m ×30	1.4m ×36	0.9m ×1	1.2m ×2	none	
Measured environmental data	Outside	Temperature /°C	24	25	23	22	25
		Humidity /%	45	48	66	64	43
	Inside	Temperature /°C	25	26	19	15	21
		Humidity /%	46	50	67	67	40
Meteorological data from the nearest weather station	Temperature /°C	Mean	17	21	18	12	14
		Max	23	26	21	16	22
		Min	11	16	16	9	7
	Humidity /%	Mean	50	53	82	80	47
		Max	54	82	100	100	77
		Min	33	26	61	52	26
	Pressure /inch Hg		30.04	30.06	29.75	29.7	29.75

Table A.3. (cont. 5)

Field trip #		26	27	28	29	30	
Date		5/22/2008	6/4/2008	6/5/2008	6/18/2008	6/19/2008	
Sites		F	A	D	B	E	
Season		Mild	Hot	Hot	Hot	Hot	
# of animals		2500	26	2350	28	2014	
Average weight (kg)		200	150	150	180	160	
Animal density (kg/m ³)		26.1	18.1	26.5	14.6	30.0	
Feed		corn and soybean ground	corn and soybean ground	corn and soybean ground	corn and soybean ground	corn and soybean ground	
Cleaning cycle		irregular	3 weeks	6 months	3 weeks	6 months	
Fans running continuously		1.2m ×4	0.9m ×1; 0.6m ×1; 0.3m ×1	1.2m ×8; 0.5m ×30	0.9m ×1; 0.6m ×1; 0.3m ×1	1.2m ×10	
Fans running intermittently		1.2m ×4	none	1.2m ×2	none	1.2m ×4	
Measured environmental data	Outside	Temperature /°C	23	28	27	27	25
		Humidity /%	57	91	94	56	75
	Inside	Temperature /°C	17	29	29	28	26
		Humidity /%	58	77	71	48	67
Meteorological data from the nearest weather station	Temperature /°C	Mean	15	24	26	20	22
		Max	18	29	30	27	28
		Min	12	19	22	14	17
	Humidity /%	Mean	58	90	80	63	61
		Max	81	100	94	94	94
		Min	41	66	58	30	30
	Pressure /inch Hg		29.83	29.95	29.63	30.04	29.94

Table A.3. (cont. 6)

Field trip #	31	32	33	34	35		
Date	7/1/2008	7/2/2008	7/10/2008	7/17/2008	7/24/2008		
Sites	C	F	K	R	Q		
Season	Hot	Hot	Hot	Hot	Hot		
# of animals	52	2500	3060	74000	449800		
Average weight (kg)	200	200	12	1.6	1.44		
Animal density (kg/m ³)	22.2	46.1	12.4	10.2	10.7		
Feed	corn and soybean ground	corn and soybean ground	corn and soybean ground	corn, soybean, DDGS, ground	corn and soybean ground		
Cleaning cycle	3 weeks	Irregular	6 months	manure: 2d; floor: 1d	manure:6h; floor: 1d		
Fans running continuously	0.9m ×3; 0.6m ×2	1.2m ×12	1.2m ×2; 0.6m ×12	1.2m ×12	1.4m ×40		
Fans running intermittently	none	none	none	1.2m ×8	1.4m ×42		
Measured environmental data	Outside	Temperature /°C	26	26	30	28	28
		Humidity /%	63	79	65	66	47
	Inside	Temperature /°C	31	30	32	29	29
		Humidity /%	42	63	51	65	45
Meteorological data from the nearest weather station	Temperature /°C	Mean	21	24	23	24	22
		Max	28	28	28	29	28
		Min	15	20	17	21	16
	Humidity /%	Mean	60	75	68	76	56
		Max	90	90	93	88	88
		Min	38	54	46	55	30
	Pressure /inch Hg	30.01	29.86	30.04	30.09	30.08	

Table A.3. (cont. 7)

#	36	37	38	39	40		
Date	7/31/2008	8/7/2008	8/13/2008	8/19/2008	8/28/2008		
Sites	P	J	J	M	O		
Season	Hot	Hot	Hot	Hot	Hot		
# of animals	243835	2380	2380	4200	4800		
Average weight (kg)	1.5	12	15	4.06	17.14		
Animal density (kg/m ³)	10.4	15.3	19.1	2.9	9.5		
Feed	corn and soybean ground	corn and soybean pellet	corn and soybean pellet	corn and soybean ground	corn and soybean pellet		
Cleaning cycle	manure: 4h; floor: 1d	6 months	6 months	2 years	2 years		
Fans running continuously	1.4m ×44	1.2m ×1; 0.9m ×1; 0.4m ×4	1.2m ×4; 0.9m ×1; 0.4m ×4	0.6m ×2	natural ventilation		
Fans running intermittently	1.4m ×44	1.2m ×3	none	none	natural ventilation		
Measured environmental data	Outside	Temperature /°C	30	28	28	29	30
		Humidity /%	65	60	57	55	61
	Inside	Temperature /°C	31	28	29	32	31
		Humidity /%	61	51	50	42	51
Meteorological data from the nearest weather station	Temperature /°C	Mean	26	22	20	21	23
		Max	32	27	27	29	28
		Min	19	17	13	13	18
	Humidity /%	Mean	77	71	70	65	78
		Max	100	94	100	94	87
		Min	35	48	42	35	69
	Pressure /inch Hg	29.79	30.04	29.85	30.03	29.85	

Table A.3. (cont. 8)

Field trip #		41	42	43	44	45	
Date		9/4/2008	9/11/2008	9/18/2008	9/25/2008	10/1/2008	
Sites		N	G	L	Q	H	
Season		Hot	Hot	Hot	Hot	Mild	
# of animals		6000	3890	550	436000	949	
Average weight (kg)		13.53	29	115	1.49	23	
Animal density (kg/m ³)		12.2	30.9	23.6	10.7	37.4	
Feed		corn and soybean pellet	corn and soybean ground	corn and soybean pellet	corn and soybean ground	corn and soybean ground	
Cleaning cycle		never	2 months	6 months	manure:6h; floor: 1d	2 months	
Fans running continuously		natural ventilation	1.2m ×6; 0.9m ×6	1.2m ×2; 0.9m ×1; 0.4m ×8	1.4m ×36	0.6m ×2; 0.3m ×2	
Fans running intermittently		natural ventilation	none	none	1.4m ×40	0.9m ×2	
Measured environmental data	Outside	Temperature /°C	22	22	26	30	25
		Humidity /%	73	88	61	50	68
	Inside	Temperature /°C	21	23	26	25	19
		Humidity /%	66	86	58	52	46
Meteorological data from the nearest weather station	Temperature /°C	Mean	17	20	19	22	11
		Max	21	21	26	30	18
		Min	13	19	12	15	5
	Humidity /%	Mean	84	95	72	60	72
		Max	94	100	93	88	93
		Min	60	93	49	18	42
	Pressure /inch Hg		29.83	30.02	30.27	30.28	29.99

Table A.3. (cont. 9)

#	46	47	48	49	50		
Date	10/8/2008	10/16/2008	10/29/2008	11/6/2008	11/17/2008		
Sites	I	J	O	N	J		
Season	Mild	Mild	Mild	Mild	Cold		
# of animals	500	1396	5000	5500	1134		
Average weight (kg)	13	60	9	9	115		
Animal density (kg/m ³)	12.2	44.7	5.2	7.4	69.7		
Feed	corn and soybean ground	corn and soybean pellet					
Cleaning cycle	2 months	6 months	2 years	never	6 months		
Fans running continuously	9" ×2	0.9m ×1; 0.4m ×4	natural ventilation	natural ventilation	0.4m ×4		
Fans running intermittently	24" ×2	1.2m ×3	natural ventilation	natural ventilation	0.9m ×1		
Measured environmental data	Outside	Temperature /°C	27	20	22	21	21
		Humidity /%	45	55	50	60	52
	Inside	Temperature /°C	22	16	17	14	4
		Humidity /%	36	50	35	52	48
Meteorological data from the nearest weather station	Temperature /°C	Mean	14	9	7	14	1
		Max	21	14	14	17	4
		Min	8	5	-1	12	-2
	Humidity /%	Mean	73	72	50	66	61
		Max	94	100	76	94	80
		Min	33	44	24	55	38
	Pressure /inch Hg	29.86	30.18	30.22	29.80	30.02	

Table A.3. (cont. 10)

#	51	52	53	54	55		
Date	11/24/2008	12/11/2008	12/18/2008	12/29/2008	1/15/2009		
Sites	G	O	M	N	Q		
Season	Cold	Cold	Cold	Cold	Cold		
# of animals	3860	4500	4000	5100	442000		
Average weight (kg)	23	16.7	8.1	18	1.44		
Animal density (kg/m ³)	24.3	8.7	5.5	13.8	10.5		
Feed	corn and soybean ground	corn and soybean pellet	corn and soybean ground	corn and soybean pellet	corn and soybean ground		
Cleaning cycle	2 months	2 years	2 years	never	manure:6h; floor: 1d		
Fans running continuously	none	natural ventilation	0.6m ×2	natural ventilation	1.4m ×20		
Fans running intermittently	0.9m ×6	natural ventilation	None	natural ventilation	1.4m ×20		
Measured environmental data	Outside	Temperature /°C	20	21	20	21	20
		Humidity /%	83	71	62	72	88
	Inside	Temperature /°C	5	1	-2	5	-17
		Humidity /%	54	64	54	65	62
Meteorological data from the nearest weather station	Temperature /°C	Mean	3	-3	-8	3	-23
		Max	6	3	-4	7	-20
		Min	1	-9	-11	0	-26
	Humidity /%	Mean	77	74	84	71	75
		Max	100	88	86	78	78
		Min	45	59	74	55	64
	Pressure /inch Hg	29.91	30.1	30.35	30.07	30.54	

Table A.3. (cont. 11)

#	56	57	58	59	60		
Date	1/26/2009	2/11/2009	4/16/2009	6/11/2009	7/8/2009		
Sites	H	I	J	H	T		
Season	Cold	Cold	Mild	Hot	Hot		
# of animals	935	750	1141	906	14000		
Average weight (kg)	11	15	80	9	1.45		
Animal density (kg/m ³)	17.6	21.1	48.8	14.0	5.5		
Feed	corn and soybean ground						
Cleaning cycle	2 months	2 months	6 months	2 months	manure: 3-5 years; floor: 70 weeks		
Fans running continuously	0.3m ×2	9" ×2	0.9m ×1; 0.4m ×4	0.3m ×2	0.9m ×4		
Fans running intermittently	0.6m ×2	24" ×1	1.2m ×3	0.9m ×2; 0.6m ×2	0.9m ×6		
Measured environmental data	Outside	Temperature °C	25	25	23	30	25
		Humidity /%	80	68	44	80	62
	Inside	Temperature °C	-7	7	19	25	27
		Humidity /%	66	76	45	71	68
Meteorological data from the nearest weather station	Temperature °C	Mean	-7	6	12	22	22
		Max	-6	11	20	27	28
		Min	-9	0	4	18	12
	Humidity /%	Mean	77	65	62	81	66
		Max	84	89	91	94	94
		Min	67	39	40	59	38
	Pressure /inch Hg	30.4	30.02	30.30	29.81	30.01	

Table A.3. (cont. 12)

#		61	62	63		
Date		9/1/2009	11/10/2009	4/22/2010		
Sites		S	G	L		
Season		Hot	Mild	Mild		
# of animals		21698	2350	2686		
Average weight (kg)		2.4	5.4	5.0		
Animal density (kg/m ³)		11.9	3.5	5.0		
Feed		corn and soybean pellet	corn and soybean pellet	corn and soybean pellet		
Cleaning cycle		1 year	2 months	6 months		
Fans running continuously		1.2m ×1; 0.9m ×1	0.9m ×2	0.9m ×1; 0.4m ×8		
Fans running intermittently		1.3m ×1; 1.2m ×7	0.9m ×2	1.2m ×1		
Measured environmental data	Outside	Temperature /°C	24	25	23	
		Humidity /%	70	44	37	
	Inside	Temperature /°C	26	15	22	
		Humidity /%	60	48	57	
Meteorological data from the nearest weather station	Temperature /°C	Mean	20	6	17	
		Max	29	13	24	
		Min	17	0	10	
	Humidity /%	Mean	n/a	69	54	
		Max	n/a	97	89	
		Min	54	30	31	
	Pressure /inch Hg		30.16	30.42	29.83	

APPENDIX B. LAYOUT OF ANIMAL FACILITIES UNDER INVESTIGATION

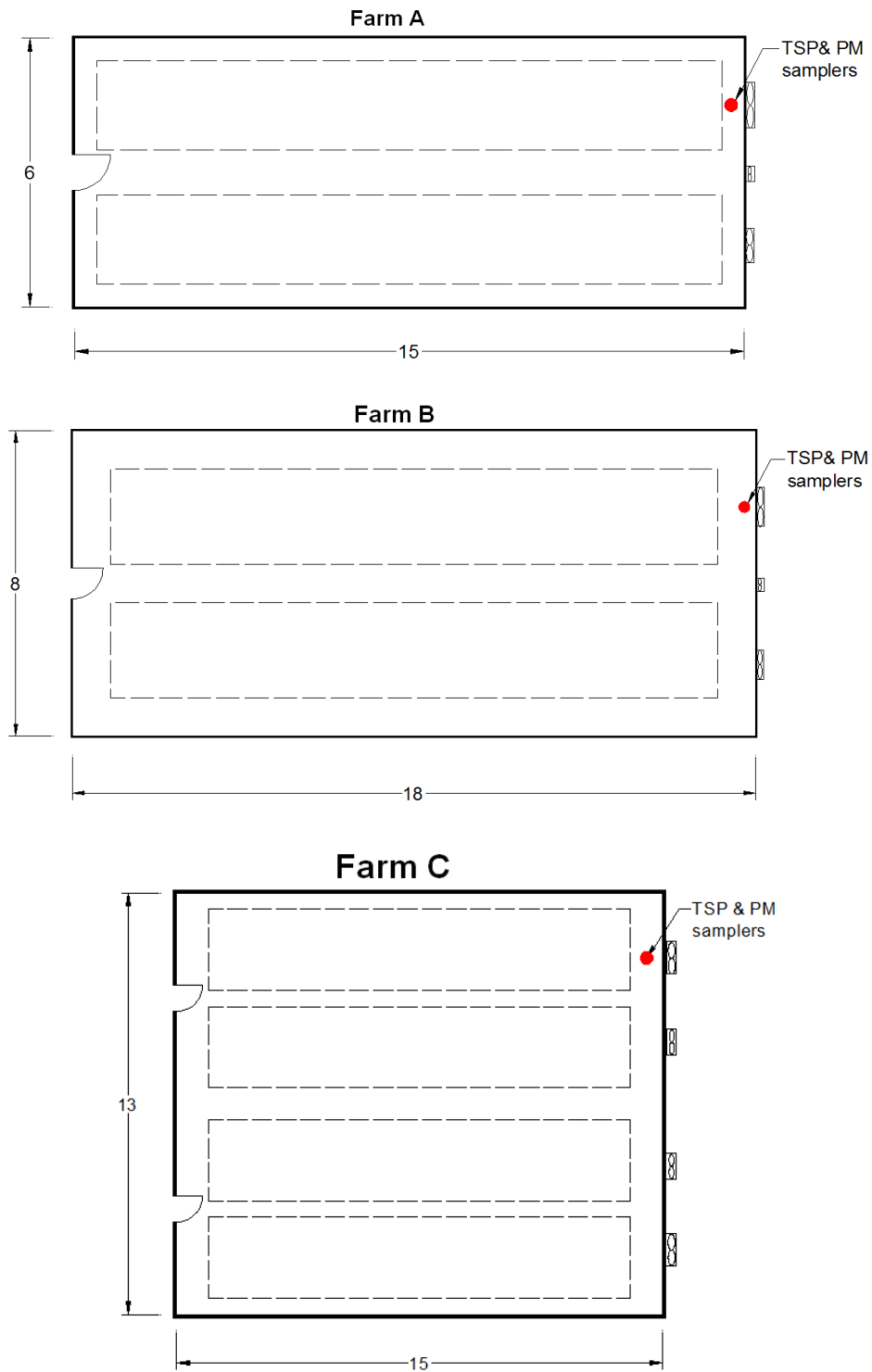


Figure B.1. Layout of animal buildings.

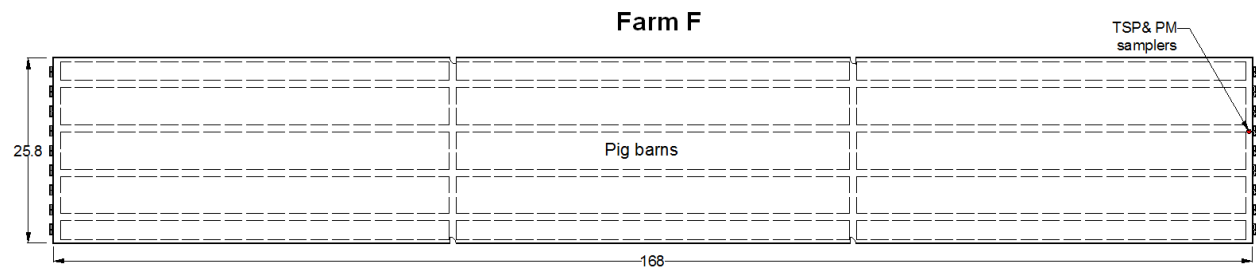
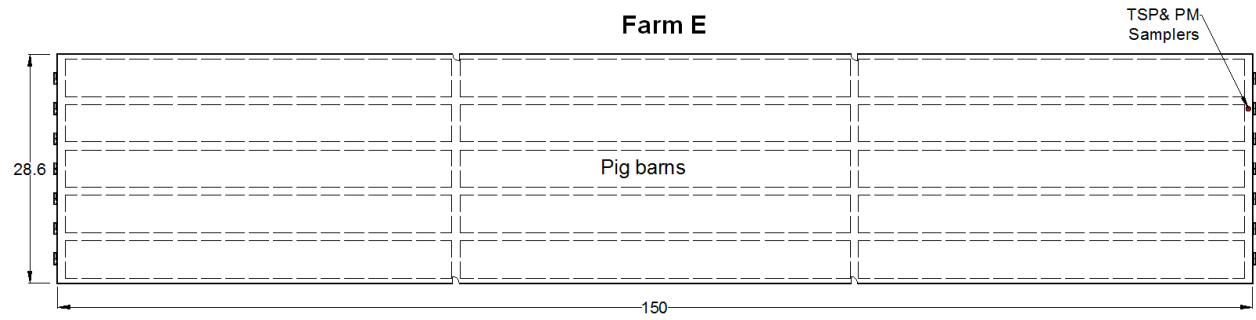
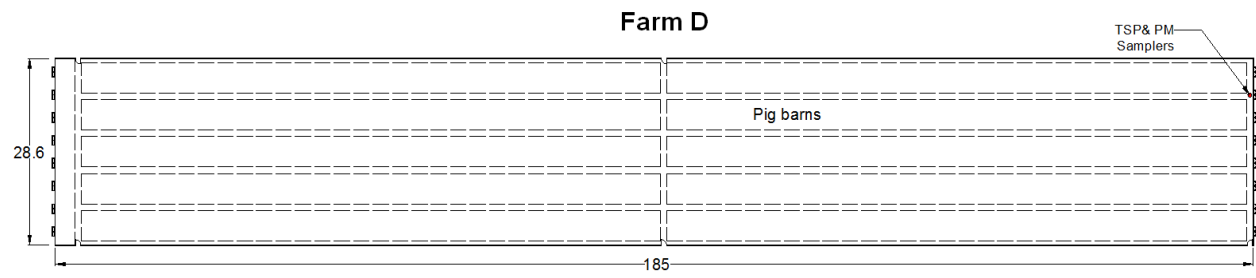


Figure B.1. Layout of animal buildings (cont. 1)

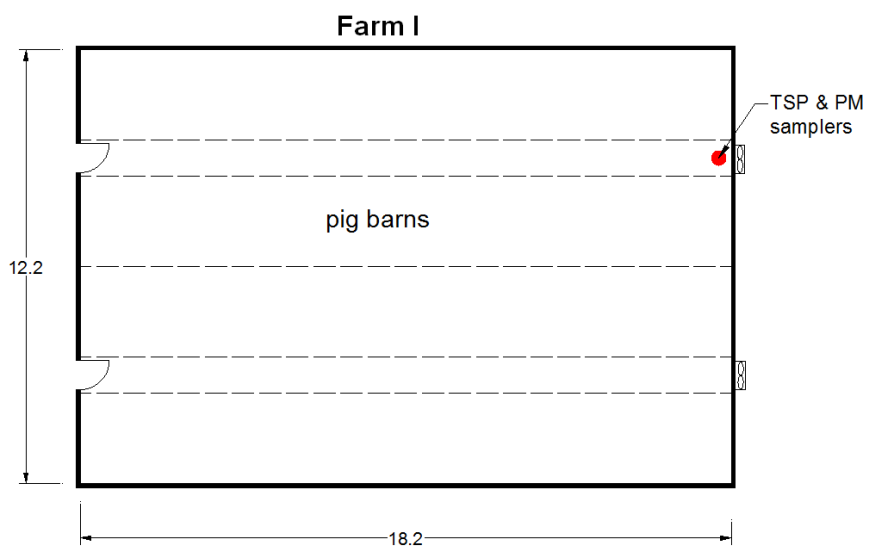
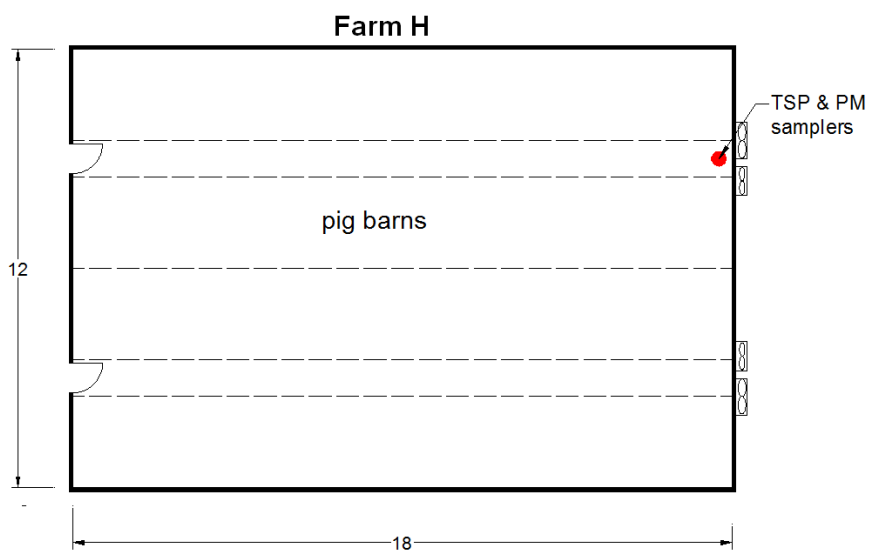
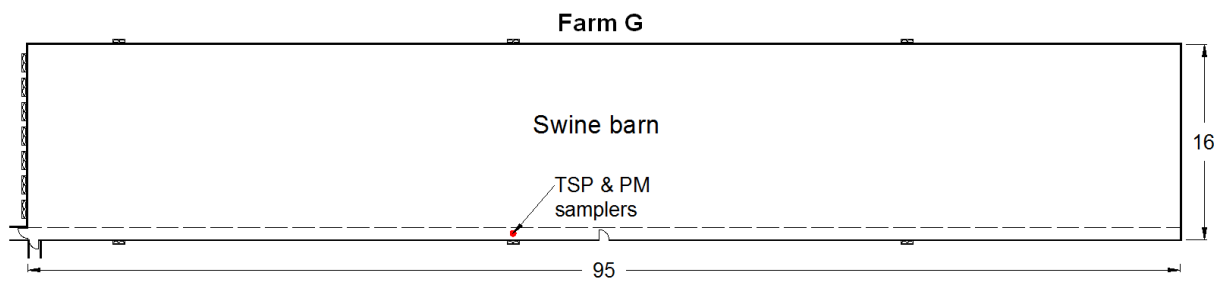


Figure B.1. Layout of animal buildings (cont. 2)

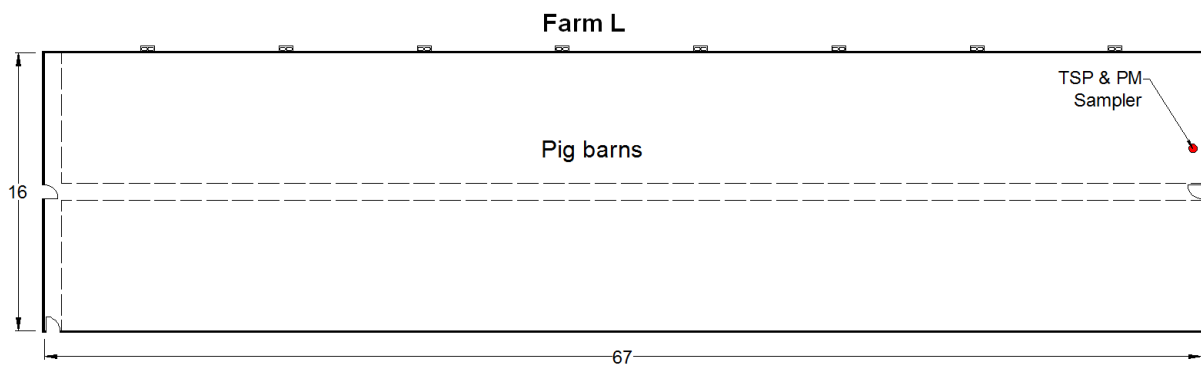
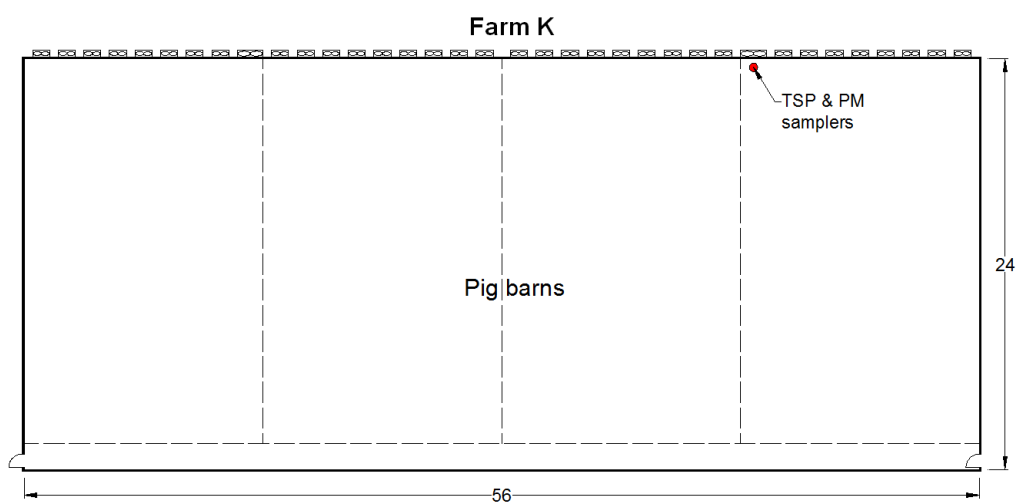
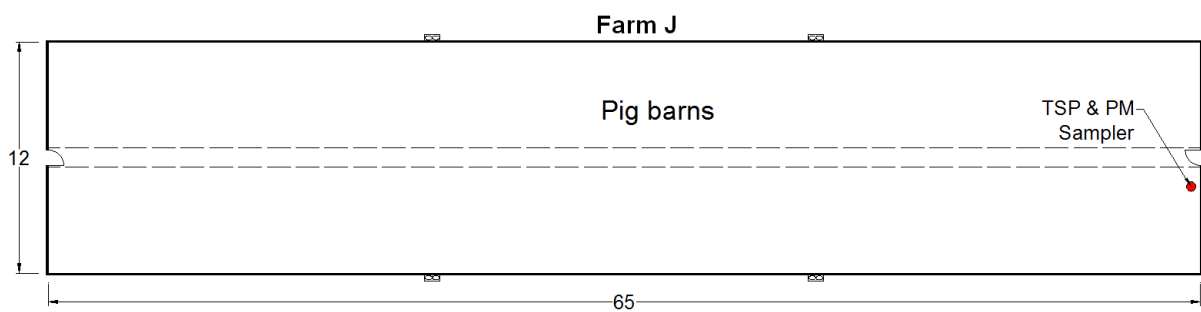


Figure B.1. Layout of animal buildings (cont. 3)

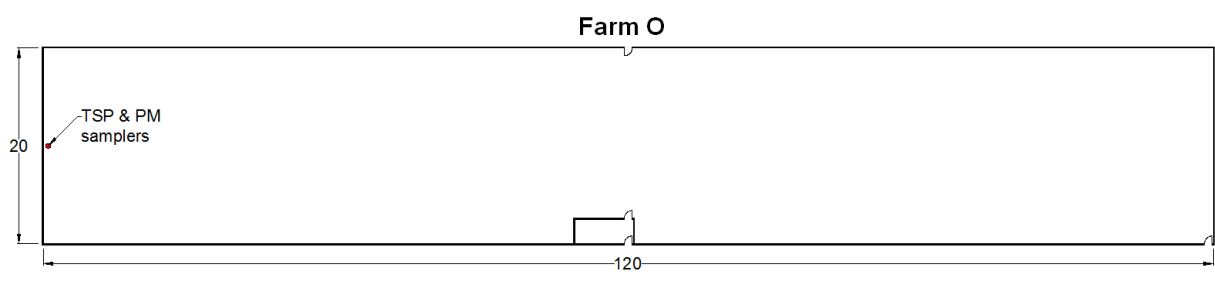
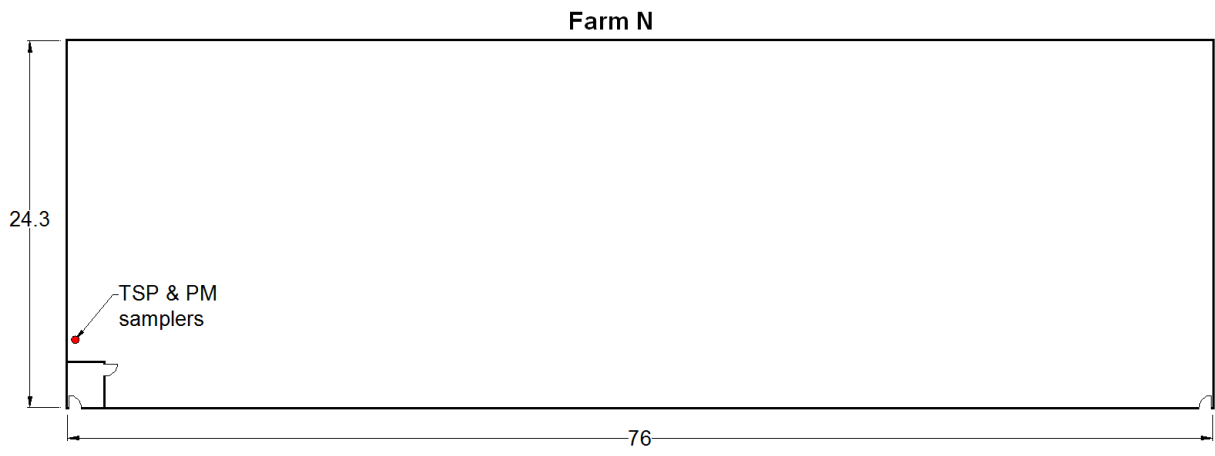
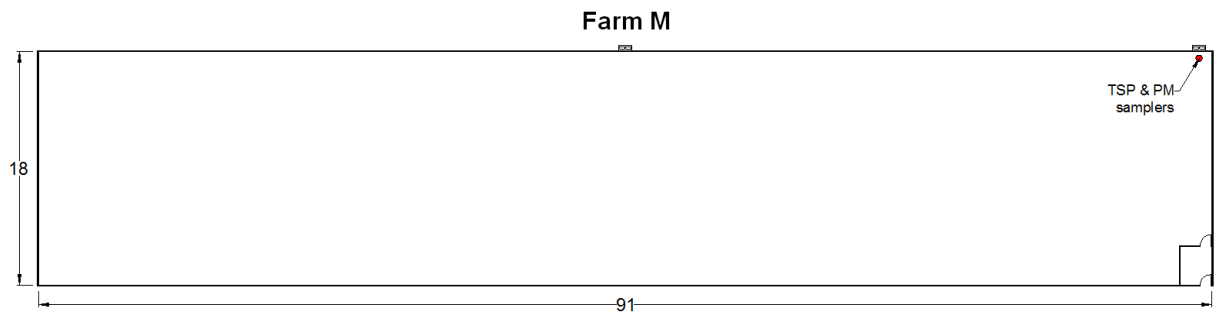


Figure B.1. Layout of animal buildings (cont. 4)

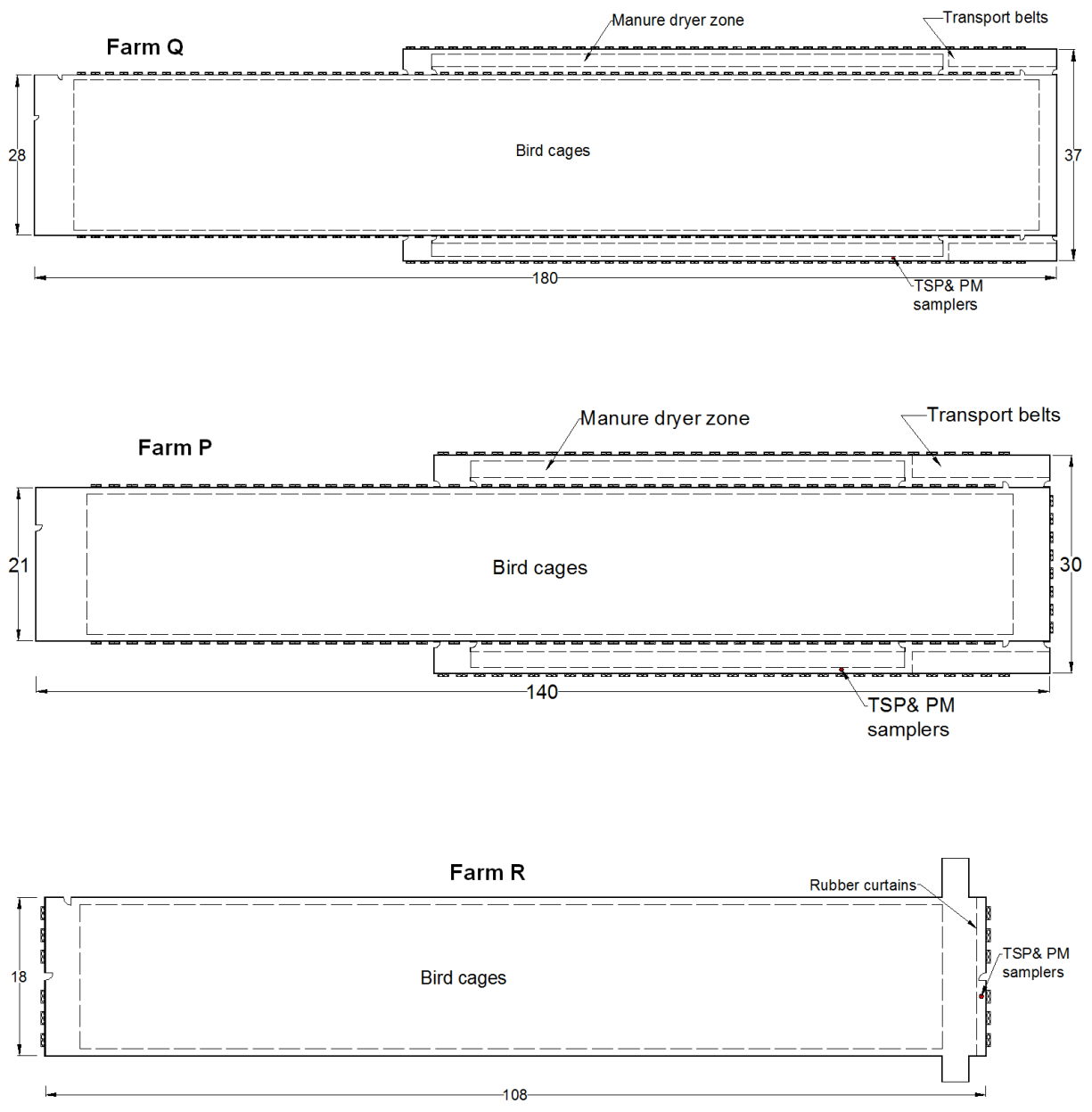


Figure B.1. Layout of animal buildings (cont. 5)

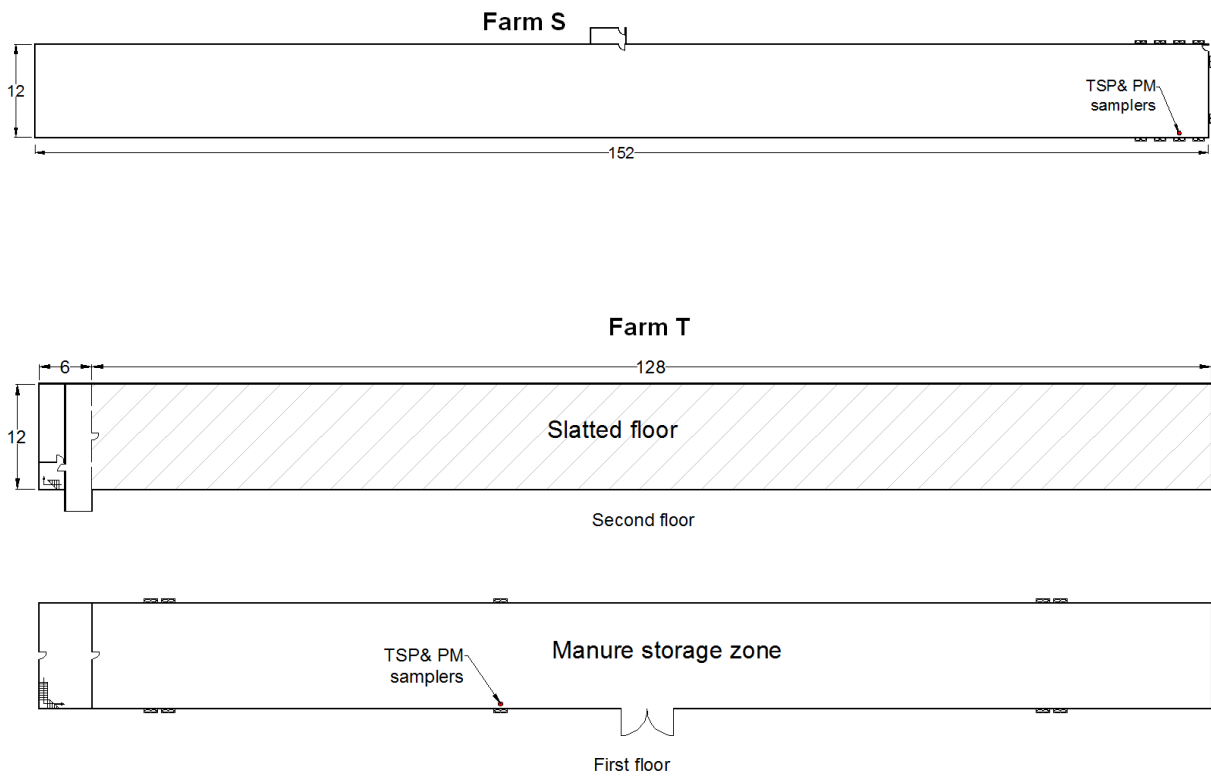


Figure B.1. Layout of animal buildings (cont. 6)

APPENDIX C. SAMPLING PROCEDURE AND MASS MEASUREMENT

The sampling procedure comprised following steps:

- (1) Clean sampling equipment. Equipment, e.g., pumps, tubing's, tools and the vehicle, was cleaned before each field trip. Items that entered animal barns were cleaned with anti-bacterial detergents.
- (2) Clean and sterilize PM samplers. All samplers were cleaned with antibacterial detergents and then rinsed with deionized water. TSP nozzles were sterilized in an autoclave (solid mode, 120 °C and 15 minutes). Polycarbonate filter cassettes and Harvard impactors were rinsed with 70% ethanol and dried under a UV light.
- (3) Sterilize filters. Glass fiber filters were sterilized in an autoclave (solid mode, 120 °C and 15 minutes) and ringed Teflon filters will be sterilized with UV light for 30 minutes in a bio-safety hood.
- (4) Pre-condition filters. Filters and support pads were conditioned in desiccators (relative humidity [RH] \leq 30 %) at room temperature (\sim 22 °C) for 24 to 48 hours. The pre-conditioning condition in this study were slightly different from that recommended by EPA for PM_{2.5} measurement (USEPA, 1999a)
- (5) Pre-weigh filters. Filters were weighed with an analytical balance (Ag245, readability of 0.01mg, Mettler Toledo, Greifensee, Switzerland). Filter weighing was repeated twice or even more times until no significant difference (\geq 0.03 mg) was detected among readings. The average reading was then recorded.
- (6) Assemble PM samplers. Filters were loaded into polycarbonate filter cassettes, or Anderson cassettes in Harvard impactors. Next, polycarbonate filters cassettes were sealed with plastic caps; while Harvard impactors were sealed with aluminum foils. For long-distance field trips, filters were loaded into Anderson cassettes first and then stored in 50 mm sterile Petri dishes (NC9074091, Fisher Scientific Inc., Franklin, MA). Loading Anderson cassettes into Harvard impactors was done in the field upon arrival.
- (7) Pre-check sampling equipment. The purpose was to ensure that pumps, timers and gauges were working properly and the sampling flow rates were correct.
- (8) Drive to animal farm. This took one to four hours depending on the location.

- (9) Install sampling system. In animal buildings, the UIUC TSP nozzles were fastened on a wood or steel frame at upstream of an exhaust fan (Figure C.1). The selected exhaust fan must be continuously running through the whole sampling period. The airflow velocity and direction were measured with an anemometer. The installation position and orientation of each TSP nozzle was then determined based on the measurement results. Harvard impactors were installed on a table near the exhaust fan. The distance between Harvard impactors and exhaust fan was at least 0.3 m, so as to avoid excessively high air velocities that could affect the sampler performance. Metal or plastic meshes were occasionally used to prevent samplers from disturbance by animals.



Figure C.1. Sampling setup in an animal building.

- (10) Check sampling flow rates to ensure the flow rate was 20 LPM for each sampler.
- (11) Start running pumps and recording the time. A time relay was occasionally used to control the sampling time.
- (12) Measure environmental conditions such as indoor and outdoor temperature and humidity, and record essential building information such as number of animals, average weight, building size, fans, ventilation stages, feeding system, feed, manure management method and cleaning cycle.
- (13) Turn off pumps after 20 to 24 hours and record the duration time. One exception was for TSP5 that only required 10 to 30 minutes' sampling time.
- (14) Dismantle the sampling system and reseal polycarbonate filter cassettes and Harvard impactors. For long-distance field trips, Anderson cassettes were taken out from Harvard impactors and stored in 50 mm sterile Petri dishes.
- (15) Drive back to campus.

- (16) Dismantle polycarbonate filter cassettes and Harvard impactors.
- (17) Transfer filters into 50 mm sterile Petri dishes.
- (18) Weigh filters. Filters were immediately weighed upon arrival in the lab. Similar to pre-weighing, filter weighing was repeated twice or even more times until no significant difference (≥ 0.05 mg) was detected among readings. The reading average was then recorded. TSP1-5 and PM3 samples were immediately sent to analysis labs, or packed and stored at around -20 °C in a freezer.
- (19) Re-condition filters. TSP6, 7 and PM1, 2, 4, 5 were conditioned in desiccators for 24 to 36 hours.
- (20) Re-weigh filters. TSP6, 7 and PM1, 2, 4, 5 were weighed again following the same protocol for pre-weighing, and then packed and stored in a freezer.
- (21) Mass concentrations were calculated with Equation C.1:

$$C_p = \frac{M_t - M_0}{Q_s \times t_s} \times \frac{T_{std}}{T_s} \times \frac{P_s}{P_{std}} \quad (C.1)$$

where C_p is mass concentration of airborne particles (mg/m^3), M_t is the mass of a filter with collected particles (mg), M_0 is the mass of that filter before sampling (mg), Q_s is the sampling flow rate (m^3/h), t_s is the sampling duration time (h), T_{std} is the standard temperature (273.2 K), T_s is the indoor temperature during sampling (K), P_s is the indoor barometric pressure (kPa), and P_{std} is the standard barometric pressure (101.325 kPa). However, only maximum indoor temperature was monitored in this study due to the availability of instrumentation. Accordingly, T_s was assumed to be 293 K (20 °C), a typical set point temperature for animal barns. The static pressure was neither monitored but generally was less than 0.2 inch water. Therefore, P_s approximately equals to the ambient atmospheric pressure available from the local weather stations.

Besides airborne particle collection, other experimental activities were conducted during field sampling. For example, feed and deposited dusts were collected; airborne bacteria and fungi were sampled on agar plates with an Anderson six-stage cascade impactor. However, those studies were not included in this thesis.

APPENDIX D. MEASUREMENT OF PSD WITH HORIBA LA-300 PARTICLE SIZER

Experimental

Horiba LA-300 particle sizer (Horiba Group, Edison, NJ) utilizes the principle of Mie scattering to measure the size distribution of polydispersed particles suspended in a light transparent liquid medium. In order to use it for aerosol study, particles have to be collected and then dispensed in a liquid. Brief experimental procedures are as follows:

- (1) Collect airborne particles on Teflon filters with the UIUC isokinetic TSP samplers.
- (2) Condition the filters in desiccators for at least 24 hours.
- (3) Transfer the filter into a 40 mL EPA vial.
- (4) Pour 20 mL 0.1 wt% NaPMP (sodium polymetaphosphate) solution into the vial.
- (5) Agitate the filter on an ultrasonicator for 20 minutes.
- (6) Dismantle and clean the optical chamber of Horiba with cotton balls and Kimberly paper towels.
- (7) Assemble the optical chamber.
- (8) Power on the particle sizer (30 minutes' warming up).
- (9) Pour deionized water into the sample chamber and clean the internal detection loop by water circulation for about five minutes.
- (10) Drain the water and repeat step (9) two to three times.
- (11) Pour a 0.1 wt% NaPMP solution into the sample chamber and start circulation
- (12) Set the proper test conditions in Horiba software (refractive index: 1.16-010i).
- (13) Perform initial alignment.
- (14) Measure the blank.
- (15) Pour 10 mL particle suspension from step (5) into the sample chamber.
- (16) Start measure the PSD of test samples.
- (17) Perform three successive replicate tests and take the average.
- (18) Export the results into a .txt file.
- (19) Drain the test sample and clean the detection loop with deionized water.
- (20) Start a new test or stop.

The data files were then imported into excel for data plotting and analysis. The Horiba calibration curve determined by Lee (2009) was used for reprocessing the raw data. Figure D.1 shows an example of obtained PSD profiles. A total of 37 samples were tested on Horiba LA-300. The measurement results were summarized in Table F-2.

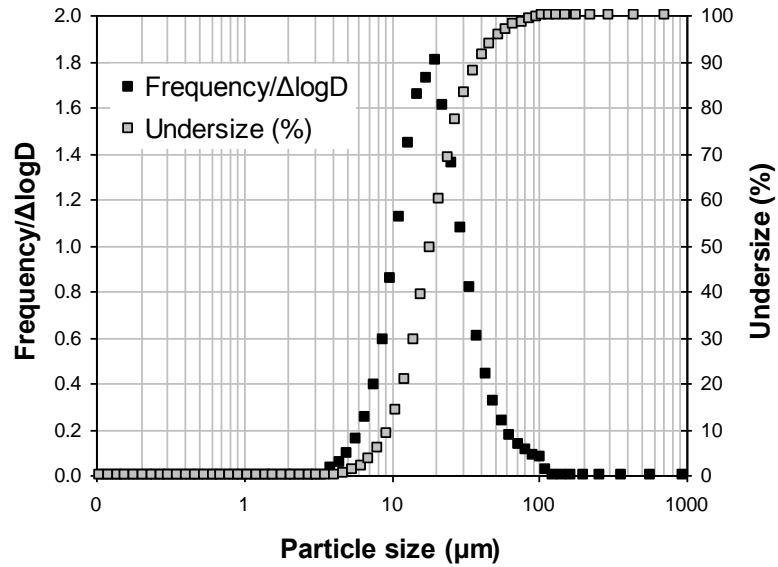


Figure D.1. A PSD profile measured by Horiba.

APPENDIX E. MEASUREMENT OF PARTICLE DENSITY WITH PYCNOMETER

Experimental

The true density of particles was measured in the lab with a pycnometer (AccuPyc II 1340, Micromeritics Instrument Cop., Norcross, GA). The smallest sample cup of this instrument is 1 mL and the corresponding test samples should be volumetrically no less than 0.5 mL. This means at least about 200 mg of dust samples need to be collected, which is impossible in practice. Therefore, in this study, the settled dust was selected as a surrogate and was collected into a Petri dish using a pre-cleaned stainless steel spoon. The collected dust samples were dried in desiccators for at least 48 hours upon arrival at the lab. Brief experimental procedures are as follows:

- (1) Turn on the helium gas.
- (2) Power on the pycnometer (30 minutes' warming-up).
- (3) Check the instrument setup to ensure that proper test parameters have been input.
- (4) Clean the 1 mL sample cup with Kimberly paper towels.
- (5) Weigh the sample cup on an analytical balance.
- (6) Carefully transfer dust samples into the sample cup with a metal spoon until 2/3 full, and then wipe off dusts on the outside surface with Kimberly paper towels.
- (7) Re-weigh the sample cup and calculate the mass of dusts inside.
- (8) Insert the sample cup into the test chamber and seal it.
- (9) Activate the analysis mode and input the sample ID and mass information.
- (10) Start the analysis program (ten replicate readings for each test).
- (11) Activated the review mode after the analysis stops, and manually record the test results displayed on the equipment screen.
- (12) Take out the sample cup, discard the test sample and then start a new test.

For each dust sample, three replicate tests were performed.

Results

A total of 16 dust samples were tested in this study. Data for other field trips can be found from Lee (2009). The true density of settled dust ranged from 1.412 to 1.567 g/cm³, with an

average of 1.489 g/cm³. Very small standard deviations were observed for each measurement, indicating a good replicability of this method.

Table E.1. Summary of density test results.

Field trip #	Sampling date	Density (g/cm ³)		Field trip #	Sampling date	Density (g/cm ³)	
		Mean	SD ^a			Mean	SD
42	9/11/2008	1.506	0.017	55	1/15/2009	1.474	0.001
43	9/18/2008	1.524	0.035	56	1/26/2009	1.474	0.013
44	9/25/2008	1.514	0.024	57	2/11/2009	1.412	0.006
45	10/1/2008	1.475	0.004	58	4/16/2009	1.496	0.010
46	10/8/2008	1.468	0.008	59	6/11/2009	1.482	0.007
47	10/16/2008	1.442	0.005	60	7/8/2009	1.567	0.006
50	11/17/2008	1.447	0.004	61	9/1/2009	1.538	0.008
51	11/24/2008	1.523	0.011	62	11/10/2009	1.488	0.009

a. SD refers to standard deviation.

APPENDIX F. LOGNORMAL REGRESSION ANALYSIS OF THE PARTICAL SIZE DISTRIBUTION DATA

Introduction

Lognormal distribution is the most commonly used model for description of particle size distribution (PSD). Many concepts (e.g., geometric standard deviation [GSD]) and mathematical and/or statistical analyses of PSD data (e.g., the Hatch-Choate equation) have been developed on the basis of a presumed lognormal distribution (Zhang, 2005). However, a deviation of measured PSD profiles from the ideal lognormal distribution is inevitable because of the complexity associated with particle formation, diminishment, aggregation and disaggregation as well as with detection. A typical size distribution of ambient aerosols can be bimodal (fine and course modes) or trimodal (nuclei, accumulation and course modes) (Wilson et al. 2002). Accordingly, two central questions related to fitting PSD data with lognormal distribution are:

- How to properly derive characteristic parameters such as mass median diameter (MMD) and GSD from a PSD profile?
- How to evaluate the goodness-of-fit of the lognormal distribution model?

Methods

There are three ways to determine MMD and GSD from a PSD profile: (1) direct reading, (2) linear regression, and (3) nonlinear regression.

Most modern particle sizers can measure cumulative mass/volume fraction of polydispersed particles. Table F.1 shows an example measured with Horiba LA-300 particle sizer (Horiba Group, Edison, NJ). MMD, i.e., the particle diameter corresponding to 50% accumulative mass fraction (D_{50}), can be determined through direct reading plus a data interpolation. Similarly, $D_{84.1}$ and $D_{15.9}$, corresponding to 84.1% and 15.9% accumulative mass fraction respectively, can be also determined. Assuming the particle size distribution is lognormal, GSD can be calculated as:

$$GSD = \left(\frac{D_{84.1}}{D_{50}} \right) = \left(\frac{D_{50}}{D_{15.1}} \right) = \left(\frac{D_{84.1}}{D_{15.9}} \right)^{0.5} \quad (\text{F.1})$$

Table F.1. A PSD example measured with Horiba LA-300 particle sizer.

Diameter (μm)	Cumulative fraction (%)	Diameter (μm)	Cumulative fraction (%)	Diameter (μm)	Cumulative fraction (%)
0.11	0.0	1.83	0.0	31.45	89.3
0.12	0.0	2.10	0.0	35.89	92.7
0.14	0.0	2.40	0.0	40.92	95.1
0.16	0.0	2.75	0.2	46.57	96.8
0.18	0.0	3.15	0.5	52.89	98.1
0.21	0.0	3.61	1.1	59.93	98.9
0.24	0.0	4.13	2.0	67.70	99.5
0.27	0.0	4.73	3.5	76.22	99.9
0.31	0.0	5.42	5.5	85.50	100.0
0.36	0.0	6.21	8.4	95.55	100.0
0.41	0.0	7.12	12.1	106.48	100.0
0.47	0.0	8.15	16.9	118.65	100.0
0.54	0.0	9.34	22.9	132.90	100.0
0.62	0.0	10.70	30.1	151.25	100.0
0.71	0.0	12.25	38.1	177.97	100.0
0.81	0.0	14.03	46.8	221.76	100.0
0.93	0.0	16.07	55.7	299.72	100.0
1.06	0.0	18.39	64.2	444.62	100.0
1.22	0.0	21.05	72.3	718.01	100.0
1.39	0.0	24.08	79.2	1233.79	100.0
1.60	0.0	27.53	84.9	2200.11	100.0

For the given example,

$$MMD = D_{50} = 14.03 + (16.07 - 14.03) \frac{(50 - 46.8)}{(55.7 - 46.8)} \approx 14.76(\mu\text{m})$$

$$D_{15.9} = 7.12 + (8.15 - 7.12) \frac{(15.9 - 12.1)}{(16.9 - 12.1)} \approx 7.93(\mu\text{m})$$

$$D_{84.1} = 24.08 + (27.53 - 24.08) \frac{(84.1 - 79.2)}{(84.9 - 79.2)} \approx 27.07(\mu\text{m})$$

$$GSD = \left(\frac{D_{84.1}}{D_{15.9}} \right)^{0.5} = \left(\frac{27.07}{7.93} \right)^{0.5} \approx 1.85$$

A more prevalent way is linear regression with the aid of a log-probability graph. This can be done by plotting data points of particle diameter versus cumulative fraction on a log-probability paper and then drawing a regression line. MMD (D_{50}), $D_{15.9}$ and $D_{84.1}$ can be read from the regression line, and GSD can be calculated subsequently. This process can also be done on an Excel sheet, as shown in Figure F.1. With Excel, the coefficient of determination (R^2) can be calculated as a measure of goodness-of-fit of lognormal distribution. For the given example, D_{50} is 14.59 μm, $D_{15.9}$ is 8.01 μm, $D_{84.1}$ is 26.56 μm and GSD is calculated to be 1.82; adjusted R^2 equals to 0.9978, indicating that the lognormal distribution model fits the PSD example data fairly well.

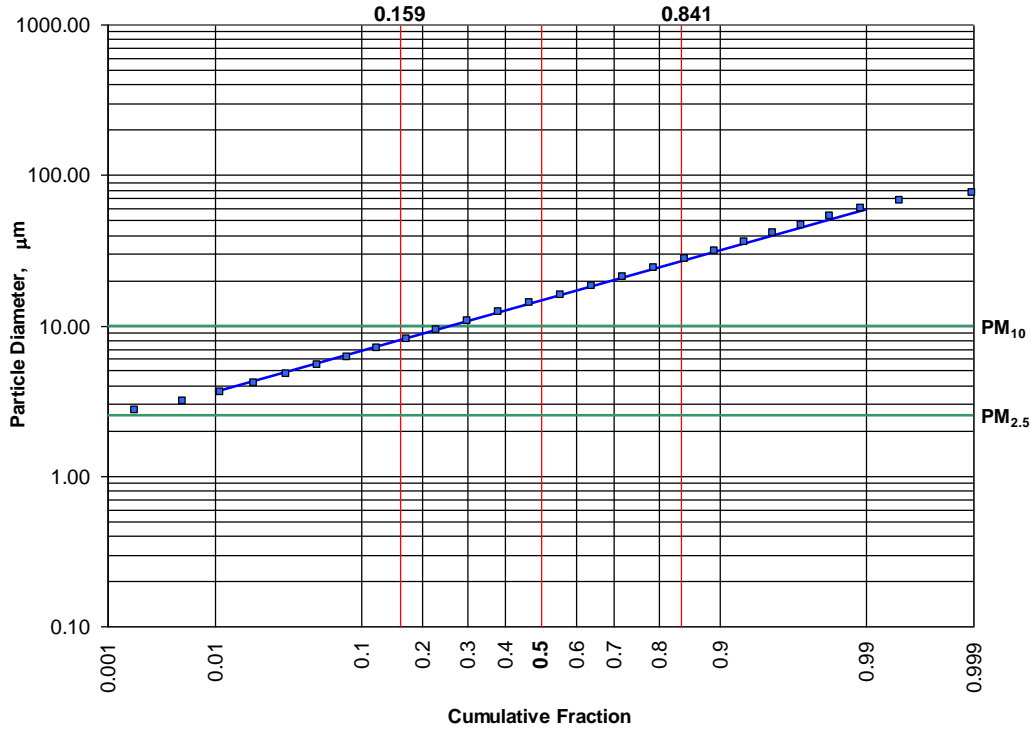


Figure F.1. Linear regression of a PSD example on an Excel sheet.

The third way is nonlinear regression. The lognormal distribution model has two variables, MMD (or CMD, SMD) and σ_g (GSD), as shown in Equation F.2. A least square nonlinear regression can be performed with a function of “nlinfit” in MATLAB 7.0. This work can also be done via an iterative optimization procedure in Excel using an add-in named SOLVER (Bah et al., 2009). In this study, the Newton iterative algorithm was selected and the initial estimates of MMD and σ_g were given by linear regression or direct reading. The tolerance was set to be 0.05%.

$$df = \frac{1}{d_p \log \sigma_g \sqrt{2\pi}} \exp\left(-\frac{(\log d_p - \log MMD)^2}{2(\log \sigma_g)^2}\right) d(d_p) \quad (F.2)$$

For evaluation of the goodness-of-fit, three parameters were calculated: adjusted R^2 , Akaike information criterion (AIC) and mean square error (MSE) (Bah et al., 2009). A good fitting performance should lead to a high adjusted R^2 , a low AIC and a low MSE, according to their respective statistical meanings.

$$R^2 = 1 - \left(\frac{RSS / (N - P)}{TSS / (N - 1)} \right) \quad (F.3)$$

$$AIC = N \ln(RSS / N) + 2P \quad (F.4)$$

$$MSE = \frac{RSS}{N - P} \quad (F.5)$$

Where, RSS is the residual sum of squares, N is the number of PSD channels, P is the number of variables (two for the lognormal distribution model), and TSS is the total sum of squares. For the given example, MMD is 14.74 μm and GSD is 1.85; adjusted R^2 is calculated to 0.9993, AIC is -921.6 and MSE is 5.4×10^{-7} , indicating a good fitting performance of lognormal distribution to the PSD example data.

Results and Discussion

Airborne particles emitted from eight swine and poultry confinement buildings were sampled on Teflon filters (ZefluorTM PTFE member filter w/ support pads, P/N P5RJ037, Pall Corporation, Ann Arbor, MI) using UIUC TSP nozzles. A total 37 TSP samples were collected and then subject to PSD measurement with a Horiba LA-300 particle sizer. The measurement data were reprocessed based on the calibration curve made by Lee (2009). Assuming an identical density for all sizes of particles, the MMD and GSD were determined by means of direct reading, linear regression and nonlinear regression, as summarized in Table F.2.

Table F.2. Summary of MMD and GSD determined by different methods.

#	Direct reading		Linear regression			Nonlinear regression					Note ^b
	MMD	GSD ^a	MMD	GSD	R ²	MMD	GSD	R ²	AIC	MSE	
1	18.5	2.90	13.5	3.10	0.9732	20.4	2.60	0.9549	-706.6	1.6×10^{-5}	bimodal
2	18.5	2.34	17.7	2.20	0.9959	18.7	2.30	0.9982	-895.3	8.2×10^{-7}	
3	13.1	1.72	9.6	2.20	0.9274	13.4	1.67	0.9944	-781.8	4.8×10^{-6}	bimodal
4	12.8	1.84	12.8	1.82	0.9985	12.7	1.83	0.9994	-929.8	4.8×10^{-7}	
5	22.1	2.05	19.2	2.09	0.9914	22.7	2.01	0.9899	-767.6	6.0×10^{-6}	
6	24.5	2.08	22.0	2.03	0.9940	25.1	2.06	0.9923	-786.6	4.5×10^{-6}	
7	63.8	3.08	53.0	4.00	0.9847	58.9	3.00	0.9134	-678.8	2.4×10^{-5}	trimodal
8	72.4	3.21	61.3	4.17	0.9872	63.8	3.18	0.8945	-665.4	3.0×10^{-5}	trimodal
9	24.0	2.09	21.2	2.10	0.9928	24.7	2.06	0.9899	-771.2	5.7×10^{-6}	
10	22.4	2.30	14.8	2.70	0.9548	24.7	1.98	0.9510	-674.1	2.6×10^{-5}	bimodal
11	20.5	2.34	15.0	2.63	0.9703	21.9	2.17	0.9729	-719.2	1.3×10^{-5}	bimodal
12	22.6	2.22	22.5	2.08	0.9945	22.6	2.23	0.9977	-872.2	1.2×10^{-6}	
13	21.4	2.94	21.5	1.89	0.9954	21.3	1.93	0.9986	-888.8	9.0×10^{-7}	
14	22.8	2.12	23.4	2.04	0.9967	22.6	2.11	0.9963	-837.5	2.0×10^{-6}	
15	21.6	2.71	15.5	3.09	0.9651	23.7	2.44	0.9608	-711.7	1.4×10^{-5}	bimodal
16	19.8	2.09	16.7	2.07	0.9884	20.6	2.04	0.9787	-720.1	1.3×10^{-5}	bimodal
17	22.8	2.39	21.1	2.37	0.9928	23.2	2.36	0.9921	-802.7	3.5×10^{-6}	

Table F.2. (cont.)

#	Direct reading		Linear regression			Nonlinear regression					Note ^b
	MMD	GSD ^a	MMD	GSD	R ²	MMD	GSD	R ²	AIC	MSE	
18	20.5	2.31	20.2	2.25	0.9963	20.5	2.29	0.9956	-836.1	2.1×10 ⁻⁶	
19	20.5	2.19	19.8	2.20	0.9975	20.6	2.18	0.9957	-831.5	2.2×10 ⁻⁶	
20	14.4	1.96	14.1	1.94	0.9975	14.4	1.96	0.9990	-909.3	6.5×10 ⁻⁷	
21	13.5	2.01	13.7	1.96	0.9969	13.4	2.01	0.9993	-932.0	4.6×10 ⁻⁷	
22	18.6	1.70	19.7	1.76	0.9960	18.3	1.68	0.9963	-806.5	3.3×10 ⁻⁶	
23	19.1	1.73	20.6	1.80	0.9947	18.7	1.70	0.9953	-793.2	4.0×10 ⁻⁶	
24	16.0	2.43	11.0	2.47	0.9645	17.7	2.06	0.9300	-651.9	3.7×10 ⁻⁵	bimodal
25	17.0	2.00	15.9	1.97	0.9971	17.2	1.99	0.9935	-792.1	4.1×10 ⁻⁶	
26	32.1	3.38	39.6	3.00	0.9865	32.6	3.45	0.9322	-695.7	1.8×10 ⁻⁵	bimodal
27	21.8	1.97	21.0	1.94	0.9960	21.8	1.96	0.9975	-851.8	1.6×10 ⁻⁶	
28	20.3	2.52	14.7	2.86	0.9692	22.1	2.29	0.9648	-710.3	1.5×10 ⁻⁵	bimodal
29	21.0	2.13	19.2	2.10	0.9931	21.3	2.11	0.9965	-841.5	1.9×10 ⁻⁶	
30	21.7	2.14	14.1	2.74	0.9486	23.5	1.85	0.9525	-668.4	2.8×10 ⁻⁵	bimodal
31	20.5	1.92	18.1	2.02	0.9943	21.0	1.87	0.9854	-735.5	9.9×10 ⁻⁶	
32	24.1	2.63	23.2	2.30	0.9873	24.1	2.63	0.9828	-761.4	6.6×10 ⁻⁶	
33	23.0	2.61	22.2	2.33	0.9905	23.0	2.62	0.9856	-772.3	5.6×10 ⁻⁶	
34	34.4	2.61	39.3	2.80	0.9696	34.1	2.56	0.9940	-832.8	2.2×10 ⁻⁶	tail peak
35	33.0	2.52	38.2	2.82	0.9664	32.6	2.48	0.9942	-831.5	2.2×10 ⁻⁶	tail peak
36	14.0	1.89	14.5	1.88	0.9977	13.9	1.88	0.9988	-893.3	8.4×10 ⁻⁷	
37	14.8	1.85	14.6	1.82	0.9978	14.7	1.85	0.9993	-921.6	5.4×10 ⁻⁷	
A ^c	15.8	1.81	23.8	2.22	0.9791	15.4	1.77	0.9959	-809.4	3.1×10 ⁻⁶	bimodal

a. $GSD = (D_{84.1}/D_{15.9})^{0.5}$.

b. Peak characteristics were obtained from direct observation.

c. An artificial PSD curve established for approach comparison: This PSD profile was a combination of two lognormal peaks: (1) MMD=15.0 μm, GSD=1.7; and (2) MMD=45 μm, GSD: 2.7. The intensity (area) ratio of two peaks is 9:1.

A drawback of the direct reading approach is that the GSD values calculated from $D_{84.1}/D_{50}$, $D_{50}/D_{15.1}$ and $(D_{84.1}/D_{15.9})^{0.5}$ can be significantly different when a PSD profile is not lognormally distributed. For example, in the 10th dataset, the calculated GSD value was 1.89 from $D_{84.1}/D_{50}$, 2.79 from $D_{50}/D_{15.1}$, and 2.30 from $(D_{84.1}/D_{15.9})^{0.5}$. To be consistent, all GSD values in Table F.2 were calculated by $GSD = (D_{84.1}/D_{15.9})^{0.5}$; however, the representativeness of those GSD values is questionable.

The values of MMD and GSD produced from three different approaches can be substantially different. For example, in the 3rd dataset, linear regression generated a MMD value of 9.6 μm, much smaller than that produced from direct reading (13.1 μm) or nonlinear regression (13.6 μm). In general, linear regression produced a smaller MMD but a greater GSD than both direct reading and nonlinear regression ($P < 0.05$). However, this might be related to the peak characteristics of measured PSD profiles and a false conclusion could be raised from a limited

number of measurements. The presence of a number of counterexamples indicates that a more appropriate comparison between linear and nonlinear approaches should be conducted on the basis of individual PSD profiles with diverse peak characteristics.

The fitting performance of lognormal distribution described by adjusted R^2 values can be inconsistent and even controversial between linear and nonlinear regression approaches. For example, in the 3rd dataset, linear regression generated an adjusted R^2 value of 0.9274, indicating a poor fitting performance; while the adjusted R^2 value produced by nonlinear regression was 0.9944, representing a good fitting. By contrast, in the 8th dataset, nonlinear regression indicated a poor fitting while linear regression predicted the opposite. Bimodal distributions were found in both PSD datasets, which implies that the inconsistency in R^2 values might be due to different treatments of “abnormal” PSD peaks by linear and nonlinear regression approaches.

Therefore, a better comparison of linear and nonlinear regression approaches would require an investigation of the influence of peak characteristics on regression coefficients (MMD and GSD) and fitting performance characterized by adjusted R^2 . To demonstrate that, an artificial and three practical PSD profiles were examined. MMD and GSD values predicted by linear and nonlinear approaches were used to plot lognormal regression curves which were then compared with the measured PSD data (Figure F.2).

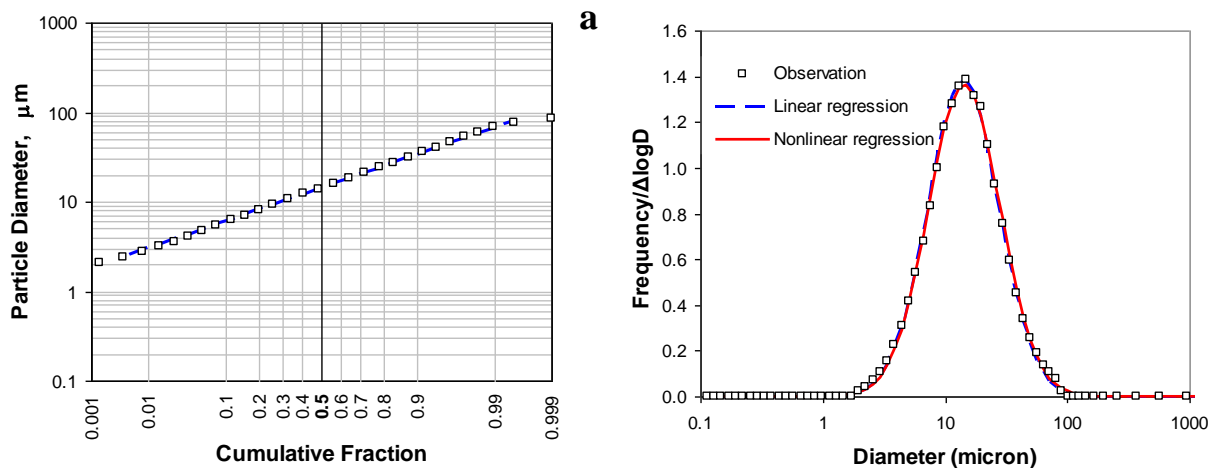


Figure F.2. Examples of PSD profiles with different peak characteristics: a- the 21st dataset, b- the 3rd dataset, c- the artificial (A) dataset, and d- the 7th dataset; Left- measured data (open square) and linear regression line (blue dash line) on the log-probability graph, and Right- observed PSD curve (open square), PSD curve from nonlinear regression (red solid line) and PSD curve from linear regression (blue dash line).

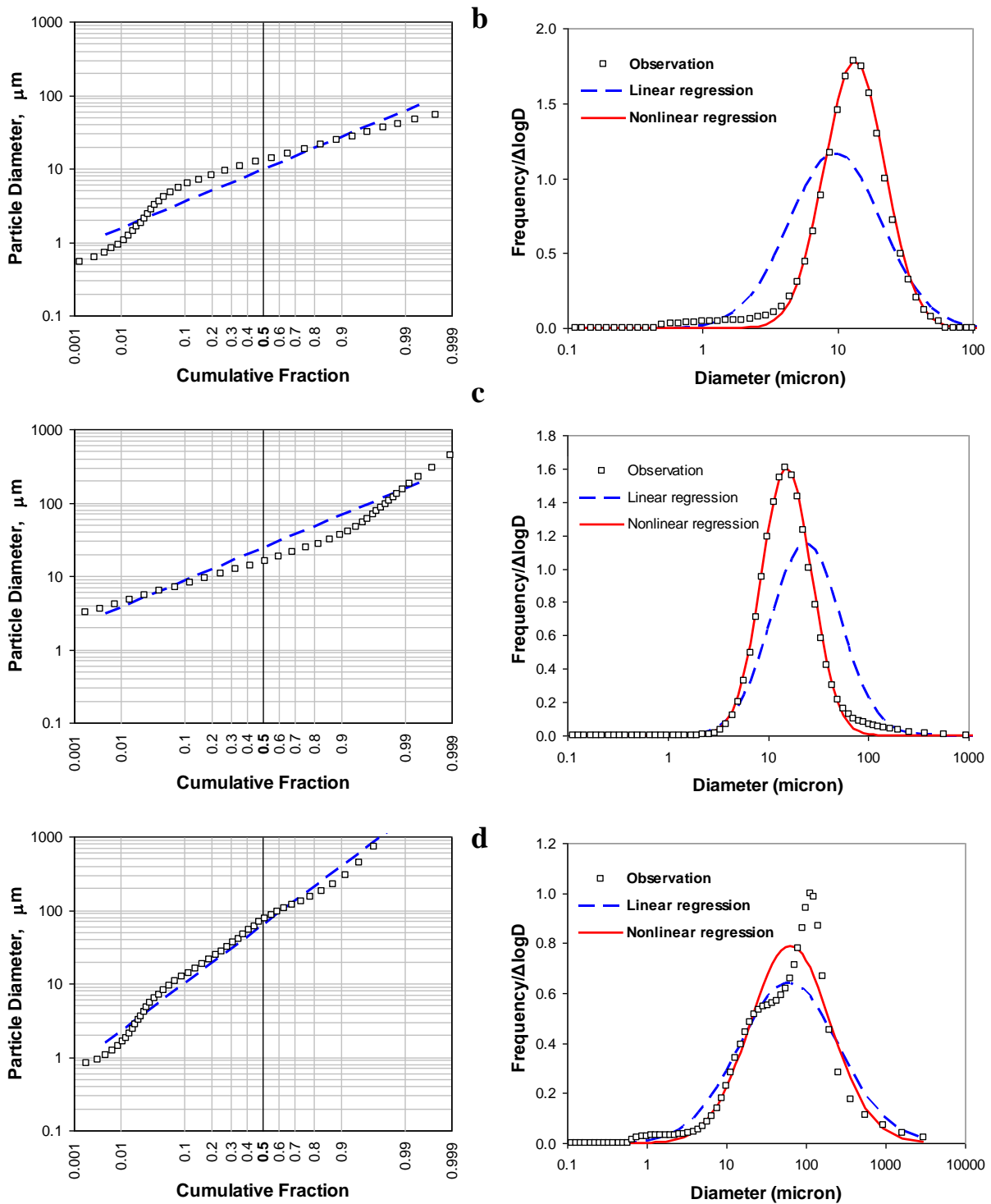


Figure F.2. (cont.)

For PSD profiles apparently well fitted with the lognormal distribution model, e.g., the 20th dataset (Figure F.2a), both linear and nonlinear regression approaches produced high adjusted R^2 and very similar MMD and GSD values. However, when a minor side or tail peak existed either

at a smaller (Figure F.2b) or higher diameter (Figure F.2c), the linear regression approach could not produce reasonable MMD and GSD results; instead, it could significantly overestimate GSD, and over- or underestimate MMD of the major peak, depending on the location of the side or tail peaks. In contrast, the MMD and GSD values produced by the nonlinear regression approach were obviously more reasonable. The sensitiveness of linear regression to minor side or tail peaks is not essentially negative: the adjusted R^2 values were found to be a good index for determination of the presence of minor side or tail peaks that were sometimes difficult to distinguish on a raw PSD profile. As shown in Table F.2, bimodal, of which the minor side peak is a special case, or tail peaks existed when the adjusted R^2 values of linear regression were less than 0.98. However, a bimodal or trimodal distribution did not always lead to an adjusted R^2 value below 0.98 (Figure F.2d): in this PSD profile, the leftmost minor peak and the rightmost major peak coincidentally made the regression line close to the measured data. As a comparison, nonlinear regression is less sensitive to the minor side or tail peaks. An adjusted R^2 value over 0.98 could be obtained even with the presence of those peaks (Figure F.2b and F.2c). However, nonlinear regression was found to be relatively sensitive to the existence of strong side peaks or a distortion of major peaks (Figure F.2d).

What causes the difference between the linear and nonlinear regression approaches? Both approaches are least squares regression methods; however, the input dataset and the targeted residual sum of squares (RSS) are fundamentally different. In the linear regression approach, the original PSD data are transformed and rescaled into a log-probability form so that a simply linear regression becomes plausible. Accordingly, the targeted residual equals $\log(D_{\text{predicted}}) - \log(D_{\text{actual}})$, where D is the particle diameter. The slope and intercept of a regression line are strongly influenced by the edge points, in this case, the data points near the minimal or maximal sizes. Although these edge data points are of less importance in describing the geometry of the major PSD peak(s) in the middle of the size range, they are sensitive to the presence/ absence of minor side or tail peaks at the edges. As a consequence, the presence of minor side or tail peaks can be over-represented in the linear-regression approach, resulting in a misestimation of MMD and GSD and a lower adjusted R^2 value (Figure F.2b and F.2c). In contrast, in the nonlinear regression approach, there is no data transformation and the targeted residual equals $F_{\text{predicted}}(D_i) - F_{\text{actual}}(D_i)$, where $F(D_i)$ refers to the occurrence frequency of particles with diameters between D_{i-1} and D_i . In this case, the presence of minor side or tail peaks becomes less significant because

usually these peaks only produce small residuals; instead, high residuals are usually caused by the presence of strong side peaks and/or a distortion of the major peak(s) (Figure F.2d), leading to a low adjusted R^2 value. Because the R^2 values from the linear and nonlinear regression approaches reflect somehow different peak characteristics of a PSD profile, they can be complementary to each other with respect to assessment of deviations from the lognormal distribution model.

From the previous discussion, an index for assessing the deviation of a PSD profile from lognormal distribution was proposed (Equation F.6). If C is equal or greater than 0.98, a PSD profile is considered to be lognormally distributed, i.e. have no significant side or distorted peaks. A total of 217 measured PSD data for animal building dust (37 from this study and 181 from Lee [2009]) were subject to the test. The results showed that the judgments made based on the proposed criterion were fully consistent with those from direct observations. The fitting performance of the lognormal distribution model was found to vary with particle size analyzer, as shown in Table F.3 and Figure F.3. The same conclusion was drawn from statistical analysis on AIC and MSE (data not shown here). A similar finding was reported by Bah et al. (2009) in efforts to investigate the size distribution of soil particles. In general, PSD profiles measured with light scattering methods (Horiba and Malvern) follow the lognormal distribution better.

$$C = \min \left(R_{adjusted_linear}^2, R_{adjusted_nonlinear}^2 \right) \quad (F.6)$$

Table F.3. Summary of lognormality tests on PSD profiles from different instruments.

	Horiba	DSP ^a	Coulter ^b	Malvern ^c
Number of profiles	83	44	45	45
Average C	0.9608	0.9338	0.8903	0.9386
Percentage passing the proposed lognormality test	34%	0%	11%	4%
Detection principle	Light scattering	Time of flight	Electrical impedance	Light scattering
Diameter type	Equivalent volumetric	Aerodynamic	Equivalent volumetric	Equivalent volumetric
Number of channels	64	100	300	100

a. Aerosizer DSP (TSI Inc., St. Paul, MN).

b. Coulter Counter Multisizer (Beckman Counter Inc., Fullerton, CA).

c. Malvern Multisizer (Malvern Instruments Ltd, Worcestershire, UK).

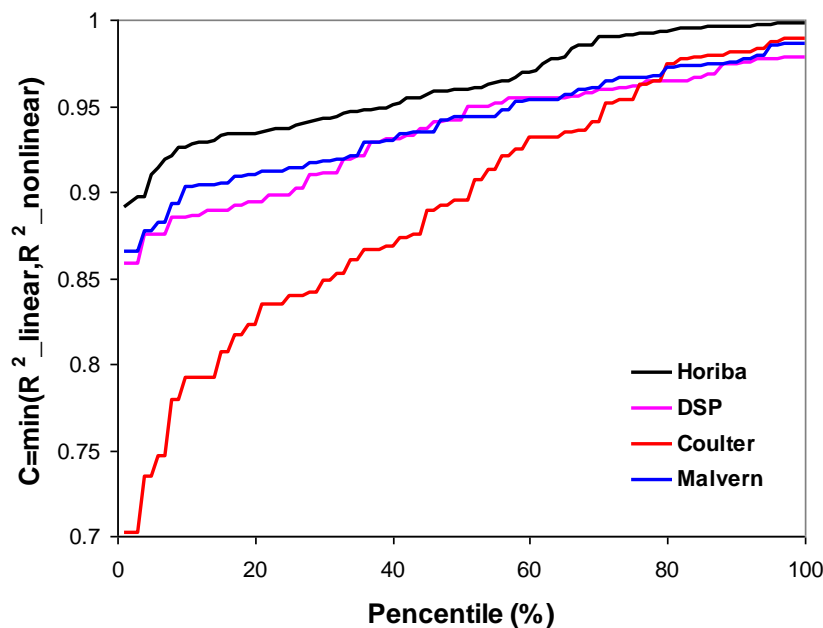


Figure F.3. Percentile plot of C values from different particle size analyzers.

Moreover, because the R^2 values from linear and nonlinear regression approaches represent somehow different manners of deviation from lognormal distribution, an R^2_{linear} versus $R^2_{\text{nonlinear}}$ plot was proposed to offer a quick and convenient overview on the lognormality of a large number of PSD profiles (Figure F.4). On this plot, PSD profiles from different particle size analyzers showed distinctly different patterns. A higher occurrence frequency of and overall stronger minor side or tail peaks were found on PSD profiles from Malvern; while PSD profiles produced from Coulter were associated with a higher occurrence frequency of distorted major peak(s) or strong side peak(s). This is consistent with our direct observations on individual PSD profiles: the Malvern to generate PSD profiles that had a single major peak with a tail or minor side peak on the left (smaller particle size); while the Coulter tended to produce PSD profiles that had no apparent side peaks but a strongly distorted and noisy major peak. Figure F.5 showed two extreme PSD examples. Differences in the lognormality of PSD profiles from different particle analyzer sizers might be caused by discrepancies in detection principles (Table F.3) and sample preparation procedures. The proposed R^2_{linear} versus $R^2_{\text{nonlinear}}$ plot may also be applied to a comparison of PSD profiles from different sampling periods and emission sources.

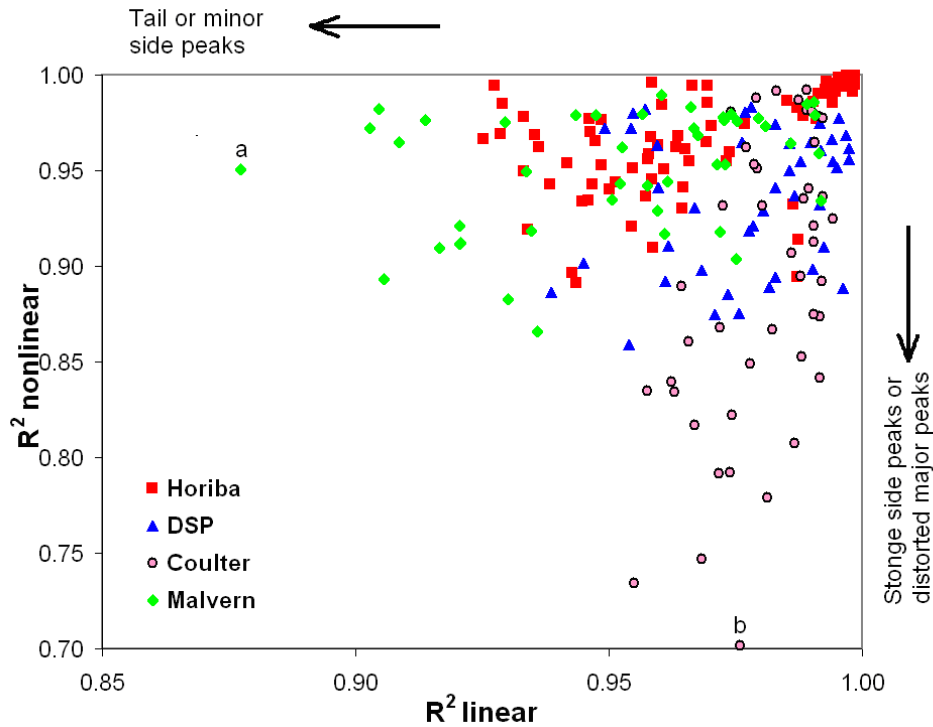


Figure F.4. Scatter plot of R^2_{linear} versus $R^2_{\text{nonlinear}}$ from different particle size analyzers.

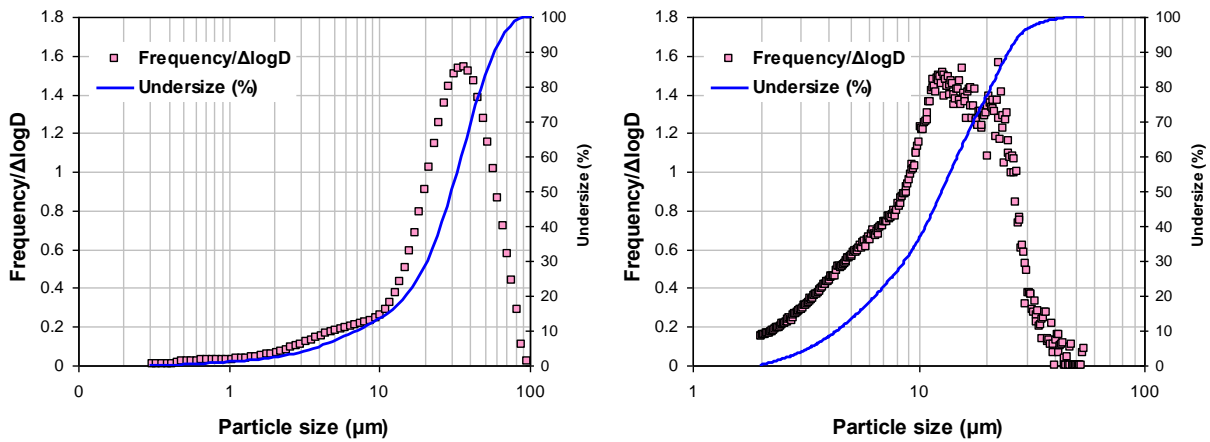


Figure F.5. Two extreme PSD examples: a- point 'a' in Figure F.4 (Malvern, $R^2_{\text{linear}}=0.8774$, $R^2_{\text{nonlinear}}=0.9503$); b- point 'b' in Figure F.4 (Coulter, $R^2_{\text{linear}}=0.9759$, $R^2_{\text{nonlinear}}=0.7018$).

Conclusion

The values of MMD and GSD derived from direct reading, linear regression and nonlinear regression can be substantially different when a PSD profile is not lognormally distributed. Among these three, the nonlinear regression approach provided the best estimates of MMD and

GSD; while the still-prevalent linear regression approach could significantly misestimate MMD and GSD with the presence of minor side or tail peaks.

The coefficients of determination derived from the linear and from the nonlinear regression approaches are associated with different manners of non-lognormality of PSD profiles. Based on that, an index ($C = \min(\text{adjust } R^2_{\text{linear}}, \text{adjust } R^2_{\text{nonlinear}})$) was proposed for evaluating the fitting performance of the lognormal distribution model. A total of 217 measured PSD datasets were tested and the results showed that the fitting performance varied with particle size analyzers used for PSD measurements. In general, PSD profiles measured with Mie scattering methods exhibited better lognormality. An R^2_{linear} versus $R^2_{\text{nonlinear}}$ plot was proposed and was found to be useful for comparing the lognormality of a large number of PSD profiles from different particle size analyzers.

APPENDIX G. FITTING PERFORMANCE OF PARTICLE SIZE DISTRIBUTION MODELS ON ANIMAL BUILDING DUST.

Introduction

Animal building dust may contain toxic, allergenic, pathogenic and even carcinogenic components and has been recognized to be associated with many public health issues (Heederik et al., 2007), e.g., occupational allergy and swine flu. Particle size is one of the most important physical characteristics of airborne dust, often presented in terms of equivalent volume diameter and aerodynamic diameter (Zhang, 2005). Particle size is strongly associated with the environmental and health effects of particles. Small dust can penetrate deeply into the respiratory tract and travel a relatively long distance in the atmosphere. Therefore, for properly assessing the potential environmental and health effects, a systematic investigation of particle size distribution (PSD) of animal building dust is of great importance.

A PSD can be derived by classifying particles into a number of size ranges. Many particle size analyzers are currently available for determining the size distribution of airborne dust. Based on their working principles, those instruments can be classified into several categories: direct observation, inertial classification, light scattering, electrical mobility and electrical impedance (Miller and Lines, 1988). Because of discrepancies in working principles and analysis protocols, different particle size analyzers may produce significantly different PSD profiles from an identical dust sample (Etzler and Sanderson, 1995). However, many previous studies on animal building dust used only a single particle size analyzer, and in most cases different analyzers were used by different research groups (Chen et al., 1995; Donham et al., 1986b; Heber et al., 1988b; Jerez, 2007; Maghirang et al., 1997; Redwine et al., 2002). As a consequence, the derived PSD profiles and parameters (e.g., MMD and GSD) were hardly comparable between studies. There is a practical need to conduct a comparison between PSD data from different particle size analyzers.

A number of mathematical models have been developed for a convenient description of PSD profiles that may consist of tens to hundreds of size ranges depending on the instrumental resolution. The proposed PSD models include the normal distribution model, the lognormal distribution model, the gamma distribution model, the Nukiyama-Tanasawa (Nukiyama and Tanasawa, 1939) or modified gamma distribution model (Liu and Liu, 1994), the Weibull (Weibull, 1951) or Rosin-Rammler model (Rosin and Rammler, 1933), the power law or Junge

model (Junge, 1963), the exponential model, the Khrgian-Mazin model (Mazin and Khrgian, 1989) and the Chen's empirical model (Chen et al., 1995). Among them, the lognormal distribution model has been most frequently employed; however, a better fitting performance of other PSD models has been reported (Chen et al., 1995). According to Knutson and Liou (1989), the lognormal distribution model could be overused, as suggested by their observations that the PSD data derived from cascade impactors showed a significant departure from lognormality. Selecting a proper PSD model requires a systematic investigation of the fitting performance of different models. Previously this work was limited by the availability of reliable PSD data for animal building dust. Fortunately, a recent effort on PSD measurements has made this examination plausible (Lee, 2009; Lee et al., 2008).

In this study, a total of 217 PSD profiles, produced from four different particle size analyzers, were subject to regression analysis. The fitting performances of six different PSD models were compared and the best-fit model was selected for each particle size analyzer.

Methods

A total of 15 animal buildings (nine swine and six poultry buildings) were selected for PSD measurements. Four state-of-the-art particle size analyzers were selected for PSD analysis, as shown in Table G.1. DSP offers a capability of in-situ, real-time measurement; while the other three are all filter-based methods, i.e., airborne dust has to be collected on filters prior to analysis. In this study, in-situ measurements and dust sample collection were conducted collocatedly right before air exhausts of an animal building. The DSP measurements were performed twice a day, one in morning and one in afternoon. A total of ten replicates were collected from each measurement. For filter-based methods, animal building dust samples were collected on Teflon filters (ZefluorTM PTFE member filter, P/N P5RJ037, Pall Corporation, Ann Arbor, MI) using UIUC isokinetic TSP samplers. Filter samples were stored at 4°C and then extracted in deionized water or chemical solutions specified by instrument manuals. The obtained extracts (dust suspension) were subsequently subject to PSD tests. A detailed description of experimental procedures can be found from Lee (2009).

Six PSD models were selected for regression analysis: the lognormal distribution model, the Weibull distribution model, the gamma distribution model, the exponential distribution model, the Khrgian-Mazin distribution model and the Chen's empirical model (Table G.2). The

Nukiyama-Tanasawa model (Equation G.1) was not selected because the Weibull, exponential, Khrgian-Mazin and gamma distribution models are all special cases of the Nukiyama-Tanasawa model. The Nukiyama-Tanasawa model would undoubtedly have superior fitting performance; however, it has more parameters and is thereby incomparable with its daughter models.

$$n(x) = ax^p e^{-bx^q} \quad (\text{G.1})$$

Table G.1. Summary of particle size analyzers used in this study.

Instrument	Horiba ^a	DSP ^b	Coulter ^c	Malvern ^d
Number of profiles	83	44	45	45
Detection principle	Light scattering	Time of flight	Electrical impedance	Light scattering
Diameter type	Equivalent volumetric	Aerodynamic	Equivalent volumetric	Equivalent volumetric
Detection range (μm)	0.1-600	0.3-700	0.4-1200	0.02-2000
Number of channels	64	100	300	100

a. Horiba LA-300 particle sizer (Horiba Group, Edison, NJ).

b. Aerosizer DSP (TSI Inc., St. Paul, MN).

c. Coulter Counter Multisizer (Beckman Counter Inc., Fullerton, CA).

d. Malvern Multisizer (Malvern Instruments Ltd, Worcestershire, UK).

Table G.2. Particle size distribution models to be tested.

PSD model	Probability density function ^a	Parameters
Lognormal	$v(x) = \frac{1}{x \log \sigma_g \sqrt{2\pi}} \exp\left(-\frac{(\log x - \log MMD)^2}{2(\log \sigma_g)^2}\right), x > 0$	MMD, σ_g (GSD)
Weibull	$v(x) = \left(\frac{k}{\lambda}\right) \left(\frac{x}{\lambda}\right)^{k-1} e^{-(x/\lambda)^k}, x > 0$	λ, k
Exponential	$n(x) = a e^{-bx}, x > 0$	a, b
Khrgian-Mazin	$n(x) = a x^2 e^{-bx}, x > 0$	a, b
Gamma	$n(x) = \frac{1}{b^a \Gamma(a)} x^{a-1} e^{-x/b}$	a, b
Chen's empirical	$n(x) = e^{-ax} \sin(bx), x > 0$	a, b

a. $v(x)$ and $n(x)$ represent the corresponding equations are for volume and number distributions respectively.

Because PSD profiles produced by particle size analyzers used in this study were exclusively of volume distribution, essential transformation was needed to convert the probability density function of number distribution to that of volume distribution. This conversion was performed with Equation G.2 (Paloposki, 1991).

$$v(x) = \frac{x^3 n(x)}{\int_0^\infty x^3 n(x) dx} \quad (\text{G.2})$$

Also it must be noted that $n(x)$ was normalized.

$$\int_0^{\infty} n(x) dx = 1 \quad (\text{G.3})$$

However, the probability density functions of volume distribution, $v(x)$, were yet not readily used for nonlinear regression. The output data from our particle size analyzers consisted of three columns: particle size, volume frequency in the nearest size range and cumulative volume fraction. To be able to utilize these data, a cumulative volume fraction function, $V(x)$, was derived.

$$V(x) = \int_0^x v(x) dx \quad (\text{G.4})$$

Accordingly, the PSD models were transformed as follows.

Lognormal:

$$V(x) = \frac{1}{2} \operatorname{erfc} \left(-\frac{\log x - \log MMD}{\sqrt{2} \log \sigma_g} \right) \quad (\text{G.5})$$

Weibull:

$$V(x) = 1 - e^{-(x/\lambda)^k} \quad (\text{G.6})$$

Exponential:

$$\int_0^{\infty} n(x) dx = \int_0^{\infty} a e^{-bx} dx = \frac{a}{b} = 1$$

So, $a = b$

$$v(x) = \frac{1}{6} b^4 x^3 e^{-bx} \quad (\text{G.7})$$

$$V(x) = 1 - \frac{1}{6} (b^3 x^3 + 3b^2 x^2 + 6bx + 6) e^{-bx} \quad (\text{G.8})$$

Khrgian-Mazin:

$$\int_0^{\infty} n(x) dx = \int_0^{\infty} a x^2 e^{-bx} dx = \frac{2a}{b^3} = 1$$

So, $a = \frac{b^3}{2}$.

$$v(x) = \frac{1}{120} b^6 x^5 e^{-bx} \quad (\text{G.9})$$

$$V(x) = 1 - \frac{1}{120} (b^5 x^5 + 5b^4 x^4 + 20b^3 x^3 + 60b^2 x^2 + 120bx + 120) e^{-bx} \quad (\text{G.10})$$

Gamma:

$$\int_0^{\infty} n(x) dx = \frac{1}{b^a \Gamma(a)} \int_0^{\infty} x^{a-1} e^{-x/b} dx = \frac{\gamma(a, x/b)}{\Gamma(a)} \Big|_0^{\infty} = 1$$

So, $\int_0^{\infty} x^{a-1} e^{-x/b} dx = b^a \Gamma(a)$

$$v(x) = \frac{x^3 n(x)}{\int_0^{\infty} x^3 n(x) dx} = \frac{\frac{1}{b^a \Gamma(a)} x^3 x^{a-1} e^{-x/b} dx}{\frac{1}{b^a \Gamma(a)} \int_0^{\infty} x^3 x^{a-1} e^{-x/b} dx} = \frac{x^{a+2} e^{-x/b} dx}{\int_0^{\infty} x^{a+2} e^{-x/b} dx}$$

Let $a' = a - 3$, then,

$$v(x) = \frac{x^{a'-1} e^{-x/b} dx}{\int_0^{\infty} x^{a'-1} e^{-x/b} dx} = \frac{1}{b^{a'} \Gamma(a')} x^{a'-1} e^{-x/b} dx \quad (\text{G.11})$$

$$V(x) = \int_0^{\infty} v(x) dx = \frac{1}{b^{a'} \Gamma(a')} \int_0^{\infty} x^{a'-1} e^{-x/b} dx = \frac{\gamma(a', x/b)}{\Gamma(a')} \quad (\text{G.12})$$

Therefore, if a PSD of number distribution follows the gamma distribution, then the PSD of volume distribution will also follow the gamma distribution. The only difference is in the parameter a , but a convenient conversion is available.

Chen's empirical:

$$\int_0^{\infty} n(x) dx = \int_0^{\infty} e^{-ax} \sin(bx) dx = \frac{b}{a^2 + b^2} = 1$$

So, $a = \sqrt{b - b^2}$

$$v(x) = \frac{(a^2 + b^2)^4}{24ab(a^2 - b^2)} x^3 e^{-ax} \sin(bx) \quad (\text{G.13})$$

$$V(x) = 1 - \frac{b^4 e^{-ax}}{24ab(a^2 - b^2)} \left\{ \left[x^3 + \frac{6a^2}{b^2} x^2 - \frac{6(-3a^2b + b^3)}{b^3} x + \frac{24ab(a^2 - b^2)}{b^4} \right] \cos(bx) \right. \\ \left. + \left[\frac{a}{b} x^3 + \frac{3(a^2 - b^2)}{b^2} x^2 - \frac{6(-a^3 + 3b^2a)}{b^3} x + \frac{6(a^4 - 6a^2b^2 + b^4)}{b^4} \right] \sin(bx) \right\} \quad (\text{G.14})$$

It can be seen that after transformation the exponential model, the Khrigian-Mazin model and the Chen's empirical model actually have only one parameter; while the lognormal model, the Weibull model and the gamma model have two parameters.

The volume frequency of particles with size ranging from x_1 to x_2 can be calculated with Equation G.15. Based on that, a least square nonlinear regression was performed with a function of "nlinfit" in MATLAB 7.0. To do it conveniently, a MATLAB program was developed to process a large number of PSD profiles in a single run. The initial values of model parameters were estimated from preliminary examination of a few typical PSD profiles. However, a trial and error process was still occasionally needed for selecting the appropriate initial values.

$$\Delta V(x_1, x_2) = V(x_2) - V(x_1) \quad (\text{G.15})$$

For evaluation of the goodness-of-fit, three parameters were calculated with the MATLAB program: adjusted R^2 , Akaike information criterion (AIC) and mean squared error (MSE) (Bah et al., 2009). A good fitting performance should lead to a high adjusted R^2 , a low AIC and a low MSE, according to their respective statistical meanings.

$$R^2 = 1 - \left(\frac{RSS / (N - P)}{TSS / (N - 1)} \right) \quad (\text{G.16})$$

$$AIC = N \ln(RSS / N) + 2P \quad (\text{G.17})$$

$$MSE = \frac{RSS}{N - P} \quad (\text{G.18})$$

Where, RSS is the residual sum of squares, N is the number of PSD channels, P is the number of variables, and TSS is the total sum of squares. A statistical analysis was then performed to compare the fitting performance of different PSD models on data from different particle size analyzers.

Results and Discussion

The PSD curves predicted by different models have an apparently similar geometry; however, differences still exist (Figure G.1). For example, the lognormal distribution model generates a symmetric peak while the Weibull distribution model results in a left-skewed peak on a semi-logarithmic (particle size) plot. The fitting performance of a PSD model is largely dependent on the geometry of a measured PSD profile, which in reality is affected by not only the “true” size distribution of dust samples but also the detection principles and experimental protocols of the particle size analyzer being used.

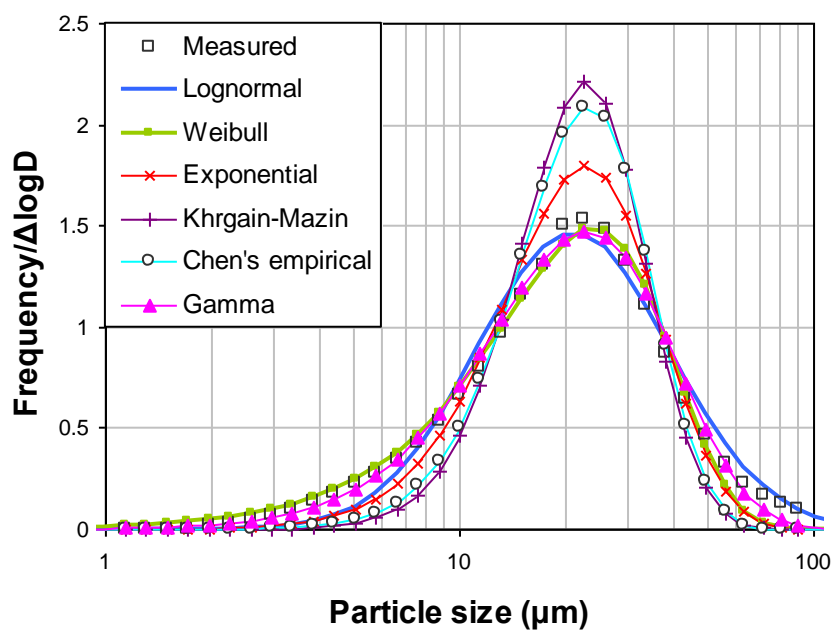


Figure G.1. PSD curves predicted by different models.

As expected, the fitting performances of different PSD models were found to differ with particle size analyzer. For Horiba and Malvern, better fits were obtained with the lognormal, Weibull and gamma models with adjusted R^2 values mostly greater than 0.9; The exponential, Chen’s empirical and Khrgian-Mazin models produced relatively poor fits (Figure G.2), and among these three the exponential model performed slightly better. The same trend was reflected by AIC and MSE values (data not shown here). For DSP, a similar observation was obtained; however the worst fit was found with the exponential model (Figure G.2). Even for models with relatively poor fits (exponential, Khrgian-Mazin and Chen’s empirical), the adjusted R^2 values were mostly greater than 0.8, better than in the Horiba and Malvern cases. For Coulter, no PSD

models provided an excellent fitting performance as the mean adjusted R^2 values were all less than 0.9. The lognormal and gamma models provided relatively the best fits, followed by the exponential model; while a poor fitting performance was found with the Weibull, Khrgian-Mazin and Chen's empirical models. One-way ANOVA tests on the mean adjusted R^2 values confirmed that for Horiba, DSP and Malvern, the lognormal, Weibull and gamma models had significantly better fitting performances ($p < 0.001$); while for Coulter, the lognormal and gamma models provided significantly better fits ($p < 0.02$) than other three. In general, two-parameter PSD models unsurprisingly offered superior fitting performance compared with one-parameter models.

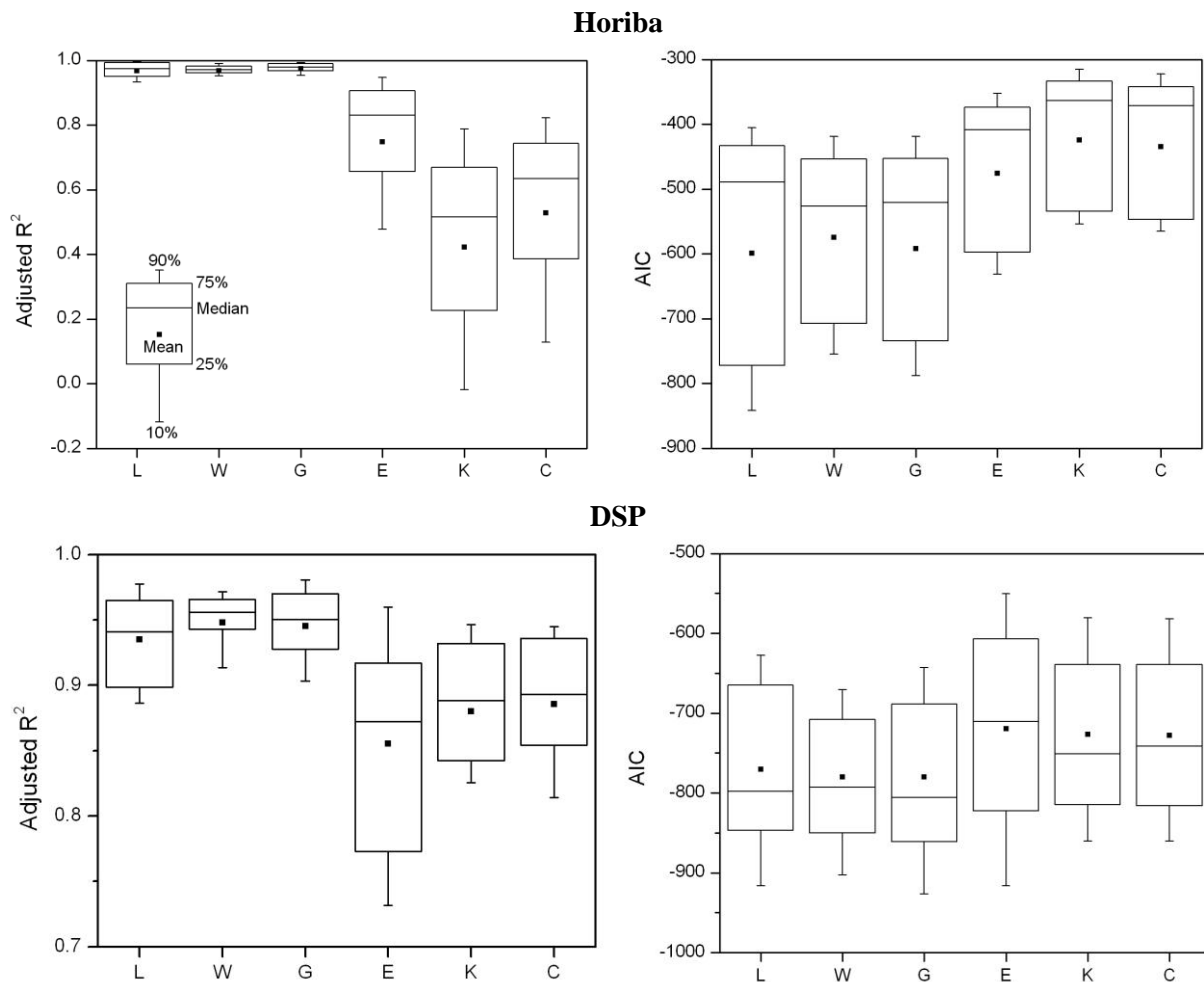


Figure G.2. Fitting performance of six particle size distribution models on data derived from four different particle size analyzers; L= lognormal, W= Weibull, G= Gamma, E= exponential, K= Khrgian-Mazin, and C= Chen's empirical.

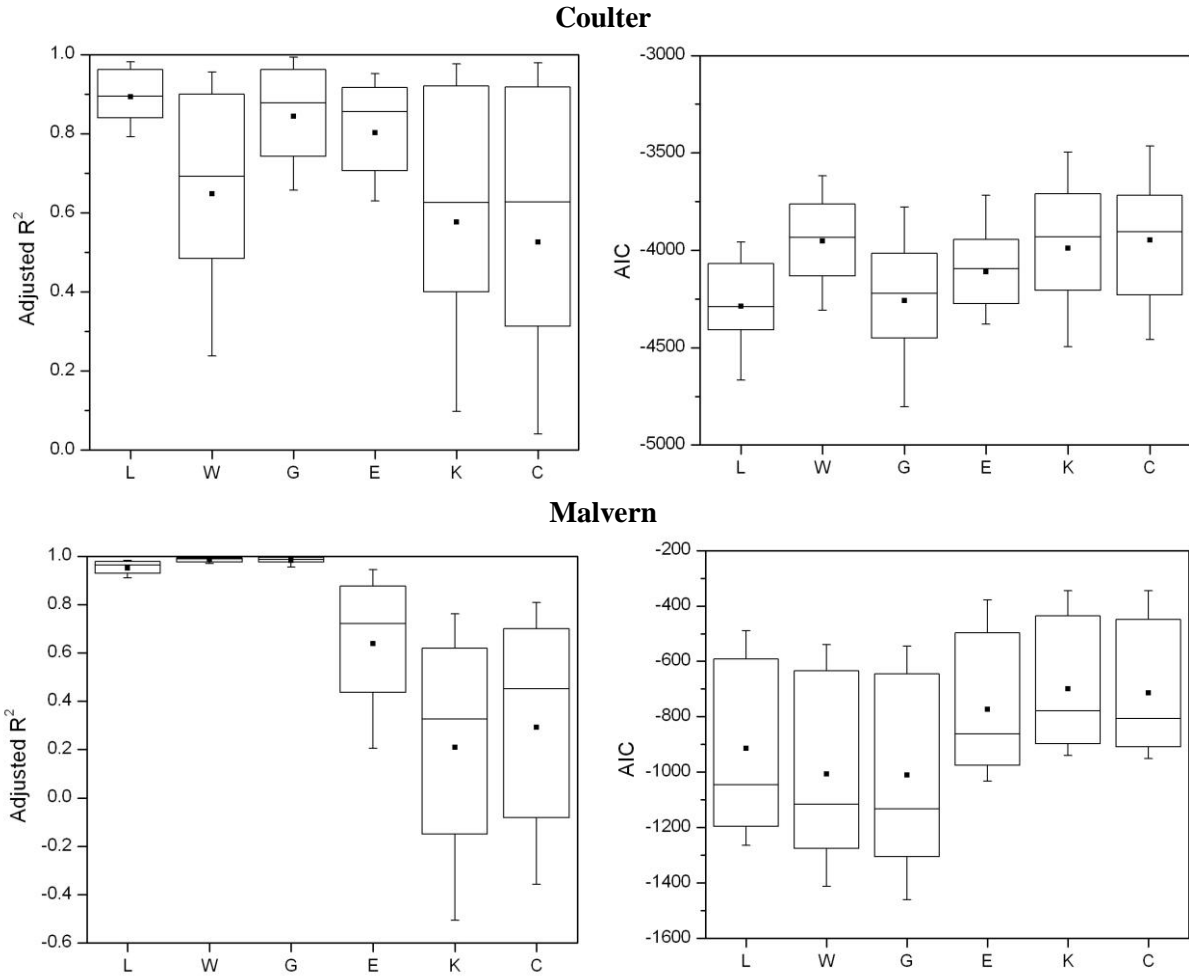


Figure G.2 (cont.)

One-way ANOVA tests compared the mean adjusted R^2 value of all PSD profiles but failed to examine the performance superiority of different PSD models on individual PSD profiles. To overcome such a limitation, PSD models were ranked according to their corresponding R^2 values for a PSD profile, i.e., the model with the highest adjustable R^2 value was ranked first, and the model with the second highest value was ranked second, and so on. The fitting performances of different models were then compared by summarizing the ranks over all PSD profiles (Figure G.3). The superiority order of fits was $\text{gamma} > \text{lognormal} \approx \text{Weibull} > \text{exponential} > \text{Chen's empirical} > \text{Khrigian-Mazin}$ for Horiba, $\text{gamma} \approx \text{Weibull} > \text{lognormal} > \text{Khrigian-Mazin} \approx \text{Chen's empirical} > \text{exponential}$ for DSP, $\text{gamma} \approx \text{lognormal} > \text{exponential} > \text{Khrigian-Mazin} \approx \text{Weibull} > \text{Chen's empirical}$ for Coulter, and $\text{gamma} \approx \text{Weibull} > \text{lognormal} > \text{exponential} > \text{Chen's empirical} > \text{Khrigian-Mazin}$ for Malvern. The gamma model was found to offer overall the best fitting performance, followed by the lognormal and Weibull models. Comparatively, one-

parameter models (exponential, Khrgian-Mazin and Chen's empirical) produced relatively poor fits. Similar results were obtained from paired t-tests (Table G.3).

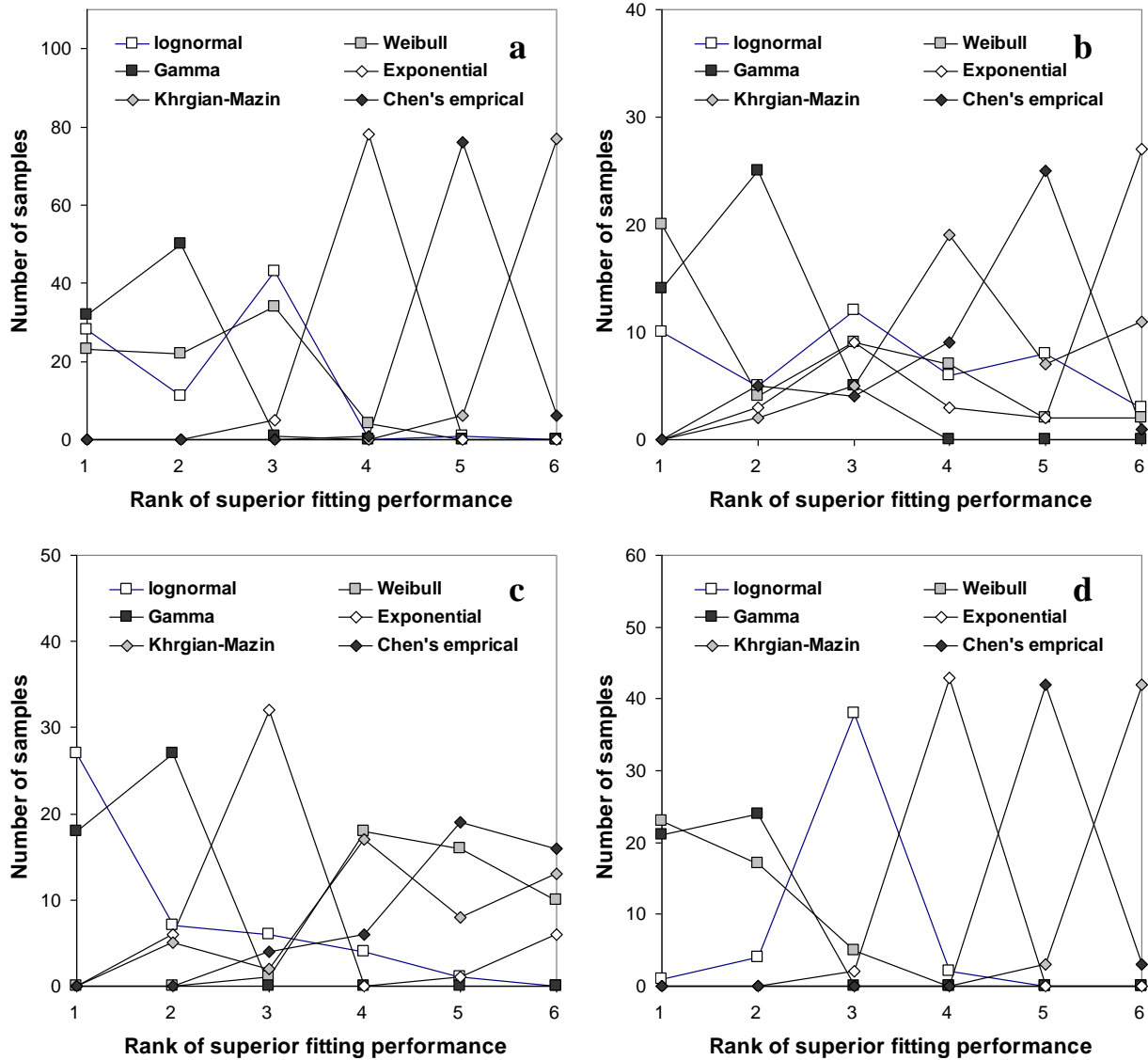


Figure G.3. Rank of fitting performances of six models on PSD data derived from: a- Horiba, b- DSP, c- Coulter, and d- Malvern.

It is noteworthy that both the exponential and Khrgian-Mazin models are special cases of the gamma model that can also be presented as $n(x) = N_0 x^a e^{-bx}$ (Liu and Liu, 1994). This explains why the gamma model always offers better fits than the exponential and Khrgian-Mazin models.

Table G.3. Paired t-tests on adjusted R² values.

Models ^a	Horiba		DSP		Coulter		Malvern	
	Δ	p value						
L-W	-0.0011	0.966	-0.0115	0.102	0.2511	<0.001	-0.0334	<0.001
L-E	0.2208	<0.001	0.0805	<0.001	0.0924	<0.001	0.3136	<0.001
L-K	0.5457	<0.001	0.0495	<0.001	0.3227	<0.001	0.7415	<0.001
L-C	0.4407	<0.001	0.0463	<0.001	0.3743	<0.001	0.6581	<0.001
L-G	-0.0063	0.020	-0.0091	0.001	0.0506	<0.001	-0.0309	<0.001
W-E	0.2209	<0.001	0.0920	<0.001	-0.1588	<0.001	0.3470	<0.001
W-K	0.5458	<0.001	0.0610	<0.001	0.0716	0.037	0.7749	<0.001
W-C	0.4409	<0.001	0.0578	<0.001	0.1231	0.004	0.6915	<0.001
W-G	-0.0062	<0.001	0.0023	0.614	-0.2005	<0.001	0.0025	0.096
E-K	0.3249	<0.001	-0.0311	0.028	0.2303	<0.001	0.4279	<0.001
E-C	0.2200	<0.001	-0.0342	0.006	0.2819	<0.001	0.3445	<0.001
E-G	-0.2271	<0.001	-0.0897	<0.001	-0.0417	<0.001	-0.3445	<0.001
K-C	-0.1050	<0.001	-0.0032	0.246	0.0516	0.002	-0.0834	<0.001
K-G	-0.5520	<0.001	-0.0586	<0.001	-0.2720	<0.001	-0.7724	<0.001
C-G	-0.4471	<0.001	-0.0554	<0.001	-0.3236	<0.001	-0.6891	<0.001

a. L- lognormal, W- Weibull, G- gamma, E- exponential, K- Khrgian-Mazin, C- Chen's empirical; L-W refers to a comparison between the lognormal and Weibull models.

Most measured PSD profiles had a single major peak. For describing the geometry of a peak, at least three basic characteristics need to be addressed: peak position, height and width. Because generally the PSD data given by an instrument are normalized, i.e., in the form of percentage, the height and width of a PSD peak are interdependent. Therefore, a 'good' PSD model should theoretically have at least two independent parameters. Unfortunately, the exponential, Khrgian-Mazin and Chen's empirical models have only one parameter that to a greater extent relates to the peak position but to a less extent to the peak height and width (Figure G.4). Because the peak height and width are relatively constant and less adjustable in these three models, the regressed PSD profiles can be substantially different from the measured profiles, leading to lower adjusted R² values even less than zero (Figure G.5). Considering such a limitation, one-parameter PSD models are not recommended for modeling animal building dust in future research; instead, the gamma, lognormal and Weibull models should be applied. This is not only because those two-parameter models provide superior fitting performances, but also for the reason that they have mathematically well-defined properties such as mean, median, mode, variance, skewness and kurtosis (Table G.4) so that a further analysis on PSD data, e.g., modeling of aerosol light extinction, can become simplified.

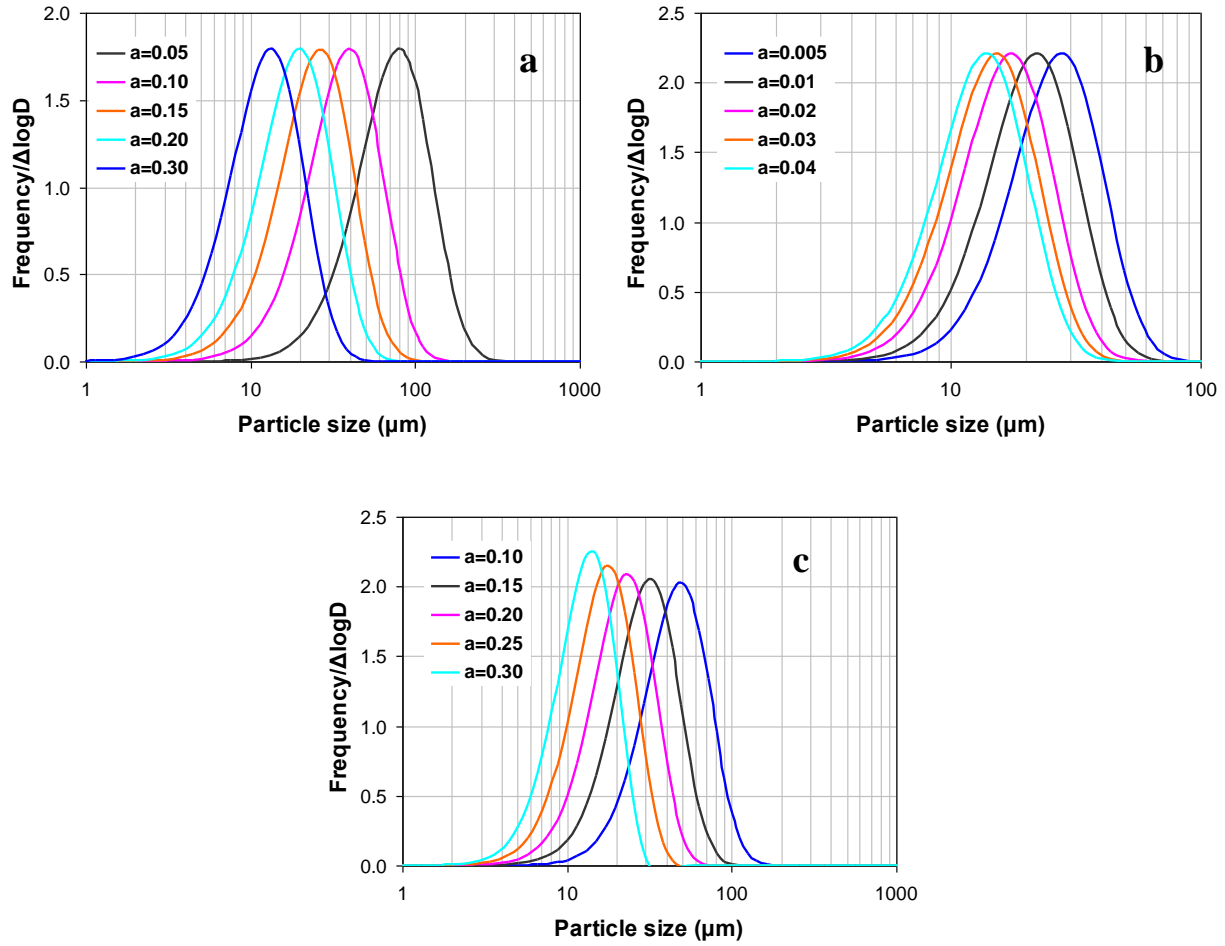


Figure G.4. PSD curves of one-parameter models: a- exponential, b- Khrgian-Mazin, c- Chen's empirical.

Table G.4. Properties of the lognormal, Weibull and gamma distributions.

	lognormal	Weibull	gamma
mean	$\mu = MMD \cdot 10^{(\log \sigma_g)^2 / 2}$	$\mu = \lambda \Gamma\left(1 + \frac{1}{k}\right)$	ab
median	MMD	$\lambda (\ln(2))^{1/k}$	No simple form
mode	$\frac{MMD}{10^{(\log \sigma_g)^2}}$	$\lambda \left(\frac{k-1}{k}\right)^{1/k}$	$(a-1)b$
variance	$\sigma^2 = \left(10^{(\log \sigma_g)^2} - 1\right) \mu^2$	$\sigma^2 = \lambda^2 \Gamma\left(1 + \frac{2}{k}\right) - \mu^2$	$\sigma^2 = ab^2$

Table G.4. (cont.)

	lognormal	Weibull	gamma
skewness	$\gamma_1 = \left(\frac{\sigma^2}{\mu^2} + 3 \right) \frac{\sigma}{\mu}$	$\gamma_1 = \frac{\Gamma\left(1 + \frac{3}{k}\right) \lambda^3 - 3\mu\sigma^2 - \mu^3}{\sigma^3}$	$\gamma_1 = \frac{2}{\sqrt{a}}$
kurtosis	$\gamma_2 = \left(\frac{\sigma^2}{\mu^2} \right)^4 + 6 \left(\frac{\sigma^2}{\mu^2} \right)^3 + 15 \left(\frac{\sigma^2}{\mu^2} \right)^2 + 16 \frac{\sigma^2}{\mu^2} + 3$	$\gamma_2 = \frac{\Gamma\left(1 + \frac{4}{k}\right) \lambda^4 - 4\gamma_1\mu\sigma^3 - 6\mu^2\sigma^2 - \mu^4}{\sigma^4}$	$\gamma_2 = \frac{6}{a}$

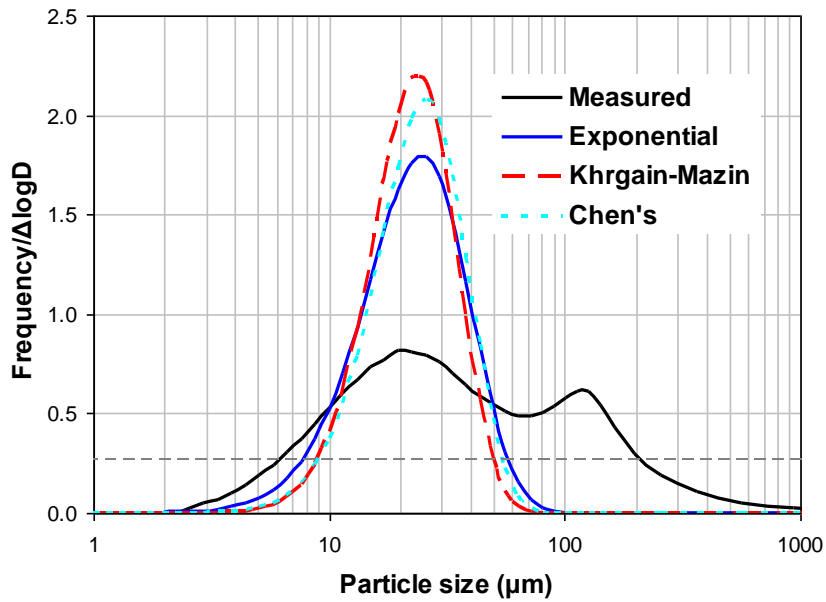


Figure G.5. Comparison of a measured PSD curve versus regression curves predicted by the exponential ($R^2=-0.5132$), Khrgain-Mazin ($R^2=-1.3017$) and Chen's empirical models ($R^2=-1.0584$).

As mentioned previously, the fitting performance of a PSD model greatly depends on the geometry of a measured PSD profile, which is affected by the detection principle of a particle size analyzer. In this study, both Horiba and Malvern are light-scattering methods. The good- and poor-fitting models and their superiority order in regard to fitting performance were found to be consistent for those two instruments (Figure G.1; Figure G.2). In fact, both instruments tended to produce PSD profiles with a left-skewed major peak. This geometry is better described by the Weibull and gamma models, which accordingly offered the best fitting performance. DSP measures the aerodynamic size distribution of particles by determining their inertias in high velocity airflow. It utilizes a time-of-flight detection principle, which is significantly different than that by Horiba and Malvern, and that by Coulter- Coulter measures the equivalent volume

diameter of particles by tracking a particle-induced, size-specific change of electrical impedance in a liquid suspension. Therefore, it is not surprising to find that the good- and poor-fitting PSD models were different for DSP than for Coulter and for Horiba and Malvern (Figure G.1; Figure G.2).

Since the lognormal, Weibull and gamma models generated relatively good fits for PSD profiles of animal building dust, it is valuable to examine and to compare regression coefficients and parameters, e.g., mean and median diameters, predicted by those three models (Table G.5). The average mean and median diameters were all greater than 10 μm , indicating the presence of a great portion of large particles in animal building dust. Similar findings were reported by other researchers (Donham et al., 1986b; Heber et al., 1988a; Jerez, 2007; Maghirang et al., 1997; Redwine et al., 2002). One-way ANOVA tests revealed that for each PSD model, significant differences in average mean and median diameters were present between Horiba and Malvern/DSP/Coulter (all $p < 0.003$) and between Malvern and Coulter (both $p < 0.007$). Among these four instruments, Horiba produced the highest mean and median diameters, followed by Malvern, DSP and then Coulter. Horiba and Malvern, which both rely on Mie scattering, tended to produce larger variances (wider peaks) than DSP and Coulter.

Table G.5. Regression coefficients and key parameters of lognormal, Weibull and gamma models^a.

Models	Parameters	Horiba	DSP	Coulter	Malvern
lognormal	MMD	23.7 (8.1)	16.9 (2.1)	13.3 (2.0)	19.1 (6.5)
	GSD (σ_g)	2.10 (0.30)	1.51 (0.15)	1.74 (0.14)	2.19 (0.28)
	mean	27.1 (10.9)	17.5 (2.3)	14.2 (2.0)	21.7 (6.7)
	median	23.7 (8.1)	16.9 (2.1)	13.3 (2.0)	19.1 (6.5)
	variance	324.2 (772.1)	25.8 (16.9)	28.7 (10.4)	139.7 (65.6)
Weibull	Λ	28.2 (11.4)	18.4 (2.5)	16.1 (1.9)	22.7 (6.8)
	K	1.52 (0.25)	2.91(0.70)	2.43 (0.23)	1.46 (0.22)
	mean	25.9 (11.8)	16.4 (2.2)	14.3 (1.7)	20.7 (5.8)
	median	21.8 (7.7)	16.1 (2.0)	13.8 (1.6)	17.7 (5.8)
	variance	535.2 (1257.6)	46.0 (28.0)	40.9 (12.7)	214.4 (88.3)
gamma	a	2.18 (0.66)	7.3 (3.2)	4.28 (0.97)	1.98 (0.57)
	b	15.1 (14.2)	2.95 (1.49)	3.54 (0.80)	11.23 (2.48)
	mean	27.1 (11.6)	17.5 (2.3)	14.6 (1.9)	21.6 (6.4)
	median ^b	22.4 (7.7)	16.5 (2.1)	13.4 (1.8)	18.1 (6.1)
	variance	559.7 (1185.0)	53.3 (32.3)	52.3 (17.0)	249.3 (110.3)

a. The numbers in parentheses are standard deviations (SD); while outside are mean values.

b. The median diameter of a gamma distribution is calculated with a function of `gammainv()` in excel.

Paired t-tests were performed to compare the mean and median diameters and variances predicted by the lognormal, Weibull and gamma models (Table G.6). The results showed that for Horiba, Malvern and DSP, the lognormal model predicted significantly higher median diameters

and lower variances (narrower peaks) than the Weibull and gamma models; the Weibull model predicted lower variances and significantly lower median diameters than the gamma model; the mean diameters derived from the lognormal and gamma models were significantly greater than those from the Weibull model. However, very dissimilar results were obtained for Coulter: the lognormal model predicted the lowest mean and median diameters and also the smallest variances; while the Weibull model predicted significantly lower variances but significantly greater median diameters than the gamma model. Such dissimilarity might be because Coulter employs a unique detection principle (electrical impedance) and accordingly may produce PSD profiles with distinctly different geometry than the other three instruments. In fact, from our measurements we found that Coulter tended to produce a noisy and strongly distorted PSD peak, which can be a possible explanation. It should be noted that from our previous discussions, the Weibull model had poor fitting performances on PSD data from Coulter with an average adjusted R^2 value of 0.640. The Weibull model therefore should not be applied to analysis of Coulter data in practice.

Table G.6. Paired t-tests on mean and median diameters and variances derived from the lognormal, Weibull and gamma models.

Model s	Parameters	Horiba		DSP		Coulter		Malvern	
		Δ	p value						
L-W	Mean	1.10	<0.001	1.09	<0.001	-0.10	0.294	1.04	<0.001
	Median	1.91	<0.001	0.78	<0.001	-0.54	<0.001	1.42	<0.001
	Variance	-210.9	<0.001	-20.1	<0.001	-12.1	<0.001	-74.7	<0.001
L-G	Mean	-0.10	0.462	0.04	<0.001	-0.39	<0.001	0.05	0.434
	Median	1.35	<0.001	0.35	<0.001	-0.13	0.009	1.08	<0.001
	Variance	-235.4	<0.001	-27.4	<0.001	-23.6	<0.001	-109.5	<0.001
W-G	Mean	-1.20	<0.001	-1.05	<0.001	-0.29	<0.001	-0.99	<0.001
	Median	-0.56	<0.001	-0.43	<0.001	0.41	<0.001	-0.34	<0.001
	Variance	-24.5	0.060	-7.3	<0.001	-11.5	<0.001	-34.9	<0.001

a. L- lognormal, W- Weibull, G- gamma; L-W refers to a comparison between the lognormal and Weibull models.

Which mean and median diameter and variance should be trusted? A reasonable criterion is the coefficient of determination (R^2). The PSD model with the highest R^2 value is recommended for estimating the PSD parameters. Based on this criterion, it can be seen that if we stick with the lognormal model, a misestimation of the PSD parameters would happen to data from Horiba, DSP and Malvern. Specifically, the lognormal model may significantly overestimate the median diameter but underestimate the variance of PSD profiles from those three analyzers. Instead, the gamma model should be selected because it provided the best fitting performance.

Chen et al. (1995) compared four PSD models (lognormal, Weibull, power law and Chen's empirical) with a total of 25 swine building dust samples and reported that the Chen's empirical model the they proposed produced the best fitting performance. However, their PSD data were of number distribution and therefore had substantially different profile geometries than the volume distribution data used in this study. Moreover, an aerodynamic particle counter (APC) was used in their study. The use of a different particle size analyzer and different PSD datasets could be the reason why different conclusions were drawn by them.

Conclusion

The fitting performances of six PSD models were evaluated with PSD data derived from four different particle size analyzers (Horiba, DSP, Coulter and Malvern), and were found to change with instruments. The gamma distribution model offered overall the best fit, followed by the lognormal and Weibull models; while one-parameter models including the exponential, Khrgian-Mazin and Chen's empirical models, produced relatively poor fitting performances, and thereby, are not recommended for future research on animal building dust. The prevalent lognormal model provided an overall good but inferior performance to the Weibull and gamma models when applied to PSD data from Horiba and Malvern that both employ a detention principle of Mie scattering. The Weibull model, another prevalent PSD model, offered fairly good fits to data from Horiba, DSP and Malvern but poor fits to data from Coulter.

The mean and median diameters calculated by the lognormal, Weibull and gamma models were numerically different but all greater than 10 μm , indicating the presence of a great portion of large particles in animal building dust. Horiba produced overall the greatest mean and median diameters, followed by Malvern. Horiba and Malvern also produced greater variances than DSP and Coulter. For Horiba, Malvern and DSP, the lognormal model predicted similar mean diameters to, but greater median diameters and lower variances than the Weibull and gamma models; the Weibull model produced lower variances and lower median diameters than the gamma model. Comparatively, for Coulter, the lognormal model predicted the lowest mean diameter, median diameters and variances. Differences in fitting performance and in calculated mean and median diameter and variance might be related to different detection principles and experimental protocols employed by different particle size analyzers.

Although the gamma distribution model showed overall the best fitting performance, this observation is not readily apply to future similar studies due to a potential difference in dust sources and particle size analyzers. However, a key point raised from this study is that the fitting performance of a PSD model must be evaluated and compared before applying it to estimation of PSD parameters. The model with the best fit should be used; otherwise, a significant misestimation may occur.

APPENDIX H. CALIBRATION OF VENTURI ORIFICES

Experimental

Calibration of venturi orifices were done separately by two means: a bench test and a simulated field test. In the bench test, venturi orifices were dismantled from sampling tubing's and calibrated with a computer programmed venturi calibration system in the Bioenvironmental Engineering Group. Detailed information on calibration procedures and operations can be found from a document *Venturi Calibration System Operating Instructions* developed by Beni Brem. In the simulated field test, venturi orifices were assembled with sampling tubing's and particle filter samplers were installed. Vacuum pumps used for practical field sampling were selected to drive the airflow. In a word, everything was set up in accordance with field sampling conditions. A DryCal flow meter (Bios International Corp., Butler, NJ) was used for measuring the airflow rate at the inlet of particle samplers. Three readings were taken for each venturi orifice and each reading was averaged from ten replicates.

Results

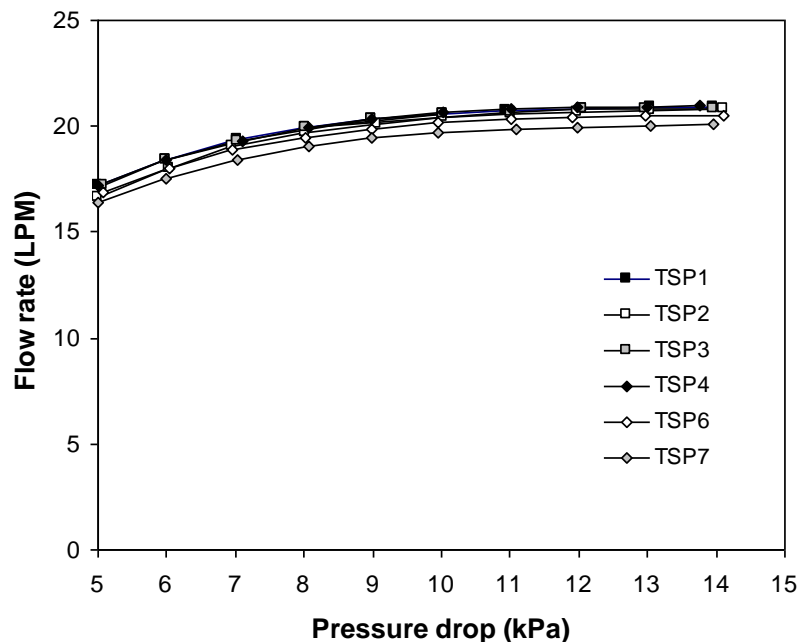


Figure H.1. Calibration curves for venturi orifices used for TSP samplers- bench test.

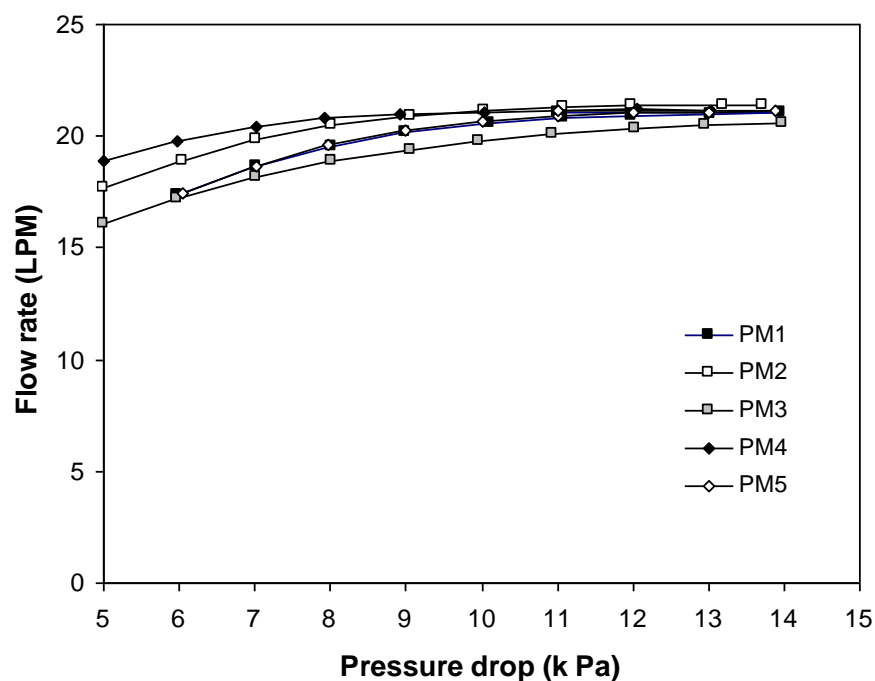


Figure H.2. Calibration curves for venturi orifices used for PM₁₀ and PM_{2.5} samplers- bench test.

Table H.1. Calibration results from the simulated field test.

	Standard flow rate ^a (LPM)					Actual flow rate ^b (LPM)				
	1	2	3	Average	SD	1	2	3	Average	SD
TSP1	21.06	21.02	21.03	21.04	0.02	21.44	21.46	21.46	21.45	0.01
TSP2	20.94	20.98	20.95	20.96	0.02	21.38	21.39	21.40	21.39	0.01
TSP3	21.00	20.98	20.98	20.99	0.01	21.46	21.46	21.46	21.46	0.00
TSP4	21.07	21.07	21.07	21.07	0.00	21.54	21.54	21.54	21.54	0.00
TSP6	20.14	20.16	20.13	20.14	0.02	20.40	20.41	20.40	20.40	0.01
TSP7	20.53	20.55	20.55	20.54	0.01	20.79	20.79	20.79	20.79	0.00
PM1	20.87	20.84	20.84	20.85	0.02	21.22	21.20	21.20	21.21	0.01
PM2	21.17	21.19	21.20	21.19	0.02	21.53	21.55	21.55	21.54	0.01
PM3	20.74	20.73	20.72	20.73	0.01	21.04	21.02	21.02	21.03	0.01
PM4	21.10	21.12	21.12	21.11	0.01	21.57	21.59	21.59	21.58	0.01
PM5	21.01	21.01	21.01	21.01	0.00	21.49	21.49	21.50	21.49	0.01

a. Standard flow rate refers to the airflow rate under standard conditions (25°C and 1 atm).

b. Actual flow rate refers to the airflow rate under calibration conditions. Based on the working principle of venturi orifices, the actual flow rate does not change with pressure and temperature (Wang, 2000).

Effects of airflow rate on cut size of PM samplers

The Harvard impactors used in this study are supposed to be working at 20 LPM such that a proper sampling performance, e.g., cut size, can be achieved. However, in practice a deviation from the ideal airflow rate is unavoidable. In this study, a sampling error might have risen due to the use of venturi orifices with controlled airflow rates greater than 20 LPM. Therefore, it is

important to assess the possible under- or oversampling at the measured flow rate. The 50% cut size of an impactor can be calculated as follows (Zhang, 2005):

$$D_{50} \sqrt{C_c} = \left(\frac{9\eta D_x^3}{4\pi\rho_p U_0 D_j^2} \right)^{1/2} \quad (\text{H.1})$$

Assume the slip correction factor is negligible. We have:

$$D_{50} \propto U_0^{-1/2} \propto Q_0^{-1/2} \quad (\text{H.2})$$

Where Q refers to the volumetric airflow rate. Based on the equation, a practical 50% cut size (D_{50}) can be calculated (Figure H.3).

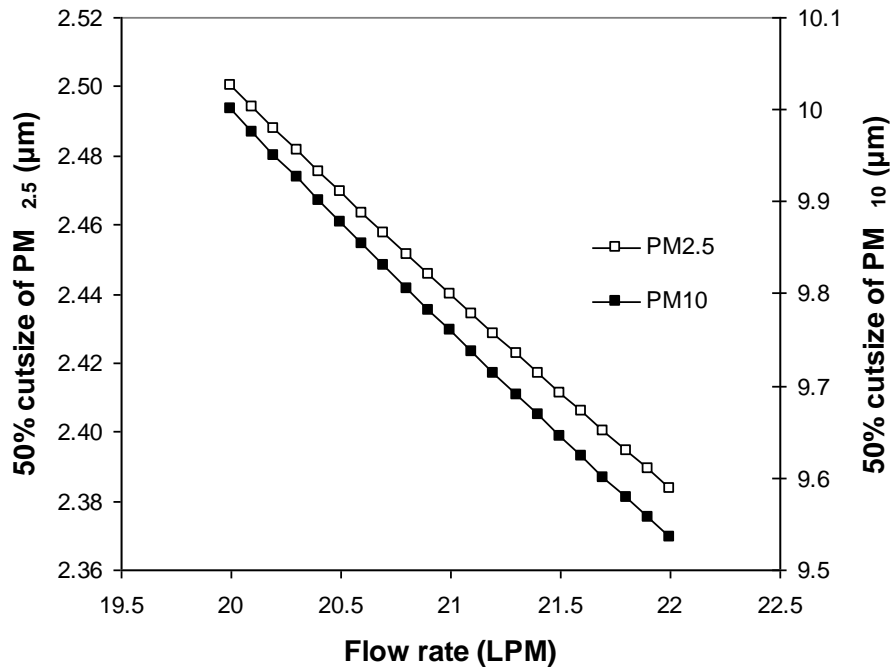
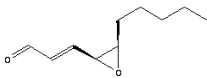
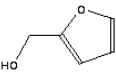


Figure H.3. Effect of airflow rate on 50% cut size (D_{50}) of PM samplers.

All PM_{10} and $PM_{2.5}$ samplers were working with D_{50} lower than supposed but greater than $9.6 \mu\text{m}$ and $2.4 \mu\text{m}$, respectively. Such cut sizes meet the sampler requirements specified by the USEPA (CFR, 2001a; CFR, 2001b). Therefore, although a slight degree of undersampling occurred, the collected PM samples were valid in terms of particle size.

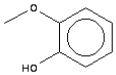
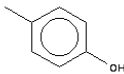
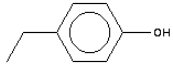
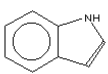
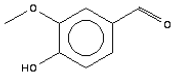
APPENDIX I. LIST OF VOLATILE ORGANIC COMPOUNDS ANALYZED IN THIS STUDY

Table I.1. Melting and boiling points of analyzed volatile organic compounds^a.

#	Compounds	ACS#	Molecular formula	Molar mass	Melting point	Boiling point
1	hexanal	66-25-1	CH ₃ (CH ₂) ₄ CHO	100.16	<-20	122
2	2-methyl-2-pentenal	623-36-9	C ₂ H ₅ CH=C(CH ₃)CHO	98.14	-95	136
3	heptanal	111-71-7	CH ₃ (CH ₂) ₅ CHO	114.19	-43.3	152.8
4	(E)-2-hexenal	6728-26-3	CH ₃ (CH ₂) ₂ CH=CHCHO	98.14		146.6
5	octanal	124-13-0	CH ₃ (CH ₂) ₆ CHO	128.21	-25	171
6	1-octen-3-one	4312-99-6	CH ₂ =CHC(=O)(CH ₂) ₄ CH ₃	126.2		178
7	(E)-2-heptenal	18829-55-5	CH ₃ (CH ₂) ₃ CH=CHCHO	112.17		166
8	(E)-2-octenal	2548-87-0	CH ₃ (CH ₂) ₄ CH=CHCHO	126.2		190.1
9	nonanal	124-19-6	CH ₃ (CH ₂) ₇ CHO	142.24	-18	195
10	decanal	112-31-2	CH ₃ (CH ₂) ₈ CHO	156.2	-3.9	208
11	benzaldehyde	100-52-7	(C ₆ H ₅)CHO	106.12	-26	178.1
12	(E)-2-nonenal	18829-56-6	CH ₃ (CH ₂) ₅ CH=CHCHO	140.22		205
13	(E,Z)-2,6-nonadienal	557-48-2	CH ₃ CH ₂ CH=CH(CH ₂) ₂ CH=CHCHO	139.21		203.3
14	(E)-2-decenal	3913-81-3	CH ₃ (CH ₂) ₆ CH=CHCHO	154.25		230
15	(E)-2-undecenal	53448-07-0	CH ₃ (CH ₂) ₇ CH=CHCHO	168.28		244.8
16	(E,E)-2,4-nonadienal	5910-87-2	CH ₃ (CH ₂) ₃ CH=CHCH=CHCHO	138.21		222
17	(E,E)-2,4-decadienal	25152-84-5	CH ₃ (CH ₂) ₄ CH=CHCH=CHCHO	152.23		245
18	trans-4,5-epoxy-(E)-2-decenal	134454-31-2		168.23		
19	ethanol	64-17-5	CH ₃ CH ₂ OH	46.07	-114.3	78.4
20	1-pentanol	71-41-0	CH ₃ (CH ₂) ₃ CH ₂ OH	88.15	-77.6	138
21	1-hexanol	111-27-3	CH ₃ (CH ₂) ₄ CH ₂ OH	102.17	-46.7	158
22	1-heptanol	111-70-6	CH ₃ (CH ₂) ₅ CH ₂ OH	116.2	-34.6	175.8
23	2-ethyl-1-hexanol	104-76-7	CH ₃ (CH ₂) ₃ CH(C ₂ H ₅)CH ₂ OH	130.23		183
24	1-octanol	111-87-5	CH ₃ (CH ₂) ₆ CH ₂ OH	130.23	-16	195
25	2-furanmethanol	98-00-0		98.1	-31	171
26	Phenylmethanol	100-51-6	C ₆ H ₅ CH ₂ OH	108.14	-15	205
27	acetic acid	64-19-7	CH ₃ COOH	60.05	16.5	118.1
28	propanoic acid	79-09-4	CH ₃ CH ₂ COOH	74.08	-21	141
29	2-methylpropanoic acid	79-31-2	(CH ₃) ₂ CHCOOH	88.11	-47	155
30	2,2-dimethyl-propanoic acid	75-98-9	(CH ₃) ₃ CCOOH	102.13	-35	163.7
31	butanoic acid	107-92-6	CH ₃ (CH ₂) ₂ COOH	88.11	-7.9	163.5
32	3-methylbutanoic acid	503-74-2	(CH ₃) ₂ CHCH ₂ COOH	102.13	-29	176

a. compiled from multiple sources, mostly from NIST Chemistry Webbook (NIST, 2010).

Table I.1. (cont.)

#	Compounds	ACS#	Molecular formula	Molar mass	Melting point	Boiling point
33	pentanoic acid	109-52-4	CH ₃ (CH ₂) ₃ COOH	102.13	-34.5	186-187
34	4-methylpentanoic acid	646-07-1	(CH ₃) ₂ CH(CH ₂) ₂ COOH	116.16		200
35	hexanoic acid	142-62-1	CH ₃ (CH ₂) ₄ COOH	116.16	-3.4	202-203
36	2-ethylhexanoic acid	149-57-5	CH ₃ (CH ₂) ₄ CH(C ₂ H ₅)COOH	144.21	-118	228
37	heptanoic acid	111-14-8	CH ₃ (CH ₂) ₅ COOH	130.18	-10.5	223
38	octanoic acid	124-07-2	CH ₃ (CH ₂) ₆ COOH	144.21	16.7	237
39	nonanoic acid	112-05-0	CH ₃ (CH ₂) ₇ COOH	158.23	12.5	254
40	decanoic acid	334-48-5	CH ₃ (CH ₂) ₈ COOH	172.26	31.6	269
41	undecanoic acid	112-37-8	CH ₃ (CH ₂) ₉ COOH	186.29	28.6	284
42	benzoic acid	65-85-0	C ₆ H ₅ COOH	122.12	122.4	249.2
43	dodecanoic acid	143-07-7	CH ₃ (CH ₂) ₁₀ COOH	200.32	44.2	298.9
44	phenylacetic acid	103-82-2	C ₆ H ₅ CH ₂ COOH	136.15	76-77	265.5
45	tridecanoic acid	638-53-9	CH ₃ (CH ₂) ₁₁ COOH	214.34	41.5	
46	phenylpropanoic acid	501-52-0	C ₆ H ₅ CH ₂ CH ₂ COOH	150.18	48	280
47	guaiacol / 2-methoxyphenol	90-05-1		124.14	28	204-206
48	o-cresol / 2-methylphenol	95-48-7		108.14	29.8	191.5
49	phenol	108-95-2	C ₆ H ₅ OH	94.11	40.5	181.7
50	p-cresol / 4-methylphenol	106-44-5		108.14	35.5	201.8
51	m-cresol / 3-methylphenol	108-39-4		108.14	11	202.8
52	4-ethylphenol	123-07-9		122.16	42-45	218
53	p-vinylguaiacol	7786-61-0		150.18		224
54	o-aminoacetophenone	551-93-9		135.16		251.8
55	indole	120-72-9		117.15	52-54	253-254
56	3-methylindole / skatole	83-34-1		131.17	93-95	265
57	vanillin / 3-methoxy-4-hydroxybenzaldehyde	121-33-5		152.15	80-81	285

APPENDIX J. EXPERIMENTAL PROCEDURE FOR ENDOTOXIN AND (1-3)-D-GLUCAN ANALYSES

J.1. Quantification of airborne endotoxin

The experimental protocol consisted of the following steps:

- (1) Extraction- A filter was extracted in a 10 mL 0.05% Tween-20 solution prepared with certified LAL reagent water (Cat. # W50-500, Lonza Group Ltd, Basel, Switzerland). A 15 mL Corning[®] pyrogen-free centrifuge tube (Corning incorporated, Acton, MA) was used as the container for extraction. Tweezers and other essential metal tools were sterilized with 70% ethanol on an alcohol burner. The extraction of endotoxins was performed on a water bath shaker (Model YB-531, American Scientific Products) at the maximum agitation rate and room temperature (~22°C) for 120 minutes. Next, the extract was centrifuged at 1,000×g for 15 minutes. After that, 1.0 mL supernatant was collected and transferred into a new pyrogen-free centrifuge tube.
- (2) Dilution- The collected supernatant was diluted with LAL reagent water. According to Spaan et al (2008), the dilution ratio should be at least 50 in order to eliminate the effects of Tween-20 on the potency of endotoxins. Additionally, the concentration of endotoxins in the diluted extract should be within the detection range of the kinetic chromogenic LAL assay (0.005 ~50 EU/mL). From existing literature, we estimated that 4 µg particles per mL extract could potentially produce an endotoxin concentration of 0.5~5 EU/mL, an optimal range for endotoxin analysis. Accordingly, two requirements were followed: (1) the dilution ratio was at least 50; (2) once the 1st requirement was satisfied, the dilution would continue until the final diluted extract contained approximately 4 µg particles /mL. Serial dilution was performed to achieve the required dilution ratio, and for each step the dilution ratio was no more than 20. The diluted extract was either immediately analyzed or stored at -20 °C in a freezer.
- (3) pH adjustment- The optimal pH range for endotoxin analysis is from 6.0 to 8.0. Accordingly, the diluted extract was tested with pH paper. A 0.01 M HCl or 0.01 M KOH solution would be used for pH adjustment if the test result was beyond the optimal range.

- (4) Analysis- Kinetic-QCL[®] assay (Cat. # 50-650U, Lonza Group Ltd, Basel, Switzerland) was employed to determine endotoxin concentrations in diluted extracts. Following the procedure given by manufacturer, an endotoxin analysis was performed on an incubating microplate reader (BioTek ELx808, BioTek Instrument Inc., Winooski, VT). Three different types of sample solutions were prepared for each 96-well microplate (Figure J.1): endotoxin standard solutions (STD), test samples (SPL) and positive product controls (SPLC). A 0.1 mL sample solution was added into each well. The stock endotoxin standard was diluted into 50, 5, 0.5, 0.05 and 0.005 EU/mL. LAL reagent water was used as the negative control (STD6). The standard solutions were analyzed in triplicate to acquire a reliable calibration curve. Test samples were measured in duplicate. A positive product control (spike sample) was prepared by adding a 10 µL 0.5 EU/mL standard solution into a test sample. The purpose of positive product control is to assess possible inhibition or enhancement effects. If the recovery efficiency is within the range of 50~150%, then there is no significant inhibition or enhancement. Further dilution would be performed if an inhibition (recovery efficiency < 50%) or enhancement (recovery efficiency > 200%) occurred. Once a microplate was ready, it was incubated at 37 °C for 10 minutes. After that, a 0.1 mL Kinetic-QCL[®] reagent per well was quickly dispensed into all 96 wells using a multichannel pipettor. The test program started immediately once the microplate was filled into the reader. The absorbance at 405 nm was monitored at 37 °C for 100 minutes. A typical absorbance curve is shown in Figure J.2.
- (5) Calculation- The reaction time in which the absorbance increases 0.20 absorbance units was recorded by the microplate reader software. A log-log linear regression of the concentration of each endotoxin standard versus its corresponding reaction time was performed to build a standard calibration curve. This curve was then used for calculating the endotoxin concentration in test samples and positive product controls. The test of a sample would be repeated if (1) the recovery efficiency was less than 50% or over 200%, or (2) the coefficient of variation (CV) between the replicate samples was over 10%. In a final report, the endotoxin concentration was presented in unit of EU/m³ air or EU/mg particles.

	1	2	3	4	5	6	7	8	9	10	11	12
A	STD1 50	STD1 50	STD1 50	SPL3	SPL3	SPLC3	SPL11	SPL11	SPLC11	SPL19	SPL19	SPLC19
B	STD2 5	STD2 5	STD2 5	SPL4	SPL4	SPLC4	SPL12	SPL12	SPLC12	SPL20	SPL20	SPLC20
C	STD3 0.5	STD3 0.5	STD3 0.5	SPL5	SPL5	SPLC5	SPL13	SPL13	SPLC13	SPL21	SPL21	SPLC21
D	STD4 0.05	STD4 0.05	STD4 0.05	SPL6	SPL6	SPLC6	SPL14	SPL14	SPLC14	SPL22	SPL22	SPLC22
E	STD5 0.005	STD5 0.005	STD5 0.005	SPL7	SPL7	SPLC7	SPL15	SPL15	SPLC15	SPL23	SPL23	SPLC23
F	STD6 0	STD6 0	STD6 0	SPL8	SPL8	SPLC8	SPL16	SPL16	SPLC16	SPL24	SPL24	SPLC24
G	SPL1	SPL1	SPLC1	SPL9	SPL9	SPLC9	SPL17	SPL17	SPLC17	SPL25	SPL25	SPLC25
H	SPL2	SPL2	SPLC2	SPL10	SPL10	SPLC10	SPL18	SPL18	SPLC18	SPL26	SPL26	SPLC26

Figure J.1. Layout of the 96-well microplate for endotoxin analysis.

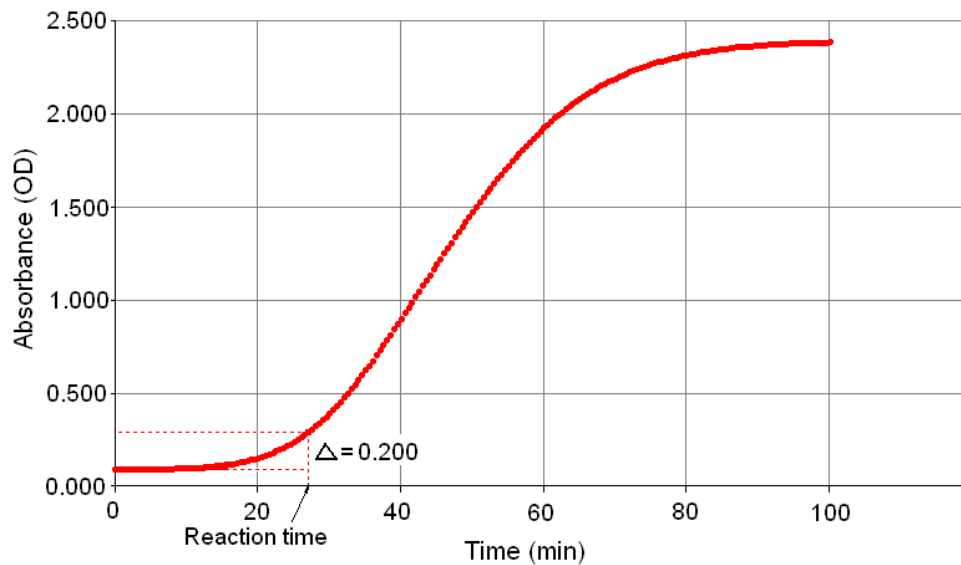


Figure J.2. Determination of the reaction time on an absorbance curve.

J.2. Quantification of airborne (1→3) β -D-glucan

The experimental protocol included the following steps:

- (1) Extraction- In the extraction step mentioned in Section J.1, a 1.0 mL supernatant per sample was collected for endotoxin analysis. Following that, a 1 mL 3M NaOH solution was added into the remaining extract. The mixture was vortexed and then agitated on a water bath shaker at the maximum agitation rate for 10 minutes with ice cooling. The

extract was centrifuged at 1,000×g for 15 minutes. A 1 mL supernatant was then collected for (1→3)-β-D-glucan analysis.

- (2) Dilution- The supernatant was diluted with reagent-grade water (Cat. # WP5001, Associates of Cape Cod Incorporated, East Falmouth, MA) until the diluted extract approximately contains 0.2 µg particles per mL solution. The diluted extract was either analyzed immediately or stored at -20 °C in a freezer.
- (4) Analysis- GlucateLL[®] Kit (Cat. # GT002, Associates of Cape Cod Incorporated, East Falmouth, MA) was used for determination of the (1→3)-β-D-glucan concentrations in the diluted extracts. (1→3)-β-D-glucan test was performed on an incubating microplate reader. Similar to the case of endotoxin analysis, three different types of sample solutions will be prepared: standard solutions (STD), test samples (SPL) and positive product controls (SPLC). The layout of the microplate was similar to that for endotoxin analysis. A 25 µL sample solution was pipetted into each well. The stock (1→3)-β-D-glucan standard was diluted in series into 100, 50, 25, 12.5, 6.25 and 3.125 pg/mL. Reagent-grade water was used as the negative control (STD7). A positive product control was prepared by adding a 5 µL 12.5 pg/mL standard solution into a test sample. The microplate was incubated at 37 °C for 10 minutes. After that, a 50 µL GlucateLL[®] reagent per well was quickly dispensed into all 96 wells of the microplate. Next, fill the microplate into a microplate reader with a temperature setting point of 37 °C, and initiate the test immediately. The absorbance at 405 nm in each well was recorded every 20 seconds. The whole test lasted for around 120 minutes.
- (5) Calculation- The reaction time required for the absorbance to increase 0.03 absorbance units was monitored. A log-log linear regression of the (1→3)-β-D-glucan concentration of each standard versus its corresponding reaction time was conducted to build a standard calibration curve. The curve was subsequently used for calculating the (1→3)-β-D-glucan concentration in test samples and positive product controls. A sample would be retested if (1) the recovery efficiency was less than 50% or over 200%, or (2) the inter-replicate CV was over 10%. In the former case, the test sample would be further diluted or be subject to pH adjustment (generally unnecessary). The concentration of airborne (1→3)-β-D-glucans was presented in unit of ng/m³ air or ng/mg particles in a final report.

AUTHOR'S BIOGRAPHY

Xufei Yang was born in Sichuan, China on August 5, 1976. He was admitted to Tsinghua University, China in 1995, and received a bachelor's degree in Environmental Engineering in 2000 and a master's degree in Environmental Science in 2002. During his BS and MS study, he worked under supervision of Dr. Weibin Li on developing advanced adsorbents and novel catalysts for mitigation of NO_x emissions from stationary and mobile sources. After graduation, he worked for a year as a research staff at Tsinghua University and was involved in construction and characterization of an indoor photochemical smog chamber system. Xufei joined the Department of Agricultural and Biological Engineering at the University of Illinois at Urbana-Champaign in fall, 2005. As a graduate research assistant supervised by Dr. Xinlei Wang, he primarily participated in a USDA CSREES air quality project titled *Physical, Chemical and Biological Characterizations of Particulate Matter from Confinement Livestock Buildings*. He also acted as a teaching assistant for multiple courses, and received the Karl. M. Snyder Teaching Excellence Award in 2008. Xufei has been a member of the American Society of Agricultural and Biological Engineering (ASABE) and the American Society of Heating, Refrigerating and Air Conditioning Engineers (ASHRAE) since 2007. He is also an inducted member of Alpha Epsilon since 2008.